Design, Synthesis and Biological Evaluation of Novel Organosilanes and Synthesis of Enantiopure Pheromones towards Crop Protection

Thesis Submitted to AcSIR

For the Award of the Degree of

DOCTOR OF PHILOSOPHY

In

CHEMICAL SCIENCES

AcSIR

By

Remya Ramesh
(Registration Number: 10CC11A26021)

Under the guidance of
Dr. D. Srinivasa Reddy

Organic Chemistry Division
CSIR-National Chemical Laboratory
Pune - 411008, India.

Dedicated

To My Parents

Thesis Certificate

This is to certify that the work incorporated in this Ph.D. thesis entitled "**Design, Synthesis and Biological Evaluation of Novel Organosilanes and Synthesis of Enantiopure Pheromones towards Crop Protection**" submitted by **Ms. Remya Ramesh** to Academy of Scientific and Innovative Research (AcSIR) in fulfilment of the requirements for the award of the Degree of Doctor of Philosophy, embodies original research work under my supervision. I further certify that this work has not been submitted to any other University or Institution in part or full for the award of any degree or diploma. Research material obtained from other sources has been duly acknowledged in the thesis. Any text, illustration, table etc., used in the thesis from other sources, have been duly cited and acknowledged.

Remya Ramesh

(Research Student)

Dr. D. Srinivasa Reddy

(Research Supervisor)

Declaration by the Candidate

I hereby declare that the original research work embodied in this thesis entitled, "**Design, Synthesis and Biological Evaluation of Novel Organosilanes and Synthesis of Enantiopure Pheromones towards Crop Protection**" submitted to Academy of Scientific and Innovative Research for the award of degree of Doctor of Philosophy (Ph.D.) is the outcome of experimental investigations carried out by me under the supervision of **Dr. D. Srinivasa Reddy**, Senior Scientist, Organic Chemistry Division, CSIR-National Chemical Laboratory, Pune. I affirm that the work incorporated is original and has not been submitted to any other academy, university or institute for the award of any degree or diploma.

September 2016   **Remya Ramesh**

CSIR-National Chemical Laboratory   **(Research Student)**

Pune-411 008

Acknowledgments

I take this opportunity to express my sincere gratitude to everyone who has helped me in this dissertation. I owe my gratitude to all those people who have made this dissertation possible and because of whom my graduate experience has been one that I will cherish forever.

My deepest gratitude is to my mentor Dr. D. Srinivasa Reddy, whose dedication to research is an inspiration to me. I thank him for giving me interesting problems and for his suggestions, ideas which has resulted in this thesis. I had gone through a tough time at the initial stages of my research and his support and advices helped me overcome it. He also gives the students free hand on chemicals and other facilities which makes our life more comfortable. He is a perfectionist and his time management and professionalism has had a lot of influence on me. I thank him for all his efforts which made me the researcher that I am today.

I express my sincere thanks to my Doctoral Advisory Committee members Dr. G.J. Sanjayan, Dr. Pradeep Kumar and Dr. M. V. Badiger for evaluating my research progress and for their continued support, guidance and suggestions. I am grateful to our Director Dr. Ashwini Nangia and former Directors Dr. Vijayamohanan K.Pillai, and Dr. Sourav Pal for providing me an opportunity to work at this prestigious institute and for providing all the research amenities necessary to carry out this work.

I extend my sincere gratitude to the head of the Organic Chemistry Division, Dr. Pradeep Kumar and Former HoDs, Dr. R. A. Joshi and Dr. Ganesh Pandey for allowing me to proceed smoothly and institutionalizing my work so as to complete within the time period. I am also thankful to all the scientists, staff and colleagues of OCD Division for their help and co-operation during this dissertation work. I owe my thanks to NMR division of NCL for providing the spectroscopic data, especially Dr. Rajamohanan, Sanoop, Srikanth, Snehal, Mayur, Dinesh, and Kavya. Help from Dr. B. Shantakumari, HRMS division is also acknowledged. I express my heartiest gratitude towards Dr. Rajesh Gonnade, and Sridhar for their help in X-Ray crystallographic analysis.

Thanks to all my collaborators Dr. Jocelyn Millar (University of California), Andrew Twidle (Plant and Food Research, New Zealand), Dr. Rajesh Gokhale (IGIB, New Delhi), Dr. Ramesh Ummani (IICT, Hyderabad), and Incozen therapeutics for providing us with data and for their suggestions which helped to take the project forward.

Acknowledgments

Acknowledgments

Finally, I bow my head in front of God, the almighty for giving me the strength to overcome all the difficulties in life. I am thankful to him for everything in my life, the good and the bad. Some were blessings and some were lessons.

Remya

September 2016

Pune

Abbreviations

AIBN	azobisisobutyronitrile
AcCl	acetyl chloride
Ac_2O	acetic anhydride
ADME	absorption, distribution, metabolism, and excretion
Å	angstrom
ATP	adenosine triphosphate
Bn	benzyl
Boc	*tertiary*-butyloxycarbonyl
brs	broad singlet
brsm	based on recovered starting material
Bu	butyl
t-Bu	*tertiary*-butyl
calcd.	calculated
cm^{-1}	1/centimetre
C–C	carbon-carbon
C–Cl	carbon-chlorine
C–Si	carbon-silicon
CNS	central nervous system
DBU	1,8-diazabicyclo[5.4.0]undec-7-ene
DCC	*N,N'*-dicyclohexylcarbodiimide
DCM	dichloromethane
DIBAL	diisobutylaluminium hydride
DIPEA	*N,N*-diisopropylethylamine
DMAP	4-dimethyl aminopyridine
DME	1,2-dimethoxyethane
DMF	*N,N*-dimethylformamide
DMSO	dimethylsulphoxide
DPPA	diphenylphosphoryl azide
dd	doublet of doublet
d	doublet

Abbreviations

EDC	1-ethyl-3-(3-dimethylaminopropyl)carbodiimide
Et	ethyl
EtOAc	ethyl acetate
EtOH	ethanol
eq.	equivalent
ESI	electron spray ionization mass spectroscopy
eV	electronvolt
FDA	food and drug administration
FGI	functional group interconversion
g	gram(s)
GI	gastrointestinal
GLP	good laboratory practice
h	hour(s)
hERG	human ether-à-go-go-related gene
HLM	human liver microsome
HOBt	hydroxybenzotriazole
HPLC	high performance liquid chromatography
HRMS	high resolution mass spectrometry
Hz	hertz
IP	intellectual property
IR	infrared
J	coupling constant (in NMR)
LAH	lithium aluminium hydride
LDA	lithium diisopropylamide
m	multiplet
m-CPBA	*meta*-chloroperoxybenzoic acid
Me	methyl
MeOH	methanol
MHz	megahertz
min	minute(s)

Abbreviations

mL	milliliter(s)
mmol	millimole(s)
MOM	methoxymethyl
Mtb	*mycobacterium tuberculosis*
Ms	methanesulfonyl
m/z	mass to charge ratio
N	normality
NaHMDS	sodium hexamethyldisilazane
NBS	*N*-bromosuccinimide
nM	nanomolar
NMR	nuclear magnetic resonance
NSAID	nonsteroidal anti-inflammatory drug
p-ABSA	*p*-acetamidobenzenesulfonyl azide
PCC	pyridinium chlorochromate
PDC	pyridinium dichromate
PK	pharmacokinetics
ppm	parts per million
psi	pounds per square inch
PTSA	*p*-toluenesulfonic acid
py	pyridine
q	quartet
RB	round bottom flask
RCM	ring closing metathesis
R_f	retention factor
RT	room temperature
s	singlet
SAR	structure – activity relationship
sec	secondary
t	triplet
TBS	*tert*-butyldimethylsilyl

Abbreviations

tert	tertiary
TEA	triethyl amine
TES	triethyl silane
Tf	trifluoromethanesulfonyl
THF	tetrahydrofuran
TFA	trifluroacetic acid
TLC	thin layer chromatography
TMEDA	tetramethylethylenediamine
TPP	triphenyl phosphine
UV	ultraviolet
WHO	world health organization
^{o}C	degree celsius
μM	micromolar
))))	sonication

General Remarks

- All reagents, starting materials, and solvents (including dry solvents) were obtained from commercial suppliers and used as such without further purification.

- Reactions were carried out in oven-dried glassware under a positive pressure of argon unless otherwise mentioned with magnetic stirring.

- Air sensitive reagents and solutions were transferred *via* syringe or cannula and were introduced to the apparatus *via* rubber septa.

- The progress of reactions was monitored by thin layer chromatography (TLC) with 0.25 mm pre-coated silica gel plates (60 F254). Visualization was accomplished with either UV light, Iodine adsorbed on silica gel or by immersion in ethanolic solution of phosphomolybdic acid (PMA), *p*-anisaldehyde or $KMnO_4$ followed by heating with a heat gun for ~15 sec.

- Column chromatography was performed on silica gel (100-200 or 230-400 mesh size) or neutral alumina.

- All the melting points are uncorrected and were recorded using a scientific melting point apparatus (Buchi B-540).

- Deuterated solvents for NMR spectroscopic analyses were used as received.

- All ^{1}H NMR and ^{13}C NMR spectra were obtained using a 200 MHz, 400 MHz or 500 MHz spectrometer. Coupling constants were measured in Hertz. All chemical shifts are quoted in ppm, relative to TMS, using the residual solvent peak as a reference standard. The following abbreviations are used to explain the multiplicities: s = singlet, d = doublet, t = triplet, q = quartet, m = multiplet, br = broad.

- HRMS (ESI) were recorded on ORBITRAP mass analyser (Q Exactive).

- Infrared (IR) spectra were recorded on a FT-IR spectrometer as thin films using NaCl plates.

- Optical rotations were recorded on a P-2000 polarimeter at 589 nm (sodium D-line).

- Chemical nomenclature (IUPAC) and structures were generated using Chem Bio Draw Ultra.

Synopsis

	Synopsis of the Thesis to be submitted to the Academy of Scientific and Innovative Research for Award of the Degree of Doctor of Philosophy in Chemistry
Name of the Candidate	Ms. Remya Ramesh
Degree Enrolment No. & Date	Ph. D in Chemical Sciences (10CC11A26021); August 2011
Title of the Thesis	Design, Synthesis and Biological Evaluation of Novel Organosilanes and Synthesis of Enantiopure Pheromones towards Crop Protection
Research Supervisor	Dr. D. Srinivasa Reddy

The thesis is divided into two chapters. Chapter I deal with the design, synthesis and biological evaluation of organosilicon compounds. The first subsection (1.1) of this chapter gives an overview about the utility of silicon in medicinal chemistry. The second subsection (1.2) deals with the synthesis and identification of silicon analogs of an anti-obesity drug rimonabant as potent anti-tubercular agents. The third part (1.3) describes a methodology for the preparation of allyl silanes and its application to the synthesis of α, β and γ amino acids with silicon incorporation. Chapter II deals with the synthesis of enantiomers of the longtailed mealybug pheromone and its biological evaluation.

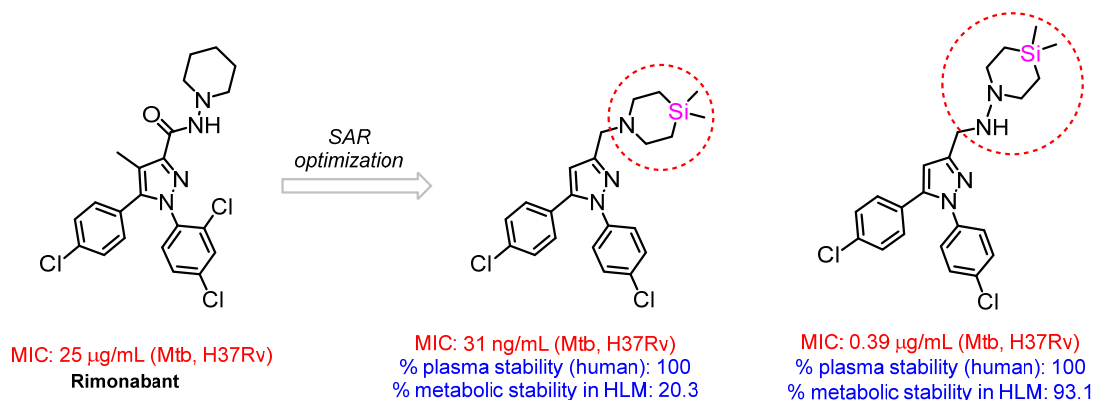**Chapter I: Design, synthesis and biological evaluation of organosilanes**

In drug discovery, isosteric replacement is one of the key tools for lead optimization. Due to similarities between carbon and silicon, the latter is considered to be an isostere of carbon. At the same time, the inherent differences between carbon and silicon can be judiciously used to modulate the potency and pharmacokinetic properties of a molecule. Silicon increases the lipophilicity of the molecule which increases the cell penetration and can be advantageous in drugs targeting the central nervous system and infectious diseases.[1]

Identification of novel sila analogs of rimonabant as potent anti-TB agents

Tuberculosis is an infectious disease caused by various strains of mycobacteria and affects mainly the lungs. Bacteria develop resistance against the known drugs, which

is a major hurdle in antibiotic drug discovery. With the emergence of multi-drug resistant tuberculosis, discovery of new drugs to combat tuberculosis is the need of the hour. BM212, a diarylpyrrole inhibits the growth of mycobacteria (MIC 0.7-1.5 μg/mL) by blocking the MmpL3 protein. MmpL3 is a transporter protein which helps in translocation of mycolic acids from the cytoplasm to the cell wall. These mycolic acids are essential for the survival of mycobacteria. Rimonabant, a cannabinoid (CB1) receptor blocker is structurally very similar to BM212. Hence, several analogs of rimonabant were synthesized and their anti-TB potential was evaluated. An increase in lipophilicity is expected to improve the potency of this series because of increased cell penetration. Keeping this in mind, analogs containing silicon atom were synthesized and they showed improved anti-tubercular activity with the best compound showing an MIC of 0.031 μg/mL. Another sila analog (MIC 0.39 μg/mL) showed very good ADME properties which include solubility, metabolic and plasma stability.[2]

MIC: 25 μg/mL (Mtb, H37Rv)
Rimonabant

SAR optimization

MIC: 31 ng/mL (Mtb, H37Rv)
% plasma stability (human): 100
% metabolic stability in HLM: 20.3

MIC: 0.39 μg/mL (Mtb, H37Rv)
% plasma stability (human): 100
% metabolic stability in HLM: 93.1

Zinc mediated allylations of chlorosilanes promoted by ultrasound: Synthesis of novel constrained sila amino acids

Due to our interest on organosilanes, novel methodologies to synthesize organosilicon building blocks were explored. Allylsilanes are generally prepared by allylation (Grignard or metal mediated reactions) of chloro or alkoxysilanes. They can be functionalized and transformed to compounds which are biologically active. Along these lines, a simple, fast and efficient method for zinc mediated allylation and propargylation of chlorosilanes promoted by ultrasound was developed. The methodology was used for the synthesis of many compounds including mono-allyl, di-allyl and tri-allyl silanes. The

known iodo intermediate prepared from diallyldimethylsilane was then transformed to α−, β− and γ− amino acids having an unusual 5,5-*trans* fusion which may be considered as GABA mimics. The constrained and lipophilic GABA analog is expected to show interesting biological features.[3]
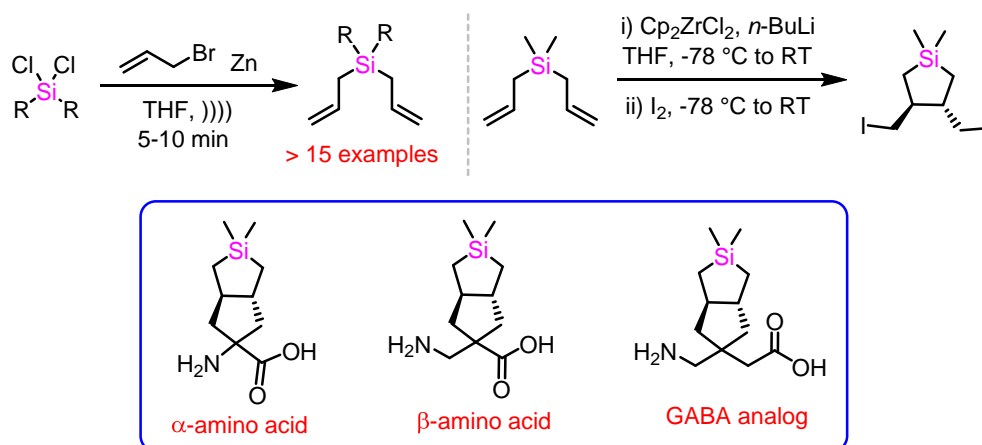

Chapter II: Synthesis of enantiopure pheromones towards crop protection

A pheromone is a chemical factor that triggers a social response in members of the same species. Synthetic pheromones can be used to lure and trap insects and find applications in pest management programs. Pheromones are highly sensitive and species specific. Since, they don't affect other beneficial organisms; pheromones are considered to be one of the environment friendly methods for controlling pests.

The longtailed mealybug is a pest that infests various crops such as avocado, coffee, citrus, guava, mango, orchids, pineapple, potato, sugarcane etc. The sex pheromone secreted by the female longtailed mealybug was isolated and characterized by Millar's group. The compound possesses a monoterpene skeleton with a chiral quaternary center whose absolute configuration was not known. The synthetic racemic pheromone showed excellent activity in field trials. One of intermediates in the racemic synthesis of our research group, an acyclic alcohol was resolved by converting into its diastereomeric derivatives. The enantiopure intermediates were then individually converted to the target compounds. Field trials of the enantiomers were conducted in California (USA) and New

Zealand. The results showed that (*S*)-(+)-pheromone is attractive to male mealybugs suggesting that it is the natural product.[4]
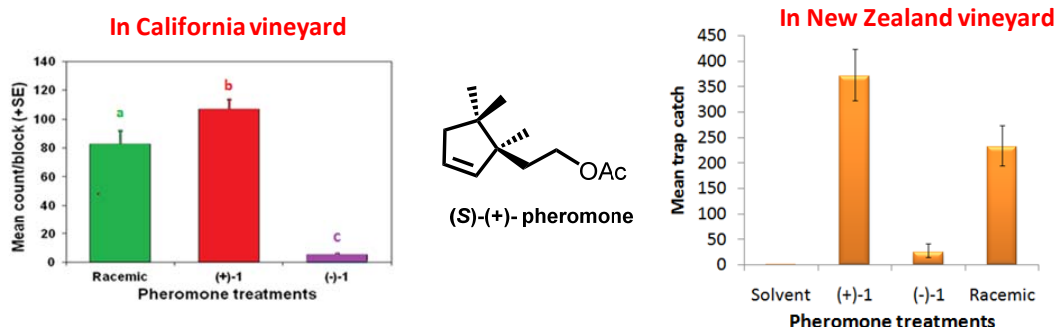
The resolution method was not suitable for making large quantities of the active enantiomer. Hence, we developed an enantiospecific route for the synthesis of pheromones starting from corresponding bornyl acetates. The highlights of this synthesis are use of cheap chiral pool starting material and translactonization of [3.2.1] bicyclic lactone.[5]
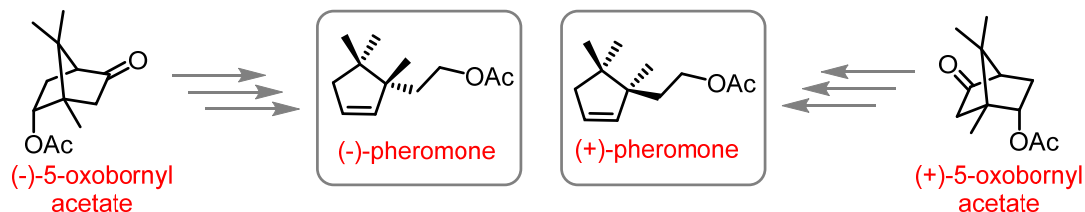
Noteworthy Findings

a) Synthesized several analogs of rimonabant and evaluated their anti-TB potential. The best compound showed an MIC of 31 ng/mL against Mtb.

b) Developed a methodology for the ultrasound promoted synthesis of allyl and propargyl silanes from chlorosilanes through zinc mediation.

c) α−, β− and γ− amino acids with unusual 5,5-*trans* fusion (GABA mimics) were synthesized starting from diallyldimethylsilane.

d) Enantiomers of the longtailed mealybug pheromone were synthesized for the first time and field trials were conducted in two geographically different locations. The (*S*)-(+)-pheromone was attracting male mealybugs following which an enantiospecific synthesis was developed.

References

1. A. K. Franz, S. O. Wilson, *J. Med. Chem.* **2013**, *56*, 388.

2. **R. Ramesh**, R. Shingare, V. Kumar, A. Anand, B Swetha, S. Veeraraghavan, S. Viswanadha, R. Ummanni, R. Gokhale, D. S. Reddy, *Eur. J. Med. Chem.* **2016**, *122*, 723.

3. **R. Ramesh**, D. S. Reddy, *Org. Biomol. Chem.* **2014**, *12*, 4093.

4. **R. Ramesh**, P. S. Swaroop, R. G. Gonnade, C. Thirupathi, R. A. Waterworth, J. G. Millar, D. S. Reddy, *J. Org. Chem.* **2013**, *78*, 6281.

5. **R. Ramesh**, V. Bell, A. M. Twidle, R. G. Gonnade, D. S. Reddy, *J. Org. Chem.* **2015**, *80*, 7785.

Contents

Chapter 1. Design, synthesis and biological evaluation of novel organosilanes

Section 1. *Prospects of organosilanes in medicinal chemistry*

Section 2. *Identification of novel sila analogs of rimonabant as potent anti-TB agents*

Contents

Contents

Chapter 2. Synthesis of enantiopure pheromones towards crop protection

Chapter 1:

Design, synthesis and biological evaluation of novel organosilanes

1.1.1. Silicon in medicinal chemistry

The switching of hydrogen with deuterium in drug discovery has been explored very well and is considered to be a successful concept.[1,2] In similar lines, the similarity between carbon and silicon makes silicon an ideal choice as a carbon bioisostere in drug discovery.[3-10] Bioisosteres are groups with similar physicochemical properties and display similar biological activity. Bioisosteric replacements are commonly practised in medicinal chemistry so as to modulate the properties of a molecule.[3,11,12] Unlike other elements such as tin, silicon does not have any inherent toxicity.[5,13] The introduction of silicon also provides freedom to operate as most of the earlier patents do not cover silicon as part of their claims. The effect of silicon substitution was also explored in agrochemicals[14,15] and odorants[16,17]. Some of the fundamental differences between carbon and silicon can be efficiently utilized in drug design and lead optimization (figure 1.1.1).

➢ *Larger Carbon-Silicon bond length:* The bond length of C-C is 1.54 Å and that of C-Si is 1.87 Å *i.e.* C-Si bond is almost 20% longer than a C-C bond.[18] This can lead to changes in shape and conformation of the molecule and can also alter the way in which the molecule interacts with the receptor.

➢ *Increase in lipophilicity:* Silicon analogs are more lipophilic than their carbon counterparts. This can lead to improved cell penetration and can ultimately result in an improvement in potency. The increase in lipophilicity can also be beneficial in the design of drugs targeting bacteria and central nervous system.[19] In some cases, it can also be detrimental as this can lead to liabilities such as poor solubility and metabolic clearance. Therefore, one needs to balance the concept depending on the target and its location.

➢ *Difference in bonding preferences:* Silicon prefers higher coordination numbers as compared to carbon.[18,20] Double bonds on silicon are not observed generally. eg. a silane diol does not undergo dehydration to form silanone whereas geminal diols are not stable in the case of carbon. Thus silicon also offers a novel chemical space and provides access to compounds for which corresponding carbon analogs

are not available. This has been exploited in designing transition state mimics. Silicon can also extend its co-ordination number up to six which is useful in the formation of coordination complexes.

➢ *Higher electropositivity of silicon:* Silicon is more electropositive than carbon which leads to difference in bond polarity. This can cause subtle differences in the behaviour of silanols and carbinols.

Larger covalent radius

Increase in lipophilicity

14 **Si**
Silicon
28.0855

Clear IP position

Access to compounds that do not have stable carbon analogs

No intrinsic element specific toxicity

More electropositive
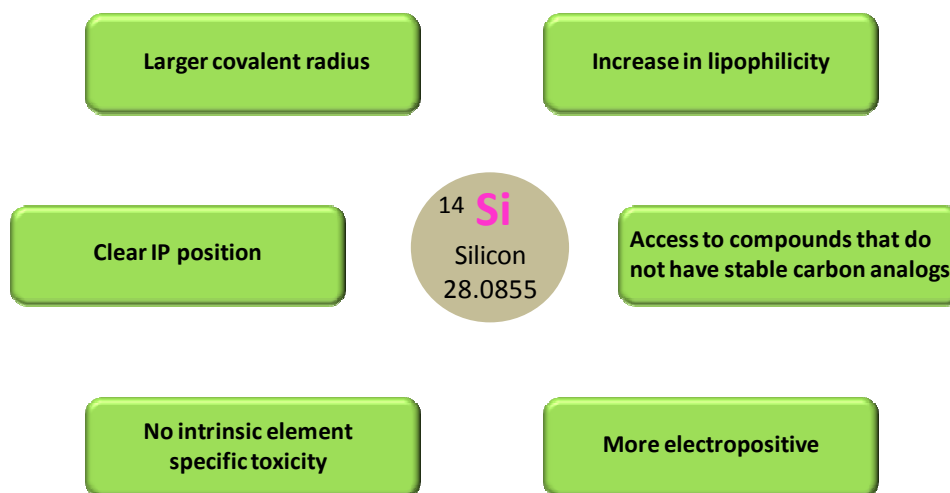
Figure 1.1.1. Silicon isosteres in medicinal chemistry

The utility of organosilanes in drug discovery has been reviewed in the past by research groups of Reinhold Tacke and Annaliese Franz.[4-10] In this section of the thesis, selected examples from the literature are discussed highlighting the potential of silicon in medicinal chemistry. The focus is on case studies where the introduction of silicon has created a benefit over its analog.

1.1.2. Modification of metabolic pathways

Any drug after reaching the body undergoes enzyme catalyzed biochemical modification called metabolism.[21] Due to the difference in bonding properties, silicon analogs can have a different metabolic fate compared to the parent carbon compound.

Johansson *et.al.* incorporated silicon in the antipsychotic drug haloperidol and found that the silicon analog follows a different metabolic pathway (figure 1.1.2).[22-25]
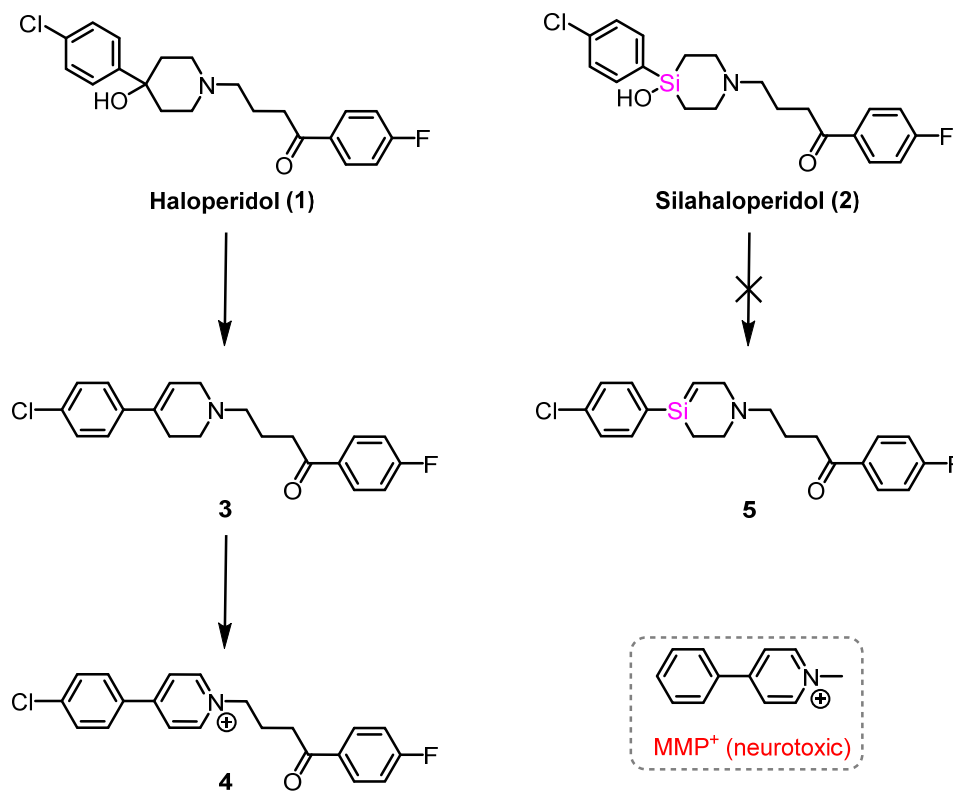
Figure 1.1.2. Metabolism of haloperidol and its silicon analog

Haloperidol causes neurotoxic side effect which is attributed to its metabolite, a pyridinium compound **4**. Compound **4** is structurally similar to 1-methyl-4-phenylpyridinium (MMP$^+$) which kills dopamine producing neurons of the brain and can induce Parkinson disease.[26-29] However, in the case of silahaloperidol (**2**) the pyridinium metabolite was not observed.[23,30] The inherent stability of the Si-O bond and the instability of the Si=C makes the molecule to adopt a different metabolic pathway.

Similar carbon/ silicon switching was also done in another related compound, trifluperidol (**6**) and analogous results were obtained (figure 1.1.3). [23,31] In the case of both the silicon analogs **2** and **7**, hydroxylation of the piperidine ring leading to opening of the ring was found to be the major metabolic pathway.
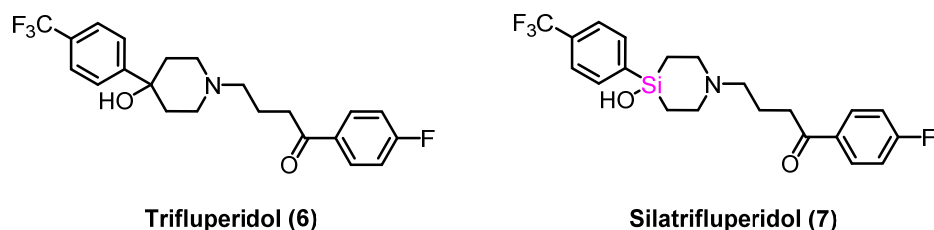
Figure 1.1.3. Trifluperidol and its silicon analog

Tacke *et.al.* incorporated silicon in loperamide, a commonly prescribed anti-diarrheal drug.[32] The structure of loperamide (**8**) is similar to haloperidol (**1**), although they act on completely different targets. The compounds **8** and **9** showed similar potency for the µ1 opioid receptor and had similar physicochemical properties.
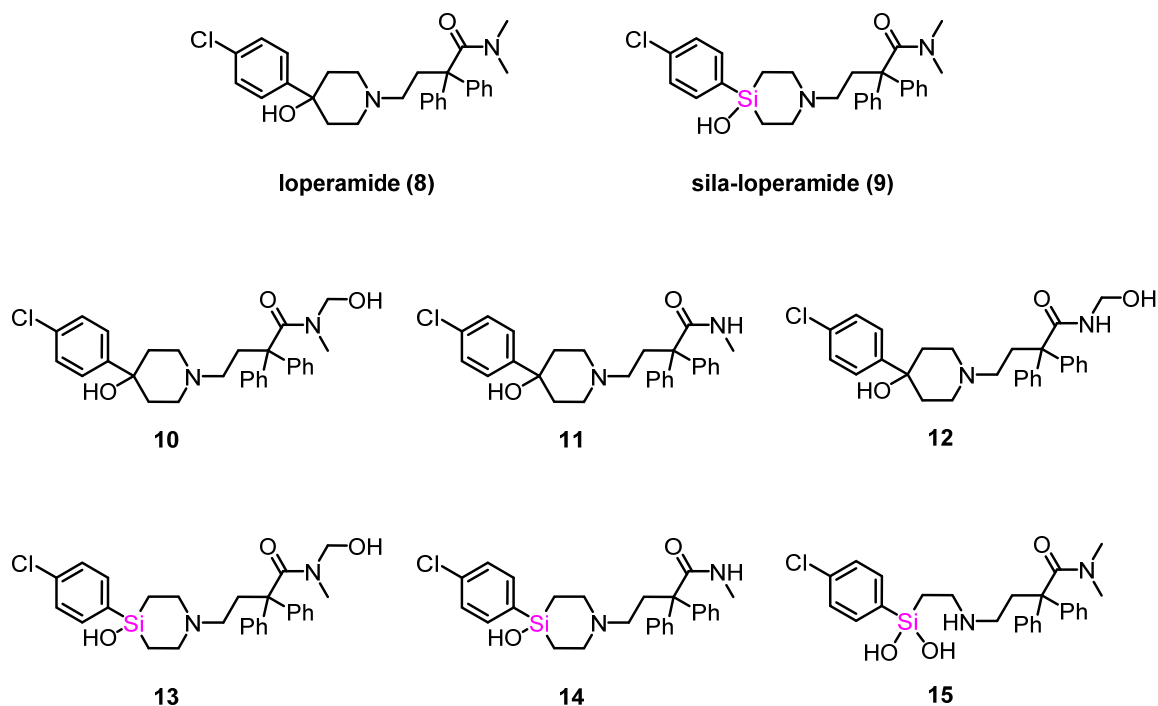
Figure 1.1.4. Metabolism of loperamide and its silicon analog

The metabolic pathways of both the compounds (**8** and **9**) were found to have marked differences (figure 1.1.4). The major metabolites of loperamide **10**, **11** and **12** were stable in circulation. Similar metabolites **13** and **14** were observed in case of the silicon analog, but the analog of **12** was not detected. Instead another metabolite **15**

resulting from the α oxidation and ring opening was found. The silanediol **15** showed high clearance and was rapidly eliminated from the circulation thus reducing the burden of metabolites. Thus, the above examples show that silicon incorporation in drugs can lead to alternate metabolic pathway which was advantageous in most cases.

1.1.3. Silanols as transition state mimics

1.1.3.1. Silane diols as protease inhibitors

Proteases are enzymes which hydrolyze the amide bond of peptides and are involved in various physiological reactions. Inhibition of specific proteases has been found to be useful in controlling several diseases and hence proteases have become an interesting pharmaceutical target.[33] Proteases stabilize the tetrahedral diol formed by the addition of water and this diol then collapses to individual peptides. Any compound which can mimic the enzyme-substrate interactions present in the tetrahedral intermediate and does not undergo hydrolysis could inhibit the enzyme (see figure 1.1.5).[34]
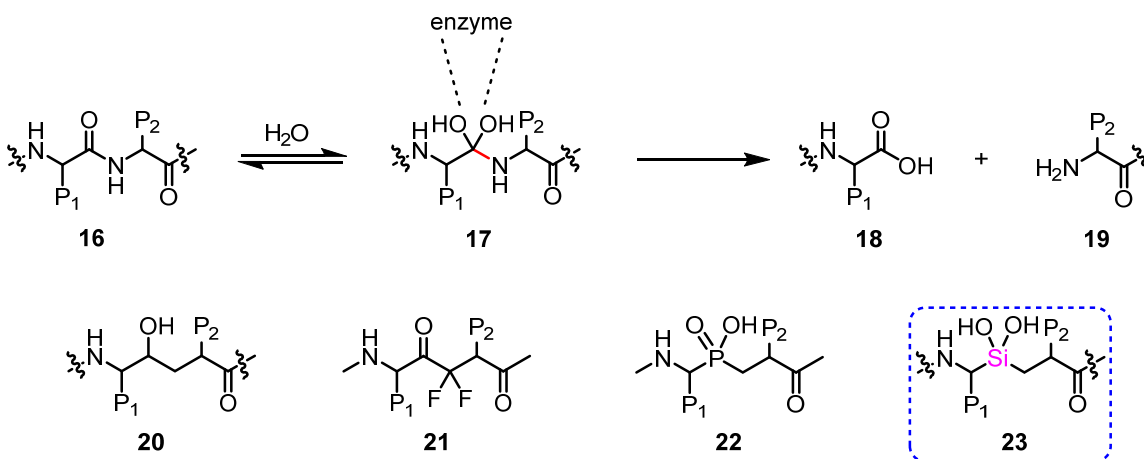
Figure 1.1.5. Design of protease inhibitors

Sieburth pioneered the use of stable silane diols to mimic the *gem* diol transition state involved in protease hydrolysis.[34-42] Silicon favors sp^3 hybridization over sp^2 and hence geminal silane diols are stable and do not undergo elimination to from the silanone (Si=O). Silane diols as bioisosteres of carbonyl hydrate has gained attraction in medicinal

chemistry and some of the inhibitors known in the literature are shown in figure 1.1.6.[34,37,38,41] Simple silane diols undergo polymerization, but sterically hindered diols are found to be stable. The biological activity of silane diols also prompted organic chemists to develop efficient synthetic routes to access them.[43] Since protease inhibitors represent an important class of therapeutic agents, silane diols have great potential and further research in this area can lead to more potent and selective inhibitors.

ACE inhibitor (24)
$IC_{50} = 3.8$ nM

HIV protease inhibitor (25)
$IC_{50} = 2.7$ nM

serine protease inhibitor (26)
$IC_{50} = 107$ nM

thermolysin inhibitor (27)
$IC_{50} = 41$ nM
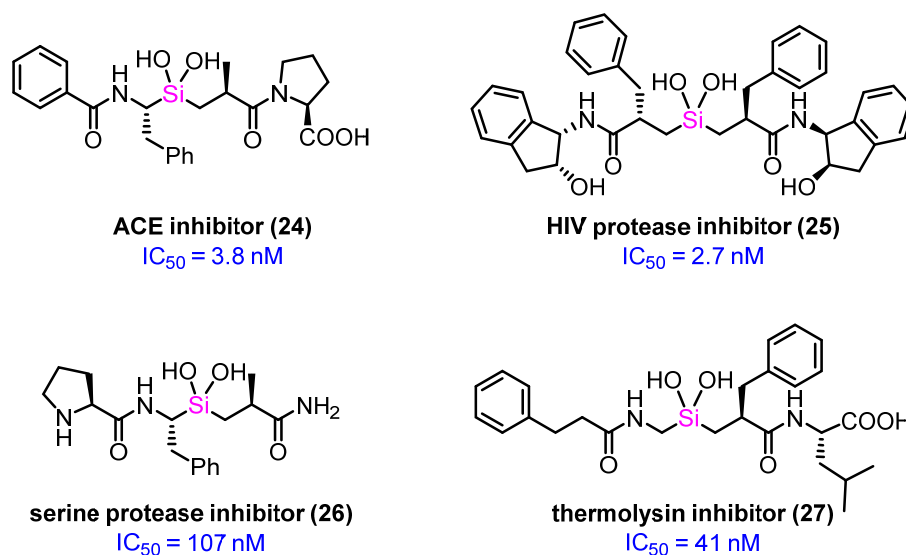
Figure 1.1.6. Silane diol based protease inhibitors

1.1.3.2. Silane triols

Blunder *et.al.* extended the concept of silane diols to silane triols in order to mimic the transition state of ester hydrolysis.[44] Silane triols with bulky substituents (**28 – 30**) were synthesized so as to prevent self- polymerization and were evaluated for their inhibition of the enzyme acetylcholinesterase (AChE). Compound **29** showed the highest inhibition rate and the IC_{50} was found to be 121 µM. The compound showed reversible inhibition of the enzyme which is a prerequisite for therapeutic agents. Irreversible inhibitors can lead to damage of the enzyme.
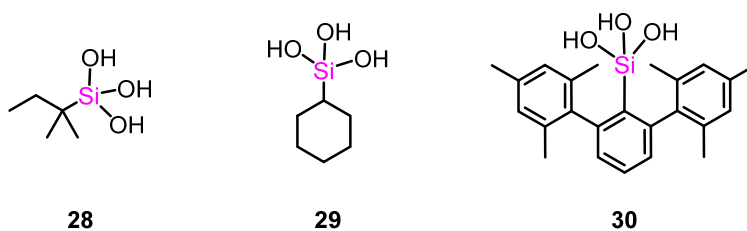
Figure 1.1.7. Silane triols as AChE inhibitors

1.1.4. Silicon containing complexes

Silicon can exhibit coordination numbers higher than four due to the presence of empty 3d orbitals. The silicon complex Pc-4 (**32**) built on the framework of phthalocyanine (**31**) is undergoing clinical trials for use in the photodynamic therapy (PDT).[45-50] In PDT, the photosensitizer when excited by light of particular wavelength interacts with molecular oxygen and generates reactive oxygen species.[51-56] This reactive oxygen species (ROS) then kills the cells in the illuminated area by inducing apoptosis. The photosensitizer is cleared from normal tissues more rapidly, which leads to their relatively more accumulation in tumour cells. The photophysical properties of phthalocyanines can be modulated by changing the ring substituents, axial ligands and the central metal atom. The silicon phthalocyanine Pc-4 has the right balance between lipophilicity and hydrophilicity. Pc-4 after cellular uptake accumulates in the mitochondria and causes photocytotoxicity. Recently, another modified phthalocyanine Pc-227 (**33**) was reported which on photolysis gives Pc-4 (figure 1.1.8).[56]
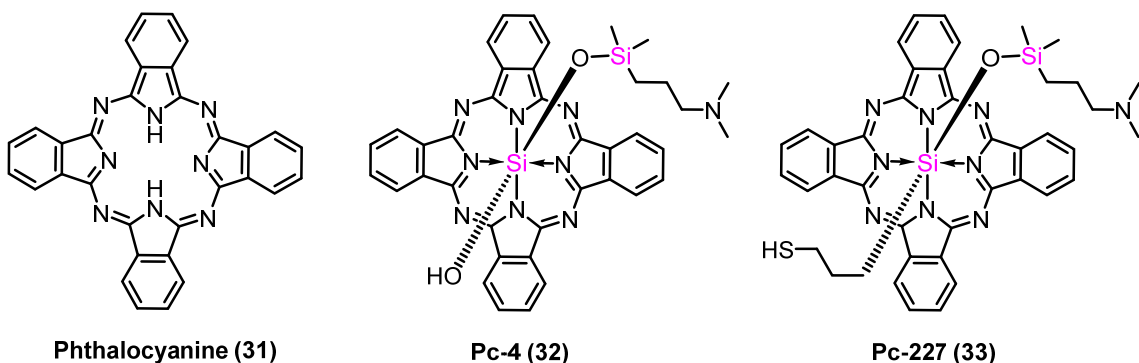
Figure 1.1.8. Silicon phthalocyanines

Meggers and co-workers recently reported the biological activity of silicon containing octahedral polypyridyl complexes **34 – 37** (figure 1.1.9).[57] Studies showed that the complexes **36** and **37** intercalate between the DNA base pairs. DNA intercalators have a variety of therapeutic applications mainly in the area of cancer therapy.[58] Silicon because of non-toxicity and natural abundance is advantageous over the commonly used transition metals in designing complexes with pharmaceutical applications.

34   **35**

36   **37**
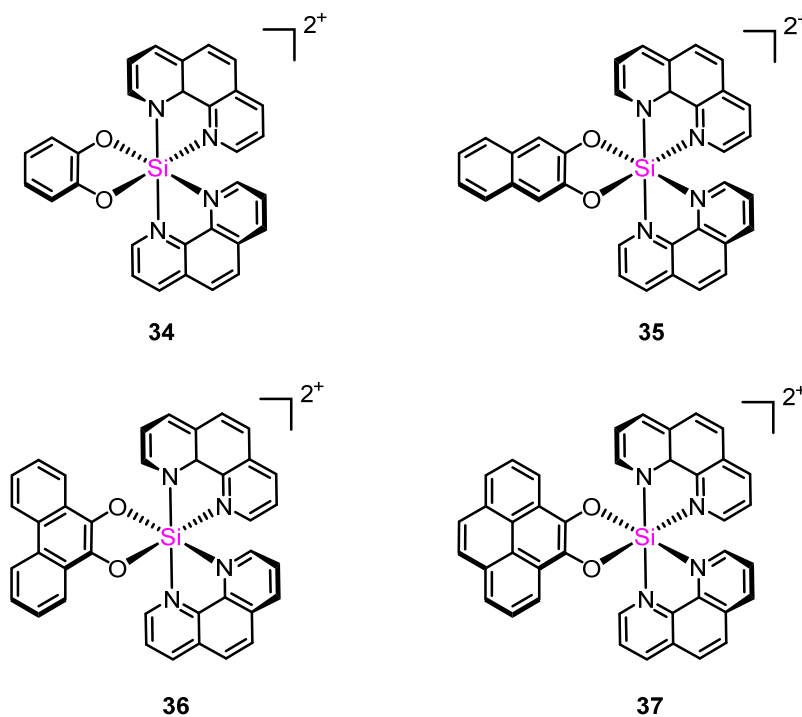
Figure 1.1.9. Hypervalent silicon complexes as DNA intercalators

Silatranes are compounds having pentavalent silicon with a transannular dative bond between N and Si (see figure 1.1.10 for a general structure).[59,60] Some of the compounds from this class are reported to have interesting biological activities (antibacterial, antifungal, anticancer, antiviral, anti-inflammatory etc.).[61-65] Mehta *et. al.* reported that 1-ethoxysilatrane (**38**) inhibits cholesterol biosynthesis and rats treated with the compound showed a decrease in serum cholesterol.[64,65]

Y = O; Silatrane
Y = N; Azasilatrane
Y = C; Carbasilatrane
Y = S; Thiasilatrane

38
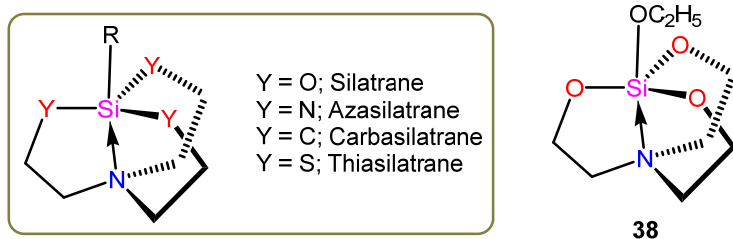
Figure 1.1.10. Silatranes

1.1.5. Increase in lipophilicity by introduction of silicon

1.1.5.1. Silicon incorporation to increase brain penetration

The endothelial cells of the brain capillaries have tight junctions which is called blood brain barrier (BBB). This barrier selectively allows the passage of certain molecules to the brain and prevents others. Hence, the BBB makes drug delivery to the brain a tough task.[19,66] It is known that small lipophilic molecules diffuse through this barrier. The incorporation of silicon into a molecule increases its lipophilicity, which can increase the BBB penetration of a drug.

ClogP = 0.17

Linezolid
(marketed antibiotic)

ClogP = 1.00

Sutezolid
(Phase-II; TB)

Silicon incorporation increases
brain/plasma ratio significantly

Siliconized linezolids

39: R = H; R' = C(O)Me; ClogP = 4.15
40: R = F; R' = C(O)Me; ClogP = 4.36
41: R = H; R' = C(S)OMe; ClogP = 5.55
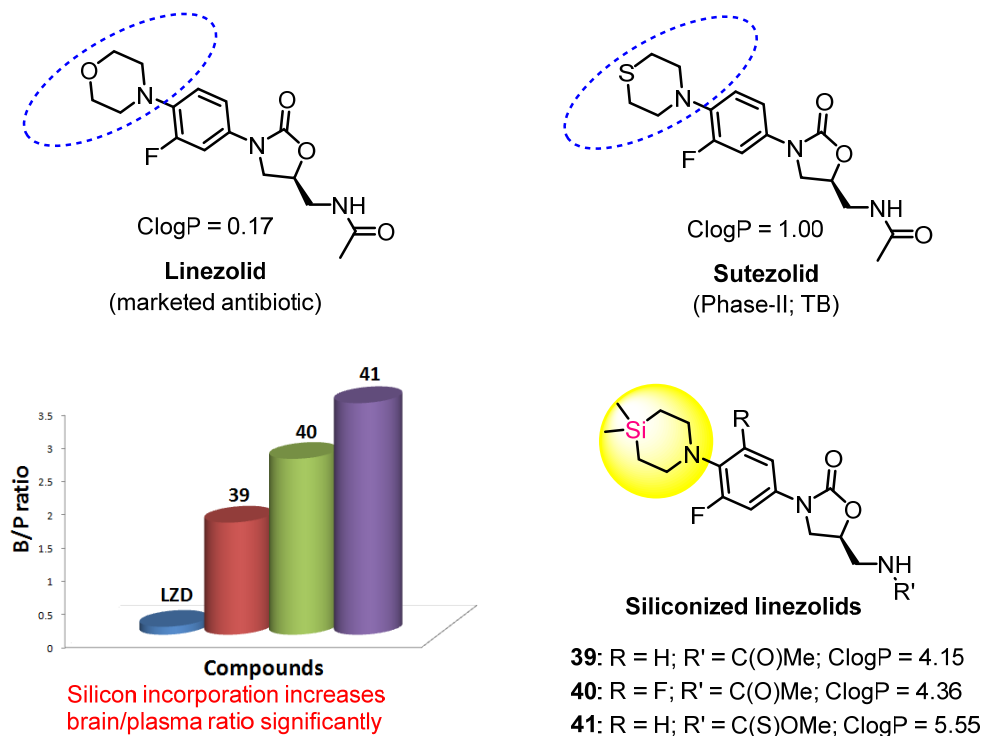
Figure 1.1.11. Silicon incorporation in linezolid

In our group, we had designed and synthesized silicon analogs of oxazolidinone antibiotics (figure 1.1.11).[67] Linezolid is the first marketed oxazolidinone drug and is used as an antibiotic.[68] The thiomorpholine sutezolid is in clinical trials for treating tuberculosis. Several compounds were synthesized with silicon replacing the O/S atom of the ring. The brain pharmacokinetics of the most active compounds revealed that silicon compounds had increased brain penetration. The compound **41** had 29-fold higher brain/plasma ratio with respect to linezolid. This increase in CNS exposures is due to the increase in lipophilicity of the compounds which is also evident from the ClogP values.[67]

1.1.5.2. Silicon analogs of campothecin

The increase in lipophilicity due to silicon incorporation was utilized in the synthesis of stable campothecin analogs. Campothecin is an anticancer natural product which inhibits the enzyme DNA topoisomerase I.[69] The δ-lactone moiety present in campothecin is susceptible to hydrolysis *in vivo*. The lactone form (**42**) which can distribute into the cell is considered to be the active form. The carboxylate **43** binds strongly to human serum albumin which causes an increase in the rate of lactone hydrolysis so as to maintain the equilibrium.
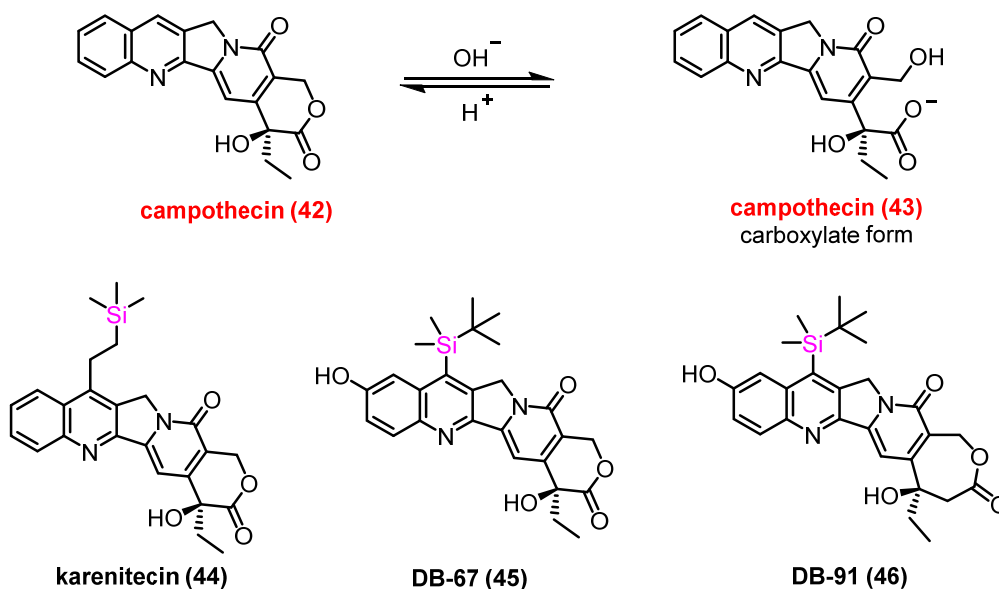
Figure 1.1.12. Silicon analogs of campothecin

An increase in lipophilicity leads to increased partitioning into red blood cells resulting in less hydrolysis of the lactone. Several silicon analogs were synthesized and two of them, karenitecin and DB-67 were evaluated in human clinical trials for cancer.[70-79] The compound DB-67 also penetrates the blood brain barrier and hence was tested for cancers of the central nervous system.

1.1.6. Drug design utilizing the electropositivity of silicon

1.1.6.1. N$^+$/ Si exchange

Zifrosilone (**49**) is a silicon compound which went to clinical trials for treating Alzheimer's disease.[80-82] It was proposed that Alzheimer's patients have a deficiency of the neurotransmitter acetylcholine and so medications which help to increase the concentration of acetylcholine would be beneficial.[83] The enzyme acetylcholineesterase (AChE) catalyzes the hydrolysis of acetylcholine (**47**) and hence inhibitors of this enzyme were tested for Alzheimer's disease. Trifluoromethyl ketones such as **48** were reported to inhibit AChE.[84,85] An ammonium/silicon switching in **48** resulted in lipophilic compound **49** which also showed AChe inhibition (figure 1.1.13). The greater electropositivity of silicon creates an ionic charge which interacts with the cation binding site of the target enzyme. This drug design strategy to create a positive center in a neutral molecule can be used in medicinal chemistry as an alternate option.

acetylcholine (47)   **48**   **zifrosilone (49)**
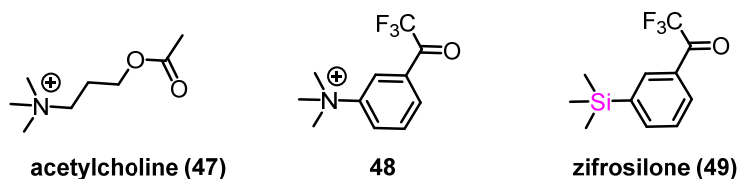
Figure 1.1.13. N$^+$/ Si exchange in zifrosilone

Tacke and co-workers applied the concept of N$^+$/ Si in the muscarinic M2 receptor modulators (figure 1.1.14).[86,87] W84 (**50**) inhibits the dissociation of [^{3}H]NMS, an orthosteric radiolabeled ligand of the receptor. The silicon analog **51** was also found to be an allosteric modulator of the receptor, but it exhibited positive allosteric modulation

(enhances binding of [³H]NMS to receptor). Here silicon switching has transformed the molecule from allosteric inhibitor to allosteric activator.

W84 (50)

51
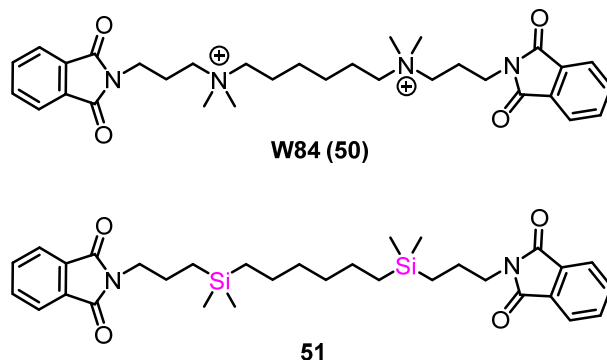
Figure 1.1.14. Silicon analog of W84

1.1.6.2. Acidity of silanols

Due to the higher electropositivity of silicon, the hydrogen bonding ability and acidity of silanols is higher. This can be useful in pharmacophores where hydrogen bonding interactions are important. Baney and co-workers showed that silicon incorporation increased the antibacterial activity in a series of alcohols (figure 1.1.15).[88]

| 52a (El = C) | 53a (El = C) | 54a (El = C) | 55a (El = C) |
| 52b (El = Si) | 53b (El = Si) | 54b (El = Si) | 55b (El = Si) |
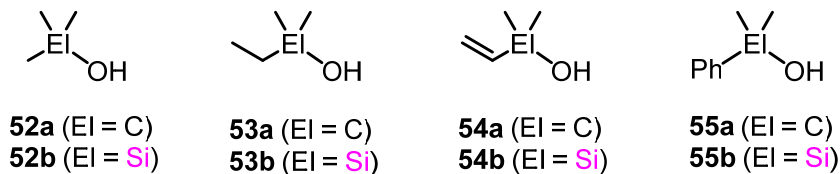
Figure 1.1.15. Alcohols and their corresponding silanols; El (element) = C/Si

This increase in activity (see table 1.1.1.) is proposed to be due to increase in hydrogen bonding ability as well as lipophilicity. The authors also proved that the hydrogen bonding ability of silanols was almost twice of that of the corresponding alcohols with the help of IR spectroscopy. Another example where an increase in potency of silanols was reported is discussed in a later section (figure 1.1.20).

Compound	Minimum Lethal Concentration (MLC in %, g/g)			
	E. coli	*S. aureus*	*P. aeruginosa*	*E. faecalis*
52a	13.54	10.61	9.79	13.33
52b	2.36	2.48	2.36	3.15
53a	5.09	4.17	3.96	5.67
53b	1.04	0.80	0.87	1.14
54a	5.23	4.37	3.67	5.63
54b	1.23	1.04	1.00	1.32
55a	0.96	0.78	0.71	0.93
55b	0.27	0.26	0.35	0.42

Table 1.1.1. Antibacterial activity of compounds

1.1.7. Taking advantage of the increased bond length of silicon

1.1.7.1. Silicon as an isostere of olefinic double bond

Combretastatin A-4, a natural product shows potent anti-cancer activity by inhibiting the tubulin polymerization. The compound has a *cis*-olefin which tends to isomerize in solution and hence there have been attempts to replace this olefin with any stable isostere.[89] Nakamura *et. al.* assumed that because of the larger C-Si bond length, a silicon linker can be used as a bioisostere of olefin. Computational calculations showed that the distance between the benzene rings (d) is almost same in combretastatin A-4 and the silicon analog **56** (figure 1.1.16). Accordingly, several silicon analogs were synthesized and evaluated using *in vitro* assays for anti-cancer activity (human breast cancer cell line). The natural product showed an IC$_{50}$ of 0.004 μM and the newly designed silicon analog (**56**) also showed activity (IC$_{50}$ 0.043 μM), but lesser than the natural product. One of the silicon analogs (**58**) showed an IC$_{50}$ of 0.007 μM similar to the natural product. The stability of the compounds in solution was also analyzed which showed that compounds **56**, **58** and **59** were stable. Under same conditions, it was observed that the concentration of combretastatin decreased to nearly 85%.[90]
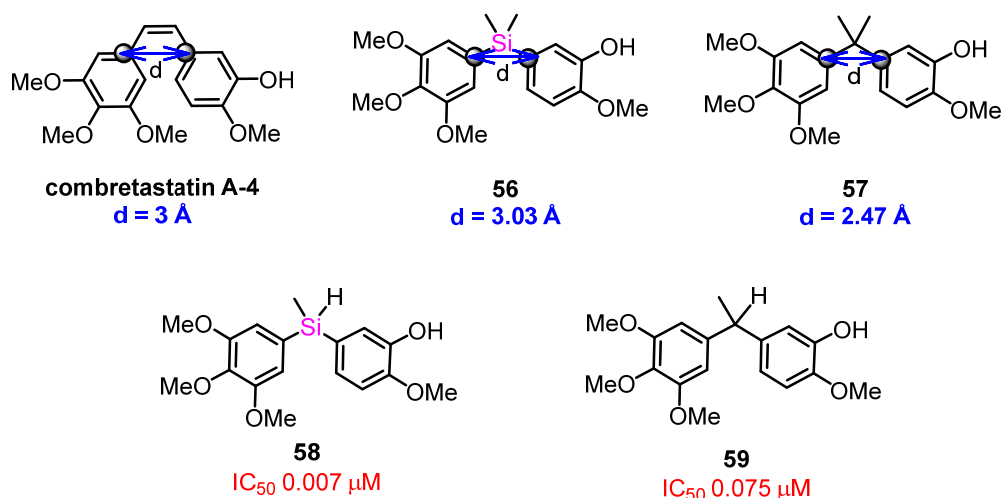
Figure 1.1.16. Silicon analogs of combretastatin A-4

1.1.7.2. Silicon as amide surrogate

Toyama *et.al.* replaced the amide functionality in retinoic acid receptor inverse agonists belonging to the phenanthridinone class (**60** and **65**) with a silyl group and studied their biological activity.[91,92] Docking studies showed that the amide is not involved in hydrogen bonding with the receptor and the binding site is hydrophobic.[93] The compounds **61 - 64** showed similar IC$_{50}$ for the inhibition of RORγ as that of parent compound **60**. The activities of **62** (IC$_{50}$ = 4.2 μM) and **64** (IC$_{50}$ = 4.4 μM) were slightly better than that of compound **60** (IC$_{50}$ = 4.7 μM). However, the inhibition of **66** was found to be 2-fold less compared to the carbon compound **65**.
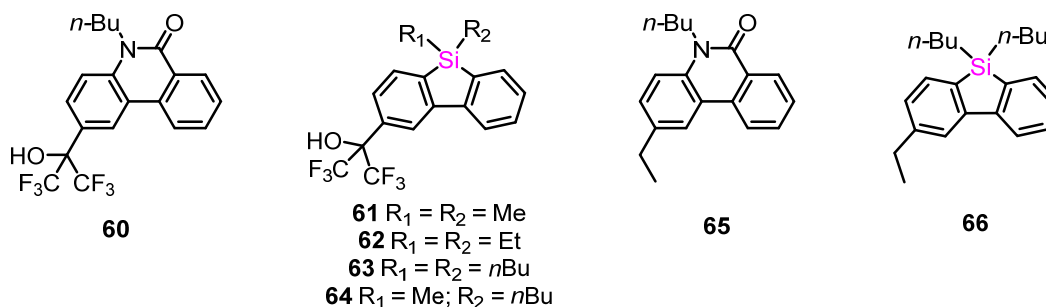
Figure 1.1.17. Silicon analogs of phenanthridinone derivatives

1.1.8. Silicon incorporation to improve the potency

The lipophilic silicon analogs display a better cell penetration compared to their carbon analogs and can lead to increase in potency in certain drugs. Other properties such as polarization of the bond, increased bond length, conformational changes etc. can also cause an increase in potency.

Kagechika and co-workers substituted silicon in place of carbon in 4-substituted phenols and evaluated their estrogenic activity.[94] Out of all tested compounds, the triethyl silicon derivative **72** showed the highest potency. Silicon substitution caused an increase in activity for all the compounds in the series (figure 1.1.18). Docking studies showed that the trialkyl group at *p* position lies in a hydrophobic pocket of the estrogen receptor which suggests that the improvement in activity may be due to the increase in lipophilicity caused by silicon substitution.
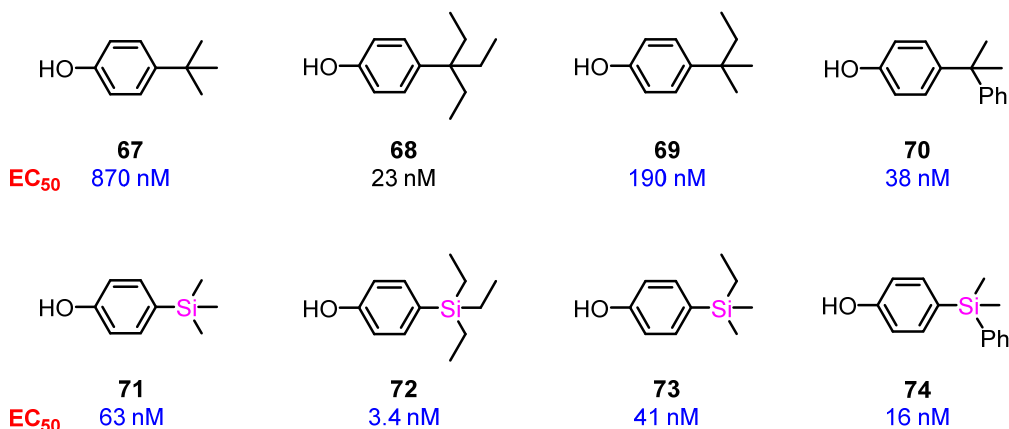
Figure 1.1.18. Estrogenic activity of phenols

Osvaldo *et. al.* studied the effect of TBS group (a protecting group commonly used in organic chemistry) on the cytotoxic activity of substituted tetrahydropyrans.[95] The cLogP of the TBS protected alcohols were found to be higher compared to free alcohols as well as other protecting groups. The growth inhibitory activities of the compounds were checked in two cancerous cell lines, HL60 and MCF7 (fig. 1.1.19). The derivatives having TBS group at 3rd position showed anti-cancer activity (**76** *vs* **75**/ **77**/ **78**; **80** *vs* **79**; **82** *vs* **81**). This observed activity by the introduction of TBS group may be due to better

cell penetration of the lipophilic TBS compounds. These results also indicate that the TBS group can be employed to increase the cellular uptake of compounds. However, TBS groups are expected to be labile under gastric (acidic pH) conditions.

	75	**76**	**77**	**78**
GI$_{50}$ (HL60)	NA	22 μg/ mL	NA	NA
GI$_{50}$ (MCF7)	NA	18 μg/ mL	NA	NA

	79	**80**	**81**	**82**
GI$_{50}$ (HL60)	NA	31 μg/ mL	NA	40 μg/ mL
GI$_{50}$ (MCF7)	NA	61 μg/ mL	NA	21 μg/ mL
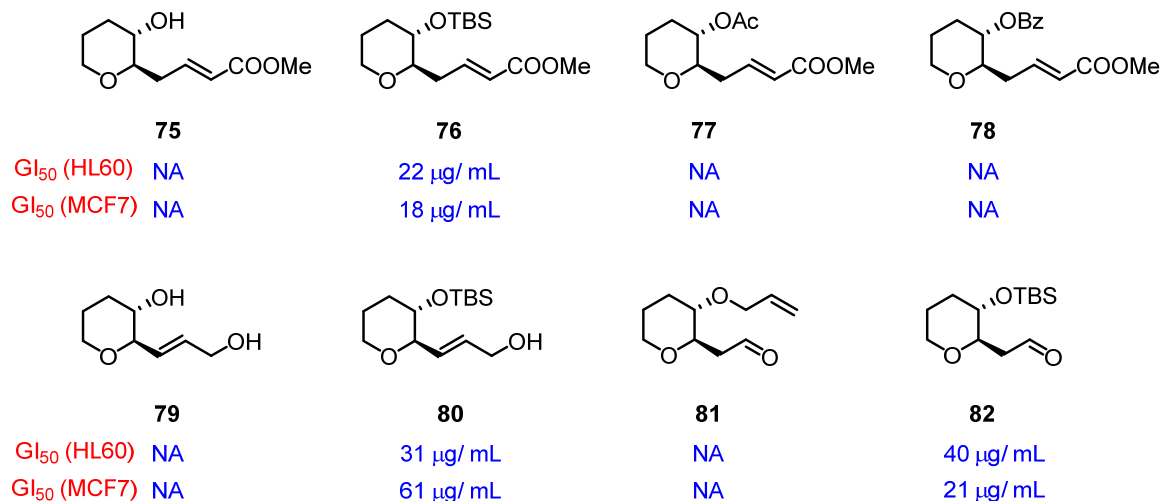
Figure 1.1.19. Cytotoxic effects of tetrahydropyran derivatives *(NA = not active)*

Tacke studied the effect of C/Si bioisosterism in muscarinic antagonists (figure 1.1.20).[96] Muscarinic acetylcholine receptors are activated by the neurotransmitter acetylcholine. Antagonists of this receptor are useful in treating Parkinson's disease.

83   **84**   **85**

86   **87**   **88**
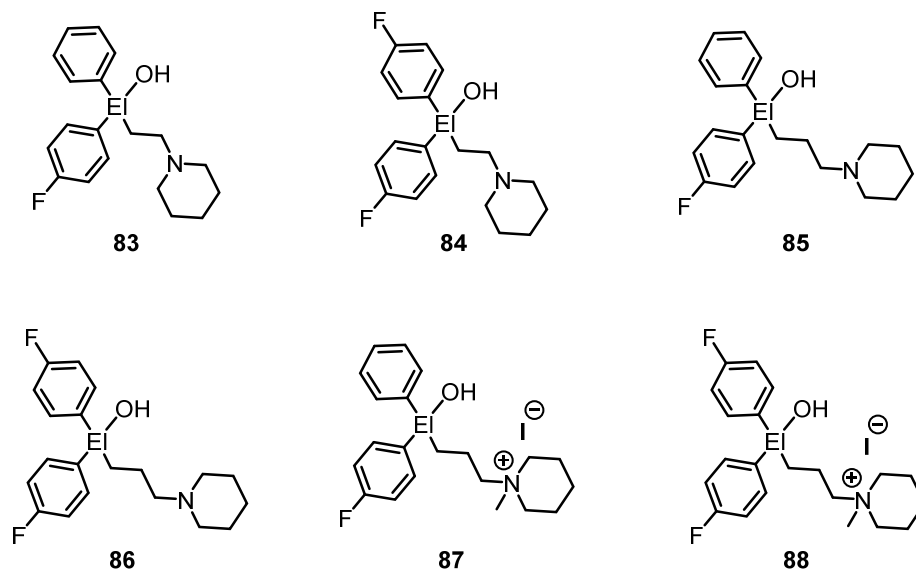
Figure 1.1.20. Silicon switch in muscarinic antagonists (El = C or Si)

16

The silanols showed increased binding affinities for all the four receptor subtypes (M1 – M4) compared to corresponding carbinols. The highest improvement in potency was found for the pair **87** (table 1.1.2).

Compound	Si/C affinity ratio			
	M1	M2	M3	M4
83	1.6	2.0	2.0	1.6
84	1.3	2.0	-	1.3
85	10.0	5.0	7.9	16
86	2.5	1.6	3.2	3.2
87	40	50	32	40
88	6.3	13	10	6.3

Table 1.1.2. Binding affinity ratios of silicon to carbon analogs

DeGrado and co-workers reported organosilyl amine inhibitors of M2 protein of influenza A virus.[97] It is known that lipophilicity can improve the potency of M2 inhibitors because the protein has a hydrophobic binding pocket. The spirane amines **89** - **92** were synthesized and the activities against A/M2-V27A were evaluated (figure 1.1.21). The silicon analogs **90** and **92** showed an increase in potency compared to their carbon counterparts **89** and **91**. The authors suggest that this is probably due to the lipophilicity as well as larger ring size which provide a better binding of the molecule with the receptor protein.

89
IC$_{50}$ 84.9 μM

90
IC$_{50}$ 31.3 μM

91
IC$_{50}$ 318.6 μM

92
IC$_{50}$ 96.3 μM
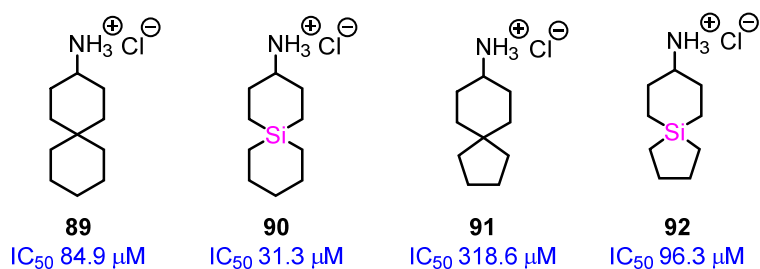
Figure 1.1.21. Antiviral activity of silaspirane amines

Tacke and co-workers studied the effect of carbon to silicon switch in the retinoid agonist SR11237 (**93**).[98] Since silicon substitution causes an enlargement in ring size, the indane derivatives **94** and **97** were also made for the sake of comparison. Due to higher C-Si bond length, the ring size of **93** and **97** are expected to be same. The potencies of **93** and **96** were found to be similar with the silicon analog **96** exhibiting a slightly higher activity. However, in the cases of indanes the sila analog **97** was found to be almost 10 fold more potent compared to its corresponding carbon compound **94**. Similar enhancement in activity (almost 10 fold) was also observed in the case of another retinoid agonist, tamibarotene (**98** *vs* **95**).[99]
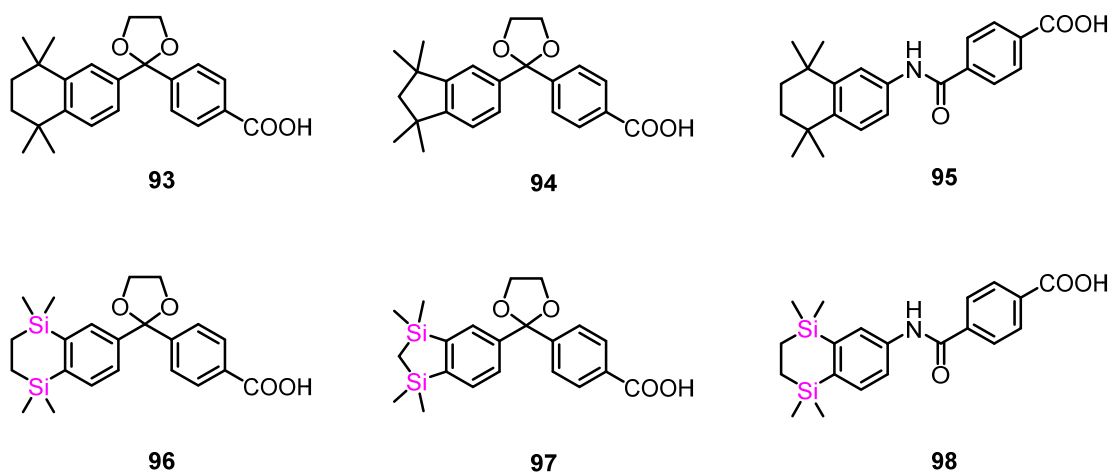
Figure 1.1.22. Silicon switching in retinoids

In our group, we studied the effect of silicon substitution in morpholine antifungals. Fenpropidin (**99**) and fenpropimorph (**100**) are marketed fungicides whereas amorolfine (**101**) is applied topically for nail infections. Several compounds were synthesized and the sila analog **102** came out as the lead of the series with better MFC (minimum fungicidal concentration) than the parent compounds (**99**, **100** and **101**) against various human pathogenic fungi (table 1.1.3). The silicon analog **103** also showed good activity.[100]

18
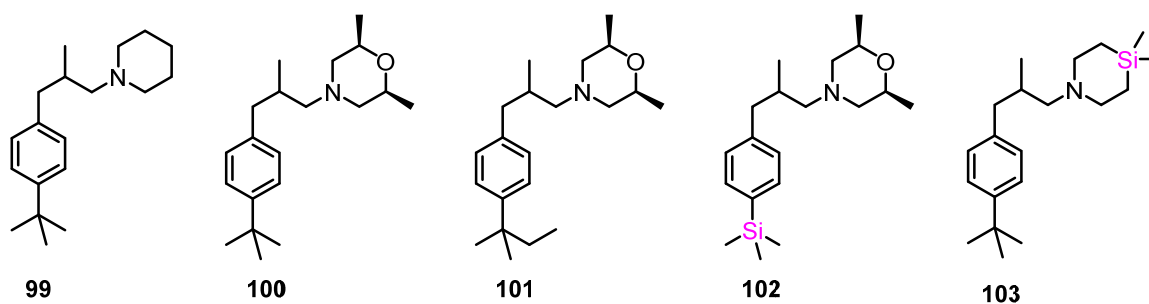
Figure 1.1.23. Silicon switching in morpholine antifungals

Compound	Minimum fungicidal concentration (MFC in μg/mL)				
	C. albicans	*C. neoformans*	*C. glabrata*	*C. tropicalis*	*A. niger*
99	0.5	32.0	16.0	> 256	> 256
100	4.0	64.0	128.0	> 256	> 256
101	8.0	64.0	32.0	> 256	> 256
102	0.5	2.0	2.0	64.0	256
103	8.0	4.0	8.0	64.0	64.0

Table 1.1.3. Antifungal activity of compounds **99 - 103**

1.1.9. Silicon substitution to modulate pharmacological selectivity

In certain compounds, silicon substitution leads to a change in receptor selectivity. In the case of W84 analog **51** (discussed in section 1.1.6.1), a silyl substitution transformed the molecule from allosteric inhibitor to allosteric activator. Hashimoto and co-workers reported a change in receptor selectivity by silicon substitution in compounds **104 – 106**.[101] It was previously reported that some of the analogs of the known vitamin D receptor (VDR) agonist **104** showed slight androgen receptor (AR) antagonistic activity.[102,103] The silicon analogs showed decreased VDR agonistic activity compared to the parent compounds. However, they displayed better androgen receptor antagonistic activity compared to carbon compounds (figure 1.1.24).

104	**105**	**106**
VDR (PC$_{50}$ in μM)	0.14; El = C 0.92; El = Si	0.68; El = C 4.8; El = Si	4.6; El = C > 30; El = Si
AR (IC$_{50}$ in μM)	>> 10; El = C 6.8; El = Si	>> 10; El = C > 10; El = Si	> 10; El = C 6.2; El = Si
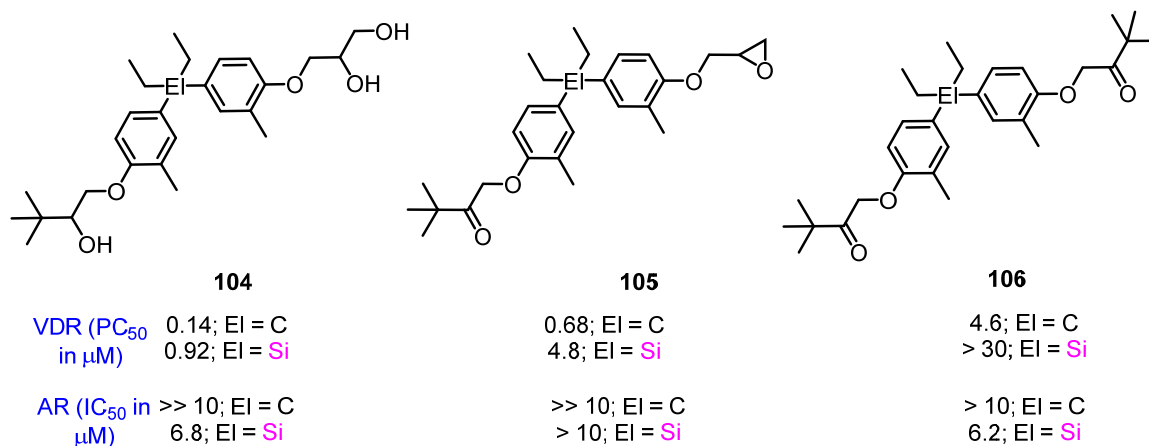
Figure 1.1.24. Silicon switch in muscarinic antagonists (El = C/Si)

Tacke and co-workers synthesized silicon analogs of venlafaxine (**107**) which is a marketed antidepressant (in racemic form) belonging to serotonin-noradrenaline reuptake inhibitor class.[104] The enhanced acidity of silanols **108** and **109** can be beneficial leading to an increased hydrogen bonding interaction with the receptor. However, it was found that the silanols **108** and **109** displayed a different pharmacological profile.

107   **108**   **109**
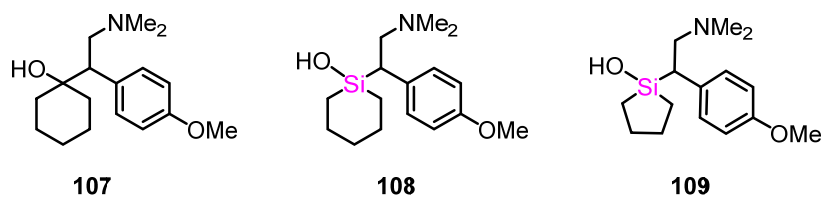
Figure 1.1.25. Silicon analogs of venlafaxine

The silicon analogs showed decreased serotonin reuptake inhibition (table 1.1.4). Interestingly sila analog **108** showed a higher selectivity for the noradrenaline reuptake transporter. The pure enantiomers were prepared by diastereomeric resolution. The authors further postulated that selective noradrenaline reuptake inhibitors maybe useful in treating emesis (vomiting). Accordingly, (**R**)-**108** was evaluated in animal models and showed anti-emetic activity at 5mg/kg. [105]

Compound	IC$_{50}$ (μM)		
	Serotonin	Noradrenaline	Dopamine
rac- **107**	0.020	0.149	4.430
(R)- **107**	0.030	0.061	19.600
(S)- **107**	0.006	0.754	6.670
rac- **108**	1.063	0.109	2.630
(R)- **108**	3.168	0.251	5.270
(S)- **108**	0.791	4.715	36.350
rac- **109**	0.904	0.275	0.707

Table 1.1.4. Monoamine reuptake transporter inhibition of venlafaxine and analogs

1.1.10. Silicon containing amino acids

Unnatural amino acids are used to probe the bioactive conformation of peptides and find applications in peptidomimetics.[106,107] Amino acids with silicon incorporation have several attractive features which can be useful in drug discovery.[108,109] But, only a few silicon amino acids are known and with limited structural variations. Cavelier group has made significant contributions in this area.[110-120] Some of the known silicon containing amino acids are shown in figure 1.1.26. In our group, we have synthesized silicon incorporated amino acids (alpha, beta and gamma) starting from allylsilanes. This is discussed in detail in the third section of this chapter. Incorporation of a lipophilic silicon moiety can improve the cell penetration as well as stability of the peptide towards biodegradation.
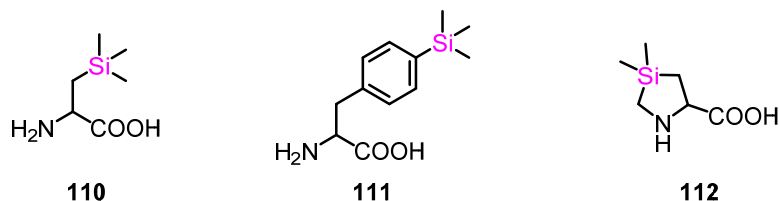

Figure 1.1.26. Silicon amino acids

The synthesis of silaproline **112** (Sip) was first reported by Cavelier group.[118] cLogP value of Fmoc-silaproline was experimentally found to be 14 times greater than Fmoc-proline which shows that it is more lipophilic than proline. The authors incorporated this proline surrogate in place of proline in the neurotensin (8-13) analog. Neurotensin is a neuropeptide containing 13 amino acids and has analgesic and hypothermic effects. The natural neurotensin undergoes proteolytic decomposition near to the proline residue and hence is injected along with enzyme inhibitors. The neurotensin analog with silaproline was active even in the absence of protease inhibitors which indicates that silicon incorporation improved the stability of the peptide *in vivo*.[119] In another report, the replacement of proline with silaproline on the hydrophobic face of a cell penetrating peptide led to a 20 fold enhancement in cellular uptake.[120]

Silaproline was also incorporated in one of Merck's lead compound MK-4882 (**113**), a hepatitis C virus (HCV) inhibitor. Several analogs were made by varying the central core and the compound **114** appeared to be a promising candidate for further development. The compound showed good half life (7.6 h, rat IV) and plasma exposure.[121]
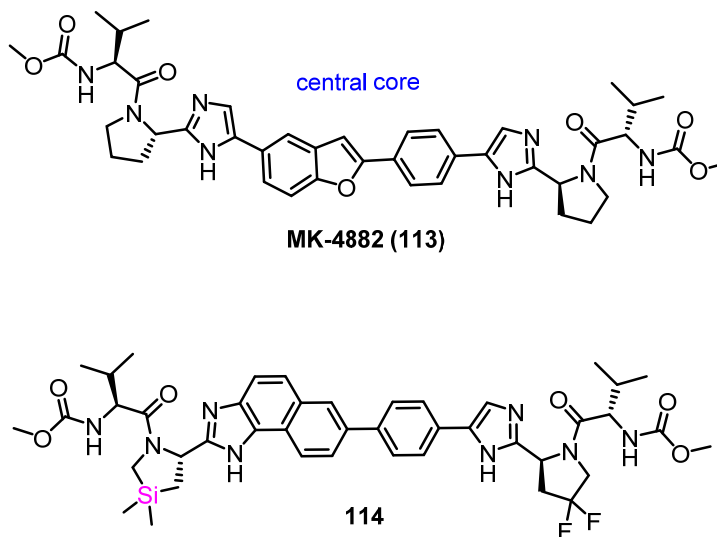

Figure 1.1.27. HCV inhibitor containing sila proline

The replacement of leucine with TMSalanine (**110**) in the neurotensin (8-13) analog led to an increased affinity for the neurotensin receptor. The peptide containing TMSalanine showed potent analgesic effects in animal models of pain.[112] Tacke and co-workers studied the effect of silicon incorporation in decapeptide cetrorelix, a GnRH (gonadotrophin-releasing hormone) antagonist. The TMSalanine containing peptide showed significant activity *in vivo* with increased duration of action.[122]

Marutake *et. al.* synthesized and evaluated the silicon analogs of pregabalin (figure 1.1.28).[123,124] Pregabalin is an analog of gamma-amino butyric acid (GABA), a neurotransmitter present in the central nervous system. It is used to treat epilepsy and neuropathic pain. The anti-allodynic activity of the compounds **116** and **117** were checked in spinal nerve ligation models. The activity of **117** was found to be comparable to that of pregabalin. Interestingly, both the silicon analogs **116** and **117** did not show any anti-convulsant activity of pregabalin. Pregabalin causes dizziness and had hypalgesic effects which were not observed in rats dosed with **116** and **117**. These results suggests that silicon analogs **116** and **117** can be considered as pregabalin analogs with reduced CNS side effects.[123]
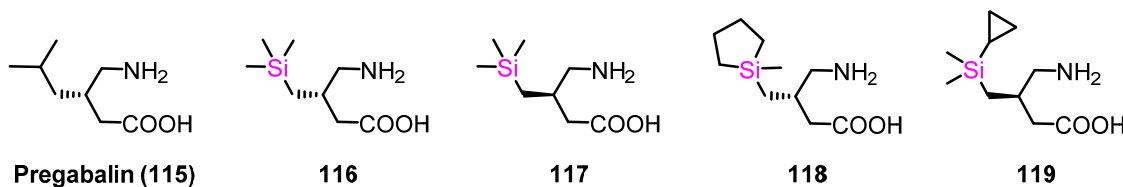
Figure 1.1.28. Silicon containing GABA analogs

Further optimization of the series led to the development of compounds **118** and **119**.[124] In rotarod experiments, rats administered with pregabalin lost their balance showing CNS side effects. The silagaba compounds were found to be devoid of any CNS side effects in rotarod experiments. PK experiments showed that the distribution of pregabalin into brain is more when compared to the silicon analogs which may be a reason for its side effects. The silagaba compounds showed weak binding to α_2-δ protein which is presumed to be the target of pregabalin. This suggests that the sila compounds may be binding to some other proteins causing similar allodynic activity as pregabalin.

1.1.11. Organosilanes which entered clinical trials

Although there are no marketed drugs containing silicon, some of the compounds have entered human clinical trials (figure1.1.29). To the best of our knowledge, 9 compounds have been tested in humans; the results of which proved that silicon incorporation does not cause any toxicity concerns.[5] Karenitecin, DB-67 and Pc-4 are currently in clinical trials for treatment of cancer.[125] Silabolin, a prodrug of the steroid nandrolone was available in Russia and used by athletes.[126,127]

Zifrosilone
Alzheimer's
(Phase II)

TAC-101
Cancer
(Phase II)

Silabolin
Cachexia
(Limited clinical use)

Cisobitan
cancer
(Phase II)

Sandoz 58-112
Muscle relaxant
(Phase I)

Silperisone
Muscle relaxant
(Phase II)

Karenitecin
Cancer
(Phase III)

DB-67
Cancer
(Phase II)

Pc 4
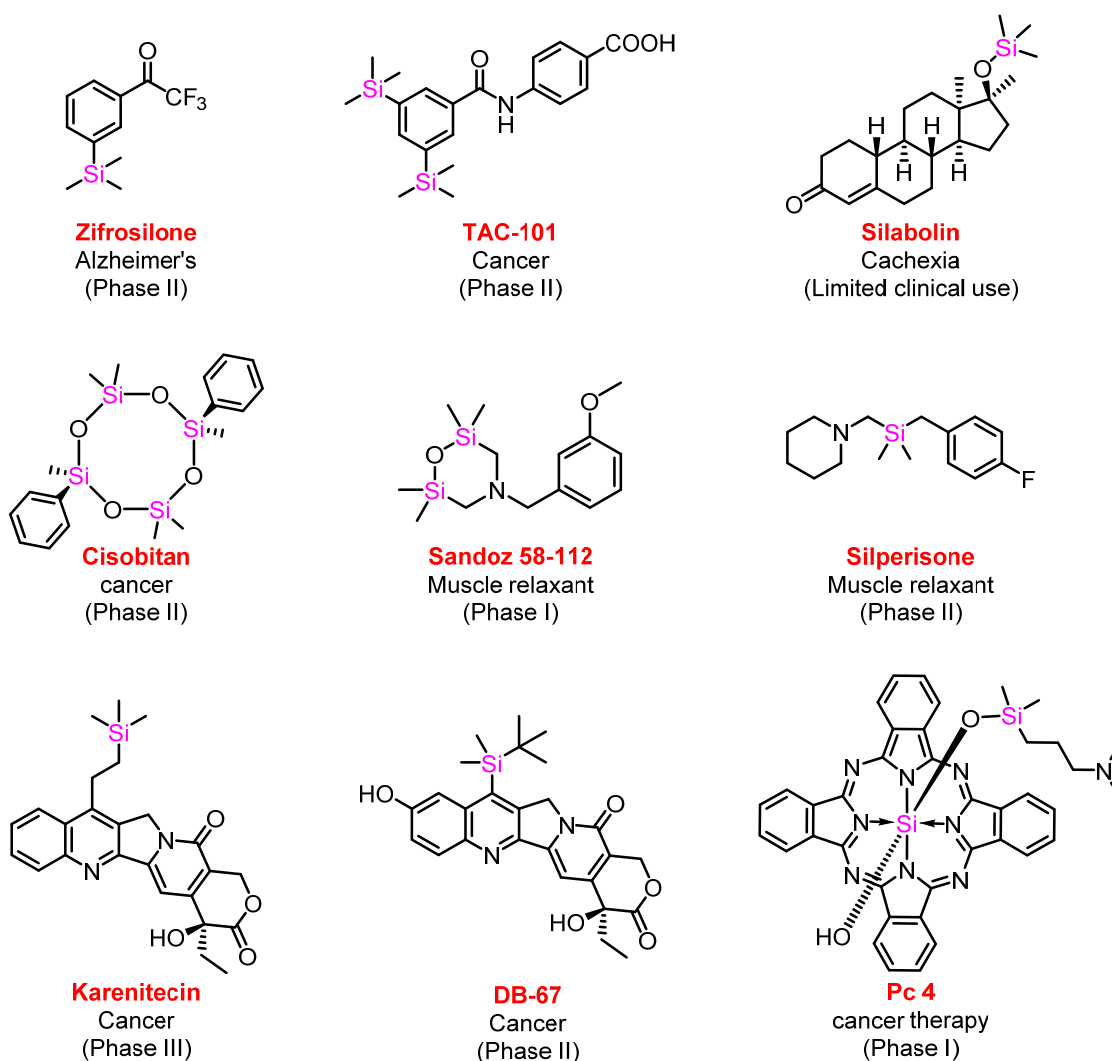cancer therapy
(Phase I)

Figure 1.1.29. Organosilanes which entered human clinical trials

1.1.12. Conclusions

Silicon is the element which shows closest similarity with carbon and is considered as a bioisostere of carbon. Some of the differences in properties of carbon and silicon can be effectively used in drug design. Silicon also provides a novel chemical space which cannot be accessed using the carbon compounds. The increase in lipophilicity of silicon is an interesting property and can be used to modulate the druggable properties of a lead. Some of the compounds have been shown to be safe in human clinical trials, but currently there are no silicon drugs approved for clinical use. Although silicon offers potential avenues to medical chemists, the area remains underexplored. It is anticipated that the success of any silicon incorporated clinical candidate will bring in more attention to this field in the future. With this background in mind, we have initiated multiple projects in our research group. Two of those projects are discussed in detail in the following sections of this chapter.

1.1.13. References

(1)   Mullard, A. *Nat. Rev. Drug Discov.* **2016**, *15*, 219-221.

(2)   Gant, T. G. *J. Med. Chem.* **2014**, *57*, 3595–3611.

(3)   Meanwell, N. A. *J. Med. Chem.* **2011**, *54*, 2529−2591.

(4)   Gately, S.; West, R. *Drug Dev. Res.* **2007**, *68*, 156−163.

(5)   Bains, W.; Tacke, R. *Curr. Opin. Drug Discovery Dev.* **2003**, *6*, 526−543.

(6)   Franz, A. K.; Wilson, S. O. *J. Med. Chem.* **2013**, *56*, 388−405.

(7)   Garson, L. R.; Kirchner, L. K. *J. Pharm. Sci.* **1971**, *60*, 1113-1127.

(8)   Mills, J. S.; Showell, G. A. *Expert Opin. Investig. Drugs* **2004**, *13*, 1149-1157.

(9)   Mills, J. S.; Showell, G. A. *Drug Discov. Today* **2003**, *8*, 551-556.

(10)   Pooni, P. K.; Showell, G. A. *Mini Rev. Med. Chem.* **2006**, 6, 1169-1177.

(11)   Patani, G. A.; LaVoie, E. J. *Chem. Rev.* **1996**, *96*, 3147-3176.

(12)   Lima, L. M.; Barreiro, E. J. *Curr. Med. Chem.* **2005**, *12*, 23-49.

(13)   Tacke, R.; Zilch, H. *Endeavour* **1986**, *10*, 191–197.

(14) Koyanagi, T.; Haga, T. In Synthesis and Chemistry of Agrochemicals IV, *ACS Symposium Series*, Chapter 2, pp 15–24, Washington DC, 1995.

(15) Sieburth, S. McN. In Designing Safer Chemicals, *ACS Symposium Series*, Chapter 4, pp 74–83, Washington DC, 1996.

(16) Doszczak, L.; Gasperi, T.; Saint-Dizier, A.; Loreto, M. A.; Enders, D. *Chem Biodivers.* **2004**, *12*, 1921-1935.

(17) Liu, J.; Zhang, Q.; Li, P.; Qu, Z.; Sun, S.; Ma, Y.; Su, D.; Zong, Y.; Zhang, J. *Eur. J. Inorg. Chem.* **2014**, 3435–3440.

(18) Clayden, J.; Greeves, N.; Warren, S. Organic Chemistry, Oxford University Press, Oxford, second edition, 668-677.

(19) Gabathuler, R. *Neurobiol. Dis.* **2010**, 37, 48-57.

(20) Bertrand, G. *Science* **2004**, *305*, 783-785.

(21) Lin, J. H.; Lu, A. Y. H.; *Pharmacol. Rev*. **1997**, *49*, 403-449.

(22) Tacke, R.; Nguyen, B.; Burschka, C.; Lippert, W. P.; Hamacher, A.; Urban, C.; Kassack, M. U. *Organometallics* **2010**, *29*, 1652–1660.

(23) Johansson, T.; Weidolf, L.; Popp, F.; Tacke, R.; Jurva, U. *Drug Metab. Dispos*. **2010**, *38*, 73-83.

(24) Tacke, R.; Popp, F.; Mueller, B.; Theis, B.; Burschka, C.; Hamacher, A.; Kassack, M. U.; Schepmann, D.; Wuensch, B.; Jurva, U.; Wellner, E. *ChemMedChem* **2008**, *3*, 152−164.

(25) Tacke, R.; Heinrich, T.; Bertermann, R.; Burschka, C.; Hamacher, A.; Kassack, M. U. *Organometallics* **2004**, *23*, 4468−4477.

(26) Dauer, W.; Przedborski, S. *Neuron* **2003**, *39*, 889-909.

(27) Subramanyam, B.; Rollema, H.; Woolf, T.; Castagnoli, N. Jr. *Biochem Biophys Res Commun.* **1990**, *166*, 238-244.

(28) Subramanyam, B.; Pond, S. M.; Eyles, D. W.; Whiteford, H. A.; Fouda, H. G.; Castagnoli, N. Jr. *Biochem Biophys Res Commun.* **1991**, *181*, 573-578.

(29) Subramanyam, B.; Woolf, T.; Castagnoli, N. Jr. *Chem Res Toxicol.* **1991**, *4*, 123-128.

(30) Svennebring, A. *J. Appl. Toxicol*. **2016**, *36*, 483-500.

(31) Tacke, R.; Nguyen, B.; Burschka, C.; Lippert, W. P.; Hamacher, A.; Urban, C.; Kassack, M. U. *Organometallics* **2010**, *29*, 1652–1660.

(32) Geyer, M.; Wellner, E.; Jurva, U.; Saloman, S.; Armstrong, D.; Tacke, R. *ChemMedChem.* **2015**, *10*, 911-924.

(33) Turk, B. *Nat. Rev. Drug Discov.* **2006**, *5*, 785-799.

(34) Chen, C. A.; Sieburth, S. McN.; Glekas, A.; Hewitt, G. W.; Trainor, G. L.; Erickson-Viitanen, S.; Garber, S. S.; Cordova, B.; Jeffry, S.; Klabe, R. M. *Chem. Biol.* **2001**, *8*, 1161-1166.

(35) Sieburth, S. McN.; Nittoli, T.; Mutahi, A. M.; Guo, L. *Angew. Chem. Int. Ed.* **1998**, *37*, 812-814.

(36) wa Mutahi, M.; Nittoli, T.; Guo, L.; Sieburth, S. McN. *J. Am. Chem. Soc.* **2002**, *124*, 7363-7375

(37) Kim, J.; Glekas, K.; Sieburth, S. McN. *Bioorg. Med. Chem. Lett.* **2002**, *12*, 3625–3627.

(38) Kim, J.; Sieburth, S. McN. *Bioorg. Med. Chem. Lett.* **2004**, *14*, 2853–2856.

(39) Juers, D. H.; Kim, J.; Matthews, B. W.; Sieburth, S. McN. *Biochemistry* **2005**, *44*, 16524−16528.

(40) Sieburth, S. McN.; Chen, C.-A. *Eur. J. Org. Chem.* **2006**, 311−322.

(41) Singh, S.; Sieburth, S. McN. *Org. Lett.* **2012**, *14*, 4422−4425.

(42) Kim, J. K.; Sieburth, S. McN. *J. Org. Chem.* **2012**, *77*, 2901–2906.

(43) Organ, M. G.; Buon, C.; Decicco, C. P.; Combs, A. P. *Org. Lett.* **2002**, *4*, 2683-2685.

(44) Blunder, M.; Hurkes, N.; Spirk, S.; List, M.; Pietschnig, R. *Bioorg. Med. Chem. Lett*. **2011**, *21*, 363–365.

(45) He, J.; Larkin, H. E.; Li, Y. -S.; Rihter, B. D.; Zaidi, S. I. A.; Rodgers, M. A. J.; Mukhtar, H.; Kenney, M. E.; Oleinick, N. L. *Photochem. Photobiol.* **1997**, *65*, 581–586.

(46) Baron, E. D.; Malbasa, C. L.; Santo-Domingo, D.; Fu, P.; Miller, J. D.; Hanneman, K. K.; Hsia, A. H.; Oleinick, N. L.; Colussi, V. C.; Cooper, K. D. *Lasers Surg. Med.* **2010**, *42*, 728–735.

(47) Oleinick, N. L.; Antunez, A. R.; Clay, M. E.; Rihter, B. D.; Kenney, M. E. *Photochem. Photobiol.* **1993**, *57*, 242–247.

(48) Anderson, C. Y.; Freye, K.; Tubesing, K. A.; Li, Y. –S.; Kenney, M. E.; Mukhtar, H.; Elmets, C. A. *Photochem. Photobiol*. **1998**, *67*, 332–336.

(49) Trivedi, N. S.; Wang, H. –W.; Nieminen, A. –L.; Oleinick, N. L.; Izatt, J. A. *Photochem. Photobiol.* **2000**, *71*, 634–639.

(50) Zaidi, S. I. A.; Agarwal, R.; Eichler, G.; Rihter, D.; Kenney, M. E.; Mukhtar, H. *Photochem. Photobiol.* **1993**, *58*, 204–210.

(51) Mfouo-Tynga, I.; Abrahamse, H. *Int. J. Mol. Sci*. **2015**, *16*, 10228-10241.

(52) Morris, R. L.; Varnes, M. E.; Kenney, M. E.; Li, Y. –S.; Azizuddin, K.; McEnery, M. W.; Oleinick, N. L. *Photochem. Photobiol*. **2002**, *75*, 652–661.

(53) Josefsen, L. B.; Boyle, R. W. *Met. Based Drugs* **2008**, Article ID 276109.

(54) Allen, C. M.; Sharman, W. M.; Van Lier, J. E. *J. Porphyrins Phthalocyanines* **2001**, *5*, 161–169.

(55) He, J.; Whitacre, C. M.; Xue, L. Y.; Berger, N. A.; Oleinick, N. L. *Cancer Res*. **1998**, *58*, 940–946.

(56) Li, J.; Yang, Y.; Zhang, P.; Sounik, J. R.; Kenney, M. E. *Photochem. Photobiol. Sci*. **2014**, *13*, 1690-1698.

(57) Xiang, Y.; Fu, C.; Breiding, T.; Sasmal, P. K.; Liu, H.; Shen, Q.; Harms, K.; Zhang, L.; Meggers, E. *Chem. Commun*. **2012**, *48*, 7131–7133.

(58) Wheate, N. J.; Brodie, C. R.; Collins, J. G.; Kemp, S.; Aldrich-Wright, J. R. *Mini Rev. Med. Chem.* **2007**, *7*, 627-648.

(59) Frve, C. L.; Vogel, G. E.; Hall, J. A. *J. Am. Chem. Soc*. **1961**, *83*, 996–997.

(60) Puri, J. K.; Singh, R.; Chahal, V. K. *Chem. Soc. Rev*. **2011**, *40*, 1791–1840.

(61) Voronkov, M. G. *Top Curr. Chem.* **1979**, *84*, 77–135.

(62) Black, C. A.; Ucci, J. W.; Vorpagel, J. S.; Mauck, M. C.; Fenlon, E. E. *Bioorg. Med. Chem. Lett*. **2002**, *12*, 3521–3523.

(63) Grna, A.; Koo, P. H.; Hogan, J. *Anticancer Res.* **1992**, *12*, 565–569.

(64) Mehta, P. P.; Ramasarma, T.; Kurup, C. K. R. *Biochim. Biophys. Acta* **1987**, *920*, 102-104.

(65) Mehta, P. P.; Ramasarma, T.; Kurup, C. K. R. *Mol. Cell Biochem.* **1990**, *97*, 75-85.

(66) Hawkins, B. T.; Davis, T. P. *Pharmacol. Rev.* **2005**, *57*, 173-185.

(67) Seetharamsingh, B.; Ramesh, R.; Dange, S. S.; Khairnar, P. V.; Singhal, S.; Upadhyay, D.; Veeraraghavan, S.; Viswanadha, S.; Vakkalanka, S.; Reddy, D. S. *ACS Med. Chem. Lett.* **2015**, *6*, 1105−1110.

(68) Barbachyn, M. R.; Ford, C. W. *Angew. Chem., Int. Ed.* **2003**, *42*, 2010-2023.

(69) Wall, M. E.; Wani, M. C.; Cooke, C. E.; Palmer, K. H.; McPhail, A. T.; Sim, G. A. *J. Am. Chem. Soc.* **1966**, *88*, 3888–3890.

(70) Pollack, I. F.; Erff, M.; Bom, D.; Burke, T.; Strode, J. T.; Curran, D. P. *Cancer Res.* **1999**, *59*, 4898–4905.

(71) Van Hattum, A. H.; Pinedo, H. M.; Schluper, H. M. M.; Hausheer, F. H.; Boven, E. *Int. J. Cancer* **2000**, *88*, 260–266.

(72) Van Hattum, A. H.; Schluper, H. M. M.; Hausheer, F. H.; Pinedo, H. M.; Boven, E. *Int. J. Cancer* **2002**, *100*, 22–29.

(73) Daud, A.; Valkov, N.; Centeno, B.; Derderian, J.; Sullivan, P.; Munster, P.; Urbas, P.; DeConti, R. C.; Berghorn, E.; Liu, Z.; Hausheer, F.; Sullivan, D. *Clin. Cancer Res.* **2005**, *11*, 3009−3016.

(74) Bom, D.; Curran, D. P.; Kruszewski, S.; Zimmer, S. G.; Strode, J. T.; Kohlhagen, G.; Du, W.; Chavan, A. J.; Fraley, K. A.; Bingcang, A. L.; Latus, L. J.; Pommier, Y.; Burke, T. G. *J. Med. Chem.* **2000**, *43*, 3970−3980.

(75) Venditto, V. J.; Simanek, E. E. *Mol. Pharmaceutics* **2010**, *7*, 307−349.

(76) Arnold, S. M.; Rinehart, J. J.; Tsakalozou, E.; Eckardt, J. R.; Fields, S. Z.; Shelton, B. J.; DeSimone, P. A.; Kee, B.K.; Moscow, J. A.; Leggas, M. *Clin. Cancer Res.* **2010**, *16*, 673–680.

(77) Lopez-Barcons, L. A.; Zhang, J.; Siriwitayawan, G.; Burke, T. G.; Perez-Soler, R. *Neoplasia* **2004**, *6*, 457–467.

(78) Tsakalozou, E.; Adane, E. D.; Kuo, K. -L.; Daily, A.; Moscow, J. A.; Leggas, M. *Drug Metab. Dispos.* **2013**, *41*, 1404–1413.

(79) Yeh, T. –K.; Li, C. –M.; Chen, C. –P.; Chuu, J. –J.; Huang, C. –L.; Wang, H. –S.; Shen, C. –C.; Lee, T. –Y.; Chang, C. –Y.; Chang, C. –M.; Chao, Y. –S.; Lin, C. –T.; Chang, J. –Y.; Chen, C. –T. *Pharmacol. Res.* **2010**, *61*, 108–115.

(80) Hornsperger, J. M.; Collard, J. N.; Heydt, J. G.; Giacobinit, E.; Funes, S.; Dow, J.; Schirlin, D. *Biochem. Soc. Trans.* **1994**, *22*, 758-763.

(81) Cutler, N. R.; Seifert, R. D.; Schleman, M. M.; Sramek, J. J.; Szylleyko, O. J.; Howard, D. R.; Barchowsky, A.; Wardle, T. S.; Brass, E. P. *Clin. Pharmacol. Ther.* **1995**, *58*, 54-61.

(82) Zhu, X. D.; Giacobini, E.; Hornsperger, J. –M. *Eur. J. Pharmacol.* **1995**, *276*, 93–99.

(83) Coyle, J. T.; Price, D. L.; Delong, M. R. *Science* **1983**, *219*, 1184-1190.

(84) Brodbeck, U.; Schweikert, K.; Gentinetta. R.; Rottenberg, M. *Biochim. Biophys. Acta* **1979**, *567*, 357-369.

(85) Nair, H. K.; Lee, K.; Quinn, D. M. *J. Am. Chem. Soc.* **1993**, *115*, 9939-9941.

(86) Daiss, J. O.; Duda-Johner, S.; Burschka, C.; Holzgrabe, U.; Mohr, K.; Tacke, R. *Organometallics* **2002**, *21*, 803–811.

(87) Duda-Johner, S.; Daiß, J. O.; Mohr, K.; Tacke, R. *J. Organomet. Chem.* **2003**, *686*, 75-83.

(88) Kim, Y. -m.; Farrah, S.; Baney, R. H. *Int. J. Antimicrob. Agents* **2007**, *29*, 217−222.

(89) Tron, G. C.; Pirali, T.; Sorba, G.; Pagliai, F.; Busacca, S.; Genazzani, A. A. *J. Med. Chem.* **2006**, *49*, 3033-3044.

(90) Nakamura, M.; Kajita, D.; Matsumoto, Y.; Hashimoto, Y. *Bioorg. Med. Chem.* **2013**, *21*, 7381–7391.

(91) Nishiyama, Y.; Nakamura, M.; Misawa, T.; Nakagomi, M.; Makishima, M.; Ishikawa, M.; Hashimoto, Y. *Bioorg. Med. Chem.* **2014**, *22*, 2799-2808.

(92) Toyama, H.; Nakamura, M.; Hashimoto, Y.; Fujii, S. *Bioorg. Med. Chem.* **2015**, *23*, 2982–2988.

(93) Fauber, B. P.; de Leon Boenig, G.; Burton, B.; Eidenschenk, C.; Everett, C.; Gobbi, A.; Hymowitz, S. G.; Johnson, A. R.; Liimatta, M.; Lockey, P.; Norman,

M.; Ouyang, W.; Rene, O.; Wong, H. *Bioorg. Med. Chem. Lett.* **2013**, *23*, 6604-6609.

(94) Fujii, S.; Miyajima, Y.; Masuno, H.; Kagechika, H. *J. Med. Chem.* **2013**, *56*, 160−166.

(95) Donadel, O. J.; Martin, T.; Martin, V. S.; Villar, J.; Padron, J. M. *Bioorg. Med. Chem. Lett.* **2005**, *15*, 3536–3539.

(96) Tacke, R.; Terunuma, D.; Tafel, A.; Muhleisen, M.; Forth, B.; Waelbroeck, M.; Gross, J.; Mutschler, E.; Friebe, T.; Lambrecht, G. *J. Organomet. Chem.* **1995**, *501*, 145-154.

(97) Wang, J.; Ma, C.; Wu, Y.; Lamb, R. A.; Pinto, L. H.; DeGrado, F. *J. Am. Chem. Soc.* **2011**, *133*, 13844–13847.

(98) Lippert, W. P.; Burschka, C.; Gotz, K.; Kaupp, M.; Ivanova, D.; Gaudon, C.; Sato, Y.; Antony, P.; Rochel, N.; Moras, D.; Gronemeyer, H.; Tacke, R. *ChemMedChem* **2009**, *4*, 1143–1152.

(99) Tacke, R.; Muller, V.; Buttner, M. W.; Lippert, W. P.; Bertermann, R.; Daiss, J. O.; Khanwalkar, H.; Furst, A.; Gaudon, C.; Gronemeyer, H. *ChemMedChem* **2009**, *4*, 1797–1802.

(100) Jachak, G. R.; Ramesh, R.; Sant, D. G.; Jorwekar, S. U.; Jadhav, M. R.; Tupe, S. G.; Deshpande, M.V.; Reddy, D. S. *ACS Med. Chem. Lett.* **2015**, *6*, 1111−1116.

(101) Nakamura, M.; Makishima, M.; Hashimoto, Y. *Bioorg. Med. Chem.* **2013**, *21*, 1643–1651.

(102) Hosoda, S.; Tanatani, A.; Wakabayashi, K.; Makishima, M.; Imai, K.; Miyachi, H.; Nagasawa, K.; Hashimoto, Y. *Bioorg. Med. Chem.* **2006**, *14*, 5489-.5502.

(103) Maruyama, K.; Noguchi-Yachide, T.; Sugita, K.; Hashimoto, Y.; Ishikawa, M. *Bioorg. Med. Chem. Lett.* **2010**, *20*, 6661-6666.

(104) Daiss, J. O.; Burschka, C.; Mills, J. S.; Montana, J. G.; Showell, G. A.; Warneck, J. B. H.; Tacke, R. *Organometallics* **2006**, *25*, 1188-1198.

(105) Showell, G. A.; Barnes, M. J.; Daiss, J. O.; Burschka, C.; Mills, J. S.; Montana, J. G.; Tacke, R. Warneck, J. B. H. *Bioorg. Med. Chem. Lett.* **2006**, *16*, 2555–2558.

(106) Voloshchuk, N.; Montclare, J. K. *Mol. BioSyst.* **2010**, *6*, 65-80.

(107) Dougherty, D. A. *Curr. Opin. Chem. Biol.* **2000**, *4*, 645–652.

(108) Mortensen, M.; Husmann, R.; Veri, E.; Bolm, C. *Chem. Soc. Rev.* **2009**, *38*, 1002−1010.

(109) Rémond, E.; Martin, C.; Martinez, J.; Cavelier, F. *Chem. Rev.* **2016**, ASAP.

(110) Cavelier, F.; Marchand, D.; Martinez, J.; Sagan, S. *J. Peptide Res.* **2004**, *63*, 290–296.

(111) Cavelier, F.; Marchand, D.; Martinez, J. *Chem. Biodivers.* **2008**, *5*, 1279-1287.

(112) Fanelli, R.; Besserer-Offroy É.; René A.; Côté J.; Tétreault, P.; Collerette-Tremblay, J.; Longpré, J. –M.; Leduc, R.; Martinez, J.; Sarret, P.; Cavelier, F. *J. Med. Chem.* **2015**, *58*, 7785−7795.

(113) Fanelli, R.; Salah, K. B. H.; Inguimbert, N.; Didierjean, C.; Martinez, J.; Cavelier, F. *Org. Lett.* **2015**, *17*, 4498−4501.

(114) Cavelier, F.; Marchand, D.; Mbassi, P.; Martinez, J.; Marraud, M. *J. Pept. Sci.* **2006**, *12*, 621–625.

(115) Dalkas, G. A.; Marchand, D.; Galleyrand, J. –C.; Martinez, J.; Spyroulias, G. A.; Cordopatisa, P.; Cavelier, F. *J. Pept. Sci.* **2010**, *16*, 91–97.

(116) Martin, C.; Legrand, B.; Lebrun, A.; Berthomieu, D. Martinez, J.; Cavelier, F. *Chem. Eur. J.* **2014**, *20*, 14240–14244.

(117) Rene´, A.; Vanthuyne, N.; Martinez, J.; Cavelier, F. *Amino Acids* **2013**, *45*, 301–307.

(118) Vivet, B.; Cavelier, F.; Martinez, J. *Eur. J. Org. Chem.* **2000**, 807−811.

(119) Cavelier, F.; Vivet, B.; Martinez, J.;Aubry, A. *J. Am. Chem. Soc.* **2002**, *124*, 2917−2923.

(120) Pujals, S.; Fernandez-Carneado, J.; Kogan, M. J.; Martinez, J.; Cavelier, F.; Giralt, E. *J. Am. Chem. Soc.* **2006**, *128*, 8479−8483.

(121) Nair, A. G. *et. al. Bioorg. Med. Chem. Lett.* **2016**, *26*, 1475–1479.

(122) Tacke, R.; Merget, M.; Bertermann, R.; Bernd, M.; Beckers, T.; Reissmann, T. *Organometallics* **2000**, *19*, 3486-3497.

(123) Muratake, H.; Ito, A.; Toda, T.; Suzuki, H.; Fukasawa, H.; Tsuda, M; Inoue, K.; Sugiyama, K.; Shudo, K. *Bioorg. Med. Chem. Lett.* **2012**, *22*, 7602−7604.

(124) Fukasawa, H.; Muratake, H.; Ito, A.; Suzuki, H.; Amano, Y.; Nagae, M.; Sugiyama, K.; Shudo, K. *ACS Chem. Neurosci.* **2014**, *5*, 525−532.

(125) Information from the internet *via* www.clinicaltrials.gov

(126) Millership, J. S.; Shanks, M. L. *Int. J. Pharm.* **1986**, *28*, 1−9.

(127) Information from website www.ergo-log.com/silabolin.html

1.2.1. Tuberculosis

1.2.1.1. Introduction

Tuberculosis (TB) is an air-borne infectious disease caused by mycobacteria, mostly *Mycobacterium tuberculosis*. Historically, this disease used to be called by different names and the popular name was 'consumption' because patients lose their weight significantly and the disease appeared to consume the individual who got affected. As of now, TB is the leading cause of death due to an infectious agent and ranks alongside HIV. The bacteria mainly affect lungs and in some cases the infection spreads to bone, brain, liver, kidney, and heart. According to reports, one-third of the human population possess latent TB, a condition where the patient does not show any symptoms of TB.[1] A person with latent TB does not transmit the pathogen. Nearly 10% of the latent TB cases transform into active TB at a later stage and the chances are more in immune-compromised patients. Currently, chest X-ray or sputum culture is used for the diagnosis of active TB.

Tuberculosis is a very old disease and humans acquired this disease almost 5000 years ago. The causative agent, *Mycobacterium tuberculosis* was first identified in 1882 by the German microbiologist Robert Koch. He was awarded the Nobel Prize in medicine (1905) for this groundbreaking discovery. Although several advances were made in the field of medicine, tuberculosis still remains a global health concern. According to WHO reports, a total of 1.5 million TB deaths occurred in 2014 (including 0.4 million HIV positive cases).[2]

1.2.1.2. Epidemiology of TB

Tuberculosis is a disease of the poor and the economic burden of TB is borne by the developing and under developed countries. The South-East Asian region accounts for almost 40% of the TB cases reported. WHO lists 22 high TB burden countries with India reporting the highest number of cases, followed by Indonesia and China. India accounts for 23% of the world's incident cases and 21% of TB deaths. The charts shown below are

drawn based on figures taken from WHO reports and prove that the global distribution of TB is highly uneven.[2, 3]
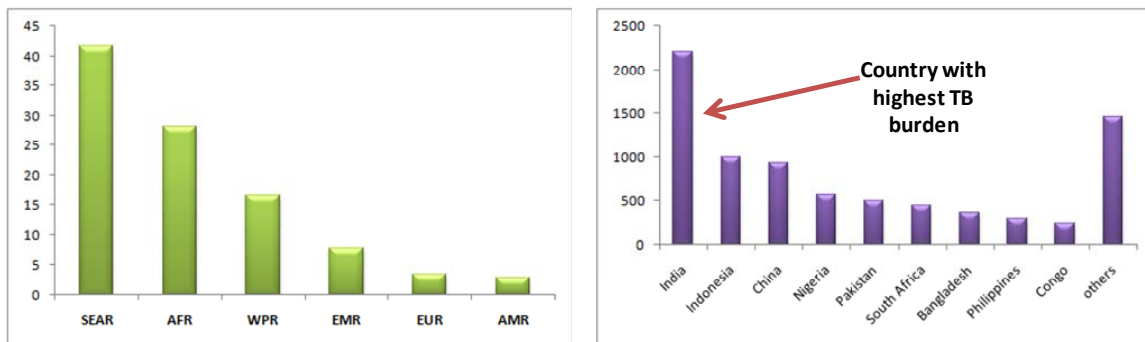

Figure 1.2.1. Global distribution of TB cases (a) among the WHO regions (b) among the highest TB burden countries (based on incident cases reported in 2014)

1.2.1.3. Current treatment for TB

The BCG vaccination given to babies is intended to protect from TB infection. In countries endemic to TB vaccination is recommended; the protection period varies between 10-20 years. After a person is diagnosed with TB, management involves a combination of several antibiotics. Treatment includes a regime of isoniazid, rifampicin, pyrazinamide, ethambutol for 2 months (intensive phase), followed by isoniazid - rifampicin combination for another 4 months (continuation phase). These four drugs are called the first line drugs (Group 1) for TB.[4-9]
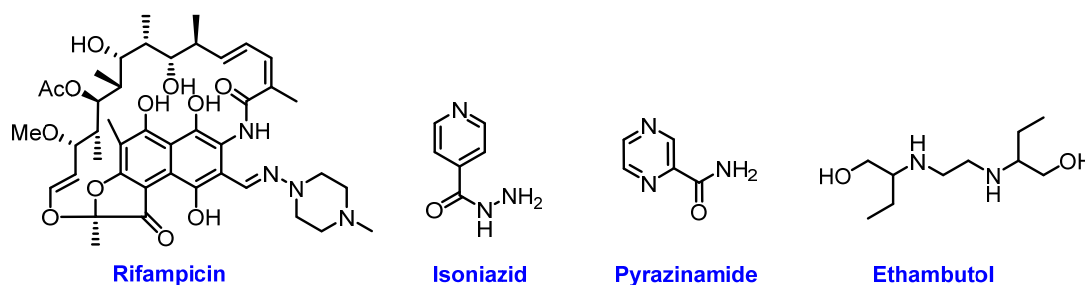
Figure 1.2.2. First line drugs for treating TB

It is observed that the mycobacteria develop resistance to existing antibiotics which necessitates development of new drugs to treat tuberculosis. In patients resistant to first line therapy, second line drugs (group 2, 3 and 4) are given which are less efficient than the first line drugs. Group 2 consists of aminoglycosides (streptomycin, kanamycin, amikacin) and polypeptides (capreomycin, viomycin). All the fluoroquinolones (ciprofloxacin, levofloxacin, moxifloxacin, ofloxacin, gatifloxacin) fall under group 3. Group 4 consists of oral drugs such as *p*-aminosalicyclic acid, cycloserine, terizidone, ethionamide, prothionamide, thioacetazone and linezolid. The third line drugs (group 5) have uncertain efficacy and safety. It includes clofazimine, linezolid, amoxicillin plus clavulanate, imipenem plus cilastatin, clarithromycin, rifabutin and bedaquiline. Some of the second line drugs are shown in figure 1.2.3.[4-9]
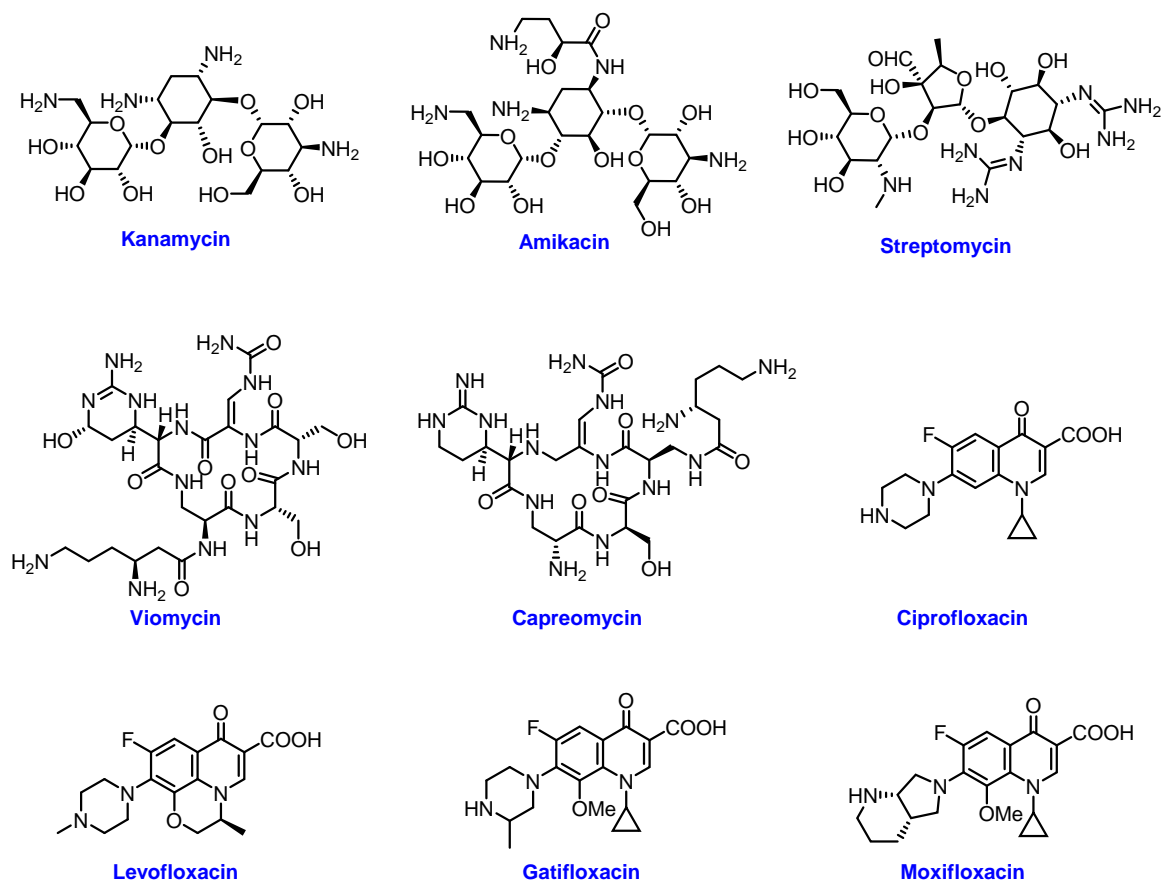

Figure 1.2.3. Second line drugs for treating TB

Treatment of TB takes longer time than that required for treating other bacterial infections. If doses are skipped or if the treatment is stopped, it can lead to development of resistance against the antibiotics. WHO recommends DOTS (Directly Observed Treatment, Short- course) therapy for effective management of TB.[10] The government sets up a centralized system for detecting and monitoring tuberculosis. A healthcare worker observes the patient and ensures that the antibiotics are taken properly. DOTS have been a huge success and is estimated that nearly 41 million people were successfully treated.

1.2.1.4. Drug resistant TB

Mycobacteria develop resistance to known drugs which poses a serious threat to currently available treatment. The treatment takes longer time (up to 2 years) and is more expensive and less effective.[11] There exists different forms of drug resistant TB which are described below.[6]

Multidrug resistant tuberculosis (MDR-TB): Resistance to the most effective first line drugs, isoniazid and rifampicin. According to WHO reports, 190000 MDR-TB deaths occurred in 2014. Only 50% of the MDR-TB cases were treated successfully asserting that drug resistant TB is a serious health concern.[2]

Extensively drug resistant tuberculosis (XDR-TB): Resistance to any fluoroquinolones (group 3), and one of the injectable drugs from group 2 (amikacin, kanamycin, capreomycin) in addition to isoniazid, rifampicin. According to latest estimates, 9.7% of MDR-TB patients have XDR-TB.

Totally drug resistant tuberculosis (TDR TB): Resistance to all first line and second line drugs. It is also known as *extremely drug resistant TB (XXDR TB)* because of the difficulty in treatment.

The emergence of drug resistance necessitates the development of new anti TB drugs. Extensively drug resistant TB has been reported in 105 countries. The more serious problem of totally drug resistant TB was reported in India (2011). Despite several

efforts from WHO and other organisations, there remains a serious gap in TB treatment.[2,3,12]

1.2.2. Drug targets in Mtb and developmental candidates

1.2.2.1. Drug pipeline for tuberculosis

There are many compounds undergoing clinical trials for treating TB (see fig. 1.2.4).[2, 13] Recently, the drug bedaquiline got FDA approval (in 2012) for the treatment of MDR-TB. Bedaquiline acts by inhibiting the mycobacterial ATP synthase which is a novel target. The global threat of drug resistant TB prompted FDA to give a fast track approval to bedaquiline based on the efficacy shown in Phase II clinical trials. It was the first TB drug to hit the market in four decades. However, bedaquiline is known to induce QT prolongation by binding to hERG and hence the drug comes with a black box warning.[14]

Discovery	Preclinical Development		Clinical Development		
Lead Optimization	**Early Stage Development**	**GLP Tox.**	**Phase 1**	**Phase 2**	**Phase 3**
Cyclopeptides	TBI-166	BTZ043	TBA-354	Sutezolid	Bedaquiline
Diarylquinolines	CPZEN-45	PBTZ169	Q203	SQ109	Delamanid
DprE Inhibitors	SQ609	TBA-7371		Rifapentine	
InhA Inhibitor, Indazoles	SQ641	GSK-070		AZD5847	Pretomanid-
LeuRS Inhibitors, ureas	DC-159a				Moxifloxacin-
Macrolides, Azaindoles					Pyrazinamide
Mycobacterial Gyrase				Bedaquiline-	regime
Inhibitors				Pretomanid-	
Pyrazinamide analogs				Pyrazinamide	
Ru (II) complexes				regime	
Spectinamides SPR-113					
Translocase-1 Inhibitors, Clp,					
MmPL3, oxazolidinones,					
Pyrimidines, DprE1, Aryl					
Sulfonamides, PKS13,					
Squaramides					

Figure 1.2.4. Pipeline for new TB drugs (information from www.newtbdrugs.org)

1.2.2.2. Drug targets in Mtb

The currently used anti-TB drugs target cell wall biosynthesis, protein synthesis, DNA replication, and other pathogen growth mechanisms.[9] The newly approved drug bedaquiline (TMC 207) has a novel mechanism of action and inhibits the mycobacterial proton pump. Rifamycins inhibit bacterial DNA dependent RNA synthesis in Mtb.

The cell wall of mycobacteria is unique consisting of fatty acids called mycolic acids and has been a popular drug target. The first line drug, isoniazid targets 2-trans-enoyl-acyl carrier protein reductase and blocks the mycolic acid biosynthesis. Ethambutol inhibits the synthesis of arabinogalactan which is a vital component of mycobacterial cell wall.[9]
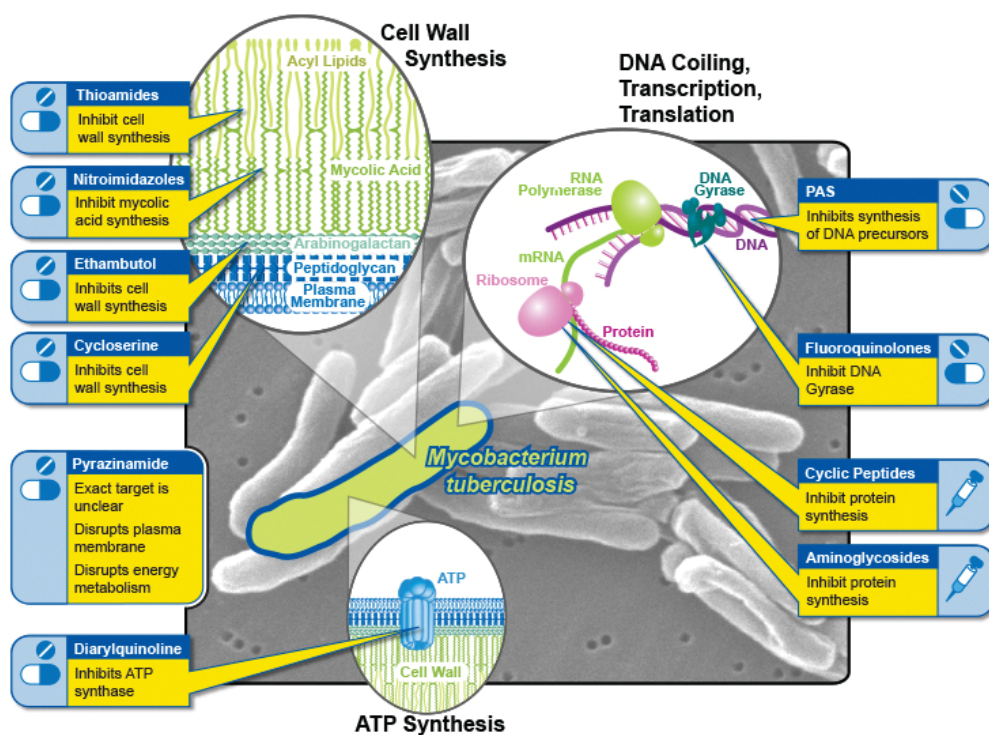
Figure 1.2.5. Drug targets in Mtb (Picture taken from National Institute of Allergy and Infectious Diseases website)[15]

1.2.2.3. MmpL3 as a potential target to treat TB

The cell wall of mycobacteria is associated with its virulence and is a promising target to develop anti-TB drugs. The cell wall consists of a peptidoglycan layer covalently linked to arabinogalactans. There is another layer made of long fatty acids called mycolic acids. The mycolic acids are either linked to arabinogalactans or bonded to sugars called trehalose *via* ester bonds forming trehalose monomycolate (TMM) or trehalose dimycolate (TDM). This mycolic acid layer protects the bacteria from any chemicals, hosts immune system and provides support to the cell wall.[16-18]
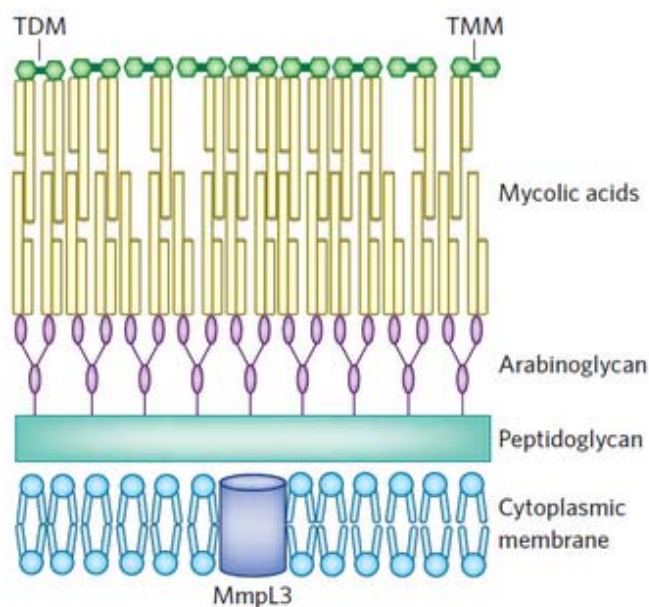
Figure 1.2.6. Schematic diagram showing cell wall of mycobacteria (picture taken from Nature publications)[17]

Mycolic acids are synthesized in the cytoplasm as TMM and then transported to the cell wall. Recently, it was discovered that the protein MmpL3 transports TMM to the cell wall. MmpL3 appears to be a promising drug target and an inhibitor of this transporter protein, SQ109 is in Phase II clinical trials for TB. Other compounds such as AU1235, BM212, C215, also inhibit Mtb by targeting MmpL3 (see fig. 1.2.7).[16-26] The target was identified by growing resistant strains and characterized by genome sequencing.
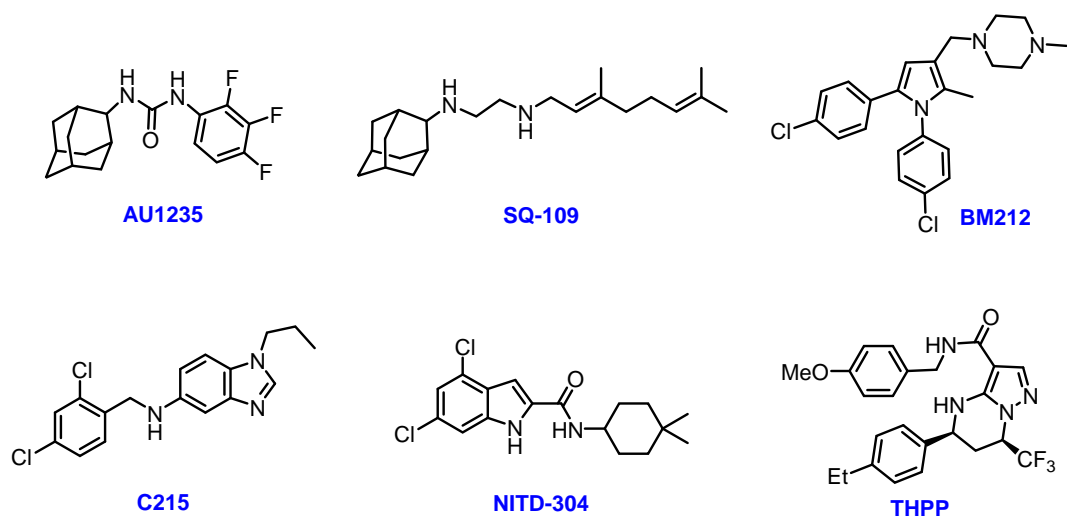
Figure 1.2.7. Selected MmpL3 inhibitors known in the literature

1.2.3. Present work

1.2.3.1. Repurposing rimonabant drug scaffold for TB

The need for new treatment for tuberculosis prompted us to develop drugs to tackle this global threat. Along these lines, the drug rimonabant (**2**) an anti-obesity drug currently withdrawn from the market received our attention due to its structural similarity with the MmpL3 inhibitor BM212 (**1**). Rimonabant reduces food intake by blocking the cannabinoid receptor CB1 and is the first marketed CB1 receptor antagonist.[27-31]
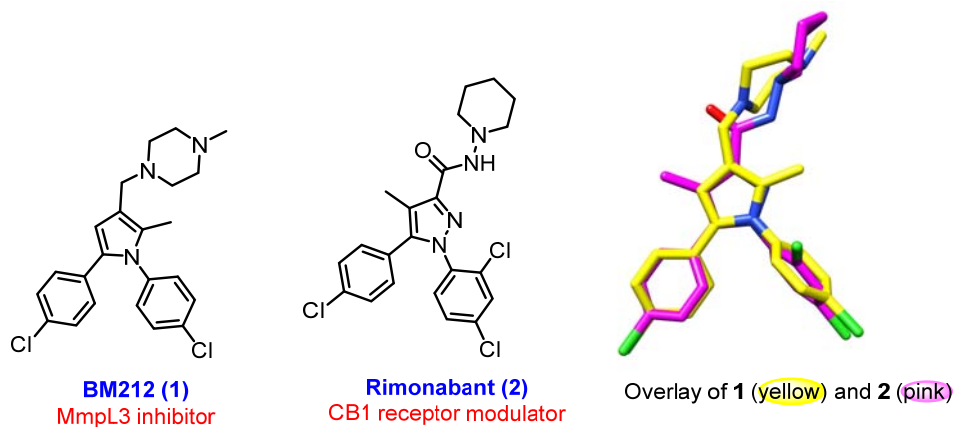
Figure 1.2.8. Structural similarity between BM212 and rimonabant

Drug repurposing (drug repositioning) is finding new therapeutic usage for an existing drug. It is a lower risk strategy because the safety and druggability of the compound is already established.[32-35] Once a new usage is identified the drug can be evaluated directly in Phase II. To launch a new drug to market, it takes approximately 10-15 years at a cost of 2.6 billion USD.[36] According to reports, nearly 40% of the overall cost to bring a drug to market can be bypassed by drug repurposing.[32] Now, many pharmaceutical companies (Pfizer, AstraZeneca, GlaxoSmithKline etc.) are actively pursuing this strategy and nearly 30% of the drugs approved per year are repurposed candidates. The drugs which failed for a particular indication are ideal candidates for repurposing.[35] A very good example for this is the controversial drug thalidomide.[37, 38] Thalidomide was prescribed to pregnant ladies for morning sickness and created birth defects in children. Later, it was found to have immunomodulatory and anti-angiogenic effects and is now used to treat multiple myeloma.

A drug is the optimized candidate out of a series of lead compounds. So the scaffold itself may have druggable properties and possess good safety profile. Molecules which are structurally close to a marketed drug are also expected to have drug like properties. Hence the concept "repurposing of a drug scaffold" was adopted by some researchers recently.[39,40] With this background, we decided to evaluate rimonabant scaffold for anti-TB activity because of its striking similarity to BM212. We expected that this scaffold may be a promising starting point because of its druggable properties. The diaryl pyrazole scaffold is also present in other drugs belonging to the class of NSAID's such as celecoxib. Since, this scaffold is known for CNS diseases it was expected that rimonabant analogs may be useful in developing therapeutic agents to treat brain tuberculosis. To our delight, initial screening of rimonabant showed moderate activity (MIC 25 μg/mL) against $H_{37}Rv$. Recently, while we were working on this project another report on the anti-TB activity of rimonabant analogs appeared in the literature.[41]

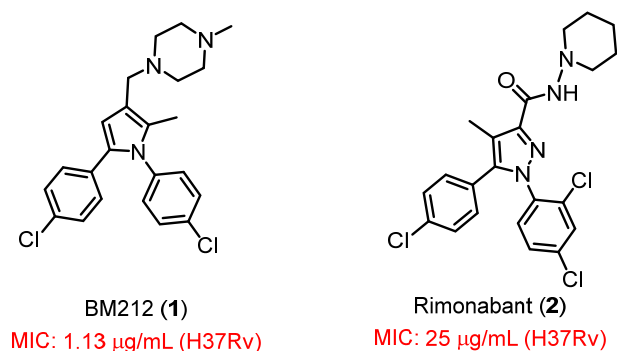BM212 (**1**)
MIC: 1.13 µg/mL (H37Rv)

Rimonabant (**2**)
MIC: 25 µg/mL (H37Rv)

Figure 1.2.9. Anti-TB activity of BM212 and rimonabant

1.2.3.2. Design and synthesis of rimonabant analogs towards anti-TB agents

To improve the anti-TB activity of rimonabant, we designed and synthesized analogs of rimonabant with varying structural features keeping in mind the structural variations between rimonabant and BM212 (fig. 1.2.10). Due to our group's interest in organosilanes we decided to synthesize a few silicon analogs as well. An increase in lipophilicity is known to enhance the anti TB activity in the BM212 series.[42-45] Hence, we assumed that the lipophilic silicon analogs may possess better cell penetration resulting in an enhanced potency. Analogs with varying functional groups were designed in such a way as to establish the effect of C-3 substituent on the anti-TB activity.

Novel modifications such as introduction of Silicon

Role of carbonyl

Effect of substituent

Effect of substituent

Silicon incorporation can increase the lipophilicity and gives good IP space
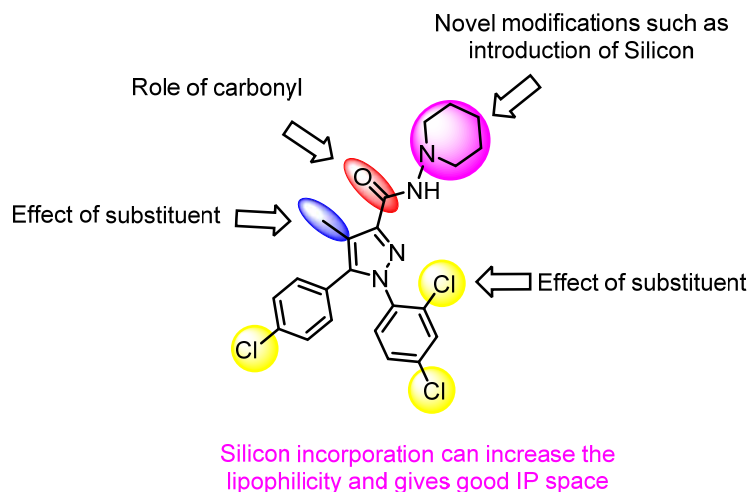
Figure 1.2.10. Design of rimonabant analogs for anti-TB activity

43

The required silicon building blocks were made in multigram quantities as shown in scheme 1.2.1. The 4,4-dimethyl silapiperidine (**6**) was prepared following procedures known in the literature.[46, 47] Commercially available dimethyldivinylsilane (**3**) on addition of freshly prepared HBr gas in presence of benzoyl peroxide in heptane gave the bromo derivative (**4**) in quantitative yield. This dibromo compound on cyclization with benzyl amine (TEA, CHCl$_3$) gave the benzylated silapiperidine **5** in moderate yield. This compound was converted to its HCl salt and debenzylated under an atmosphere of hydrogen to give the required silapiperidine (**6**) as its HCl salt. The NMR was compared with the reported values and found to be identical. In a similar way, the dibromo derivative **4** was cyclized with Boc hydrazine to give the compound **7** as a crystalline solid in low yield (38%). In ^{1}H NMR, the singlet at δ 1.44 ppm indicated the *t*-butyl group from Boc. In ^{13}C NMR, the carbamate carbonyl appeared at δ 154.3 ppm and the quaternary carbon of Boc appeared at δ 79.9 ppm all of which are in agreement with the structure. The deprotection of Boc using HCl in dioxane gave the *N*-aminosilapiperidine (**8**) in its salt form.
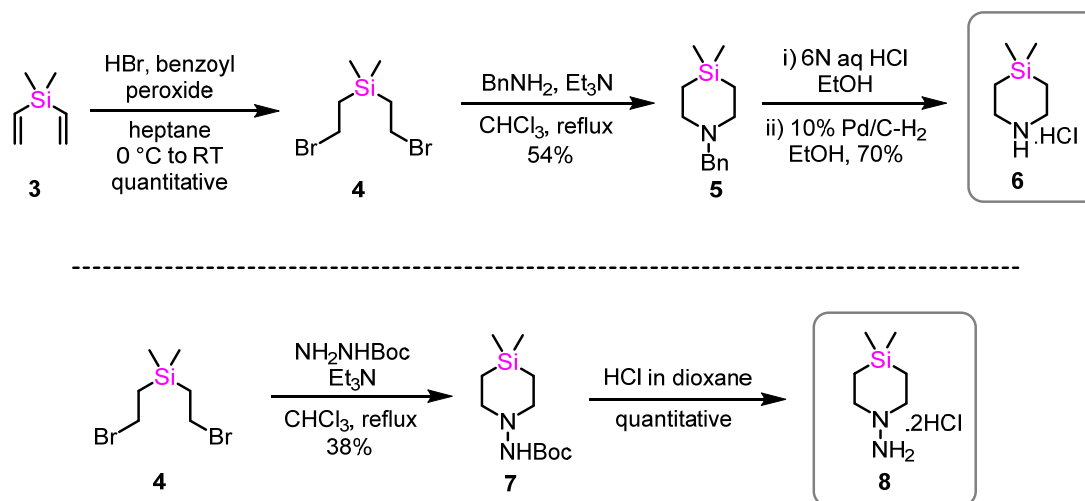
Scheme 1.2.1. Syntheses of silicon containing building blocks

The pyrazole starting material **9** was synthesized according to the literature protocol and was coupled with several amines using EDC and HOBt to give a series of amides (**10 - 20**).[48]
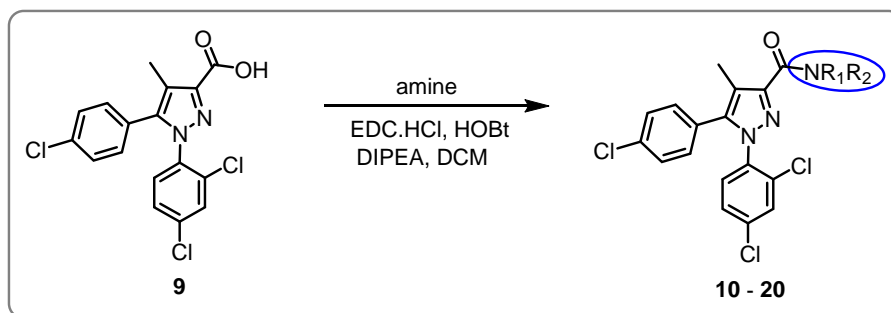
Scheme 1.2.2. General scheme for syntheses of amides **10 - 20**

The compounds **10**, **11**, **14**, **15** and **20** are already known in the literature and the ^{1}H NMR spectra of all these compounds were found to be identical with the reported data.[48-50] The acid on coupling with the 4,4-dimethyl-silapiperidine **6** gave the silicon analog **12** in 89% yield. In ^{1}H NMR, the highly shielded methyls attached to silicon appeared at δ 0.12 ppm. The silicon attached protons in the ring appeared at δ 0.9 ppm as a multiplet. The ring protons attached to amide appeared at δ 3.8 ppm as a multiplet. The aromatic methyl resonated at δ 2.17 ppm as a singlet. In ^{13}C NMR, the characteristic amide carbonyl was observed at δ 163.9 ppm. The silicon methyls were observed at δ - 3.0 ppm. The HRMS analysis also matched with the molecular formula $C_{23}H_{24}ON_3Cl_3SiNa$ $[M + Na]^+$ thus confirming the structure. 2-(trimethylsilyl)ethanamine required for synthesis of silicon analog **13** was synthesized from commercially available 2-(trimethylsilyl)ethanol. In ^{1}H NMR, the silicon attached methyls appeared at δ 0.05 ppm. The methylene attached to silicon appeared at δ 0.92 ppm as a multiplet and that attached to amide appeared at δ 3.47 ppm. The other newly synthesized amides **16**, **17**, **18** and **19** were also fully characterized with the help of spectral data (NMR, IR, HRMS). The known amide **21** was synthesized from the corresponding acid chloride by following reported procedure.[51]

10 (78%)

11 (83%)

12 (89%)

13 (72%)

14 (42%)

15 (72%)

16 (89%)

17 (62%)

18 (52%)

19 (83%)

20 (72%)

21 (73%)
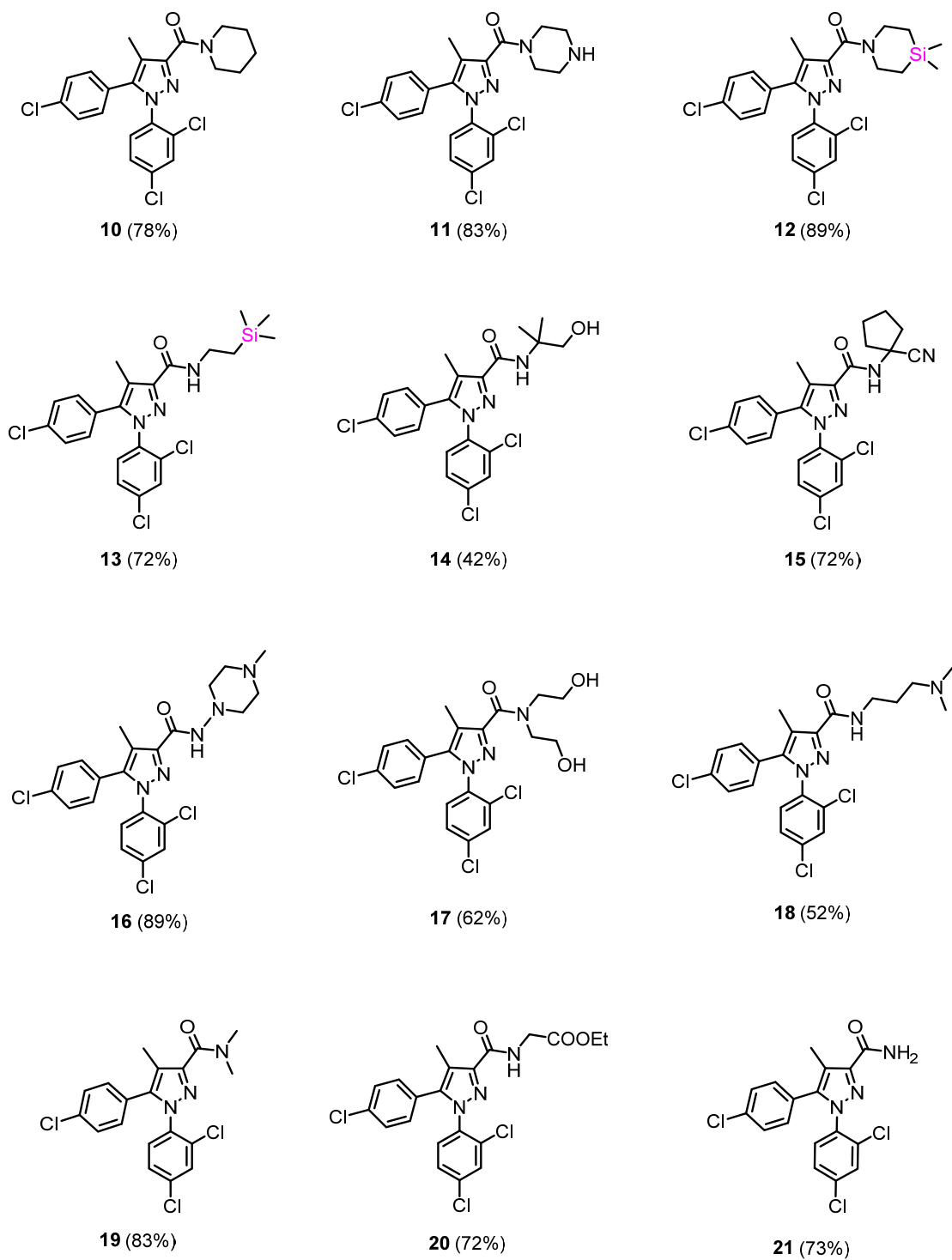
Figure 1.2.11. List of amides synthesized from carboxylic acid **9**

The ester group in **20** on hydrolysis gave the carboxylic acid **22**.[50] The known hydrazide **24** was prepared from the corresponding ester **23** and hydrazine hydrate.[49]
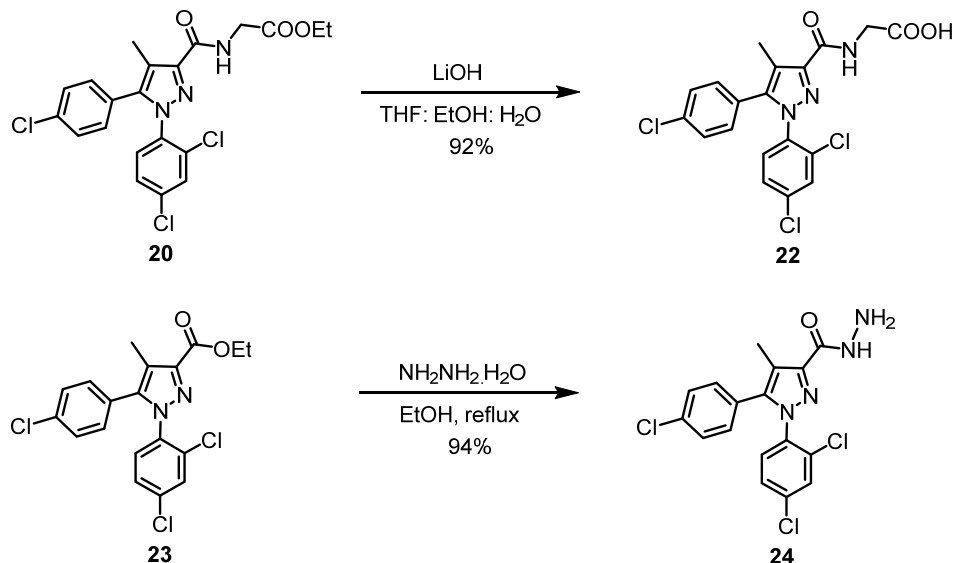

Scheme 1.2.3. Syntheses of compounds **22** and **24**

The thioamide **25** was synthesized from the amide **12** using Lawesson's reagent in excellent yields (98%). On TLC, the product appeared non-polar when compared to the starting material. In ^{1}H NMR, the gem methyls attached to silicon appeared at δ 0.16 ppm. The thioamide attached protons appeared as two sets; δ 4.49 ppm (m, 2H) and δ 3.89 ppm (t, J = 5.6 Hz, 2H). The characteristic thiocarbonyl appeared at δ 190.2 ppm in ^{13}C NMR. The HRMS analysis showed a mass peak at 508.0596 corresponding to $C_{23}H_{25}N_3Cl_3SSi$ which further confirmed the structure.
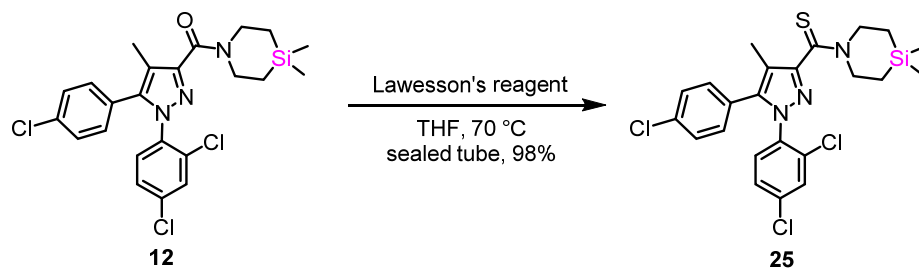
Scheme 1.2.4. Synthesis of thioamide **25**

Next, we decided to introduce a more polar substituent into the scaffold. The ester **23** was converted to the hydroxyl acid **27** by using reported procedures.[52] The benzylic position was first brominated using NBS in CCl_4 solvent. The bromide and starting material **23** appeared at same R_f on TLC and the reaction did not go for completion (even after refluxing for 18h). The ^{1}H NMR indicated that the product and starting material were present in a 1:1 ratio and this mixture was used for the next step. The bromide was converted to the alcohol **26** in presence of $AgNO_3$ using water as the nucleophile (unreacted **23** recovered). The ester **26** on basic hydrolysis gave the acid **27** which was coupled to silicon amines 4,4-dimethylsilapiperidine and 2-(trimethylsilyl)ethanamine to give compounds **28** and **29** respectively (Scheme 1.2.5). The ^{1}H NMR of compound **28** showed a singlet at δ 4.47 ppm which corresponds to the benzylic protons. In ^{13}C NMR, the amide carbonyl appeared at δ 163.5 ppm. Both the structures of compounds **28** and **29** were further confirmed by HRMS.
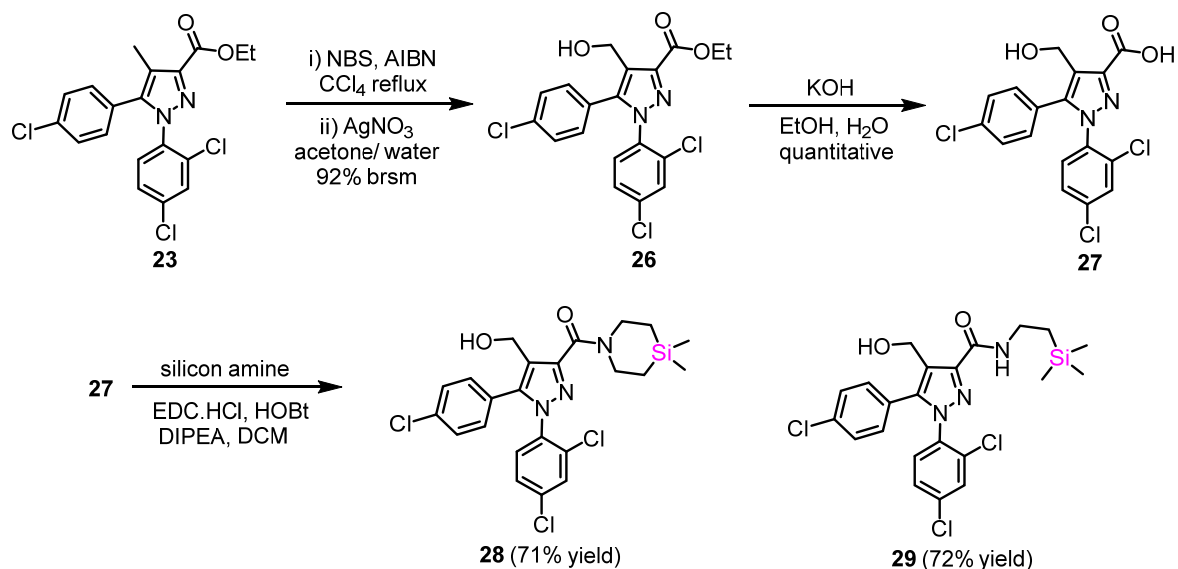
Scheme 1.2.5. Syntheses of sila amides **28** and **29**

After synthesis of amides, we turned our attention towards the amine series. For this purpose, the known alcohol **30** was converted to mesylate and then displaced with various amines to give compounds **31 – 36** (Scheme 1.2.6).
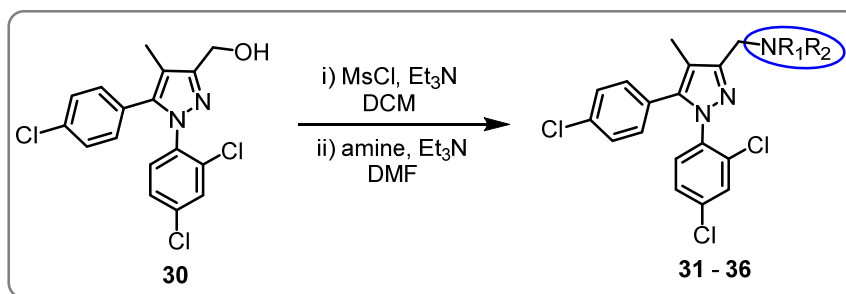
Scheme 1.2.6. General scheme for syntheses of amines **31 – 36**

The compound **31** is known in the literature, but was synthesized from the corresponding aldehyde using reductive amination.[53] The ^{1}H NMR of **31** synthesized by the present route was consistent with that of the reported NMR. All the compounds (**31 – 36**) were purified by silica gel column chromatography and the products were fully characterized with the help of spectroscopic techniques (NMR, IR, HRMS).
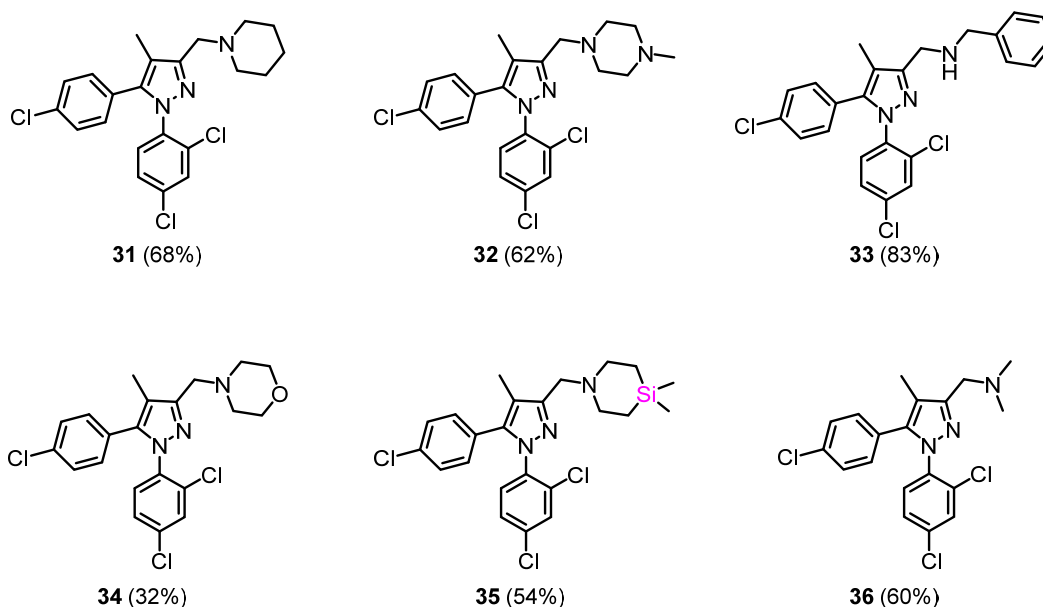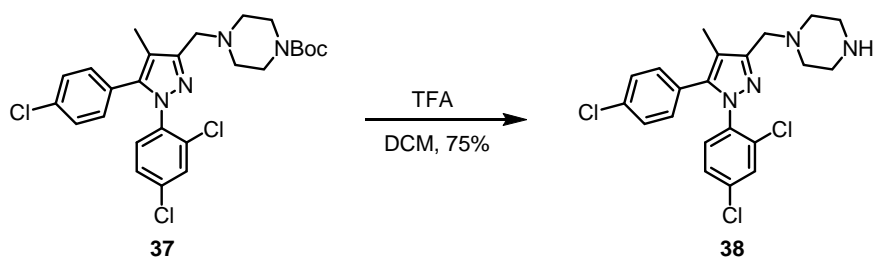

31 (68%)   **32** (62%)   **33** (83%)

34 (32%)   **35** (54%)   **36** (60%)

Figure 1.2.12. List of amines synthesized from alcohol **30**

The compound **37** was synthesized from alcohol **30** by displacement of the mesylate with *N*-Boc piperazine as shown in scheme 1.2.6 (70% yield). The Boc group was then deprotected using TFA in DCM to give the amine **38** (scheme 1.2.7).

Scheme 1.2.7. Synthesis of amine **38**

The known ether **39** was prepared from alcohol **30** by alkylation with benzyl bromide in presence of base, sodium hydride in DMF (Scheme 1.2.8).[54]
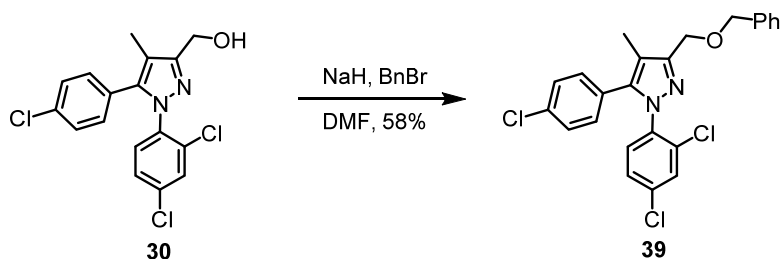
Scheme 1.2.8. Synthesis of ether **39**

The hydroxymethyl amine **42** was synthesized as shown in scheme 1.2.9. The benzylic alcohol **26** described in scheme 1.2.5 was protected to give its TBS ether **40**. The ester group was then reduced with LAH in THF solvent, and the resultant alcohol was mesylated and displaced with 4,4-dimethylsilapiperidine (**6**) to give compound **41**. Ultimately, the TBS group was deprotected using TBAF to give compound **42**. In ^{1}H NMR, the singlet at δ 4.52 ppm corresponds to the methylene protons attached to hydroxyl and a singlet at δ 3.73 ppm corresponds to the benzylic methylene attached to amine. The protons of silapiperidine attached to nitrogen appeared at δ 2.86 ppm as a triplet with J = 5.5 Hz. Another triplet at δ 0.84 ppm (J = 5.9 Hz, 4H) corresponds to the ring protons adjacent to silicon. The highly shielded gem dimethyl groups appeared further upfield at δ 0.08 ppm. The HRMS analysis revealed a peak at 496.0954 corresponding to the molecular ion $C_{23}H_{27}ON_3Cl_2{}^{37}ClSi$ [M+H]$^+$ further confirming the structure.
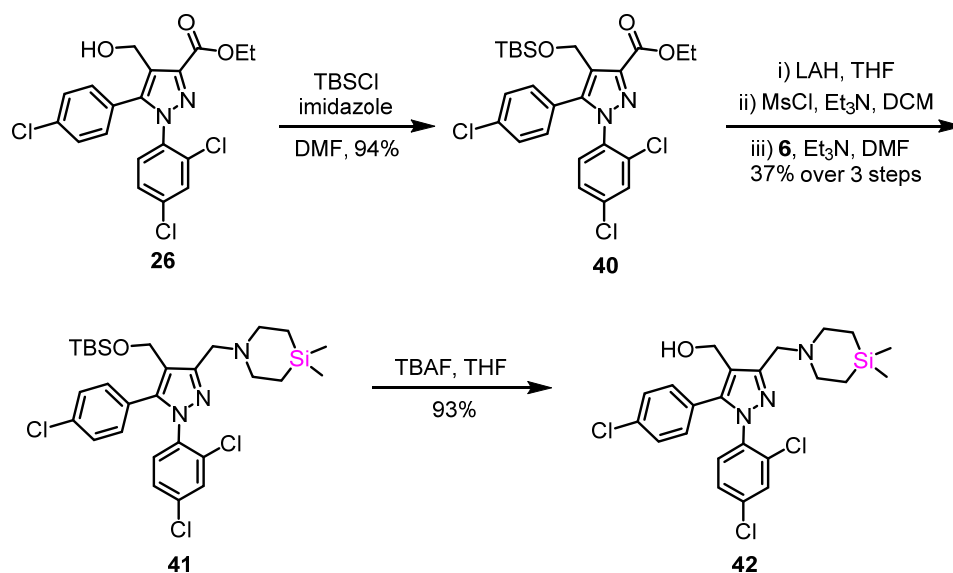
Scheme 1.2.9. Synthesis of silicon amine **42**

Since, triazoles are gaining more importance in medicinal chemistry; we planned to introduce a triazole in the rimonabant scaffold.[55,56] Triazoles are also considered as surrogates of amide. The Cu(I) catalyzed azide alkyne cycloaddition, a variant of the click reaction gives exclusively the 1,4-substituted 1,2,3-triazole. This reaction has gained immense popularity in recent times.[57-60] Accordingly, the azide **43** was synthesized from alcohol **30** using DPPA, DBU in THF solvent. This crude azide was treated with ethyl propiolate in presence of catalytic CuI in CH_3CN to give the triazole ester **44** (Scheme 1.2.10). In ^1H NMR, the characteristic aromatic proton of triazole ring appeared at δ 8.20 ppm as a singlet. The methylene attached to triazole appeared at δ 5.69 ppm. All the NMR values and HRMS analysis were in agreement with the structure.
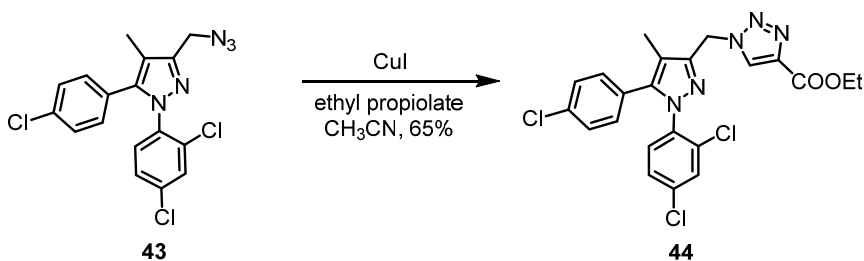
Scheme 1.2.10. Synthesis of triazole **44**

Rimonabant is a 1,5-diarylpyrazole with a methyl substituent at C4. BM212 contains a 1,5-diarylpyrrole and the C4 position is unsubstituted. Hence, we decided to make a few analogs of rimonabant without C4 substituent. Towards this, the acid **45** prepared using known procedures[61] was coupled with various amines to give amides **46 – 50** (Scheme 1.2.11). The pyrazole proton was clearly distinguishable in ^{1}H NMR and resonated upfield compared to the other aromatic protons. In **46** this proton appeared at δ 6.88 ppm and the C4 carbon appeared at 110.1 ppm in ^{13}C NMR.
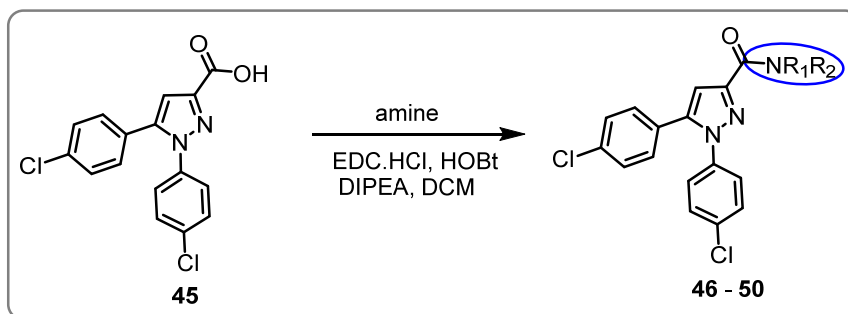
Scheme 1.2.11. General scheme for syntheses of amides **46 - 50**
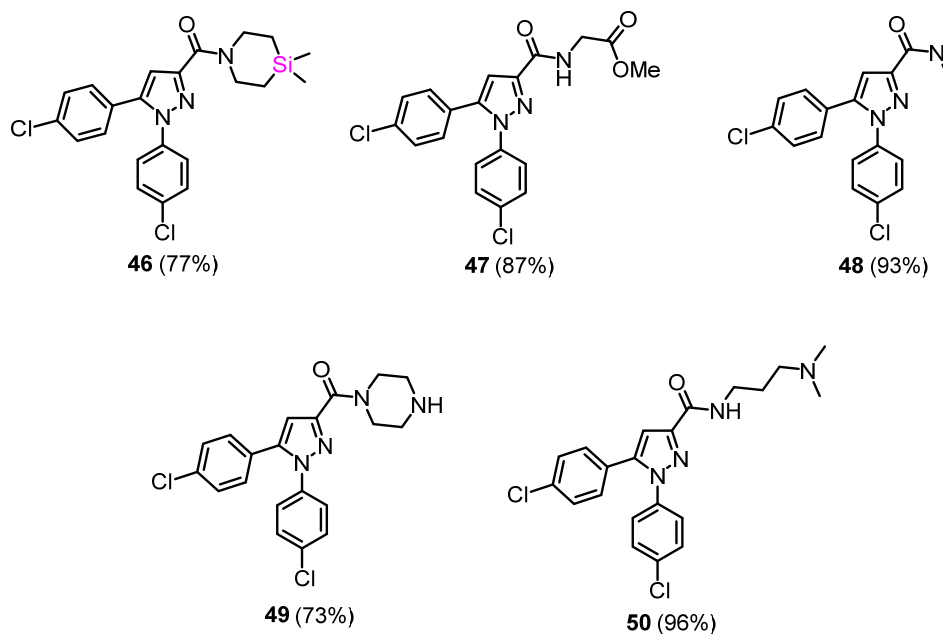
Figure 1.2.13. List of amides synthesized from acid **45**

For the synthesis of amines, alcohol **51** was mesylated and displaced with different amines to give compounds **52 – 56**. All the synthesized compounds were characterized with the help of spectral data (^{1}H and ^{13}C NMR) and HRMS.

Scheme 1.2.12. General scheme for syntheses of amines **52 – 56**
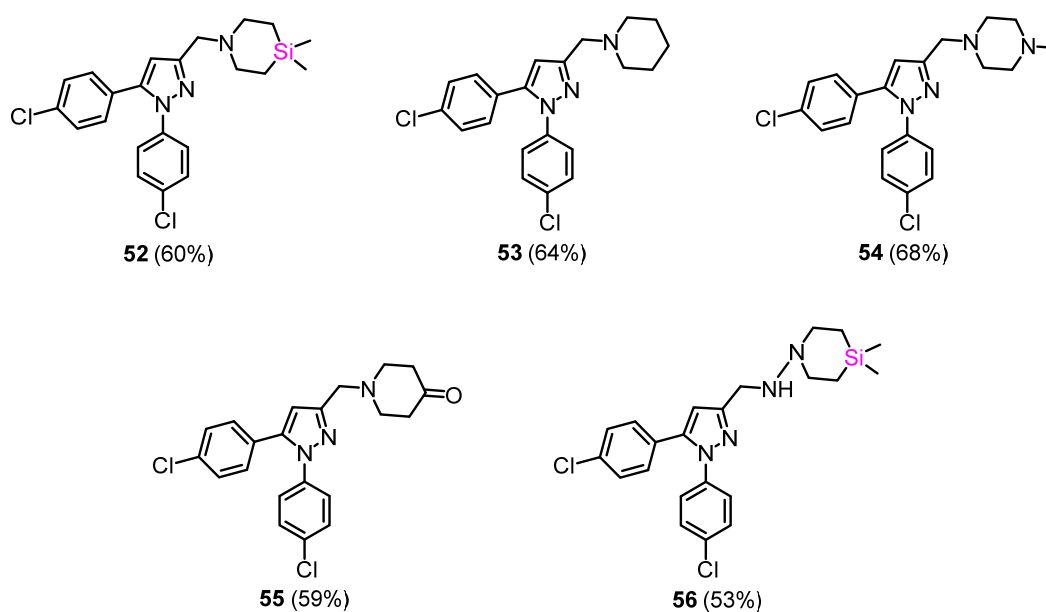
Figure 1.2.14. List of amines synthesized from alcohol **51**

1.2.3.3. Biological evaluation and SAR

The anti-TB activity of all the compounds was evaluated in collaboration with Dr. Rajesh Gokhale group, Institute of Genomics and Integrative Biology, New Delhi. Initially, the percentage inhibition of the compounds against *Mycobacterium smegmatis* was determined (collaborator: Dr. Ramesh Ummanni, Indian Institute of Chemical

Technology, Hyderabad) and the active compounds were selected for determination of minimum inhibitory concentration (MIC) against Mtb. MIC is the lowest concentration at which the compound can prevent the growth of the bacteria after overnight incubation. The MIC of the compounds against the virulent strain H37Rv was determined using alamar blue assay.[62] In alamar blue assay the colour change of the redox indicator, resazurin is used to determine the bacterial growth. Resazurin is blue in colour and can penetrate the cell of microorganisms. In growing cells resazurin gets reduced to fluorescent red resorufin whose fluorescence is detected by a detector. So, the fluorescence is an indication of bacterial growth. The compound at different concentrations is added to the cells and incubated followed by addition of resazurin. From the fluorescent intensity of the cells at varying concentrations of compound, MIC is determined. The MIC's of compounds active below a concentration of 100 μg/mL are shown in table 1.2.1. In our assay, rimonabant showed an MIC of 25 μg/mL and BM212 an MIC of 1.13 μg/mL.

Most of the compounds from the amide series were not active. Some of the compounds (**11**, **16**, **18**, **46**, **48, 49**, and **50**) showed moderate activity similar to or better than rimonabant. The silaamide **46** showed an of MIC 6.25 μg/mL and was the most active among the amides. The thioamide **25**, the ether analog **39**, as well as the triazole **44** did not show any activity. However, most of the amines showed moderate to good activity. The basic nitrogen may be crucial for the activity of the compound. It was also observed that the silicon analogs showed an increase in potency. The activity of sila analog **35** (MIC 1.17 μg/mL) was similar to that of BM212 (MIC 1.13 μg/mL). The amines **32** (MIC 12.5 μg/mL) and **38** (MIC 25 μg/mL) showed less activity compared to **35** clearly indicating the advantage of incorporating silicon. The silicon amines **52** (MIC 0.031 μg/mL) and **56** (MIC 0.39 μg/mL) also showed excellent activity. Silicon incorporation makes the compound more lipophilic, which in turn increases the cell penetration. It is interesting to note that analogs which lack the C4 methyl were more active (**46** *vs* **12** and **52** *vs* **35**).

Table 1.2.1. Antitubercular activity of the compounds

Compd	Y	R₁	MIC (H37Rv)	Compd.	Y	R₁	MIC (H37Rv)
2	CO	HN—N⟨piperidine⟩	25	46	CO	-N⟨Si⟩	6.25
11	CO	-N⟨⟩NH	25	47	CO	N(H)-CH₂-C(=O)-OMe	50
16	CO	HN—N⟨⟩N—	25	48	CO	-N(CH₃)₂	25
18	CO	N(H)-(CH₂)₃-N(CH₃)	25	49	CO	-N⟨⟩NH	25
19	CO	-N(CH₃)₂	50	50	CO	N(H)-(CH₂)₃-N(CH₃)	25
31	CH₂	-N⟨piperidine⟩	12.5	51	CH₂	-OH	50
32	CH₂	-N⟨⟩N—	12.5	52	CH₂	-N⟨Si⟩	0.031
33	CH₂	N(H)-CH₂-Ph	6.25	53	CH₂	-N⟨piperidine⟩	1.56
34	CH₂	-N⟨⟩O	50	54	CH₂	-N⟨⟩N—	25
35	CH₂	-N⟨Si⟩	1.17	55	CH₂	-N⟨⟩=O	25
36	CH₂	-N(CH₃)₂	6.25	56	CH₂	HN—N⟨Si⟩	0.39
38	CH₂	-N⟨⟩NH	25	1	-	-	1.13
42	CH₂OH	-N⟨Si⟩	6.25	INH	-	-	0.3

MIC values are in μg/mL

The compound **53** (MIC 1.56 μg/mL) containing piperidine is similar to BM212 in potency and indicates that replacement of pyrrole to pyrazole in BM212 retains the activity. The activity can be efficiently modulated by changing the substituents at C3 and C4. As previously reported, we could observe that increase in lipophilicity increased the activity in the BM212 series.[42-45] For instance, the introduction of a polar hydroxyl group to compound **35** resulted in a 5 fold decrease in potency (MIC of **42** = 6.25 μg/mL). Compound **52** (MIC 0.031 μg/mL) emerged as the most potent compound from this series and is 36 fold more active than the known compound BM212. The SAR conclusions of this series are given in figure 1.2.15. It is also interesting that the lead compounds do not contain the amide moiety. The amide oxygen is important in conferring the CB1 activity and associated side effects of rimonabant.[63, 64]
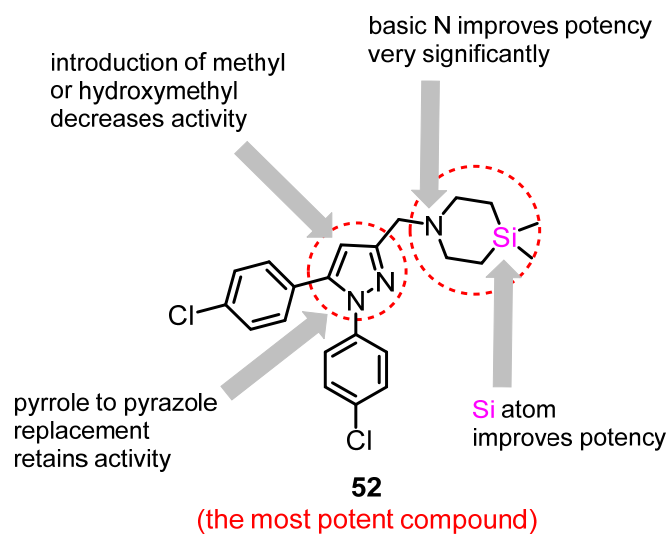
Figure 1.2.15. SAR conclusions (using anti-TB potential) of the current series

Cytotoxicity studies were done to examine the selectivity of the compounds for Mtb. Selectivity index is the ratio between cytotoxicity and MIC (both in μM). The potent compounds **52** and **56** showed excellent selectivity for Mtb over the cancerous cell lines A549 and Hep G2 (Table 1.2.2). The most potent compound **52** showed selectivity indices of 841 and 306 against A549 and Hep G2 cell lines respectively. The anticancer drug doxorubicin was used as the positive control.

Table 1.2.2. Cytotoxicity effects of the selected compounds

compd	IC$_{50}$ (µM)		selectivity index	
	A549 IC$_{50}$ ± Std dev	HEP G2 IC$_{50}$ ± Std dev	A549	HEP G2
BM212	91.6 ± 5.2	71.0 ± 5.3	33.6	26.0
32	80.3 ± 3.1	85.0 ± 4.4	2.9	3.1
33	55.8 ± 1.1	57.4 ± 3.4	4.1	4.2
35	54.2 ± 9.6	51.9 ± 3.3	22.2	21.3
36	57.2 ± 5.4	36.3 ± 2.4	3.6	2.3
42	61.9 ± 3.6	30.4 ± 1.2	4.9	2.4
46	68.3 ± 2.1	59.0 ± 0.5	4.9	4.2
52	58.9 ± 0.5	21.4 ± 2.6	841.3	306.3
56	73.2 ± 3.4	86.8 ± 3.7	84.2	99.8
Doxorubicin	5.3 ± 3.2	5.3 ± 1.8	-	-

Data obtained from Dr. Ramesh Ummanni, CSIR-IICT, Hyderabad

Since Mtb resides and multiplies in macrophages, the cytotoxicity studies were also carried out in RAW macrophages and THP-1 monocytes. The graph showing percentage viability of cells at different concentrations is shown in fig 1.2.16. Cytotoxicity was apparent at ≥ 3 µM for all the compounds tested and varied in the range of 40-60% across both cell lines.
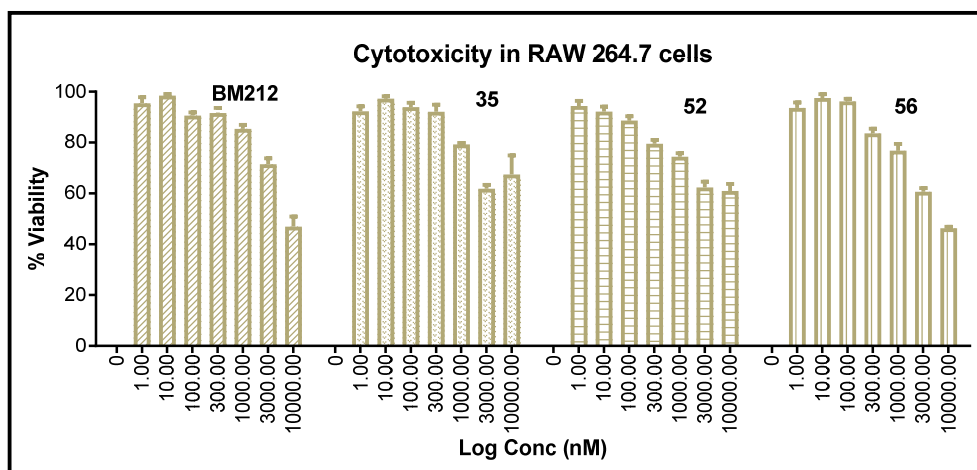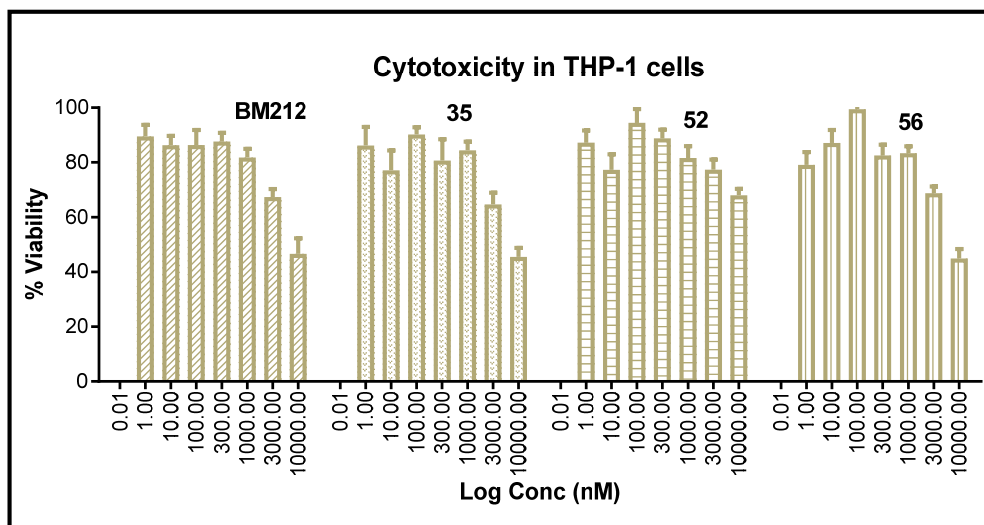
Data obtained from Incozen therapeutics, Hyderabad

Figure 1.2.16. Cytotoxicity studies on RAW macrophages and THP-1 monocytes

The best compounds were taken for further *in vitro* studies to check their druggable properties. Solubility is an important parameter in drug discovery and poor solubility can lead to less absorption of drugs from the GI tract. In the solubility assays, a solution of the compound is added to buffers of varying pH and then centrifuged. The supernatant solution is subjected to HPLC analysis to determine the solubility at a particular pH.

Table 1.2.3. *In-vitro* solubility data.

compd.	solubility (µM) at pH				
	1.2	2.2	4.5	7.4	10.2
BM212	45.19	42.21	36.73	26.68	5.38
35	40.98	40.58	34.24	1.05	10.94
42	44.02	42.47	41.62	5.31	2.39
46	0.16	0.18	0.13	0.05	1.28
52	43.04	42.28	41.87	3.72	1.99
53	44.96	44.65	43.56	11.40	1.49
56	43.14	43.20	44.28	39.76	38.00

Data obtained from Incozen therapeutics, Hyderabad

58

All the amines, **35**, **42**, **52**, **53** and **56** showed good solubility at acidic pH (table 1.2.3). Amines are expected to show good solubility at lower pH because of their basic nature. However at higher pH, compounds **35**, **42**, **52** and **53** showed poor solubility. The compound, **56** was the standout among all the tested compounds and showed good solubility at acidic as well as basic pH. The amide **46** displayed very poor solubility at all the pH tested.

The enzymes present in plasma hydrolyse certain functional groups which can affect the overall bioavailability of the drug. The most active silicon compounds **35**, **52** and **56** showed excellent plasma stability. Plasma stability was measured by incubating the compounds with plasma followed by LC-MS analysis to measure the amount of compound present (table 1.2.4).

Table 1.2.4. *In-vitro* Physchem and ADME Data.

compd.	% plasma stability (human)	% metabolic stability in liver microsomes (after 30 min.)		% human PPB
		mouse	human	
BM212	100	62.4	79.8	99.23
35	99.18	9.2	18.5	99.95
42	88.12	3.7	2.1	99.96
46	89.72	3.9	2.1	99.99
52	100.0	6.3	20.3	99.93
53	91.7	26	60.1	99.89
56	100.0	100.0	93.1	99.31

Data obtained from Incozen therapeutics, Hyderabad

The plasma contains proteins such as serum albumin, globulin, glycoprotein and lipoprotein to which the drugs can bind. In our assays, all the active compounds and BM212 were found to show high binding to the plasma proteins (> 99%). Since only the unbound drug (free drug) shows the pharmacological effect, some researchers believe that drugs should not possess high plasma protein binding (PPB). But some others believe

that PPB data generated by *in vitro* experiment cannot be used to determine the efficacy of a drug. Inside body several other factors such as metabolism come into action. According to a recent review article by Liu *et al.*, 45% of the new drugs have plasma protein binding > 95% which also supports the theory that drugs with high PPB can still be valuable.[65, 66]

Several enzymes present in the body biochemically modify the drug. This process called drug metabolism, introduces polar functionalities into the drug and the hydrophilic metabolites are easily cleared from the body. Liver is the major site of metabolism and is rich in metabolising enzymes such as cytochrome P450. Drugs get absorbed from the gut into blood and go to liver before reaching the systemic circulation. The rate of metabolism is a critical factor in determining the bioavailability, half life and dosage of the drug. In laboratory assays, liver microsomes which are rich in cytochrome P450 are used to determine the metabolic stability.[67,68] The metabolic stability of active compounds was evaluated using mouse and human liver microsomes after 60 min incubation at 1μM concentration. Unfortunately, compounds **35**, **42**, **46** and **52** showed poor microsomal stability. To our joy, the silicon amine **56** showed very good metabolic stability and was better than BM212. The overall PK profile of **56** is excellent and is superior in all the tested parameters compared to the parent compound BM212. This compound had an MIC 0.39 μg/mL and is 12 times less potent than the most potent compound **52**.

1.2.3.4. Scale up of lead compounds for animal experiments

From the biological studies, two compounds **52** and **56** emerged as the leads in the series. Although, the compound **52** showed excellent potency, the PK profile of the compound was not impressive. On the other hand, compound **56** which is less potent than **52** showed very good ADME profile. These two compounds had to be scaled up for further biological profiling in animal models.
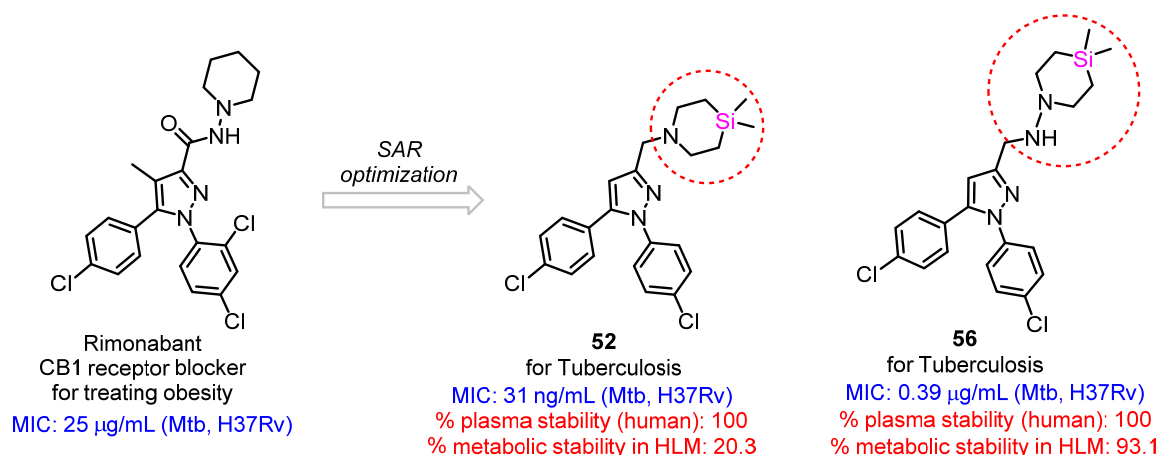
Figure 1.2.17. Lead compounds from the series (**52** and **56**)

The initial route for the amine synthesis was giving moderate yields. The yield was improved by converting the alcohol **51** to bromide instead of mesylate as in the earlier examples. The bromide was synthesized from alcohol **51** by an Appel reaction (TPP, CBr$_4$ in acetonitrile). The crude bromide was displaced with silicon amines **6** and **8** in DMF solvent. The compound **52** was obtained in a better yield of 74% after purification by column chromatography. In the case of **56**, the product precipitated from the reaction mixture upon addition of crushed ice and was purified by filtration (86% yield). Both the compounds were prepared in gram scale (~3 grams) and sent to CSIR-Central Drug Research Institute (CDRI) for *in vivo* studies using mouse models in collaboration with Dr. Sidharth Chopra.
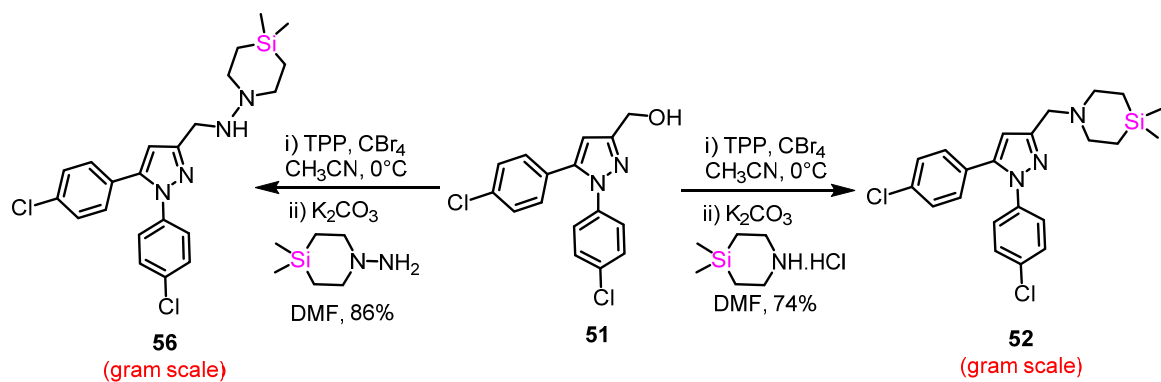
Scheme 1.2.13. Scale up of lead compounds **52** and **56**

1.2.4. Conclusions

The structural resemblance of the anti-obesity drug rimonabant with the anti-TB agent BM212 impelled us to investigate the anti-TB potential of rimonabant drug scaffold. Rimonabant as such showed moderate potency with MIC 25 µg/mL against H37Rv. Several analogs with varying structural features were synthesized and the biological activity was evaluated. It was observed that introduction of silicon increased the anti-TB activity of the series. The silicon compound **52** emerged as the most active compound in the series (MIC 0.031 µg/mL). Thus, we could successfully repurpose the rimonabant scaffold for the development of anti-TB agents. However, the metabolic stability of the compound (**52**) was poor. Another compound from this series, **56** (MIC 0.39 µg/mL) which was 3 fold more active than BM212 showed very good pharmacokinetic profile. Further optimization of the identified leads to improve the PK properties is underway in our group.

1.2.5. Experimental section

***Tert*-butyl (4,4-dimethyl-1,4-azasilinan-1-yl)carbamate (7)**
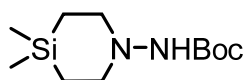
Bis(2-bromoethyl)dimethylsilane **4** (150 mg, 0.55 mmol), Boc protected hydrazine (361 mg, 2.7 mmol) and triethylamine (0.23 mL, 1.6 mmol) were dissolved in chloroform (10 mL) and refluxed for 24 hours. The reaction mass was cooled and 2N NaOH was added and the organic layer was separated, dried, concentrated and purified by silica gel column chromatography to give the compound **7** as a white crystalline solid (50 mg, 38 %).

IR ν_{max} (thin film, CHCl$_3$) 3262, 2977, 2925, 1709, 1523, 1366 cm^{-1}

^{1}H NMR (400 MHz, CDCl$_3$): δ 5.67 (s, 1H), 3.01 (t, J = 6.3 Hz, 4H), 1.44 (s, 9H), 0.85 (t, J = 6.3 Hz, 4H), 0.04 (s, 6H).

^{13}C NMR (100 MHz, CDCl$_3$): δ 154.3, 79.9, 55.5, 28.3, 13.0, -3.5

HRMS (ESI): m/z calculated for C$_{11}$H$_{25}$O$_2$N$_2$Si [M+H]$^+$ 245.1680; found, 245.1679.

4,4-dimethyl-1,4-azasilinan-1-amine hydrochloride (8)
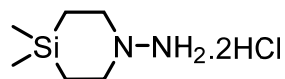
To the compound **7** (50 mg), HCl in dioxane (1 mL, 2.5M) was added and stirred at RT for 2 h. The reaction mass was concentrated and the solid obtained was washed with diethyl ether to give pure **8**.

^{1}H NMR (500 MHz, MeOD): δ 3.49 (m, 4H), 1.10 (t, J = 6.7 Hz, 4H), 0.19 (s, 6H).
^{13}C NMR (125 MHz, MeOD): δ 57.7, 11.6, -4.1

General procedure for synthesis of analogs

The generalised procedure for the synthesis of amides and amines are given below. The purity of products was determined by reverse phase HPLC analysis using Agilent technologies 1200 series; column: ZORBAX Eclipse XBD-C-18 (4.6 x 250 mm, 5 μ). Flow rate 1.00 mL/min, UV 254 nm; using mobile phases, Method A: 95/5 CH_3OH/H_2O for 20 min; Method B: 90/10 CH_3CN/H_2O for 20 min.

A. *Procedure for amide coupling:*

   To a solution of the carboxylic acid (1 eq) in dry dichloromethane, was added *N*-(3-Dimethylaminopropyl)-*N'*-ethylcarbodiimide hydrochloride (EDC.HCl, 1.2 eq), Hydroxybenzotriazole (1.2 eq) and diisopropylethyl amine (3 eq) at 0°C. Then the amine (1.1 eq) was added and stirred at RT for 6 h. To the reaction mixture water was added and the organic layer was separated, washed with saturated $NaHCO_3$, 1N HCl, dried over Na_2SO_4 and concentrated under reduced pressure. This crude mixture was purified by column chromatography to give the pure compound.

B. *Procedure for preparation of amines:*

   To a solution of the alcohol (1 eq) in dry dichloromethane (DCM), was added triethylamine (2.5 eq) followed by Mesyl chloride (1.1 eq) at 0°C and stirred at the same temperature for 30 min. To the reaction mixture water was added and

the organic layer was separated, dried over Na_2SO_4 and concentrated under reduced pressure. This crude product was immediately taken for the next step. The mesylate was dissolved in dry dimethyl formamide (DMF), triethylamine (4 eq) and corresponding amine partner (1.2 eq) was added at 0°C and left to stir at RT for 4h. To the reaction mixture water was added and the organic layer was separated, the aqueous layer was extracted using dichloromethane, dried over Na_2SO_4 and concentrated under reduced pressure. The crude was then purified by column chromatography to give the required compound.

(5-(4-Chlorophenyl)-1-(2,4-dichlorophenyl)-4-methyl-1*H*-pyrazol-3-yl)(4,4-dimethyl-1,4-azasilinan-1-yl)methanone (12)
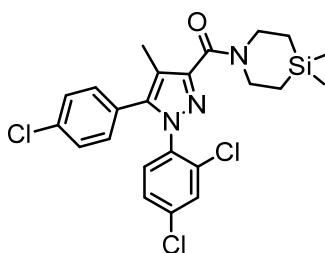
The title compound was synthesized from the carboxylic acid **9** and 4,4-dimethyl-4-silapiperidine[46,47] by following general procedure A.

Yield: 89%.

IR ν_{max} (thin film, CHCl₃) 2930, 1627, 1493, 1264 cm⁻¹

¹H NMR (200 MHz, CDCl₃): δ ppm 7.44 (d, *J* = 2.1 Hz, 1H), 7.31 − 7.05 (m, 6H), 3.91 − 3.78 (m, 4H), 2.17 (s, 3H), 0.97 - 0.84 (m, 4H), 0.12 (s, 6H).

¹³C NMR (100 MHz, CDCl₃): δ ppm 163.9, 147.4, 141.5, 136.0, 135.5, 134.7, 133.1, 130.6, 130.5, 130.3, 128.9, 127.8, 127.5, 115.7, 46.9, 42.2, 15.4, 13.9, 8.9, -3.0

HRMS (ESI): m/z calculated for $C_{23}H_{24}ON_3Cl_3SiNa$ [M + Na]⁺ 514.0646; found, 514.0645

HPLC analysis (Method B): t_R 8.13 min, purity 99.98 %

5-(4-Chlorophenyl)-1-(2,4-dichlorophenyl)-4-methyl-*N*-(2-(trimethylsilyl)ethyl)-1*H*-pyrazole-3-carboxamide (13)
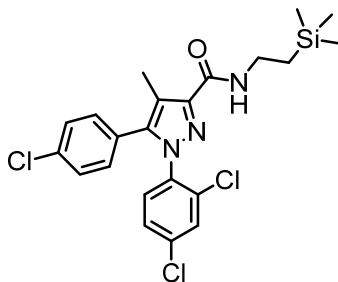
The title compound was synthesized from the carboxylic acid **9** and 2-(trimethylsilyl)ethan-1-amine hydrochloride[69, 70] by following general procedure A.

Yield: 72% brsm.

IR ν_{max} (thin film, CHCl$_3$) 3421, 3013, 1661, 1537, 1488 cm^{-1}

^{1}H NMR (400 MHz, CDCl$_3$): δ ppm 7.43 (d, *J* = 1.9 Hz, 1H), 7.31 - 7.24 (m, 4H), 7.07 - 7.05 (m, 2H), 6.91 (m, 1H), 3.50 - 3.44 (m, 2H), 2.38 (s, 3H), 0.94 - 0.90 (m, 2H), 0.05 (s, 9H).

^{13}C NMR (100 MHz, CDCl$_3$): δ ppm 162.4, 145.2, 142.9, 136.0, 135.9, 134.8, 133.0, 130.8, 130.5, 130.3, 128.8, 127.8, 127.3, 117.6, 35.4, 17.8, 9.4, -1.7

HRMS (ESI): m/z calculated for C$_{22}$H$_{25}$ON$_3$Cl$_2$^{37}ClSi [M+H]$^+$ 482.0797; found, 482.0789

HPLC analysis (Method B): t$_R$ 8.71 min, purity 96.62 %

5-(4-Chlorophenyl)-1-(2,4-dichlorophenyl)-4-methyl-*N*-(4-methylpiperazin-1-yl)-1*H*-pyrazole-3-carboxamide (16)
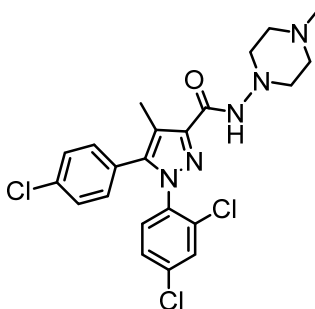
The title compound was synthesized from the carboxylic acid **9** by following general procedure A.

Yield: 89%.

IR ν_{max} (thin film, CHCl$_3$) 3406, 3319, 2944, 2807, 1680, 1533, 1491 cm^{-1}

^{1}H NMR (400 MHz, CDCl$_3$): δ ppm 7.61 (s, 1H), 7.42 (m, 1H), 7.29 - 7.26 (m, 4H), 7.04 (m, 2H), 2.95 (m, 4H), 2.63 (m, 4H), 2.35 (s, 3H), 2.31 (s, 3H).

^{13}C NMR (100 MHz, CDCl$_3$): δ ppm 160.1, 144.1, 143.0, 136.1, 135.8, 134.9, 132.9, 130.8, 130.5, 130.3, 128.9, 127.9, 127.1, 118.3, 55.5, 54.4, 45.7, 9.3

HRMS (ESI): m/z calculated for C$_{22}$H$_{23}$ON$_5$Cl$_3$Na [M+H]$^+$ 478.0963; found, 478.0959

HPLC analysis (Method A): t$_R$ 4.82 min, purity 97.93 %

5-(4-Chlorophenyl)-1-(2,4-dichlorophenyl)-*N,N*-bis(2-hydroxyethyl)-4-methyl-1*H*-pyrazole-3-carboxamide (17)
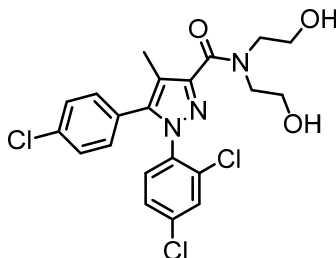
The title compound was synthesized from the carboxylic acid **9** by following general procedure A.

Yield: 62%.

IR ν_{max} (thin film, CHCl$_3$) 3376, 2930, 1622, 1494, 1446, 1362 cm^{-1}

^{1}H NMR (400 MHz, CDCl$_3$): δ ppm 7.49 (d, *J* = 2.2 Hz, 1H), 7.32 (d, *J* = 8.3 Hz, 2H), 7.24 (dd, *J* = 8.6, 2.0 Hz, 1H), 7.09 – 7.05 (m, 3H), 3.85 (m, 8H), 2.24 (s, 3H).

^{13}C NMR (100 MHz, CDCl$_3$): δ ppm 165.8, 145.8, 142.5, 136.2, 135.24, 135.15, 132.7, 130.7, 130.6, 130.2, 129.1, 128.1, 126.7, 118.2, 60.8, 59.4, 51.8, 50.4, 9.1

HRMS (ESI): m/z calculated for C$_{21}$H$_{20}$O$_3$N$_3$Cl$_3$Na [M+Na]$^+$ 490.0462; found, 490.0466

HPLC analysis (Method A): t$_R$ 1.98 min, purity 95.1 %

5-(4-Chlorophenyl)-1-(2,4-dichlorophenyl)-*N*-(3-(dimethylamino)propyl)-4-methyl-1*H*-pyrazole-3-carboxamide (18)
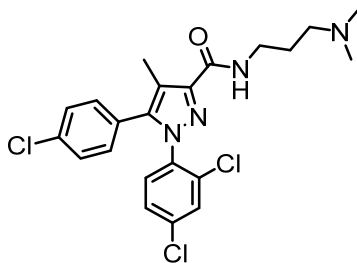
The title compound was synthesized from the carboxylic acid **9** by following general procedure A.

Yield: 94%.

IR ν_{max} (thin film, CHCl$_3$) 3417, 2939, 1662, 1540, 1485, 1387 cm^{-1}

¹H NMR (400 MHz, CDCl$_3$): δ ppm 7.43 (m, 2H), 7.31 - 7.28 (m, 4H), 7.08 -7.06 (m, 2H), 3.54 (q, *J* = 6.4 Hz, 2H), 2.91 (m, 2H), 2.64 (s, 6H), 2.36 (s, 3H), 2.10 – 2.03 (m, 2H).

¹³C NMR (100 MHz, CDCl$_3$): δ ppm 163.2, 144.6, 143.0, 135.9, 135.8, 134.9, 132.7, 130.7, 130.5, 130.2, 128.9, 127.9, 127.1, 117.6, 56.5, 43.8, 36.6, 25.9, 9.3

HRMS (ESI): m/z calculated for C$_{22}$H$_{24}$ON$_4$Cl$_3$ [M+H]$^+$ 465.1010; found, 465.1023

HPLC analysis (Method A): t$_R$ 2.10 min, purity 98.8 %

5-(4-Chlorophenyl)-1-(2,4-dichlorophenyl)-*N*,*N*,4-trimethyl-1*H*-pyrazole-3-carboxamide (19)
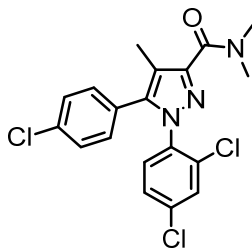
The title compound was synthesized from the carboxylic acid **9** by following general procedure A.

Yield: 83%.

IR ν_{max} (thin film, CHCl₃) 3013, 2931, 1630, 1493 cm^{-1}

¹H NMR (500 MHz ,CDCl₃): δ ppm 7.43 (d, *J* = 1.8 Hz, 1H), 7.29 (d, *J* = 8.5 Hz, 2H), 7.24 (dd, *J* = 2.0, 8.4 Hz, 1H), 7.17 (d, *J* = 8.2 Hz, 1H), 7.10 - 7.02 (m, *J* = 8.2 Hz, 2H), 3.26 (s, 3H), 3.13 (s, 3H), 2.20 (s, 3H).

¹³C NMR (125 MHz, CDCl₃): δ ppm 164.7, 146.8, 141.8, 136.0, 135.7, 134.7, 133.0, 130.6, 130.5, 130.2, 128.9, 127.8, 127.4, 116.7, 39.1, 35.3, 9.0

HRMS (ESI): m/z calculated for $C_{19}H_{16}ON_3Cl_3Na$ [M+Na]$^+$ 430.0251; found, 430.0241

HPLC analysis (Method B): t_R 4.40 min, purity 98.31 %

(5-(4-Chlorophenyl)-1-(2,4-dichlorophenyl)-4-methyl-1*H*-pyrazol-3-yl)(4,4-dimethyl-1,4-azasilinan-1-yl)methanethione (25)
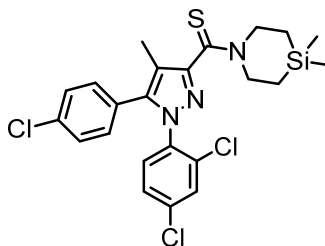
The compound **12** (100 mg, 0.20 mmol) was taken in a sealed tube and dry tetrahydrofuran (THF, 3 mL) was added followed by Lawesson's reagent (41 mg, 0.10 mmol). It was then sealed and heated at 70 ºC for 5 h. The reaction mixture was cooled; solvent was removed under reduced pressure and purified by column chromatography to give the title compound **25** as a yellow solid (100 mg, 98 %).

IR ν_{max} (thin film, CHCl₃) 3375, 2968, 1598, 1498, 1435 cm^{-1}

¹H NMR (400 MHz ,CDCl₃): δ ppm 7.44 (d, *J* = 1.7 Hz, 1H), 7.29 (d, *J* = 8.3 Hz, 2H), 7.25 – 7.19 (m, 2H), 7.09 (d, *J* = 8.3 Hz, 2H), 4.49 (m, 2H), 3.89 (t, *J* = 5.6 Hz, 2H), 2.15 (s, 3H), 1.13 (t, *J* = 6.3 Hz, 2H), 0.96 (m, 2H), 0.16 (s, 6H).

¹³C NMR (100 MHz, CDCl₃): δ ppm 190.2, 152.6, 141.6, 136.0, 135.5, 134.7, 133.2, 130.8, 130.6, 130.2, 128.9, 127.8, 127.5, 113.7, 51.9, 49.2, 15.8, 12.9, 9.1, -3.1

HRMS (ESI): m/z calculated for $C_{23}H_{25}N_3Cl_3SSi$ [M+H]$^+$ 508.0599; found, 508.0596

(5-(4-Chlorophenyl)-1-(2,4-dichlorophenyl)-4-(hydroxymethyl)-1H-pyrazol-3-yl)(4,4-dimethyl-1,4-azasilinan-1-yl)methanone (28)
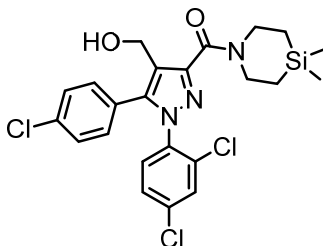
The title compound was synthesized from the carboxylic acid **27** and 4,4-dimethyl-4-silapiperidine by following general procedure A.

Yield: 71%.

IR ν$_{max}$ (thin film, CHCl$_3$) 3377, 3019, 2927, 1605, 1492, 1432 cm^{-1}

^{1}H NMR (400 MHz, CDCl$_3$): δ ppm 7.50 (d, J = 2.0 Hz, 1H), 7.32 - 7.23 (m, 3H), 7.16 - 7.11 (m, 3H), 4.47 (s, 2H), 4.12 (m, 2H), 3.92 (m, 2H), 0.95 (m, 4H), 0.13 (s, 6H).

^{13}C NMR (100 MHz, CDCl$_3$): δ ppm 163.5, 147.3, 142.2, 135.9, 135.6, 135.3, 133.1, 130.9, 130.45, 130.40, 129.0, 127.8, 126.4, 122.7, 54.7, 47.1, 43.3, 15.5, 14.0, -3.0

HRMS (ESI): m/z calculated for C$_{23}$H$_{25}$O$_2$N$_3$Cl$_3$Si [M+H]$^+$ 508.0776; found, 508.0776

HPLC analysis (Method B): t$_R$ 6.90 min, purity 94.66 %

5-(4-Chlorophenyl)-1-(2,4-dichlorophenyl)-4-(hydroxymethyl)-N-(2-(trimethylsilyl)ethyl)-1H-pyrazole-3-carboxamide (29)
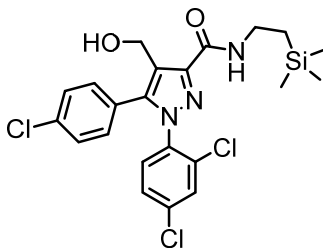
The title compound was synthesized from the carboxylic acid **27** and 2-(trimethylsilyl)ethan-1-amine hydrochloride by following general procedure A.

Yield: 72%.

IR ν_{max} (thin film, CHCl$_3$) 3415, 3021, 2964, 1649, 1549 cm^{-1}

^{1}H NMR (400 MHz, CDCl$_3$): δ ppm 7.47 (m, 1H), 7.33 - 7.24 (m, 3H), 7.10 - 7.08 (m, 3H), 5.41 (brs, 1H), 4.63 (s, 2H), 3.56 - 3.50 (m, 2H), 0.98 – 0.94 (m, 2H), 0.08 (s, 9H)

^{13}C NMR (100 MHz, CDCl$_3$): δ ppm 162.6, 145.7, 142.7, 136.3, 135.50, 135.47, 133.0, 131.0, 130.5, 130.4, 129.0, 127.9, 126.2, 122.3, 54.9, 35.8, 17.7, -1.7

HRMS (ESI): m/z calculated for C$_{22}$H$_{24}$O$_2$N$_3$Cl$_3$SiNa [M+Na]$^+$ 518.0596; found, 518.0596

HPLC analysis (Method B): t$_R$ 7.59 min, purity 97.59 %

1-((5-(4-Chlorophenyl)-1-(2,4-dichlorophenyl)-4-methyl-1H-pyrazol-3-yl)methyl)-4-methylpiperazine (32)
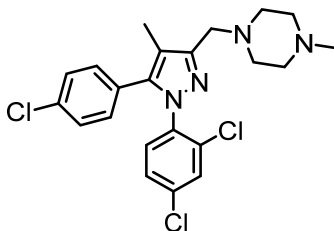
The title compound was synthesized from alcohol **30** and *N*-methylpiperazine by following general procedure B.

Yield: 62%.

IR ν_{max} (thin film, CHCl$_3$) 3351, 2938, 1494, 1451 cm^{-1}

^{1}H NMR (400 MHz, CDCl$_3$): δ ppm 7.36 (t, J = 1.1 Hz, 1H), 7.25 - 7.20 (m, 4H), 7.06 - 7.00 (m, 2H), 3.67 (s, 2H), 2.79 (m, 8H), 2.49 (s, 3H), 2.07 (s, 3H).

^{13}C NMR (100 MHz, CDCl$_3$): δ ppm 148.5, 141.6, 136.4, 135.3, 134.4, 133.1, 130.7, 130.5, 130.1, 128.7, 128.0, 127.7, 114.9, 54.4, 53.6, 51.2, 44.8, 8.6

HRMS (ESI): m/z calculated for C$_{22}$H$_{24}$N$_4$Cl$_3$ [M+H]$^+$ 449.1061; found, 449.1054

HPLC analysis (Method A): t$_R$ 4.70 min, purity 94.75 %

***N*-Benzyl-1-(5-(4-chlorophenyl)-1-(2,4-dichlorophenyl)-4-methyl-1H-pyrazol-3-yl)methanamine (33)**
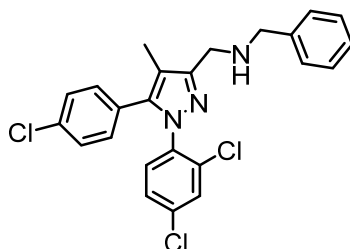
The title compound was synthesized from alcohol **30** and benzylamine by following general procedure B.

Yield: 83%.

IR ν_{max} (thin film, CHCl$_3$) 3330, 2856, 1647, 1593, 1493, 1392 cm^{-1}

^{1}H NMR (400 MHz, CDCl$_3$): δ ppm 7.42 - 7.39 (m, 3H), 7.34 - 7.31 (m, 2H), 7.28 - 7.24 (m, 5H), 7.06 - 7.03 (m, 2H), 3.95 (s, 2H), 3.92 (s, 2H), 2.08 (s, 3H).

^{13}C NMR (100 MHz, CDCl$_3$): δ ppm 150.3, 141.6, 138.8, 136.4, 135.2, 134.3, 133.0, 130.7, 130.5, 130.1, 128.7, 128.6, 128.4, 128.1, 127.7, 127.2, 114.0, 53.0, 44.4, 8.4

HRMS (ESI): m/z calculated for C$_{24}$H$_{21}$N$_3$Cl$_3$ [M+H]$^+$ 456.0796; found, 456.0796

HPLC analysis (Method A): t$_R$ 3.44 min, purity 93.97 %

4-((5-(4-Chlorophenyl)-1-(2,4-dichlorophenyl)-4-methyl-1*H*-pyrazol-3-yl)methyl)morpholine (34)
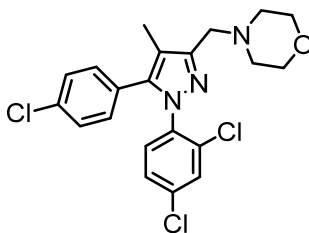
The title compound was synthesized from alcohol **30** and morpholine by following general procedure B.

Yield: 32%.

IR ν_{max} (thin film, CHCl$_3$) 3348, 3021, 2926, 1422, 1216 cm^{-1}

^{1}H NMR (200 MHz, CDCl$_3$): δ ppm 7.39 (t, *J* = 1.3 Hz, 1H), 7.31 - 7.24 (m, 4H), 7.10 - 7.03 (m, 2H), 3.74 (t, *J* = 4.7 Hz, 4H), 3.62 (s, 2H), 2.57 (t, *J* = 4.6 Hz, 4H), 2.13 (s, 3H).

^{13}C NMR (100 MHz, CDCl$_3$): δ ppm 149.2, 141.5, 136.5, 135.2, 134.3, 133.2, 130.7, 130.5, 130.1, 128.7, 128.2, 127.7, 114.9, 67.0, 54.8, 53.5, 8.6

HRMS (ESI): m/z calculated for C$_{21}$H$_{21}$ON$_3$Cl$_3$ [M+H]$^+$ 436.0745; found, 436.0745

HPLC analysis (Method A): t$_R$ 5.16 min, purity 94.30 %

1-((5-(4-Chlorophenyl)-1-(2,4-dichlorophenyl)-4-methyl-1*H*-pyrazol-3-yl)methyl)-4,4-dimethyl-1,4-azasilinane (35)
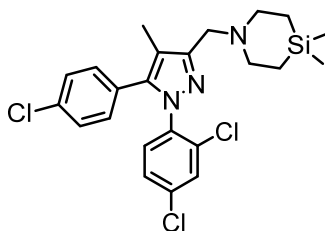
The title compound was synthesized from alcohol **30** and 4,4-dimethyl-silapiperidine by following general procedure B.

Yield: 54%.

IR ν$_{max}$ (thin film, CHCl$_3$) 3336, 2924, 1596, 1493, 1403 cm^{-1}

^{1}H NMR (500 MHz, CDCl$_3$): δ ppm 7.39 (m, 1H), 7.28 – 7.24 (m, 4H), 7.07 (d, *J* = 8.5 Hz, 2H), 3.69 (s, 2H), 2.84 (t, *J* = 5.5 Hz, 4H), 2.13 (s, 3H), 0.81 (t, *J* = 5.8 Hz, 4H), 0.05 (s, 6H).

^{13}C NMR (125 MHz, CDCl$_3$): δ ppm 150.1, 141.3, 136.6, 135.0, 134.2, 133.3, 130.7, 130.6, 130.1, 128.7, 128.4, 127.6, 115.0, 54.1, 52.3, 13.6, 8.8, -3.1

HRMS (ESI): m/z calculated for C$_{23}$H$_{27}$N$_3$Cl$_3$Si [M+H]$^+$ 478.1034; found, 478.1050

HPLC analysis (Method A): t$_R$ 14.72 min, purity 92.92 %

1-(5-(4-Chlorophenyl)-1-(2,4-dichlorophenyl)-4-methyl-1H-pyrazol-3-yl)-*N*,*N*-dimethylmethanamine (36)
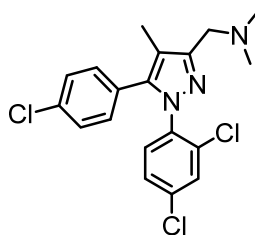
The title compound was synthesized from alcohol **30** by following general procedure B.

Yield: 60%.

IR ν_{max} (thin film, CHCl$_3$) 3330, 2930, 2860, 1597, 1493, 1396 cm^{-1}

^{1}H NMR (400 MHz, CDCl$_3$): δ ppm 7.39 (m, 1H), 7.28 – 7.25 (m, 4H), 7.08 – 7.05 (m, 2H), 3.56 (s, 2H), 2.36 (s, 6H), 2.13 (s, 3H).

^{13}C NMR (100 MHz, CDCl$_3$): δ ppm 149.8, 141.5, 136.5, 135.1, 134.2, 133.2, 130.7, 130.5, 130.1, 128.7, 128.2, 127.6, 114.8, 55.2, 45.3, 8.6

HRMS (ESI): m/z calculated for C$_{19}$H$_{19}$N$_3$Cl$_3$ [M+H]$^+$ 394.0639; found, 394.0641

HPLC analysis (Method A): t$_R$ 5.02 min, purity 94.55 %

1-((5-(4-Chlorophenyl)-1-(2,4-dichlorophenyl)-4-methyl-1*H*-pyrazol-3-yl)methyl)piperazine (38)
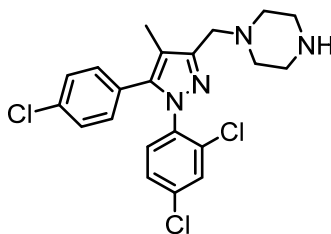
Tert-butyl carbamate **37** was synthesized from alcohol **30** and *N*-Boc piperazine by following general procedure B. Yield: 70%. This compound (90 mg, 0.17 mmol) was then dissolved in DCM (3mL) and trifluoroacetic acid (0.5 mL) was added at 0 °C and stirred at RT or 3h. The reaction mixture was cooled to 0 °C and neutralized using 2N NaOH solution. The organic layer was separated, dried over Na$_2$SO$_4$ and the solvent was removed under vacuum. The crude product was further purified by column chromatography on silica gel (100- 200) using 5% MeOH- DCM mixture to give the product as a white solid (55 mg, 75% yield).

IR ν_{max} (thin film, CHCl₃) 3297, 2934, 2811, 1494, 1447 cm⁻¹

IR ν_{max} (thin film, CHCl$_3$) 3297, 2934, 2811, 1494, 1447 cm^{-1}

^{1}H NMR (400 MHz, CD$_3$OD): δ ppm 7.55 (m, 1H), 7.41 (m, 2H), 7.33 (d, J = 8.6 Hz, 2H), 7.15 (d, J = 8.6 Hz, 2H), 3.64 (s, 2H), 3.05 (t, J = 4.9 Hz, 4H), 2.66 (m, 4H), 2.11 (s, 3H).

^{13}C NMR (100 MHz, CDCl$_3$): δ ppm 149.5, 141.4, 136.6, 135.1, 134.2, 133.2, 130.7, 130.6, 130.1, 128.7, 128.3, 127.6, 114.9, 55.0, 54.4, 46.1 (2C), 8.7

HRMS (ESI): m/z calculated for C$_{21}$H$_{22}$N$_4$Cl$_3$ [M+H]$^+$ 435.0905; found, 435.0901

HPLC analysis (Method A): t_R 3.28 min, purity 95.8 %

Ethyl   4-(((tert-butyldimethylsilyl)oxy)methyl)-5-(4-chlorophenyl)-1-(2,4-dichlorophenyl)-1H-pyrazole-3-carboxylate (40)
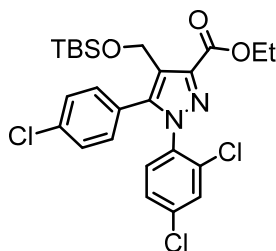
To a solution of **23** (80 mg, 0.18 mmol) in dry DMF (2 mL), was added imidazole (29 mg, 0.43 mmol) and TBDMSCl (0.36 mg, 0.24 mmol) at 0°C and stirred at RT for 4 h. To the reaction mixture water and ethyl acetate was added and the organic layer was separated, washed with brine, dried over Na$_2$SO$_4$ and concentrated under reduced pressure. This crude mixture was purified by column chromatography to give **40** (95 mg) as a sticky gum in 94% yield.

IR ν_{max} (thin film, CHCl$_3$) 3020, 2941, 1721, 1489, 1100 cm^{-1}

^{1}H NMR (500 MHz, CDCl$_3$): δ ppm 7.41 (d, J = 1.7 Hz, 1H), 7.33 - 7.24 (m, 6H), 4.83 (s, 2H), 4.46 (q, J = 7.2 Hz, 2H), 1.42 (t, J = 7.0 Hz, 3H), 0.88 (s, 9H), 0.07 (s, 6H).

^{13}C NMR (125 MHz, CDCl$_3$): δ ppm 162.2, 144.8, 142.6, 136.2, 135.7, 135.3, 133.1, 131.0, 130.7, 130.2, 128.6, 127.8, 126.7, 122.3, 61.1, 54.8, 25.8, 18.3, 14.4, -5.4

HRMS (ESI): m/z calculated for $C_{25}H_{29}O_3N_2Cl_3SiNa$ [M+Na]$^+$ 561.0905; found, 561.0906

1-((4-((((tert-butyldimethylsilyl)oxy)methyl)-5-(4-chlorophenyl)-1-(2,4-dichlorophenyl)-1H-pyrazol-3-yl)methyl)-4,4-dimethyl-1,4-azasilinane (41)
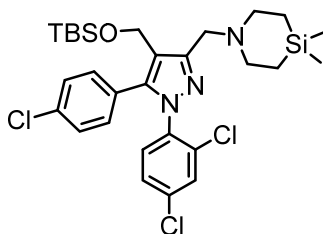
To a solution of lithium aluminium hydride (7.5 mg, 0.17 mmol) in dry THF (5 mL), was added dropwise a solution of **40** (95 mg, 0.17 mmol) in THF at 0°C and stirred at the same temperature for 2h. The reaction mixture was quenched by careful addition of saturated solution of NH$_4$Cl (2 mL), then extracted with ethyl acetate and the organic layer was separated, dried over Na$_2$SO$_4$ and concentrated under reduced pressure. The compound obtained was dissolved in dry DCM (5 mL), Triethylamine (35 µL, 0.25 mmol) was added followed by Mesylchloride (11 µL, 0.15 mmol) at 0°C and stirred at the same temperature for 2 h. To the reaction mixture water was added and the organic layer was separated, dried over Na$_2$SO$_4$ and concentrated under reduced pressure. This crude product was immediately taken to the next step. The mesylate was dissolved in dry DMF (2 mL), Triethylamine (0.56 µL, 0.40 mmol) and 4,4-dimethyl-1,4-azasilinane hydrochloride (33 mg, 0.20 mmol) was added at 0°C and left to stir at RT for 2h. To the reaction mixture water was added and the organic layer was separated, the aqueous layer was extracted using ethylacetate, dried over Na$_2$SO$_4$ and concentrated under reduced pressure. The crude was then purified by column chromatography (silica gel 100 – 200 mesh) using 2% MeOH-DCM to give **41** (40 mg, 37% yield over 3 steps).

IR ν_{max} (thin film, CHCl$_3$) 3367, 3022, 1599 cm^{-1}

^{1}H NMR (400 MHz, CDCl$_3$): δ ppm 7.43 (m, 1H), 7.28 - 7.18 (m, 6H), 4.60 (s, 2H), 3.78 (s, 2H), 2.85 (m, 4H), 0.91 (s, 9H), 0.80 (m, 4H), 0.07 (s, 6H), 0.04 (s, 6H).

^{13}C NMR (100 MHz, CDCl$_3$): δ ppm 143.1, 136.4, 135.3, 134.7, 133.4, 130.8, 130.7, 130.2, 128.6, 127.7, 119.1, 54.9, 54.1, 52.5, 25.9, 18.3, 13.6, -3.1, -5.3

HRMS (ESI): m/z calculated for C$_{29}$H$_{41}$ON$_3$Cl$_2$^{37}ClSi$_2$ [M+H]$^+$ 610.1819; found, 610.1807

(5-(4-Chlorophenyl)-1-(2,4-dichlorophenyl)-3-((4,4-dimethyl-1,4-azasilinan-1-yl)methyl)-1*H*-pyrazol-4-yl)methanol (42)
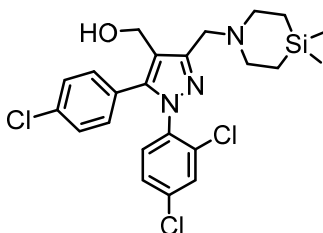
The compound **41** (40 mg, 0.06 mmol) was dissolved in dry THF (3 mL) and 0.13 mL Tetrabutylammonium fluoride solution (1M sol in THF, 0.13 mmol) was added. The reaction mixture was stirred at RT for 2h. Solvent was removed under reduced pressure and purified by column chromatography (silica gel 100 – 200) using 5% MeOH – DCM to give the title compound **42** as a yellow gummy solid (30 mg, 93 %).

IR ν$_{max}$ (thin film, CHCl$_3$) 3272, 2924, 2856, 1596, 1493, 1399 cm^{-1}

^{1}H NMR (400 MHz, CDCl$_3$): δ ppm 7.42 (m, 1H), 7.29 – 7.26 (m, 4H), 7.10 (d, *J* = 8.3 Hz, 2H), 4.52 (s, 2H), 3.73 (s, 2H), 2.86 (t, *J* = 5.5 Hz, 4H), 0.84 (t, *J* = 5.9 Hz, 4H), 0.08 (s, 6H).

^{13}C NMR (100 MHz, CDCl$_3$): δ ppm 151.4, 141.9, 136.0, 135.5, 134.9, 133.4, 130.8, 130.7, 130.2, 128.8, 127.7, 127.2, 120.3, 55.2, 54.8, 52.5, 13.3, -3.4

HRMS (ESI): m/z calculated for C$_{23}$H$_{27}$ON$_3$Cl$_2$^{37}ClSi [M+H]$^+$ 496.0954; found, 496.0942

HPLC analysis (Method A): t$_R$ 8.05 min, purity 99.72 %

Ethyl   1-((5-(4-chlorophenyl)-1-(2,4-dichlorophenyl)-4-methyl-1*H*-pyrazol-3-yl)methyl)-1*H*-1,2,3-triazole-4-carboxylate (44)
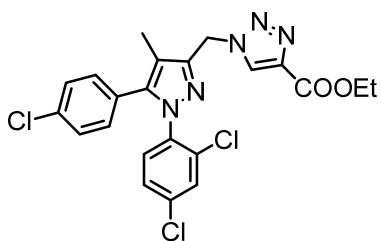
The alcohol **30** (200 mg, 0.54 mmol) was dissolved in dry THF (5 mL), diphenylphosphoryl azide (275 mg, 0.65 mmol) was added followed by DBU (0.1 mL, 0.65 mmol) and stirred at RT overnight. Water was added and the compound was extracted using DCM, dried over Na_2SO_4 and the solvent was removed in a rotary evaporator. The crude azide **43** was used for the next step without further purification. To a solution of **43** (50 mg, 0.127 mmol) in dry acetonitrile (5 mL), Copper iodide (2.4 mg, 0.013 mmol) and ethyl propiolate (24 µL, 0.254 mmol) was added and stirred at RT overnight. To the reaction mixture water was added and the compound was extracted using ethyl acetate. The solvent was removed in a rotary evaporator and the crude was purified by column chromatography on silica gel (100-200 mesh) to give the product as a white solid (40 mg, 65 % yield).

IR ν_{max} (thin film, CHCl$_3$) 3347, 2988, 2928, 1730, 1493, 1384, 1212 cm^{-1}

^{1}H NMR (400 MHz, CDCl$_3$): δ ppm 8.20 (s, 1H), 7.44 (d, J = 2.3 Hz, 1H), 7.31 − 7.24 (m, 4H), 7.06 - 7.02 (m, 2H), 5.69 (s, 2H), 4.42 (q, J = 6.9 Hz, 2H), 2.04 (s, 3H), 1.40 (t, J = 6.9 Hz, 3H)

^{13}C NMR (100 MHz, CDCl$_3$): δ ppm 160.8, 145.7, 142.6, 140.6, 135.8, 135.8, 134.9, 133.0, 130.5, 130.4, 130.3, 128.9, 127.9, 127.5, 127.2, 114.6, 61.3, 46.7, 14.3, 8.2

HRMS (ESI): m/z calculated for $C_{22}H_{18}O_2N_5Cl_3Na$ [M+Na]$^+$ 512.0418; found, 512.0416

HPLC analysis (Method A): t_R 4.08 min, purity 93.67 %

(1,5-Bis(4-chlorophenyl)-1*H*-pyrazol-3-yl)(4,4-dimethyl-1,4-azasilinan-1-yl)methanone (46)
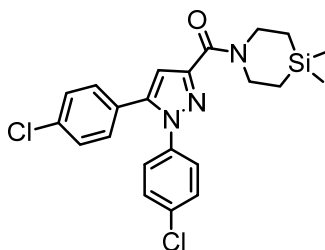
The title compound was synthesized from carboxylic acid **45**[61] by following general procedure A.

Yield: 77%.

IR ν_{max} (thin film, CHCl$_3$) 3021, 1615, 1487, 1216 cm^{-1}

^{1}H NMR (400 MHz, CDCl$_3$): δ ppm 7.36 - 7.33 (m, 4H), 7.25 (d, J = 8.3 Hz, 2H), 7.19 (d, J = 8.1 Hz, 2H), 6.88 (s, 1H), 4.07 (m, 2H), 3.92 (m, 2H), 0.96 (m, 4H), 0.16 (s, 6H).

^{13}C NMR (100 MHz, CDCl$_3$): δ ppm 162.8, 148.5, 142.4, 138.0, 135.0, 133.7, 130.0, 129.2, 129.0, 128.1, 126.2, 110.1, 46.7, 43.0, 15.5, 13.8, -3.0

HRMS (ESI): m/z calculated for C$_{22}$H$_{24}$ON$_3$Cl$_2$Si [M+H]$^+$ 444.1060; found, 444.1060

HPLC analysis (Method B): t$_R$ 7.55 min, purity 95.36 %

Methyl (1,5-bis(4-chlorophenyl)-1H-pyrazole-3-carbonyl)glycinate (47)
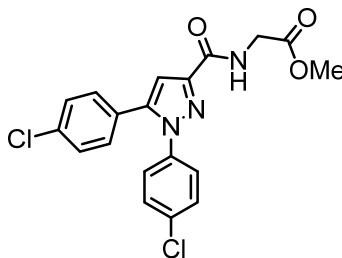
The title compound was synthesized from carboxylic acid **45** and glycine methyl ester by following general procedure A.

Yield: 87%.

IR ν_{max} (thin film, CHCl$_3$) 3686, 3022, 2976, 1740, 1626 cm^{-1}

^{1}H NMR (400 MHz, CDCl$_3$): δ ppm 7.41 (m, 1H), 7.38 - 7.31 (m, 4H), 7.26 - 7.23 (m, 2H), 7.16 – 7.13 (m, 2H), 7.04 - 7.03 (m, 1H), 4.25 (d, J = 5.5 Hz, 2H), 3.79 (s, 3H)

^{13}C NMR (100 MHz, CDCl$_3$): δ ppm 170.2, 161.6, 146.7, 143.8, 137.7, 135.2, 134.3, 130.0, 129.4, 129.1, 127.8, 126.5, 108.6, 52.4, 40.9

HRMS (ESI): m/z calculated for C$_{19}$H$_{17}$O$_3$N$_3$Cl$_2$Si [M+H]$^+$ 404.0563; found, 404.0561

HPLC analysis: (Method B) t$_R$ 3.36 min, purity 95.33 %

1,5-Bis(4-chlorophenyl)-*N*,*N*-dimethyl-1*H*-pyrazole-3-carboxamide (48)
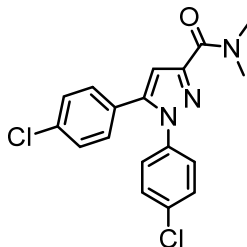
The title compound was synthesized from carboxylic acid **45** and *N*,*N*-dimethyl amine hydrochloride by following general procedure A.

Yield: 93%.

IR ν$_{max}$ (thin film, CHCl$_3$) 2935, 1630, 1489, 1365, 1184 cm^{-1}

^{1}H NMR (400 MHz, CDCl$_3$): δ ppm 7.33 (m, 4H), 7.24 - 7.15 (m, 4H), 6.91 (s, 1H), 3.43 (s, 3H), 3.15 (s, 3H).

^{13}C NMR (100 MHz, CDCl$_3$): δ ppm 163.6, 148.3, 142.4, 137.9, 134.9, 133.8, 129.9, 129.3, 129.0, 127.9, 126.3, 110.4, 39.0, 36.1

HRMS (ESI): m/z calculated for C$_{18}$H$_{16}$ON$_3$Cl$_2$ [M+H]$^+$ 360.0665; found, 360.0657

HPLC analysis (Method A): t$_R$ 5.77 min, purity 94.96 %

(1,5-Bis(4-chlorophenyl)-1*H*-pyrazol-3-yl)(piperazin-1-yl)methanone (49)
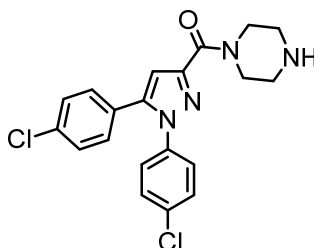
Tert-butyl   4-(1,5-bis(4-chlorophenyl)-1*H*-pyrazole-3-carbonyl)piperazine-1-carboxylate was synthesized from carboxylic acid **45** (100 mg) and *N*-Boc piperazine by following general procedure A. This compound was then dissolved in DCM (5 mL) and trifluoroacetic acid (1 mL) was added at 0 °C and stirred at RT or 3h. The reaction mixture was cooled to 0 °C and neutralized using 2N NaOH solution. The organic layer was separated, dried over Na_2SO_4 and the solvent was removed under vacuum. The crude product was further purified by column chromatography on silica gel (100- 200) using 5% MeOH- DCM mixture to give the product as a white solid (88 mg, 73% yield over two steps).

IR ν_{max} (thin film, $CHCl_3$) 3417, 2926, 1627, 1486, 1364, 1240 cm^{-1}

^{1}H NMR (400 MHz, CDCl$_3$): δ ppm 7.37 - 7.16 (m, 8H), 6.91 (m, 1H), 4.10 (m, 2H), 3.84 (m, 2H), 3.01 (m, 4H), 2.34 (br.s, 1H).

^{13}C NMR (100 MHz, CDCl$_3$): δ ppm 162.2, 147.9, 142.6, 137.8, 135.0, 133.9, 130.0, 129.3, 129.0, 127.9, 126.4, 110.6, 48.1, 46.5, 45.8, 43.4

HRMS (ESI): m/z calculated for $C_{20}H_{19}ON_4Cl_2$ [M+H]$^+$ 401.0930; found, 401.0925

HPLC analysis (Method A): t$_R$ 3.93 min, purity 99.86 %

1,5-Bis(4-chlorophenyl)-*N*-(3-(dimethylamino)propyl)-1*H*-pyrazole-3-carboxamide (50)
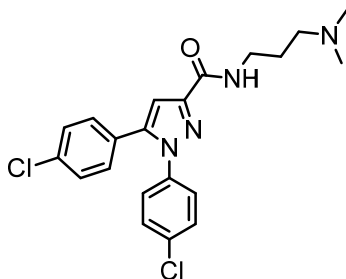
The title compound was synthesized from carboxylic acid **45** by following general procedure A.

Yield: 96%.

IR ν_{max} (thin film, $CHCl_3$) 3417, 3318, 2946, 1662, 1548, 1489, 1232 cm^{-1}

¹H NMR (200 MHz, CDCl₃): δ ppm 7.86 (t, J = 5.6 Hz, 1H), 7.37 - 7.12 (m, 8H), 7.01 (s, 1H), 3.54 (q, J = 6.4 Hz, 2H), 2.56 (t, J = 6.9 Hz, 2H), 2.36 (s, 6H), 1.86 (quintet, J = 6.8 Hz, 2H).

¹³C NMR (50 MHz, CDCl₃): δ ppm 161.6, 147.5, 143.5, 137.7, 134.9, 133.9, 129.9 (2C), 129.2 (2C), 128.9 (2C), 127.8, 126.2 (2C), 108.3, 57.3, 44.9 (2C), 37.8, 26.4

HRMS (ESI): m/z calculated for $C_{21}H_{23}ON_4Cl_2$ [M+H]⁺ 417.1243; found, 417.1240

HPLC analysis (Method A): t_R 3.90 min, purity 98.03 %

(1,5-Bis(4-chlorophenyl)-1*H*-pyrazol-3-yl)methanol (51)
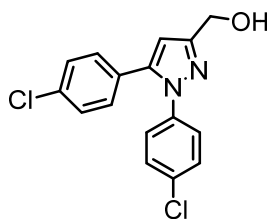
A solution of the the ester[61] ethyl 1,5-bis(4-chlorophenyl)-1H-pyrazole-3-carboxylate (1 g, 2.77 mmol) in dry THF (20 mL) was cooled to 0 °C and LAH (210 mg, 5.54 mmol) was added cautiously in portions and stirred at RT for 3h. The reaction mixture was cooled to 0 °C and quenched with sat. Na₂SO₄. The inorganics were filtered through celite and to the filtrate water and ethyl acetate was added and the organic layer was separated. The aqueous layer was again extracted with ethyl acetate, dried over Na₂SO₄ and concentrated under reduced pressure. The crude product was purified by column chromatography over silica gel (100 – 200) to give the product as a white solid (760 mg, 86%).

IR ν_{max} (thin film, CHCl₃) 3347, 1599, 1533, 1268 cm⁻¹

¹H NMR (200 MHz, CDCl₃): δ ppm 7.36 – 7.28 (m, 4H), 7.24 – 7.11 (m, 4H), 6.52 (s, 1H), 4.78 (d, J = 4.8 Hz, 2H), 2.05 (m, 1H).

¹³C NMR (100 MHz, CDCl₃): δ ppm 153.2, 143.0, 138.2, 134.7, 133.4, 129.9 (2C), 129.2 (2C), 129.0 (2C), 128.5, 126.3 (2C), 106.7, 59.0

HRMS (ESI): m/z calculated for $C_{16}H_{12}ON_2Cl_2Na$ [M+Na]⁺ 341.0219; found, 341.0221

HPLC analysis (Method B): t_R 3.49 min, purity 91.70 %

1-((1,5-Bis(4-chlorophenyl)-1*H*-pyrazol-3-yl)methyl)-4,4-dimethyl-1,4-azasilinane (52)
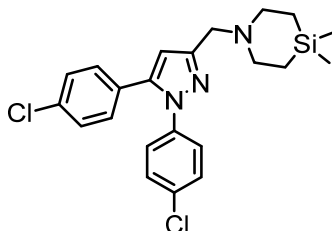
The title compound was synthesized from alcohol **51** by following general procedure B.

Yield: 60%.

**IR** v_{max} (thin film, CHCl$_3$) 3376, 2971, 1606, 1497, 1416 cm^{-1}

^{1}H NMR (400 MHz, CDCl$_3$): δ ppm 7.33 – 7.28 (m, 4H), 7.23 (d, *J* = 8.6 Hz, 2H), 7.17 (d, *J* = 8.6 Hz, 2H), 6.54 (s, 1H), 3.72 (s, 2H), 2.85 (t, *J* = 6.4 Hz, 4H), 0.83 (t, *J* = 6.1 Hz, 4H), 0.07 (s, 6H).

^{13}C NMR (100 MHz, CDCl$_3$): δ ppm 151.5, 142.4, 138.3, 134.4, 133.0, 129.8, 129.1, 128.8, 126.2, 108.3, 55.7, 52.6, 13.6, -3.1

HRMS (ESI): m/z calculated for C$_{22}$H$_{26}$N$_3$Cl$_2$Si [M+H]$^+$ 430.1268; found, 430.1267

HPLC analysis (Method A): t_R 10.46 min, purity 90.94 %

1-((1,5-Bis(4-chlorophenyl)-1*H*-pyrazol-3-yl)methyl)piperidine (53)
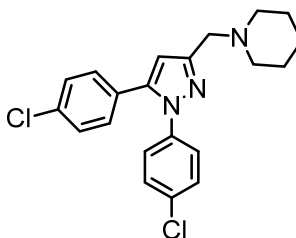
The title compound was synthesized from alcohol **51** by following general procedure B.

Yield: 64%.

IR v_{max} (thin film, CHCl$_3$) 3330, 3022, 2926, 1600, 1420 cm^{-1}

¹H NMR (500 MHz, CDCl₃): δ ppm 7.33 - 7.27 (m, 4H), 7.24 - 7.20 (m, 2H), 7.17 - 7.14 (m, 2H), 6.56 (s, 1H), 3.66 (s, 2H), 2.58 (m, 4H), 1.66 (quin, J = 5.5 Hz, 4H), 1.47 (m, 2H).

¹³C NMR (125 MHz, CDCl₃): δ ppm 150.3, 142.6, 138.2, 134.4, 133.1, 129.8, 129.1, 128.8, 128.7, 126.3, 108.6, 56.3, 54.4, 25.6, 24.0

HRMS (ESI): m/z calculated for $C_{21}H_{22}N_3Cl_2$ [M+H]⁺ 386.1185; found, 386.1179

HPLC analysis (Method A): t_R 4.49 min, purity 91.21 %

1-((1,5-Bis(4-chlorophenyl)-1*H*-pyrazol-3-yl)methyl)-4-methylpiperazine (54)
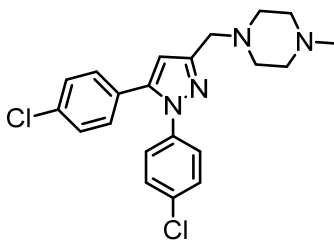
The title compound was synthesized from alcohol **51** by following general procedure B.

Yield: 68%.

IR v_{max} (thin film, CHCl₃) 3363, 3022, 2976, 1425 cm⁻¹

¹H NMR (400 MHz, CDCl₃): δ ppm 7.33 - 7.27 (m, 4H), 7.24 − 7.21 (m, 1H), 7.19 − 7.15 (m, 2H), 7.13 − 7.10 (m, 1H), 6.48 (s, 1H), 3.66 (s, 2H), 2.63 − 2.50 (m, 8H), 2.30 (s, 3H).

¹³C NMR (100 MHz, CDCl₃): δ ppm 150.1, 142.6, 138.2, 134.5, 133.2, 129.8, 129.2, 128.9, 128.6, 126.3, 108.5, 55.4, 54.8, 52.4, 45.6

HRMS (ESI): m/z calculated for $C_{21}H_{23}N_4Cl_2$ [M+H]⁺ 401.1294; found, 401.1288

HPLC analysis (Method A): t_R 4.96 min, purity 91.35%

1-((1,5-Bis(4-chlorophenyl)-1*H*-pyrazol-3-yl)methyl)piperidin-4-one (55)
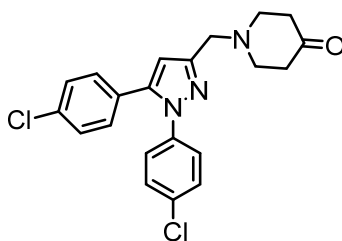
The title compound was synthesized from alcohol **51** by following general procedure B.

Yield: 59%.

IR ν_{max} (thin film, CHCl$_3$) 2957, 2805, 1716, 1497 cm^{-1}

^{1}H NMR (400 MHz, CDCl$_3$): δ ppm 7.34 - 7.16 (m, 8H), 6.54 (m, 1H), 3.77 (m, 2H), 2.91 (m, 4H), 2.52 (m, 4H).

^{13}C NMR (100 MHz, CDCl$_3$): δ ppm 209.0, 150.5, 142.8, 138.1, 134.6, 133.3, 129.8, 129.2, 128.9, 128.5, 126.2, 108.2, 54.8, 53.0, 41.2

HRMS (ESI): m/z calculated for C$_{21}$H$_{20}$ON$_3$Cl$_2$ [M+H]$^+$ 400.0978; found, 400.0971

HPLC analysis (Method A): t$_R$ 3.78 min, purity 96.0%

N-**((1,5-bis(4-chlorophenyl)-1H-pyrazol-3-yl)methyl)-4,4-dimethyl-1,4-azasilinan-1-amine (56)**
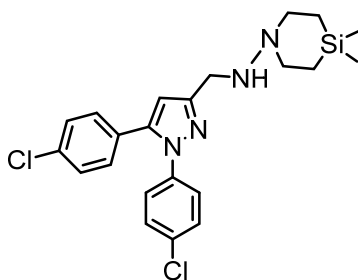
The title compound was synthesized from alcohol **51** and 4,4-dimethyl-1,4-azasilinan-1-amine hydrochloride (**8**) by following general procedure B.

Yield: 53%.

IR ν_{max} (thin film, CHCl$_3$) 3373, 2925, 2857, 1736, 1670, 1457, 1255 cm^{-1}

^{1}H NMR (200 MHz, CDCl$_3$): δ 7.38 - 7.12 (m, 8H), 6.23 (m, 2H), 4.99 (s, 2H), 4.30 – 4.16 (m, 2H), 3.90 – 3.77 (m, 2H), 1.30 - 1.09 (m, 4H), 0.27 (s, 3H), 0.21 (s, 3H).

^{13}C NMR (100 MHz, CDCl$_3$): δ 143.5, 141.6, 137.7, 135.0, 134.1, 130.1, 129.3, 128.9, 127.6, 126.4, 112.4, 63.0, 61.1, 9.4, -3.6

HRMS (ESI): m/z calculated for C$_{22}$H$_{27}$N$_4$Cl$_2$Si [M+H]$^+$ 445.1377; found, 445.1367

HPLC analysis (Method A): t$_R$ 6.58 min, purity 95.4%.

1.2.6. References

(1)   Information from WHO site www.who.int/mediacentre/factsheets/fs104/en

(2)   WHO global tuberculosis report 2015

(3)   Tuberculosis control in the South-East Asia Region: annual report 2015.

(4)   Poce, G.; Cocozza, M.; Consalvi, S.; Biava, M. *Eur. J. Med. Chem.* **2014**, *86*, 335-351.

(5)   Biava, M.; Porretta, G. C.; Deidda, D.; Pompei, R. *Infect. Disord. Drug Targets* **2006**, *6*, 159-172.

(6)   Zumla, A.; Nahid, P.; Cole, S. T. *Nature* **2013**, *12*, 388-404.

(7)   Slepikas, L.; Salys, J.; Rodovičius, H.; Tarasevičius, E. *Medicina* **2011**, *47*, 39-48.

(8)   Ballell, L.; Field, R. A.; Duncan, K.; Young, R. J. *Antimicrob. Agents Chemother.* **2005**, *49*, 2153-2163.

(9)   Janin, Y. L. *Bioorg. Med. Chem.* **2007**, *15*, 2479–2513.

(10)   Treatment of Tuberculosis: Guidelines- Fourth edition; World Health Organization. WHO/HTM/TB/2009.420

(11)   www.tbonline.info/medicines

(12)   www.newtbdrugs.org/pipeline.php

(13)   Green, K. D.; Garneau-Tsodikova, S. *Front Microbiol.* **2013**, *4*, Article 208.

(14)   Jones, D. *Nat. Rev. Drug Discov.* **2013**, *12*, 175-176.

(15)   www.niaid.nih.gov/topics/tuberculosis/pages/default.aspx?wt.ac=bcNIAIDTopics Tuberculosis

(16)   Rayasam, G. V. *Expert Opin. Ther. Targets* **2013**, *18*, 1-10.

(17)   Cole, S. T. *Nat. Chem. Biol.* **2012**, *8*, 326-327.

(18) Grzegorzewicz, A. E.; Pham, H.; Gundi, V. A.; Scherman, M. S.; North, E. J.; Hess, T.; Jones,V.; Gruppo, V.; Born, S. E. M.; Korduláková, J.; Chavadi, S. S.; Morisseau, C.; Lenaerts, A. J.; Lee, R. E.; McNeil, M. R.; Jackson, M. *Nat. Chem. Biol.* **2012**, *8*, 334-341.

(19) Stanley, S. A.; Grant, S. S.; Kawate, T.; Iwase, N; Shimizu, M.; Wivagg, C.; Silvis, M.; Kazyanskaya, E.; Aquadro, J.; Golas, A.; Fitzgerald, M.; Dai, H.; Zhang, L.; Hung, D. T. *ACS Chem. Biol*. **2012**, *7*, 1377-1384.

(20) Stec, J.; Onajole, O. K.; Lun, S.; Guo, H.; Merenbloom, B.; Vistoli, G.; Bishai, W. R.; Kozikowski, A. P. *J. Med. Chem*. **2016**, *59*, 6232-6247.

(21) Rao, S. P. S. et.al. *Sci. Transl. Med*. **2013**, *5*, 214ra168.

(22) Li, W.; Upadhyay, A.; Fontes, F. L.; North, E. J.; Wang, Y.; Crans, D. C.; Grzegorzewicz, A. E.; Jones, V.; Franzblau, S. G.; Lee, R. E.; Crick, D. C.; Jackson, M. *Antimicrob. Agents Chemother.* **2014**, *58*, 6413-6423.

(23) Lun, S.; Guo, H.; Onajole, O. K.; Pieroni, M.; Gunosewoyo, H.; Chen, G.; Tipparaju, S. K.; Ammerman, N. C.; Kozikowski, A. P.; Bishai, W. R. *Nat Commun*. **2013**, *4*, 2907.

(24) Deidda, D.; Lampis, G.; Fioravanti, R.; Biava, M.; Porretta, G. C.; Zanetti, S.; Pompei, R. *Antimicrob. Agents Chemother.* **1998**, *42*, 3035-3037.

(25) La Rosa, V.; Poce, G.; Canseco, J. O.; Buroni, S.; Pasca, M. R.; Biava, M.; Raju, R. M.; Porretta, G. C.; Alfonso, S.; Battilocchio, C.; Javid, B.; Sorrentino, F.; Loerger, T. R.; Sacchettini, J. C.; Manetti, F.; Botta, M.; De Logu, A.; Rubin, E. J.; De Rossi, E. *Antimicrob. Agents Chemother.* **2012**, *56*, 324-331.

(26) Tahlan, K.; Wilson, R.; Kastrinsky, D. B.; Arora, K.; Nair, V.; Fischer, E.; Barnes, S. W.; Walker, J. R.; Alland, D.; Barry III, C. E.; Boshoff, H. I. *Antimicrob. Agents Chemother.* **2012**, *56*, 1797–1809.

(27) Bifulco, M.; Grimaldi, C.; Gazzerro, P.; Pisanti, S.; Antoro, A. *Mol. Pharmacol*. **2007**, *71*, 1445–1456.

(28) Xie, S.; Furjanic, M. A.; Ferrara, J. J.; McAndrew, N. R.; Ardino, E. L.; Ngondara, A.; Bernstein, Y.; Thomas, K. J.; Kim, E.; Walker, J. M.; Nagar, S.; Ward, S. J.; Raffa, R. B. *J. Clin. Pharm. Ther.* **2007**, *32*, 209–231

(29) van Diepen, H.; Schlicker, E.; Michel, M. C. *Naunyn Schmiedebergs Arch Pharmacol*. **2008**, *378*, 345-369.

(30) Sam, A. H.; Salem, V.; Ghatei, M. A. *J. Obes*. **2011**, article ID 432607.

(31) Pertwee, R. G. *Int. J. Obes*. **2006**, *30*, S13-S18.

(32) Chong, C. R.; Sullivan, D. J. *Nature* **2007**, *448*, 645-646.

(33) Tartaglia, L. A. *Expert Opin. Investig. Drugs* **2006**, *15*, 1295-1298.

(34) Nosengo, N. *Nature* **2016**, *534*, 314-316.

(35) Petsko, G. A. *BMC Biol*. **2010**, *8*, 61.

(36) http://csdd.tufts.edu/news/complete_story/pr_tufts_csdd_2014_cost_study

(37) Singhal, S.; Mehta, J.; Desikan, R.; Ayers, D.; Roberson, P.; Eddlemon, P.; Munshi, N.; Anaissie, E.; Wilson, C.; Dhodapkar, M.; Zeldis, J.; Siegel, D.; Crowley, J.; Barlogie, B. *N. Engl. J. Med*. **1999**, *341*, 1565-1571.

(38) Therapontos, C.; Erskine, L.; Gardner, E. R.; Figg, W. D.; Vargesson, N. *Proc. Natl. Acad. Sci. USA* **2009**, *106*, 8573-8578.

(39) Patel, P.; Karver, C. E.; Behera, R.; Guyett, P. J.; Sullenberger, C.; Edwards, P.; Roncal, N. E.; Mensa-Wilmot, K.; Pollastri, M. P. *J. Med. Chem.* **2013**, *56*, 3820−3832.

(40) Chen, H.; Wu, J.; Gao, Y.; Chen, H.; Zhou, J. *Curr. Top. Med. Chem*. **2016**, *16*, 2107-2114.

(41) Gajbhiye, J. M.; More, N. A.; Patil, M. D.; Ummanni, R.; Kotapalli, S. S.; Yogeeswari, P.; Sriram, D.; Masand, V. H. *Med. Chem. Res*. **2015**, *24*, 2960-2971.

(42) Biava, M.; Porretta, G. C.; Poce, G.; De Logu, A.; Meleddu, R.; De Rossi, E.; Manetti, F.; Botta, M. *E. J. Med. Chem*. **2009**, *44*, 4734–4738.

(43) Biava, M.; Porretta, G. C.; Poce, G.; Deidda, D.; Pompei, R.; Tafic, A.; Manetti, F. *Bioorg. Med. Chem.* **2005**, *13*, 1221–1230.

(44) Biava, M.; Porretta, G. C.; Poce, G.; Battilocchio, C.; Alfonso, S.; De Logu, A.; Manetti, F. Botta, M. *ChemMedChem.* **2011**, *6*, 593–599.

(45) Biava, M.; Porretta, G. C.; Poce, G.; De Logu, A.; Saddi, M.; Meleddu, R.; Manetti, F.; De Rossi, E.; Botta, M. *J. Med. Chem*. **2008**, *51*, 3644-3648.

(46) Wendeborn, S. V.; Lamberth, C.; Nebel, K.; Crowley, P. J.; Nussbaumer, H. Patent WO 2006066872.

(47) Heinrich, T.; Burschka, C.; Penka, M.; Wagner, B.; Tacke, R. *J. Organomet. Chem.* **2005**, *690*, 33-47.

(48) Sasmal, P. K.; Reddy, D. S.; Talwar, R.; Venkatesham, B.; Balasubrahmanyam, D.; Kannan, M.; Srinivas, P.; Shiva Kumar, K.; Neelima Devi, B.; Jadhav, V. P.; Khan, S. K.; Mohan, P.; Chaudhury, H.; Bhuniya, D.; Iqbal, J.; Chakrabarti, R. *Bioorg. Med. Chem. Lett.* **2011**, *21*, 562-568.

(49) Sasmal, P. K.; Talwar, R.; Swetha, J.; Balasubrahmanyam, D.; Venkatesham, B.; Rawoof, K. A.; Neelima Devi, B.; Jadhav, V. P.; Khan, S. K.; Mohan, P.; Reddy, D. S.; Nyavanandi, V.; Nanduri, S.; Shiva Kumar, K.; Kannan, M.; Srinivas, P.; Nadipalli, P.; Chaudhury, H.; Sebastian, V. J. *Bioorg. Med. Chem. Lett.* **2011**, *21*, 4913-4918.

(50) Zhang, Y.; Gilliam, A.; Maitra, R.; Damaj, M. I.; Tajuba, J. M.; Seltzman, H. H.; Thomas. B. F. *J. Med. Chem.* **2010**, *53*, 7048–7060.

(51) Kang, S. Y.; Lee, S. -H; Seo, H. J.; Jung, M. E.; Ahn, K.; Kim, J.; Lee, J. *Bioorg. Med. Chem. Lett.* **2008**, *18*, 2385-2389.

(52) Barth, F.; Congy, C.; Martinez, S.; Pointeau, P.; Rinaldi-Carmona, M. Patent US 7297710 B1.

(53) Kobayashi, K.; Uchiyama, M.; Ito, H.; Takahashi, H.; Yoshizumi, T.; Sakoh, H.; Nagatomi, Y.; Asai, M.; Miyazoe, H.; Tsujita, T.; Hirayama, M.; Ozaki, S.; Tani, T.; Ishii, Y.; Ohta, H.; Okamoto, O. *Bioorg. Med. Chem. Lett.* **2009**, *19*, 3627-3631.

(54) Wiley, J. L.; Jefferson, R. G.; Grier, M. C.; Mahadevan, A.; Razdan, R. K.; Martin, B. R. *J. Pharm. Exp. Ther.* **2001**, *296*, 1013-1022.

(55) Kharb, R.; Sharma, P. C.; Yar, M. S. *J. Enzyme Inhib. Med. Chem.* **2011**, *26*, 1-21.

(56) Zhou, C. H.; Wang, Y. *Curr. Med. Chem.* **2012**, *19*, 239-280.

(57) Kolb, H. C.; Sharpless, K. B. *Drug Discov. Today* **2003**, *8*, 1128-1137.

(58) Meldal, M.; Tornøe, C. W. *Chem. Rev.* **2008**, *108*, 2952–3015.

(59) Kolb, H. C.; Finn, M. G.; Sharpless, K. B. *Angew. Chem. Int. Ed.* **2001**, *40*, 2004-2021.

(60) Moses, J. E.; Moorhouse, A. D. *Chem. Soc. Rev*. **2007**, *36*, 1249–1262.

(61) Alvarado, M.; Goya, P.; Macías-González, M.; Pavón, F. J.; Serrano, A.; Jagerovic, N.; Elguero, J.; Gutiérrez-Rodríguez, A.; García-Granda, S.; Suardíaz, M.; de Fonseca, F. R. *Bioorg. Med. Chem.* **2008**, *16*, 10098–10105.

(62) Andrews, J. M. *J. Antimicrob. Chemother*. **2001**, *48*, 5-16.

(63) Hurst, D.; Umejiego, U.; Lynch, D.; Seltzman, H.; Hyatt, S.; Roche, M.; McAllister, S.; Fleischer, D.; Kapur, A.; Abood, M.; Shi, S.; Jones, J.; Lewis, D.; Reggio, P. *J. Med. Chem*. **2006**, *49*, 5969-5987.

(64) Hurst, D. P.; Lynch, D. L.; Barnett-Norris, J.; Hyatt, S. M.; Seltzman, H. H.; Zhong, M.; Song, Z. –H.; Nie, J.; Lewis, D.; Reggio, P. H. *Mol. Pharmacol.* **2002**, *62*, 1274–1287.

(65) Smith, D. A.; Di, L.; Kerns, E. H. *Nat. Rev. Drug Discov.* **2010**, *9*, 929-939.

(66) Liu, X.; Wright, M.; Hop, C. E. *J. Med. Chem.* **2014**, *57*, 8238-8248.

(67) Lin, J. H.; Lu, A. Y. H.; *Pharmacol. Rev*. **1997**, *49*, 403-449.

(68) Tanaka, E. *J. Clin. Pharm. Ther.* **1998**, *23*, 403-416.

(69) Lee, Y. J.; Ling, R.; Mariano, P. S. *J. Org. Chem.* **1996**, *61*, 3304-3314.

(70) Nishimura, S. –I.; Shimawaki, K. Patent, WO 2010103857 A1, 2010.
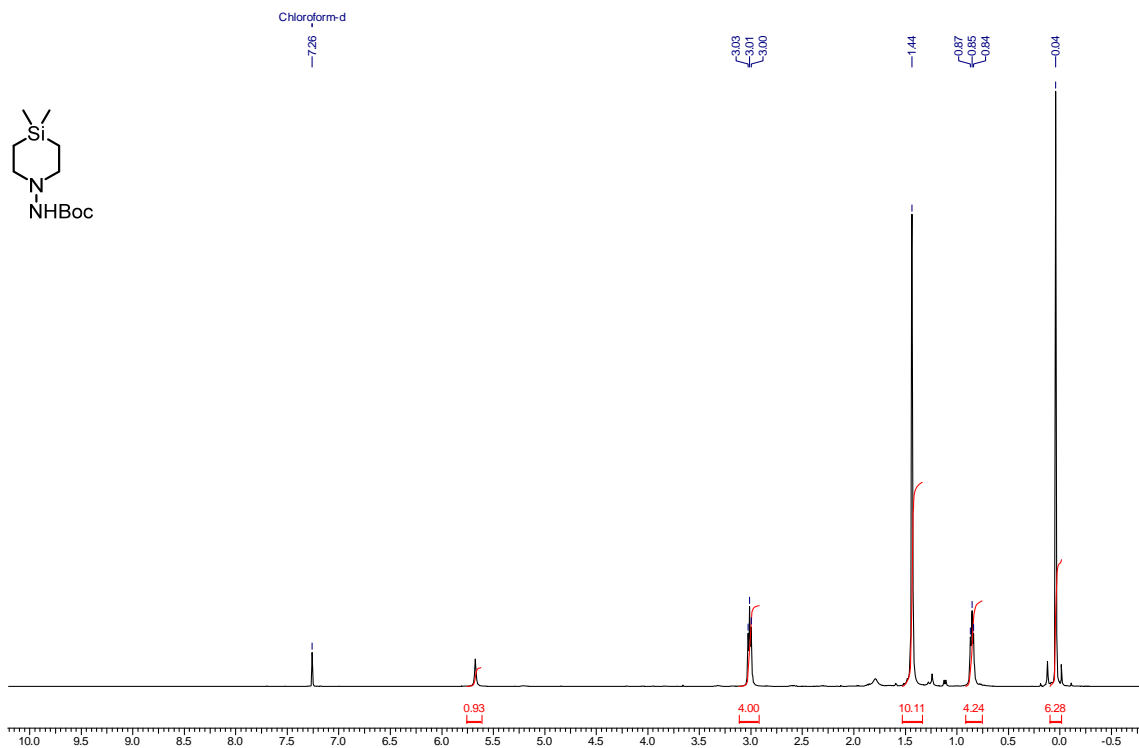
Figure 1.2.18. ^{1}H NMR of **7** (400 MHz, CDCl$_3$)
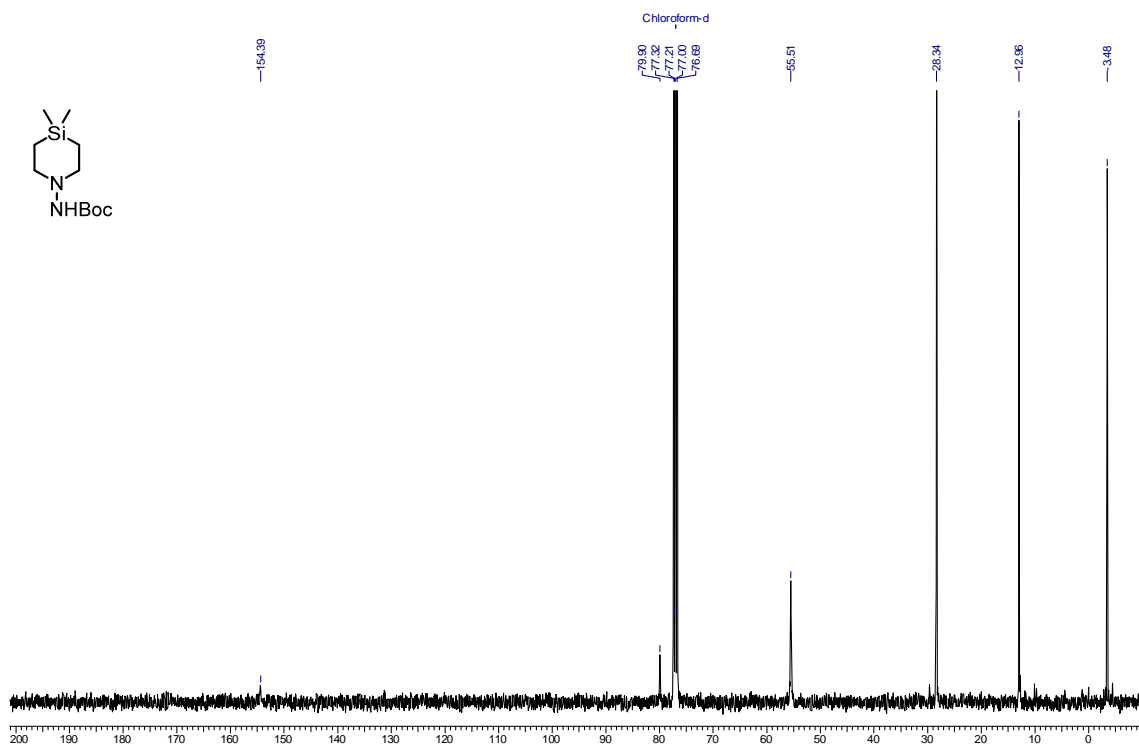
Figure 1.2.19. ^{13}C NMR of **7** (100 MHz, CDCl$_3$)
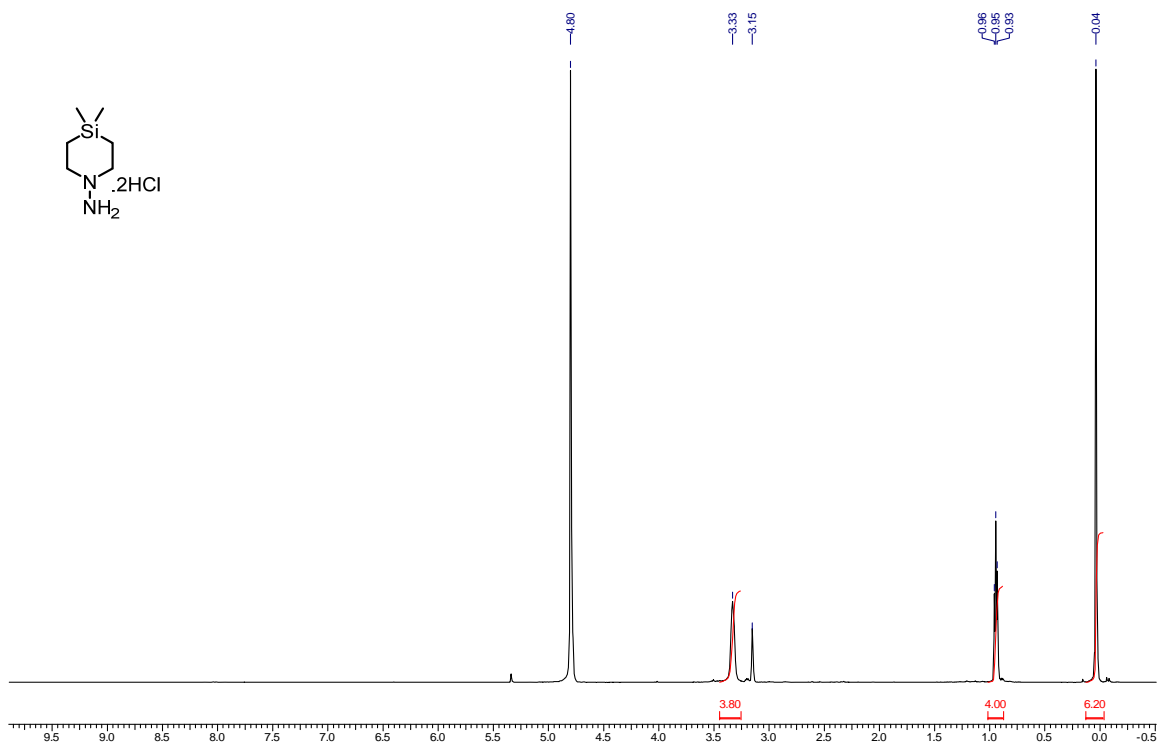
Figure 1.2.20. ^{1}H NMR of **8** (500 MHz, MeOD)
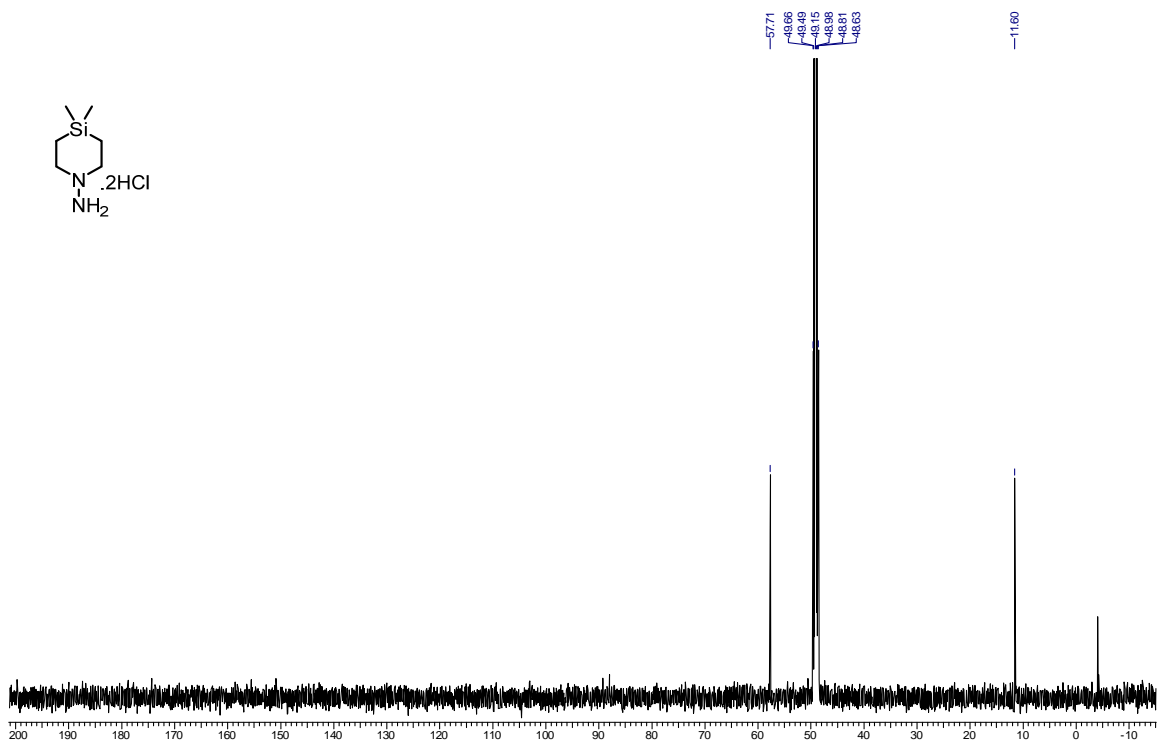
Figure 1.2.21. ^{13}C NMR of **8** (125 MHz, MeOD)

Figure 1.2.22. ^{1}H NMR of **12** (200 MHz, CDCl$_3$)

Figure 1.2.23. ^{13}C NMR of **12** (100 MHz, CDCl$_3$)
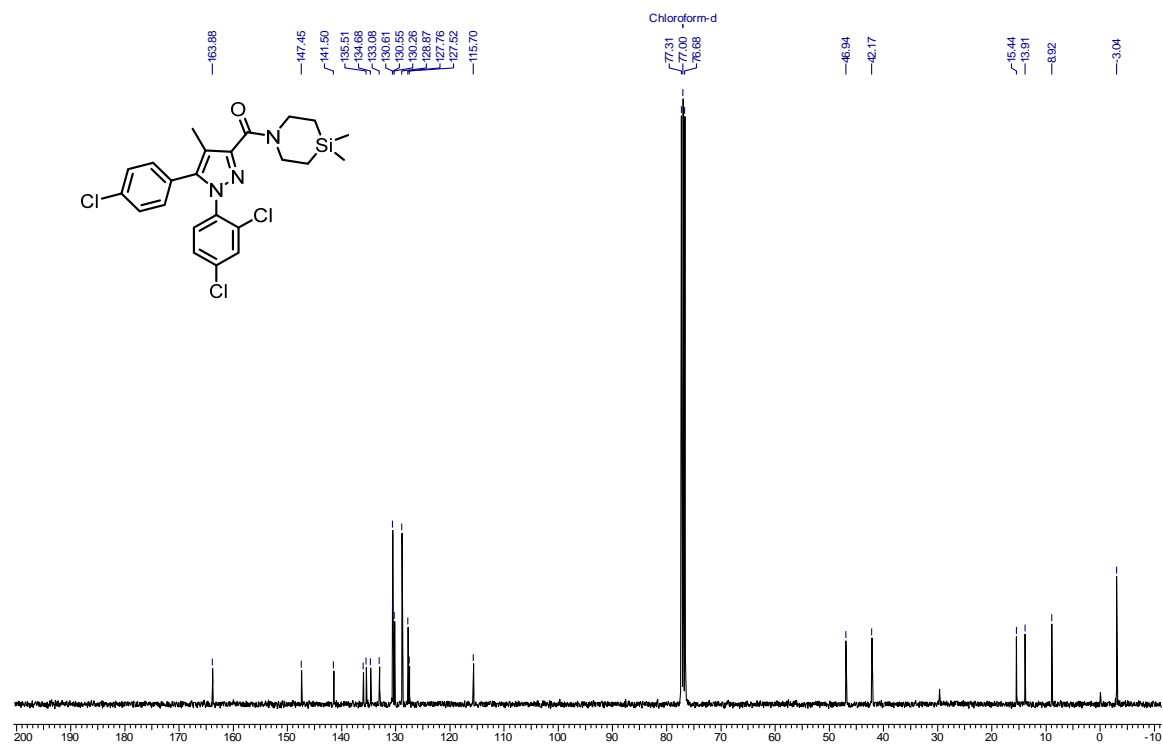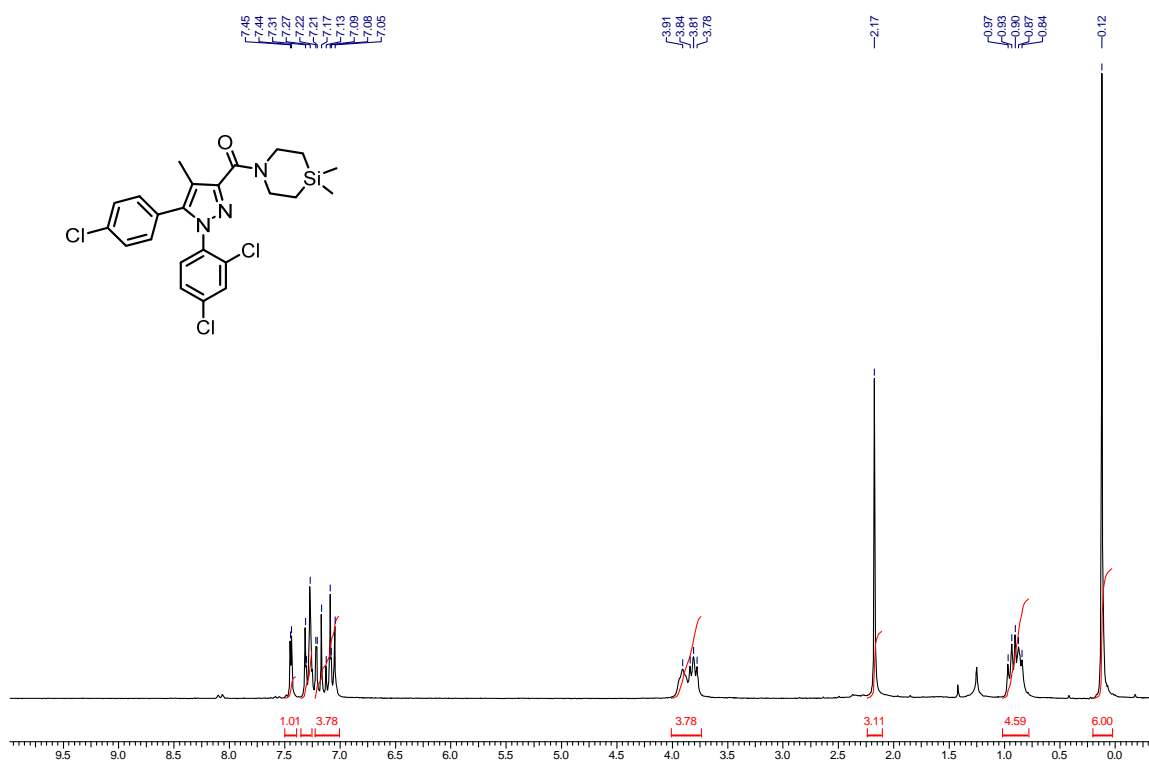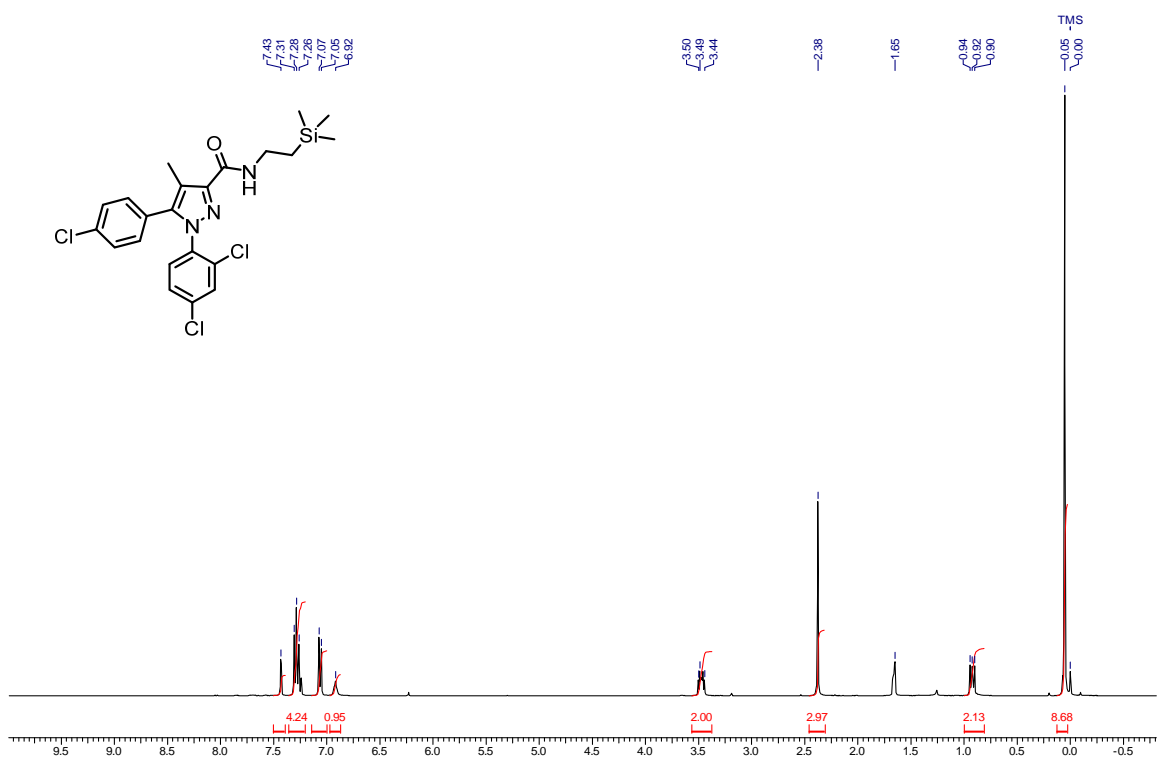
Figure 1.2.24. ^{1}H NMR of **13** (400 MHz, CDCl$_3$)
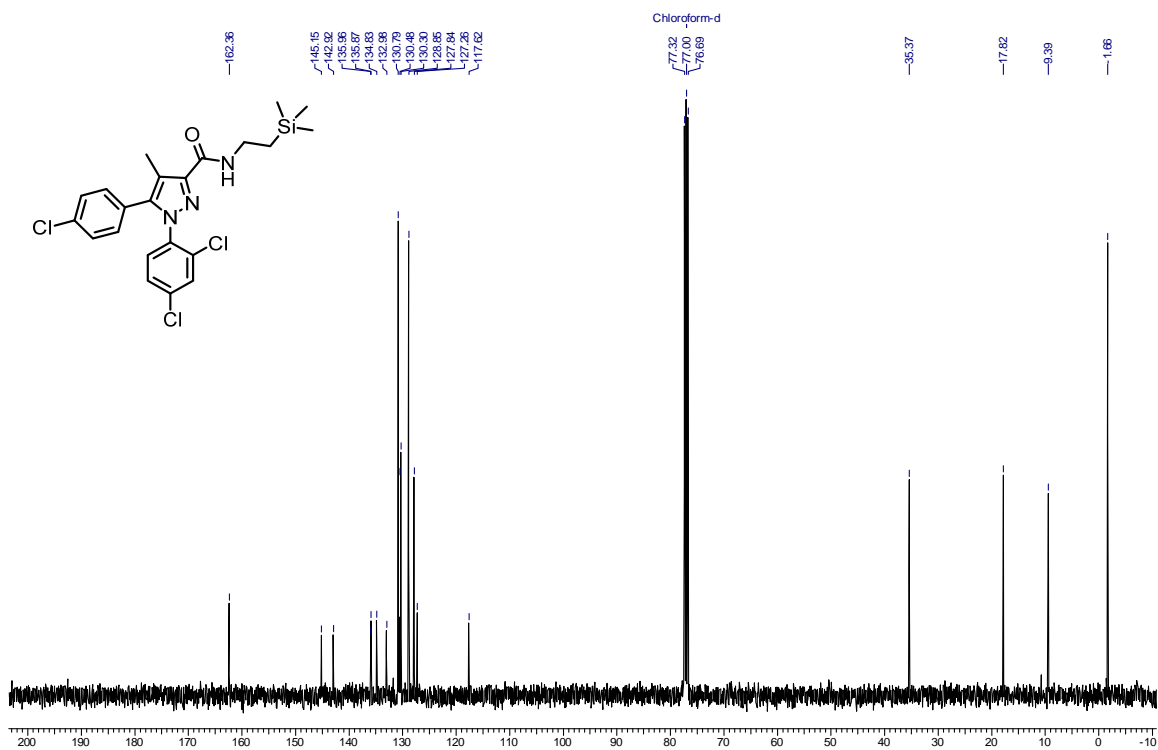
Figure 1.2.25. ^{13}C NMR of **13** (100 MHz, CDCl$_3$)
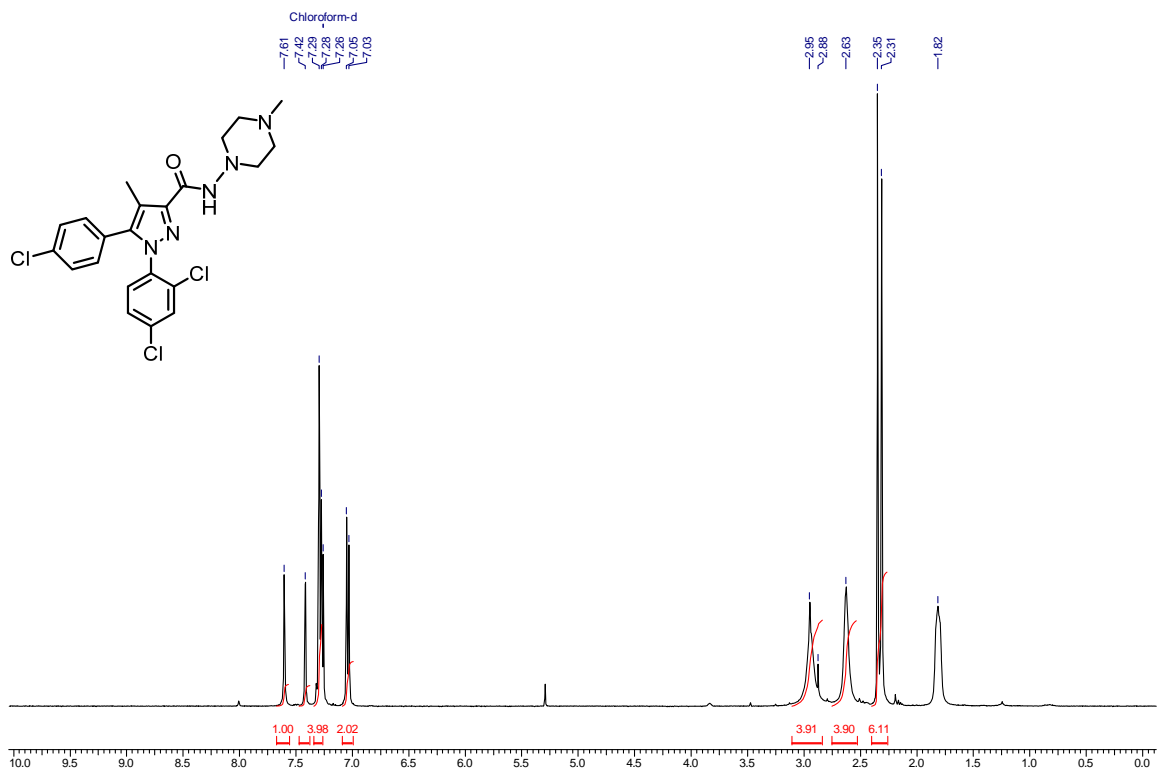
Figure 1.2.26. ^{1}H NMR of **16** (400 MHz, CDCl$_3$)
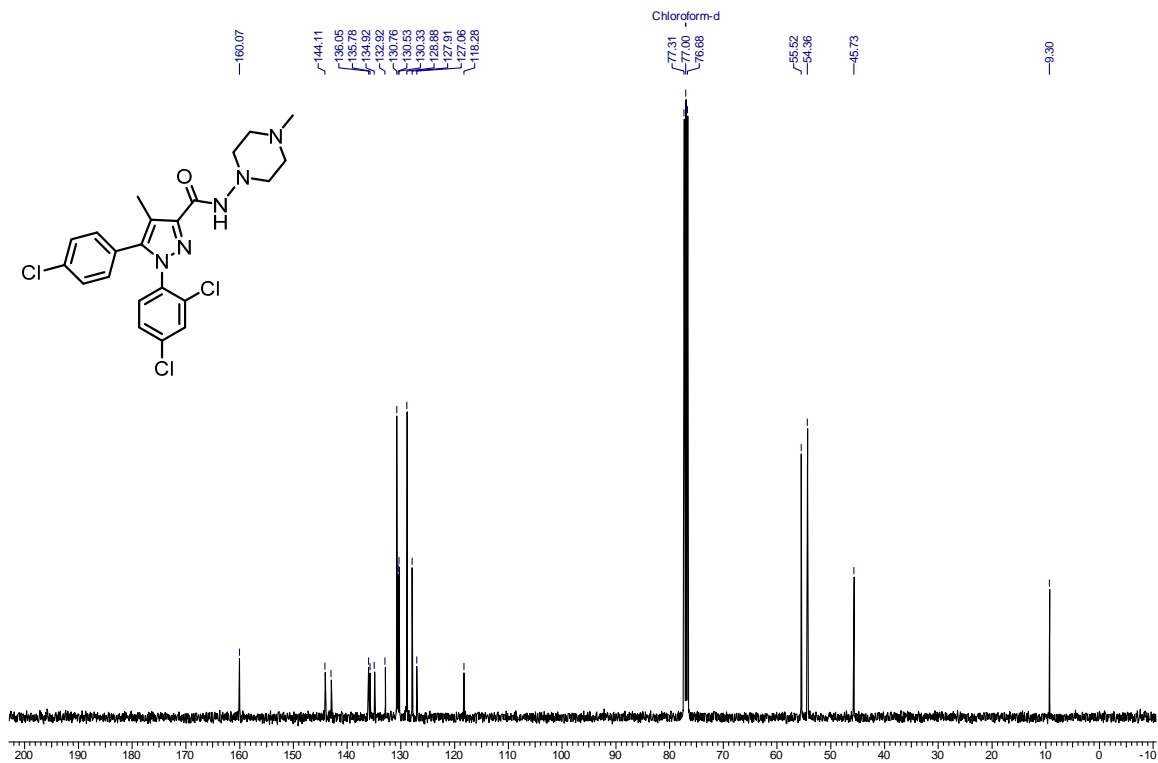
Figure 1.2.27. ^{13}C NMR of **16** (100 MHz, CDCl$_3$)
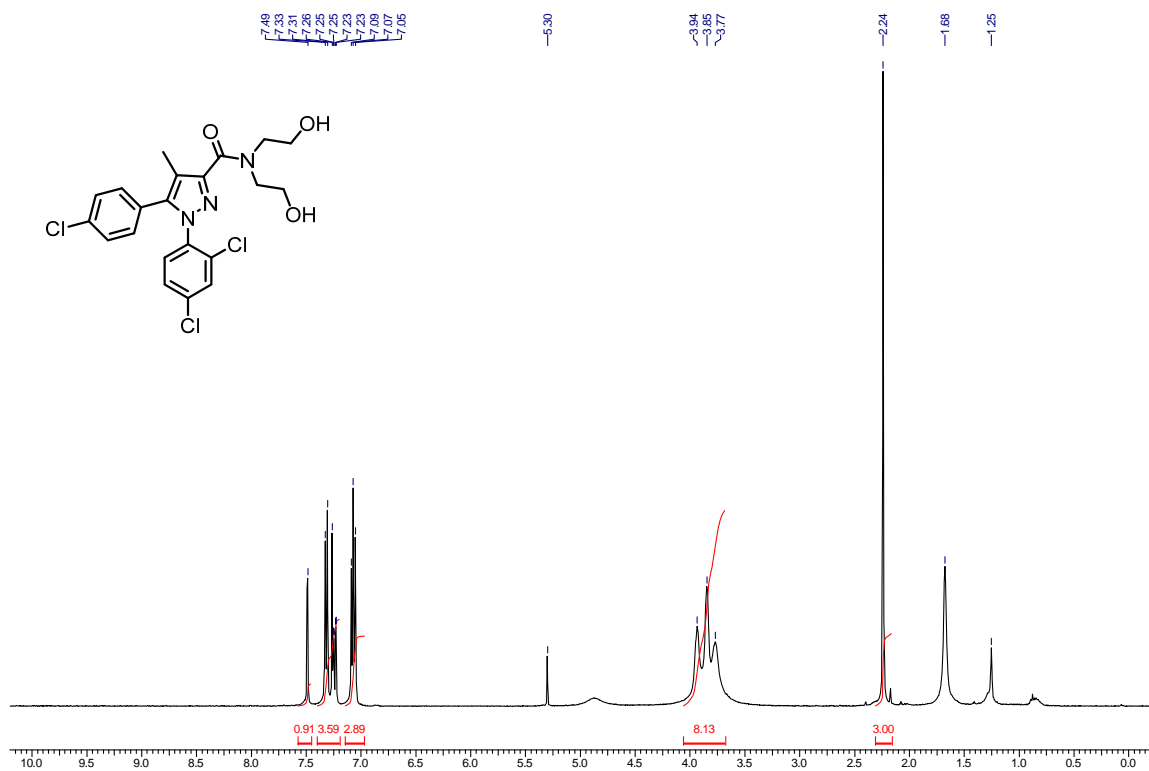
Figure 1.2.28. ^{1}H NMR of **17** (400 MHz, CDCl$_3$)
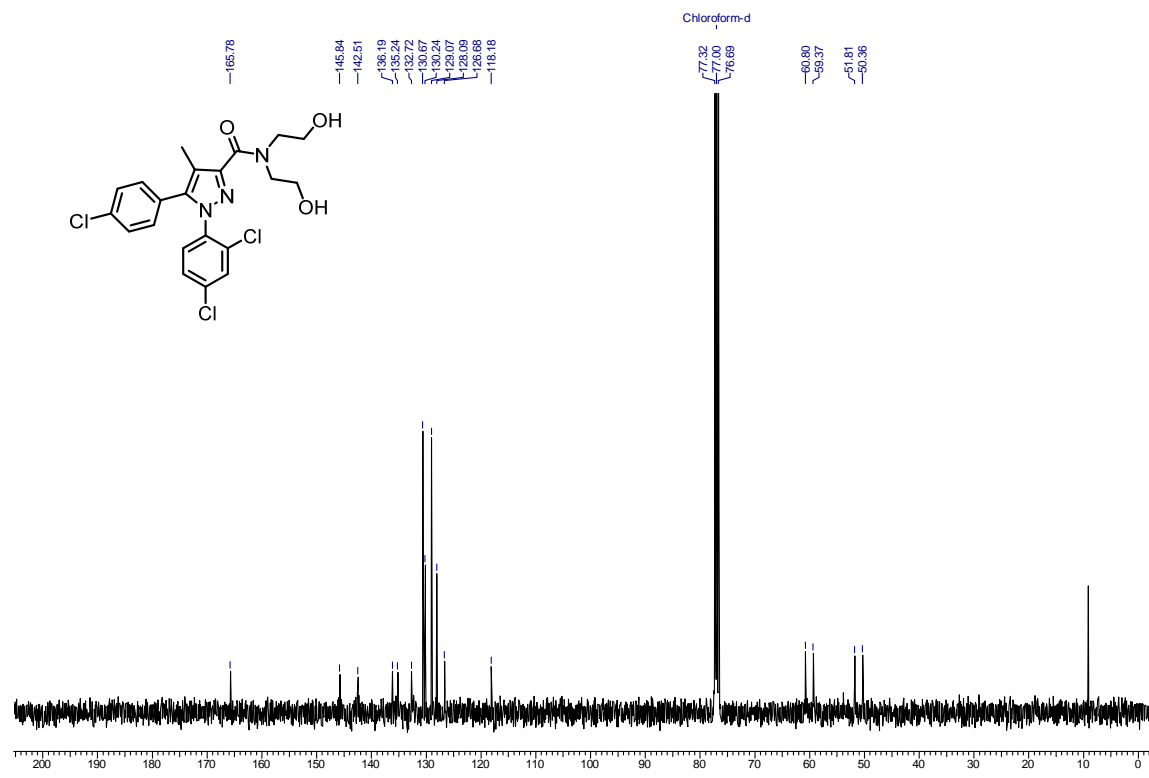
Figure 1.2.29. ^{13}C NMR of **17** (100 MHz, CDCl$_3$)

Figure 1.2.30. ^{1}H NMR of **18** (400 MHz, CDCl$_3$)

Figure 1.2.31. ^{13}C NMR of **18** (100 MHz, CDCl$_3$)
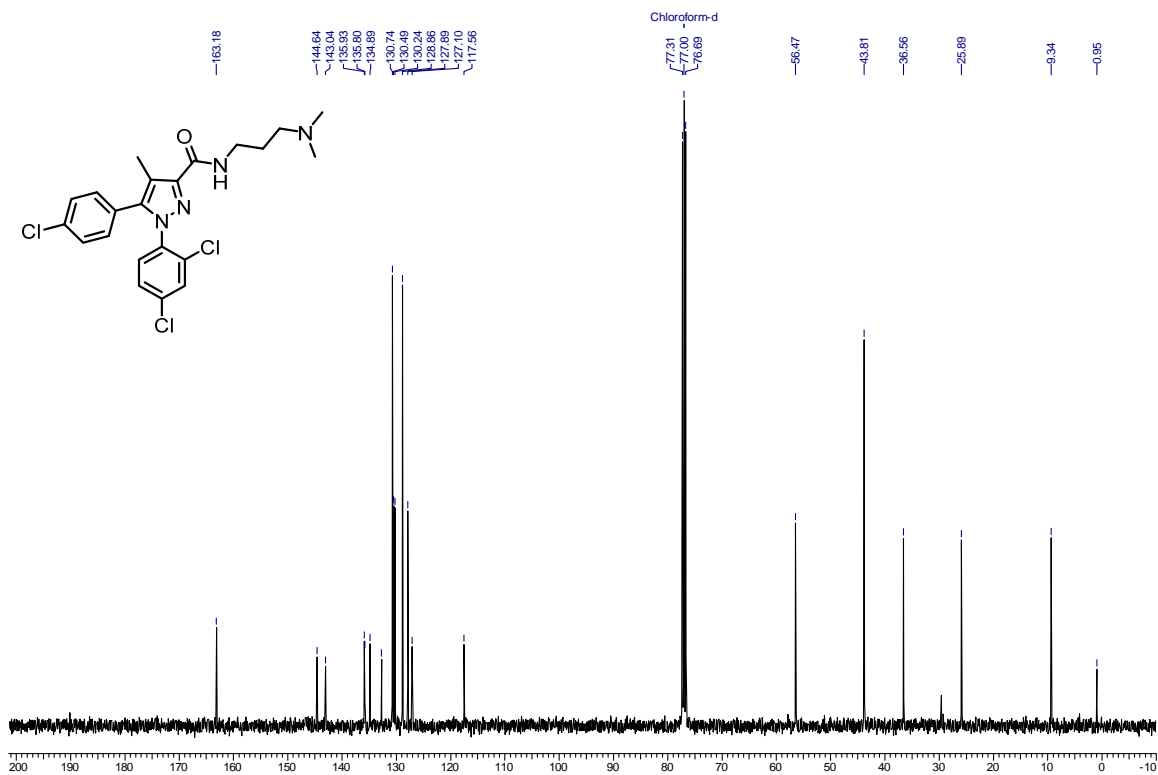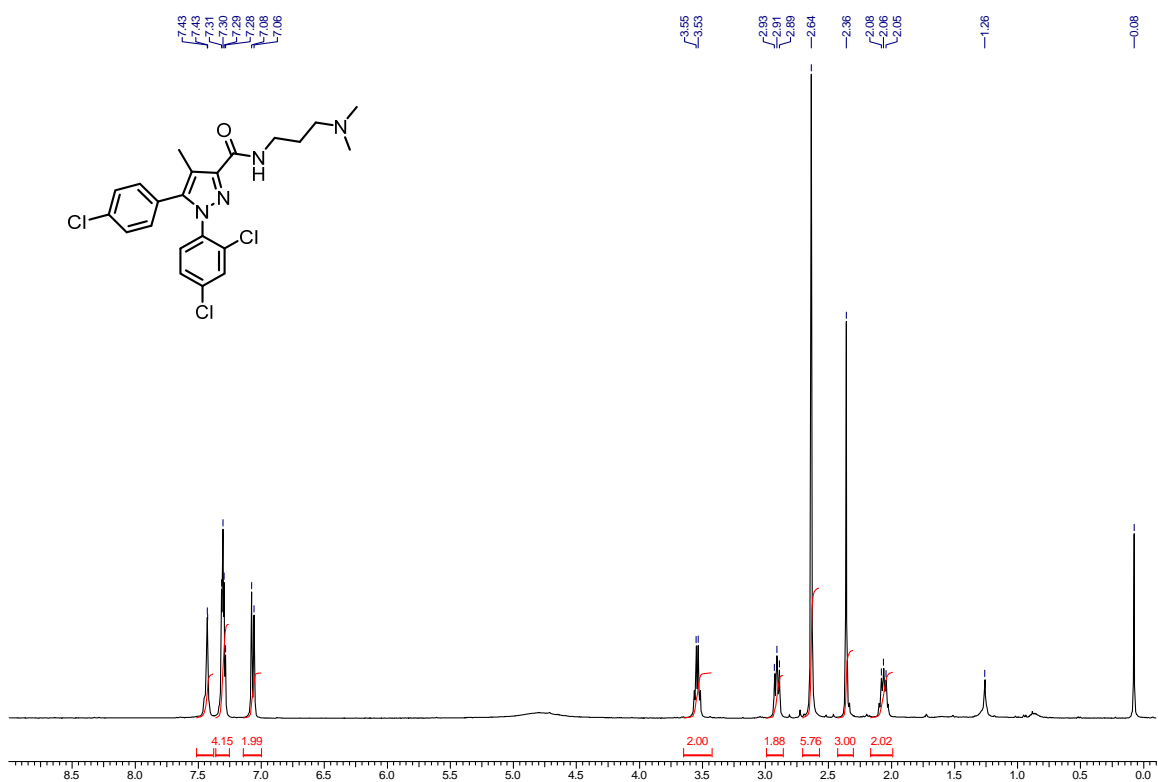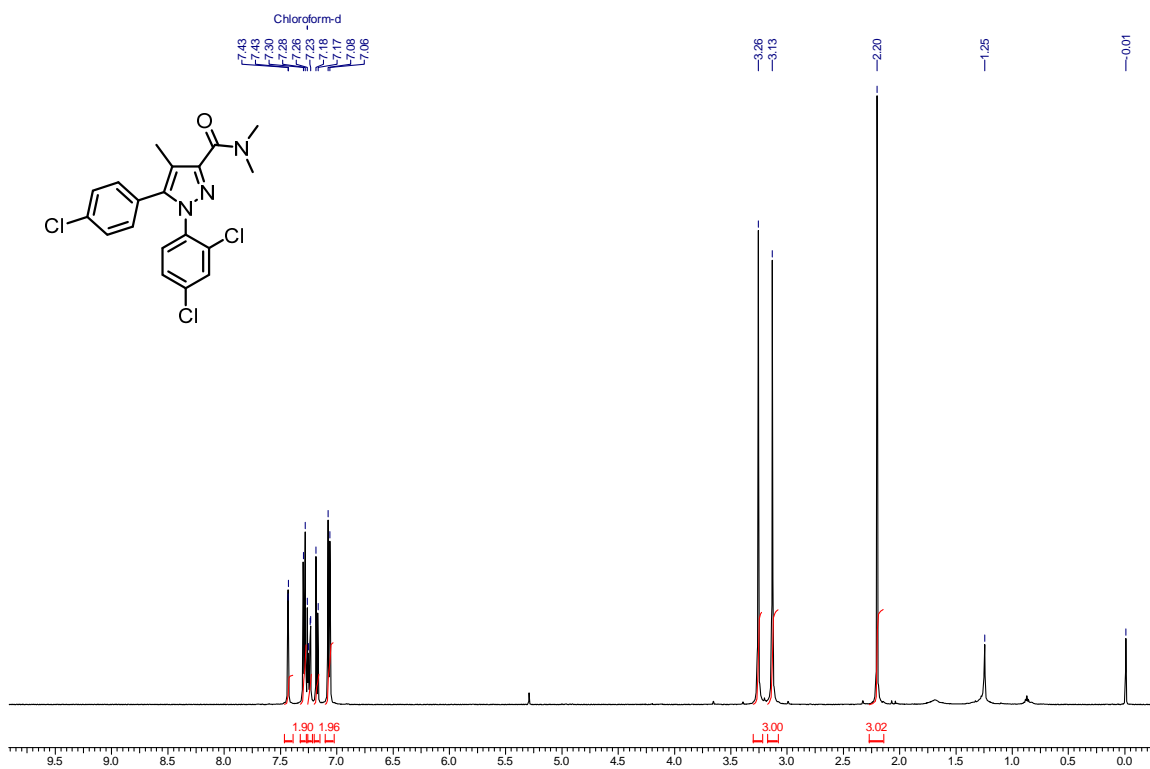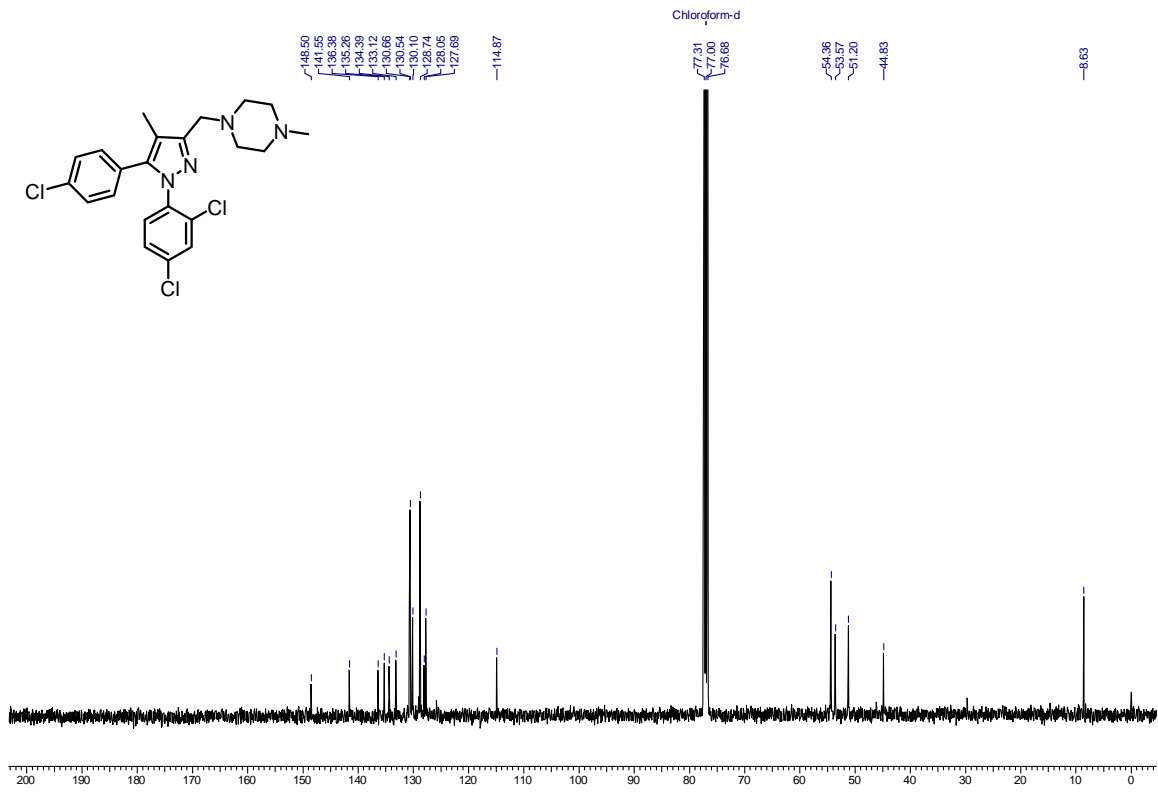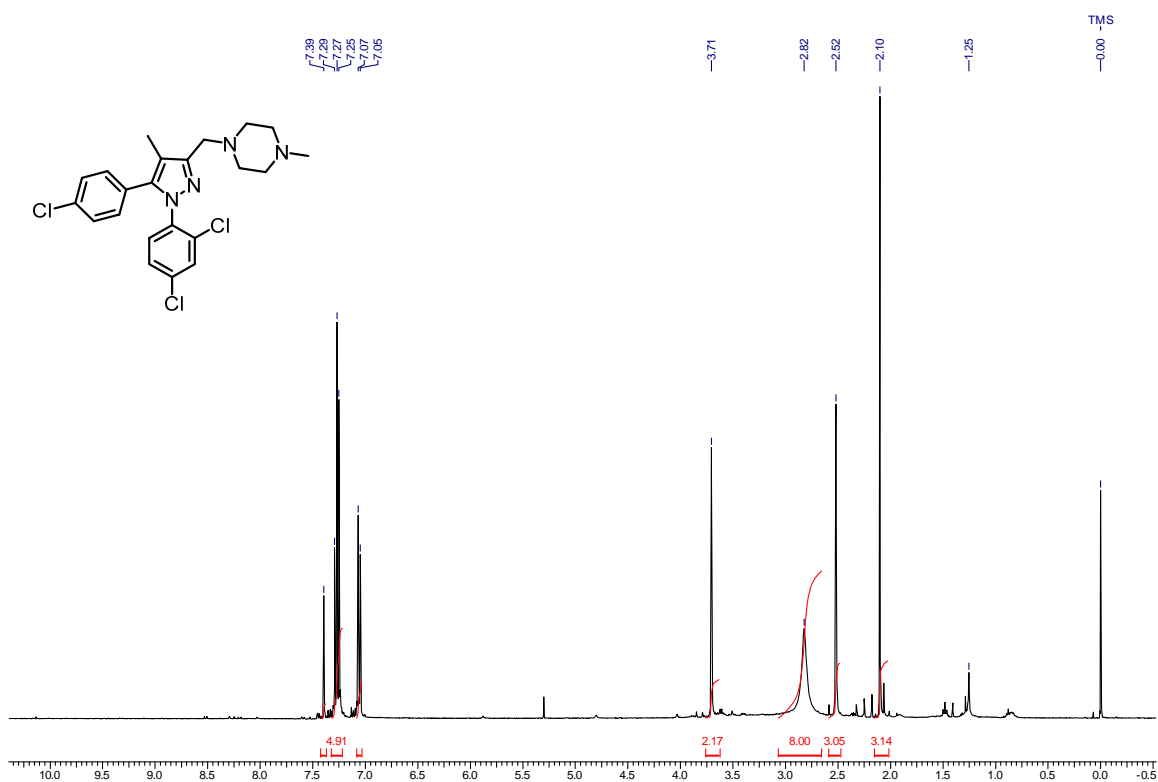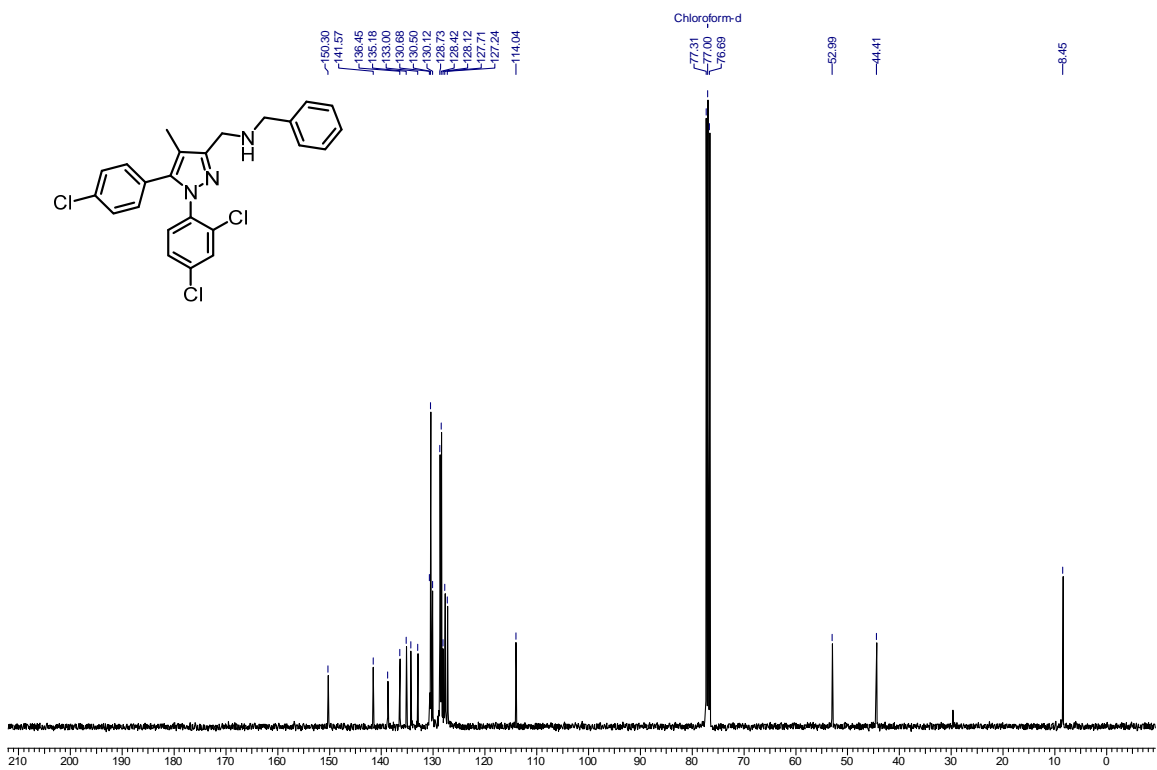
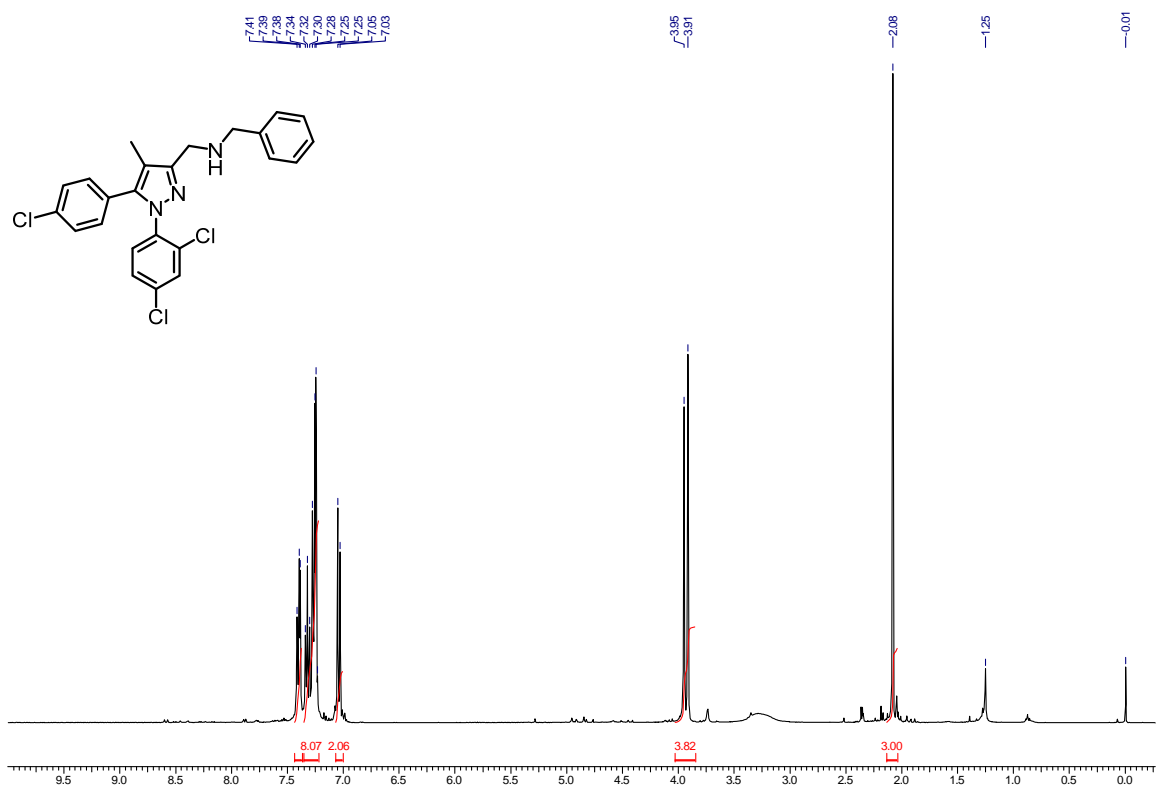**Figure 1.2.32.** ^{1}H NMR of **19** (500 MHz, CDCl$_3$)
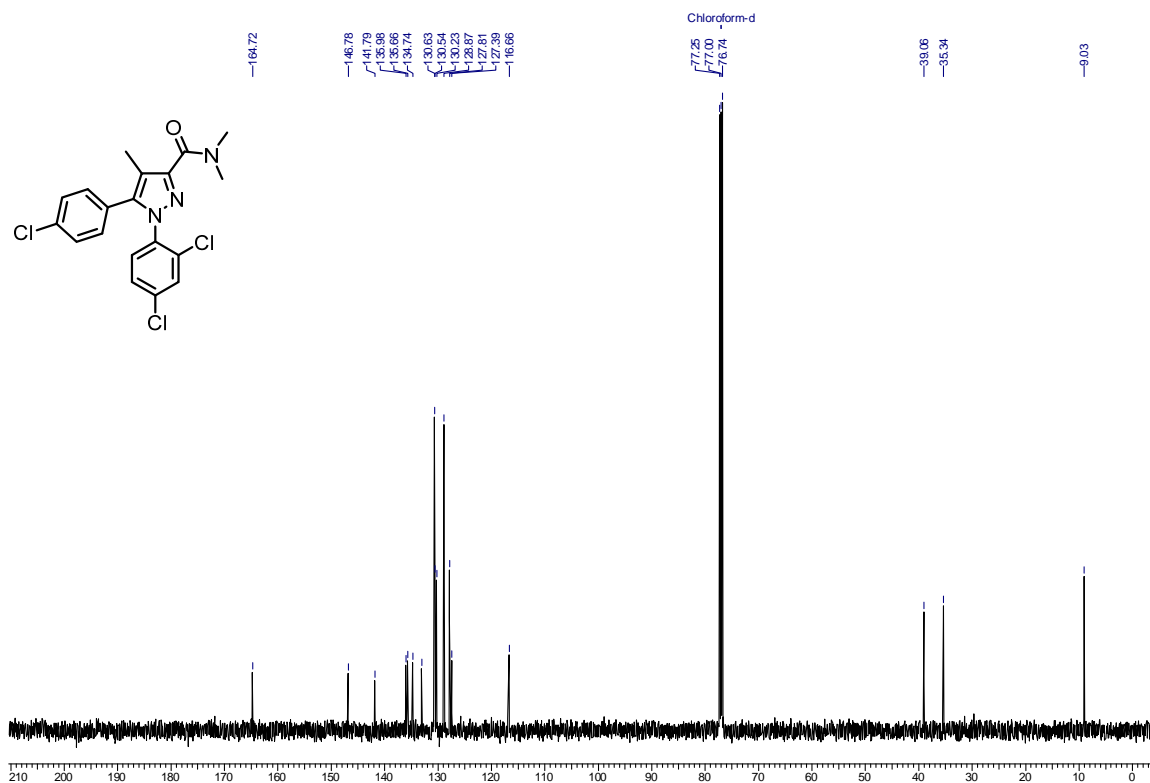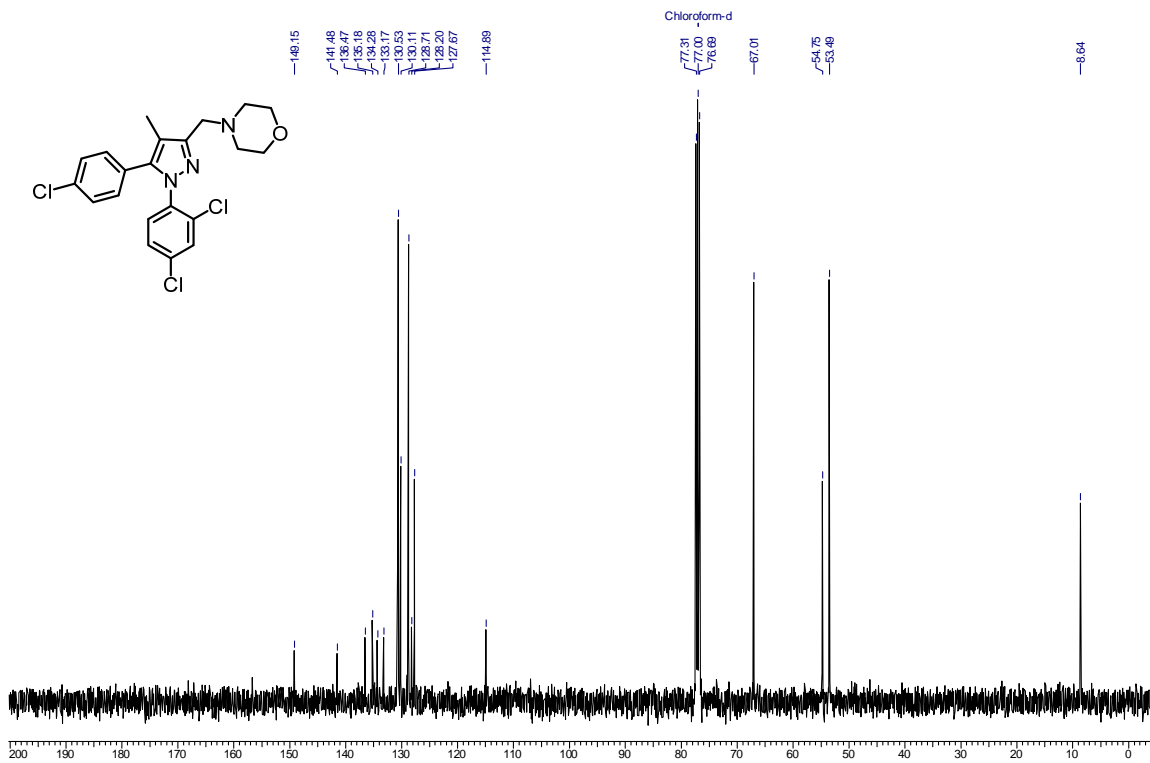

Figure 1.2.33. ^{13}C NMR of **19** (125 MHz, CDCl$_3$)

Figure 1.2.34. ^{1}H NMR of **25** (400 MHz, CDCl$_3$)

Figure 1.2.35. ^{13}C NMR of **25** (100 MHz, CDCl$_3$)

98

Figure 1.2.36. ^{1}H NMR of **28** (400 MHz, CDCl$_3$)

Figure 1.2.37. ^{13}C NMR of **28** (100 MHz, CDCl$_3$)

Figure 1.2.38. ^{1}H NMR of **29** (400 MHz, CDCl$_3$)

Figure 1.2.39. ^{13}C NMR of **29** (100 MHz, CDCl$_3$)

100

Figure 1.2.40. ^{1}H NMR of **32** (400 MHz, CDCl$_3$)

Figure 1.2.41. ^{13}C NMR of **32** (100 MHz, CDCl$_3$)

Figure 1.2.42. ^{1}H NMR of **33** (400 MHz, CDCl$_3$)

Figure 1.2.43. ^{13}C NMR of **33** (100 MHz, CDCl$_3$)

Figure 1.2.44. ^{1}H NMR of **34** (200 MHz, CDCl$_3$)

Figure 1.2.45. ^{13}C NMR of **34** (100 MHz, CDCl$_3$)

Figure 1.2.46. ^{1}H NMR of **35** (500 MHz, CDCl$_3$)

Figure 1.2.47. ^{13}C NMR of **35** (125 MHz, CDCl$_3$)

Figure 1.2.48. ^{1}H NMR of **36** (400 MHz, CDCl$_3$)
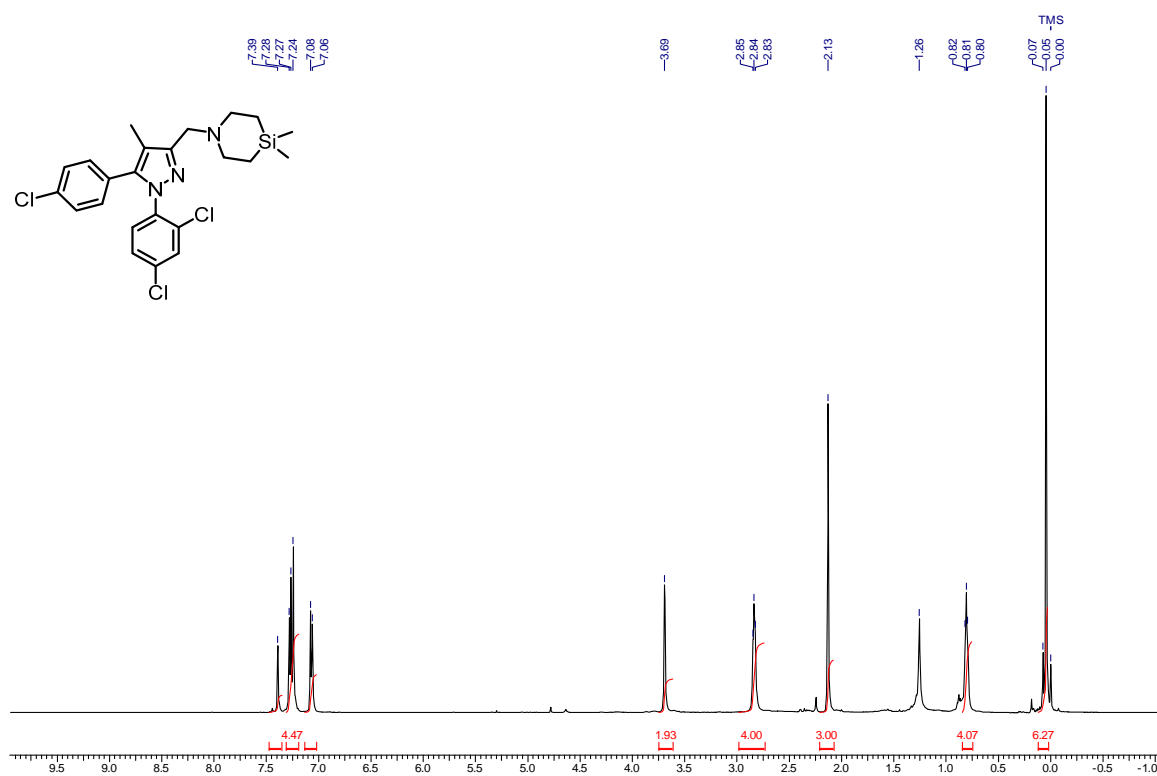

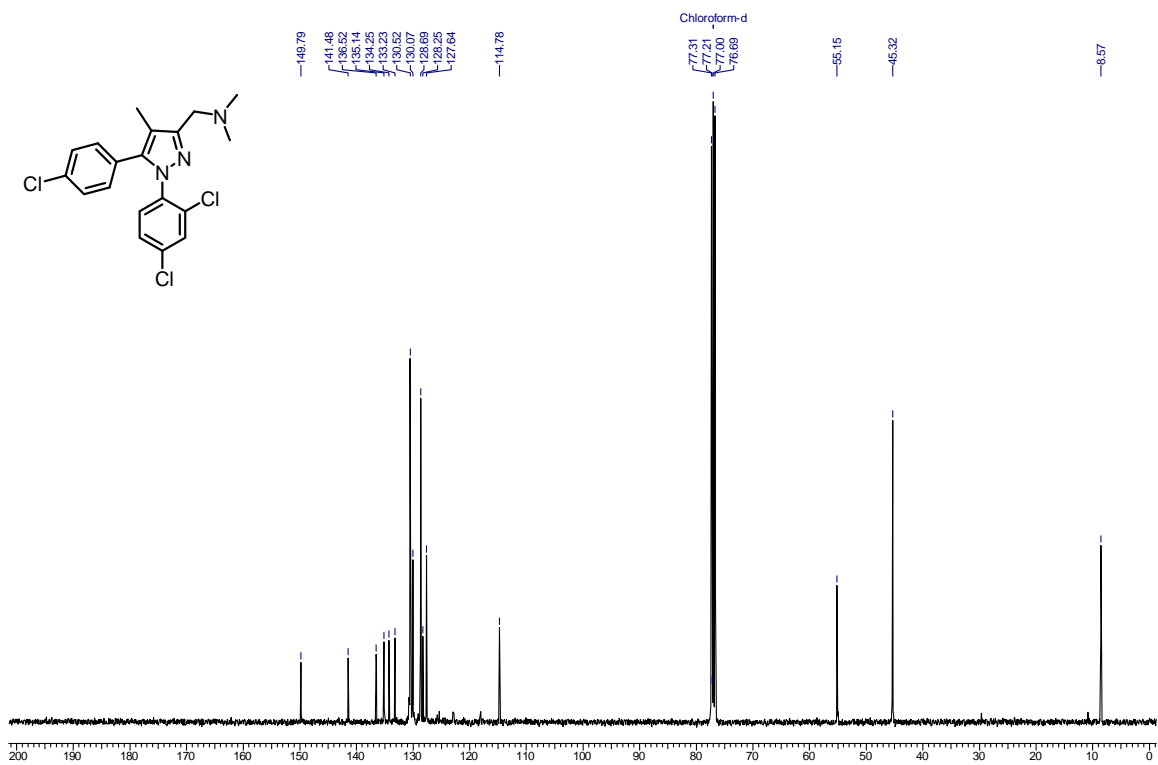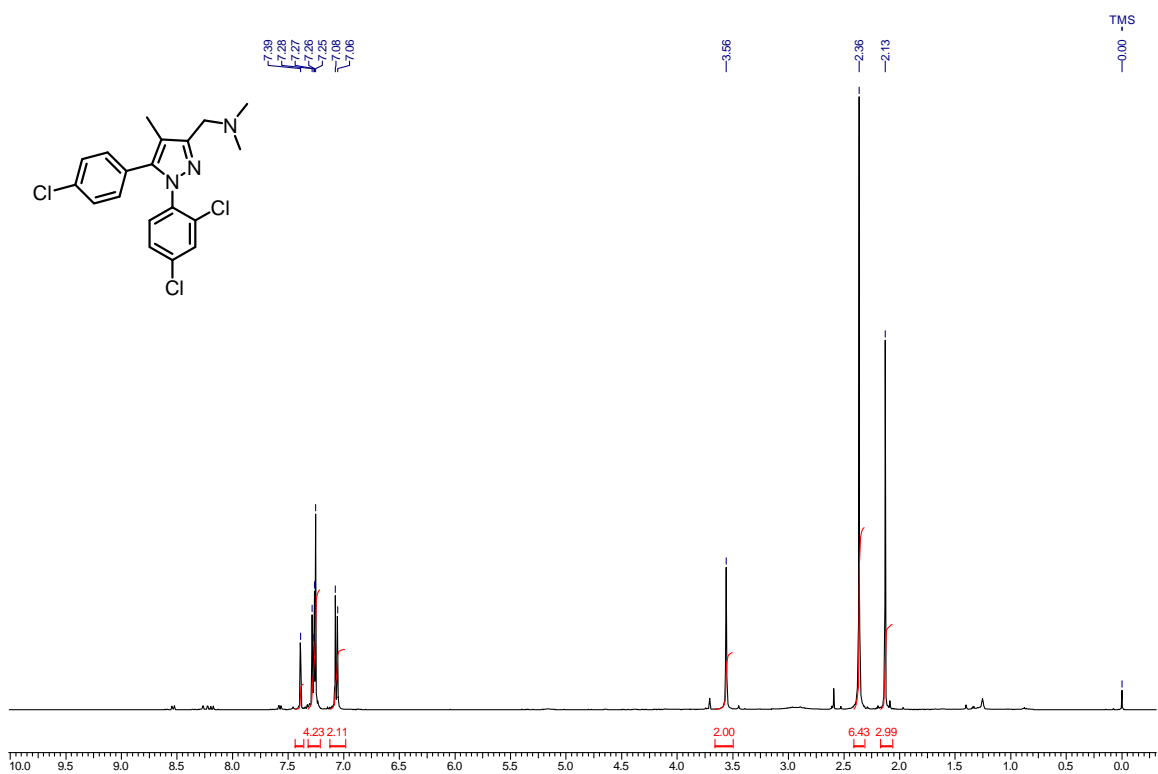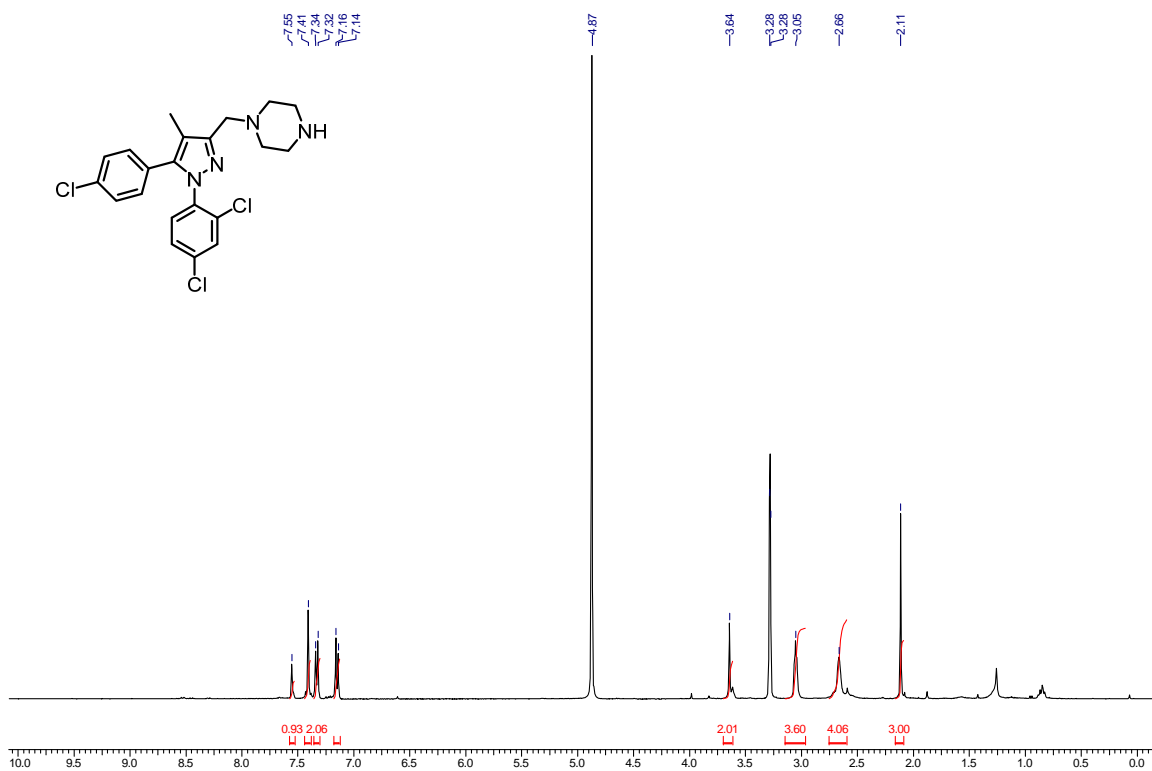**Figure 1.2.49.** ^{13}C NMR of **36** (100 MHz, CDCl$_3$)

105

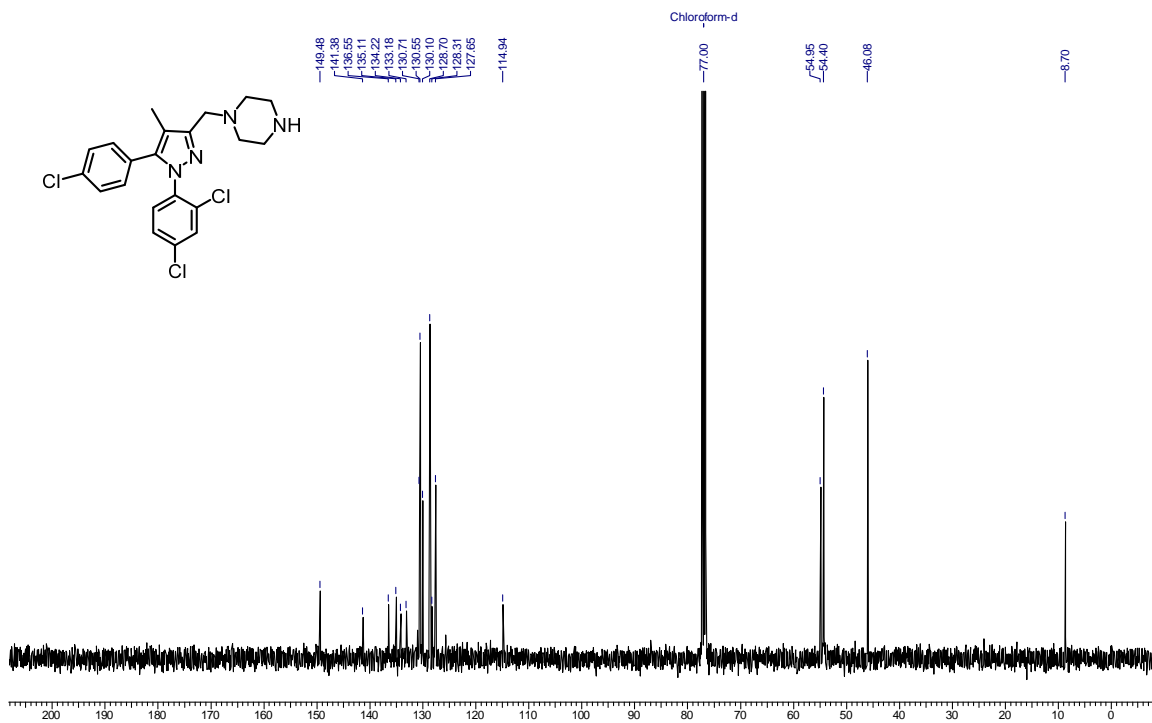**Figure 1.2.50.** ^{1}H NMR of **38** (400 MHz, MeOD)

Figure 1.2.51. ^{13}C NMR of **38** (100 MHz, CDCl$_3$)

Figure 1.2.52. ^{1}H NMR of **40** (500 MHz, CDCl$_3$)

Figure 1.2.53. ^{13}C NMR of **40** (125 MHz, CDCl$_3$)

Figure 1.2.54. ^{1}H NMR of **41** (400 MHz, CDCl$_3$)

Figure 1.2.55. ^{13}C NMR of **41** (100 MHz, CDCl$_3$)
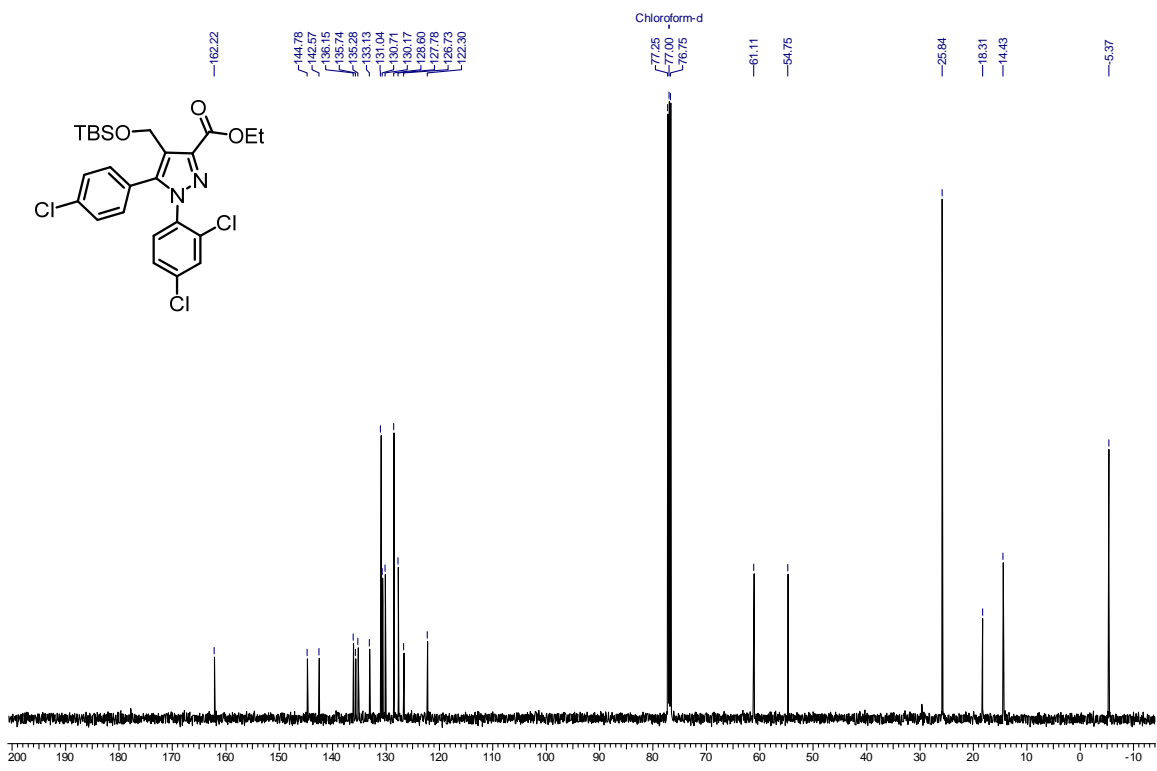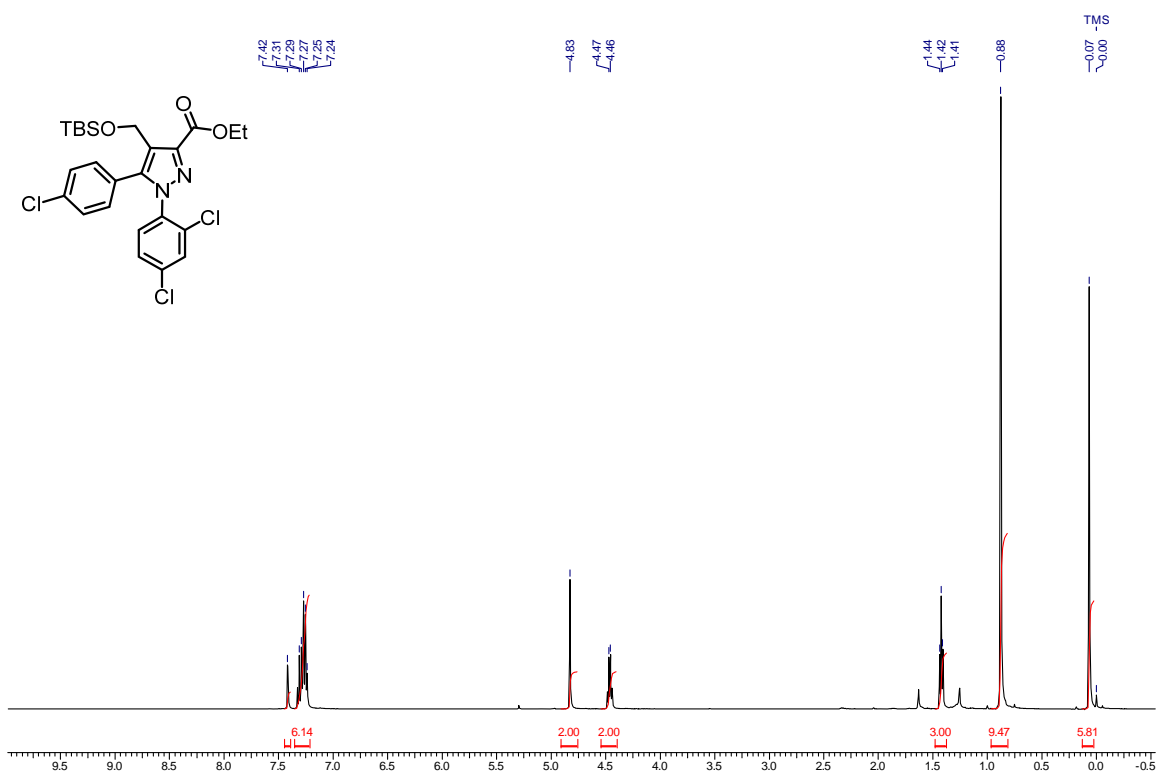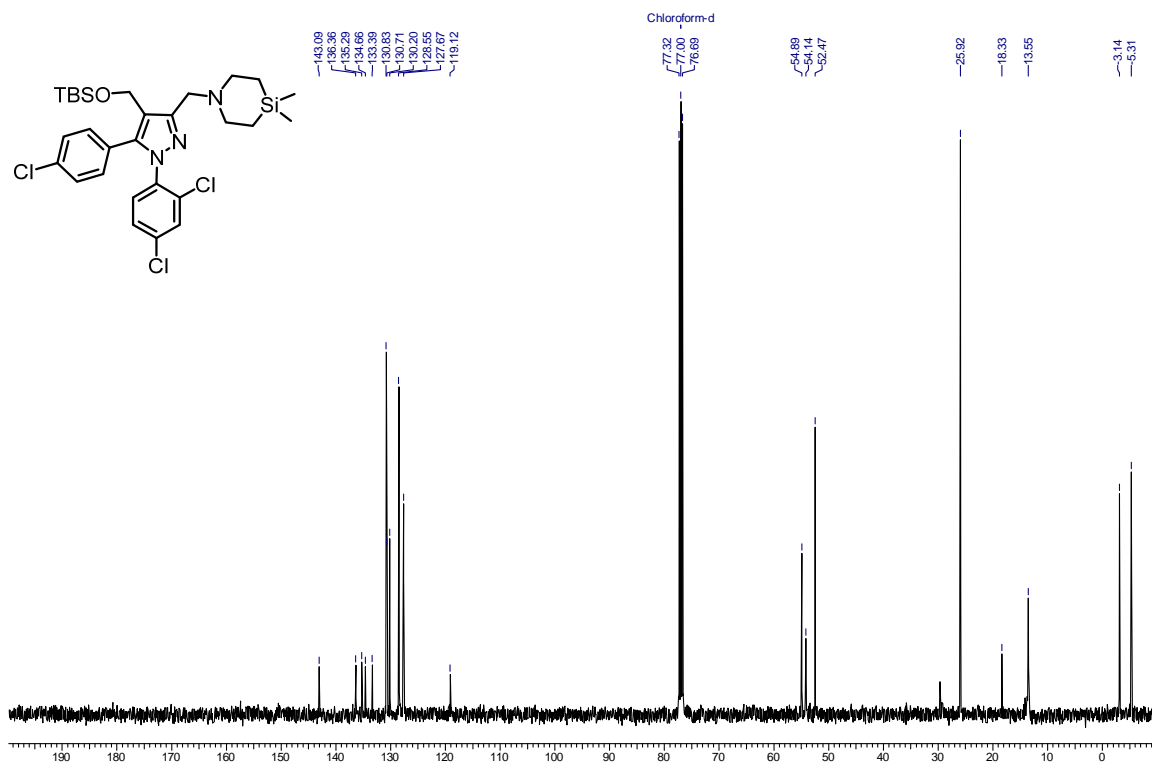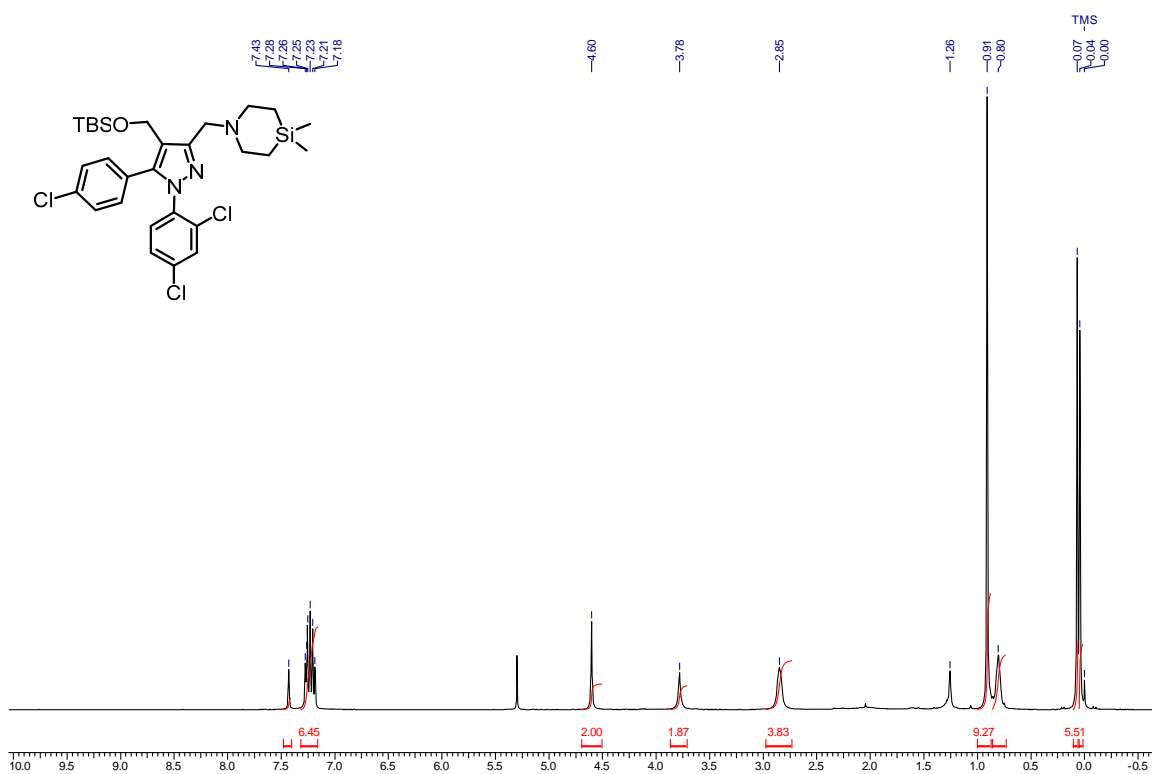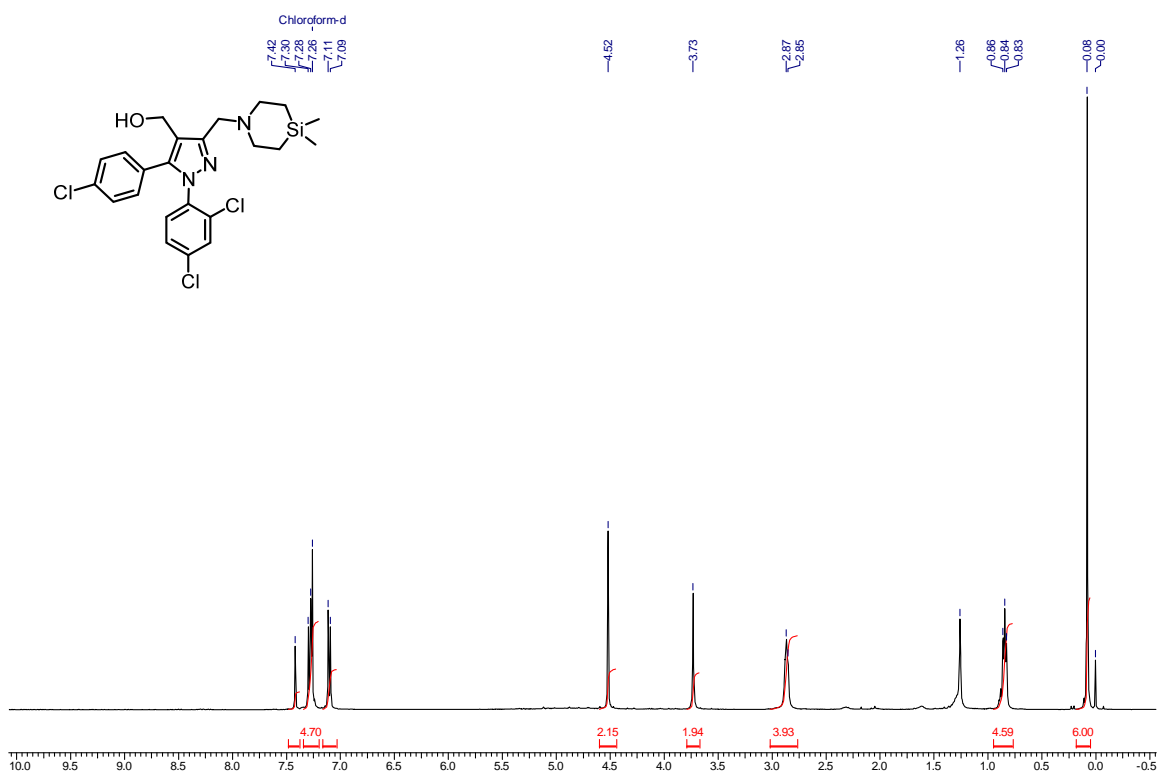
Figure 1.2.56. ^{1}H NMR of **42** (400 MHz, CDCl$_3$)
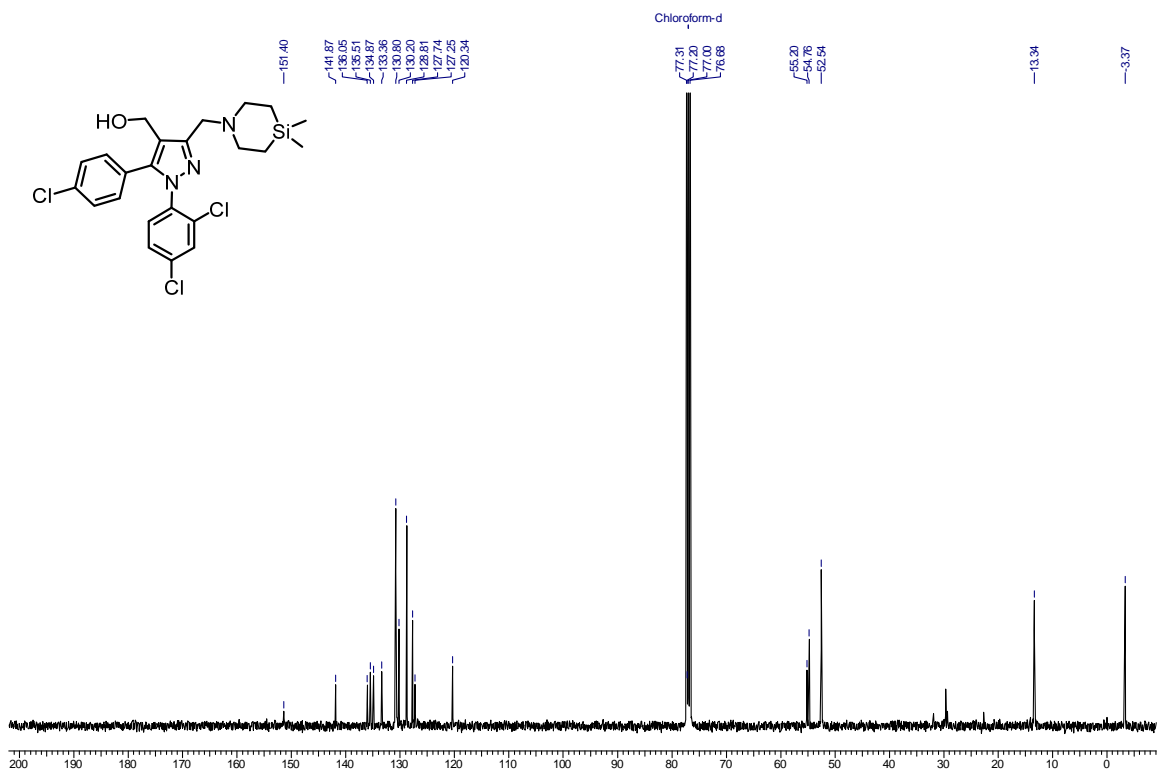
Figure 1.2.57. ^{13}C NMR of **42** (100 MHz, CDCl$_3$)

Figure 1.2.58. ^{1}H NMR of **44** (400 MHz, CDCl$_3$)

Figure 1.2.59. ^{13}C NMR of **44** (100 MHz, CDCl$_3$)

Figure 1.2.60. ^{1}H NMR of **46** (400 MHz, CDCl$_3$)

Figure 1.2.61. ^{13}C NMR of **46** (100 MHz, CDCl$_3$)
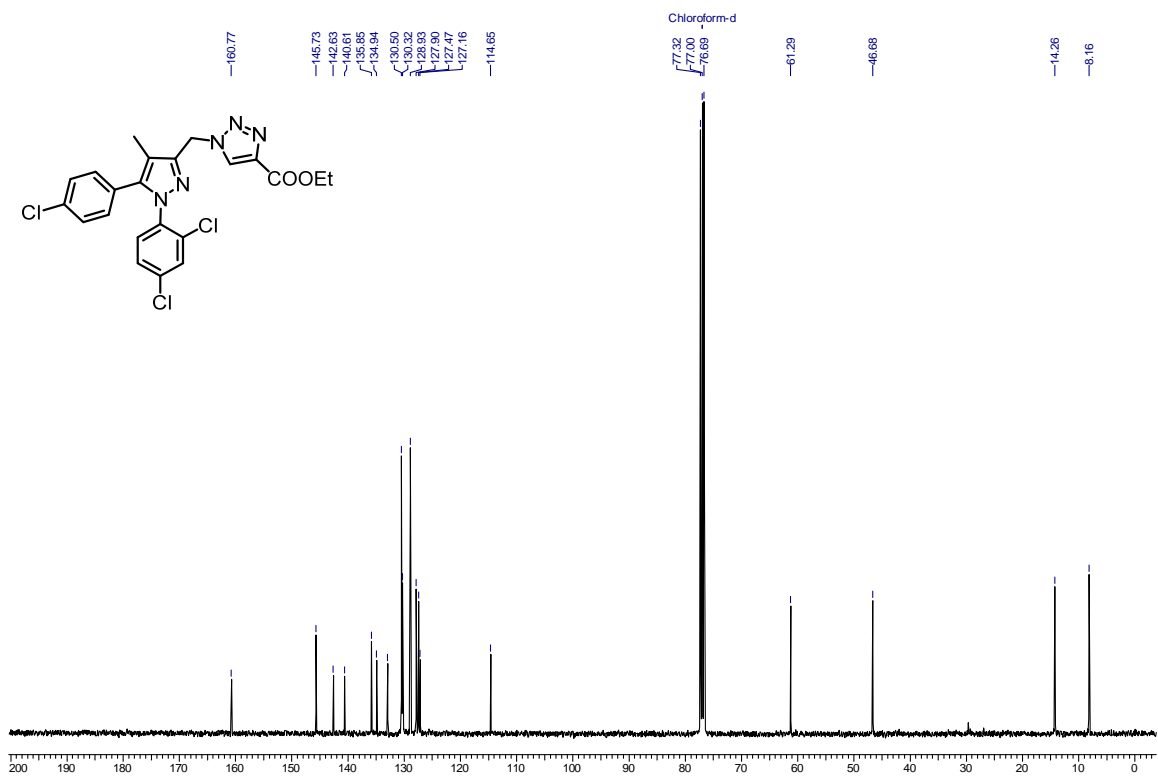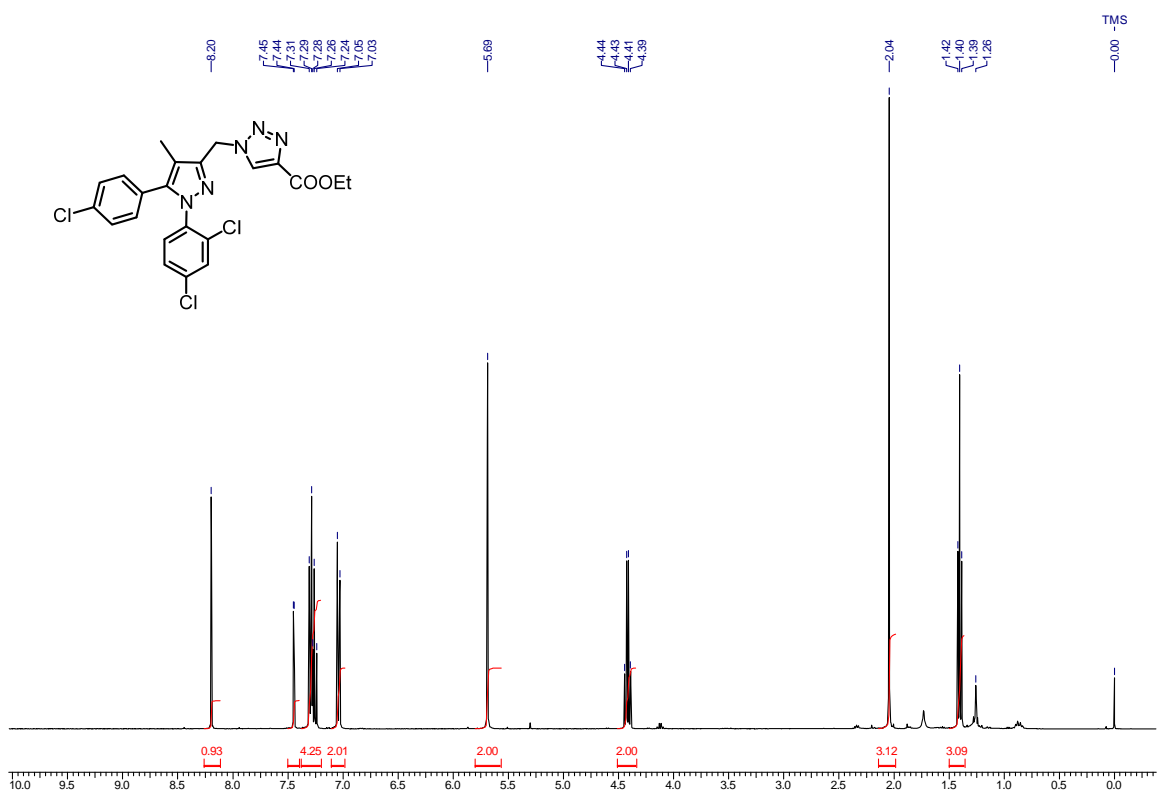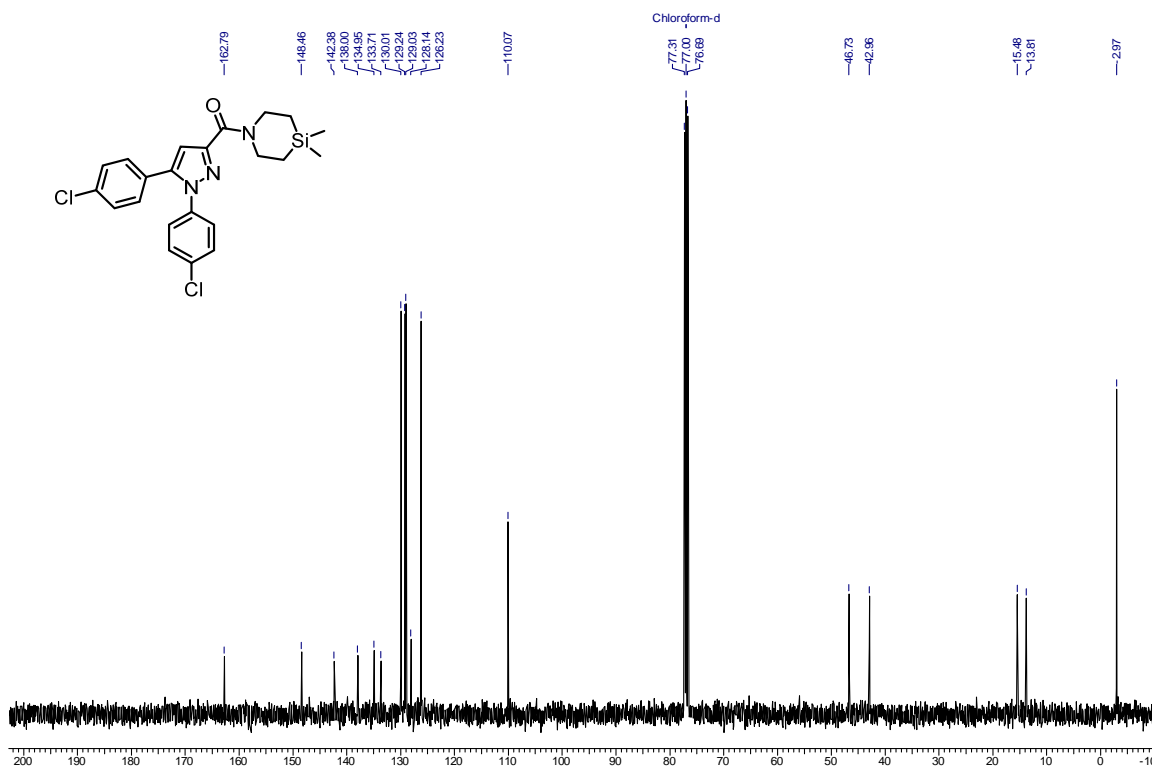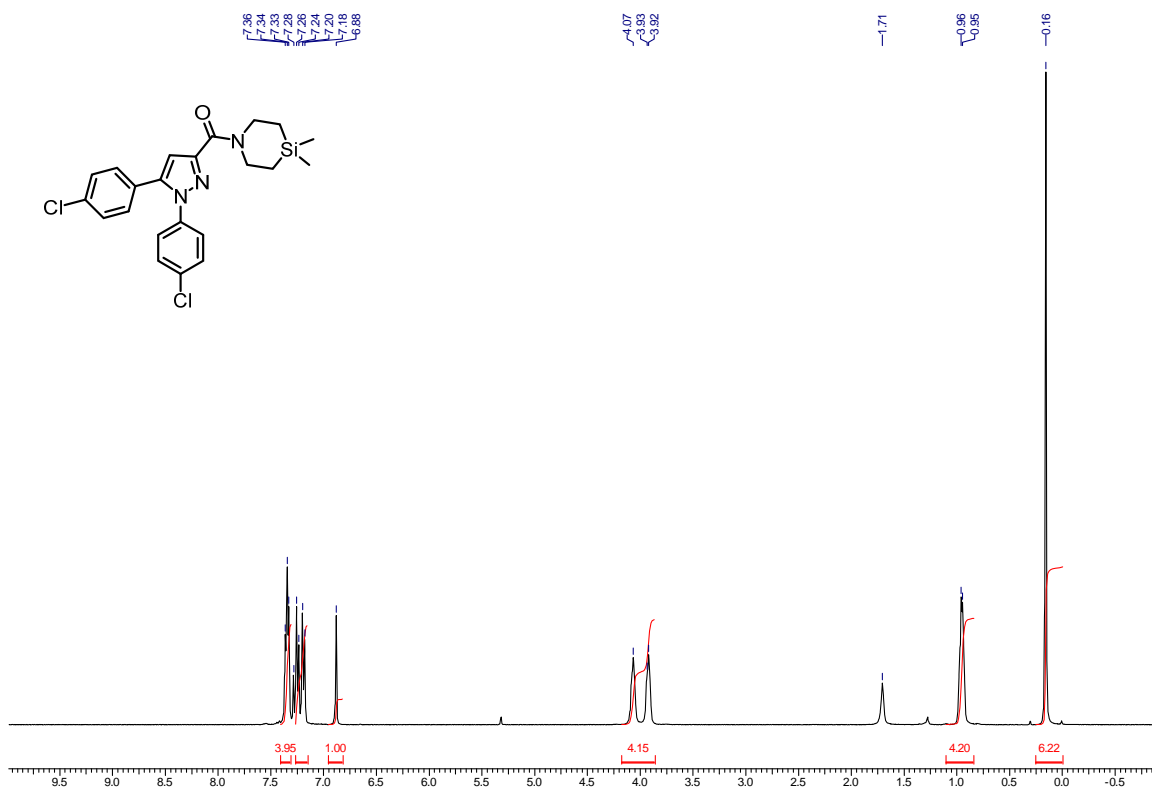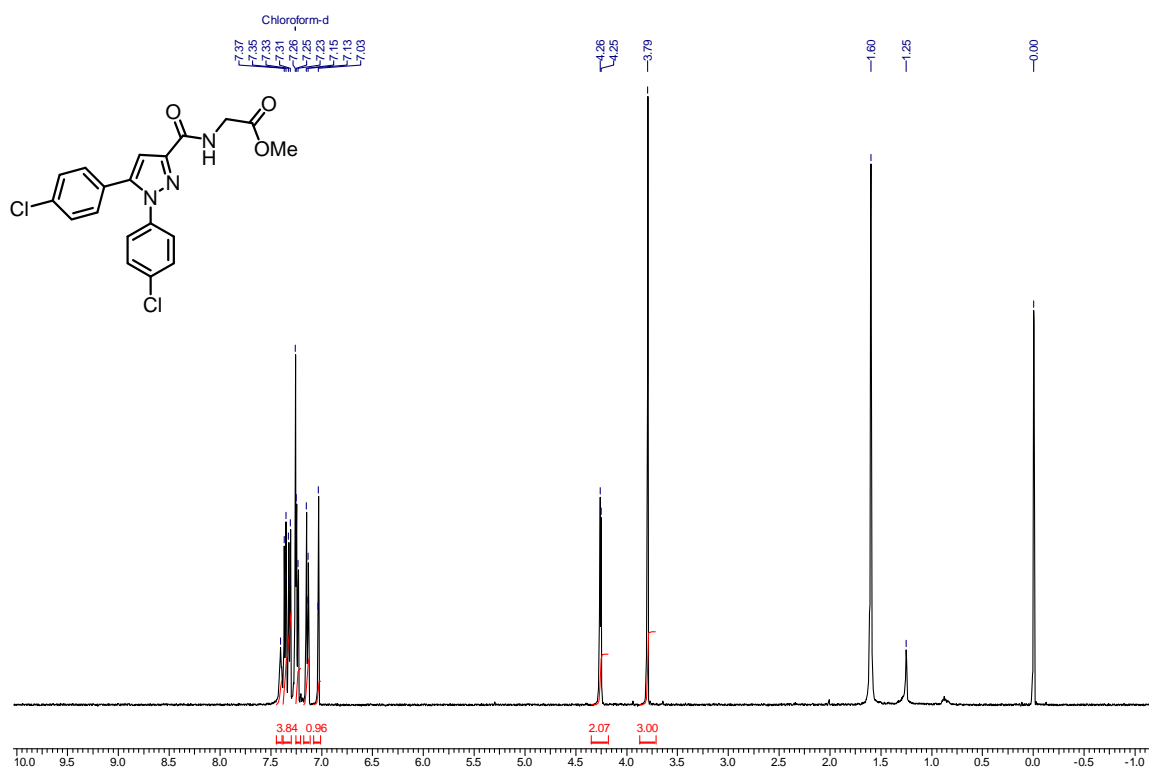
Figure 1.2.62. ^{1}H NMR of **47** (400 MHz, CDCl$_3$)
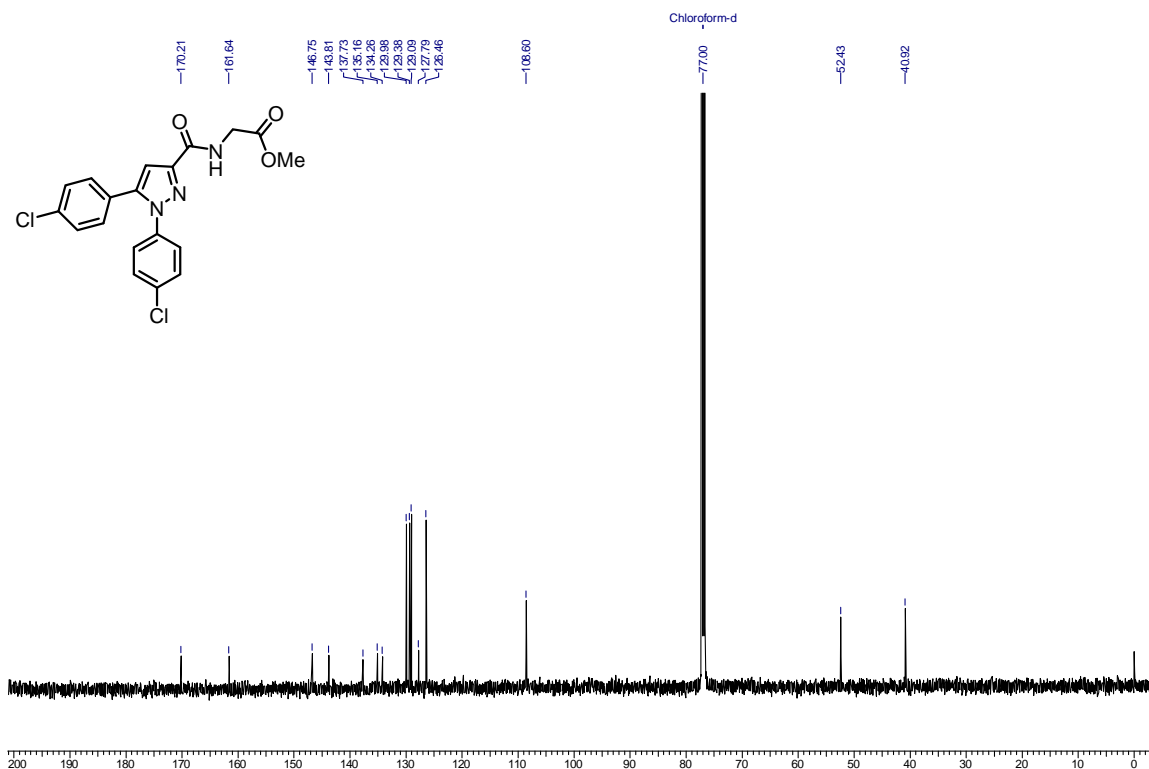
Figure 1.2.63. ^{13}C NMR of **47** (100 MHz, CDCl$_3$)
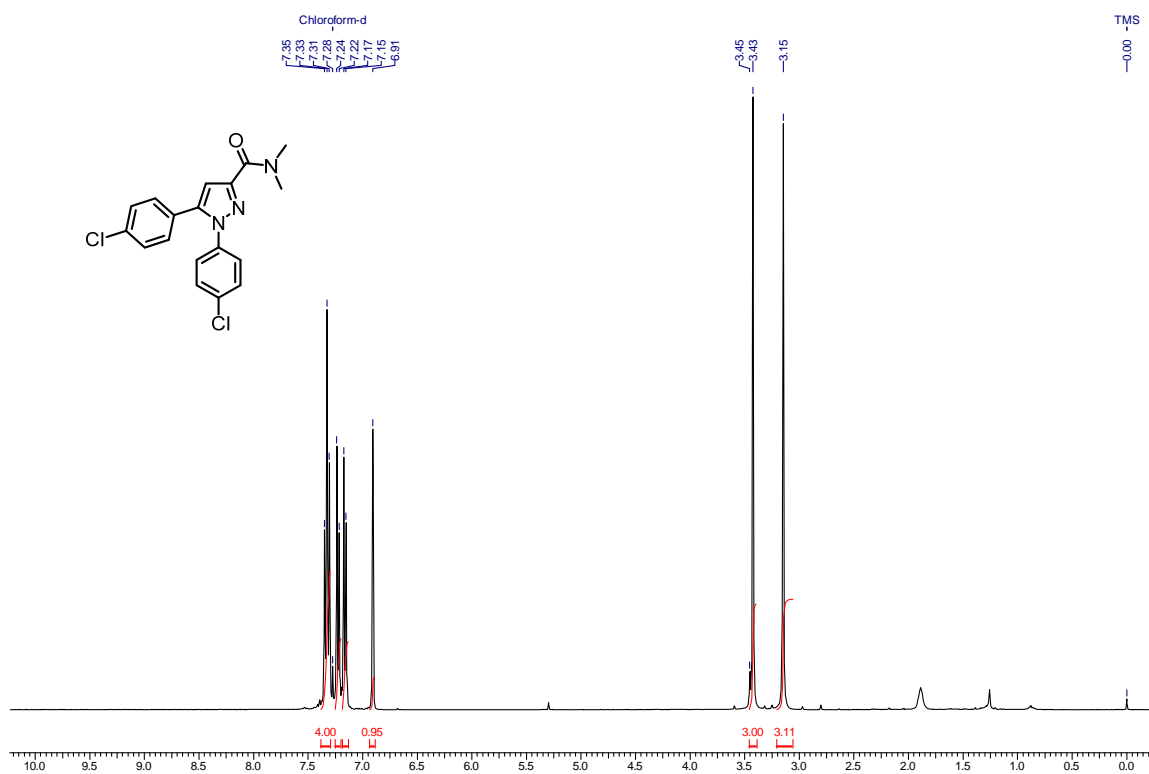
Figure 1.2.64. ^{1}H NMR of **48** (400 MHz, CDCl$_3$)
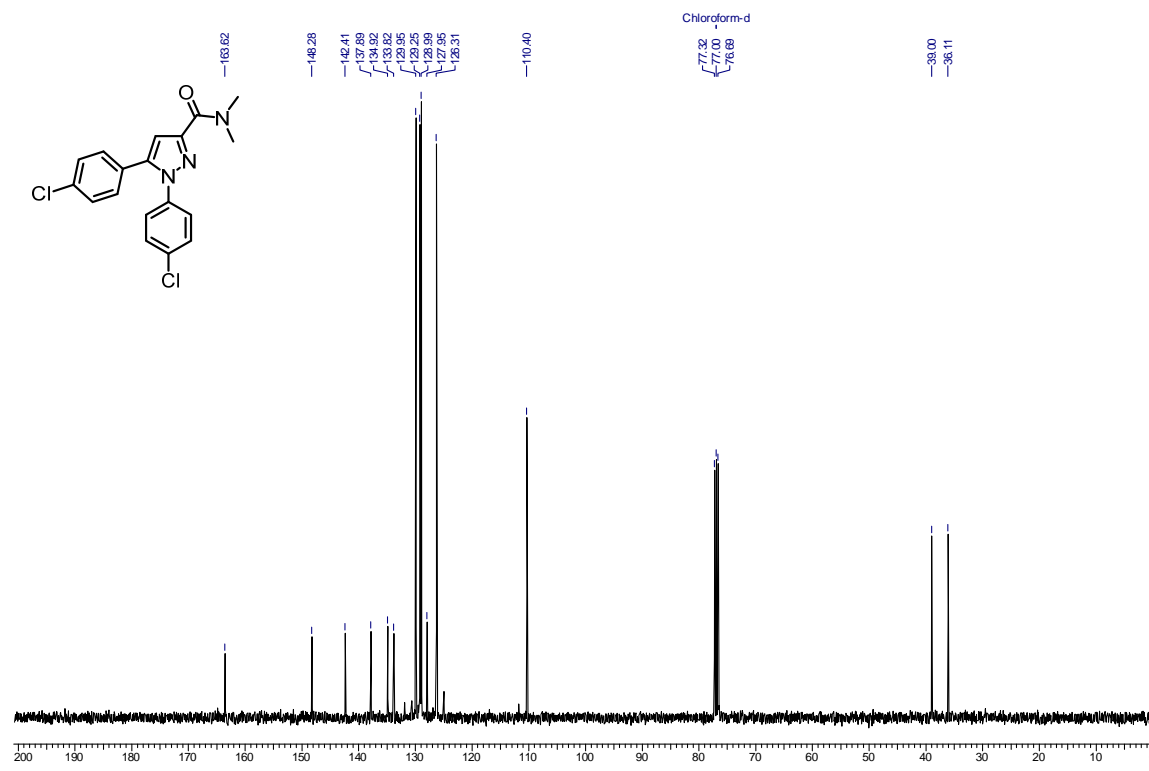
Figure 1.2.65. ^{13}C NMR of **48** (100 MHz, CDCl$_3$)

113

Figure 1.2.66. ^{1}H NMR of **49** (400 MHz, CDCl$_3$)

Figure 1.2.67. ^{13}C NMR of **49** (100 MHz, CDCl$_3$)

Figure 1.2.68. ^{1}H NMR of **50** (200 MHz, CDCl$_3$)

Figure 1.2.69. ^{13}C NMR of **50** (50 MHz, CDCl$_3$)

115
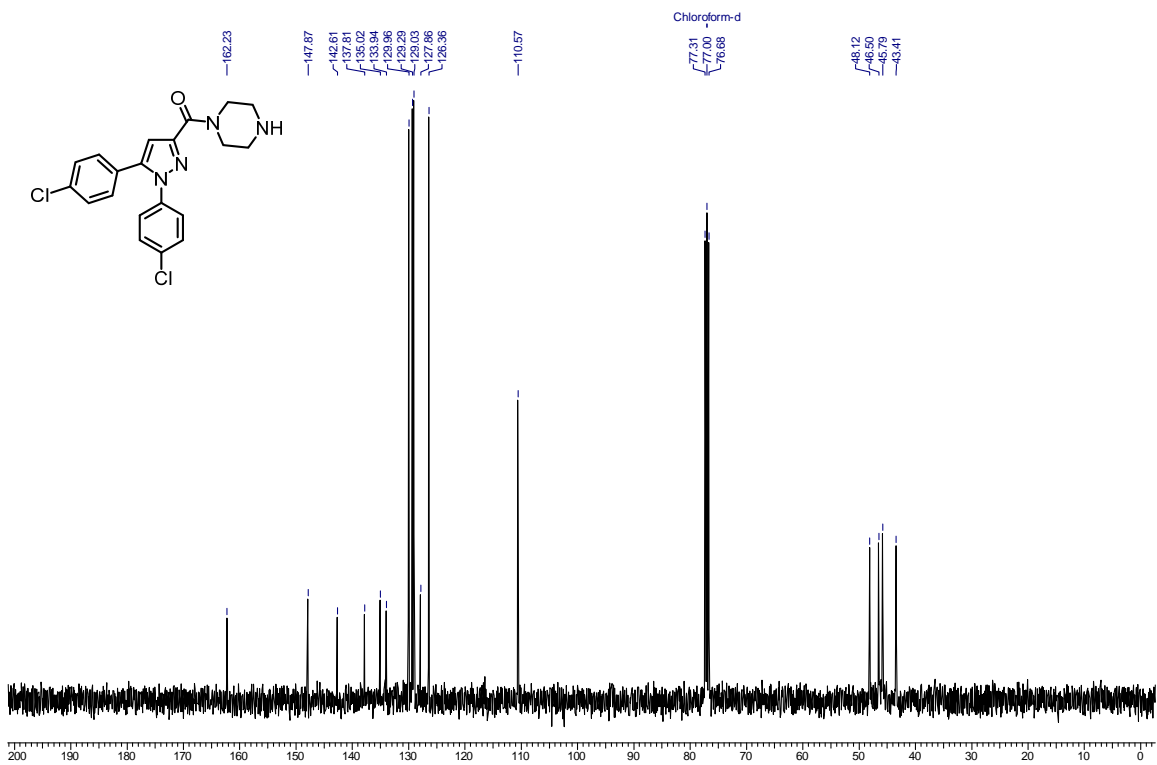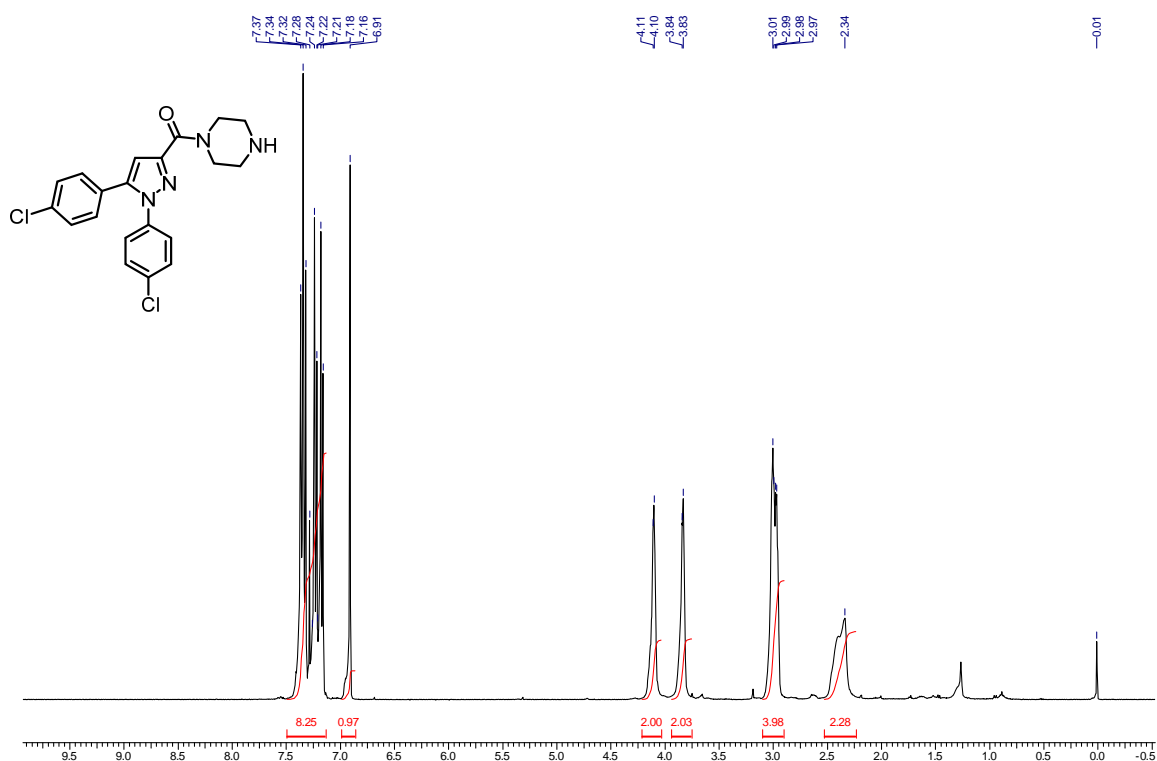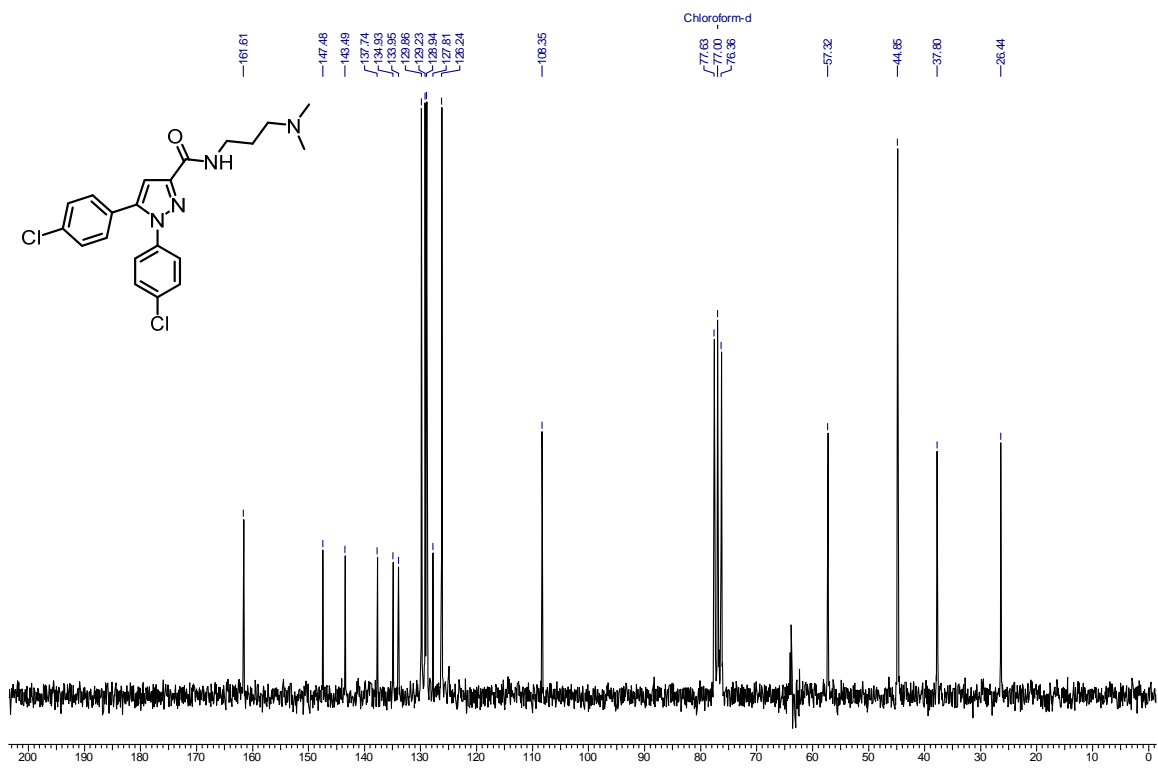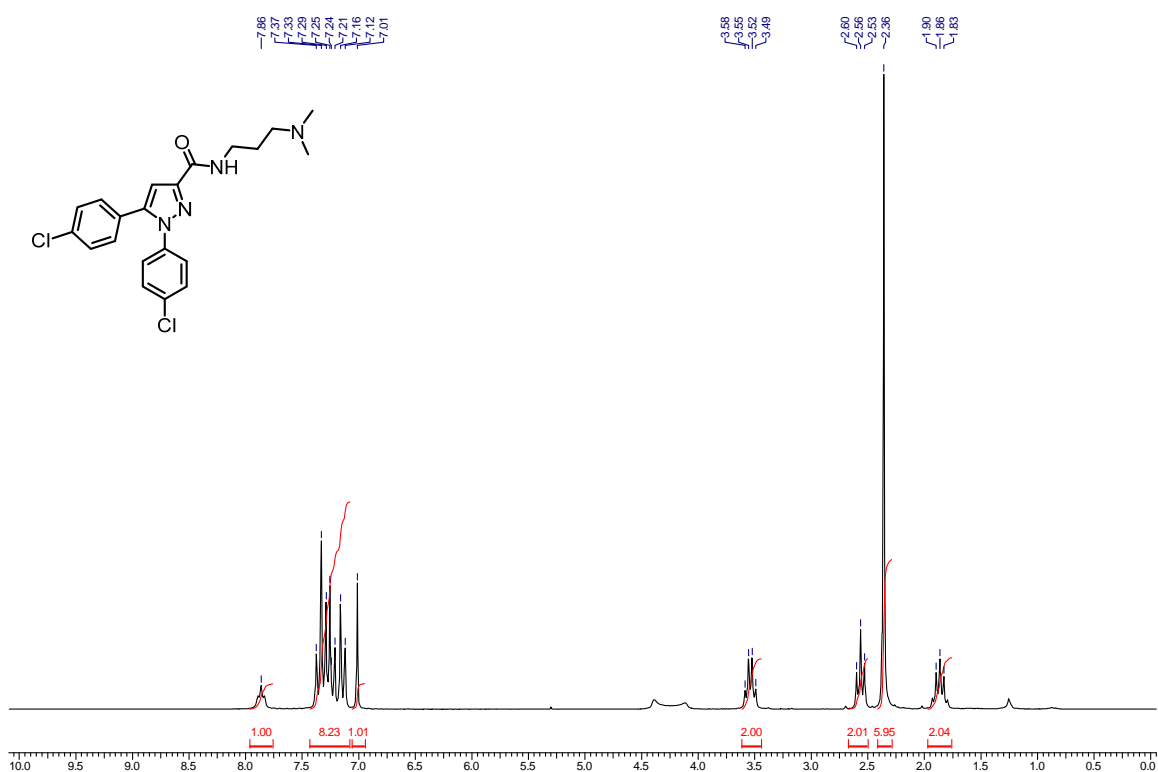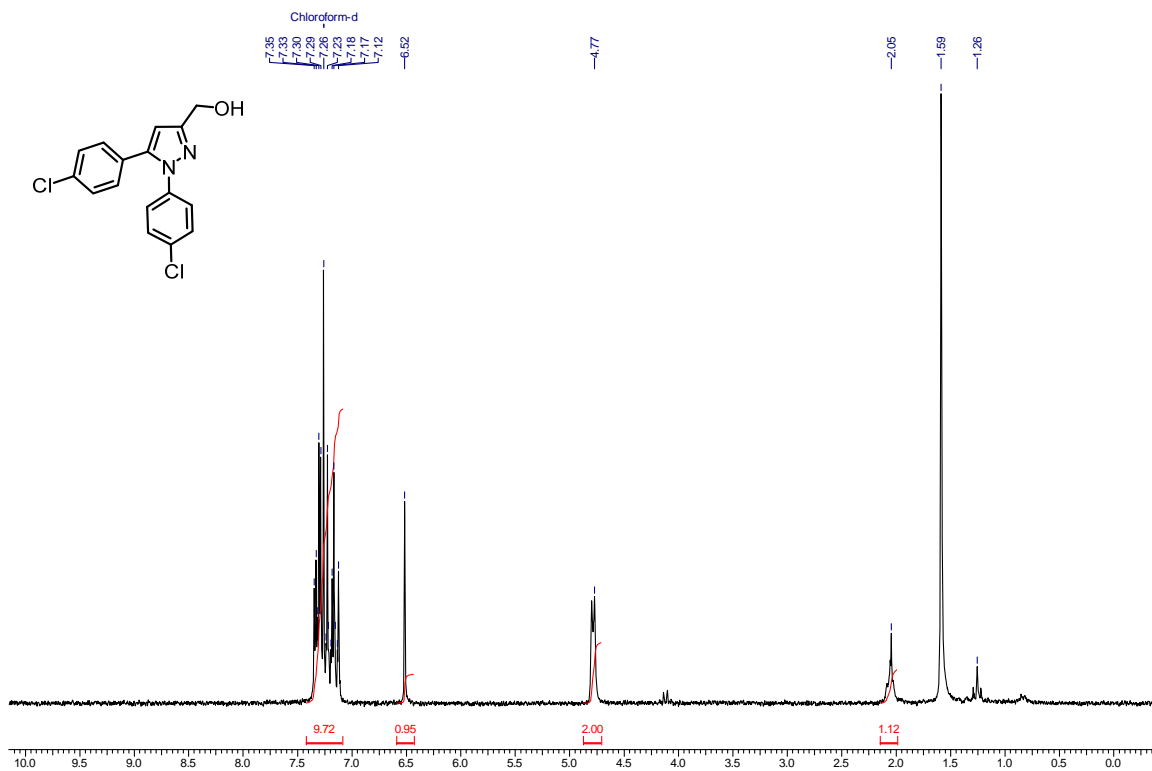
Figure 1.2.70. ^{1}H NMR of **51** (200 MHz, CDCl$_3$)
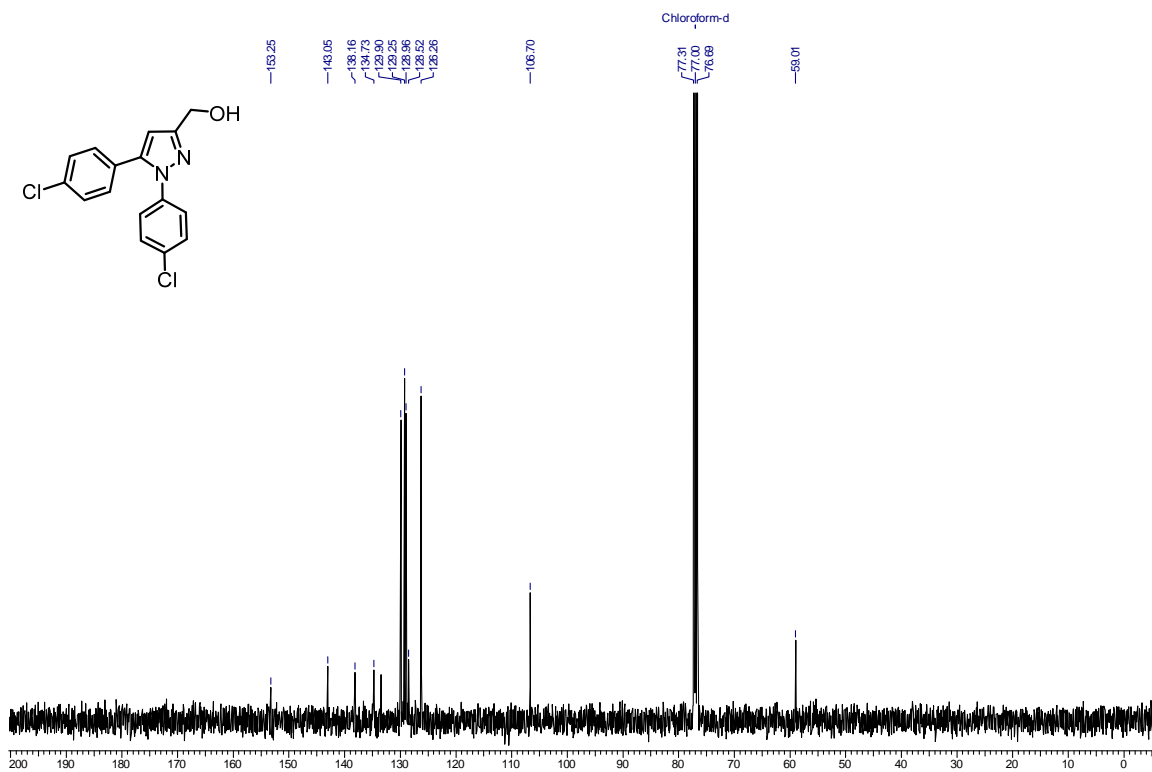
Figure 1.2.71. ^{13}C NMR of **51** (100 MHz, CDCl$_3$)
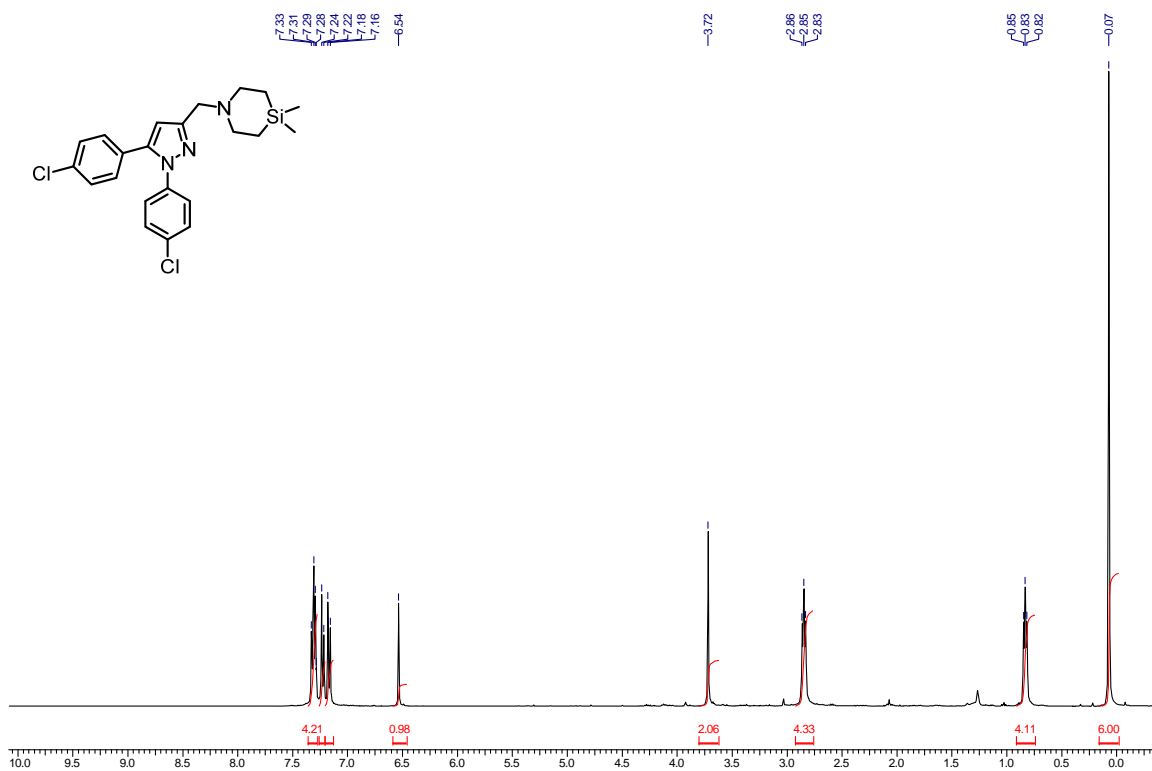
Figure 1.2.72. ^{1}H NMR of **52** (400 MHz, CDCl$_3$)
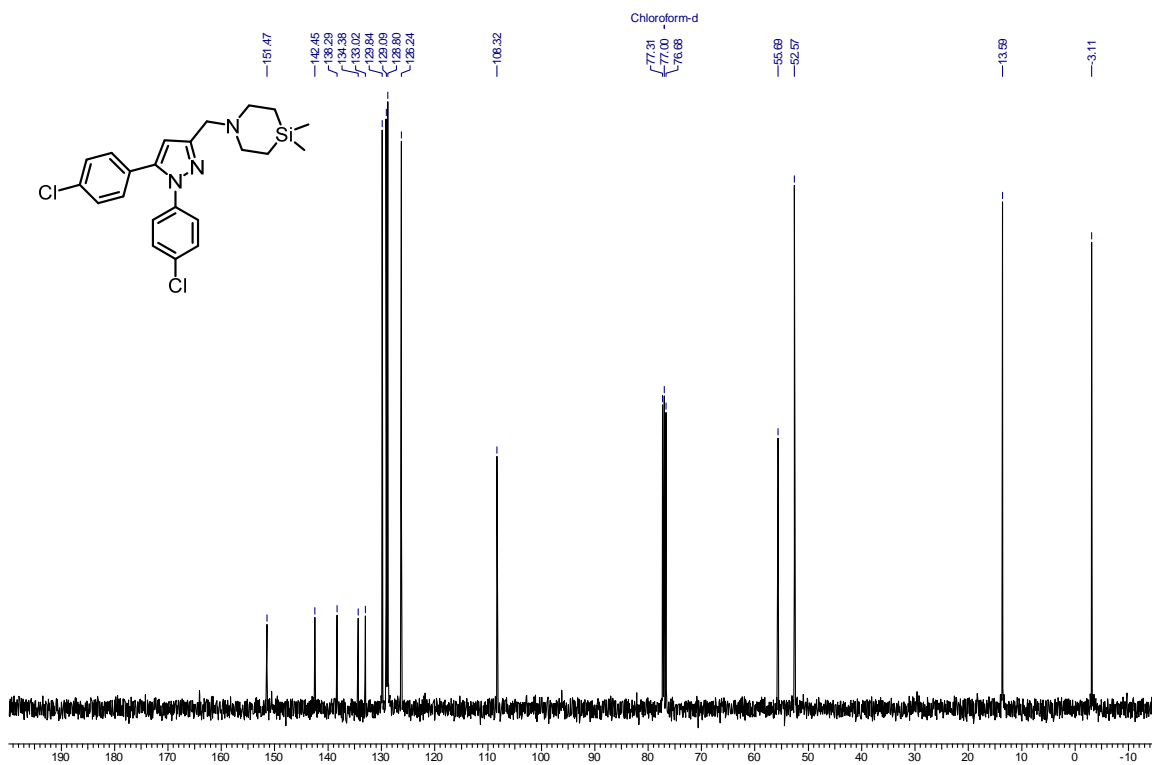
Figure 1.2.73. ^{13}C NMR of **52** (100 MHz, CDCl$_3$)

Figure 1.2.74. ^{1}H NMR of **53** (500 MHz, CDCl$_3$)

Figure 1.2.75. ^{13}C NMR of **53** (125 MHz, CDCl$_3$)
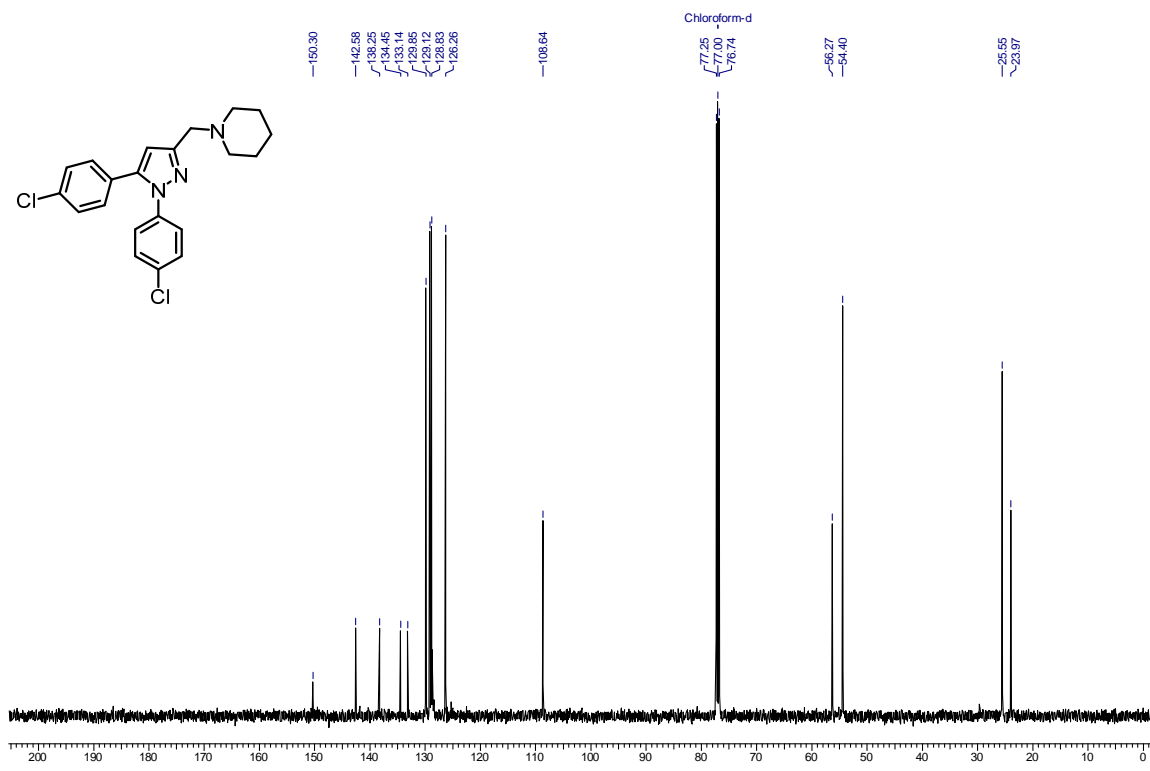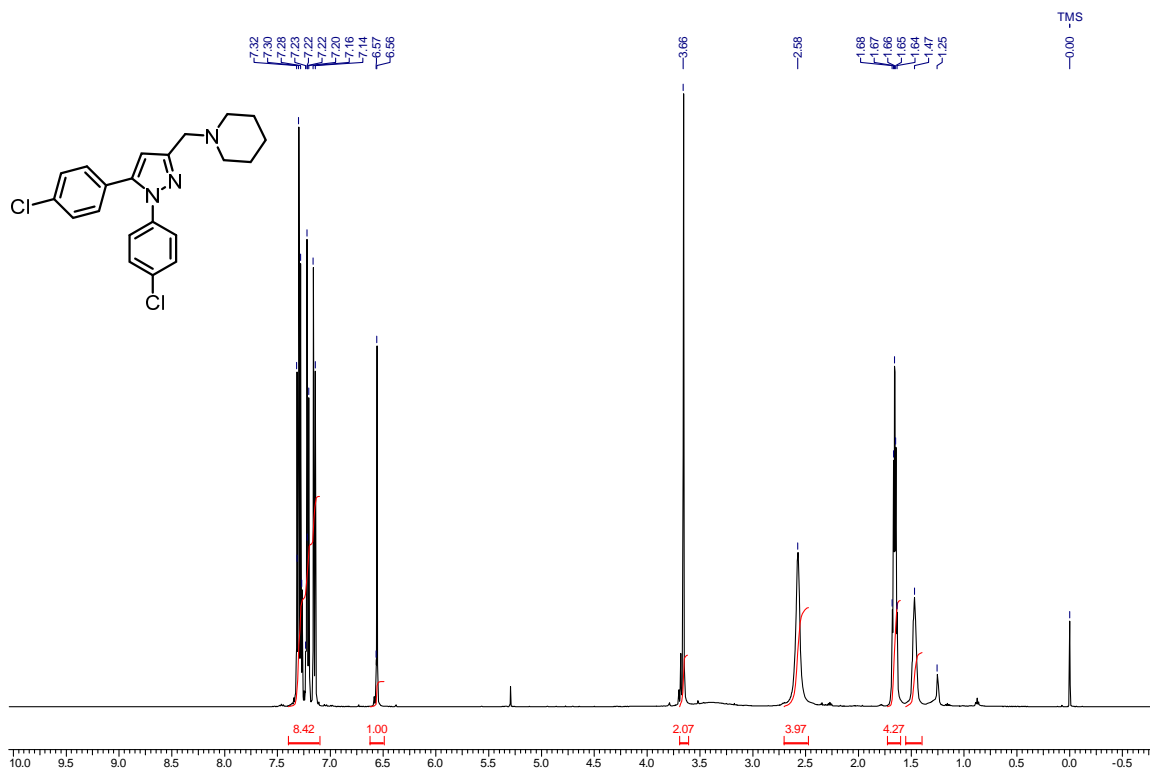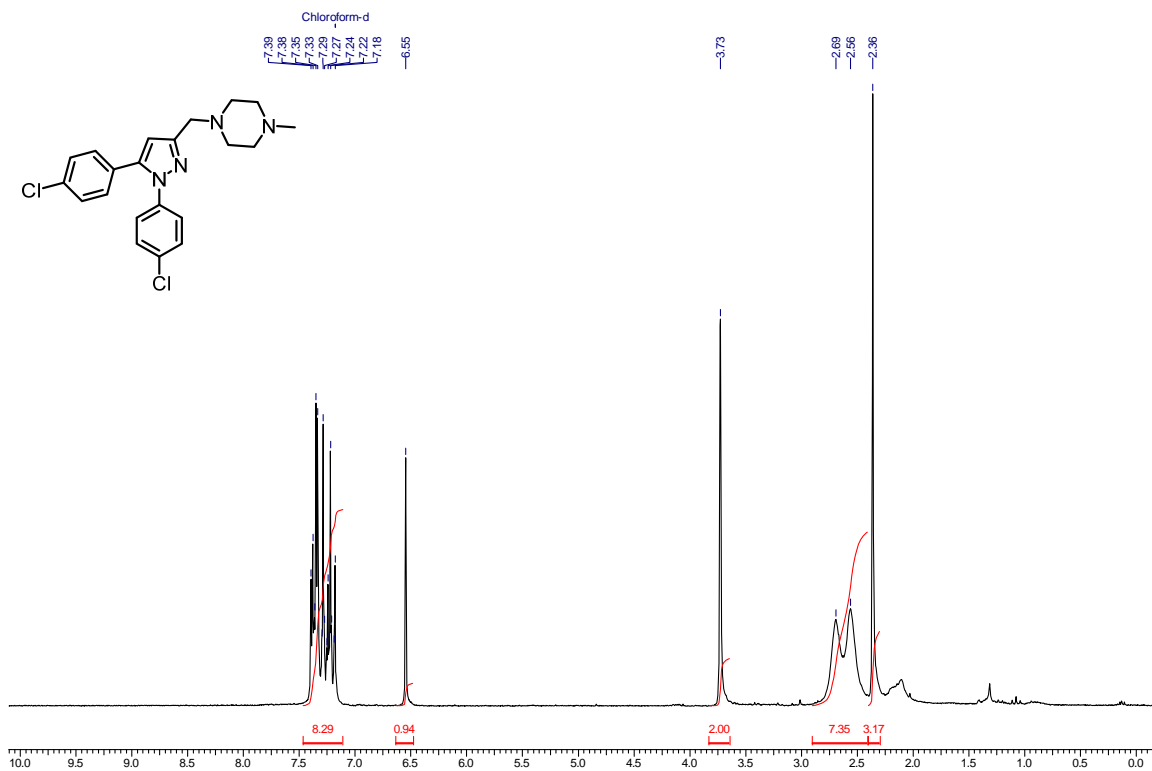
Figure 1.2.76. ^{1}H NMR of **54** (400 MHz, CDCl$_3$)
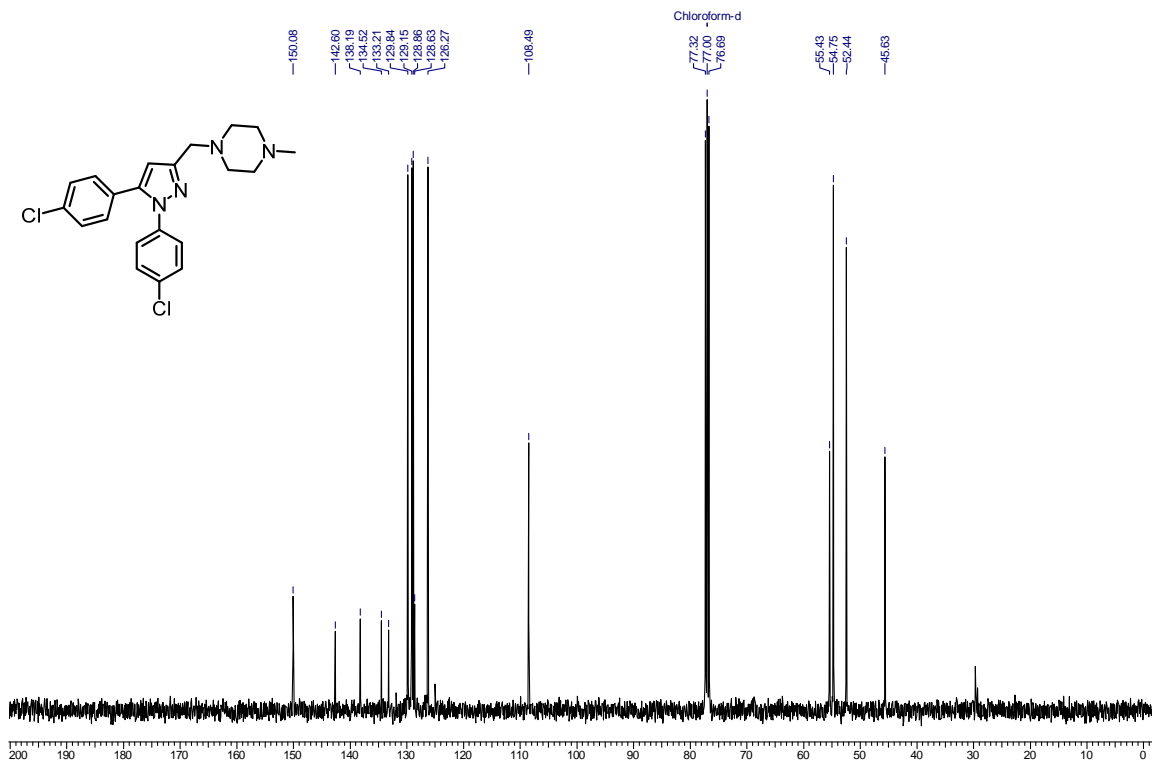
Figure 1.2.77. ^{13}C NMR of **54** (100 MHz, CDCl$_3$)

119
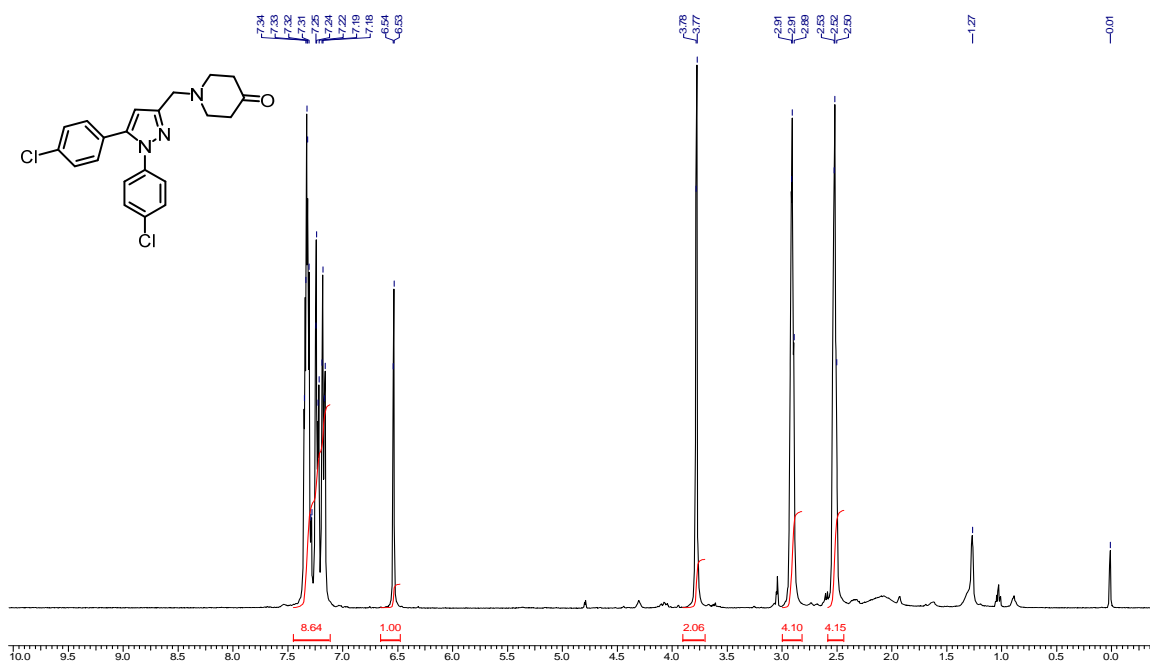
Figure 1.2.78. ^{1}H NMR of **55** (400 MHz, CDCl$_3$)
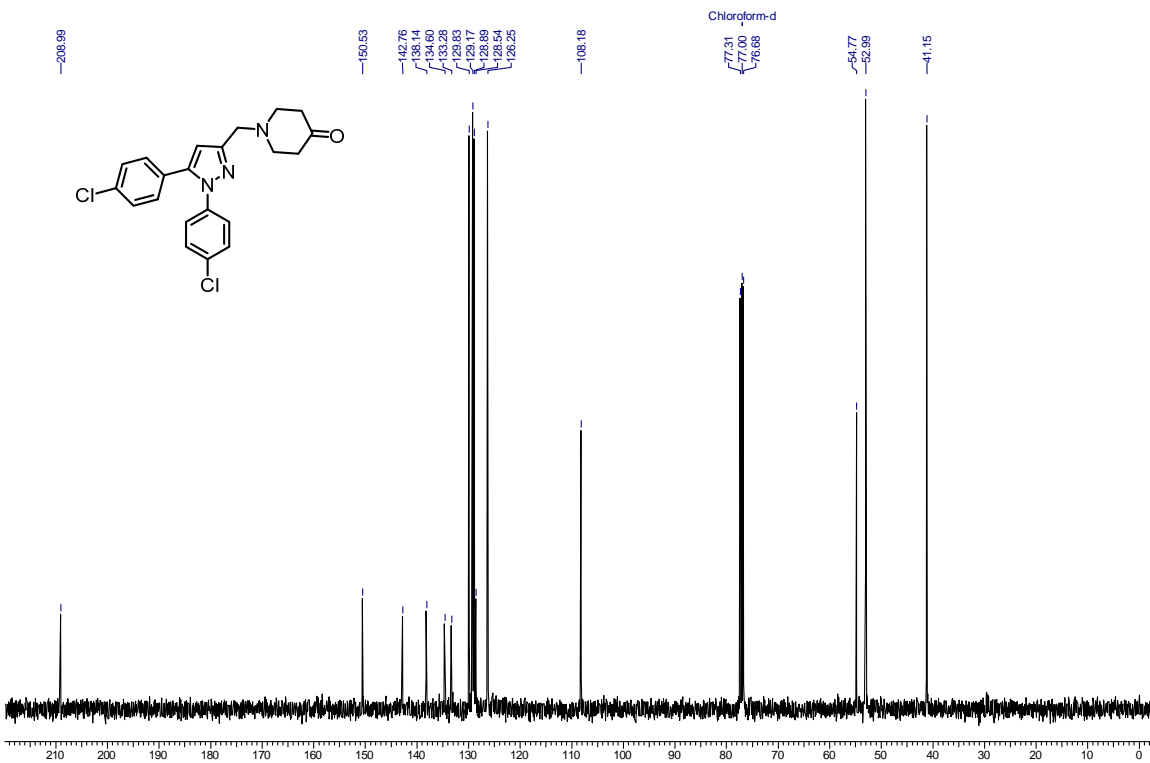
Figure 1.2.79. ^{13}C NMR of **55** (100 MHz, CDCl$_3$)
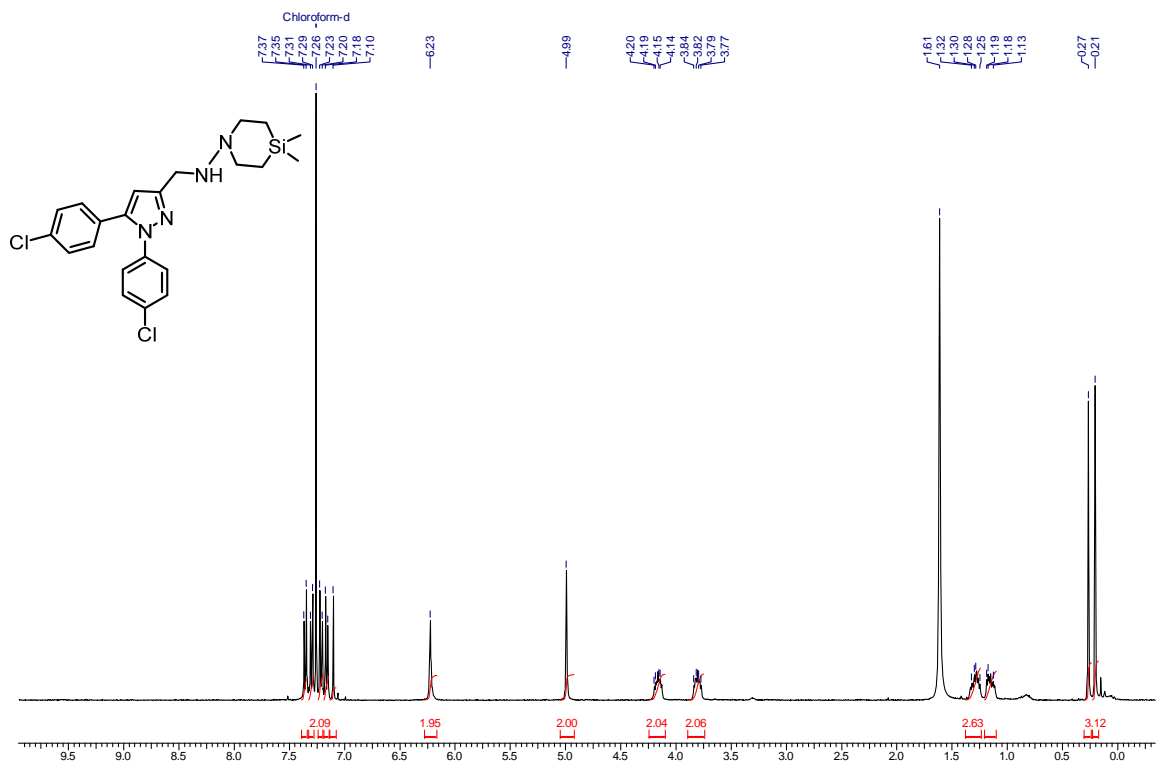
Figure 1.2.80. ^{1}H NMR of **56** (200 MHz, CDCl$_3$)
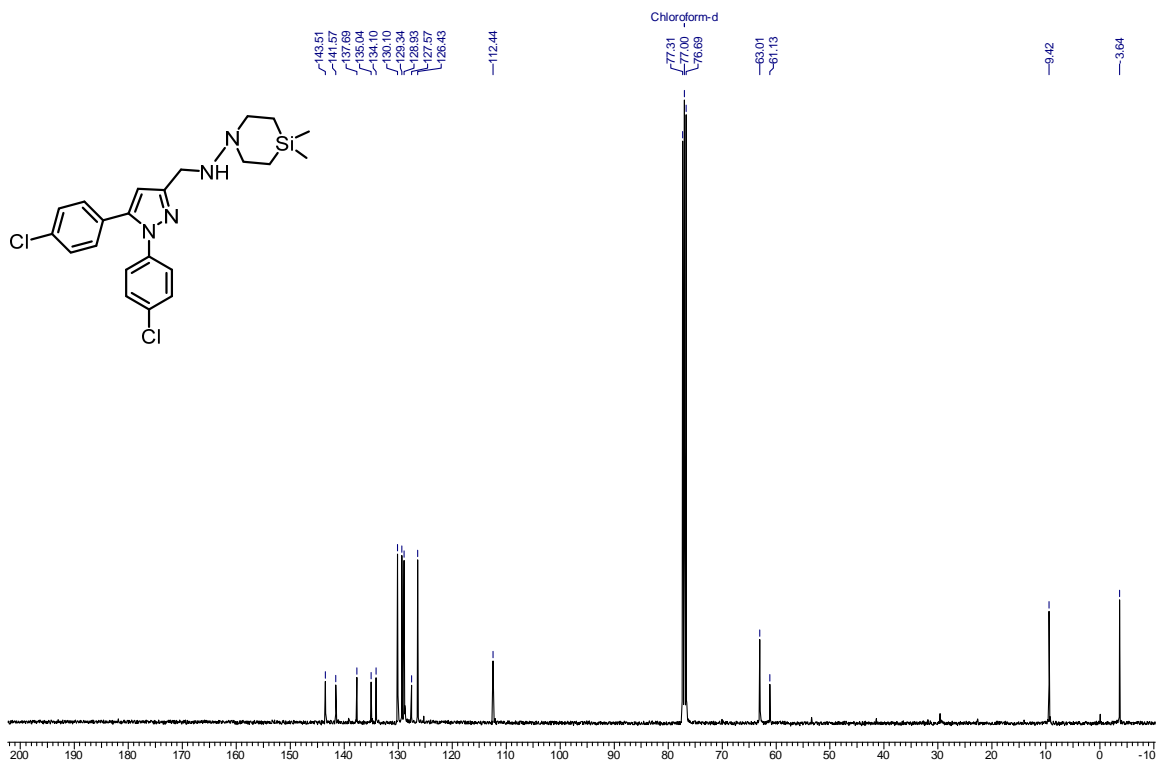
Figure 1.2.81. ^{13}C NMR of **56** (100 MHz, CDCl$_3$)

1.3.1. Allylsilanes

Organosilanes are extensively used in organic[1-9] as well as polymer chemistry.[10-12] Also, they are commonly encountered as protecting groups in organic chemistry. Silicon is found in nature as its oxide, but organosilanes are synthesized in the laboratory by a variety of methods.[13,14] The chemistry and reactivity of organosilanes can be reasoned on the basis of a few fundamental principles such as the β silicon effect.[15] The carbon-silicon bond (C-Si) is comparatively weaker than a C-C bond and hence can be broken more easily. A silyl group is also called a fat proton or super proton because it is used as a substitute for proton.[16]

Organosilanes do not occur in nature and are synthesized in the laboratory. Charles Friedel and James Crafts prepared the first organosilicon compound, tetraethylsilane by the reaction of tetrachlorosilane and diethylzinc (1863).[17] Later Kipping used Grignard reagents to displace the chloro group of silane and this is one of the most popular methods as of now to prepare organosilanes.[18,19] The electropositive nature of silicon makes it prone for attack by nucleophilic reagents, whereas a C-Cl bond would be inert under these conditions.

$$2\,ZnEt_2 \;+\; SiCl_4 \longrightarrow SiEt_4 \;+\; 2\,ZnCl_2$$
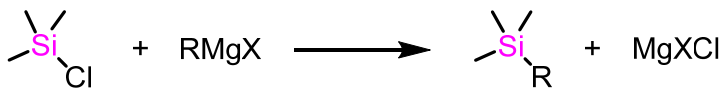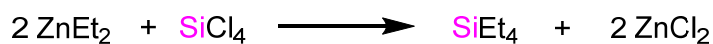
Figure 1.3.1. Synthesis of organosilanes

Allylsilanes are compounds in which a silicon atom is bonded to an allyl group. It is commonly used as an allylating reagent, although several other applications are also known.[20-29] They are usually prepared from chlorosilanes using organometallic reagents such as Grignard reagents.[30,31] Sakurai and co-workers used the more cheap metal, zinc for allylation of chlorosilanes in dimethylimidazolidinone (DMI) as solvent. DMI was chosen because regular solvents such as THF and DMF did not give satisfactory results.

The authors also reported that it was difficult to remove the excess DMI.[32] It is interesting to note that the first organosilane (tetraethylsilane) was also synthesized using zinc metal.[17]
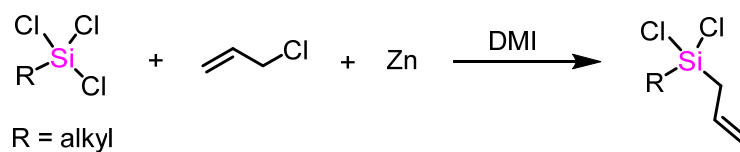
Figure 1.3.2. Synthesis of allylsilanes using zinc

Li *et.al.* used organosamarium reagent for the synthesis of allylsilanes from chlorosilanes. It is possible to control the number of allyl groups introduced on polychlorosilanes by changing the equivalents of samarium (fig. 1.3.3).[33]
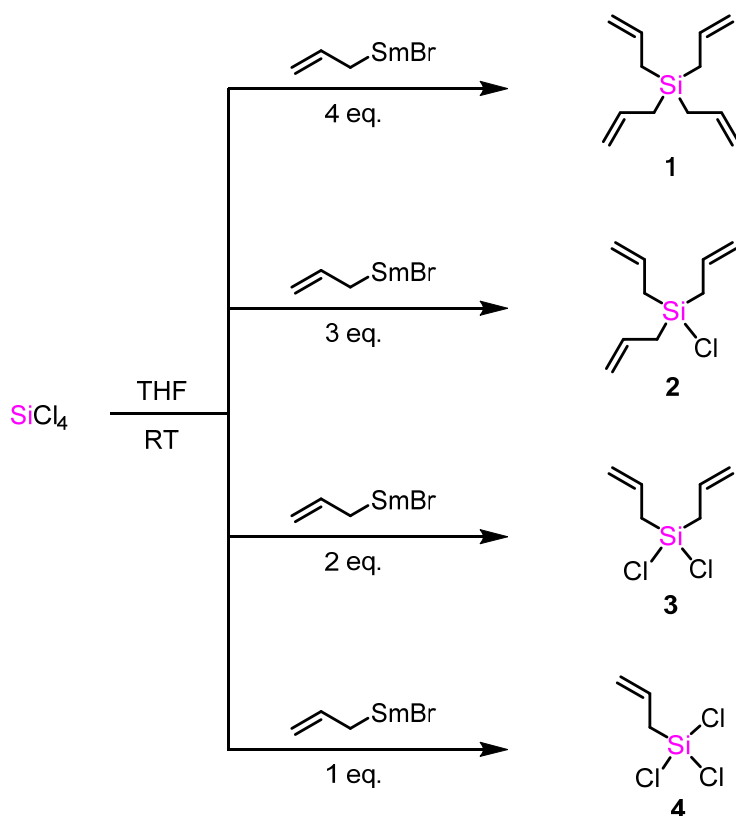
Figure 1.3.3. Synthesis of allylsilanes using samarium

Later Lai and co-workers reported the selective allylation and allenylation of chlorosilanes mediated by organoindium reagents.[34] In the case of unsymmetrical olefins

such as prenyl bromide, the rearranged product was observed (see compound **8**, fig. 1.3.4). Reactions using propargyl bromide gave the allene exclusively (compound **9**). They were also able to control the number of chloro groups replaced by changing the equivalents of indium and bromide (compound **7**).
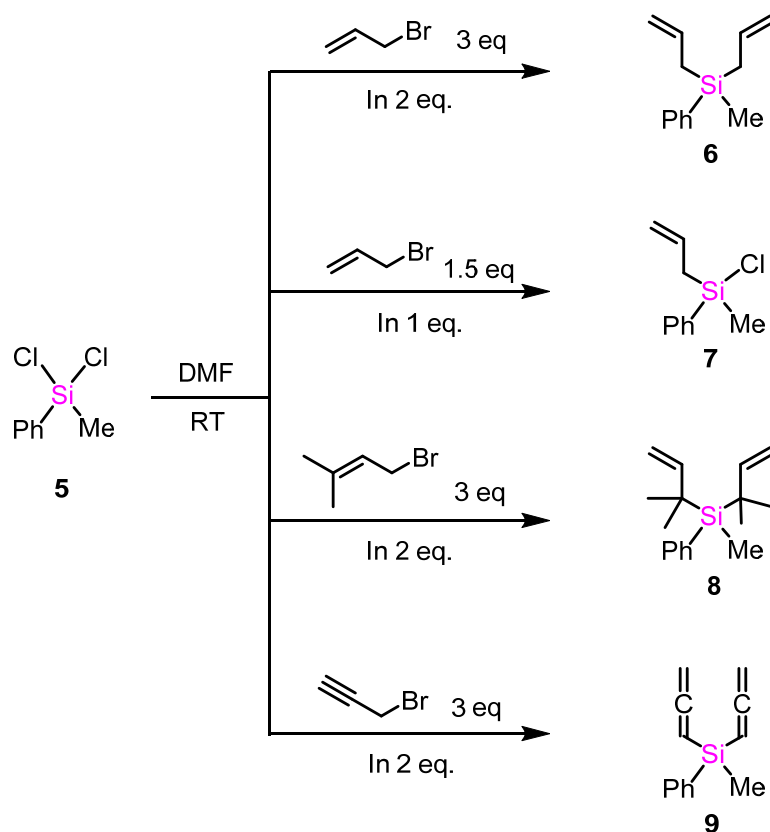
Figure 1.3.4. Synthesis of allylsilanes and allenylsilanes using indium

1.3.2. Present work

1.3.2.1. Ultrasound promoted synthesis of allyl and propargyl silanes

As discussed in the first section of this chapter, due to similarity with carbon, the study of biological properties of organosilanes is an interesting area of research. As part of an ongoing activity on the synthesis of silicon analogs of bioactive molecules, we became interested in exploring novel methodologies to access organosilanes. We reasoned that allylsilanes would be good starting points as they could be readily

functionalised and transformed to desired building blocks with silicon incorporation, which can be used for making biologically active compounds. The reported method for the conversion of chlorosilanes to allylsilanes using zinc has certain drawbacks and was not generalised.[32] We assumed that rate of the reaction could be enhanced by ultrasound waves (sonication).[35,36] The rate of Barbier reactions have been reported to be enhanced by sonications[37,38] and the sonochemical variant of the Reformatsky reaction is also known in the literature.[39,40]

In heterogenous reaction mixtures, the ultrasound waves disperse the solid, thereby increasing the surface area and enhancing the reaction rates.[35] Sonochemical reactions can be performed even in aqueous solutions contrary to the extreme dryness required for organometallic reactions. In the light of these literature reports we explored the reactions of various chlorosilanes with allyl bromide in presence of ultrasound waves.

Table 1.3.1. Optimization of reaction conditions
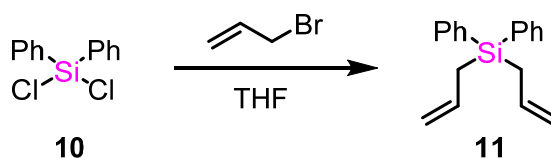
Sl. No.	Conditions	Time	Yield
1	Zn, RT	10 min	No reaction
2	Zn, RT	1 h	48%
3	Zn, RT	5 h	60%
4	Zn, RT,))))	10 min	88%

For the initial optimizations, we chose diphenyldichlorosilane (**10**) and allylbromide. Diphenyldichlorosilane (1 eq.), zinc dust (4 eq.) and allylbromide (4 eq.) were taken in dry THF and sonicated for 10 min in an ultrasound bath (37 kHz). The excess reagent was quenched with 1N aq. HCl and the pure product was isolated by column chromatography (88% yield). The ^{1}H NMR of the product was compared with

the reported values and was found to be identical.[34] The same reaction when carried out under conventional reaction conditions gave a yield of 60% of the product after 5h (table 1.3.1). This clearly indicates that the reaction rate was enhanced by sonication. The experiment is also simple, good yielding and uses the cheap metal zinc.
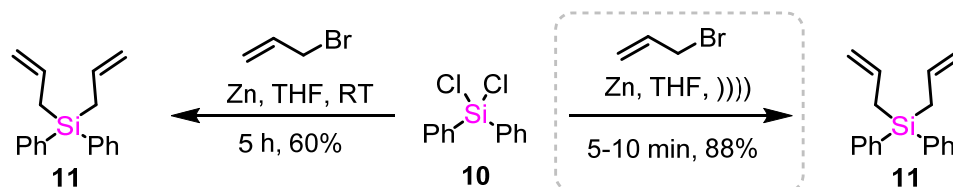
Scheme 1.3.1. Ultrasound promoted synthesis of allylsilanes
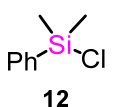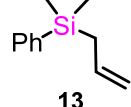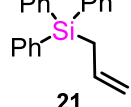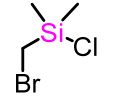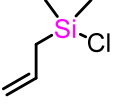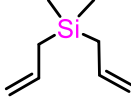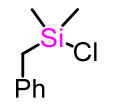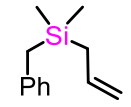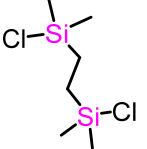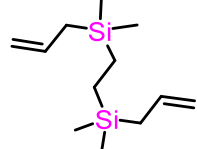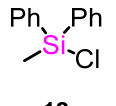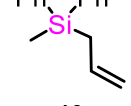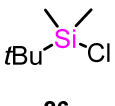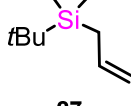
The reaction was then generalised by taking different chlorosilanes. Chlorosilanes having aromatic substitution or any higher molecular weight groups were preferred for the ease of isolation of product. For each equivalent of chlorine to be displaced, 2 equivalents of bromide and 2 eq. of zinc were used. All chlorosilanes used in the present study were purchased from commercial sources. The starting materials were taken in THF, sonicated for 10 min and then the product was isolated by column chromatography. All the products were highly non polar and was eluted using pet ether.
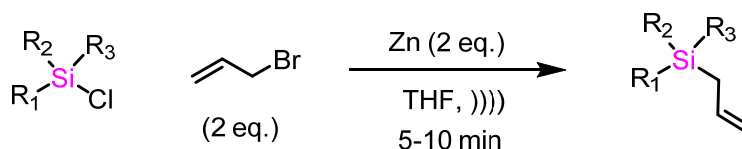
Scheme 1.3.2. General scheme for allylation of monochlorosilanes

Addition of one allyl group was demonstrated using monochlorosilanes **12**, **14**, **16**, **18**, **20** and **22**. The compound **23** was isolated in lesser yields (22%) which may be due to its volatility. The reaction went well with compound **24** having two chlorosilanes in the same molecule. The ^{1}H NMR of all the compounds were compared with the reported values and found to be matching. Unfortunately, the reaction did not work with *tert*-butyl(chloro)diphenylsilane (TBDPSCl, **26**) which may be due to steric crowding of *t*-butyl group.

Table 1.3.2. Allylation of monochlorosilanes

chlorosilane	product	yield	chlorosilane	product	yield
12	**13**	98%	**20**	**21**	88%
14	**15**	71%	**22**	**23**	22%
16	**17**	95%	**24**	**25**	81%
18	**19**	71%	**26**	**27**	No reaction

The addition of two allyl groups on dichlorosilanes gave products **6**, **23**, **28**, and **29**. The volatile compound **23** was earlier prepared by monoallylation of allyl(chloro)dimethylsilane **22**.
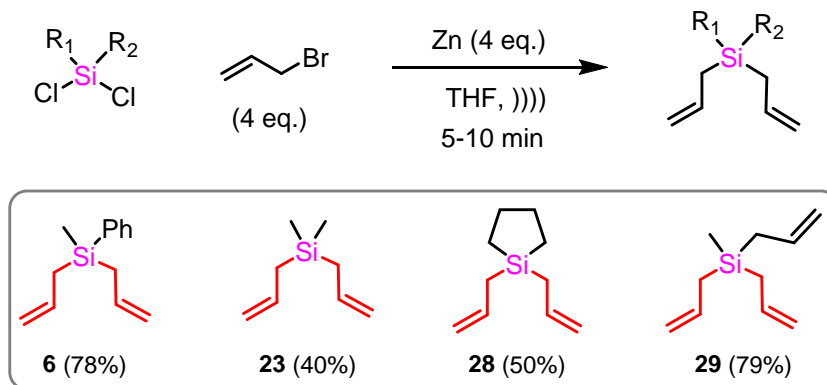
Scheme 1.3.3. Allylation of dichlorosilanes

Triallylation was done on phenyltrichlorosilane **30** and the product **31** was obtained with a moderate yield of 60%. All the compounds were colourless liquids with the exception of **21** obtained as a colourless solid. The synthesized allyl silanes are known in the literature and ^{1}H NMR values were found to be consistent with the literature reports.
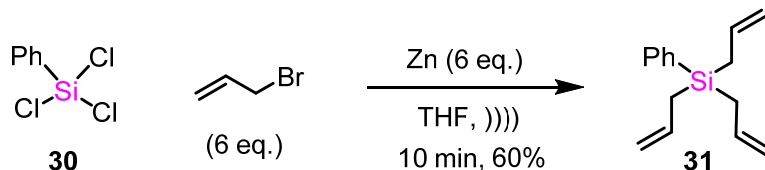
Scheme 1.3.4. Allylation of trichlorosilane **30**

After the successful experiments with allylation, we explored the reaction of chlorosilanes with propargyl halides. The reaction of monochlorosilanes **12** and **16** with propargyl bromide proceeded smoothly to give exclusively the propargyl compounds **32** (98% yield) and **33** (82% yield) respectively. The rearranged allene product was not observed in both the cases. The reported indium mediated reaction of chlorodimethyl(phenyl)silane (**12**) with propargyl bromide gave exclusively the allene (96% yield). The reaction of monochlorosilane **12** with Grignard reagent is known to give a mixture of propargyl and allene derivatives with the propargyl compound **32** as the major product.[41] The ^{1}H NMR values of **32** were found to be in agreement with the reported values.[41,42] The acetylenic proton appeared at δ 1.86 ppm (t, J = 2.9 Hz) and the propargylic protons were observed at δ 1.72 ppm (d, J = 2.9 Hz). The ^{1}H NMR of compound **33** showed a triplet at δ 1.88 ppm (J = 3.0 Hz) corresponding to the acetylenic proton. The propargylic protons resonated upfield at δ 1.44 ppm further confirming the product formation. The benzylic proton was seen at δ 2.21 ppm as a singlet. In ^{13}C NMR, the acetylene carbons appeared at δ 82.1 and 67.3 ppm. The benzylic carbon was observed at δ 24.2 ppm and the propargylic carbon was found to be highly shielded and showed at δ 4.9 ppm. The gem dimethyls attached to silicon appeared at δ -4.2 ppm.
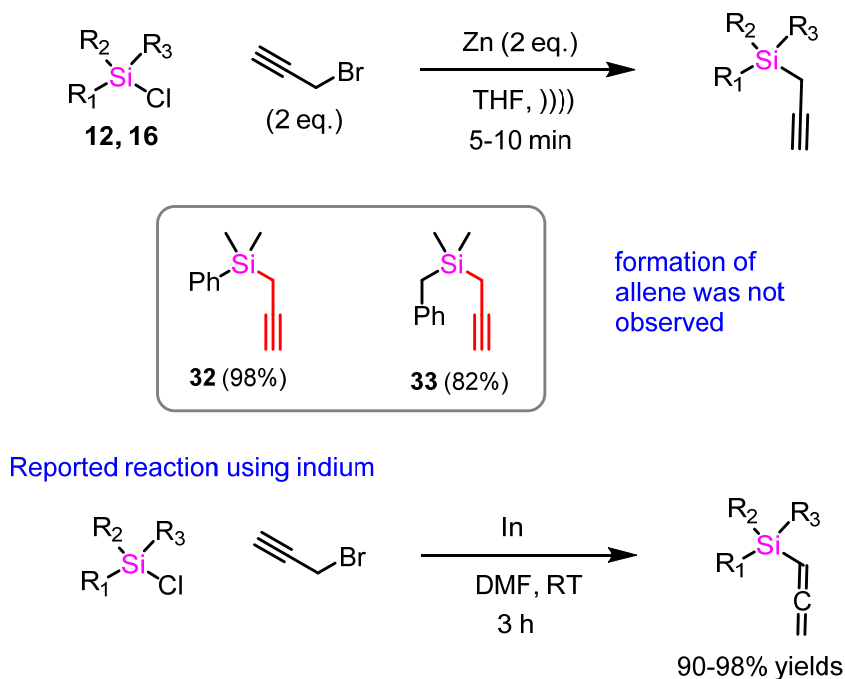
Scheme 1.3.5. Propargylation of monochlorosilanes

Dichlorosilanes **5** and **10** gave the dipropargyl compound (**34**, **36**) as the major product along with minor amount of the propargylallenyl compound (**35**, **37**). On thin layer chromatography, the allene was non polar compared to the propargyl compounds. The compounds could be cleanly separated by column chromatography on silica gel using pet ether as the eluent. The compounds **34** and **36** are already known in the literature and NMR spectra were matching with the reports.[43] In **37**, the allene protons were observed at δ 5.33 (t, J = 7.1 Hz, 1H) and δ 4.47 (d, J = 7.2 Hz, 2H) ppm. The propargylic protons appeared at δ 2.14 (d, J = 3.0 Hz, 2H) ppm and the acetylenic proton at δ 1.86 (t, J = 2.9 Hz, 1H) ppm confirming the structure. In ^{13}C NMR, the characteristic sp hybridised carbon of allene appeared at δ 215.1 ppm. The sp^{2} hybridised carbons of allene appeared at δ 75.9 and 68.7 ppm. The acetylene carbons appeared at δ 80.9 and 68.6 ppm. In IR spectra of **37** the alkyne stretching was observed at 2252 cm^{-1} and the allene stretching at 1930 cm^{-1}.
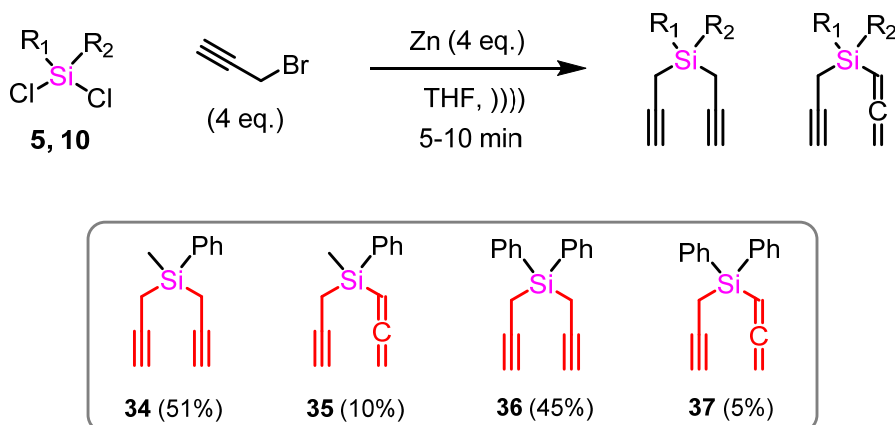
Scheme 1.3.6. Propargylation of dichlorosilanes

1.3.2.2. Synthesis of constrained sila amino acids

After successfully developing a new methodology for the synthesis of allyl and propargyl silanes, our next goal was to utilize these building blocks for the synthesis of biologically active compounds. In this context, the zirconacyclization of allyl silanes caught our attention. Nugent *et. al.* first reported the zirconium mediated cyclization of 1,6-dienes to give cyclopentanes such as **38**.[44] The zirconocene equivalent (developed by Negishi) is generated by the reaction of zirconocene dichloride and *n*-BuLi.[45] This zirconocene (Cp_2Zr) generated in situ reacts with 1,6-dienes to give a zirconacycle intermediate which on reaction with electrophiles give cyclic products.[46-49] The relative stereochemistry of the product depends on several factors such as substrate and ligands on zirconium. Diallyldimethylsilane (**23**) on zirconacyclization followed by treatment with iodine gives the compound **38** with a *trans* stereochemistry. We sought to use this compound for the synthesis of constrained silicon containing amino acids.
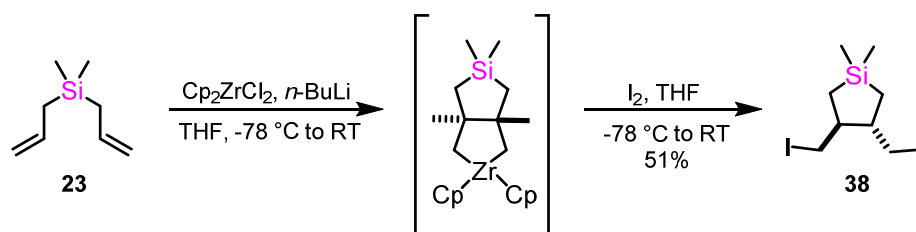
Scheme 1.3.7. Zirconacyclization of diallylsilane

As mentioned in the first section of this chapter, there is considerable interest on silicon amino acids and some of them have been incorporated into biologically active peptides.[50-54] Peptides incorporated with sila amino acids showed greater cell penetration as well as increased resistance to biodegradation. Although silicon amino acids have several attractive features, they are few in number with limited structural variations. Unnatural amino acids are good building blocks in drug discovery and are also used to probe the conformation of peptides.[55-59]

Compound **38** was prepared following procedures known in the literature.[47,49] After addition of diene **23** to zirconocene, a blood red colour was observed indicating the formation of zirconacycle. This reaction mixture was treated with iodine and the product **38** was purified by column chromatography. The NMR values were in agreement with previously reported data.[49] The reaction of ethylisocyanoacetate with the iodo derivative **38**, base K_2CO_3 and phase transfer catalyst 18-crown-6 went well in acetonitrile solvent and the isocyanoester **39** was obtained in good yield (74%). It is analogous to the procedure reported by Kotha and co-workers on carbon version to synthesize unnatural α-amino acids.[60,61] The IR spectra showed a strong absorption at 2134 cm^{-1} characteristic of isocyanide. The ^{1}H NMR indicated the presence of ethyl ester; 4.26 (q, J = 7.0 Hz, 2H), 1.33 (t, J = 7.0 Hz, 3H). The ^{13}C NMR showed the presence of ester carbonyl at δ 170.4 ppm and isocyanide at δ 157.3 ppm further confirming the structure. In an all carbon 5,5-fused system, the *cis* junction is generally favoured over the more strained *trans* isomer. The increased Si-C bond length compared to C-C bond may result in more flexibility for this system over a carbon analog.[62] The isocyanide **39** on exposure to HCl gave the amine **40** by hydrolysis. The amine was protected as carbamate to give the orthogonally protected α–amino acid **41**. The NMR data agreed with the structure and HRMS analysis showed peak at 364.1910 corresponding to $C_{17}H_{31}NO_4NaSi$ [M + Na]$^+$ further justifying the structure. The ester was subjected to base hydrolysis followed by deprotection of Boc in acidic conditions. The solid obtained after evaporation of the solvent was washed with diethyl ether to obtain the pure α- amino acid **42**. The spectral data was in agreement with the structure.
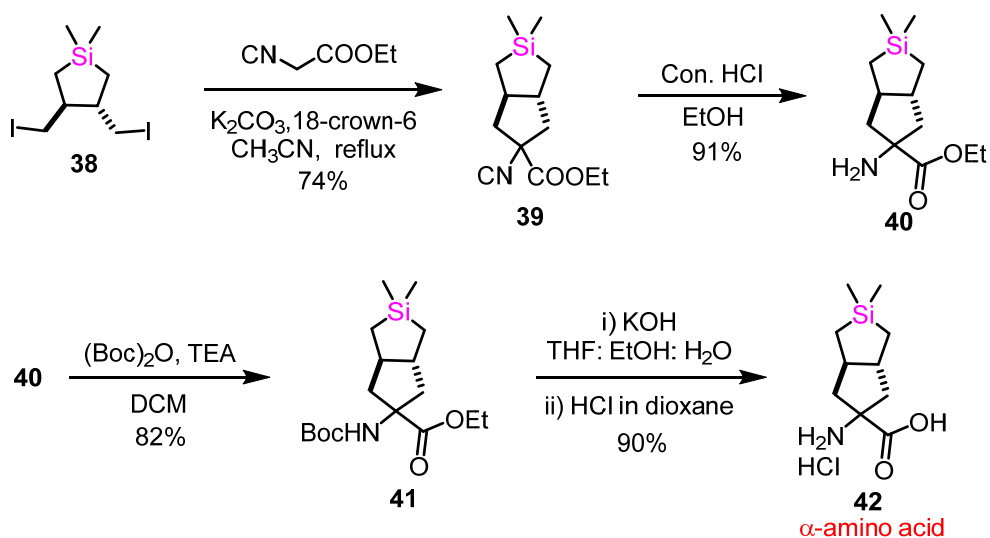
Scheme 1.3.8. Synthesis of constrained sila α− amino acid

The same protocol was expanded for the synthesis of β− and γ− amino acids. The compound **38** on reaction with ethylcyanoacetate under the similar conditions gave the cyanoester **43** (86% yield). Dilution was found to an important factor in this reaction ($\sim 10^{-2}$ M). The peak at δ 122.2 ppm in ^{13}C NMR and IR peak at 2200 cm^{-1} confirmed the presence of cyano group.
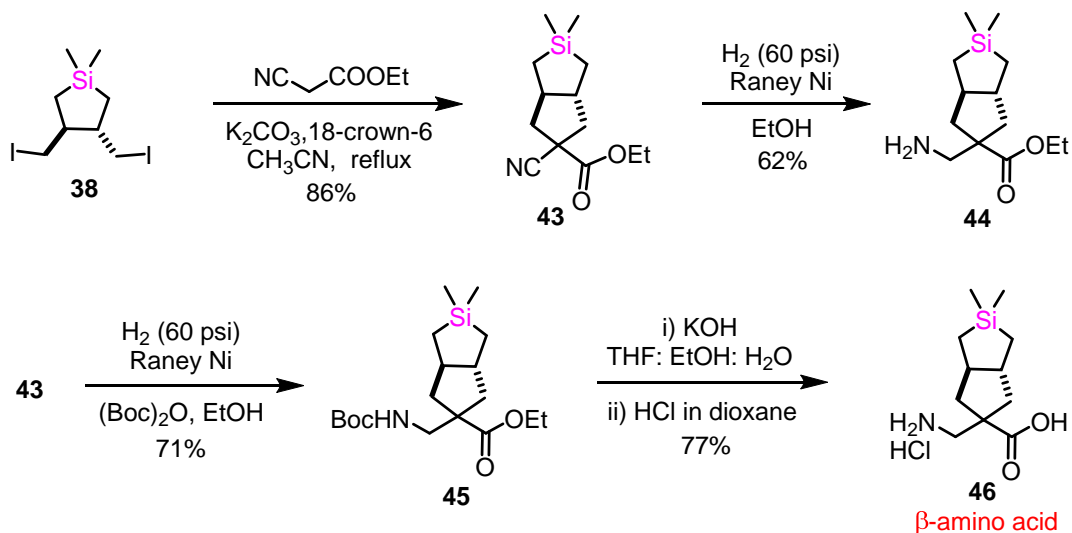
Scheme 1.3.9. Synthesis of constrained β−amino acid

The cyano group in **43** was chemoselectively reduced by catalytic hydrogenation (60 psi pressure, Raney Ni) to give the β–amino acid as its ethyl ester (**44**). The reduction was also carried out in presence of Boc anhydride to give the orthogonally protected β–amino acid **45** in better yield. The peaks at δ 4.15 and 1.29 ppm in ^{1}H NMR correspond to the ethyl ester. The methylene attached to amine appeared at δ 3.35 - 3.22 ppm as a multiplet. In ^{13}C NMR, the ester carbonyl appeared at δ 177.9 ppm and Boc carbonyl at δ 156.3 ppm. The HRMS analysis showed a peak at $C_{18}H_{33}NO_4NaSi$ [M + Na]$^+$ which is also in agreement with the structure. Ester hydrolysis followed by carbamate deprotection gave the β–amino acid **46** in moderate yield.

After successfully synthesizing α–and β–amino acids with a novel skeleton, we turned our attention towards the synthesis of a γ–amino acid/ GABA analog. GABA (γ–amino butyric acid) is the major inhibitory neurotransmitter present in the central nervous system of mammals. Neurotransmitters are molecules which help to transmit the signals across a synapse. Deficiency of GABA leads to several neurological disorders. GABA is synthesized inside the brain by decarboxylation of amino acid glutamic acid. GABA when administered externally cannot reach the brain because it cannot cross a protective barrier called the blood brain barrier (BBB).[63,64]
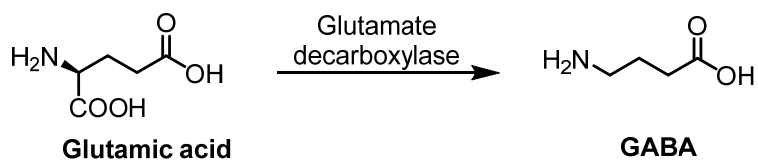
Figure 1.3.5. Biosynthesis of GABA

The knowledge of BBB traces back to 1885 when bacteriologist Paul Ehrlich discovered that all organs except brain was stained by aniline dyes. The endothelial cells of the brain capillaries have tight junctions which is called blood brain barrier. This barrier selectively allows the passage of certain molecules to the brain. Small lipophilic molecules can diffuse through this barrier. Also, certain polar compounds such as amino acids cross BBB with the help of carrier proteins. On one hand the BBB protects the

brain from pathogens, but on the other hand it makes drug delivery to the brain a tough task.[65-69] According to some reports, nearly 98% of small molecule drugs do not cross BBB.[66]

Atagabalin
(insomnia
Phase II)

Gabapentin
(epilepsy
marketed)

Mirogabalin
(neuropathic pain
Phase III)

Baclofen
(skeletal muscle
relaxant, marketed)

Phenibut
(psychotropic drug
limited clinical use)

Pregabalin
(anticonvulsant
marketed)

Vigabatrin
(epilepsy
marketed)

Picamilon
(dietary supplement)

Hopantenic acid
(psychotropic
limited clinical use)
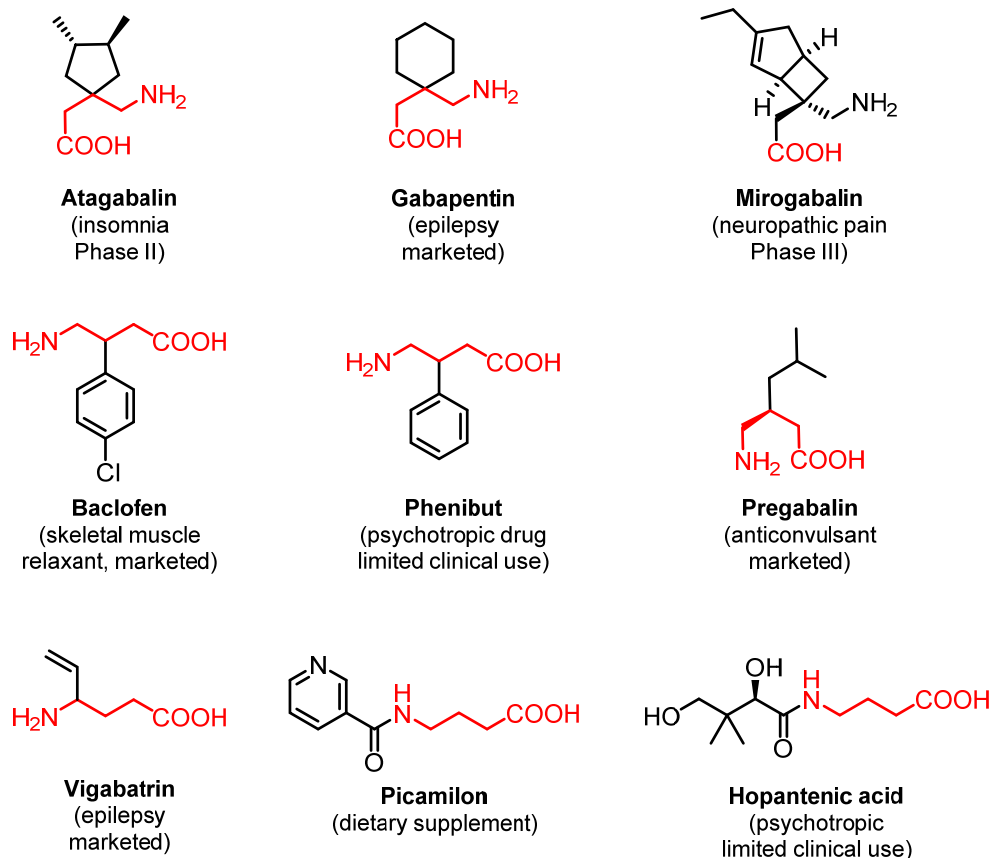
Figure 1.3.6. Some of the known GABA analogs

Low levels of GABA can lead to anxiety, depression, chronic pain, muscle tension and so on. To treat GABA deficiency, lipophilic and rigid analogs of GABA have been synthesized (fig. 1.3.6).[63,64,70] GABA analogs typically have anti-anxiety and anti-convulsive effects. Since GABA binds to different receptors with different conformations, GABA analogs have rigid structures so as to control their binding to the target. In gabapentin, the cyclohexane ring makes the molecule to adopt a particular conformation which mimics the amino acids and then the molecule is transported to the brain by the amino acid transporter.[63]
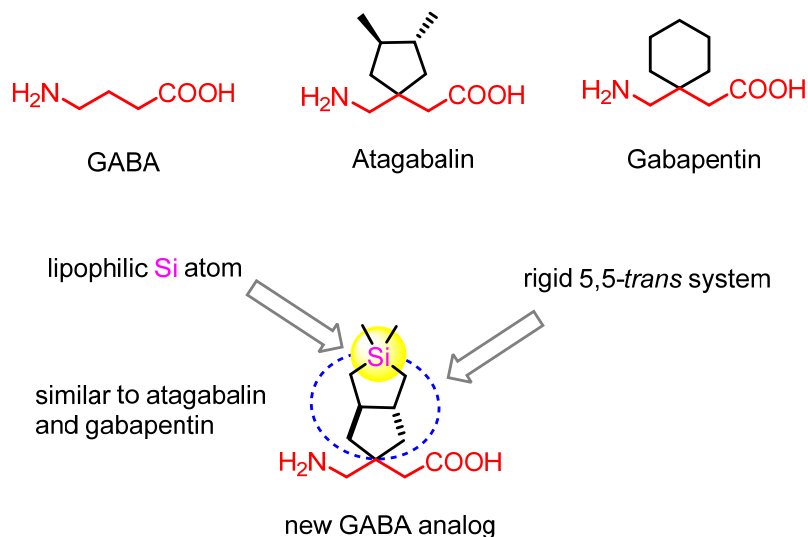
Figure 1.3.7. Design of sila GABA

Considering the importance of GABA analogs, we designed a novel silicon analog of GABA as shown in figure 1.3.7. The intermediate **43** could be transformed to the newly designed sila GABA analog by simple functional group interconversions.[71] The compound **43** was converted to nitrile **48** by ester hydrolysis followed by decarboxylation of acid **47**. The methine α to cyano appeared at δ 3.03 ppm in ^{1}H NMR as a multiplet. The characteristic IR stretching of nitrile was observed at 2260 cm^{-1}. Our initial attempt to synthesize nitrile **48** from **43** in one step by Krapcho decarboxylation (LiCl, DMSO, 150 °C, microwave) was not successful.[72]
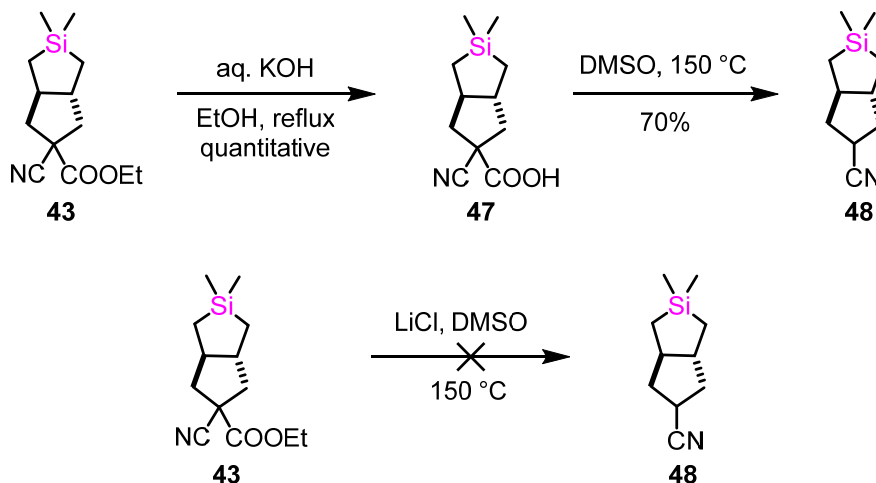
Scheme 1.3.10. Synthesis of nitrile **48**

The nitrile **48** was then alkylated with prenyl bromide and NaHMDS to give the olefin **49**. On TLC, the product appeared non polar compared to starting material along with another very close spot. We were not able to obtain pure **49** and hence the impure material was used for the next step. The olefin was subjected to cleavage under ozonolysis (met. NaOH) to get the ester **50**.[73] Although this reaction was clean, the overall yield from **48** to **50** was less (26%) because of poor yields obtained in alkylation. In ^{1}H NMR, the methyl ester appeared at δ 3.74 ppm as a singlet. The ^{13}C NMR also showed a peak at δ 169.8 ppm indicating ester and another peak at δ 125.7 ppm suggesting the presence of nitrile group. The HRMS analysis also confirmed the formation of product. The IR stretching of nitrile was observed at 2233 cm^{-1}.
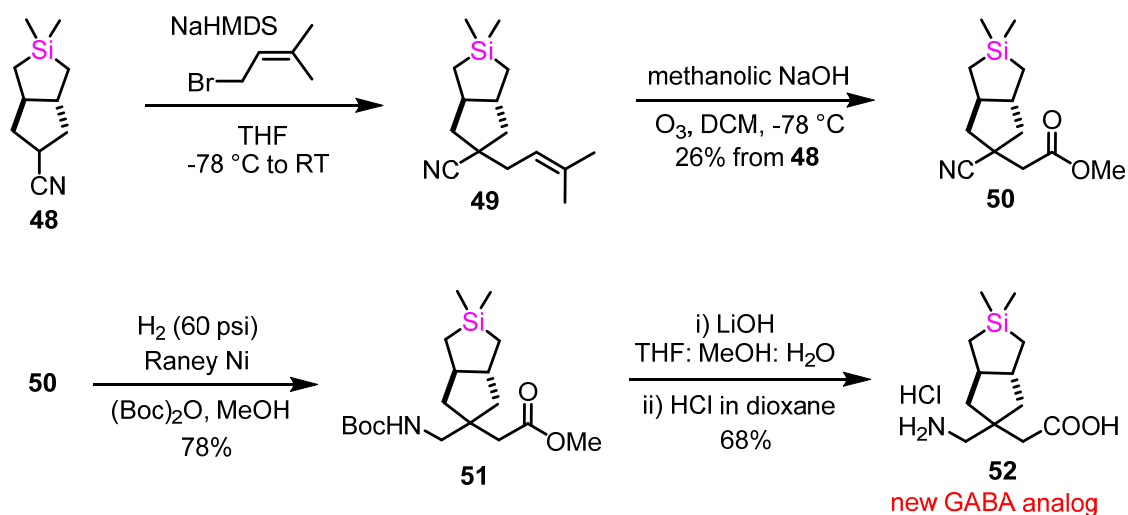
Scheme 1.3.11. Synthesis of silicon containing GABA analog

The cyano **50** was then hydrogenated (60 psi pressure, Raney nickel catalyst) in presence of Boc anhydride. TLC indicated clean conversion with the formation of a slightly non polar spot which was isolated by column chromatography. The ^{1}H NMR matched with the gross structure and ^{13}C NMR showed presence of ester carbonyl (δ 172.8 ppm) and carbamate carbonyl (δ 156.4 ppm) further confirming the structure. The HRMS analysis also revealed a mass peak at 378.2068 corresponding to $C_{18}H_{33}NO_4NaSi$ matching with the structure **51**. The compound **51** was transformed to the γ-amino acid

52 by using similar procedures; ester hydrolysis and Boc deprotection. This compound is a lipophilic and constrained analog of GABA and is expected to show interesting biological activity. Also, the compound is similar to the marketed anti-epileptic drug gabapentin[74,75] and another preclinical candidate atagabalin.[71]

1.3.3. Conclusions

A new methodology has been developed which provides easy and rapid access to allyl and propargyl silanes. The synthesis of propargyl silanes is interesting because, classical methods lead to the formation of allenes. The reaction conditions are mild, easy to operate, use the cheap metal zinc and are rapid (~10 min). One of the products, diallyldimethylsilane was used as starting material to synthesize $\alpha-$, $\beta-$ and $\gamma-$amino acids with 5,5-*trans* fusion. Unnatural amino acids find applications in drug discovery and peptidomimetics. The new GABA analog with silicon incorporation is an attractive candidate for biological evaluation. Lipophilic and conformationally rigid GABA analogs are known to cross BBB and are used for treating several CNS disorders.

1.3.4. Experimental Section

1.3.4.1. General procedure for allylations / propargylations of chlorosilanes.

Allyl bromide (2 mmol), Zn dust (2 mmol) and monochlorosilane (1 mmol) were taken in dry THF (5 mL) and sonicated by placing in an ultrasound cleaning bath (37 kHz, 320 W). After consumption of starting material (approx. 10 min.), the reaction mixture was cooled to 0 °C and saturated ammonium chloride was added till the excess Zn dissolved. Diethyl ether was added and the organic layer was separated. The aqueous layer was then extracted twice with diethyl ether, dried over Na_2SO_4 and the solvent was removed. The crude reaction mass was then purified by column chromatography on silica gel (100-200) using pet ether to afford the pure compound. In the case of polychlorosilanes, for each equivalent of chloro to be displaced 2 eq of Zinc and 2 eq. of bromide was used. In order to synthesize propargyl derivatives, propargyl bromide was used and similar procedure was followed.

Benzyldimethyl(prop-2-yn-1-yl)silane (33)
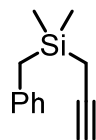
Yield: 82%

IR υ_{max}(thin film, CHCl$_3$): 3313, 3025, 2959, 2117, 1726, 1601, 1494 cm^{-1}

^{1}H NMR (200 MHz, CDCl$_3$): δ 7.24 - 6.96 (m, 5H), 2.21 (s, 2 H), 1.88 (t, J = 3.0 Hz, 1H), 1.46 - 1.43 (m, 2H), 0.09 (s, 6H).

^{13}C NMR (125 MHz, CDCl$_3$): δ 139.3, 128.3, 128.1, 124.2, 82.1, 67.3, 24.2, 4.9, -4.2

MS (70 eV) m/z 188.

Methyl(phenyl)(prop-2-yn-1-yl)(propa-1,2-dien-1-yl)silane (35)
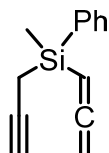
Yield: 10%

IR υ_{max}(thin film, CHCl$_3$): 3295, 3071, 2924, 2182, 2104, 1931, 1429 cm^{-1}

^{1}H NMR (500 MHz, CDCl$_3$): δ 7.64 - 7.58 (m, 2H), 7.43 - 7.35 (m, 3H), 5.14 (t, J = 7.1 Hz, 1H), 4.45 (d, J = 7.2 Hz, 2H), 1.86 - 1.84 (m, 3H), 0.51 (s, 3H).

^{13}C NMR (125 MHz, CDCl$_3$): δ 214.2, 135.4, 134.0, 129.8, 127.9, 81.3, 77.1, 68.2, 67.9, 5.3, -4.9

MS (70 eV) m/z 197.

Diphenyl(prop-2-yn-1-yl)(propa-1,2-dien-1-yl)silane (37)
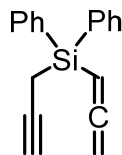
Yield: 5%

IR υ_{max}(thin film, CHCl$_3$): 3256, 3070, 2951, 2252, 1930, 1653, 1557 cm^{-1}

^{1}H NMR (200 MHz, CDCl$_3$): δ 7.67 - 7.59 (m, 4H), 7.44 - 7.33 (m, 6H), 5.33 (t, J = 7.1 Hz, 1H), 4.47 (d, J = 7.2 Hz, 2H), 2.14 (d, J = 3.0 Hz, 2H), 1.86 (t, J = 2.9 Hz, 1H).

^{13}C NMR (125 MHz, CDCl$_3$): δ 215.1, 135.0, 133.3, 130.0, 127.9, 80.9, 75.9, 68.7, 68.6, 4.3

MS (70 eV): m/z 260.

1.3.4.2. Synthesis of unnatural α- amino acid

Synthesis of (3*S**,4*S**)-3,4-bis(iodomethyl)-1,1-dimethylsilolane (38)[49]
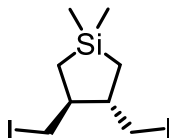
A two neck RB was charged with dichlorozirconocene (3.2 g, 10.94 mmol) and flushed with Argon. Dry THF (15 mL) was added, cooled to -78 °C and *n*-BuLi (16.4 mL, 1.6 M in hexanes, 26.3 mmol) was added dropwise so as to generate bis(cyclopentadienyl)zirconium. The yellow solution obtained was stirred at the same temperature for 1h. Then a solution of diallyldimethylsilane (2 mL, 10.94 mmol) in dry THF was added and the reaction was allowed to warm to rt and stirring was continued. After 10 h, the reaction mixture was cooled to -78 °C and a solution of Iodine (5.6 g, 21.88 mmol) in THF was added, warmed to RT and stirred at the same temperature for 1h. The reaction mixture was quenched with 1N H$_2$SO$_4$, diethyl ether was added and the organic layer was separated. This layer was then washed with aq. Sodium thiosulphate solution so as to remove excess iodine, dried over Na$_2$SO$_4$ and concentrated. The crude was then purified by column chromatography (silica gel 100-200, pet ether) to afford the compound as a light yellow liquid (2.2 g, 51%).

Ethyl (3a*S**,6a*S**)-5-isocyano-2,2-dimethyloctahydrocyclopenta[c]silole-5-carboxylate (39)
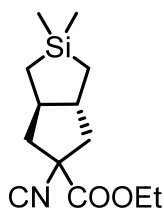
Ethylisocyanoacetate (0.06 mL, 0.51 mmol) was taken in dry acetonitrile (5 mL), added K_2CO_3 (282 mg, 2.04 mmol), a pinch of 18-crown-6 and stirred for 5 min. Then a solution of **38** (200 mg, 0.51 mmol) in acetonitrile (5 mL) was added and refluxed overnight. The reaction mass was cooled to RT, added water, DCM and the organic layer was separated, washed with brine, dried over Na_2SO_4 and concentrated under reduced pressure. The crude mass was then purified by column chromatography (silica gel 100-200, 2% ethyl acetate- pet ether) to afford the compound as a light yellow liquid (95 mg, 74%).

IR υ_{max}(thin film, $CHCl_3$): 2134, 1742, 1253 cm^{-1}

^{1}H NMR (500 MHz, $CDCl_3$): δ 4.26 (q, J = 7.0 Hz, 2H), 2.65 - 2.61 (m, 1H), 2.36 - 2.32 (m, 1H), 1.97 - 1.81 (m, 2H), 1.75 - 1.65 (m, 2H), 1.33 (t, J = 7.0 Hz, 3H), 0.94 - 0.88 (m, 2H), 0.29 – 0.05 (m, 8H).

^{13}C NMR (125 MHz, $CDCl_3$): δ 170.4, 157.3, 69.0, 62.6, 50.3, 49.2, 47.0, 46.9, 16.9, 16.4, 14.0, -0.8

HRMS (ESI): m/z calculated for $C_{13}H_{21}NO_2NaSi$ [M + Na]$^+$ 274.1234, found 274.1228.

Ethyl (3a*S,6a*S**)-5-amino-2,2-dimethyloctahydrocyclopenta[c]silole-5-carboxylate (40)**
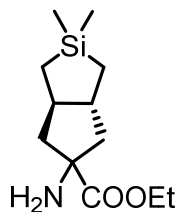
To a solution of **39** (80 mg, 0.32 mmol) in ethanol (2 mL) was added a drop of con. HCl and stirred at RT for 30 min. Ethanol was removed and to the residue DCM and water were added and the aqueous layer was separated. It was then neutralized with *2N* NaOH,

and the aqueous layer was extracted with DCM, dried over Na_2SO_4 and concentrated under vacuum to give the pure compound (70 mg, 91%).

IR υ_{max}(thin film, CHCl$_3$): 3220, 2955, 2933, 1728, 1248 cm^{-1}

^{1}H NMR (400 MHz, CDCl$_3$): δ 4.17 (q, J = 7.0 Hz, 2H), 2.39 - 2.34 (m, 1H), 1.90 – 1.78 (m, 1H), 1.73 - 1.60 (m, 5H), 1.28 (t, J = 7.0 Hz, 3H), 1.10 (t, J = 11.5 Hz, 1H), 0.88 - 0.82 (m, 2H), 0.25 – 0.07 (m, 8H).

^{13}C NMR (125 MHz, CDCl$_3$): δ 178.0, 66.6, 61.2, 51.2, 49.0, 46.6, 45.9, 17.4, 17.0, 14.2, -0.7

HRMS (ESI): m/z calculated for $C_{12}H_{24}NO_2Si$ [M + H]$^+$ 242.1571, found 242.1568

Ethyl   (3aS*,6aS*)-5-((tert-butoxycarbonyl)amino)-2,2-dimethyloctahydrocyclopenta[c]silole-5-carboxylate (41)
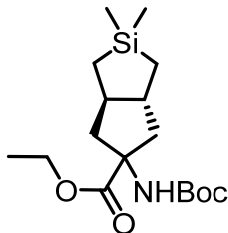
To a solution of **40** (20 mg, 0.083 mmol) in DCM (2 mL) was added triethylamine (17 μL, 0.124 mmol), Boc anhydride (28 μL, 0.124 mmol) and stirred at RT for 3h. To the reaction mixture, water was added and the organic layer was separated. The aqueous layer was extracted with DCM and the combined organic layer was dried over Na_2SO_4, concentrated under reduced pressure and purified by column chromatography (silica gel 100-200 mesh, 5% ethyl acetate - pet ether). The product was obtained as a yellow solid (23 mg, 82%).

IR υ_{max}(thin film, CHCl$_3$): 3300, 2955, 1707, 1499, 1249 cm^{-1}

^{1}H NMR (400 MHz, CDCl$_3$): δ 5.03 (br s, 1H), 4.17 (q, J = 7.1 Hz, 2H), 2.55 (m, 1H), 1.97 – 1.58 (m, 5H, merged with CDCl$_3$ moisture), 1.43 (s, 9H), 1.26 (t, J = 7.2 Hz, 3H), 0.89 – 0.83 (m, 2H), 0.23 – 0.08 (m, 8H).

¹³C NMR (100 MHz, CDCl₃): δ 175.3, 155.0, 79.5, 67.6, 61.2, 50.1, 49.1, 45.5, 44.5, 28.3, 17.2, 17.0, 14.2, -0.71

HRMS (ESI): m/z calculated for $C_{17}H_{31}NO_4NaSi$ $[M + Na]^+$ 364.1915, found 364.1910

(3a*R**,6a*R**)-5-amino-2,2-dimethyloctahydrocyclopenta[c]silole-5-carboxylic   acid hydrochloride (42)
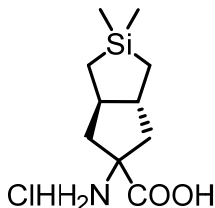
To a solution of **41** (40 mg, 0.118 mmol) in THF (1 mL): Ethanol (1 mL), KOH (20 mg, 0.353 mmol) in H_2O (0.5 mL) was added and stirred at RT overnight. Solvent was removed under reduced pressure and the residue was acidified with 1 N HCl (pH ~ 3) and extracted with ethyl acetate (5 mL X 3). The combined organic layer was dried over anhydrous Na_2SO_4, and concentrated under reduced pressure to afford the free acid as a solid. This solid was then dissolved in dioxane (1 mL) and then HCl in dioxane (4M, 1 mL) was added and stirred at RT for 2 h. The reaction mixture was concentrated under vacuum and the residue was washed with diethyl ether to obtain the product as a light brown solid (27 mg, 90% yield).

¹H NMR (400 MHz, MeOD): δ 2.45 – 2.42 (m, 1H), 2.09 – 2.07 (m, 1H), 1.92 (m, 3H), 1.42 (m, *J* = 12.2 Hz, 1H), 0.95 – 0.92 (m, 2H), 0.34 - 0.14 (m, 8H).

¹³C NMR (100 MHz, MeOD): δ 175.0, 67.4, 51.7, 50.0, 43.9, 43.0, 17.6, 17.5, -0.78

HRMS (ESI): m/z calculated for $C_{10}H_{20}NO_2Si$ $[M\ ]^+$ 214.1258, found 214.1253

1.3.4.3. Synthesis of unnatural β- amino acid

Ethyl (3a*S**,6a*S**)-5-cyano-2,2-dimethyloctahydrocyclopenta[c]silole-5-carboxylate (43)
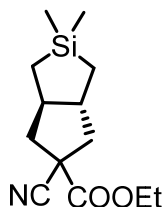
To a solution of ethylcyanoacetate (0.11 mL, 1.01 mmol) in dry acetonitrile (40 mL) was added K_2CO_3 (419 mg, 3.03 mmol), a pinch of 18-crown-6 and stirred for 5 min. Then a solution of **38** (400 mg, 1.01 mmol) in acetonitrile (20 mL) was added and refluxed overnight. The reaction mass was cooled to RT, added DCM (30 mL) and water (10 mL) and the organic layer was separated, washed with brine, dried over Na_2SO_4 and concentrated under vacuum. The crude mass was then purified by column chromatography (silica gel 100-200 mesh, 2% ethyl acetate- pet ether) to afford the compound as a colorless liquid (220 mg, 86%).

IR υ_{max}(thin film, CHCl$_3$): 2894, 2200, 1742, 1250, 1211, 1159 cm^{-1}

^{1}H NMR (400 MHz, CDCl$_3$): δ 4.25 (q, J = 7.3 Hz, 2H), 2.55 - 2.47 (m, 2H), 1.86 - 1.70 (m, 4H), 1.33 (t, J = 7.3 Hz, 3H), 0.94 - 0.88 (m, 2H), 0.26 – 0.03 (m, 8H).

^{13}C NMR (100 MHz, CDCl$_3$): δ 170.3, 122.2, 62.7, 50.4, 50.1, 48.1, 43.7, 43.1, 16.7, 16.4, 14.0, -0.71, -0.74

HRMS (ESI): m/z calculated for $C_{13}H_{22}NO_2Si$ [M + H]$^+$ 252.1414, found 252.1412.

Ethyl   (3aS*,6aS*)-5-(aminomethyl)-2,2-dimethyloctahydrocyclopenta[c]silole-5-carboxylate (44)
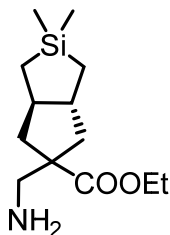
A solution of **43** (45 mg, 0.179 mmol) in ethanol (5 mL) was taken in a hydrogenation reaction bottle, Raney Ni in EtOH (cat. amount) was added and hydrogenated under a pressure of 60 psi in a parr hydrogenator for 4h. The reaction mass was filtered through

celite, excess Ni was quenched with 1N HCl and the filtrate was concentrated under reduced pressure. The crude was purified by column chromatography (neutral alumina, 2% methanol- DCM) to afford the compound as a light yellow sticky solid (28 mg, 62%).

IR υ_{max}(thin film, CHCl$_3$): 3300, 2933, 1722, 1248 cm^{-1}

^{1}H NMR (400 MHz, CDCl$_3$): δ 4.14 (q, J = 7.1 Hz, 2H), 2.91 - 2.76 (m, 2H), 2.28 - 2.23 (m, 1H), 1.79 - 1.74 (m, 1H), 1.67 - 1.41 (m, 5H, merged with CDCl$_3$ moisture), 1.25 (t, J = 7.1 Hz, 3H), 1.01 (t, J = 12.0 Hz, 1H), 0.87- 0.79 (m, 2H), 0.21 – 0.07 (m, 8H).

^{13}C NMR (100 MHz, CDCl$_3$): δ 177.7, 60.4, 58.1, 50.8, 50.3, 49.5, 41.1, 40.2, 17.4, 17.2, 14.2, -0.69, -0.72

HRMS (ESI): m/z calculated for C$_{13}$H$_{26}$NO$_2$Si [M + H]$^+$ 256.1727, found 256.1726.

Ethyl   (3aS*,6aS*)-5-(((tert-butoxycarbonyl)amino)methyl)-2,2-dimethyloctahydrocyclopenta[c]silole-5-carboxylate (45)
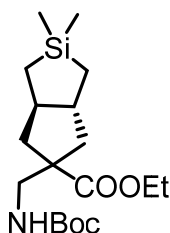
To a solution of **43** (40 mg, 0.159 mmol) in ethanol (5 mL) was added Boc anhydride (55 µL, 0.238 mmol), Raney Ni in EtOH (catalytic) and hydrogenated under a pressure of 60 psi in a parr hydrogenator for 4h. The reaction mass was filtered through celite and the filtrate was concentrated under reduced pressure and purified by column chromatography (silica gel 100-200, 5% ethyl acetate- pet ether) to afford the compound as a light yellow liquid (40 mg, 71%).

IR υ_{max}(thin film, CHCl$_3$): 3460, 3379, 1716, 1502, 1247 cm^{-1}

^{1}H NMR (400 MHz, CDCl$_3$): δ 5.03 (br s, 1H), 4.13 (q, J = 7.1 Hz, 2H), 3.33 - 3.20 (m, 2H), 2.09 (dd, J = 12.8, 6.2 Hz, 1H), 1.81 - 1.48 (m, 4H), 1.41 (s, 9H), 1.25 (t, J = 7.1 Hz, 3H), 1.07 (t, J = 11.8 Hz, 1H), 0.86 - 0.79 (m, 2H), 0.20 – 0.06 (s, 8H).

^{13}C NMR (100 MHz, CDCl$_3$): δ 177.9, 156.3, 79.0, 60.7, 56.2, 50.5, 49.3, 47.5, 41.2, 39.9, 28.4, 17.3, 17.1, 14.1, -0.71, -0.68

HRMS (ESI): m/z calculated for C$_{18}$H$_{33}$NO$_4$NaSi [M + Na]$^+$ 378.2071, found 378.2069.

(3a*R,6a*R**)-5-(aminomethyl)-2,2-dimethyloctahydrocyclopenta[c]silole-5-carboxylic acid hydrochloride (46)**
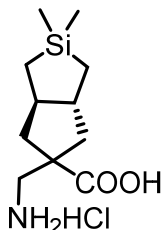
To a solution of **45** (60 mg, 0.169 mmol) in THF (1.5 mL): Ethanol (1 mL), KOH (28 mg, 0.507 mmol) in H$_2$O (0.5 mL) was added and stirred at RT overnight. Solvent was removed under reduced pressure and the residue was acidified with 1 N HCl (pH ~ 3) and extracted with ethyl acetate (5 mL X 3). The combined organic layer was dried over anhydrous Na$_2$SO$_4$, and concentrated under reduced pressure to afford a solid product. This solid was then dissolved in dioxane (1 mL) and then HCl in dioxane (4M, 1 mL) was added and stirred at RT for 3 h. The reaction mixture was concentrated under vacuum and the residue was washed with diethyl ether to obtain the product as a colorless solid (34 mg, 77% yield).

^{1}H NMR (400 MHz, MeOD): δ 3.18 – 3.15 (m, 1H), 3.05 – 3.03 (m, 1H), 2.25 - 2.21 (m, 1H), 1.90 - 1.86 (m, 2H), 1.72 – 1.64 (m, 2H), 1.18 (t, *J* = 11.9 Hz, 1H), 0.93 - 0.86 (m, 2H), 0.26 – 0.10 (m, 8H).

^{13}C NMR (100 MHz, MeOD): δ 179.4, 54.2, 51.7, 50.7, 47.2, 42.4, 41.5, 17.9, 17.8, -0.6

HRMS (ESI): m/z calculated for C$_{11}$H$_{22}$NO$_2$Si [M]$^+$ 228.1414, found 228.1411

1.3.4.4. Synthesis of new GABA analog

(3a*S,6a*S**)-5-cyano-2,2-dimethyloctahydrocyclopenta[c]silole-5-carboxylic acid (47)**

To a solution of **43** (1.5 g, 5.97 mmol) in ethanol (20 mL) was added aq. KOH (670 mg, 11.94 mmol) and refluxed for 3h. The reaction mass was cooled to RT and the solvent was removed under reduced pressure. The solid obtained was dissolved in minimal amount of water and washed with diethyl ether. The aqueous layer was separated, neutralized with 1N HCl and the product was extracted with ethylacetate, dried over Na_2SO_4 and concentrated under vacuum to afford the compound as a light brown solid (1.35 g, 100%).

IR υ_{max}(thin film, $CHCl_3$): 3100 (broad peak), 2953, 1718, 1250 cm^{-1}

^{1}H NMR (400 MHz, $CDCl_3$): δ 2.61 - 2.52 (m, 2H), 1.91 - 1.72 (m, 4H), 0.95 - 0.85 (m, 2H), 0.28 – 0.11 (m, 8H).

^{13}C NMR (100 MHz, $CDCl_3$): δ 175.2, 121.4, 50.4, 50.2, 48.2, 43.7, 43.2, 16.7, 16.4, -0.72

HRMS (ESI): m/z calculated for $C_{11}H_{17}NO_2NaSi$ [M + Na]$^+$ 246.0921, found 246.0917.

(3aS*,6aS*)-2,2-dimethyloctahydrocyclopenta[c]silole-5-carbonitrile (48)
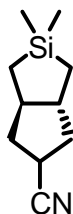
The carboxylic acid **47** (150 mg, 0.671 mmol) was dissolved in DMSO (2 mL) and heated at 150 °C for 6h. The reaction mass was cooled to rt, added diethyl ether and the organic layer was separated. The aqueous layer was again extracted with ether, dried over Na_2SO_4 and the solvent was removed. The crude mass was then purified by column

chromatography (silica gel 100-200, 20% DCM- pentane) to afford the compound as a colorless liquid (84 mg, 70%).

IR v_{max}(thin film, CHCl$_3$): 2260, 1259 cm^{-1}

^{1}H NMR (400 MHz, CDCl$_3$): δ 3.07- 3.00 (m, 1H), 2.30 - 2.23 (m, 1H), 2.15 - 2.10 (m, 1H), 1.75 - 1.63 (m, 1H), 1.56 - 1.37 (m, 3H), 0.92 - 0.86 (m, 2H), 0.26 – 0.07 (m, 8H).

^{13}C NMR (100 MHz, CDCl$_3$): δ 124.5, 50.8, 50.0, 37.0, 36.3, 27.9, 16.8 (2C), -0.75 (2C)

MS (70 eV) m/z 179.

Methyl 2-((3a*S**,6a*S**)-5-cyano-2,2-dimethyloctahydrocyclopenta[c]silol-5-yl)acetate (50)
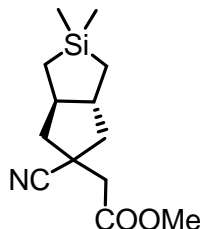
A solution of **48** (70 mg, 0.39 mmol) in dry THF (2 mL) was cooled to -78 °C, NaHMDS in THF (0.6 mL, 1M in THF, 0.59 mmol) was added and stirred for 5 min. Then a solution of 3,3-dimethylallylbromide (54 μL, 0.47 mmol) in THF (1 mL) was added at the same temperature, the reaction mass was allowed to warm to 0 °C and then quenched by drop wise addition of sat. NH$_4$Cl. Diethyl ether was added, the organic layer was separated and the aqueous layer was extracted again with diethyl ether, dried over Na$_2$SO$_4$ and concentrated. The crude mass was then subjected to purification by column chromatography (silica gel 100-200 mesh, 1% ethyl acetate- pet ether) to afford the compound **49** as a mixture along with a very close spot (40 mg, 0.162 mmol). This mixture was dissolved in DCM (10 mL), added 2.5 *M* methanolic NaOH (0.32 mL, 0.808 mmol) cooled to -78 °C and a stream of ozone was passed till the initial yellow precipitate disappeared and the characteristic blue color of ozone was attained (10 - 15 min). The reaction mass was warmed to RT, water was added and the organic layer was separated. The aqueous layer was re-extracted with DCM, the combined organic layers were dried over Na$_2$SO$_4$ and concentrated. The crude was then purified by column

chromatography (silica gel 100-200, 5% ethylacetate- pet ether) to give the product as a colorless liquid (25 mg, 26% over two steps starting from **48**).

IR υ_{max}(thin film, CHCl$_3$): 2233, 1740, 1437, 1248, 1196 cm^{-1}

^{1}H NMR (400 MHz, CDCl$_3$): δ 3.74 (s, 3H), 2.68 (AB quartet, 2H), 2.51 - 2.47 (m, 1H), 2.13 - 2.08 (m, 1H), 1.87 - 1.73 (m, 2H), 1.57 - 1.47 (m, 1H), 1.33 - 1.25 (m, 1H), 0.93 - 0.85 (m, 2H), 0.27 – 0.13 (m, 8H).

^{13}C NMR (100 MHz, CDCl$_3$): δ 169.8, 125.7, 52.0, 50.1, 49.2, 45.1, 43.99, 43.97, 39.9, 17.0, 16.8, -0.77

HRMS (ESI): m/z calculated for C$_{13}$H$_{21}$NO$_2$NaSi [M + Na]$^+$ 274.1234, found 274.1232.

Methyl   2-((3aS*,6aS*)-5-(((((l1-methyl)(l1-oxidanyl)boranyl)amino)methyl)-2,2-dimethyloctahydrocyclopenta[c]silol-5-yl)acetate (51)
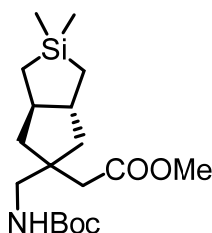
To a solution of **50** (20 mg, 0.08 mmol) in methanol (5 mL) was added Boc anhydride (28 μL, 0.119 mmol), Raney Ni in MeOH (catalytic) and hydrogenated under a pressure of 60 psi in a parr hydrogenator for 4h. The reaction mass was filtered through celite and the filtrate was concentrated under reduced pressure and purified by column chromatography (silica gel 100-200, 5% ethyl acetate- pet ether) to afford the compound as a light yellow liquid (22 mg, 78%).

IR υ_{max}(thin film, CHCl$_3$) 3376, 2950, 1717, 1509, 1247 cm^{-1}

^{1}H NMR (500 MHz, CDCl$_3$): δ 4.97 (br s, 1H), 3.67 (s, 3H), 3.23 (dd, J = 13.7, 7.3 Hz, 1H), 3.00 (dd, J = 13.7, 5.5 Hz, 1H), 2.36 (AB quartet, 2H), 1.83 - 1.78 (m, 2H), 1.56 – 1.43 (m, 11H), 1.01– 0.97 (m, 2H), 0.88 - 0.80 (m, 2H), 0.16 – 0.07 (m, 8H).

^{13}C NMR (125 MHz, CDCl$_3$): δ 172.8, 156.4, 79.0, 51.4, 49.6, 49.4, 49.2, 48.1, 44.0, 42.6, 42.2, 28.4, 17.60, 17.57, -0.70, -0.74

HRMS (ESI): m/z calculated for $C_{18}H_{33}NO_4NaSi$ [M + Na]$^+$ 378.2071, found 378.2068.

2-((3a*R**,6a*R**)-5-(aminomethyl)-2,2-dimethyloctahydrocyclopenta[c]silol-5-yl)acetic acid hydrochloride (52)
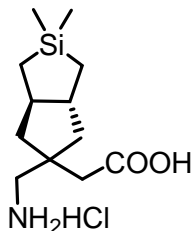
To a solution of **51** (15 mg, 0.042 mmol) in THF (1 mL): Methanol (1 mL), LiOH.H$_2$O (5 mg, 0.126 mmol) in H$_2$O (0.5 mL) was added and stirred at RT overnight. Solvent was removed under reduced pressure and the residue was acidified with 1 N HCl (pH ~ 3) and extracted with ethyl acetate (5 mL X 3). The combined organic layer was dried over anhydrous Na$_2$SO$_4$, and concentrated under reduced pressure to afford the free acid as a solid. This solid was then dissolved in dioxane (1 mL) and then HCl in dioxane (4M, 0.5 mL) was added and stirred at RT for 3 h. The reaction mixture was concentrated under vacuum and the residue was washed with diethyl ether to obtain the product as a light brown solid (8 mg, 68% yield).

^{1}H NMR (400 MHz, MeOD): δ 3.15 - 3.01 (AB quartet, 2H), 2.57 - 2.48 (AB quartet, 2H), 1.88 - 1.80 (m, 2H), 1.71 - 1.47 (m, 2H), 1.19 - 1.07 (m, 2H), 0.89 - 0.85 (m, 2H), 0.25 - 0.10 (m, 8H).

^{13}C NMR (100 MHz, MeOD): δ 175.3, 50.9, 50.4, 49.3 (merged with MeOD peaks), 46.3, 44.3, 43.8, 43.7, 18.2, 18.1, -0.8

HRMS (ESI): m/z calculated for $C_{12}H_{24}NO_2Si$ [M]$^+$ 242.1571, found 242.1566

1.3.5. References

(1) West, R.; Barton, T. J. *J. Chem. Ed.* **1980**, *57*, 165-169.

(2) Fleming, I. *Chem. Soc. Rev*. **1981**, *10*, 83-111.

(3) Larson, G. L. Recent Synthetic Applications of Organosilanes, in Organic Silicon Compounds Volume 1 and Volume 2. 2004.

(4) Denmark, S. E.; Sweis, R. F.; *Chem. Pharm. Bull.* **2002**, *50*, 1531–1541.

(5) Denmark, S. E.; Regens, C. S. *Acc. Chem. Res*. **2008**, *41*, 1486–1499.

(6) Brook, M. A. Silicon in Organic, Organometallic and Polymer Chemistry; Wiley Interscience: New York, 2000.

(7) Fleming, I. In Comprehensive Organic Synthesis; Trost, B. M., Fleming, I., Eds.; Pergamon Press: Oxford, 1991; Vol. 2, pp 563-593.

(8) Zhang, H, -J.; Priebbenow, D. L.; Bolm, C. *Chem. Soc. Rev*. **2013**, *42*, 8540-8571.

(9) Denmark, S. E.; Liu, J. H. -C. *Angew. Chem. Int. Ed*. **2010**, *49*, 2978 – 2986.

(10) Son, D. Y. *Chem Comm.* **2013**, *49*, 10209-10210.

(11) Thames, S.; Panjnani, K. *J. Inorg. Organomet. Polym*. **1996**, *6*, 59-94.

(12) Richter, R.; Roewer, G.; Böhme, U.; Busch, K.; Babonneau, F.; Martin, H. P.; Müller, E. *Appl. Organometal. Chem*. **1997**, *11*, 71−106 and refs cited therein.

(13) Burkhard, C. A.; Rochow, E. G.; Booth, H. S.; Hartt, J. *Chem. Rev*. **1947**, 41, 97−149.

(14) Rousseau, G.; Blanco, L. *Tetrahedron* **2006**, *62*, 7951−7993.

(15) Cox, L. 2009. Recent advances in organosilicon chemistry. SCI Annual Review Meeting December 2009. University of Birmingham.

(16) Fuchs, P. L. Handbook of reagents for organic synthesis, reagents for silicon-mediated organic synthesis, John Wiley and Sons, 2013.

(17) Friedel, C.; Crafts, J. M. *Annalen.* **1865**, *136*, 203.

(18) Kipping, F. S. *Proc. Chem. Soc.* **1904**, *20*, 15-16.

(19) Kipping, F. S.; Loyd, L. L. *J. Chem. Soc.* **1901**, *79*, 449-459.

(20) Sakurai, H. *Pure & Appl. Chem.* **1982**, *54*, 1-22.

(21) Hosomi, A. *Acc. Chem. Res.* **1988**, *21*, 200-206.

(22) Hwu, J. R.; Chen, B.-L.; Shiao, S.-S. *J. Org. Chem*. **1995**, *60*, 2448-2455.

(23) BouzBouz, S.; Boulard, L.; Cossy, J. *Org. Lett*. **2007**, *9*, 3765-3768.

(24) Chan, T. H.; Wang, D. *Chem. Rev*. **1995**, 1279–1292.

(25) Masse, C. E.; Panek, J. S. *Chem. Rev.* **1995**, *95*, 1293–1316.

(26) Wu, J.; Chen, Y.; Panek, J. S. *Org. Lett*. **2010**, *12*, 2112–2115.

(27) Grote, R. E.; Jarvo, E. R. *Org. Lett*. **2009**, *11*, 485–488.

(28) Kinnaird, J. W. A.; Ng, P. Y.; Kubota, K.; Wang,X.; Leighton, J. L. *J. Am. Chem. Soc*. **2002**, *124*, 7920–7921.

(29) Panek, J. S.; Yang, M. *J. Am. Chem. Soc*. **1991**, *113*, 9868–9870.

(30) Rosenberg, S. D.; Walburn, J. J.; Ramsden, H. E. *J. Org. Chem.* **1957**, *22*, 1606-1607.

(31) Scott, R. E.; Frisch, K. C. *J. Am. Chem. Soc*. **1951**, *73*, 2599-2600.

(32) Sanji, T.; Iwata, M.; Watanabe, M.; Hoshi, T.; Sakurai, H. *Organometallics* **1998**, *17*, 5068-5071.

(33) Li, Z.; Cao, X.; Lai, G.; Liu, J.; Ni, Y.; Wu, J.; Qiu, H. *J. Organomet. Chem.* **2006**, *691*, 4740-4746.

(34) Li, Z.; Yang, C.; Zheng, H.; Qiu, H.; Lai, G. *J. Organomet. Chem.* **2008**, *693*, 3771-3779.

(35) Cravotto, G.; Gaudino, E. C.; Cintas, P. *Chem. Soc. Rev*. **2013**, *42*, 7521-7534.

(36) Einhorn, C., Einhorn, J., Luche, J- L. *Synthesis*. **1989**, 787-813.

(37) Shih-Yuan, L. A.; Wen-Chin, D. *Tetrahedron Lett*. **1996**, *37*, 495-498.

(38) Aurell, M. J.; Einhorn, C.; Einhorn, J.; Luche, J. L. *J. Org. Chem*. **1995**, *60*, 8–9.

(39) Han, B. H.; Boudjouk, P. *J. Org. Chem.* **1982**, *47*, 5030–5032.

(40) Ross, N. A.; Bartsch, R. A. *J. Heterocyclic Chem*. **2001**, *38*, 1255-1258.

(41) Nelson, B.; Hiller, W.; Pollex, A.; Hiersemann, M. *Org. Lett.* **2011**, *13*, 4438-4441.

(42) Menez, P. L.; Fargeas, V.; Berque, I.; Poisson, J.; Ardisson, J. *J. Org. Chem.* **1995**, *60*, 3592-3599.

(43) Kim, Y. -H.; Gal, Y. -S.; Kim, U. -Y.; Choi, S. –K. *Macromolecules*, **1988**, *21*, 1991- 1995.

(44) Nugent, W. A.; Taber, D. F. *J. Am. Chem. Soc*. **1989**, *111* , 6435-6437

(45) Negishi, E. -i.; Cederbaum, F. E.; Takahashi, T. *Tetrahedron Lett.* **1986**, *27*, 2829-2832.

(46) Mirza-Aghayan, M.; Boukherroub, R.; Etemad-Moghadam, G.; Manuel, G.; Koenig, M. *Tetrahedron Lett.* **1996,** *37*, 3109-3112.

(47) Oba, G.; Moreira, G.; Manuel, G.; Koenig, M. *J. Organomet. Chem.* **2002**, *643–644*, 324–330.

(48) Knight, K. S.; Wang, D.; Waymouth, R. M.; Ziller, J. *J. Am. Chem. Soc*. **1994**, *116*, 1845-1854.

(49) Nair, A. G.; Keertikar, K. M.; Kim, S. H.; Kozlowski, J. A.; Rosenblum, S.; Selyutin, O. B.; Wong, M.; Yu, W.; Zeng, Q. WO Patent WO2011/112429.

(50) Cavelier, F.; Marchand, D.; Martinez, J.; Sagan, S. *J. Peptide Res*. **2004**, *63*, 290–296.

(51) Fanelli, R.; Besserer-Offroy, E.; René, A.; Côté, J.; Tétreault, P.; Collerette-Tremblay, J.; Longpré, J. –M.; Leduc, R.; Martinez, J.; Sarret, P.; Cavelier, F. *J. Med. Chem.* **2015**, *58*, 7785−7795.

(52) Fanelli, R.; Salah, K. B. H.; Inguimbert, N.; Didierjean, C.; Martinez, J.; Cavelier, F. *Org. Lett*. **2015**, *17*, 4498−4501.

(53) Cavelier, F.; Vivet, B.; Martinez, J.; Aubry, A. *J. Am. Chem. Soc*. **2002**, *124*, 2917-2923.

(54) Pujals, S.; Fernandez-Carneado, J.; Kogan, M. J.; Martinez, J.; Cavelier, F.; Giralt, E. *J. Am. Chem. Soc*. **2006**, *128*, 8479-8483.

(55) Voloshchuk, N.; Montclare, J. K. *Mol. BioSyst*. **2010**, *6*, 65.

(56) Dougherty, D. A. *Curr. Opin. Chem. Biol*. **2000**, *4*, 645-652.

(57) Tanaka, M.; Anan, K.; Demizu, Y.; Kurihara, M.; Doi, M.; Suemune, H. *J. Am. Chem. Soc*. **2005**, *127*, 11570-11571.

(58) Mortensen, M.; Husmann, R.; Veri, E.; Bolm, C. *Chem. Soc. Rev.* **2009**, *38*, 1002–1010.

(59) Stevenazzi, A.; Marchini, M.; Sandrone, G.; Vergani, B.; Lattanzio, M. *Bioorg. Med. Chem. Lett*. **2014**, *24*, 5349–5356.

(60) Kotha, S.; Brahmachary, E. *J. Org. Chem.* **2000,** *65,* 1359-1365.

(61) Kotha, S.; Goyal, D.; Chavan, A. S. *J. Org. Chem.* **2013,** *78,* 12288-12313.

(62) Handbook of Chemistry and Physics, CRC Press, 81st edn, 2000.

(63) Gajcy, K.; Lochynski, S.; Librowski, T. *Curr. Med. Chem.* **2010**, *17,* 2338-2347.

(64) Yogeeswari, P.; Ragavendran, J. V.; Sriram, D. *Recent Pat. CNS Drug Discov.* **2006**, *1*, 113-118.

(65) Weiss, N.; Miller, F.; Cazaubon, S.; Couraud, P. –O. *Biochim. Biophys. Acta* **2009**, *1788*, 842–857.

(66) Gabathuler, R. *Neurobiol. Dis.* **2010**, *47*, 48-57.

(67) Hawkins, B. T.; Davis, T. P. *Pharmacol. Rev.* **2005**, *57*, 173-185.

(68) Ballabh, P.; Braun, A.; Nedergaard, M. *Neurobiol. Dis.* **2004**, *16*, 1 – 13.

(69) Banks, W. A. *Nat. Rev. Drug Discov.* **2016**, *15*, 275-292.

(70) Bryans, J. S.; Wustrow, D. J. *Med. Res. Rev.*, **1999**, *19*, 149–177.

(71) Blakemore, D. C.; Bryans, J. S.; Carnell, P.; Carr, C. L.; Chessum, N. E. A.; Field, M. J.; Kinsella, N.; Osborne, S. A.; Warren, A. N.; Williams, S. C. *Bioorg. Med. Chem. Lett.* **2010,** *20*, 461-464.

(72) Mason, J. D.; Murphree, S. S. *Synlett* **2013**, *24*, 1391–1394.

(73) Marshall, J. A.; Garofalo, A. W. *J. Org. Chem.* **1993**, *58*, 3675-368.

(74) Sills, G. J.; *Curr. Opin. Pharmacol.* **2006**, *6*, 108–113.

(75) Gee, N. S.; Brown, J. P.; Dissanayake, U. K.; Offord, J.; Thurlow, R.; Woodruff, G. N. *J. Biol. Chem.* **1996**, *271*, 5768-5776.
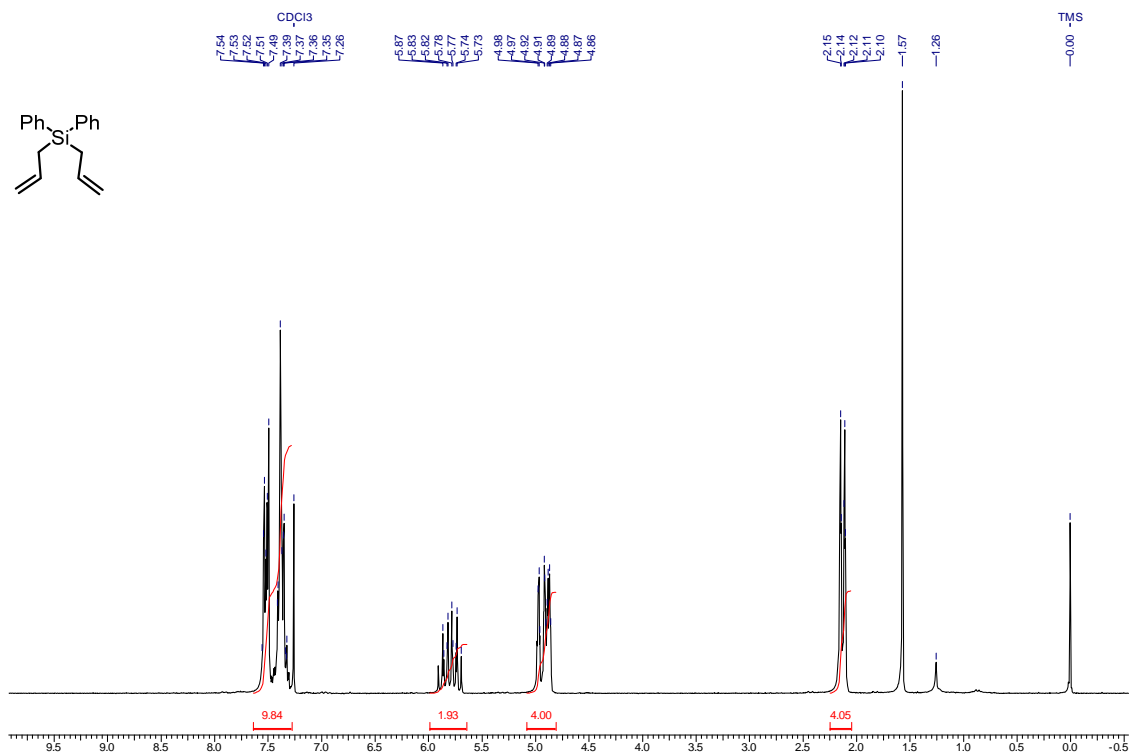
Figure 1.3.8. ^{1}H NMR of **11** (200 MHz, CDCl$_3$)
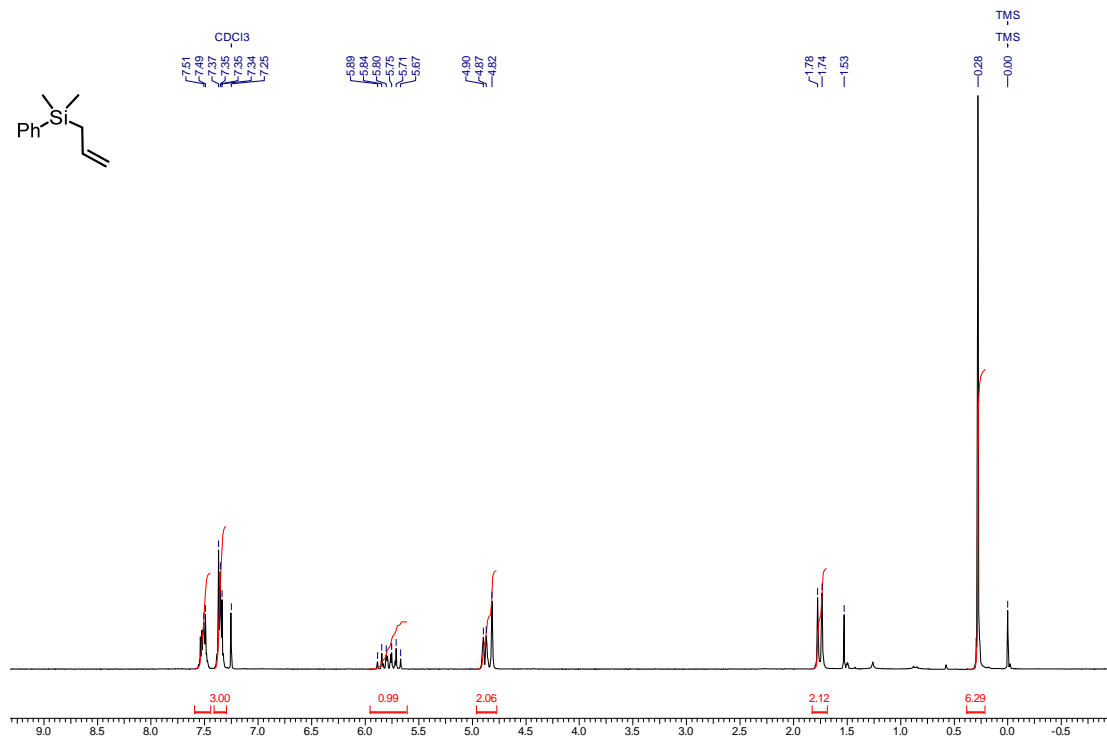
Figure 1.3.9. ^{1}H NMR of **13** (200 MHz, CDCl$_3$)
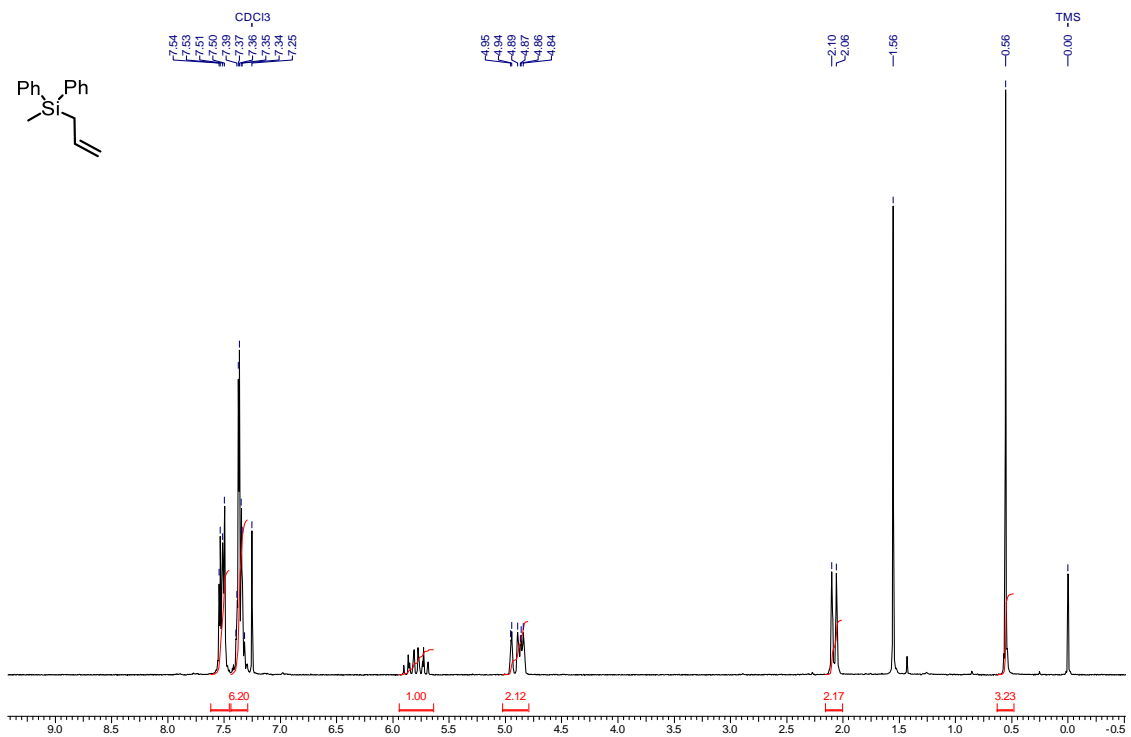
Figure 1.3.10. ^{1}H NMR of **19** (200 MHz, CDCl$_3$)
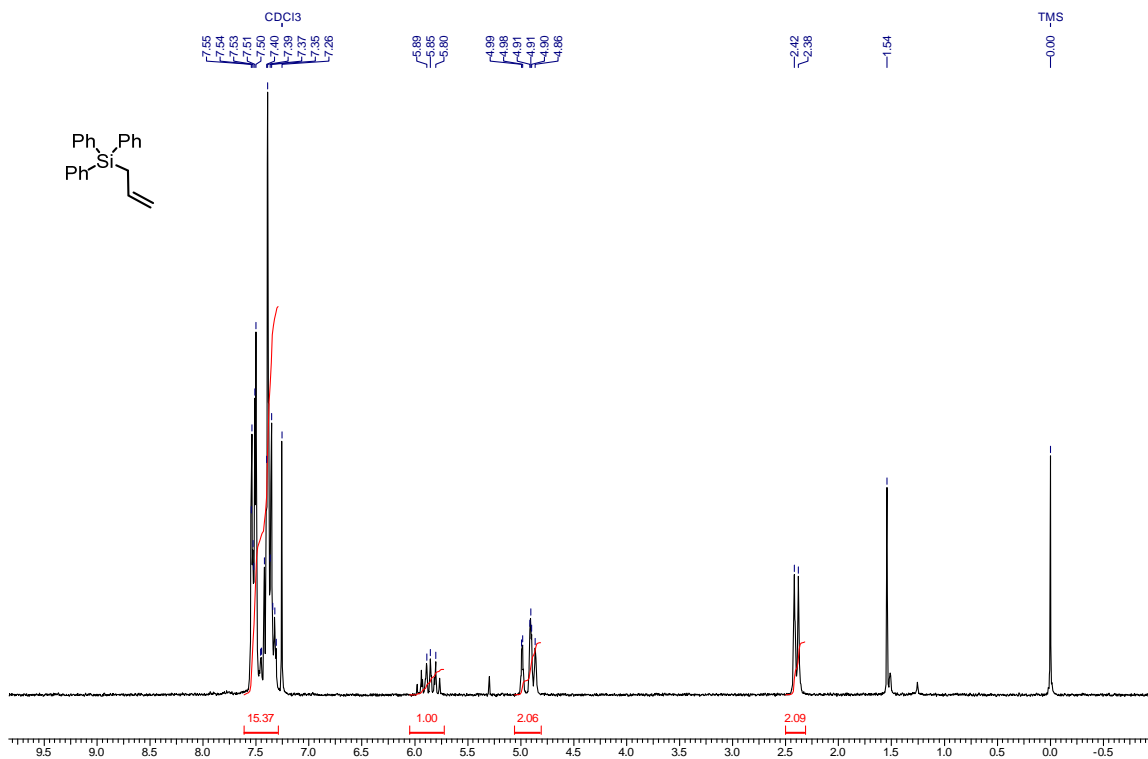
Figure 1.3.11. ^{1}H NMR of **21** (200 MHz, CDCl$_3$)
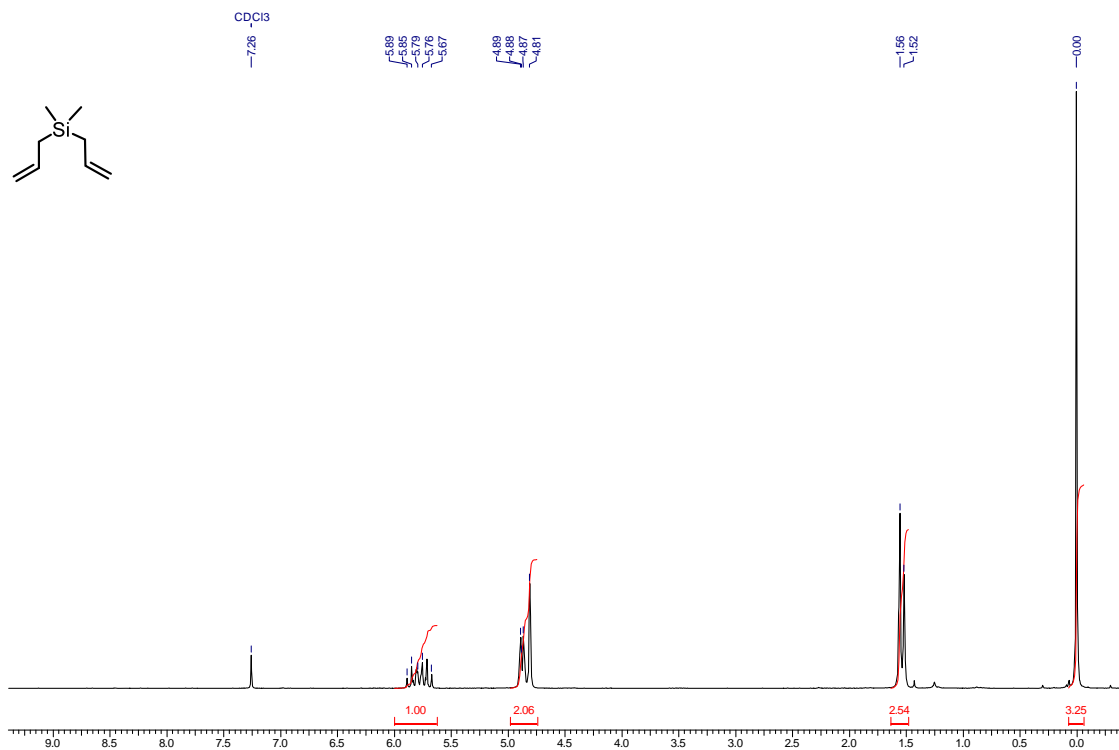
Figure 1.3.12. ^{1}H NMR of **23** (200 MHz, CDCl$_3$)
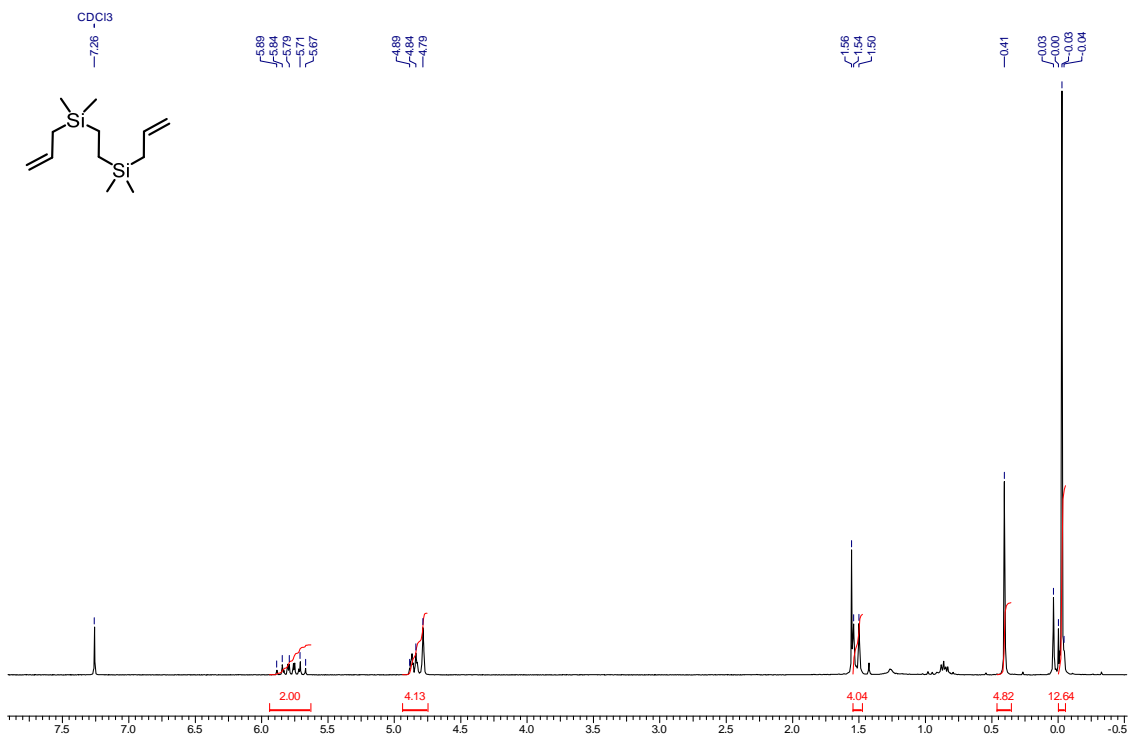
Figure 1.3.13. ^{1}H NMR of **25** (200 MHz, CDCl$_3$)
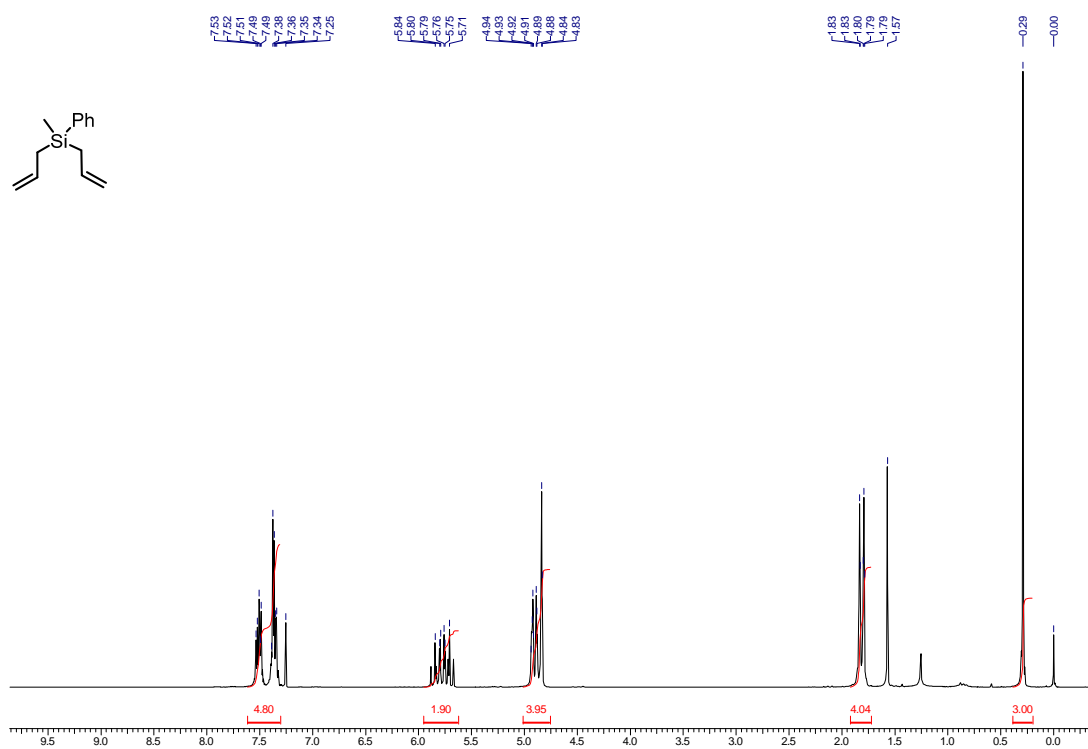
Figure 1.3.14. ^{1}H NMR of **6** (200 MHz, CDCl$_3$)
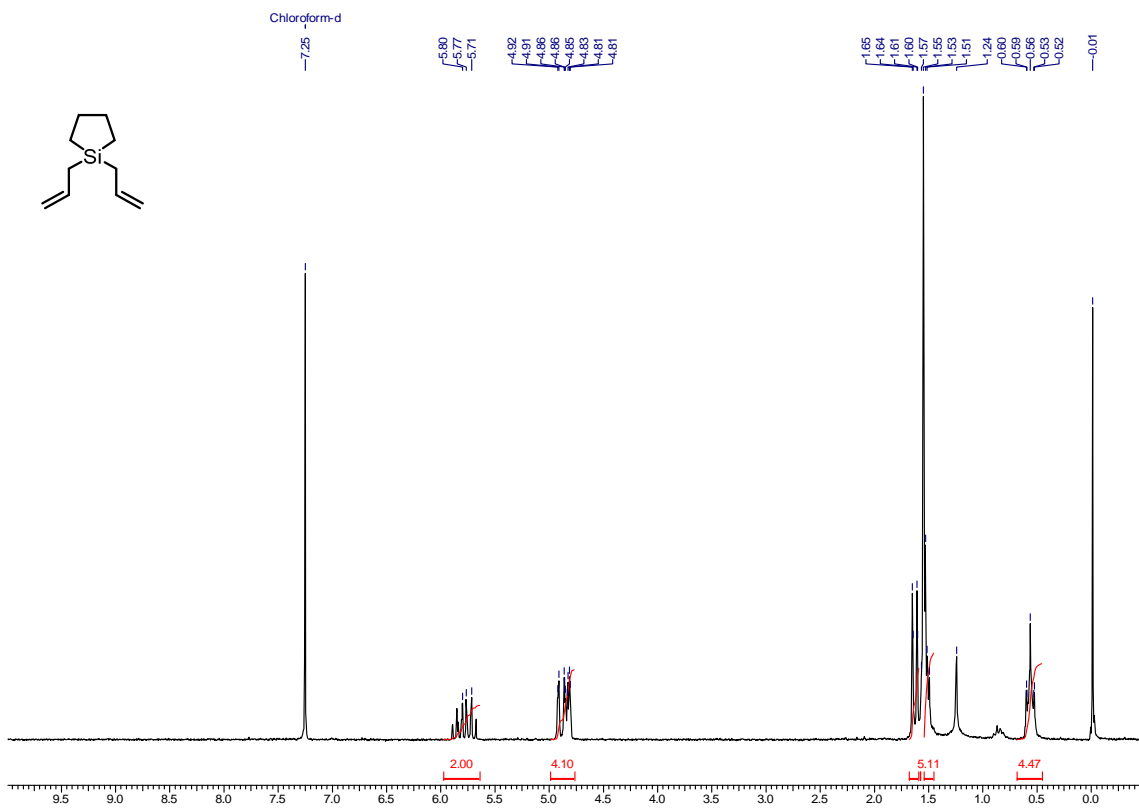
Figure 1.3.15. ^{1}H NMR of **28** (200 MHz, CDCl$_3$)
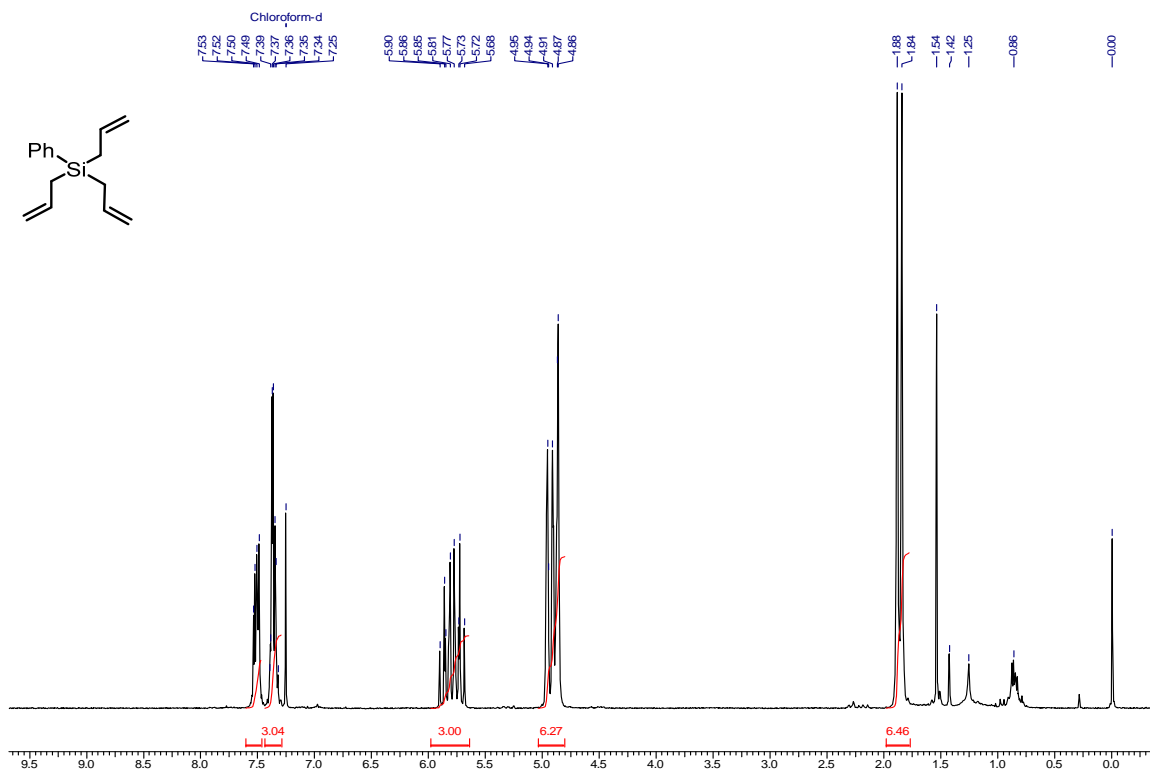
Figure 1.3.16. ^{1}H NMR of **31** (200 MHz, CDCl$_3$)
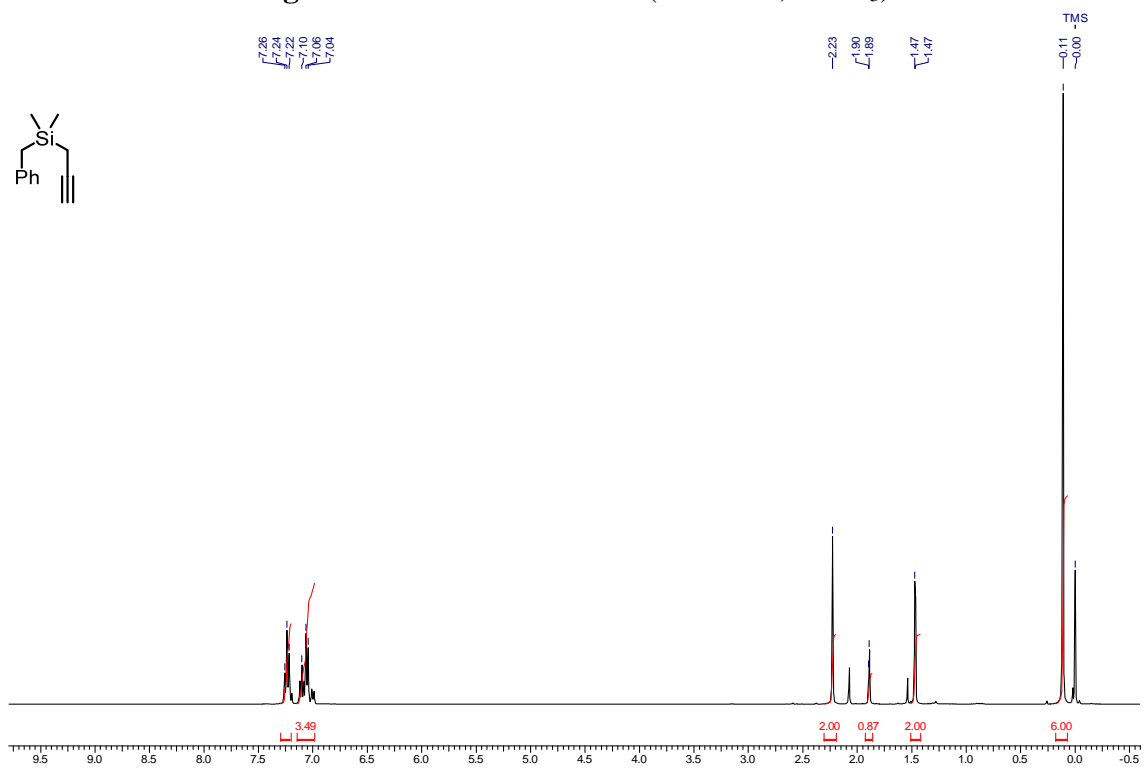
Figure 1.3.17. ^{1}H NMR of **33** (200 MHz, CDCl$_3$)
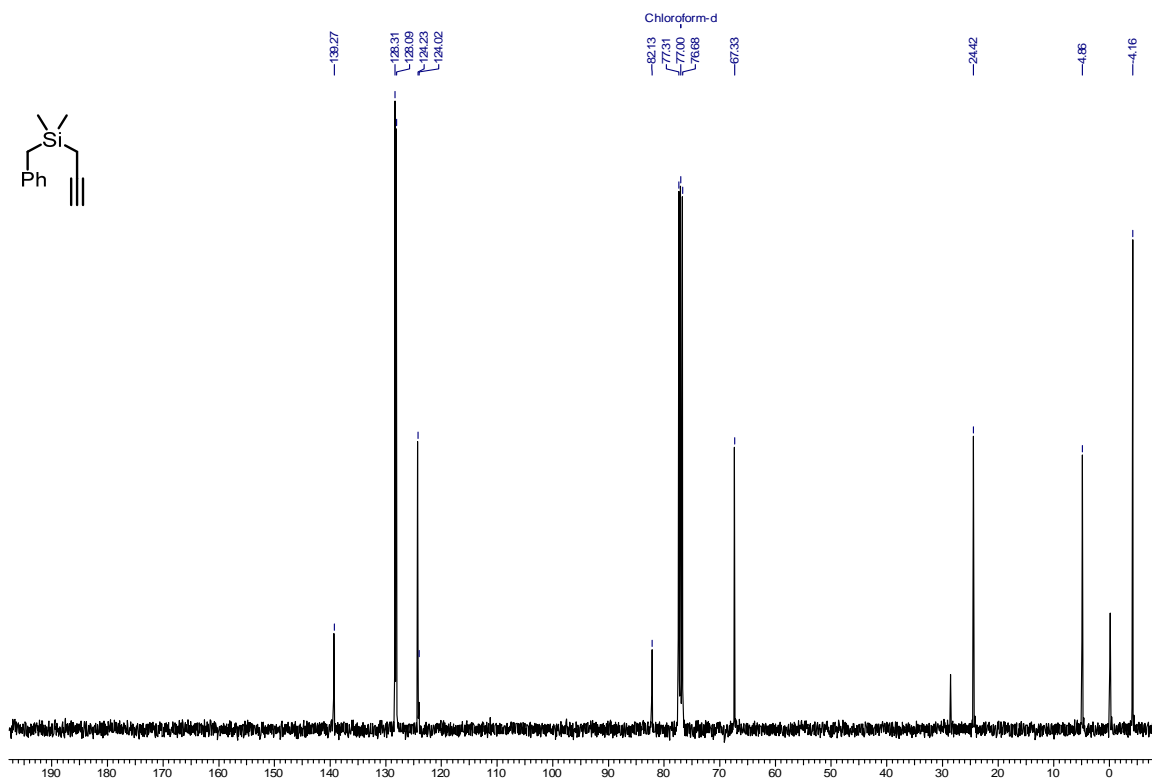
Figure 1.3.18. ^{13}C NMR of **33** (100 MHz, CDCl$_3$)
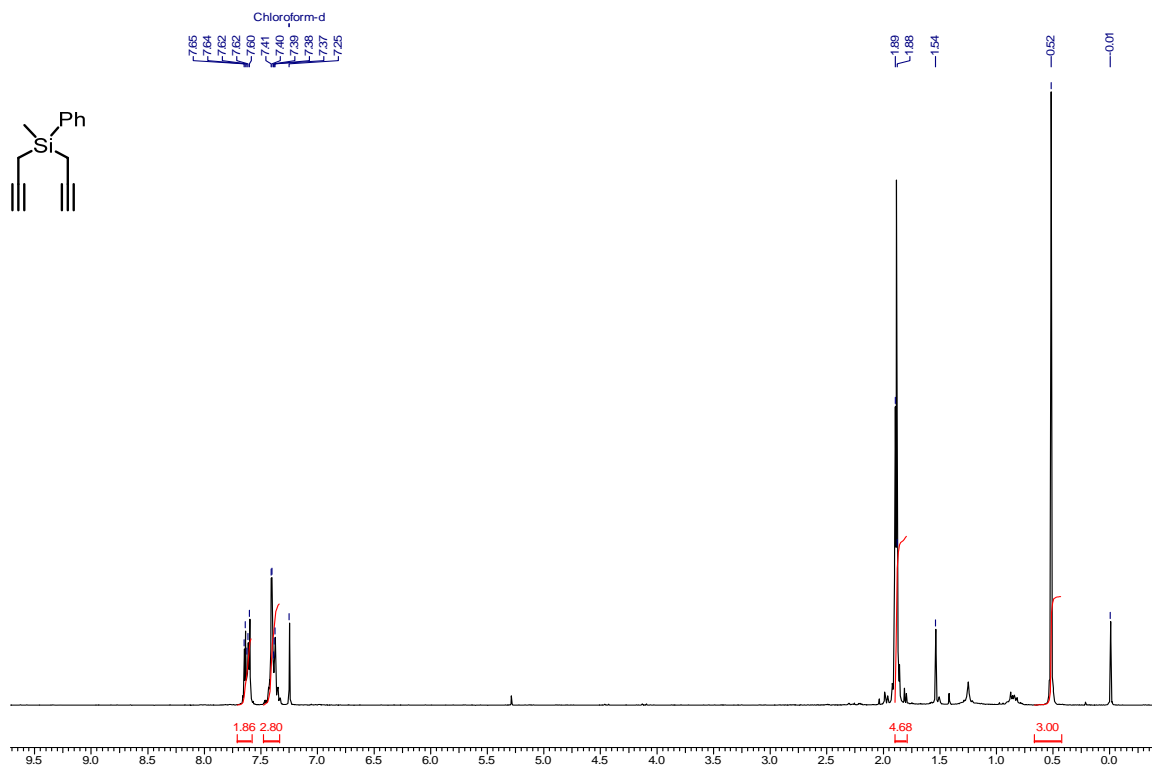
Figure 1.3.19. ^{1}H NMR of **34** (200 MHz, CDCl$_3$)

Figure 1.3.20. ^{1}H NMR of **35** (500 MHz, CDCl$_3$)

Figure 1.3.21. ^{13}C NMR of **35** (125 MHz, CDCl$_3$)
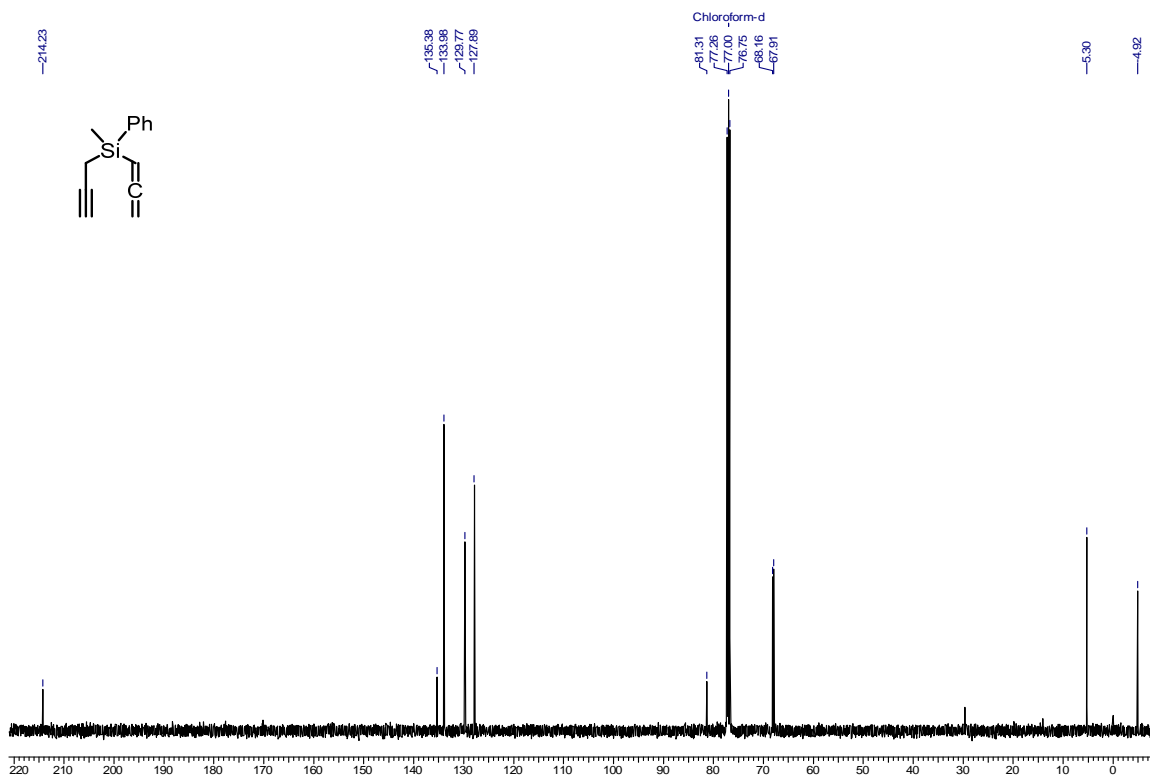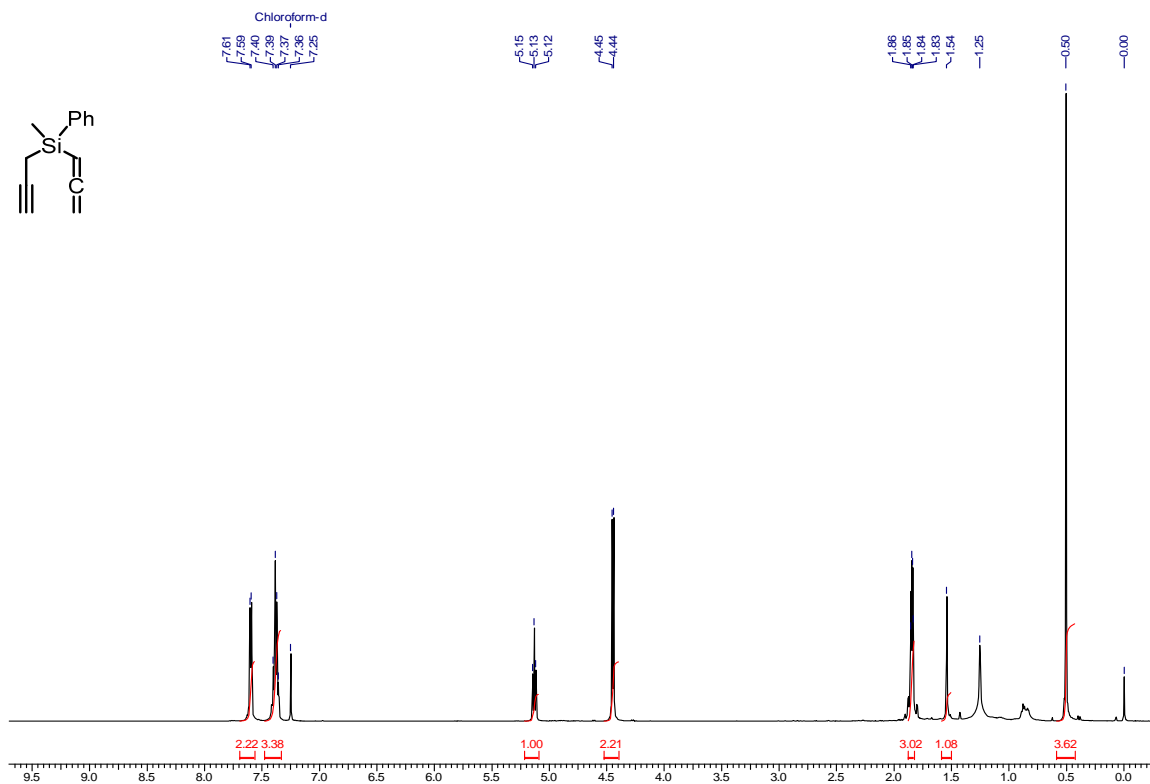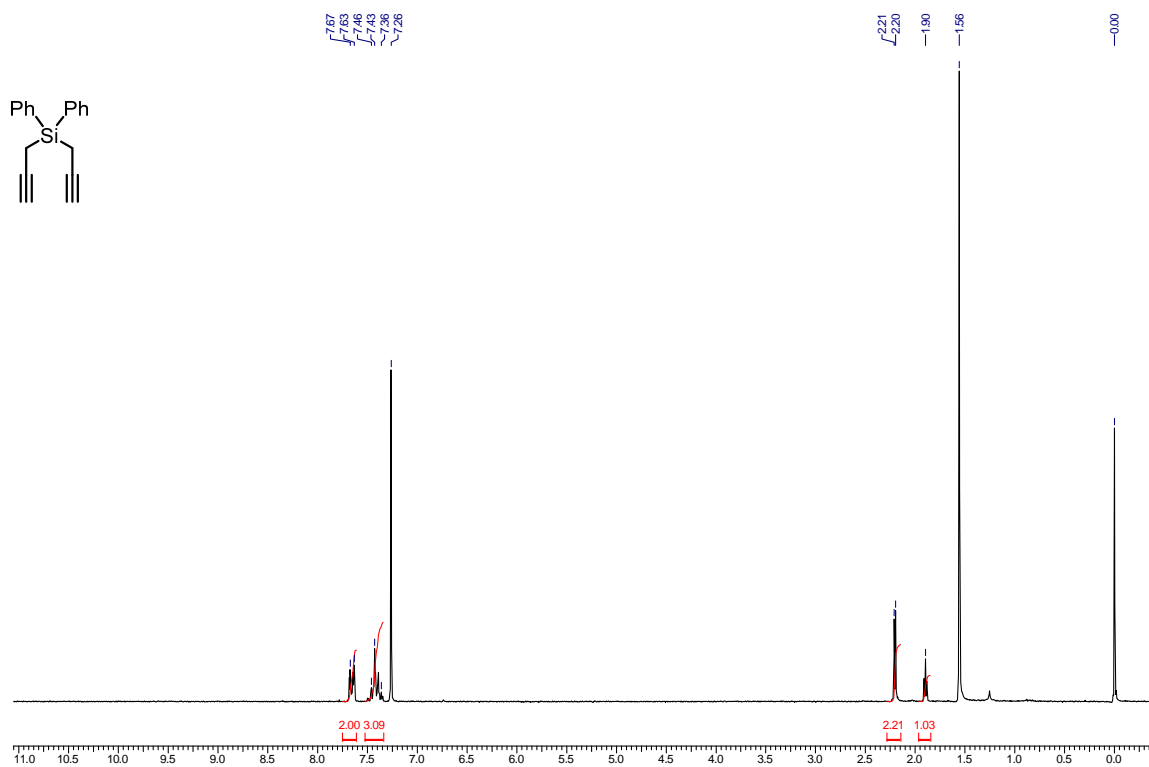
Figure 1.3.22. ^{1}H NMR of **36** (200 MHz, CDCl$_3$)
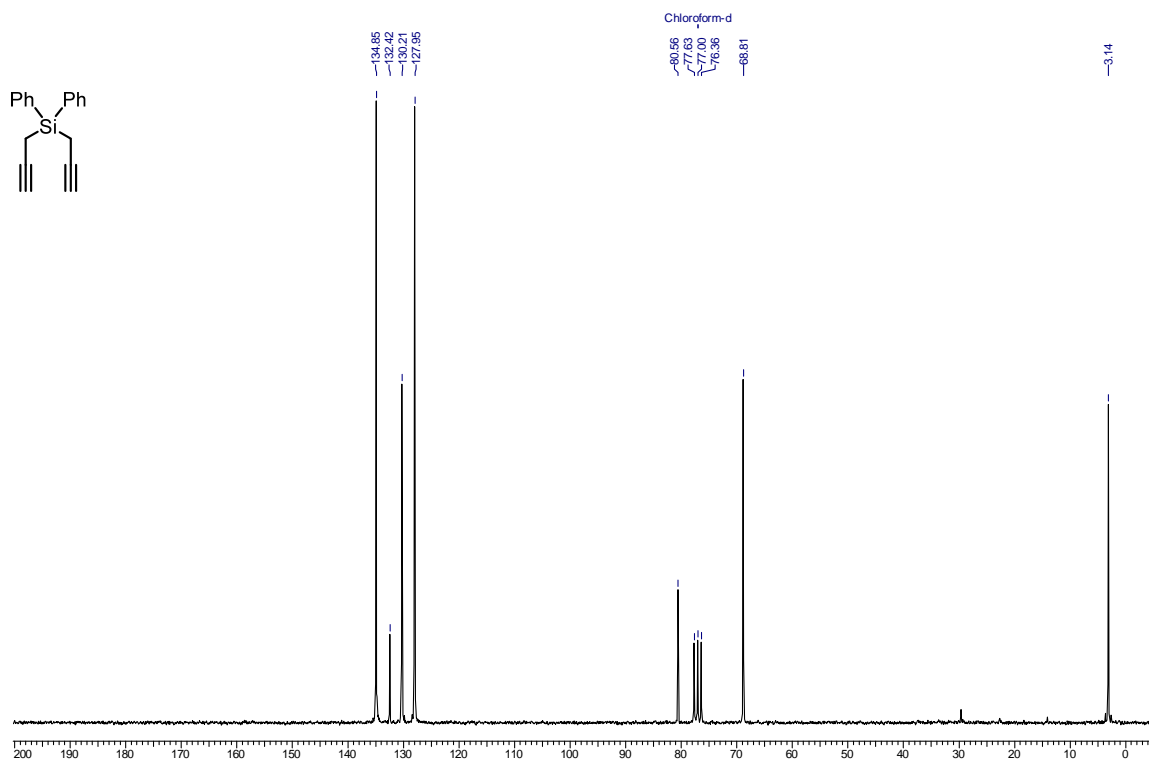
Figure 1.3.23. ^{13}C NMR of **36** (50 MHz, CDCl$_3$)
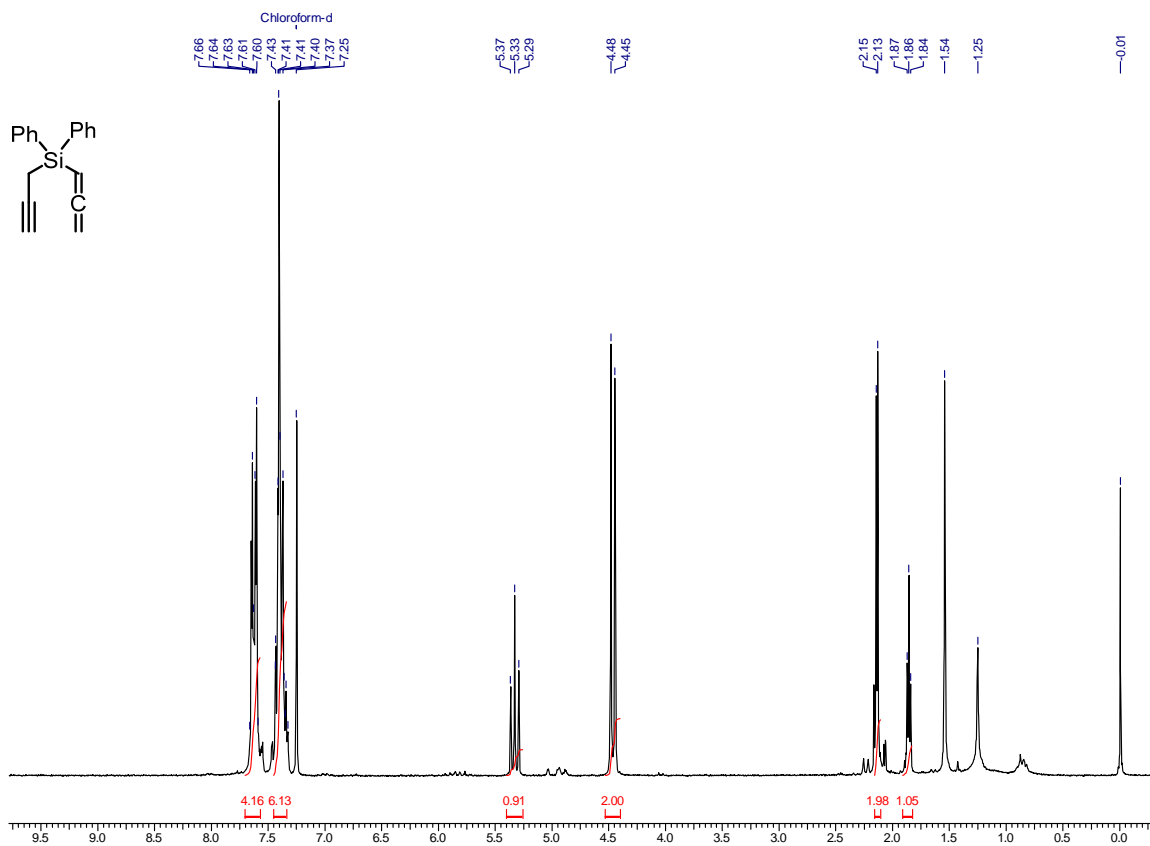
Figure 1.3.24. ^{1}H NMR of **37** (200 MHz, CDCl$_3$)
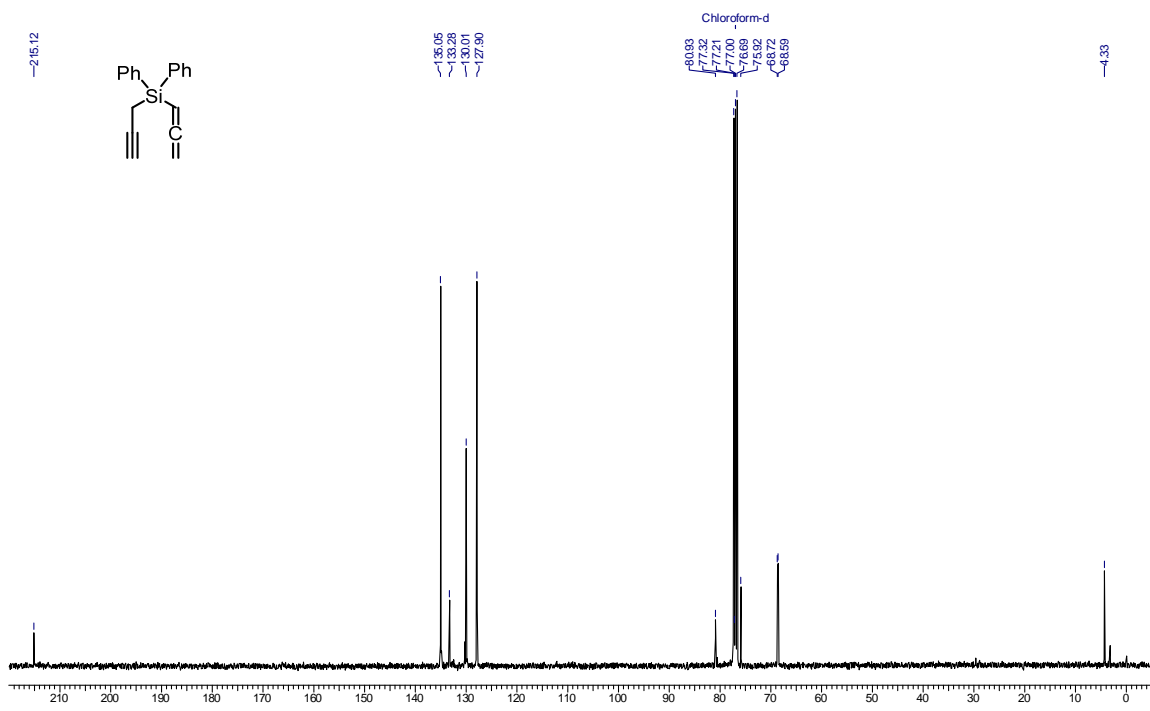
Figure 1.3.25. ^{13}C NMR of **37** (125 MHz, CDCl$_3$)
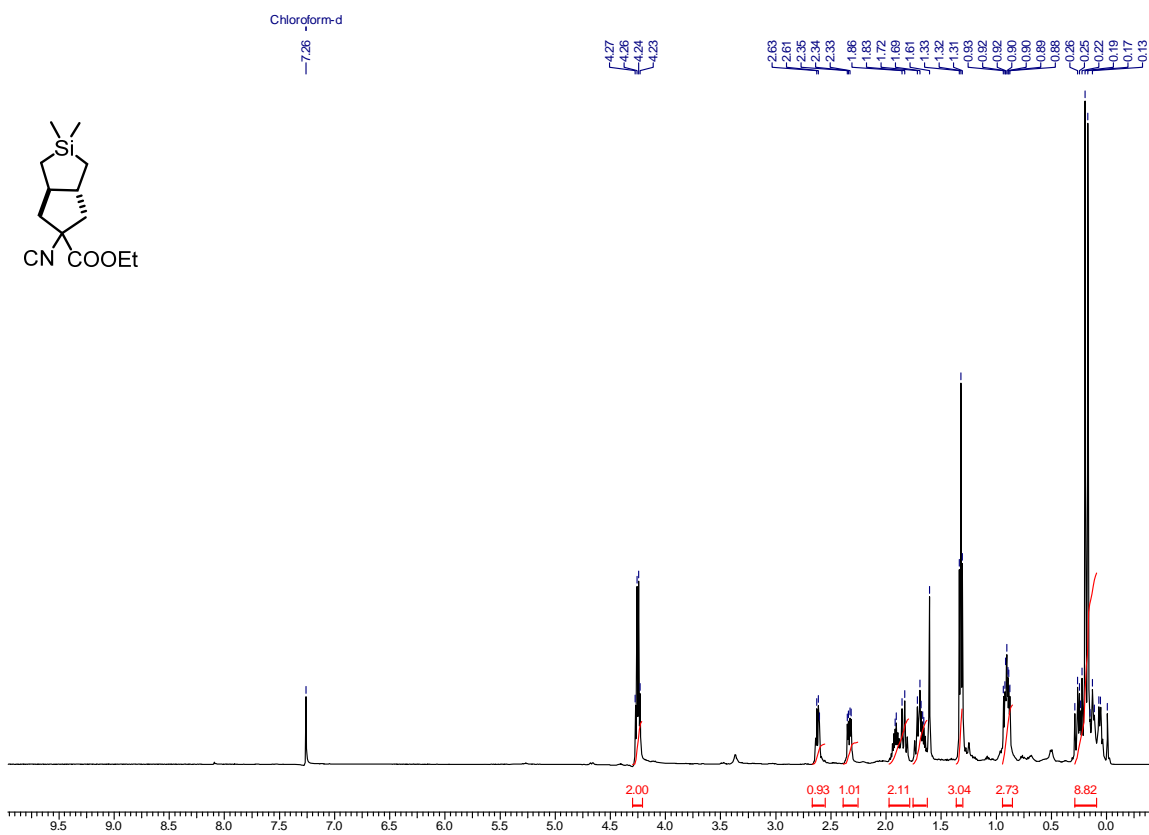
Figure 1.3.26. ^{1}H NMR of **39** (500 MHz, CDCl$_3$)
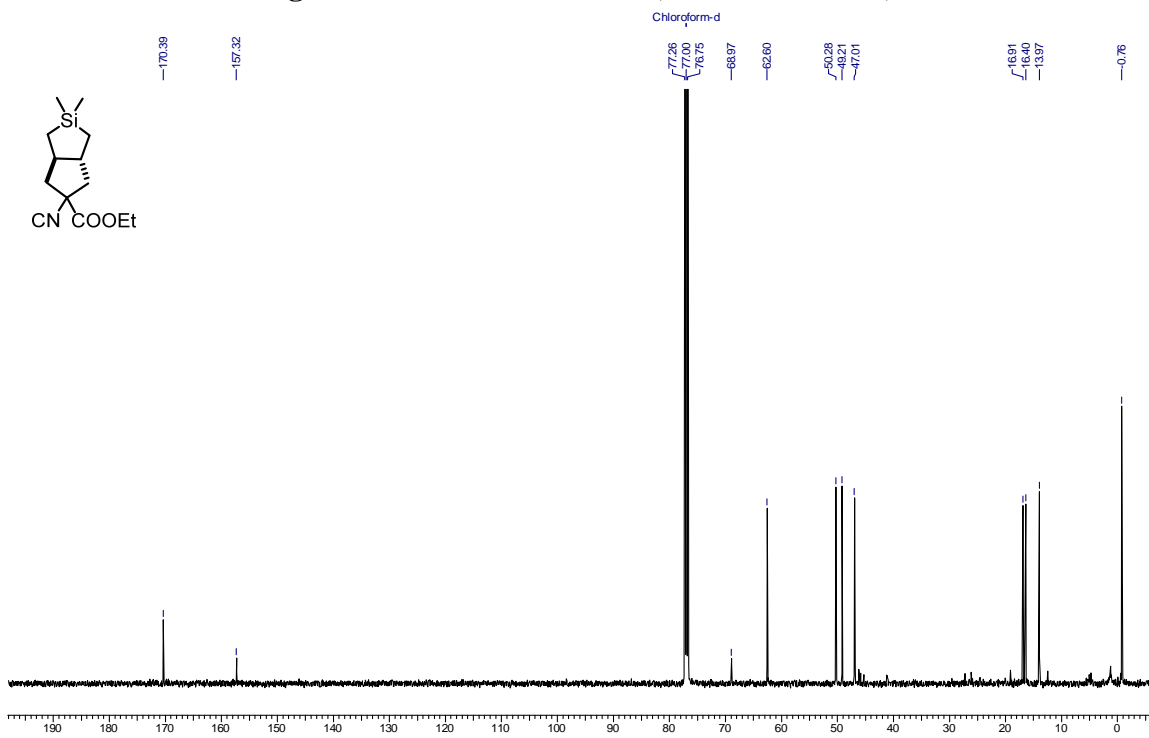
Figure 1.3.27. ^{13}C NMR of **39** (125 MHz, CDCl$_3$)
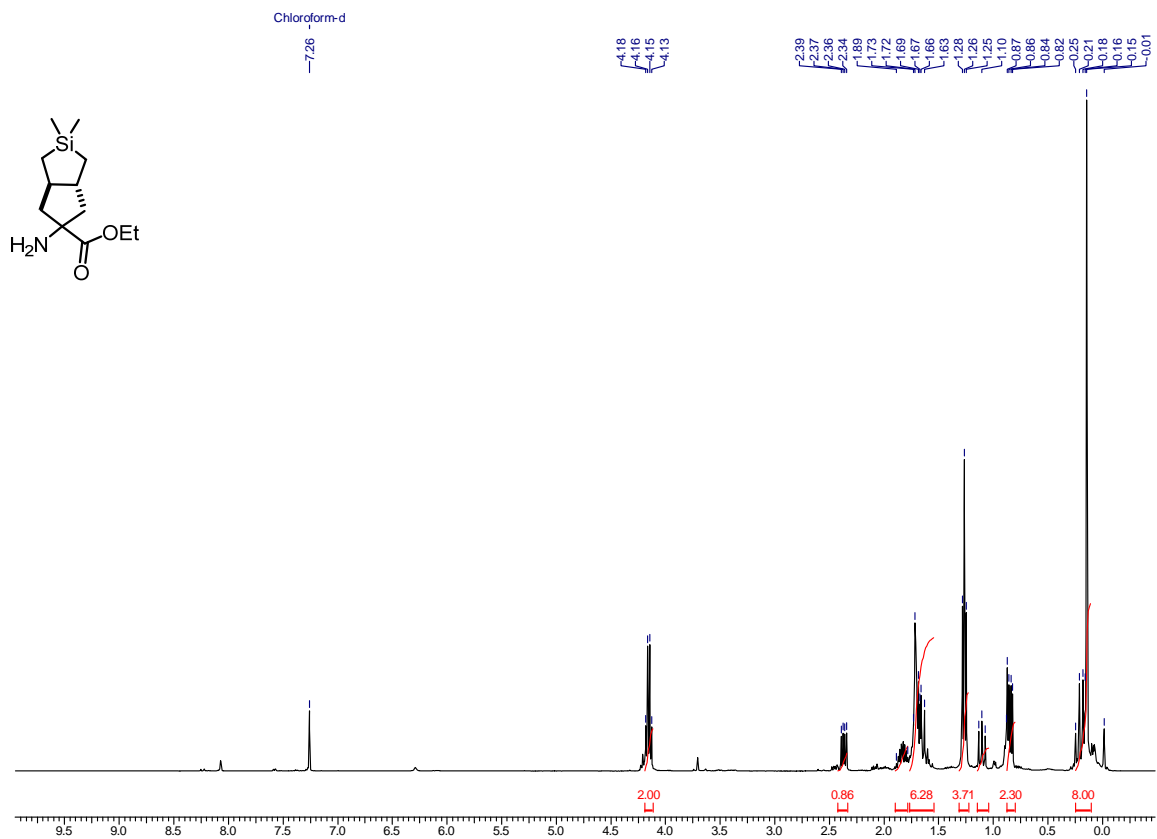
Figure 1.3.28. ^{1}H NMR of **40** (400 MHz, CDCl$_3$)
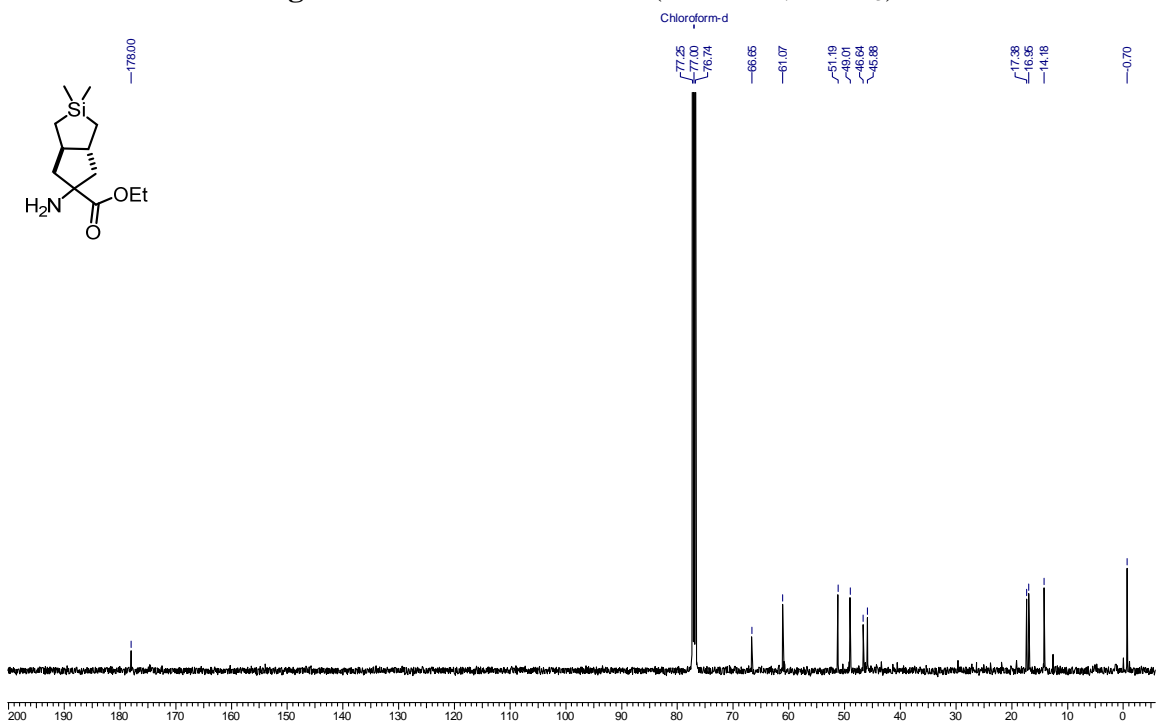
Figure 1.3.29. ^{13}C NMR of **40** (125 MHz, CDCl$_3$)
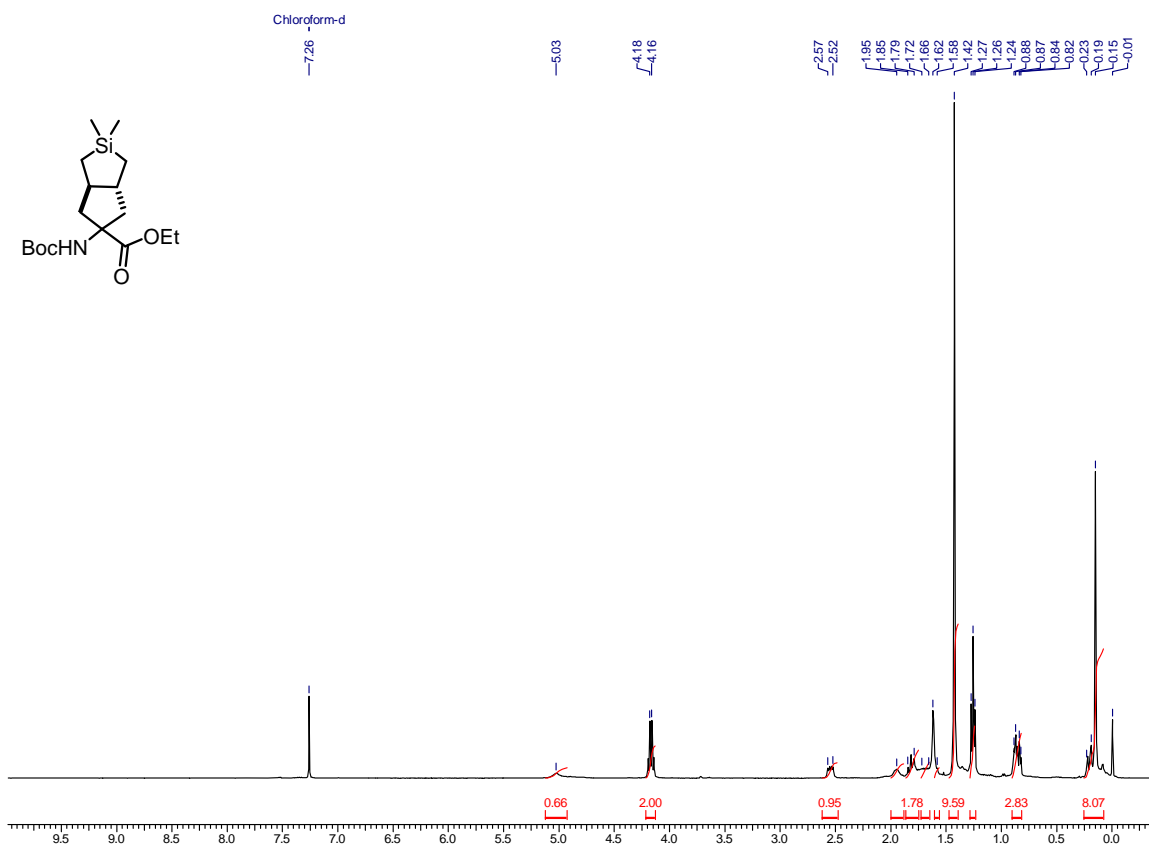
Figure 1.3.30. ^{1}H NMR of **41** (400 MHz, CDCl$_3$)
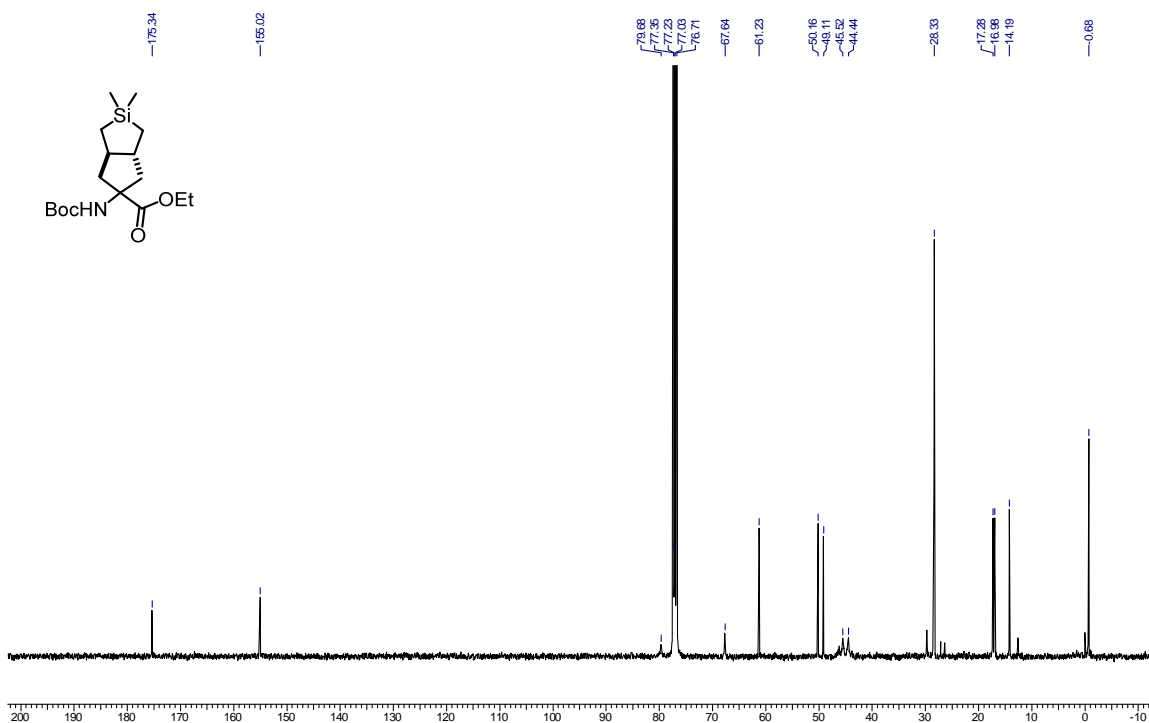
Figure 1.3.31. ^{13}C NMR of **41** (100 MHz, CDCl$_3$)

Figure 1.3.32. ^{1}H NMR of **42** (400 MHz, MeOD)

Figure 1.3.33. ^{13}C NMR of **42** (100 MHz, MeOD)
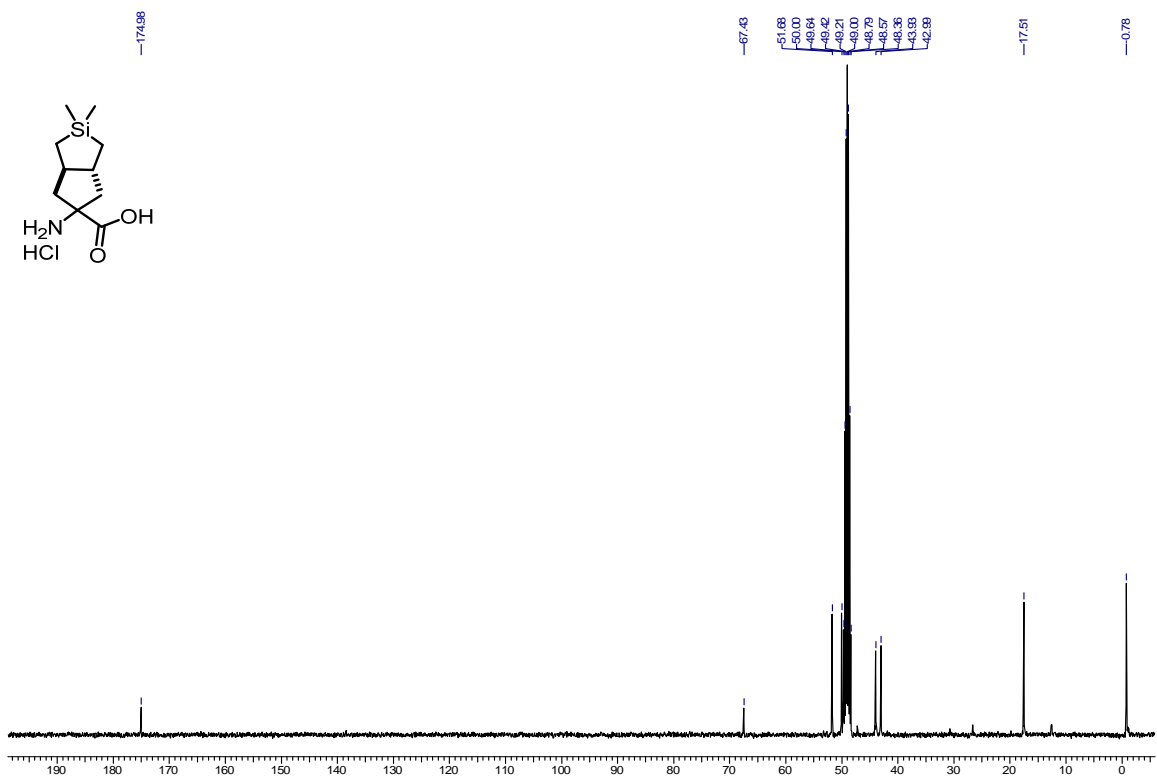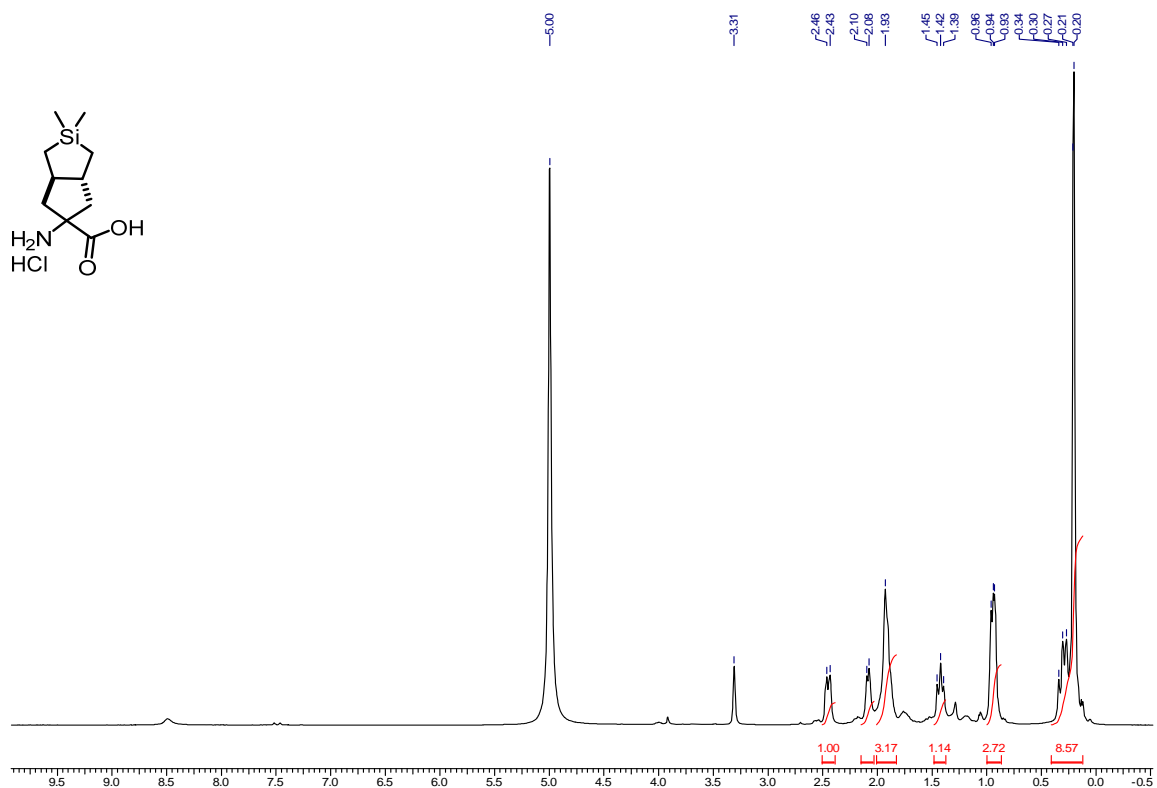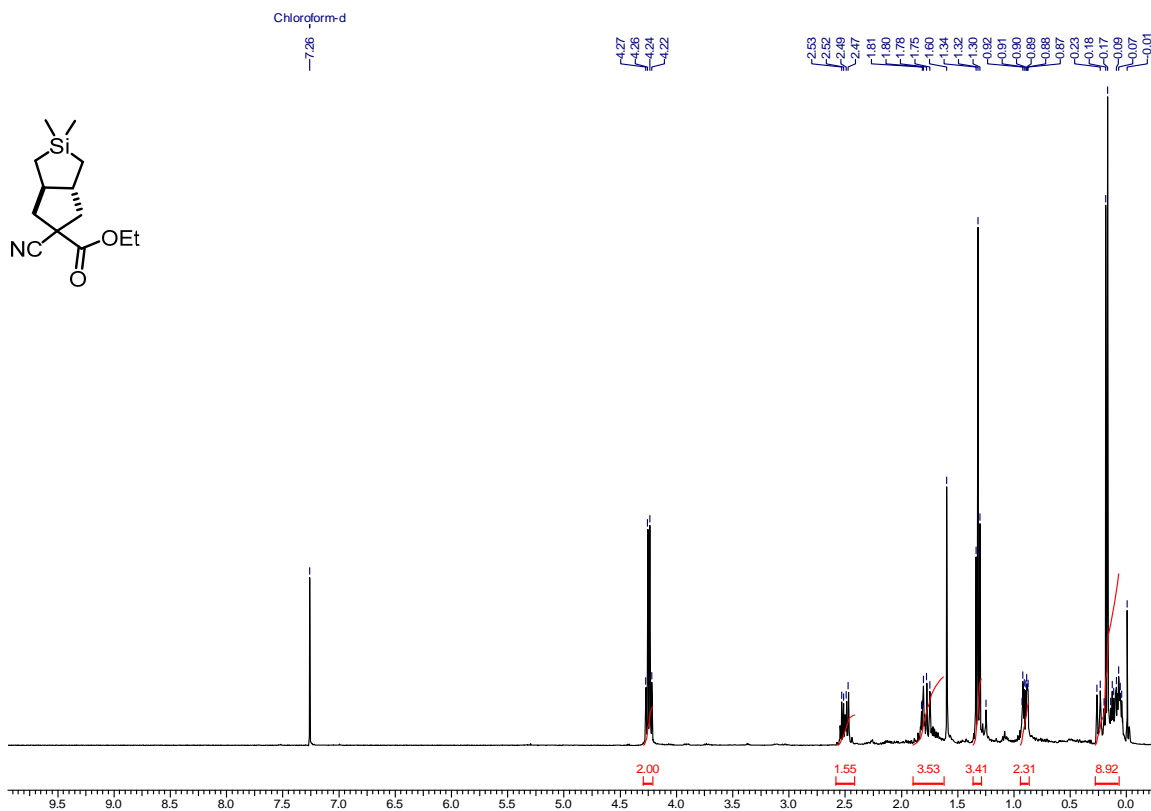
Figure 1.3.34. ^{1}H NMR of **43** (400 MHz, CDCl$_3$)
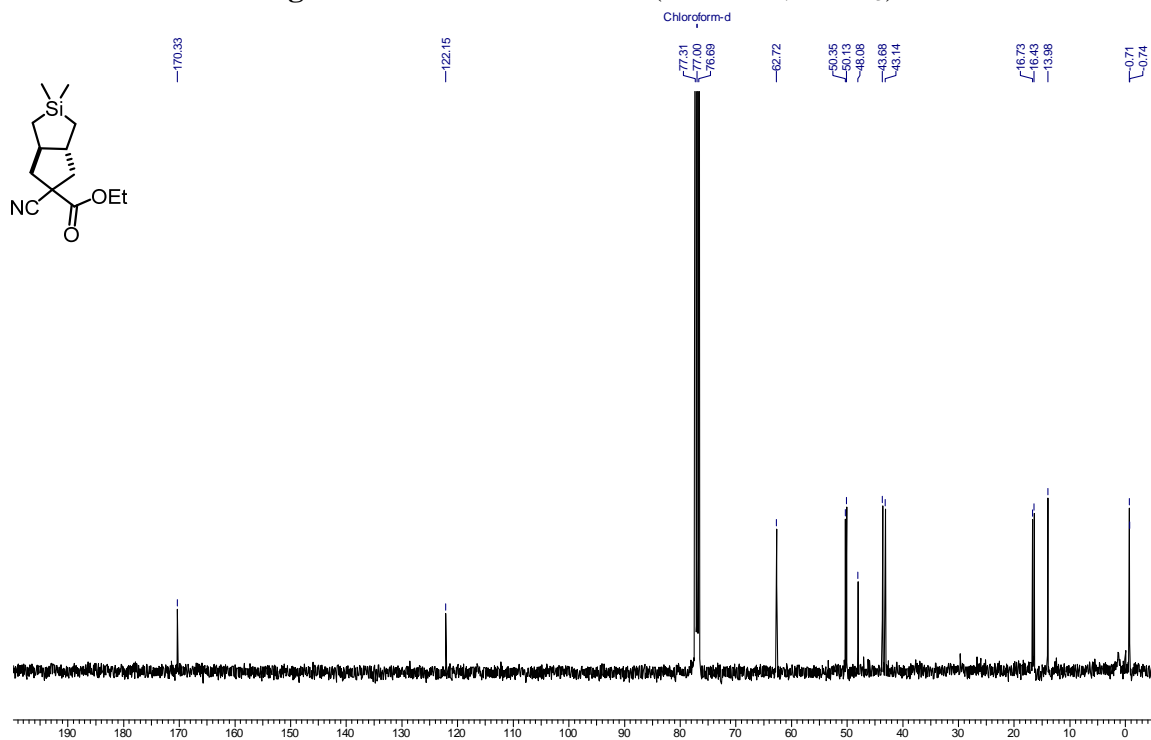
Figure 1.3.35. ^{13}C NMR of **43** (100 MHz, CDCl$_3$)

Figure 1.3.36. ^{1}H NMR of **44** (400 MHz, CDCl$_3$)

Figure 1.3.37. ^{13}C NMR of **44** (100 MHz, CDCl$_3$)
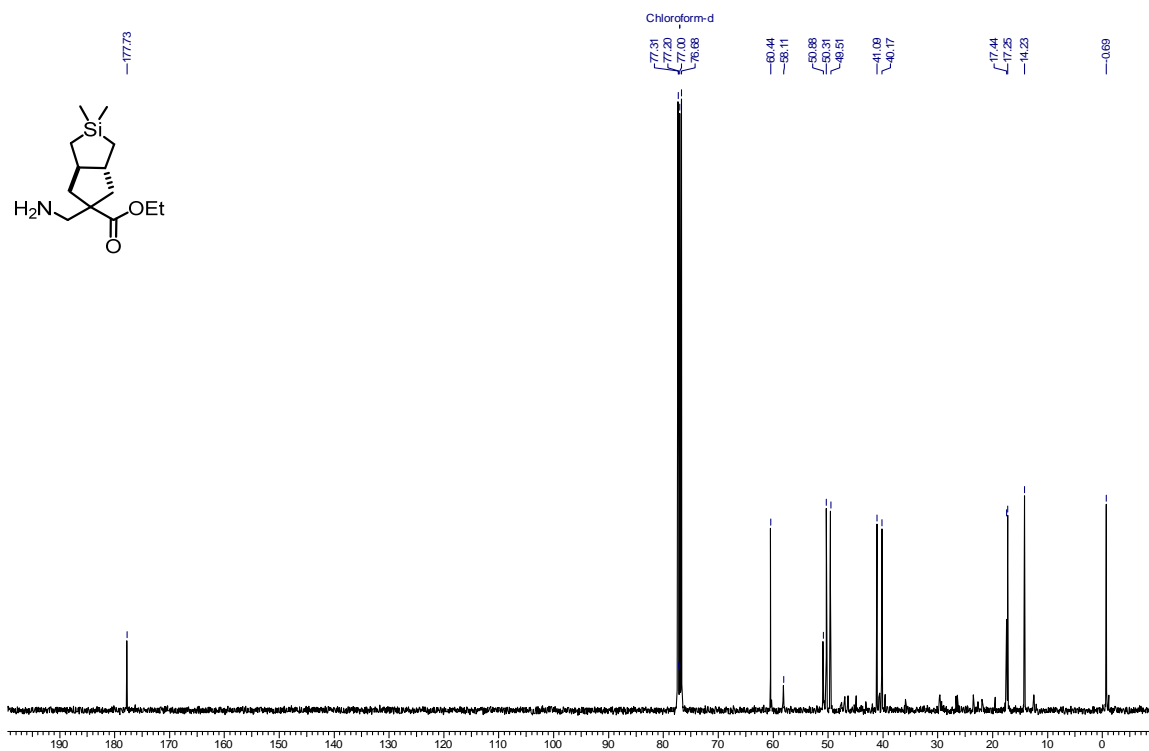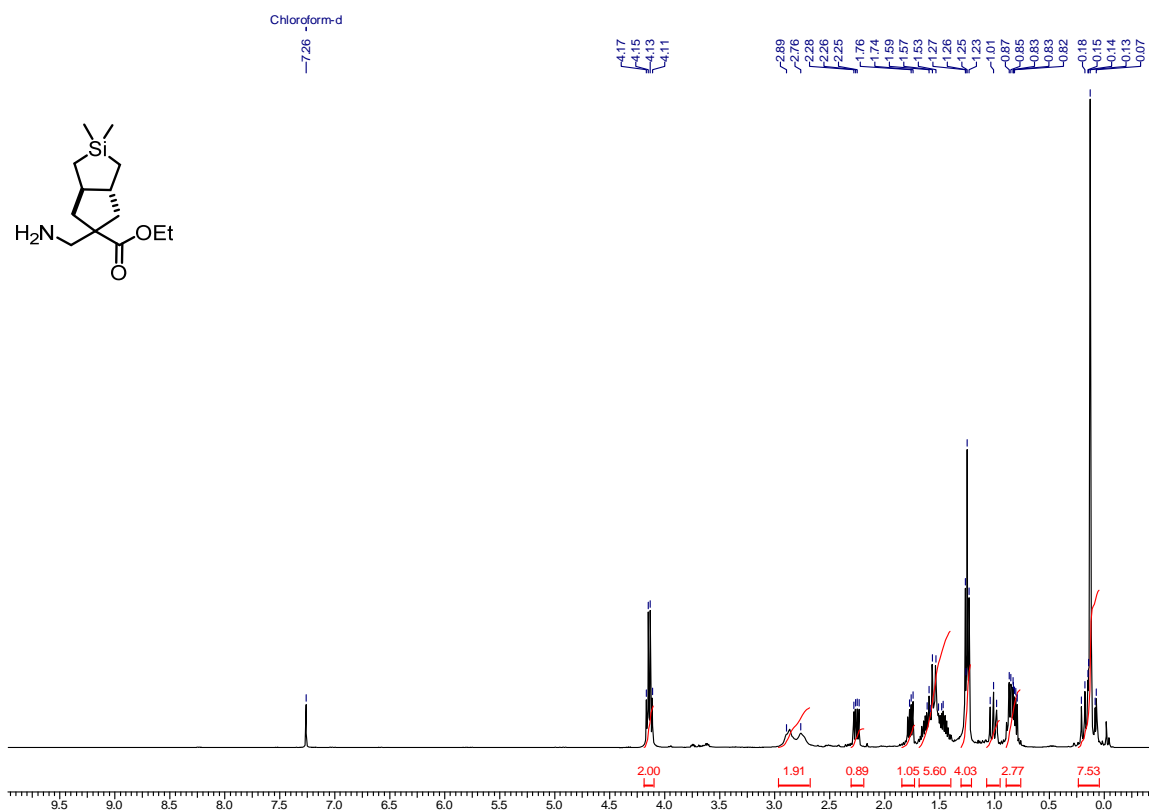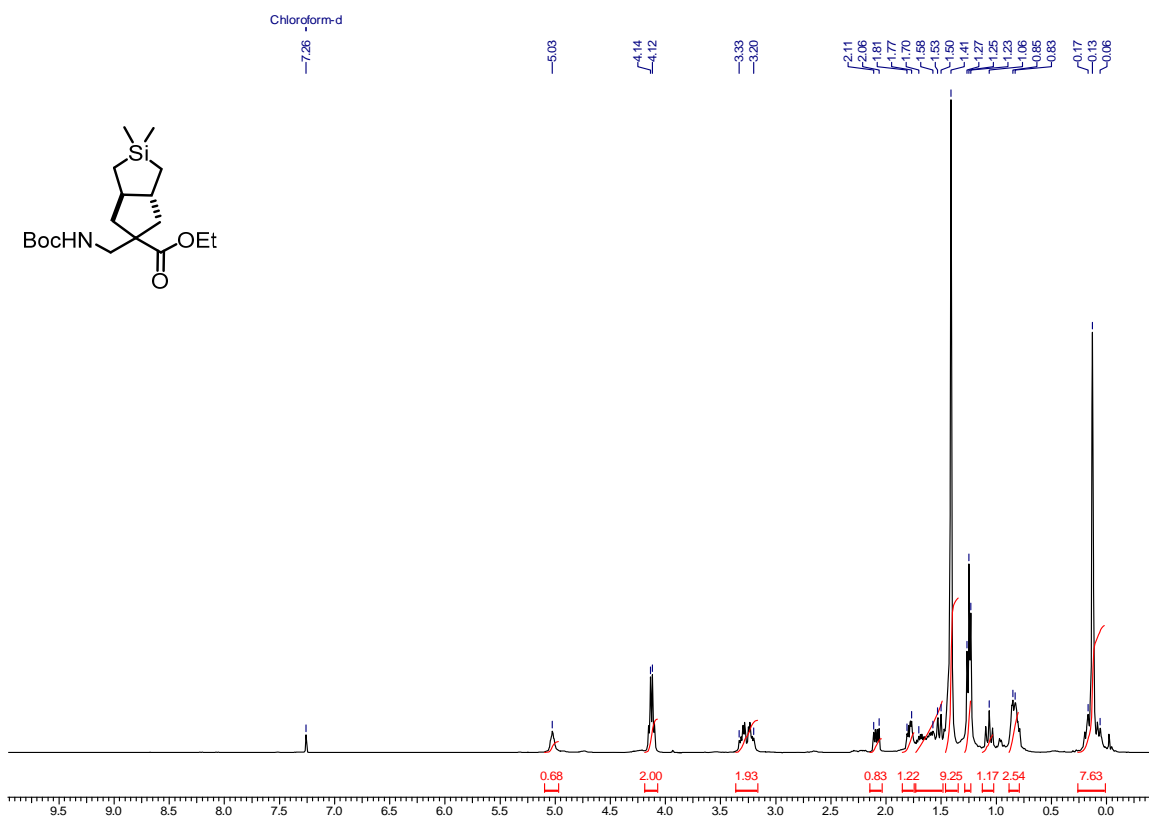
Figure 1.3.38. ^{1}H NMR of **45** (400 MHz, CDCl$_3$)
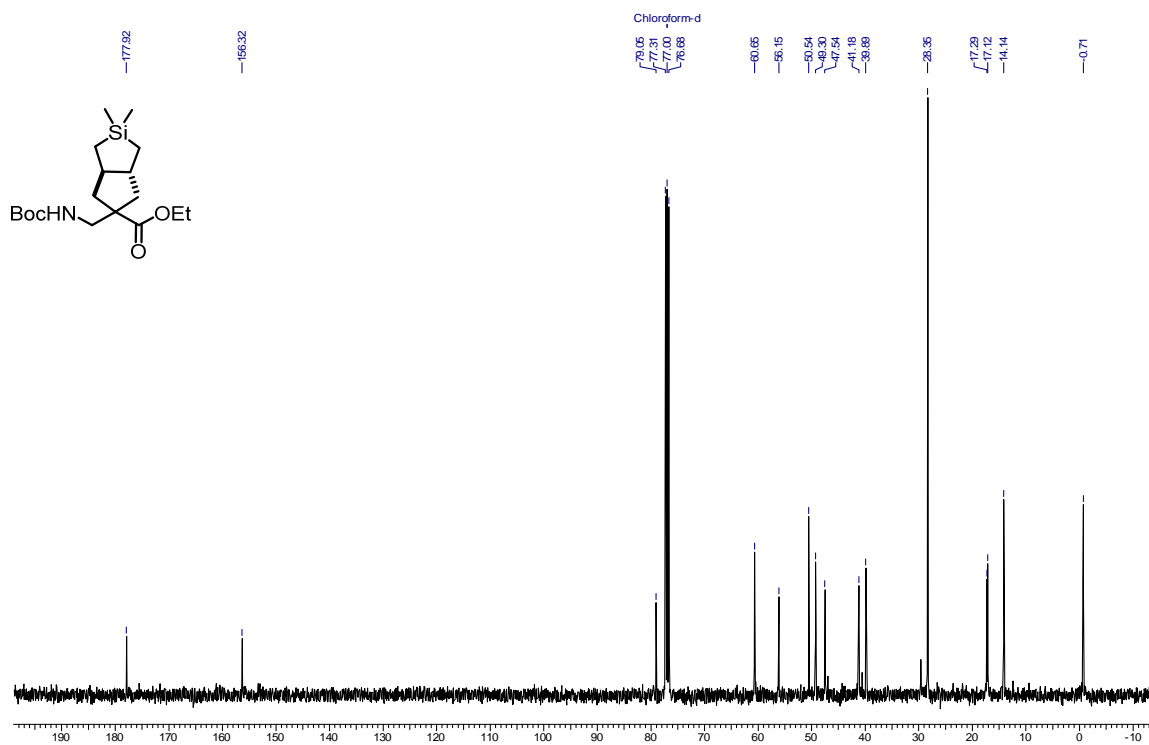
Figure 1.3.39. ^{13}C NMR of **45** (100 MHz, CDCl$_3$)

Figure 1.3.40. ^{1}H NMR of **46** (400 MHz, MeOD)

Figure 1.3.41. ^{13}C NMR of **46** (100 MHz, MeOD)

Figure 1.3.42. ^{1}H NMR of **47** (400 MHz, CDCl$_3$)

Figure 1.3.43. ^{13}C NMR of **47** (100 MHz, CDCl$_3$)
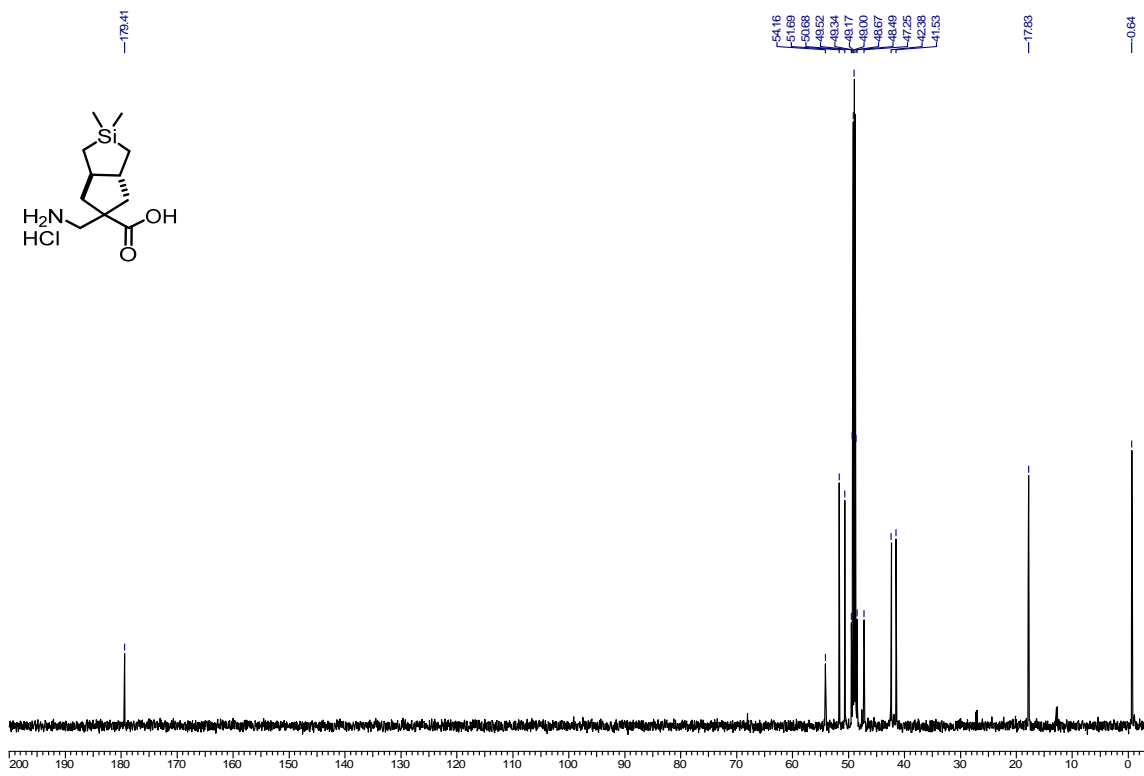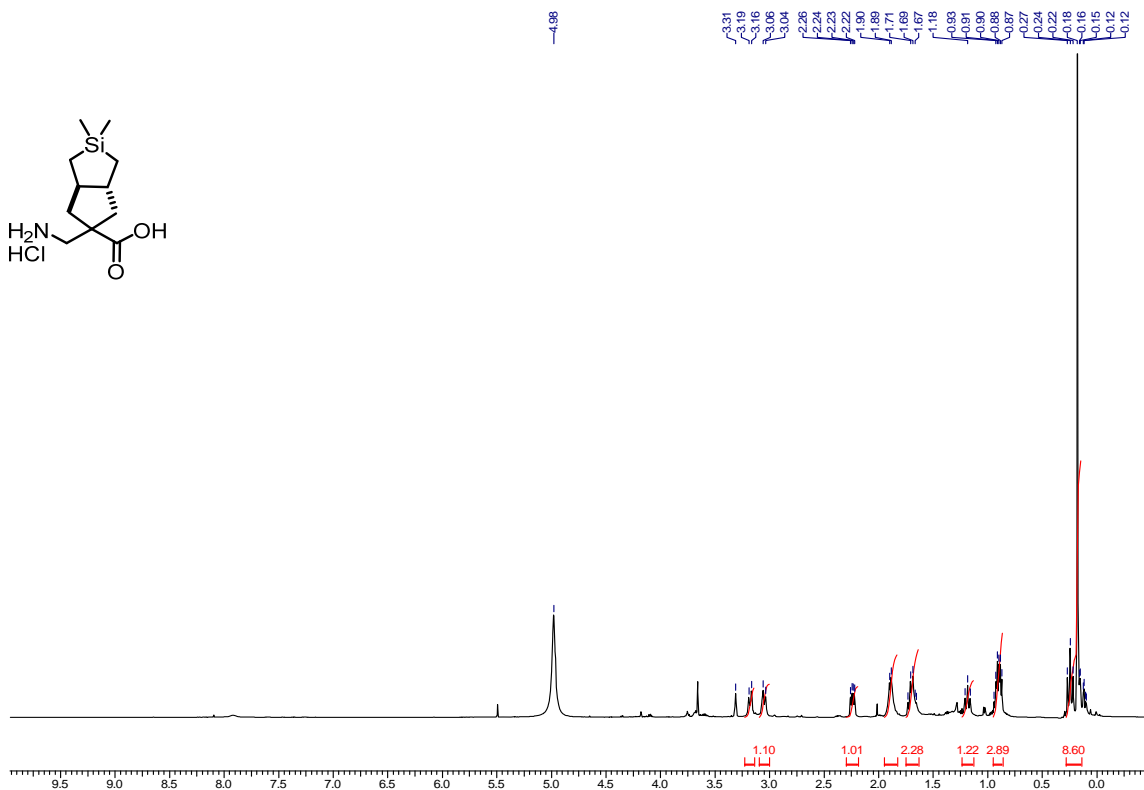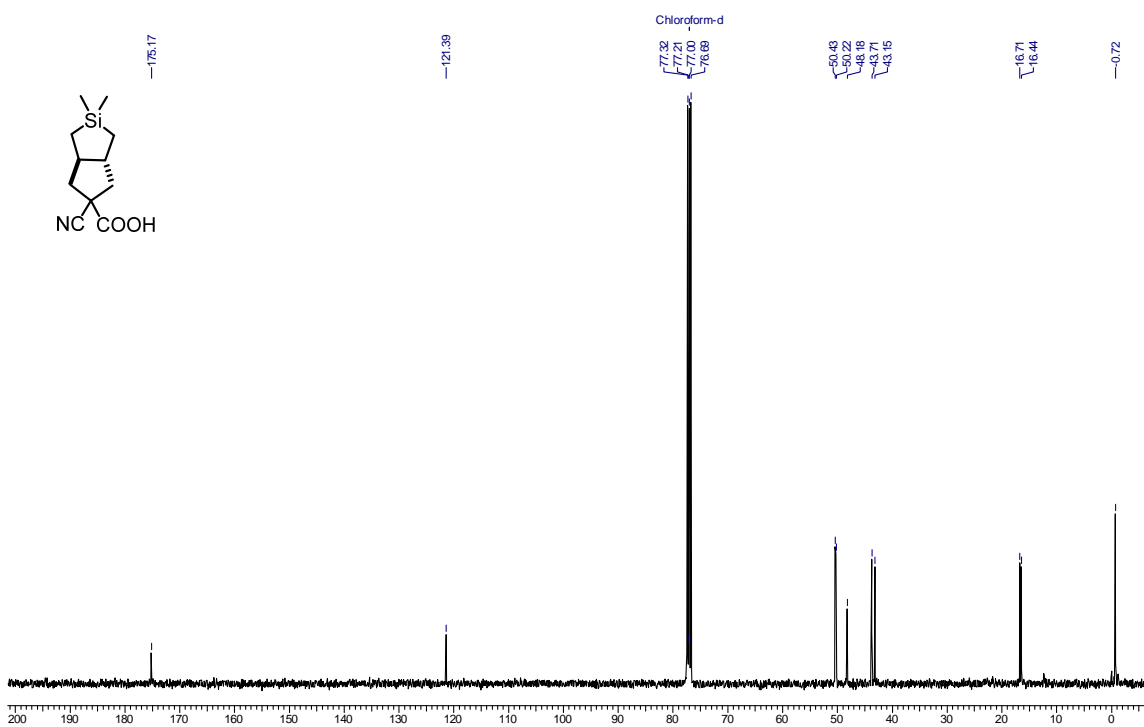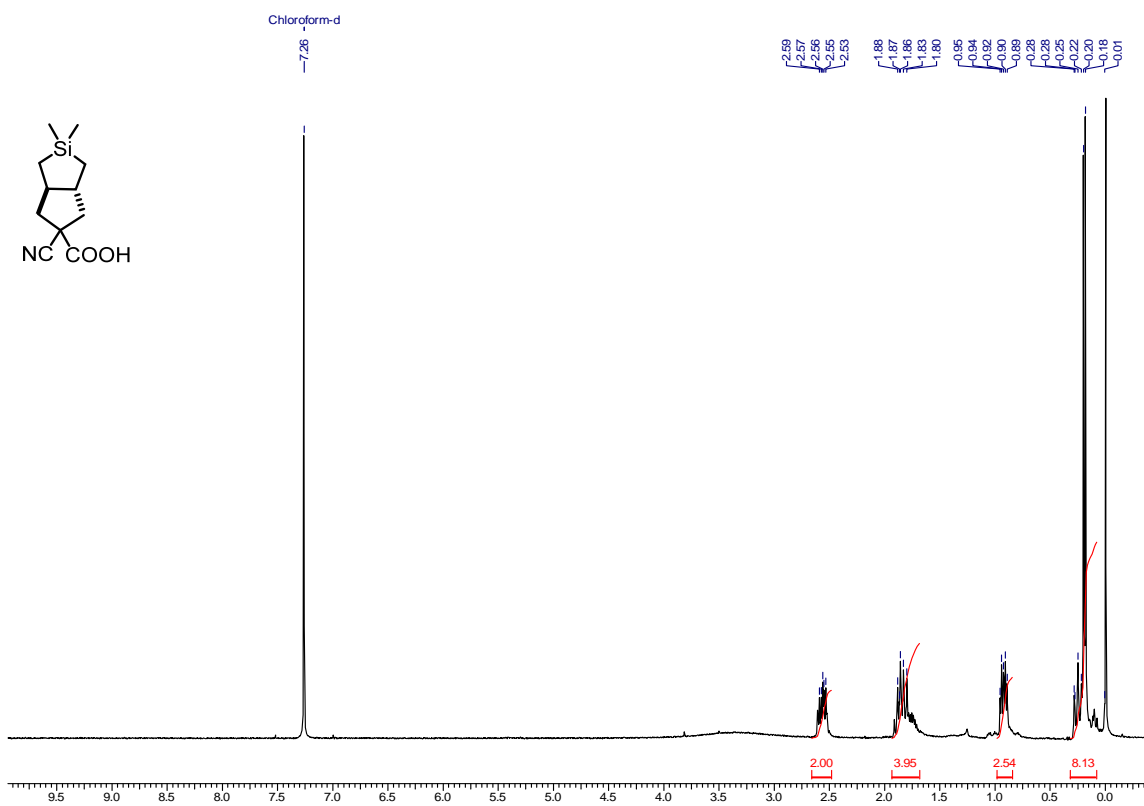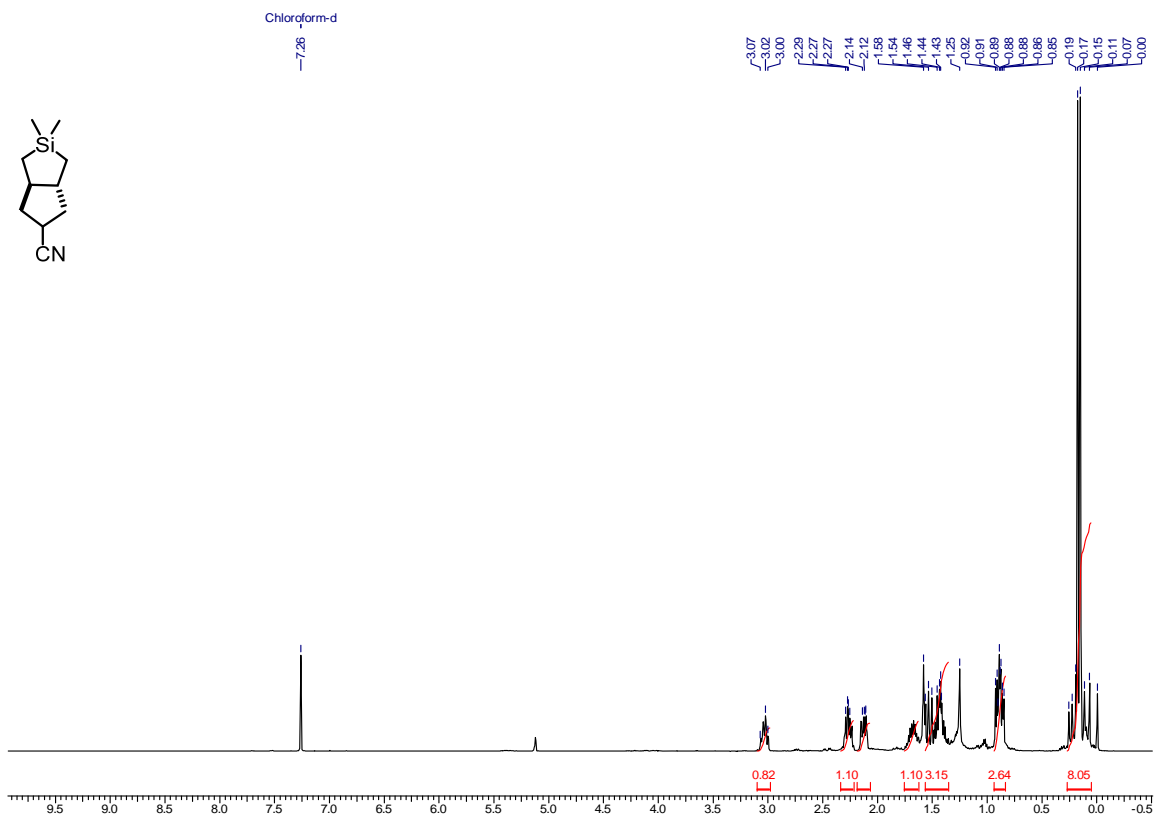
Figure 1.3.44. ^{1}H NMR of **48** (400 MHz, CDCl$_3$)
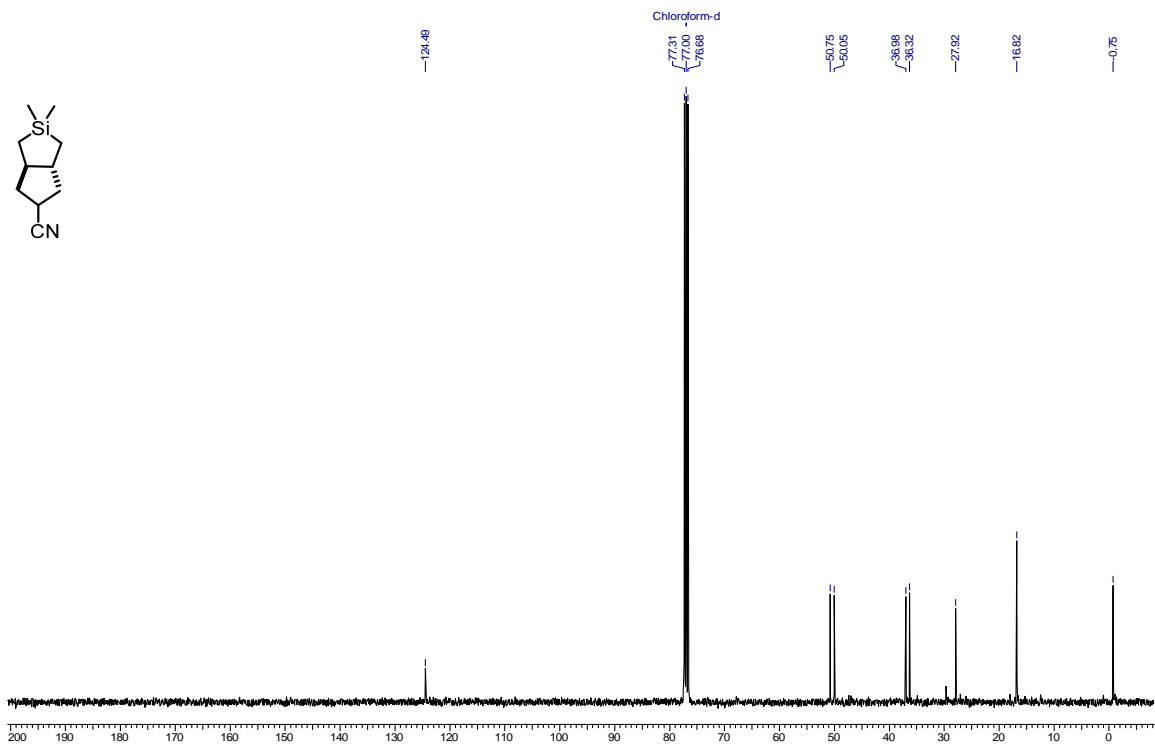
Figure 1.3.45. ^{13}C NMR of **48** (100 MHz, CDCl$_3$)

172

Figure 1.3.46. ^{1}H NMR of **50** (400 MHz, CDCl$_3$)

Figure 1.3.47. ^{13}C NMR of **50** (100 MHz, CDCl$_3$)
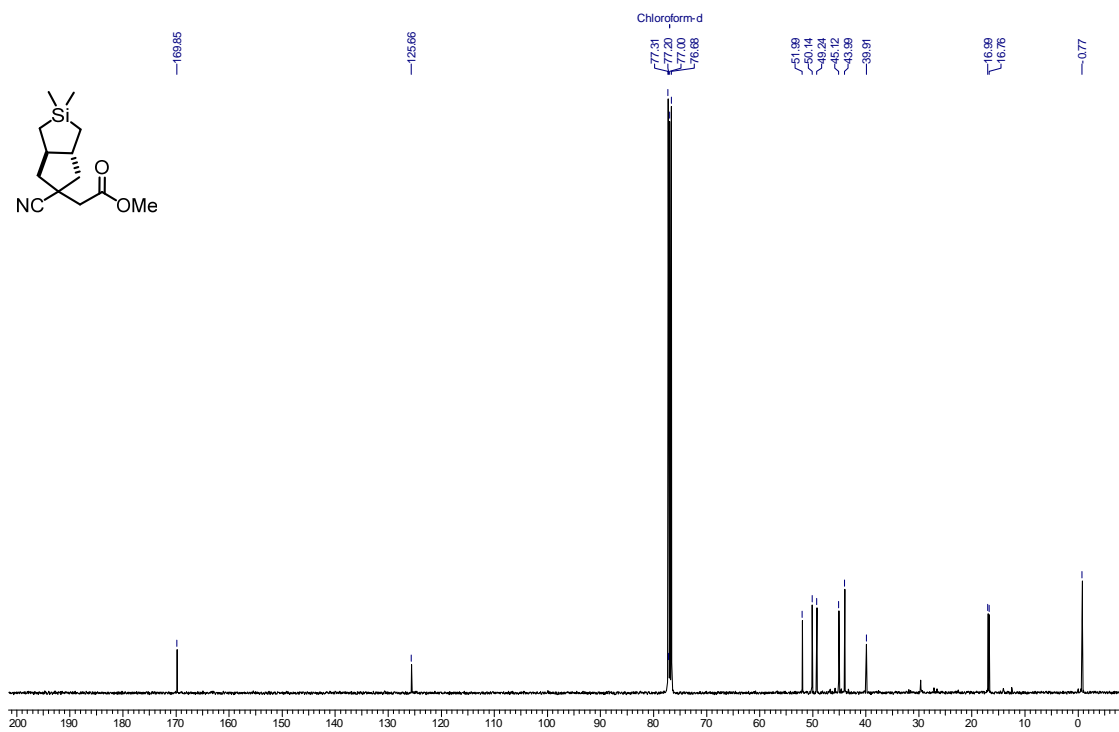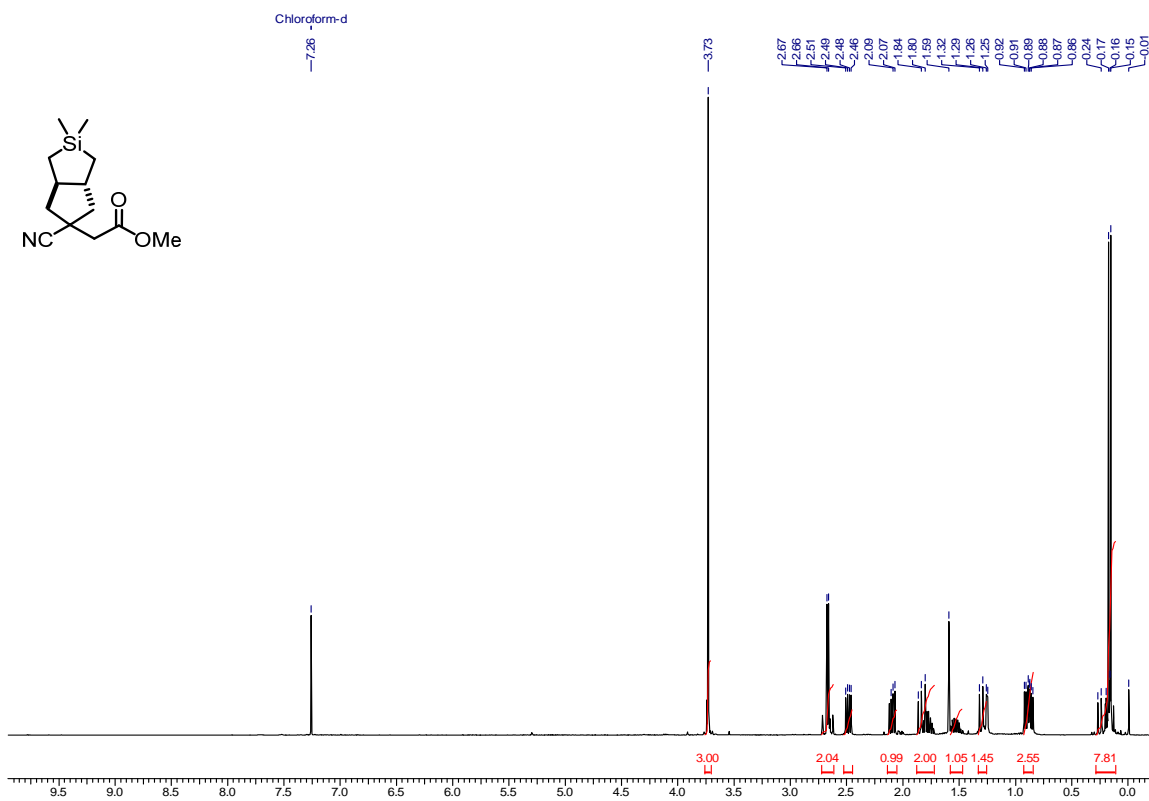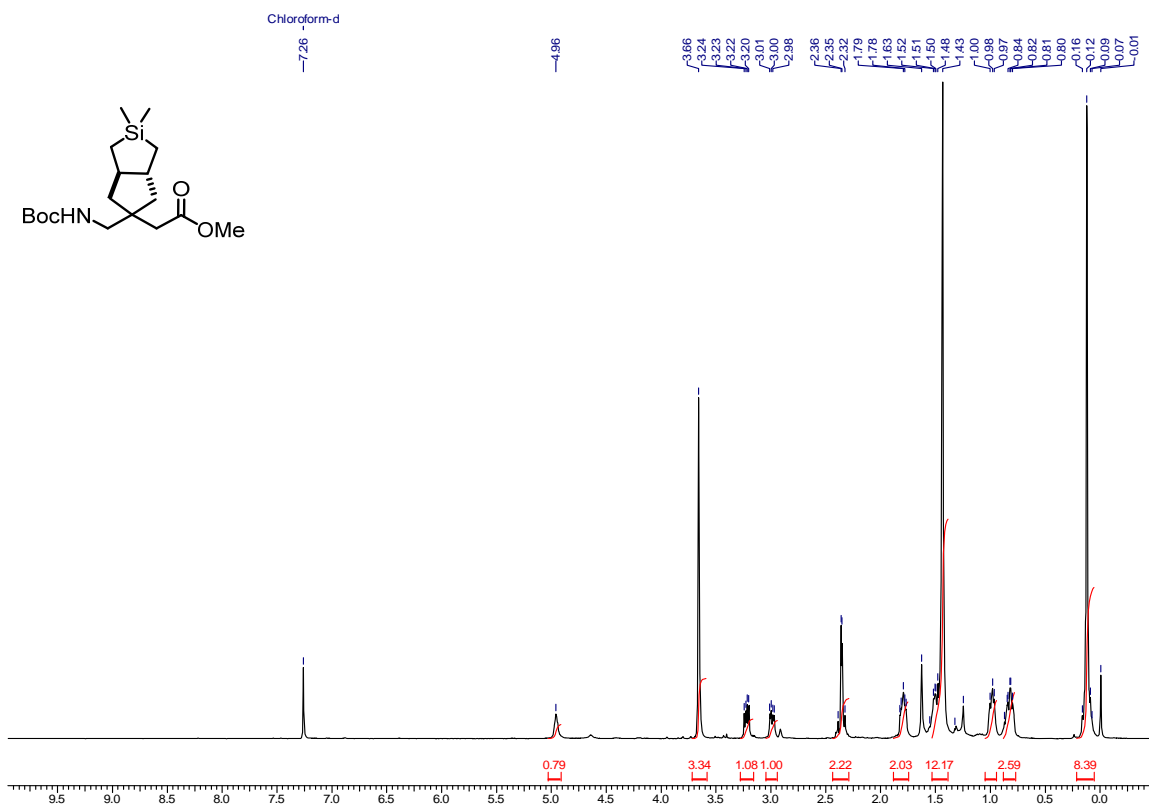
Figure 1.3.48. ^{1}H NMR of **51** (500 MHz, CDCl$_3$)
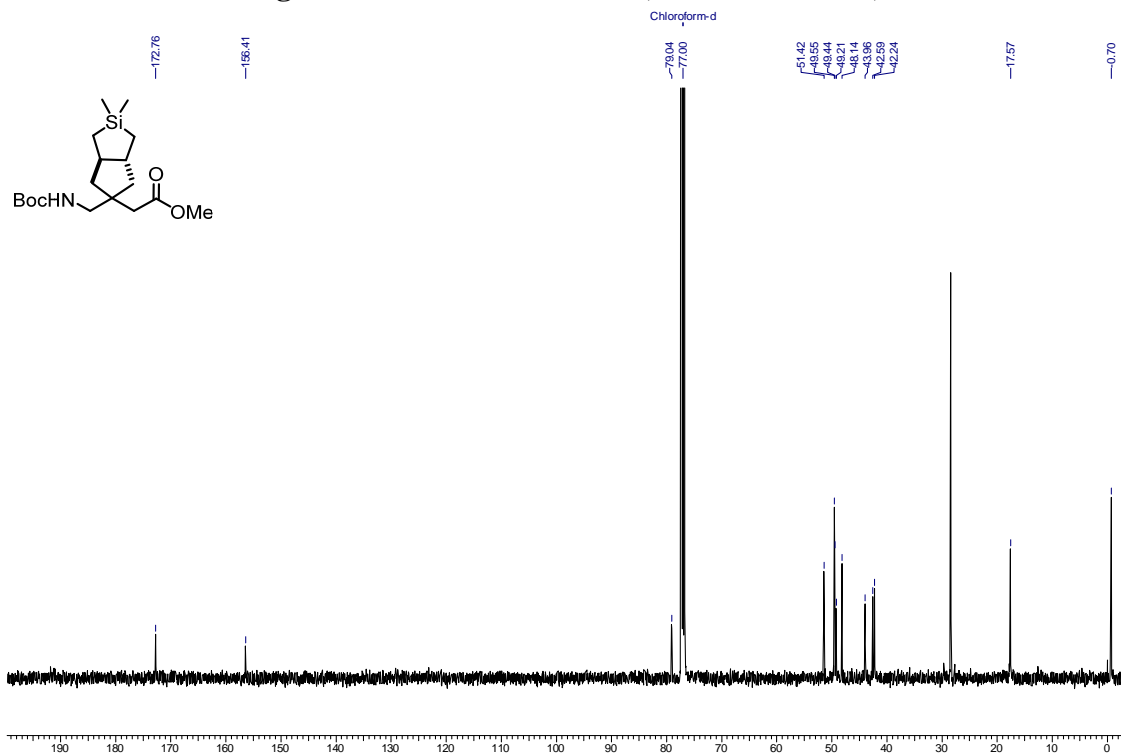
Figure 1.3.49. ^{13}C NMR of **51** (125 MHz, CDCl$_3$)
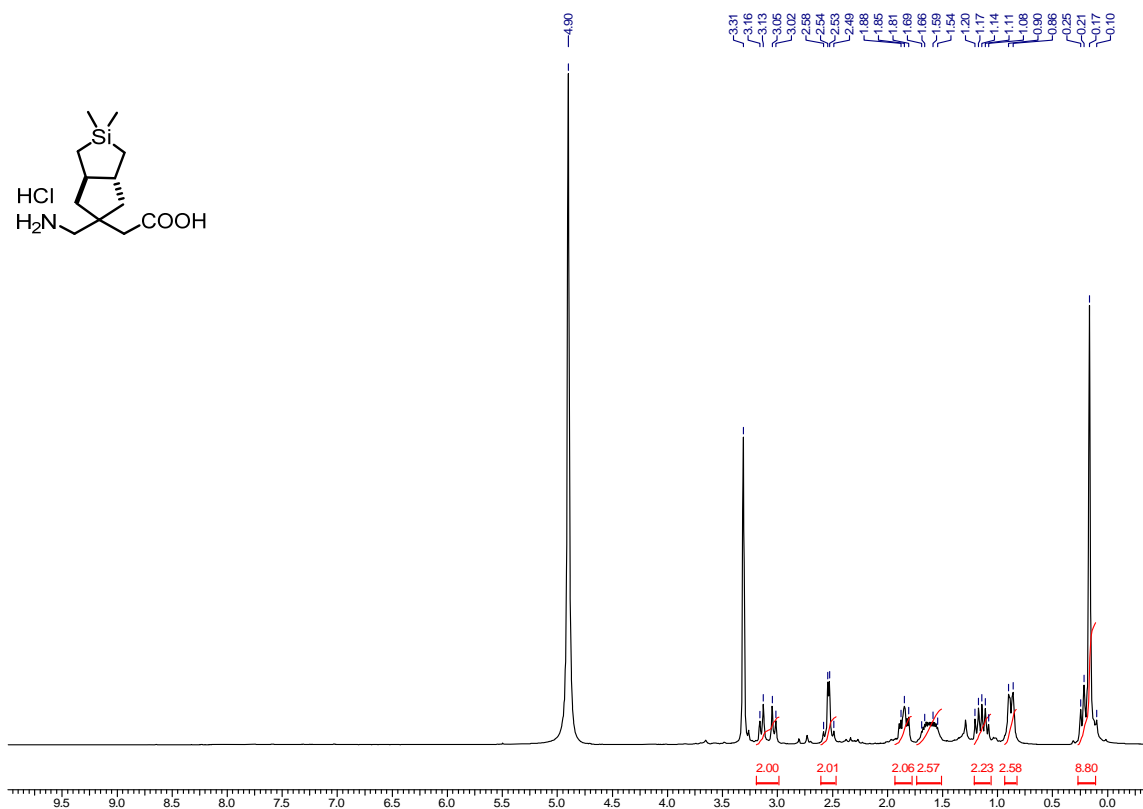
Figure 1.3.50. ^{1}H NMR of **52** (400 MHz, MeOD)
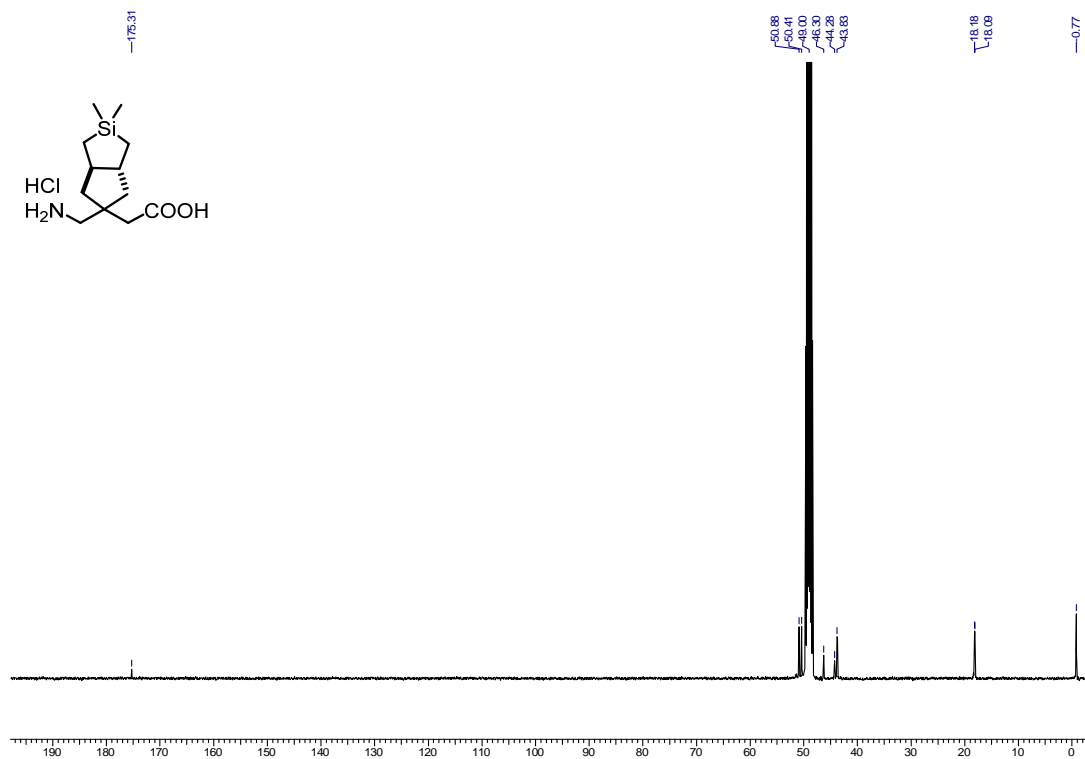
Figure 1.3.51. ^{13}C NMR of **52** (100 MHz, MeOD)

Chapter 2

Synthesis of enantiopure pheromones towards crop protection

2.1. Pheromone

2.1.1. Introduction

Semiochemicals are substances secreted by organisms as a means of communication. The term is derived from the Greek word 'semeon' which means 'signal'. Chemical ecology is an interdisciplinary field, involving both chemistry and biology and deals with the study of semiochemicals. Semiochemicals involved in interspecific communication are called allelochemicals and those involved in intraspecific communication are called pheromones. Allelochemicals are again subdivided into allomones, kairomones, and synomones.[1,2]
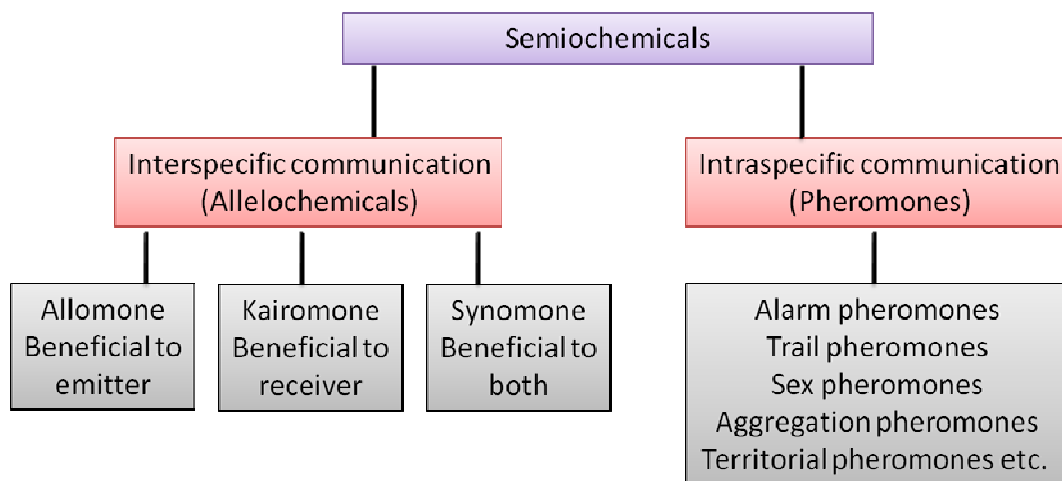
Figure 2.1. Classification of semiochemicals

Allomone: These are semiochemicals released by an individual and affect the behaviour of a member of other species and are beneficial to the emitter. Allomones are part of defense.

Kairomone: Kairomones are released by an individual and creates a response in members of other species beneficial to the receiver. They either indicate a food source or give warning about a predator.

Synomone: These chemical signals are beneficial for both emitter and receiver.

Pheromones are intraspecific signals and depending on the message conveyed, they are of different types such as: Alarm pheromones, Trail pheromones, Sex pheromones, Aggregation pheromones, Territorial pheromones etc.

Bombykol, secreted by female silkworm moth was the first pheromone to be isolated and characterized. This sex pheromone was discovered by Nobel Laureate Adolf Butenandt in the year 1959. Butenandt synthesized four geometrical isomers of bombykol. Of all the compounds synthesized, only one isomer (10*trans*, 12*cis*) was active. Hence, Butenandt confirmed that the active (10*E*, 12*Z*) isomer is the natural product.[3,4] Most of the moths are sexually dimorphic and the male antennae can sense the female pheromone. The female moths contain scent glands which secrete the pheromone.

Bombykol
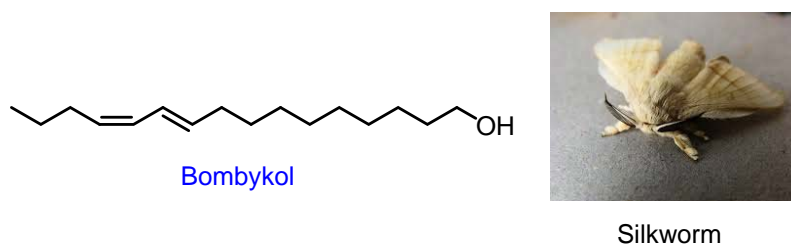
Silkworm

Figure 2.2. Sex pheromone of silkworm

Later this field gained more attention and as a result, pheromones of several other species were discovered. The name pheromone originated from the Greek words pherein (to transport) and hormon (to excite). Pheromones are generally obtained in very less quantities and therefore for further studies to establish the structure, chemical synthesis is essential.

2.1.2. Pheromones for pest control

Pheromones are now used in pest management programs, where synthetic pheromones are used to lure and trap insects. Sex pheromones and aggregation pheromones are used for this purpose. Pheromones are highly sensitive and species specific. Since, they don't affect other beneficial organisms; pheromones are considered to be one of the environment friendly methods of pest control. There are also some

disadvantages such as (i) Different pheromones have to be deployed for each pest as they are specific (ii) Field trials have to be conducted in large areas covering up to a few kilometres as pests can be attracted from nearby fields. In spite of this, pheromones of several species have been identified and commercialized. Pheromone traps can be used for pest control in three different ways.[5]

Mating disruption: Mating disruption is a pest management technique which uses artificial pheromone traps to control pests. A high concentration of the pheromone masks the natural pheromone secreted by the females and therefore the males cannot locate the female. Also since the traps are placed at many places, it creates confusion and the males get diverted from the natural pheromone. Since, males are unable to locate the natural pheromone of females, mating is prevented and blocks the reproductive cycle. Mating disruption is employed to control vine mealybugs in California.

Mass trapping: Pheromone traps are placed at different positions in the field and the insects caught are removed later. This is the most commonly used method to control pests.

Attract and kill: A toxic material is mixed with pheromone and placed in traps. The insects get attracted and die.

2.1.3. Isolation of pheromones

Since, the pheromones are present in minor quantities (ng to μg) as volatiles, isolation and characterization is very challenging. Behavioural assays can be used to confirm the activity of the isolated material. For example, when a glass rod dipped in female pheromone is shown to male silkworm, they immediately respond and display a "flutter dance''. The pheromones can be collected from an insect by solvent extraction or by effluvial extraction. For solvent extraction either the whole insect, part of abdomen or glands can be used. In effluvial extraction, volatile pheromones are collected from headspace odours of several insects and then analyzed by gas chromatography (GC). The electroantennogram (EAG) technique uses the isolated antenna from the insect to check

the response to a particular component/ chemical. When the antenna comes in contact with a pheromone, it creates an olfactory receptor potential which is amplified and recorded. GC coupled to EAG detector is used to find out pheromones from a complex mixture.[6,7]

2.1.4. Importance of stereochemistry in pheromone synthesis

Although the importance of geometrical isomerism in activity of pheromone was known from the beginning, stereochemistry-pheromone activity relationship was not known till 1970's. Since pheromones are isolated in minor quantities, stereochemical assignment is almost impossible. Significant work done by Kenji Mori proved that chirality plays an important role in determining the activity of pheromone. Mori categorized pheromones based on the stereochemistry-activity relationships (see figure 2.3).[8-10]

The category A is most commonly encountered (~60%) and here only one enantiomer is active, but the other enantiomer does not inhibit the pheromonal activity of the natural one. In pheromones belonging to category B, enantiomer has inhibitory effect whereas in category C, the diastereomer displays inhibition. In category D, although the natural pheromone is enantiopure, the other stereoisomer also exhibits activity. In some cases (category E and G), the natural pheromone itself is a stereoisomeric mixture. In pheromones belonging to category G, both the enantiomers are required for the activity. Hence, it is clear that stereochemistry plays a significant role in pheromonal activity. After identifying the gross structure, a bioassay of pheromone enantiomers can reveal more insights into the stereochemistry-activity relationship. This knowledge is essential for commercialization and practical utility of the product. For instance, the enantiopure disparlure which belongs to category B is now used to control the gypsy moth. The synthesis of enantiopure pheromones may also help in establishing the absolute configuration of the natural product.

Category A

one of the enantiomer is active and
the other enantiomer is not inhibitory
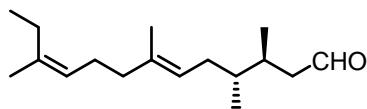
faranal (trial pheromone of pharaoh's ant)

Category B

one of the enantiomer is active and the
other enantiomer inhibits the activity
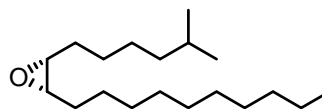
disparlure (sex pheromone of gypsy moth)

Category C

one of the enantiomer is active and the
other diastereomer inhibits the activity
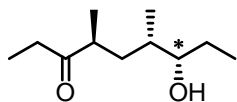
serricornin (sex pheromone
of cigarette beetle)
diastereomer at * is inhibitory

Category D

natural pheromone is enantiopure, but its
enantiomer/ diastereomer is also active
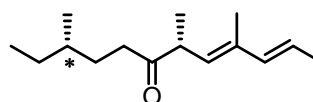
sex pheromone of maritime pine scale
diastereomer at * is also active

Category E

natural pheromone is enantiomeric mixture,
but the enantiomers are active separately

n-$C_{18}H_{37}$
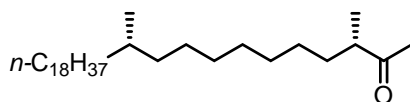
sex pheromone of German cockroach

Category F

In the same genus, different species have
different enantiomers as pheromones
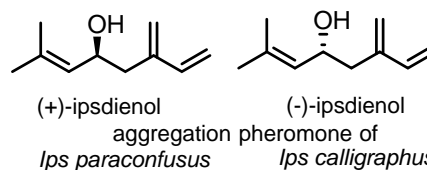
(+)-ipsdienol   (-)-ipsdienol
aggregation pheromone of
Ips paraconfusus   *Ips calligraphus*

Category G

both enantiomers are required for activity
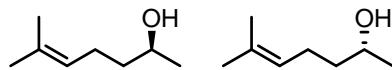
(+)-sulcatol   **(-)-sulcatol**

aggregation pheromone of
Gnathotrichus sulcatus

Category H

stereoisomeric mixture is more active
than the most active enantiomer alone
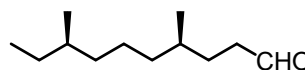
tribolure (aggregation pheromone
of red flour beetle)

Category I

one enantiomer is active on males,
and the other is active on females
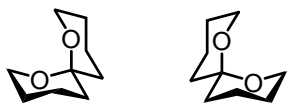
(-)-olean   **(+)-olean**
(male)   (female)
sex pheromone of olive fruit fly

Category J

only the optically inactive
meso isomer is active

n-$C_{12}H_{25}$ n-$C_{12}H_{25}$
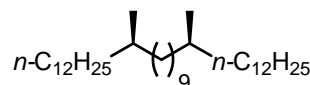
sex pheromone of tsetse fly

Figure 2.3. Classification of pheromones by Kenji Mori

2.2. Pheromones to control mealybugs

Mealybugs are insects belonging to the family *Pseudococcidae*. They are serious pests which infest a variety of plants and causes huge economic loss. Mealybugs are also vectors and transmit various plant pathogens. The mealybugs feed on plant sap and also produce a waxy coating which acts as a protective layer. Widely employed methods of control include pesticides, use of bug blaster and beneficial insects such as ladybird (*Cryptolaemus montrouzieri*). Controlling mealybugs using pesticides is inefficient and conserving natural enemies is important in reducing the damage. The conventional methods suffer from several drawbacks and there is a need to develop new methods to control mealybugs.[7]

Figure 2.4. Pictures illustrating damage caused by mealybugs (taken from internet)

One of the upcoming methods to control mealybugs is the use of pheromone traps. The female mealybugs produce volatile sex pheromone to attract their male counterparts. The sex pheromones of several mealybugs have been identified and found to be active at very less concentrations (in microgram levels). Pheromones can also be used to detect and monitor mealybug infestation in fields. The structures of selected mealybug pheromones are shown in fig. 2.5. All of them are monoterpenes with interesting structures.[7]

Matsumoto mealybug

Vine mealybug

Japanese mealybug

Passionvine mealybug

Banana mealybug

Comstock mealybug

Madeira mealybug

Citrophilous mealybug

Citrus mealybug

Pink hibiscus mealybug

Obscure mealybug

Grape mealybug
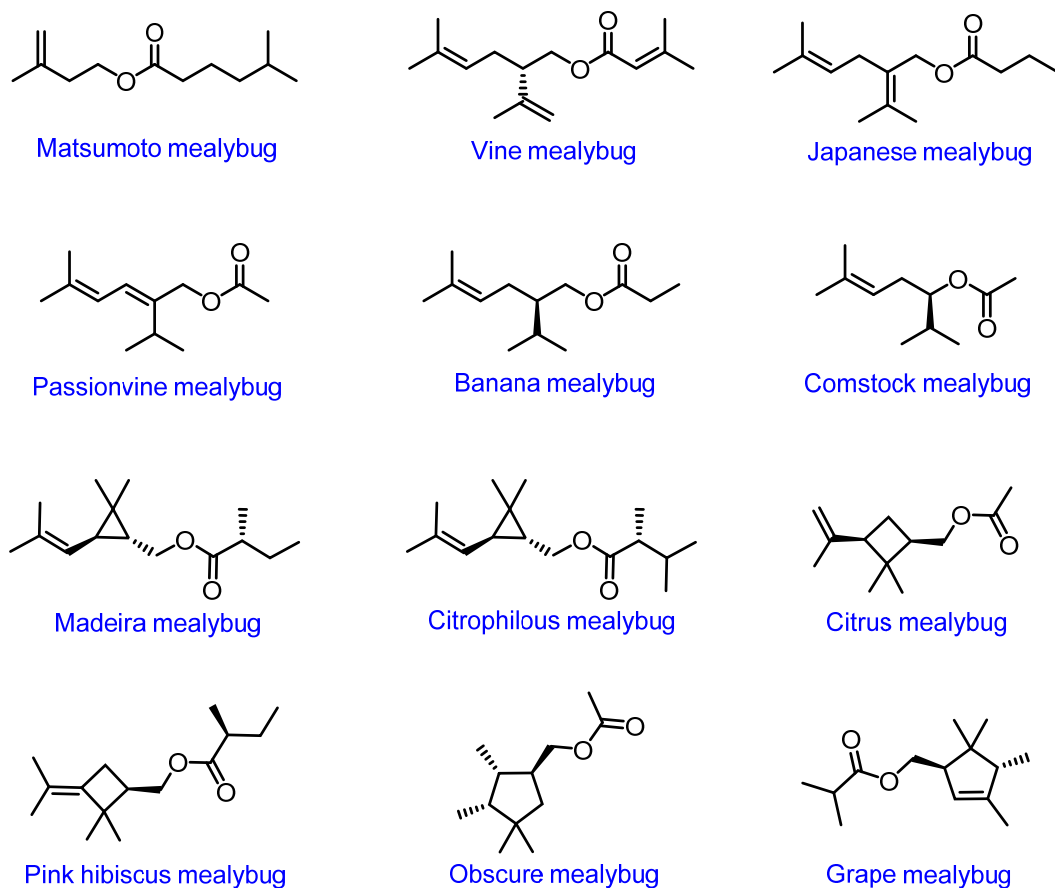
Figure 2.5. Pheromone of mealybugs

2.3. Pheromone of the longtailed mealybug

2.3.1. The longtailed mealybug

Longtailed mealybug (*Pseudococcus longispinus*) is a pest commonly found in America, Europe, Africa and Australia. It infests a variety of plants (26 families) including grapes, apples, citrus, avocado, potato, sugarcane, guava, hibiscus, mango, pineapple, orchids, lilies and so on. They affect the beauty of the plant, reduce yield and damages the fruits causing huge economic loss.

Figure 2.6. Longtailed mealybug and taxonomy

2.3.2. Isolation of sex pheromone of the longtailed mealybug

The sex pheromone produced by the female longtailed mealybug was isolated and characterized by J.G. Millar's group in 2009.[11] The headspace odours of unmated adult females were analyzed by GC and GC-MS which indicated a monoterpenoid structure. To establish the structure further, the odours collected over more than a year was purified by preparative GC to give a few micrograms of the sex pheromone. All the available data indicated two possible structures **1** and **2**.
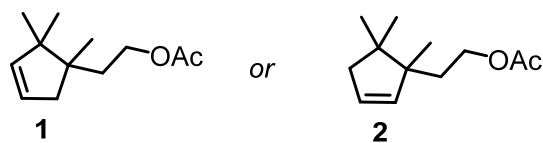
synthesis was needed to confirm the structure

Figure 2.7. Possible structures of the mealybug pheromone

To further confirm the structure both the compounds, **1** and **2** were synthesized (schemes 2.1 and 2.2) and NMR data was compared with that of the isolated compound. The known alcohol **3** was oxidized and homologated to aldehyde **6** *via* a MOM Wittig reaction. The aldehyde **6** on reduction followed by acetylation gave the target compound **1** (scheme 2.1). However, the spectrum was not matching with that of the natural product and hence **2** should be the required compound.

183
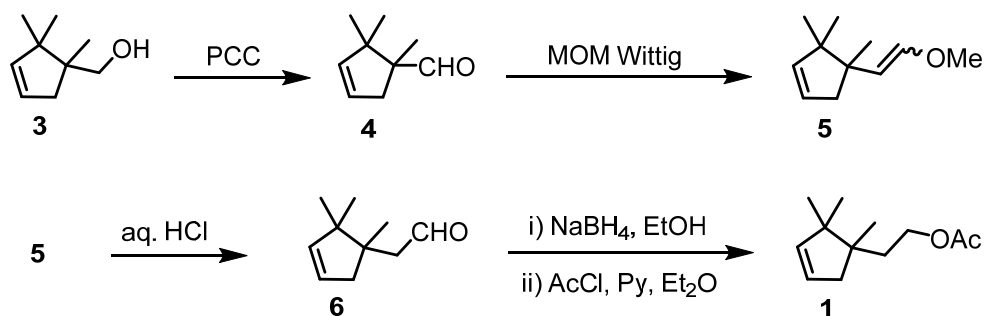
Scheme 2.1. Synthesis of compound **1**

The natural product **2** was prepared by following scheme 2.2. A *n*-BuLi mediated [2,3] sigmatropic rearrangement on allyl stannane **8** gave the olefin **9** in less yield (25%). Oxidation of alcohol followed by one carbon homologation gave aldehyde **11**. Further functional group transformations gave the compound **2** whose NMR data matched exactly with that of the isolated compound.
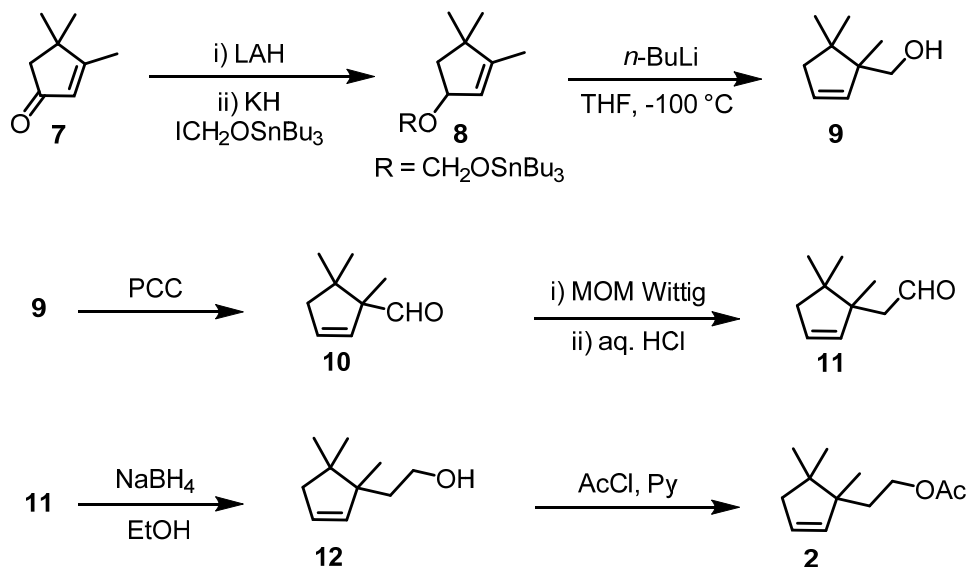
Scheme 2.2. Synthesis of compound **2**

Hence, the Millar group could identify the chemical structure of pheromone of the longtailed mealybug. But they were not able to establish the absolute configuration at the quaternary center because the racemic compound or intermediates could not be resolved

in chiral GC columns. Pheromone with cyclopentane skeleton is rare, and was previously reported in the case of obscure mealybug and grape mealybug. All these three insects (longtailed mealybug, obscure mealybug and grape mealybug) belong to the same genus Pseudococcus and the pheromones of all these mealybugs were isolated by Prof. Millar.[12,13] The female grape mealybug produces an enantiomeric mixture (85:15), with the (*R*, *R*) enantiomer as the major component.[7] The pheromone of the obscure mealybug was previously synthesized in our group in its enantiopure form.[14]
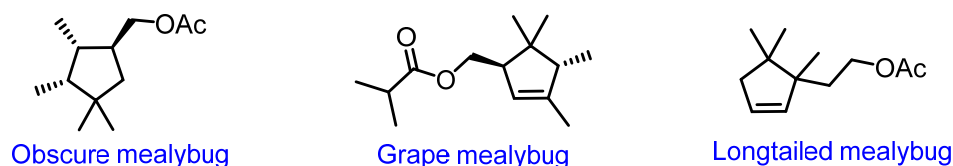
Figure 2.8. Pheromones with cyclopentane skeleton

2.3.3. Synthetic approaches for the longtailed mealybug pheromone

Although, the initial synthesis helped to confirm the structure of natural product, the synthetic sequence was lengthy and suffered from poor yields. The need for large quantities of the material prompted Millar's group and others to develop more efficient synthetic routes for the racemic pheromone.

Millar's approach II

The diazo derivative **14** was converted to cyclopentanone **15** by a Rh-catalyzed C-H insertion reaction. The active position was then methylated to give compound **16**. Conversion to enol triflate **17** followed by Pd catalyzed reduction resulted in the cyclopentene **18**. Further functional group transformations gave the natural product **2**. The authors prepared >5g of pheromone by following this scheme with an overall yield of 13.5%.[15]
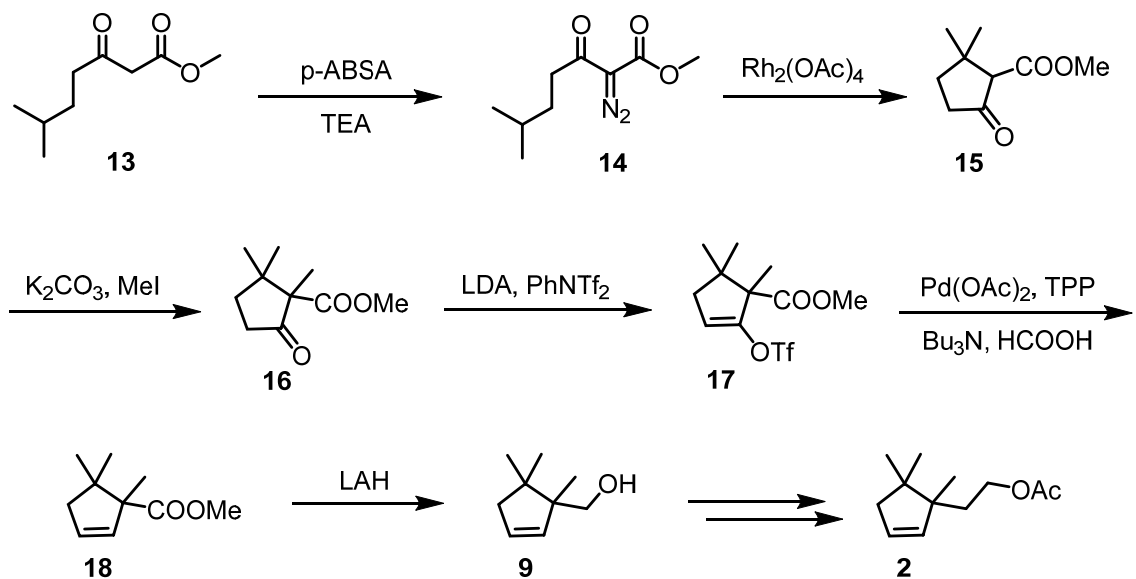
Scheme 2.3. Millar's synthesis of pheromone (approach II)

Millar's approach III

The known allylic alcohol **19** was acetylated to give the allyl acetate **20**. It was then converted to the TBS enolate **21** and subjected to Ireland Claisen rearrangement to give the acid **22**. This carboxylic acid on reduction followed by acetylation gave pheromone **2**.[16]
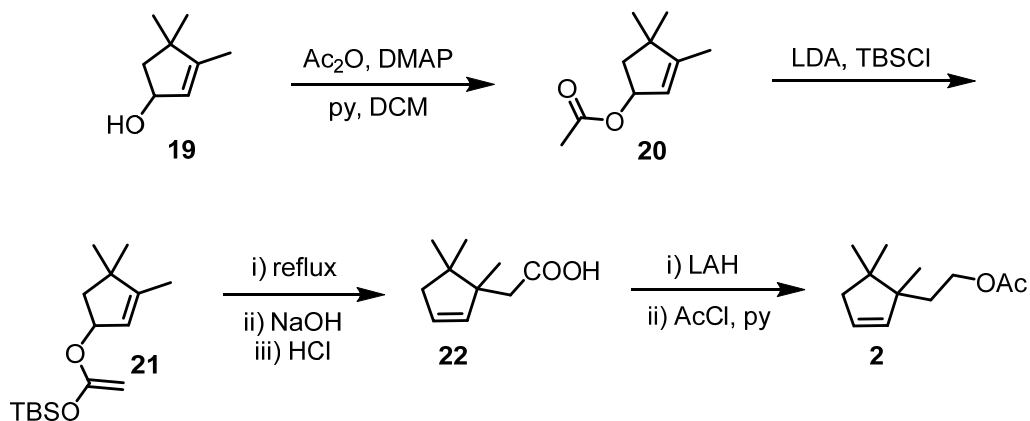
Scheme 2.4. Millar's synthesis of pheromone (approach III)

Bailey's approach

Bailey and co-workers developed a short synthesis for the racemic pheromone by employing intramolecular carbolithiation as the key step. The vinyl iodide **23** was treated with *t*-BuLi at -78 °C to give the vinyl lithium intermediate **24**. Addition of TMEDA followed by warming the reaction to RT resulted in ring closure to give intermediate **25**. The reaction was again cooled to -78 °C and the anion was treated with paraformaldehyde to give the known alcohol **12** which was converted to the natural product **2**. Although the developed route was short and efficient, reactions (use of *t*-BuLi) were not easy to operate.[17]
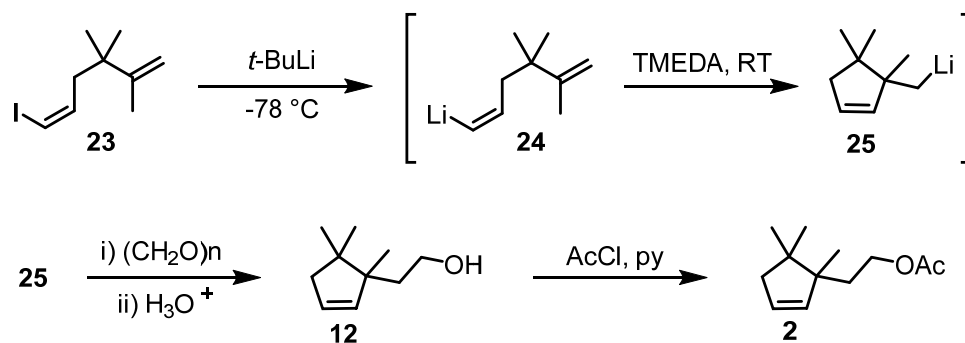
Scheme 2.5. Bailey's synthesis of pheromone

Previous synthesis from our group

Our synthesis of the racemic pheromone started from known ketone **26**. The ketone was treated with lithiated ethoxyacetylene and the tertiary alcohol obtained was subjected to Sc(OTf)$_3$ mediated Meyer-Schuster rearrangement to give the α-β-unsaturated ester **27** as a mixture of geometrical isomers. The conjugated ester on DIBAL-H reduction gave the allylic alcohol **28**. The Claisen rearrangement of alcohol **28** under conventional conditions was not successful. The reaction did not go for completion and the product **30** and starting material **28** were inseparable. Hence, the allyl vinyl ether **29** prepared from alcohol **28** was subjected to Claisen rearrangement promoted by DIBAL-H. The aldehyde formed after the sigmatropic rearrangement was reduced in situ to give the alicyclic alcohol **30**. This diene **30** on ring closing metathesis gave the

cyclopentene **12** which was acetylated to give the pheromone **2**. Alternately the alcohol **30** was acetylated and then subjected to RCM to give the target compound. In this case, the yield was found to be slightly better.[18]
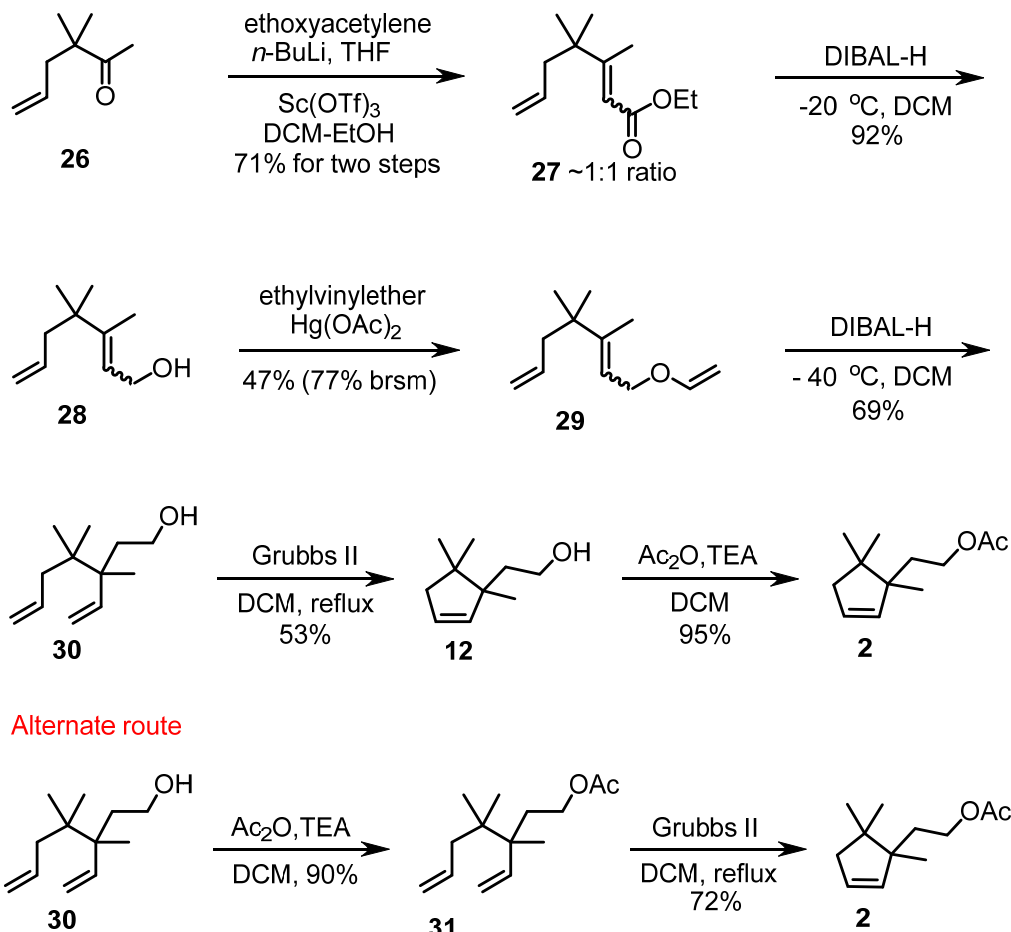
Scheme 2.6. Reddy's synthesis of pheromone

2.4. Present work

The pheromone of the longtailed mealybug caught our group's attention due to the following reasons.

- *Remarkable biological activity:* In field trials, lures containing 25 μg of racemate attracted male mealybugs for almost three months.

- *No access to optically pure pheromone:* The synthesis of enantiopure pheromones and field trials will give more insight into the role of stereochemistry in pheromonal activity.

- *Interesting chemical structure:* A sterically congested uncommon monoterpenoid with two adjacent quaternary carbons in a cyclopentene ring.

- *Unknown absolute configuration:* The Millar group could not determine the absolute configuration of the natural pheromone due to scarcity of the natural pheromone.

- *Use in crop protection:* Ultimately, present exercise may help in protecting high value crops such as grapes, citrus, apples, pears, and ornamental plants.

2.4.1. First access to enantiomers of the longtailed mealybug pheromone

In our initial efforts to access both the pheromone enantiomers so as to find the better and natural one, we planned to resolve one of the intermediates of our racemic synthesis. For this purpose, chiral auxiliary approach was explored.

A chiral auxiliary which can also be helpful in determining the absolute configuration through crystal structure analysis was required. After careful analysis of various possible options, camphorsultam phthalic acid (CSP acid), an auxiliary developed by Harada seemed to fit well with our needs. Since, the acid has three chiral centres with known configuration, the absolute configuration at the required centre can be determined without ambiguity. The heavy atom effect due to the presence of sulphur is another advantage of this auxiliary.[19-22] Although Harada group reported the resolution of alcohols using CSP acid, it was not used for establishing absolute configuration of natural products to the best of our knowledge.[23] Some of the chiral acids helpful in determining absolute configuration by crystal structure analysis are shown in figure 2.9.
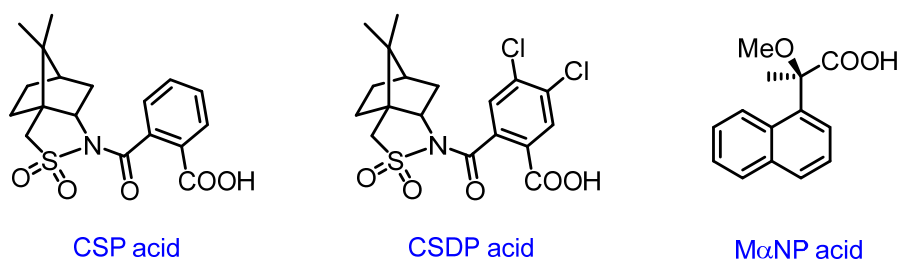
Figure 2.9. Chiral acids useful in absolute configuration determination

The CSP acid was prepared from camphorsulfonic acid **32** by adopting procedures known in the literature (Scheme 2.7).[24] The sulfonamide **33** was converted to camphorsulfonimine **34** in presence of acidic resin amberlyst-15. The imine on reduction using $NaBH_4$ resulted in camphorsultam **35**. This is a well known chiral auxiliary, also called as Oppolzer's sultam. The sultam **35** was treated with NaH and phthalic anhydride to give the required CSP acid in moderate yield and it was prepared in gram scale. All the spectral data including optical rotations were recorded and compared with that of reports from Harada's publications.
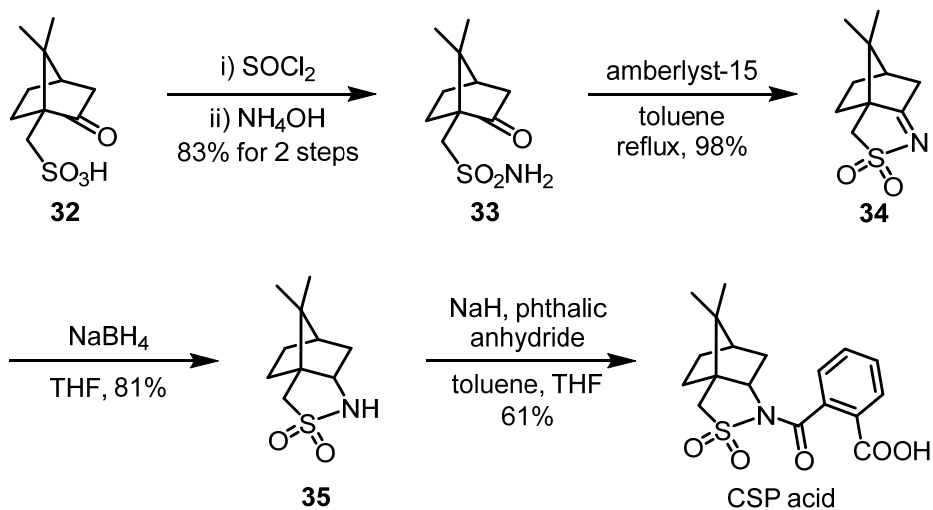
Scheme 2.7. Preparation of CSP acid

The alcohol **30**, prepared according to scheme 2.6 was converted into diastereomers **36a** and **36b** by Steglich esterification (DMAP, DCC). On TLC plate, the esters appeared more polar compared to the alcohol **30**, probably due to the presence of

sulfonamide moiety in the product. We have made a few attempts to separate the diastereomers on normal silica gel columns, but with no success. The diastereomers were resolved on an enantioselective Daicel Chiralpak® AD-H chiral stationary phase column. The chiral stationary phase in AD-H column is amylose-tris (3,5-dimethyl phenyl carbamate) coated on 5 micron silica gel. Mobile phase consisting of *n*-Hexane / Ethanol / Methanol (90/10/2, v/v/v) was used at a flow rate of 40 mL/min and the elution of enantiomers were monitored on UV detector at 225 nm. The mixture was dissolved in the mobile phase to make a solution of concentration 10 mg/mL and 3 mL was injected onto the chromatographic system and the elution of diastereomers, **36a** and **36b** were found to be at 9 min & 12 min respectively. From 400 mg of diastereomeric mixture, 160 mg of **36a** (> 96% ee) and 110 mg of **36b** (> 98% ee) were obtained.
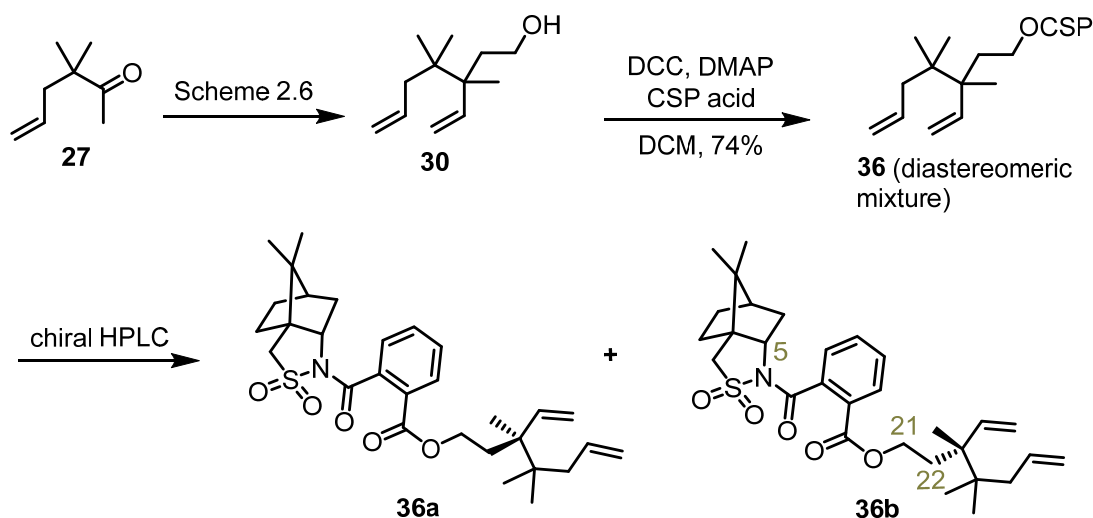
Scheme 2.8. Resolution of alcohol **30**

The ^{13}C NMR of both the diastereomers looked very similar although, there was some difference in ^{1}H NMR. The protons attached to C_{21} appeared as a triplet at δ 4.19 ppm in the case of **36a**. In the case of diastereomer **36b**, H_{21} appeared as a multiplet (δ 4.26-4.10 ppm) almost merging with H_5 multiplet (δ 4.07 ppm). The diastereomer, **36b** was crystallized from petroleum ether and the crystal structure analysis revealed that it had an (*R*) configuration at the chiral quaternary center.

191
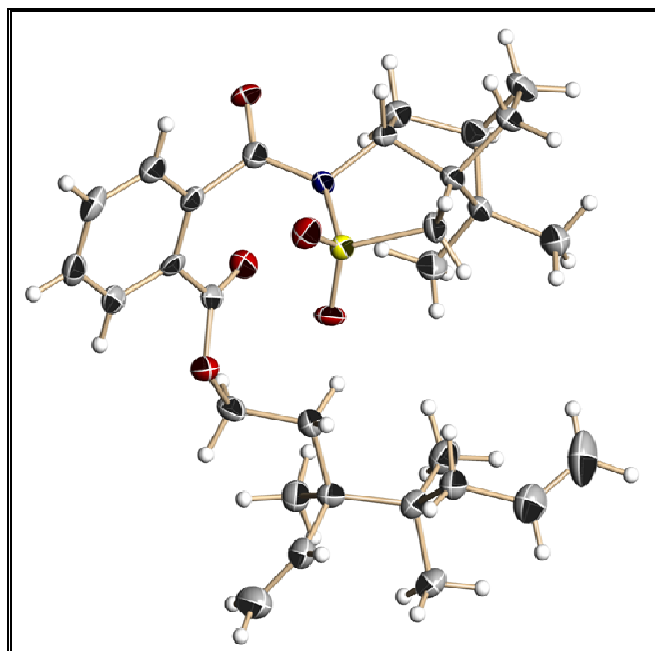
Figure 2.10. ORTEP of diastereomer **36b**

After separation, both the diastereomers were individually hydrolyzed with K_2CO_3 in MeOH to obtain the enantiopure alcohols (*S*)-**30** and (*R*)-**30**. The ^1H and ^{13}C NMR spectra of the enantiopure alcohols (*S*)-**30** and (*R*)-**30** were compared with that of the racemic compound and found to be identical. Both the enantiopure alcohols (*S*)-**30** and (*R*)-**30** were then individually acetylated and subjected to ring-closing metathesis (using Grubbs II generation catalyst) to give both the pheromone enantiomers (*S*)-**2** and (*R*)-**2** (Scheme 2.9).
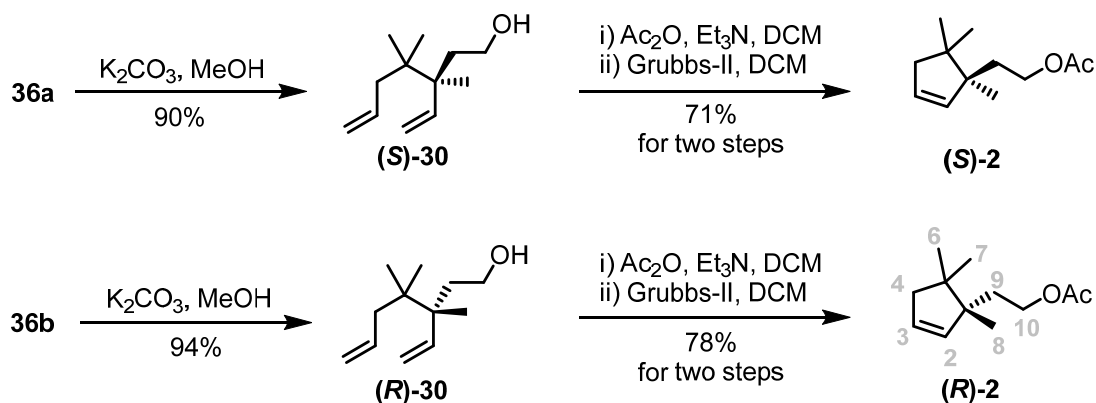
Scheme 2.9. Synthesis of pheromone enantiomers

The spectral data of both the compounds were in agreement with that of the racemate (Table 2.1).[11] The (*S*)-pheromone was found to be dextrorotatory, $[\alpha]_D^{25}$ +27.8 (c 0.16, DCM) and (*R*)-pheromone was levorotatory, $[\alpha]_D^{25}$ -24.0 (c 0.13, DCM). Although, the absolute configuration of each enantiomer was known, stereochemistry of the natural product could not be established at this stage because its optical rotation was not reported.

Table 2.1. ^{1}H NMR comparison of reported and synthesized pheromone enantiomers

Atom no:	^{1}H NMR (Reported) CDCl$_3$, 400 MHz	^{1}H NMR of (*S*)-2 CDCl$_3$, 400 MHz	^{1}H NMR of (*R*)-2 CDCl$_3$, 400 MHz
H-8	0.90 (s, 3H)	0.88 (s, 3H)	0.88 (s, 3H)
H-6 / H-7	0.94 (s, 3H)	0.93 (s, 3H)	0.93 (s, 3H)
H-6 / H-7	0.95 (s, 3H)	0.94 (s, 3H)	0.94 (s, 3H)
H-9	1.56 (ddd, *J* = 6.2, 10.2, 13.3 Hz, 1H)	1.52 – 1.58 (m, merged with moisture)	1.51 – 1.59 (m, merged with moisture)
H-9	1.70 (ddd, *J* = 6.3, 10.2, 13.3 Hz, 1H)	1.70 (ddd, *J* = 6.1, 10.1, 13.4 Hz, 1H)	1.70 (ddd, *J* = 5.9, 9.9, 13.2 Hz, 1H)
H-11 (OAc)	2.04 (s, 3H)	2.03 (s, 3H)	2.03 (s, 3H)
H-4	2.12 (br t, *J* = 2.0 Hz, 2H)	2.11 (br t, *J* = 2.0 Hz, 2H)	2.11 (br t, *J* = 1.9 Hz, 2H)
H-10	4.08 (ddd, *J* = 6.3, 9.4, 10.9 Hz, 1H)	4.10 - 4.05 (m, 1H)	4.11 - 4.04 (m, 1H)
H-10	4.19 (ddd, *J* = 6.3, 10.15, 10.5 Hz, 1H)	4.20 - 4.15 (m, 1H)	4.21 - 4.15 (m, 1H)
H-2 / H-3	5.55 (dt, *J* = 2.0 and 6.4 Hz, 1H)	5.54 - 5.53 (m, 1H)	5.55 - 5.53 (m, 1H)
H-2 / H-3	5.62 (dt, *J* = 2.0, 5.6 Hz, 1H)	5.62 - 5.61 (m, 1H)	5.63 - 5.60 (m, 1H)

2.4.2. Field trials of the pheromone enantiomers

After having both the pheromone enantiomers in hand, the next task was to evaluate their biological activity in fields. The field trials were conducted in Bonsall, California, U.S.A (0.49 ha plot) containing *Ruscus hypoglossum*. These experiments were done in collaboration with Prof. Jocelyn Millar, University of California. 1 mg each of pheromone enantiomers were used for this study. Delta sticky traps were placed at different positions in the field. The compounds were dissolved in hexane and placed in rubber septa kept inside the traps. Both the enantiomers were tested at 5 μg concentration and racemic pheromone at 10 μg concentration per trap. Some of the traps contained only hexane and served as the control. The results are shown in fig. 2.11. The mealybug attack which is seasonal, occurs during the winter and so the trials have to be conducted during that period itself (March - June).
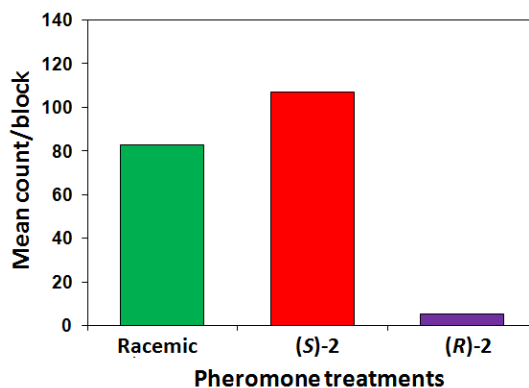
Figure 2.11 (a) Delta trap (b) Male longtailed mealybugs caught in traps baited with each of the enantiomers of the pheromone, and the racemate

The traps loaded with (*S*)-(+)-pheromone caught more male mealybugs (Fig. 2.11b), and was found to be more attractive than the racemic pheromone. This indicates that (*S*)-(+)-pheromone is the natural product. The (*R*)-(-)-pheromone showed minimal attraction which may be due to the contamination with active enantiomer.

After successful field trials in California, the enantiopure pheromones were tested in New Zealand vineyards in collaboration with Mr. Andrew Twidle (Plant and Food Research, New Zealand). A field trial was established in a Hawke's Bay vineyard

containing Sauvignon blanc vines affected with longtailed mealybug. Traps containing any of the following treatments were placed randomly in fields: 10 µg **(+)-2**, 10 µg **(-)-2**, 20 µg racemate or a solvent control. The results are shown in fig. 2.12. The (+)-enantiomer **(S)-(+)-2** was significantly more attractive than the racemate. The racemic pheromone caught significantly less male mealybugs than **(+)-2** alone. This suggests that **(-)-2** presence in the racemate may have a slight inhibitory effect on trap catch.
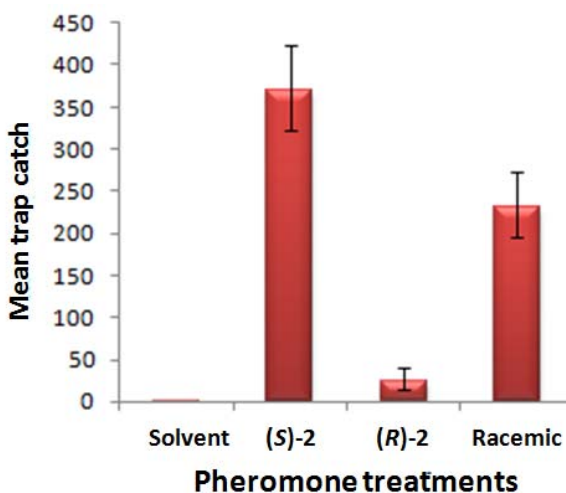
Figure 2.12. Mean numbers of male mealybugs caught per trap in a New Zealand vineyard using pheromone enantiomers, racemate, or solvent controls

2.4.3. Enantiospecific synthesis of the mealybug pheromone

After successful synthesis of pheromone enantiomers, establishment of absolute configuration and having shown superior activity of (+)-pheromone in field trials in two geographically different locations (USA and NZ), we turned our attention towards an enantiopure synthesis mainly due to the following reasons.

- The resolution approach to access enantiopure pheromones was not scalable and economic.
- The use of chiral HPLC is not desirable.
- As we are employing a diastereomeric resolution, only 50% of the required enantiomer is obtained.

Since, the pheromone is a monoterpene, it could be obtained from cheaply available chiral terpenes by appropriate synthetic transformations. The initial synthetic plan for the target molecules is shown in Scheme 2.10. The known chiral building block (-)-5-oxobornyl acetate **(-)-37**, which in turn was prepared from (-)-bornylacetate, serves as starting material for the present purpose.[25,26]
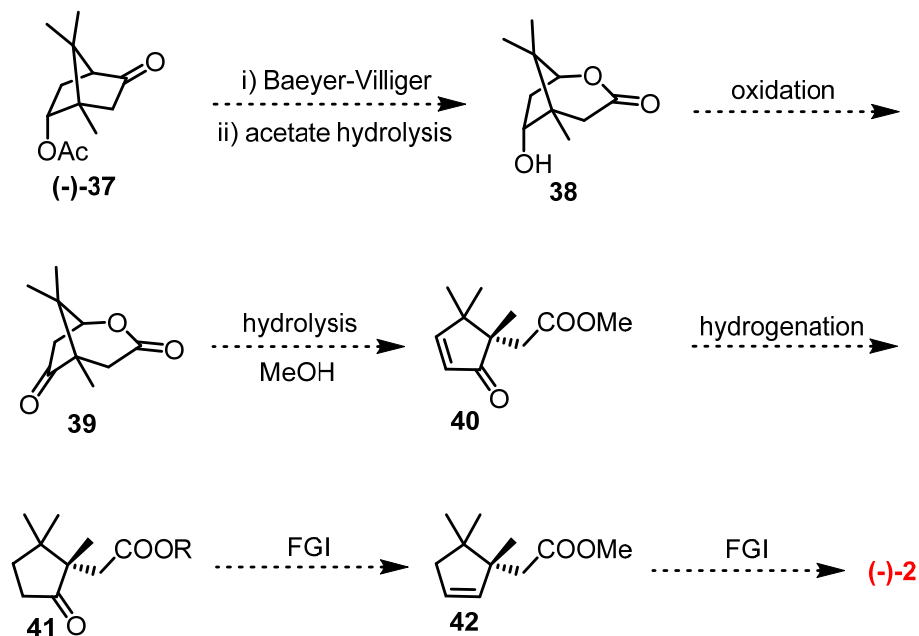
Scheme 2.10. Plan towards enantiopure pheromone

It was decided to carry out the synthesis of unnatural (-)-pheromone, **(-)-2** initially because it could be obtained from commercial (-)-bornylacetate. Regioselective Baeyer-Villiger oxidation of **(-)-37** followed by conversion of acetate to ketone can give the keto-lactone **39**. Lactone hydrolysis followed by dehydration would give the cyclopentenone ester **40**. Hydrogenation of **40** can lead to cyclopentane **41** which could be converted to the cyclopentene **42**. The cyclopentene **42** represents the complete pheromone skeleton with the opposite stereochemistry. Compound **42** can be transformed to the target **(-)-2** by simple functional group interconversions. In a similar fashion, the natural isomer **(+)-2** could be prepared by using the other enantiomeric series commencing with **(+)-37**.

The Baeyer- Villiger oxidation is a key reaction in this scheme and can lead to two products, **38** and **38'** of which **38** is required for the present route (scheme 2.11). The nucleophilic attack of peroxy anion on the protonated carbonyl of intermediate **A** leads to the formation of intermediate **B** which then rearranges to give products **38a** or **38a'**. The product formation is controlled by two factors: steric and electronic.[27-29] The acetate **38a'** is formed by the migration of methylene and is more favoured considering the steric factors. The compound **38a** is obtained when the electron rich bridgehead migrates and is more favoured according to electronic factors. The hydrolysis of the acetate **38a** can give alcohol **38** which could be transformed to the target compound.
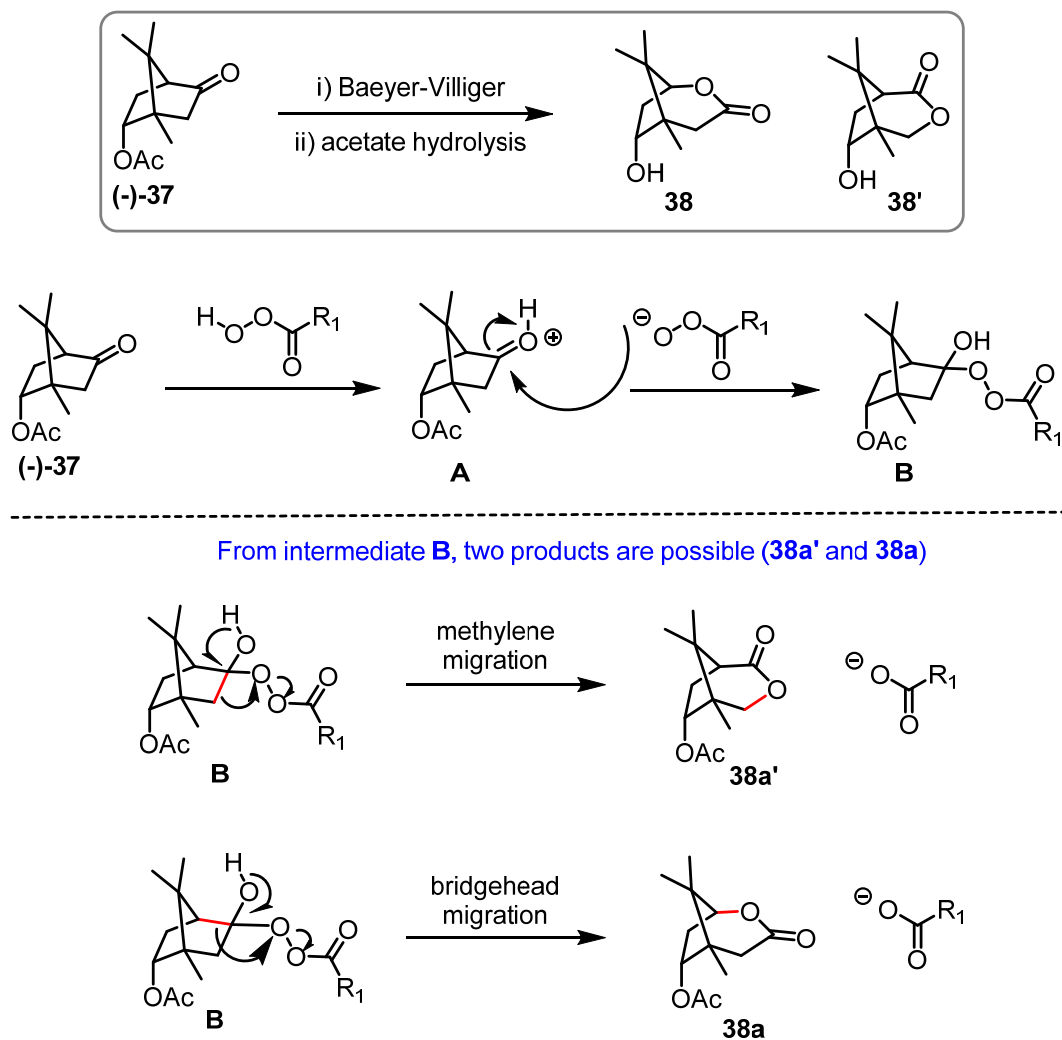
Scheme 2.11. Baeyer Villiger oxidation of **(-)-37**

The initial attempts to synthesize **38** with *m*-CPBA were unsuccessful. The reaction (*m*-CPBA, PTSA, DCM) did not go for completion and NMR indicated that a mixture of both the regioisomers were present. Although the NMR was not clean, it suggested that the major product was **38a'**. Both the regioisomeric lactones could be easily identified by NMR spectroscopy because **38a** has an –OCH– group and **38a'** has –OCH$_2$– group. In order to facilitate the migration of electron rich bridgehead it was decided to carry out the reaction in a more polar solvent. [29] In fact, the reaction went smoothly with H$_2$O$_2$-H$_2$SO$_4$ in acetic acid solvent and a more polar spot was observed in TLC. Although both of the regioisomeric lactones were formed and was inseparable on TLC, NMR data indicated that the required regioisomer **38a** was the major product. Luckily, the alcohols obtained after acetate hydrolysis were cleanly separated. The major isomer formed in the reaction had a peak at δ 177.9 ppm in ^{13}C NMR which indicated the presence of lactone carbonyl. The peaks at δ 90.5 and 81.4 ppm were CH according to DEPT. From this, we assumed that this major isomer (50% yield) is compound **38** and went forward with the synthesis. The minor isomer (~20% yield) had a peak at δ 174.9 ppm in ^{13}C NMR indicating the presence of lactone carbonyl. The peak at δ 76.3 ppm was a CH, which may be the one attached to hydroxyl. There was a CH$_2$ at δ 70.4 ppm which correspond to the carbon attached to lactone fitting to the structure **38'**. The HRMS analysis of both compounds matched with the formula C$_{10}$H$_{16}$O$_3$Na [M + Na]$^+$. Both the compounds were colourless, crystalline solids.

The required alcohol was oxidized to the corresponding ketone with PDC in DCM solvent (89% yield) and the peak at δ 216.4 ppm in ^{13}C NMR indicated the presence of ketone carbonyl. IR spectrum clearly showed the presence of two carbonyls (1783 and 1747 cm^{-1}). The peak at 1747 cm^{-1} is due to the stretching vibration of ketone carbonyl, which is very similar to the carbonyl stretching in cyclopentanone (1748 cm^{-1}). The lactone opening was done using PTSA in methanol[30] and the cyclopentenone methyl ester was isolated as the sole product along with a small amount of starting material recovered (88% brsm). Two doublets at δ 7.71 and 6.08 ppm in ^{1}H NMR indicated the presence of a conjugated olefin and the compound was UV active as well. A singlet at δ 3.71 ppm

indicated the methyl ester. In ^{13}C NMR the olefin carbons appeared at δ 168.5 and 129.0 ppm. The ketone carbonyl and ester carbonyl appeared at δ 213.5 and 171.9 ppm respectively. The HRMS analysis showed a peak at 197.1173 matching with the formula $C_{11}H_{17}O_3$ $[M + H]^+$. This compound was hydrogenated (H_2-Pd/C, MeOH) and a few conditions were tried to obtain the cyclopentene core.

Initially, we tried to achieve the synthesis of **42** by the Pd catalyzed reduction of enol triflate **43**. Millar group had reported this reaction on similar substrate (Scheme 2.3).[15] But in our hands, the enolisation (LDA, PhNTf$_2$) did not work and always starting material was recovered. Later, the ketone was reduced to alcohol (assigned structure of **44** revised to **47** later) which could be dehydrated to obtain the desired cyclopentene **42** (Scheme 2.12).
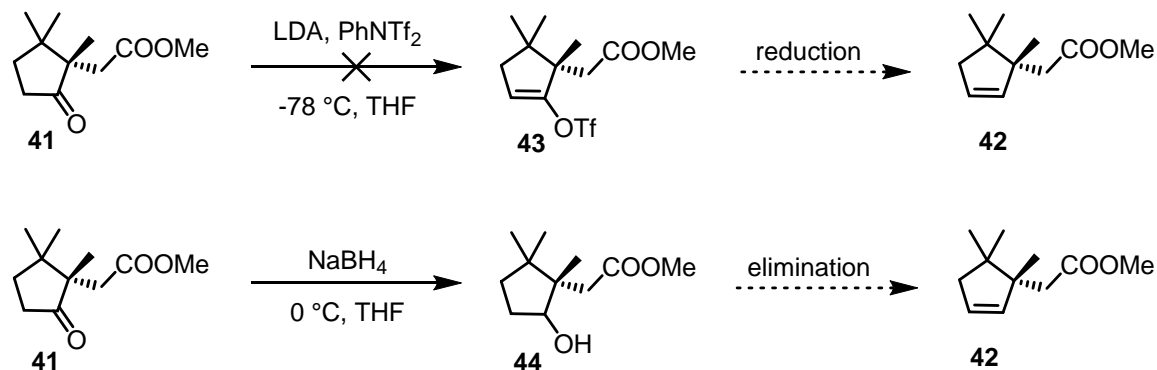
Scheme 2.12. Attempts to obtain cyclopentene **42**

Under dehydrating conditions (P_2O_5 in benzene),[31] TLC indicated formation of a non polar spot and the compound was isolated. Unfortunately, the ^{1}H NMR did not show any olefinic protons, but ^{13}C NMR showed peaks at δ 136.0 and 131.3 ppm indicating that a substituted double bond is present in the molecule. Such a product (**45**) could be formed possibly due to a 1,2-methyl shift classically known as the Wagner-Meerwein rearrangement.[32-34] A close look at the NMR data suggested that it was not matching with compound **45**. In ^{1}H NMR, two methyl groups were observed at δ 1.58 and 1.49 ppm which indicated that they were attached to a sp^2 carbon. Also, the presence of an AB

quartet at δ 2.26 ppm showed that the chiral center was still present in the molecule indicating a possible structure **46**.

Only compound **46** was isolated (confirmed by NMR)
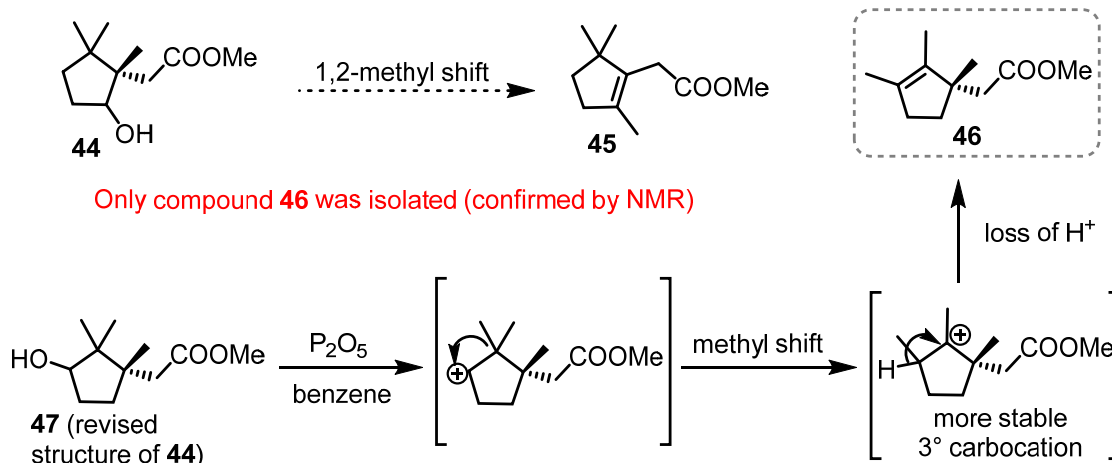
Scheme 2.13. Observation of a structural misassignment

Table 2.2. NMR analysis of compound **46**
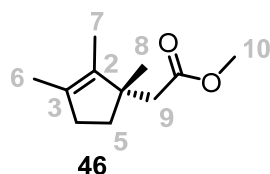
^{13}C NMR analysis
- two tetra-substituted olefin carbons (δ 131.3, 136.0 ppm)
- ester carbonyl (δ 173.0 ppm)

Atom no:	^{1}H NMR of 46 CDCl$_3$, 400 MHz	Atom no:	^{1}H NMR of 46 CDCl$_3$, 400 MHz
H-8	1.05 (s, 3H)	H-5	2.05 – 1.98 (m, 1H)
H-6 / H-7	1.49 (s, 3H)	H-4	2.16 (m, 2H)
H-6 / H-7	1.58 (s, 3H)	H-9	2.26 (AB quartet, 2H)
H-5	1.64 – 1.55 (m, merged with moisture, 1H)	H-10	3.61 (s, 3H)

It is not possible to explain the formation of **46** from **44**. But, the compound **46** could be formed from **47** by a Wagner Meerwein rearrangement. The compound **47** is a structural isomer of **44** and is expected to show similar NMR data. This observation raised a

question on the structures assigned to of all the intermediates. We then went back and took X-ray crystal structure of the alcohol obtained by Baeyer-Villiger oxidation. The crystal structure analysis revealed that there was a misassignment in the structure and the actual structure is shown in scheme 2.14. Under the reaction conditions, the initially formed [3.2.1] bicyclic lactone had undergone a translactonization/ lactone-lactone rearrangement to form **(-)-48** which relieved the extra ring strain.

ORTEP of **(-)-48**
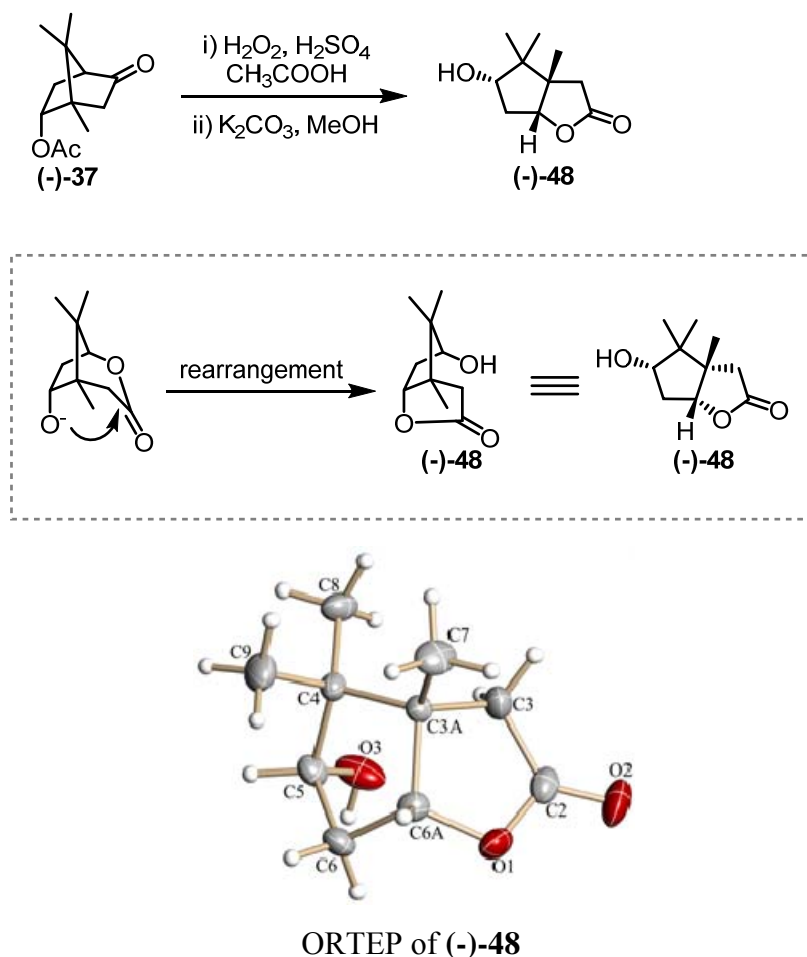
Scheme 2.14. Observation of trans-lactonization (lactone-lactone rearrangement)

Even the IR spectra of compounds **(-)-48** and the bicyclic lactone **38'** indicated some difference in the nature of carbonyl. In compound **(-)-48**, the carbonyl peak appeared at 1764 cm^{-1}, whereas the lactone **38'** showed a C=O stretching at 1716 cm^{-1}. After this observation, the structures of all intermediates were changed as shown in

scheme 2.15. The rearranged lactone **(-)-48** on PDC oxidation gives the ketolactone **(-)-49** (89% yield). Lactone hydrolysis with concomitant dehydration using PTSA, resulted in the cyclopentenone derivative **(-)-50**.

Structure of **(-)-48** confirmed by X.ray crystal structure analysis
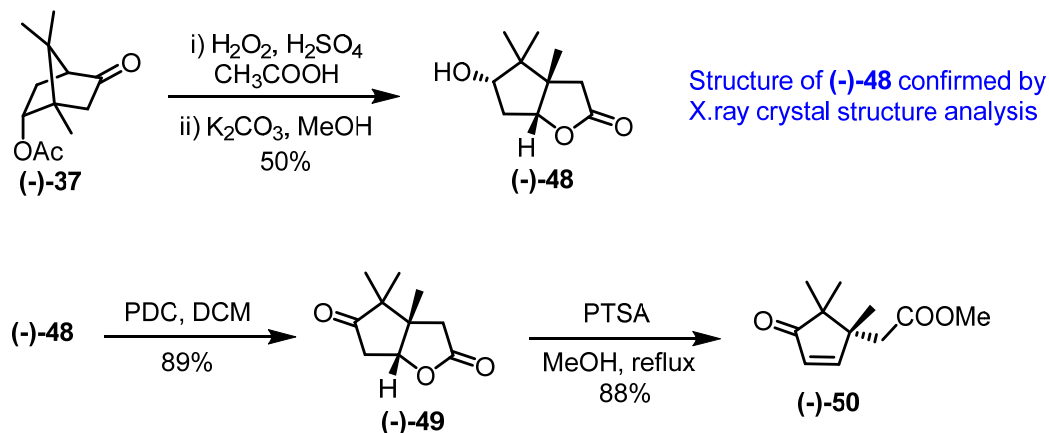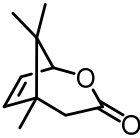
Scheme 2.15. Scheme showing revised structures

After solving the puzzle, we decided to move ahead with the same rearranged intermediates by slightly modifying the original plan. The α-β-unsaturated ketone **(-)-50** was subjected to Luche reduction to obtain the allylic alcohol **51** as a diastereomeric mixture. Deoxygenation of this allyl alcohol can lead to the cyclopentene core of pheromone. The reaction was tried under several conditions using different reagents (all details are compiled in Table 2.3), and it was found that the deoxygenation was accompanied by a migration of the double bond and both the olefin regioisomers **42a** and **42** could not be separated.
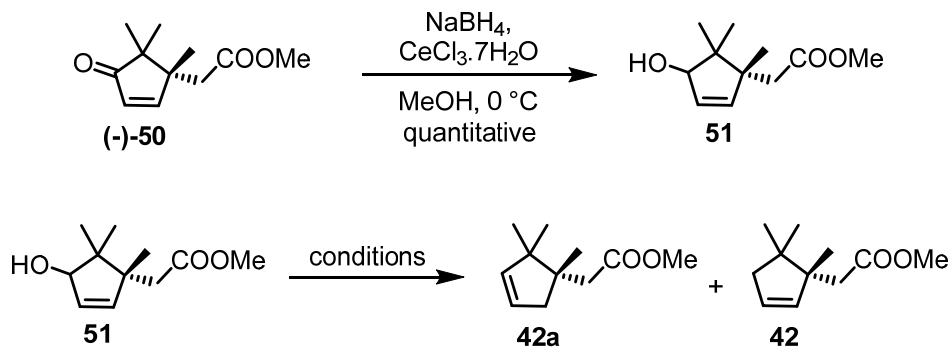
Scheme 2.16. Deoxygenation of allyl alcohol

Table 2.3. Conditions tried for deoxygenation of **51**

Sl. No.	Conditions	Observation
1.	NaBH$_3$CN (3 eq.), BF$_3$.Et$_2$O (3 eq.), THF reflux[35]	**42** and **42a** formed in 10:3 ratio
2.	i) Ac$_2$O, TEA, DCM ii) HCOOH (2 eq.), TEA (3 eq.), Pd$_2$(dba)$_3$ (2.5 mol%), PBu$_3$ (5 mol%), THF[36]	No reaction at RT and reflux
3.	i) Ac$_2$O, TEA, DCM ii) TES (5 eq.), BF$_3$.Et$_2$O (2 eq.), DCM[37]	**42** and **42a** formed in 1:1 ratio
4.	LiClO$_4$ (12 eq.), TES (3 eq.), Et$_2$O[38]	Compound **52** was formed.
5.	i) Ac$_2$O, TEA, DCM ii) LiBH$_4$ (5 eq.), Pd$_2$(dba)$_3$ (0.125 eq.), PBu$_3$ (0.5 eq.), DMF[39]	**42** and **42a** formed in 5:3 ratio
6.	i) LAH, THF ii) LiClO$_4$ (10 eq.), TES (3 eq.), Et$_2$O	No reaction
7.	i) LAH, THF ii) NaBH$_3$CN (3 eq.), BF$_3$.Et$_2$O (3 eq.), THF reflux	**(-)–12** and **(+)–12a** formed in 1:2 ratio
8.	i) ClCOOMe, TEA, DCM ii) LiBH$_4$ (5 eq.), Pd$_2$(dba)$_3$ (0.125 eq.), PBu$_3$ (5 eq.), DME[39]	No reaction. Methyl carbonate was recovered.
9.	NaBH$_3$CN (3 eq.), BF$_3$.Et$_2$O (3eq.), THF, RT	No reaction.
10.	NaBH$_4$ (3 eq.), BF$_3$.Et$_2$O (3 eq.), THF, reflux	Complex reaction mixture
11.	NaBH$_3$CN (3 eq.), BF$_3$.Et$_2$O (3 eq.), DME, reflux	**42** and **42a** formed in 10:3 ratio
12.	i) Tf$_2$O, TEA, DCM ii) LAH, THF, RT	**(-)–12** and **(+)–12a** formed in 10:3 ratio

A combination of lithium perchlorate and triethyl silane in diethyl ether is known for chemoselective deoxygenation of allylic alcohols.[38] But, under these reaction conditions, the allyl alcohol **51** gave the lactone **52** (entry 4). However, deoxygenation using $BF_3.Et_2O$ and sodium cyanoborohydride in THF reflux (Prof. Srikrishna protocol) gave the required regioisomer **42** as the major product (10:3 ratio) with a yield of 86% for the mixture (entry 1).[35] The spectral data was in agreement with the gross structure as drawn. However, at the ester stage it was not possible to distinguish between the compounds.
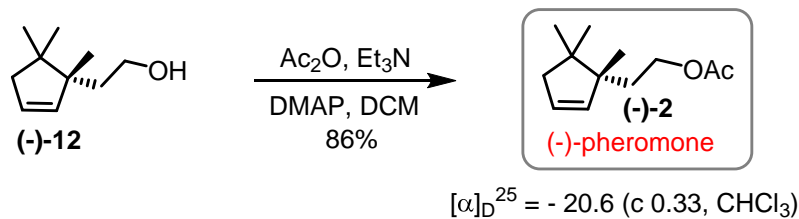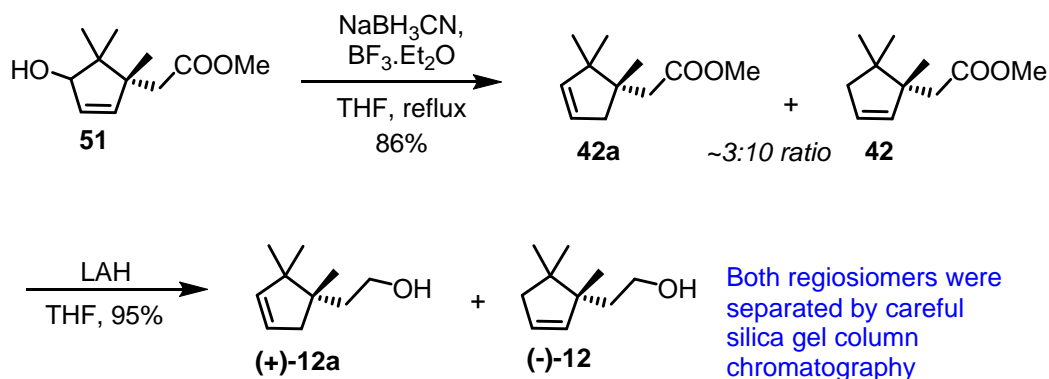
Scheme 2.17. Synthesis of (*R*)-(-)-pheromone

The alcohols obtained by ester reduction ($LiAlH_4$ in THF, 82% yield), **(+)-12a** and **(-)-12** were separated by strenuous column chromatography, but were inseparable on TLC. The compounds **(+)-12a** and **(-)-12** were reported by Prof. Millar's group in racemic form. The structures of **(+)-12a** and **(-)-12** were confirmed after comparing the NMR data with Millar's compounds.[11] In **(+)-12a**, the allylic protons were observed as

two sets of peaks, a td at δ 2.30 ppm (J = 15.6, 2.2 Hz) and a multiplet at δ 2.03 – 1.98 ppm; the olefin protons resonated at δ 5.54 – 5.51 ppm and δ 5.44 – 5.42 ppm. The allyl protons of **(-)-12** appeared as a quartet at δ 2.10 ppm with a coupling constant J = 2.2 Hz and the olefins appeared at δ 5.62 – 5.59 ppm and δ 5.56 – 5.53 ppm. The alcohol **(-)-12** was acetylated to give the unnatural pheromone **(-)-2**. The NMR data and optical rotation of **(-)-2** was measured, compared with the previous values and found to be matching.

For the synthesis of (+)-pheromone, (+)-bornylacetate was synthesized in multi-gram quantities from (+)-camphor and converted to **(+)-37**.[40] In a very similar fashion as described for the synthesis of (-)-pheromone, **(+)-37** was then transformed to the target compound **(+)-2**.
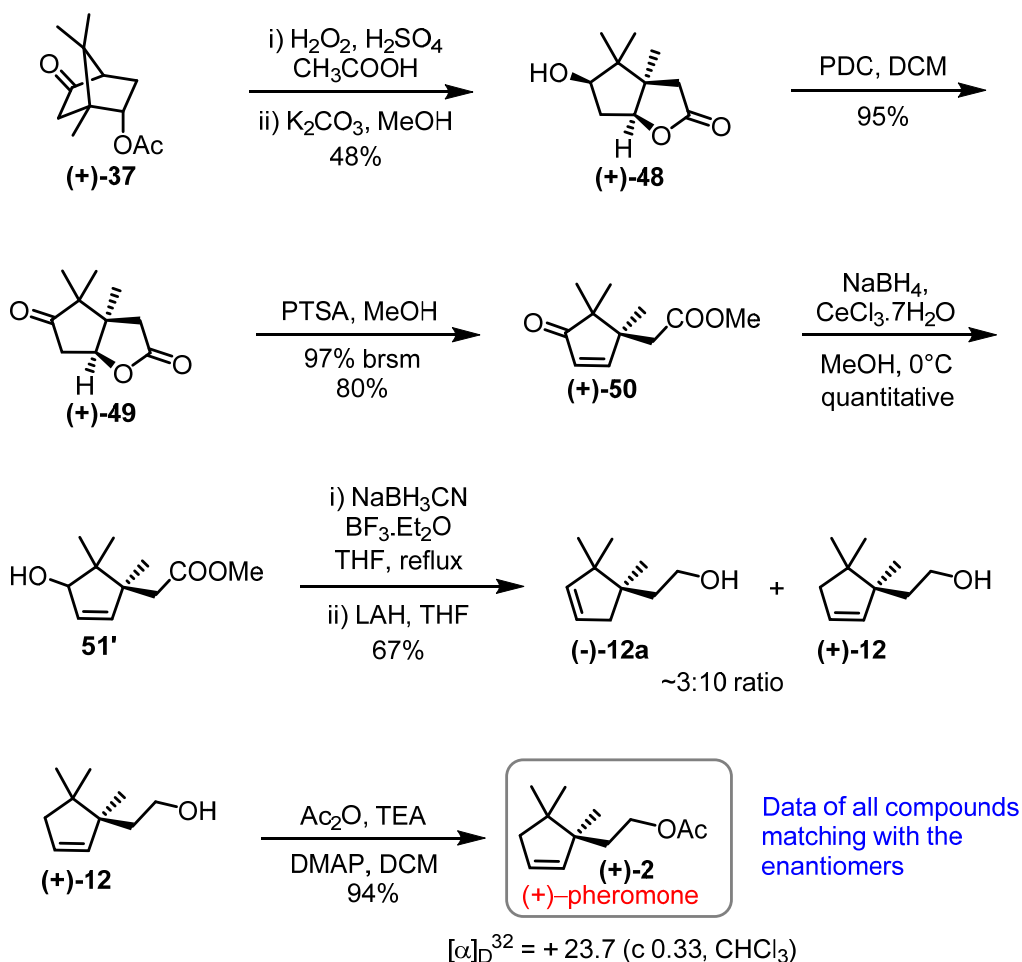
Scheme 2.18. Synthesis of (*S*)-(+)-pheromone

All the intermediates, **(+)-48**, **(+)-49**, **(+)-50**, **51'**, **(-)-12a**, **(+)-12** and pheromone **(+)-2** were characterized by spectral data (^{1}H, ^{13}C, HRMS) and optical rotation. The specific rotation of (+)-pheromone was found to be $[\alpha]_D^{32}$ +23.7 (CHCl$_3$). Thus, we could achieve the synthesis of both the enantiomers of the sex pheromone by an enantiospecific route starting from readily accessible chiral pool. Although the initial strategy did not work as planned, an unexpected rearrangement product was diverted to the target molecule.

2.5. Conclusions

Pheromones are chemicals secreted by organisms to communicate between members of the same species. Synthetic pheromones can be used to monitor and control pests without affecting other organisms. Considering the importance of synthetic pheromones in crop protection, we have made the following contributions to the project.

- Both the enantiomers of the sex pheromone of the longtailed mealybug were synthesized and absolute configuration was assigned based on crystal structure analysis of one of the derivatives.

- Field trials conducted in California, United States showed that (*S*)-(+)-pheromone is highly attractive to male mealybugs suggesting that it is the natural product. The activity of the material was further confirmed by field trials conducted in Hawke's Bay, New Zealand.

- An enantiospecific synthesis was developed in which both the pheromone enatiomers was synthesized from corresponding bornyl acetates. The synthesis features an unanticipated translactonization (lactone-lactone rearrangement) and relies on cheap chiral starting materials.

2.6. Experimental Section

2.6.1. Synthesis of pheromone enantiomers by resolution

CSP esters (36a and 36b)
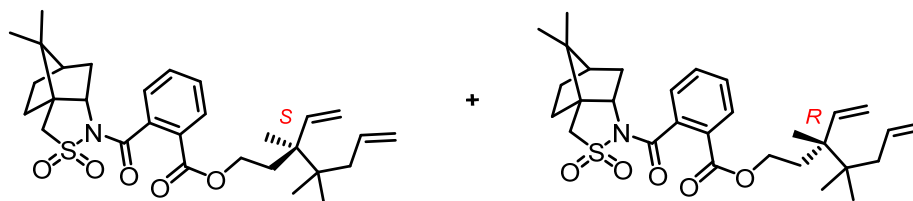
A solution of alcohol **30** (50 mg, 0.27 mmol) and CSP acid (131 mg, 0.36 mmol) in DCM (5 mL) was treated with dimethylaminopyridine (DMAP, 44 mg, 0.36 mmol) followed by dicyclohexylcarbodiimide (DCC, 61 mg, 0.30 mmol) at 0 °C. After stirring at RT for 24 h, the reaction mixture was filtered, and the filtrate was concentrated under reduced pressure. The residue was purified by column chromatography to give the mixture of diastereomers (105 mg, 74%). The mixture was resolved by chiral preparative HPLC on a Daicel CHIRALPAK® AD-H column. The purity of the collected fractions was checked on a 4.6 x 250 mm Chiralpak® IA-3 column (3μ particle size) eluted with n-hexane: EtOH (95/5), flow 1.0 mL/min, 25°C, monitoring by UV at 224 nm.

(S)-3,4,4-trimethyl-3-vinylhept-6-en-1-yl   2-((3aR,6R)-8,8-dimethyl-2,2-dioxidohexahydro-3H-3a,6-methanobenzo[c]isothiazole-1-carbonyl)benzoate (36a)

Optical rotation: $[\alpha]_D^{26}$ −106.6 (c 0.2, CHCl$_3$).

¹H NMR (400 MHz, CDCl$_3$): δ 7.99 (d, J = 7.5 Hz, 1H), 7.50-7.60 (m, 2H), 7.45 (d, J = 7.3 Hz, 1H), 5.76-5.87 (m, 2H), 5.14 (d, J = 10.8 Hz, 1H), 4.95-5.03 (m, 3H), 4.20 (t, J = 7.5 Hz, 2H), 4.08 (br s, 1H), 3.35-3.43 (m, 2H), 2.47 (br s, 1H), 2.16 (m, 1H), 2.04 (d, J = 7.3 Hz, 2H), 1.69-1.96 (m, 5H), 1.39-1.47 (m, 2H), 1.23 (s, 3H), 1.02 (s, 3H), 0.97 (s, 3H), 0.84 (s, 6H).

¹³C NMR (100 MHz, CDCl$_3$): δ 167.8, 165.2, 142.8, 136.2, 135.5, 131.7, 130.2, 129.5, 129.2, 128.9, 117.0, 114.5, 65.6, 63.7, 53.0, 48.3, 47.7, 44.7, 44.1, 41.3, 38.5, 37.7, 33.0, 32.6, 26.4, 21.6 (2C), 20.7, 20.0, 16.6

IR ν_{max} (thin film, CHCl$_3$) 2963, 1721, 1686, 1635, 1336, 1300, 1168, 1112 cm^{-1}

HRMS (ESI): m/z calculated for C$_{30}$H$_{42}$NO$_5$S [M + H]$^+$ 528.2778, found 528.2787

Chiral HPLC purity = 98.3% (96.6% ee); t$_R$ 10.57 min
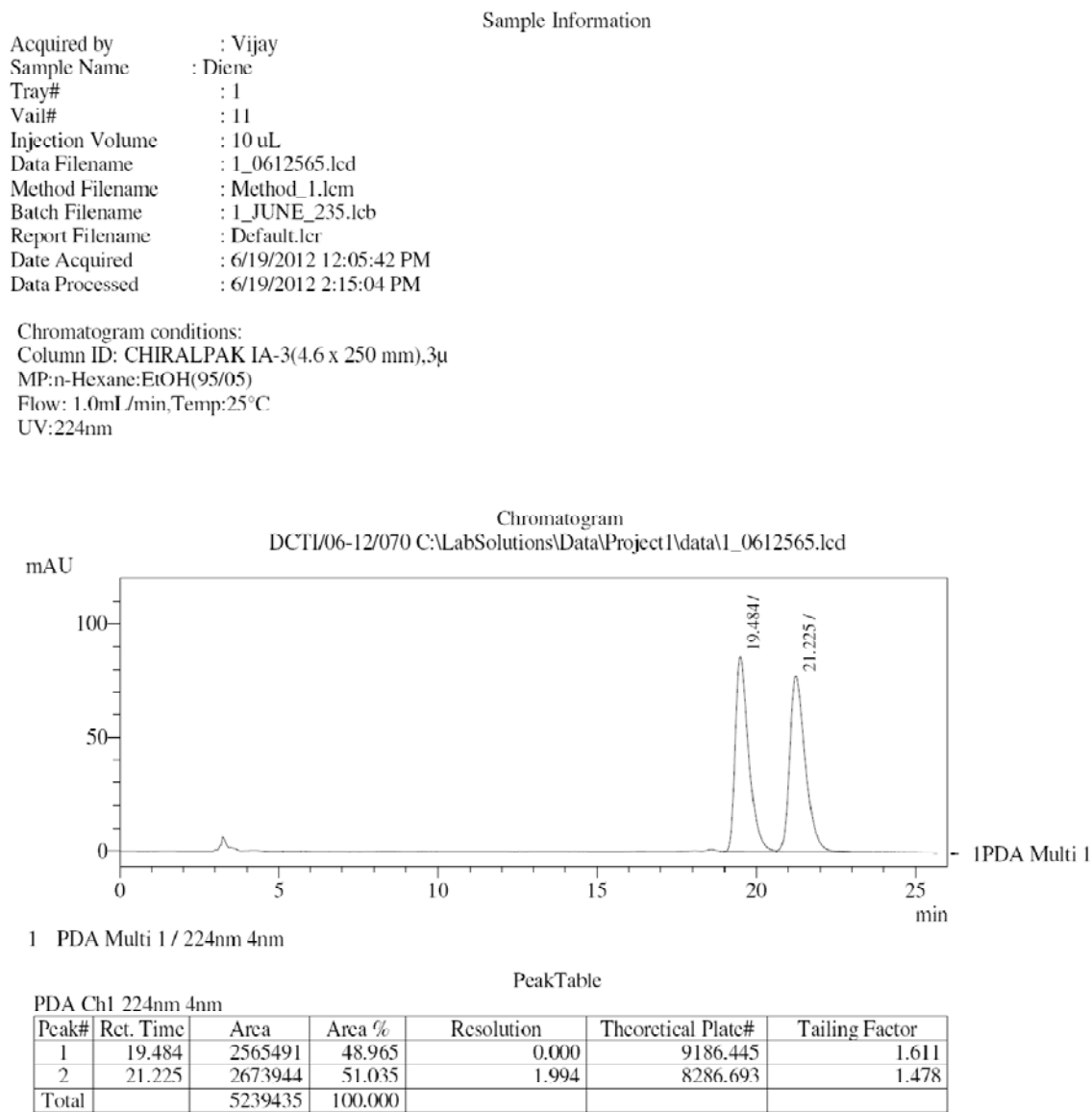
Figure 2.13. Chiral HPLC report

(R)-3,4,4-trimethyl-3-vinylhept-6-en-1-yl   **2-((3aR,6R)-8,8-dimethyl-2,2-dioxidohexahydro-3H-3a,6-methanobenzo[c]isothiazole-1-carbonyl)benzoate (36b)**

Optical rotation: $[\alpha]_D^{24}$ −71.0 (c 0.2, CHCl$_3$).

^{1}H NMR (400 MHz, CDCl$_3$): δ 7.99 (d, J = 7.8 Hz, 1H), 7.56-7.60 (m, 1H), 7.50-7.54 (m, 1H), 7.45 (d, J = 6.9 Hz, 1H), 5.76-5.89 (m, 2H), 5.13-5.16 (m, 1H), 4.95-5.03 (m,

3H), 4.08-4.27 (m, 3H), 3.36-3.43 (m, 2H), 2.47 (br s, 1H), 2.11-2.19 (m, 1H), 2.03 (d, J = 7.8 Hz, 2H), 1.81-1.97 (m, 5H), 1.36-1.47 (m, 2H), 1.23 (s, 3H), 1.01 (s, 3H), 0.97 (s, 3H), 0.84 (s, 6H).

^{13}C NMR (100 MHz, CDCl$_3$): δ 167.8, 165.2, 142.8, 136.2, 135.5, 131.7, 130.2, 129.6, 129.2, 129.0, 117.0, 114.5, 65.7, 63.7, 53.0, 48.3, 47.7, 44.8, 44.2, 41.4, 38.5, 37.7, 33.1, 32.7, 26.6, 21.6 (2C), 20.7, 20.0, 16.6

IR v_{max} (thin film, CHCl$_3$) 2963, 1720, 1685, 1635, 1333, 1299 cm^{-1}

HRMS (ESI): m/z calculated for C$_{30}$H$_{42}$NO$_5$S [M + H]$^+$ 528.2778, found 528.2787

Chiral HPLC purity = 99.3% (98.6 % ee); t$_R$ 13.63 min.

X-ray crystal structure details: Single crystals of compound **36b** were obtained from petroleum ether. X-ray intensity data were collected on a Bruker SMART APEX II CCD diffractometer with graphite-monochromatized (Mo Kα = 0.71073 Å) radiation at low temperature 150(2) K. The X-ray generator was operated at 50 kV and 30 mA. Diffraction data were collected with a ω scan width of 0.5° and at different settings of φ and 2θ. The sample-to-detector distance was fixed at 5.00 cm. The X-ray data acquisition was monitored by the APEX2 program suite. All the data were corrected for Lorentz-polarization and absorption effects using SAINT and SADABS programs integrated in the APEX2 program package. The structures were solved by the direct method and refined by full matrix least squares, based on F^2, using SHELX-97. Molecular diagrams were generated using XSHELL program integrated in SHELXTL package. All the H-atoms were placed in geometrically idealized position (C-H = 0.95 Å for phenyl H-atoms, C-H = 0.99 Å for methylene H-atoms, C-H = 1.00 Å for methine H-atoms and C-H = 0.98 Å for methyl H-atoms) and constrained to ride on their parent atoms [U_{iso}(H) = 1.2U_{eq}(C) for the phenyl, methylene, and methine group and U_{iso}(H) = 1.5U_{eq}(C) for the methyl group]. Crystallographic data for **36b** (C$_{30}$H$_{41}$NO$_5$S): M = 527.70, Crystal dimensions 0.40 x 0.22 x 0.02 mm^3, monoclinic, space group P 2$_1$, a = 9.8209(13), b = 11.2394(16), c = 13.1369(18) Å, β= 107.284(10)°, V = 1384.6(3) Å^3, Z = 2, ρ_{calcd} = 1.266 gcm^{-3}, μ (Mo-K$_\alpha$) = 0.157 mm^{-1}, $F(000)$ = 568, 2θ_{max} = 50.00°, T = 150(2) K, 8872 reflections collected, 4482 unique, 3055 observed (I > 2σ (I)) reflections, 340 refined

parameters, R value 0.0524, $wR2 = 0.0902$, (all data $R = 0.0954$, $wR2 = 0.1053$), $S = 0.996$, minimum and maximum transmission 0.940 and 0.997; maximum and minimum residual electron densities +0.26 and −0.23 e Å^{-3}. The absolute configuration was established by anomalous dispersion effect (Flack parameter of 0.07(11)) in X-ray diffraction measurements, caused by the presence of the sulphur atom in the molecule.

(*S*)-3,4,4-trimethyl-3-vinylhept-6-en-1-ol ((*S*)-30)
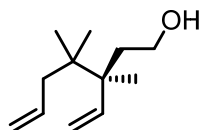
K$_2$CO$_3$ (282 mg, 2.04 mmol) was added to a solution of **36a** (90 mg, 0.170 mmol) in methanol at RT. After stirring for 2 h, the reaction mixture was concentrated under reduced pressure and purified by column chromatography to give the product **(*S*)-30** (28 mg, 90%).

Optical rotation: $[\alpha]_D^{25}$ +1.7 (*c* 0.38, CHCl$_3$).
^{1}H NMR (400 MHz, CDCl$_3$): δ 5.76-5.95 (m, 2H), 5.12 (dd, $J = 10.8, 1.5$ Hz, 1H), 4.93-5.03 (m, 3H), 3.60 (t, $J = 7.3$ Hz, 2H), 2.02 (d, $J = 7.3$ Hz, 2H), 1.78-1.85 (m, 1H), 1.64-1.71 (m, 1H), 0.98 (s, 3H), 0.82 (s, 6H).

(*S*)-3,4,4-trimethyl-3-vinylhept-6-en-1-yl acetate
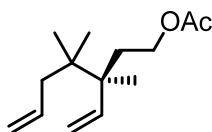
A solution of **(*S*)-30** (24 mg, 0.13 mmol) and Et$_3$N (73 µL, 0.52 mmol) in dry DCM (3 mL) was treated with acetic anhydride (26 µL, 0.26 mmol) and a catalytic amount of DMAP (2.5 mg) at RT. After stirring for 2 h, the reaction mixture was concentrated under reduced pressure and directly purified by column chromatography to give the product (28 mg, 95%).

Optical rotation: $[\alpha]_D^{23}$ –4.6 (*c* 0.1, CHCl$_3$).

^{1}H NMR (500 MHz, CDCl$_3$): δ 5.77-5.84 (m, 2H), 5.13 (dd, *J* = 11.0, 1.5 Hz, 1H), 4.93-5.02 (m, 3H), 3.95-4.02 (m, 2H), 2.01-2.04 (m, 5H), 1.70-1.83 (m, 2H), 0.97 (s, 3H), 0.82 (s, 6H).

(*S*)-2-(1,5,5-trimethylcyclopent-2-en-1-yl)ethyl acetate ((*S*)-2)
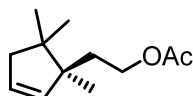
A solution of (*S*)-(3,4,4-trimethyl-3-vinyl-hept-6-enyl) acetate (22 mg, 0.10 mmol) in dry DCM (5 mL) was degassed for 10 min with a stream of argon and then treated with Grubbs' 2nd generation catalyst (9 mg, 10 mol%; Aldrich, cat# 569747) in one portion. After heating at 40 °C for 16 h, the mixture was treated with a drop of DMSO and stirring was continued for 1 hour. Evaporation of the solvent and purification by column chromatography furnished the product (14.2 mg, 75%).

Optical rotation: $[\alpha]_D^{25}$ +27.8 (*c* 0.16, CH$_2$Cl$_2$)

^{1}H NMR (400 MHz, CDCl$_3$): δ 5.55-5.64 (m, 2H), 4.05-4.23 (m, 2H), 2.13 (t, *J* = 1.6 Hz, 2H), 2.04 (s, 3H), 1.66-1.74 (m, 1H), 1.52-1.58 (m, merged with CDCl$_3$ moisture, 1H), 0.95 (s, 3H), 0.94 (s, 3H), 0.89 (s, 3H).

HRMS (ESI): m/z calculated for C$_{11}$H$_{17}$O$_3$ [M + H]$^+$ 197.1172, found 197.1173

Diastereomer **36b** was converted to (*R*)-2 in analogous fashion**.** Spectral data matched those of the corresponding enantiomers described above. Yields and optical rotations are given.

(*R*)-3,4,4-trimethyl-3-vinylhept-6-en-1-ol ((*R*)-30)
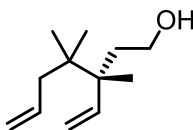
Yield: 94%

Optical rotation: $[\alpha]_D^{25}$ −2.0 (*c* 0.15, CHCl$_3$).

(*R*)-3,4,4-trimethyl-3-vinylhept-6-en-1-yl acetate
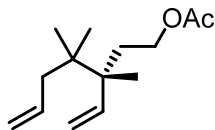
Yield: 94%

Optical rotation: $[\alpha]_D^{25}$ +3.3 (*c* 0.15, CHCl$_3$).

(*R*)-2-(1,5,5-trimethylcyclopent-2-en-1-yl)ethyl acetate ((*R*)-2)
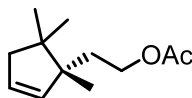
Yield: 83%

Optical rotation: $[\alpha]_D^{25}$ −24.0 (*c* 0.13, DCM).

2.6.2. Field trial of the pheromone enantiomers (California, USA)

A field bioassay of the pheromone was conducted at a nursery in Bonsall, California, USA, in a 0.49 ha plot of *Ruscus hypoglossum* L. (plot coordinates: 33º 17'18.36″ N, 117º16'55.61″W elev 113 m) that was known to be infested with *P. longispinus*. The plot was divided into seven hoop houses (63 m long x 7 m wide), six of which were used in this study. Each house (= block) was covered in plastic with open ends. Airflow between houses was not restricted because the plastic cover began 1 m above the plant canopy. Four delta sticky traps were spaced every 12.5 m along a transect within each house, suspended directly above the ruscus canopy. Each trap contained a gray rubber septa (11 mm) impregnated with hexane solutions of one of four treatments: solvent control, 5 µg (*S*)-(+)-enantiomer, 5 µg (*R*)-(-)-enantiomer, 10 µg of the racemate. Treatments were assigned randomly along each transect. Traps were replaced and treatments were repositioned once after 6 d. Traps remained in place for another 11 d. Trap count data were analyzed with SAS version 9.1.3 (SAS Institute, Cary, NC) after $\sqrt{(x + 0.5)}$

transformation of the data to meet the assumptions of normality and equal variances. The PROC MIXED routine was used, and the blocks were entered as a component of the RANDOM statement. Differences among means were tested using Tukey's honestly significant different (HSD) test. There was no significant interaction between the two sampling periods (= date) and the treatments (F = 3.23, df = 2, 30, and P = 0.054). Thus, data for each date were combined for the final analysis. There was both a significant effect of date (F = 10.19, df = 2, 32, P = 0.0032) and treatment (F = 130.04, df = 2, 32, P < 0.0001). Controls were not included in the analysis because their zero values and lack of variance violate the assumptions of ANOVA. Instead, SAS was used to construct confidence intervals, showing that the low trap counts for the (**R**)-(**-**)-enantiomer were significantly different than zero, i.e., that the (-)-enantiomer was slightly more attractive than controls.

2.6.3. Synthesis of pheromone enantiomers from chiral pool

Synthesis of (R)–(-)–pheromone

(3a*S*,5*S*,6a*R*)-5-Hydroxy-3a,4,4-trimethylhexahydro-2*H*-cyclopenta[*b*]furan-2-one((-)–48)
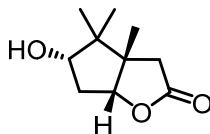
Acetic acid (6 mL) and H_2O_2 (35 wt% in water, 5 mL) were taken in a single neck round-bottomed flask, cooled to 0 ºC and H_2SO_4 (1 mL) was added. Then a solution of (-)–37[25,26] (1.9 g, 9.03 mmol) in acetic acid (3 mL) was added and stirred at RT for 24 h. Ethyl acetate was added and the aqueous layer was extracted thrice (30 mL X 3). The combined organic layer was dried over Na_2SO_4 and the solvent was evaporated under reduced pressure. The crude thus obtained was dissolved in methanol (20 mL), added K_2CO_3 (3.74 g, 27.09 mmol) and stirred at RT for 3 h. The reaction mixture was passed through celite and the filtrate was concentrated and purified by column chromatography (230–400 silica gel) using 25 – 30 % Ethyl acetate: pet ether to afford the product (-)–48

as a colourless crystalline solid (832 mg, 50%) along with minor amount of **(-)–38'** (5:2 ratio in this experiment).

Melting Point: 224 – 226 °C

Optical rotation: $[\alpha]_D^{29}$ –9.2 (c 0.33, CHCl₃).

¹H NMR (400 MHz, CDCl₃): δ 4.55 (dd, J = 8.6 , 2.0 Hz, 1H), 3.92 (dd, J = 5.6, 1.7 Hz, 1H), 3.35 (d, J = 18.1 Hz, 1H), 2.51 (ddd, J = 15.9, 8.6, 5.9 Hz, 1H), 2.07 (d, J = 18.1 Hz, 1H), 1.88 (dt, J = 16.1, 2.0 Hz, 1H), 1.73 (brs, 1H), 1.14 (s, 3H), 1.04 (s, 3H), 0.85 (s, 3H).

¹³C NMR (100 MHz, CDCl₃): δ 177.9, 90.5, 81.4, 50.7, 46.5, 40.2, 39.8, 24.2, 22.1, 18.2.

IR ν_{max} (thin film, CHCl₃) 3470 (broad peak), 2969, 1764, 1069 cm^{-1}

HRMS (ESI): m/z calculated for C₁₀H₁₆O₃Na [M + Na]⁺ 207.0992, found 207.0985

X-ray crystal structure details: Single crystals of compound **(-)–48** was obtained from chloroform.

Crystallographic data (C₁₀H₁₆O₃): M = 184.23, Crystal dimensions 0.64 x 0.60 x 0.20 mm³, orthorhombic, space group $P2_12_12_1$, a = 6.9872(7), b = 11.6575(12), c = 11.8586(12) Å, V = 965.92(17) Å³, Z = 4, ρ_{calcd} = 1.267 gcm^{-3}, μ (Mo-K$_\alpha$) = 0.092 mm^{-1}, $F(000)$ = 400, $2\theta_{max}$ = 50.00°, T = 296(2) K, 5178 reflections collected, 1648 unique, 1532 observed (I > 2σ (I)) reflections, 122 refined parameters, R value 0.0329, wR2 = 0.0806, (all data R = 0.0356, wR2 = 0.0824), S = 1.091, minimum and maximum transmission 0.943 and 0.982; maximum and minimum residual electron densities +0.09 and –0.11 e Å^{-3}.

(1*S*,5*R*,6*R*)-6-Hydroxy-5,8,8-trimethyl-3-oxabicyclo[3.2.1]octan-2-one ((-)–38')

In the above experiment compound **(-)–38'** was also isolated as a colourless solid (330 mg, 20%)
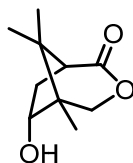
Melting point: 264 – 267 °C

Optical rotation: $[\alpha]_D^{28}$ −10.8 (c 0.28, CHCl$_3$).

^{1}H NMR (400 MHz, CDCl$_3$): δ 4.54 (d, J = 12.7 Hz, 1H), 4.23 (dd, J = 9.6, 2.9 Hz, 1H), 3.84 (d, J = 12.5 Hz, 1H), 2.63 – 2.55 (m, 1H), 2.46 (d, J = 7.6 Hz, 1H), 1.81 (brs, 1H), 1.64 (dd, J = 14.9, 3.9 Hz, 1H), 1.08 (s, 3H), 0.93 (s, 3H), 0.89 (s, 3H).

^{13}C NMR (100 MHz, CDCl$_3$): δ ppm 174.9, 76.3, 70.4, 51.7, 46.3, 42.0, 36.0, 21.5, 20.2, 13.2

IR ν_{max} (thin film, CHCl$_3$) 3480 (broad peak), 2965, 1716, 1461, 1246, 1057 cm^{-1}

HRMS (ESI): m/z calculated for C$_{10}$H$_{16}$O$_3$Na [M + Na]$^+$ 207.0992, found 207.0992

(3aS,6aR)-3a,4,4-Trimethyltetrahydro-2H-cyclopenta[b]furan-2,5(3H)-dione ((-)−49)
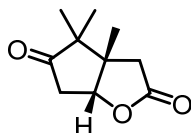
To a solution of **(-)−48** (1.2 g, 6.5 mmol) in dry DCM (20 mL), 4 Å molecular sieves was added followed by PDC (3.7 g, 9.8 mmol) and stirred at RT overnight. The reaction mass was filtered through celite. The filtrate was washed with 1N HCl, dried over Na$_2$SO$_4$ and concentrated. The crude mass was purified by column chromatography (100–200 silica gel) using 15% ethyl acetate: pet ether to give the compound as a white crystalline solid (1.05 g, 89% yield).

Melting point: 169 – 171 °C

Optical rotation: $[\alpha]_D^{29}$ −98.3 (c 0.32, CHCl$_3$).

^{1}H NMR (400 MHz, CDCl$_3$): δ 4.79 (dd, J = 9.0, 4.2 Hz, 1H), 3.02 (dd, J = 20.3, 8.8 Hz, 1H), 2.44 (dd, J = 20.3, 4.2 Hz, 1H), 2.32 (AB quartet, 2H), 1.27 (s, 3 H), 1.08 (s, 3H), 1.02 (s, 3H).

¹³C NMR (100 MHz, CDCl₃): δ 216.3, 175.3, 82.7, 52.4, 50.1, 41.1, 39.0, 21.2, 19.3, 18.8

IR ν$_{max}$ (thin film, CHCl₃) 2973, 2884, 1783, 1747, 1460, 1288 cm⁻¹

HRMS (ESI): m/z calculated for C₁₀H₁₅O₃ [M + H]⁺ 183.1016, found 183.1011

Methyl (*R*)-2-(1,5,5-trimethyl-4-oxocyclopent-2-en-1-yl)acetate ((-)−50)
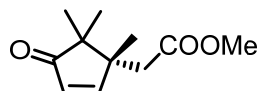
The compound **(-)–49** (900 mg, 4.95 mmol) was dissolved in dry methanol (20 mL), PTSA monohydrate (3.8 g, 19.8 mmol) was added and refluxed for 24 h. The reaction mass was cooled to RT and solvent was removed under reduced pressure. Water (10 mL) and DCM (25 mL) was added and the organic layer was separated, aqueous layer was extracted with DCM (20 ml x 2) and the combined organics were dried over Na₂SO₄ and concentrated under reduced pressure. The pure product was obtained by column chromatography (silica gel 100–200) using 10% ethyl acetate: pet ether to afford the product as a colourless liquid (850 mg, 88% yield) along with recovery of starting material (60 mg, 94% brsm).

Optical rotation: [α]$_D^{29}$ –4.4 (c 0.34, CHCl₃).

¹H NMR (500 MHz, CDCl₃): δ 7.71 (d, *J* = 5.8 Hz, 1H), 6.08 (d, *J* = 5.8 Hz, 1H), 3.71 (s, 3H), 2.51 (d, *J* = 14.9 Hz, 1H), 2.39 (d, *J* = 14.9 Hz, 1H), 1.18 (s, 3H), 1.09 (s, 3H), 1.06 (s, 3H).

¹³C NMR (125 MHz, CDCl₃): δ 213.5, 171.9, 168.5, 129.0, 51.6, 51.3, 48.5, 41.5, 23.0, 22.7, 20.9

IR ν$_{max}$ (thin film, CHCl₃) 2969, 2883, 1715, 1594, 1203 cm⁻¹

HRMS (ESI): m/z calculated for C₁₁H₁₇O₃ [M + H]⁺ 197.1172, found 197.1173

Methyl (*R*)-2-(1,5,5-trimethylcyclopent-2-en-1-yl)acetate (42)

~3:10 ratio
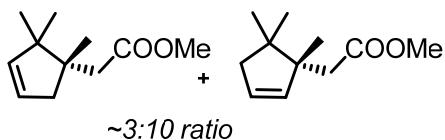
A solution of **(-)–50** (70 mg, 0.356 mmol) in dry methanol (3 mL) was cooled to 0 ºC, added CeCl₃.7H₂O (146 mg, 0.392 mmol), followed by sodium borohydride (27 mg, 0.712 mmol) and stirred at RT for 1 h. The reaction mass was cooled to 0 ºC, quenched with sat. NH₄Cl and methanol was removed in rotary evaporator. Ethyl acetate (10 mL) was added and the aqueous layer was extracted (10 mL x 3), dried over Na₂SO₄ and concentrated to give the allyl alcohol **51** as a colourless liquid (70 mg, quantitative).

A solution of **51** (70 mg, 0.353 mmol) in dry THF (3 mL) was cooled to 0 ºC, added BF₃.Et₂O (0.13 mL, 1.059 mmol) followed by sodium cyanoborohydride (66 mg, 1.059 mmol) and refluxed overnight. The reaction was quenched with 2N NaOH, added DCM (10 mL) and the organic layer was separated. It was then dried over Na₂SO₄, concentrated and purified by column chromatography (silica gel 230–400 gel) using 2% ethyl acetate: pet ether to give the product **42** as a mixture with its regioisomer **42a** (55 mg, 86% combined yield, 10:3 ratio by NMR). Data for the major isomer **42**:

¹H NMR (400 MHz, CDCl₃): δ 5.80 – 5.76 (m, 1H), 5.68 –5.65 (m, 1H), 3.68 (s, 3H), 2.44 – 2.07 (m, 4H), 0.99 (s, 6H), 0.96 (s, 3H).

¹³C NMR (100 MHz, CDCl₃): δ 173.6, 138.7, 127.9, 51.2, 49.8, 46.7, 44.1, 40.6, 24.4, 24.0, 19.8

HRMS (ESI): m/z calculated for $C_{11}H_{17}O_3$ $[M + H]^+$ 197.1172, found 197.1173

(*R*)-2-(1,5,5-Trimethylcyclopent-2-en-1-yl)ethan-1-ol ((-)–12)
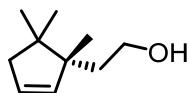
The regioisomeric mixture (**42** and **42a**) obtained in the above step was used to prepare the title compound. This mixture (50 mg, 0.275 mmol) was dissolved in dry THF (3 mL), cooled to 0 ºC, added LAH (31 mg, 0.824 mmol) and stirred at RT for 2 h. The reaction

mixture was quenched with saturated Na$_2$SO$_4$ solution, ethyl acetate (10 mL) was added and the organic layer was separated, the aqueous layer was again extracted (10 mL X 2), dried over Na$_2$SO$_4$, concentrated in a rotary evaporator and purified by column chromatography (silica gel 230 –400 mesh) using 5% ethyl acetate: pet ether to give the product as a colourless liquid (40 mg, 95% yield along with its regioisomer **(+)–12a**). Both the regioisomers could be separated by flash column chromatography although they were inseparable in TLC.

Optical rotation: $[\alpha]_D^{26}$ –10.4 (c 1.14, CHCl$_3$).

^{1}H NMR (400 MHz, CDCl$_3$): δ 5.63 – 5.60 (m, 1H), 5.56 – 5.54 (m, 1H), 3.77 – 3.69 (m, 2H), 2.13 – 2.11 (m, 2H), 1.67 – 1.61 (m, 1H), 1.56 – 1.51 (m, 1H), 0.95 (s, 3H), 0.93 (s, 3H), 0.88 (s, 3H).

HRMS (ESI): m/z calculated for C$_{11}$H$_{17}$O$_3$ [M + H]$^+$ 197.1172, found 197.1173

(*S*)-2-(1,2,2-Trimethylcyclopent-3-en-1-yl)ethan-1-ol ((+)-12a)
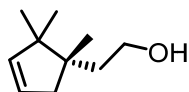
Optical rotation: $[\alpha]_D^{25}$ +14.5 (c 0.17, CHCl$_3$).

^{1}H NMR (400 MHz, CDCl$_3$): δ 5.54 – 5.51 (m, 1H), 5.44 – 5.43 (m, 1H), 3.79 – 3.64 (m, 2H), 2.32 – 2.28 (m, 1H), 2.03 – 1.98 (m, 1H), 1.73 – 1.60 (m, 2H), 0.91 (s, 3H), 0.90 (s, 3H), 0.89 (s, 3H).

^{13}C NMR (100 MHz, CDCl$_3$): δ 141.6, 126.2, 61.1, 48.7, 44.9, 44.7, 39.6, 23.8, 22.3, 22.2.

(*R*)-2-(1,5,5-Trimethylcyclopent-2-en-1-yl)ethyl acetate ((-)−2)
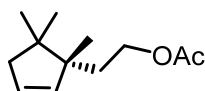
To a solution of **(-)–12** (10 mg, 0.065 mmol) in dry DCM (2 mL), triethylamine (36 μL, 0.26 mmol) and acetic anhydride (12 μL, 0.13 mmol) was added followed by a pinch of

DMAP and stirred at RT for 3 h. The reaction mixture was diluted with DCM, water was added, the organic layer was separated, dried over Na$_2$SO$_4$, concentrated and purified by column chromatography (100–200 silica gel) using 20% DCM: pentane to afford the product as a colourless liquid (11 mg, 86%). NMR spectrum was found to be identical with the previous one.

Optical rotation: $[\alpha]_D^{25}$ –20.6 (c 0.33, CHCl$_3$).

Synthesis of (S)–(+)–pheromone

The same route was followed for the synthesis of the other antipode (S)–(+)–pheromone starting from (+)–**37**.[25,26,40] The NMR data of all the compounds in this series were found to be exactly matching with the other enantiomeric series. The optical rotations also showed the same magnitude but with an inverse sign.

(3a*R*,5*R*,6a*S*)-5-Hydroxy-3a,4,4-trimethylhexahydro-2*H*-cyclopenta[*b*]furan-2-one (+)–48
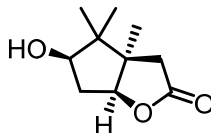
Yield: 48%
Optical rotation: $[\alpha]_D^{28}$ +6.8 (c 0.34, CHCl$_3$).

(3a*R*,6a*S*)-3a,4,4-Trimethyltetrahydro-2*H*-cyclopenta[*b*]furan-2,5(3*H*)-dione (+)–49
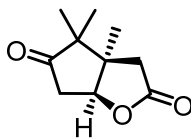
Yield: 95%
Optical rotation: $[\alpha]_D^{28}$ +98.3 (c 0.27, CHCl$_3$).

Methyl(*S*)-2-(1,5,5-trimethyl-4-oxocyclopent-2-en-1-yl)acetate (+)–50
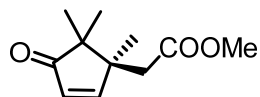
Yield: 80%, 97% brsm

Optical rotation: $[\alpha]_D^{25}$ +4.5 (c 0.50, CHCl₃).

(*S*)-2-(1,5,5-Trimethylcyclopent-2-en-1-yl)ethan-1-ol ((+)–12)
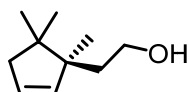
Optical rotation: $[\alpha]_D^{26}$ +11.3 (c 0.30, CHCl₃).

(*R*)-2-(1,2,2-Trimethylcyclopent-3-en-1-yl)ethan-1-ol ((-)–12a)
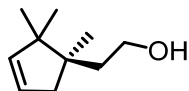
Optical rotation: $[\alpha]_D^{24}$ −13.8 (c 0.17, CHCl₃).

(*S*)-2-(1,5,5-Trimethylcyclopent-2-en-1-yl)ethyl acetate ((+)–2)
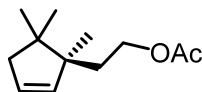
Yield: 94%

Optical rotation: $[\alpha]_D^{32}$ +23.7 (c 0.33, CHCl₃).

Methyl (*S*)-2-(1,2,2-trimethyl-3-oxocyclopentyl)acetate (Reassigned structure of **41**)
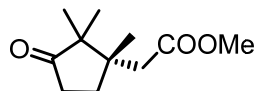
The compound **(-)–50** (350 mg, 1.79 mmol) was dissolved in methanol (5 mL), palladium on carbon (35 mg, 10 wt %) was added and was stirred under an atmosphere of hydrogen for 1 h. The reaction mass was then filtered through celite and washed with DCM, dried

over Na$_2$SO$_4$ and solvent was removed under reduced pressure to give the product as a colourless liquid (330 mg, 93%).

Optical rotation: [α]$_D^{27}$ −74.5 (c 1.33, CHCl$_3$).

^{1}H NMR (400 MHz, CDCl$_3$): δ 3.64 (s, 3H), 2.36 – 2.17 (m, 4H), 2.04 – 1.96 (m, 1H), 1.87 – 1.80 (m, 1H), 0.97 (s, 3H), 0.90 (s, 3H), 0.89 (s, 3H).

^{13}C NMR (100 MHz, CDCl$_3$): δ 222.3, 172.4, 52.5, 51.4, 43.1, 41.1, 33.6, 30.9, 21.3, 19.8, 18.2

IR ν$_{max}$ (thin film, CHCl$_3$) 2968, 1737, 1450, 1206, 1105 cm^{-1}

HRMS C$_{11}$H$_{18}$O$_3$Na [M + Na]$^+$ 221.1148, found 221.1147

Methyl (*S*)-2-(1,2,3-trimethylcyclopent-2-en-1-yl)acetate (46)
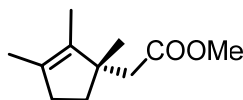
The saturated ketone (50 mg, 0.25 mmol) obtained in the above reaction was dissolved in dry methanol (3 mL), cooled to 0 °C and NaBH$_4$ (10 mg, 0.25 mmol) was added cautiously and stirred at RT for 1 h. Reaction mass was cooled to 0 °C and quenched with sat. NH$_4$Cl and methanol was removed in a rotary evaporator. Ethyl acetate (10 mL) was added and the organic layer was separated, aqueous layer was again extracted (20 mL x 3) and the combined extracts were dried over Na$_2$SO$_4$, and concentrated under reduced pressure to give **47** (40 mg). The crude mass was used for the next step without further purification.

The compound **47** (40 mg, 0.20 mmol) was dissolved in dry benzene (3 mL), P$_2$O$_5$ (170 mg, 0.599 mmol) was added and refluxed overnight. The reaction mixture was cooled to RT, diluted with DCM (10 mL) and 2N NaOH was added. The organic layer was separated, washed with brine, dried over Na$_2$SO$_4$ and solvent was removed in a rotary evaporator. The reaction mixture was purified by column chromatography (silica gel 100–200) using 2-3% ethyl acetate: pet ether to afford the product as a colourless liquid (28 mg, 78% yield).

Optical rotation: $[\alpha]_D^{30}$ −6.4 (c 0.19, CHCl$_3$).

^{1}H NMR (400 MHz, CDCl$_3$): δ 3.61 (s, 3H), 2.26 (AB quartet, 2H), 2.16 (m, 2H), 2.05 − 1.98 (m, 1H), 1.64 − 1.55 (m, 1H, merged with methyl singlet), 1.58 (s, 3H), 1.49 (s, 3H), 1.05 (s, 3H).

^{13}C NMR (100 MHz, CDCl$_3$): δ 173.0, 136.0, 131.3, 51.1, 49.7, 43.4, 35.6, 35.2, 25.0, 14.2, 9.4

IR ν_{max} (thin film, CHCl$_3$) 3022, 2926, 2856, 1729, 1446, 1322, 1214 cm^{-1}

HRMS C$_{11}$H$_{19}$O$_2$ [M + H]$^+$ 183.1380, found 183.1379

(1S,5R)-5,8,8-Trimethyl-2-oxabicyclo[3.2.1]oct-6-en-3-one (52)

Compound **51** (50 mg, 0.25 mmol) was dissolved in dry diethyl ether, added lithium perchlorate (319 mg, 3 mmol) followed by triethylsilyl hydride (0.12 mL, 0.75 mmol). The reaction mixture was then stirred at RT overnight. Water was added and the organic layer was separated. The aqueous layer was again extracted with diethyl ether, combined organics were dried over Na$_2$SO$_4$ and concentrated under reduced vacuum. The product was purified by column chromatography (silica gel 100-200) eluting with 2% ethylacetate-pet ether to give the product as colourless oil (28 mg, 68%).

Optical rotation: $[\alpha]_D^{27}$ −207.3 (c 1.1, CHCl$_3$).

^{1}H NMR (400 MHz, CDCl$_3$): δ 5.85 (d, J = 5.9 Hz, 1H), 5.65 (dd, J = 5.8, 1.3 Hz, 1H), 5.05 (m, 1H), 2.62 (d, J = 17.1 Hz, 1H), 2.04 (d, J = 17.1 Hz, 1H), 1.19 (s, 3H), 1.03 (s, 3H), 0.98 (s, 3H).

^{13}C NMR (100 MHz, CDCl$_3$): δ 176.9, 146.3, 125.8, 93.8, 51.7, 47.6, 40.0, 26.4, 22.6, 18.4

IR ν_{max} (thin film, CHCl$_3$) 3023, 2967, 2876, 1774, 1611, 1457, 1346, 1215 cm^{-1}

HRMS C$_{10}$H$_{15}$O$_2$ [M + H]$^+$ 167.1067, found 167.1066

2.7. References

(1)   Mori, K. *Acc. Chem. Res*. **2000**, *33*, 102-110.

(2)   Mori, K. *Tetrahedron* **1989**, *45*, 3233-3298.

(3)   Butenandt, A.; Beckman, R.; Stamm, D.; Hecker, E. *Z. Naturforsch*. **1959**, *14B*, 283-284.

(4)   Kasang, G.; Kaissling, K. E.; Vostrowsky, O.; Bestmann, H. J. *Angew. Chem. Int. Ed. Engl*. **1978**, *17*, 60.

(5)   Witzgall, P.; Kirsch, P.; Cork, A. *J Chem Ecol.* **2010**, *36*, 80-100.

(6)   Byers, J. A. *Biol. Rev.* **1991**, *66*, 347-378.

(7)   Zou, Y.; Millar, J. G. *Nat. Prod. Rep.* **2015**, *32*, 1067-1113.

(8)   Mori, K. *Proc. Jpn. Acad., Ser. B* **2014**, *90*, 373-388.

(9)   Mori, K. *Chemcomm.* **1997**, 1153-1158.

(10)   Mori, K. *Biosci. Biotech. Biochem.* **1996**, *60*, 1925-1932.

(11)   Millar, J. G.; Moreira, J. A.; McElfresh, J. S.; Daane, K. M.; Freund, A. S. *Org. Lett.* **2009**, *11*, 2683-2685.

(12)   Millar, J. G.; Midland, S. L.; McElfresh, J. S.; Daane, K. M. *J. Chem. Ecol.* **2005**, *31*, 2999-3005.

(13)   Figade`re, B. A.; McElfresh, J. S.; Borchardt, D.; Daane, K. M.; Bently, W.; Millar, J. G. *Tetrahedron Lett.* **2007**, *48*, 8434-8437.

(14)   Hajare, A. K.; Datrange, L. S.; Vyas, S.; Bhuniya, D.; Reddy, D. S. *Tetrahedron Lett.* **2010**, *51*, 5291-5293.

(15)   Zou, Y.; Millar, J. G. *J. Org. Chem.* **2009**, *74*, 7207-7209.

(16)   Zou, Y.; Millar, J. G. *Synlett* **2010**, 2319-2321.

(17)   Bailey, W. F.; Bakonyi, J. M. *J. Org. Chem.* **2013**, *78*, 3493−3495.

(18)   Kurhade, S. E.; Siddaiah, V.; Bhuniya, D.; Reddy, D. S. *Synthesis*, **2013**, *45*, 1689-1692.

(19)   Harada, N.; Nehira, T.; Soutome, T.; Hiyoshi, N.; Kido, F. *Enantiomer* **1996**, *1*, 35-39.

(20)   Harada, N.; Koumura, N.; Robillard, M. *Enantiomer* **1997**, *2*, 303-309.

(21) Kosaka, M.; Sugito, T.; Kasai,Y.; Kuwahara, S.; Watanabe, M.; Harada, N.; Job, G. E.; Shvet, A.; Pirkle, W. H. *Chirality* **2003**, *15*, 324-328.

(22) Harada, N. *Chirality* **2008**, *20*, 691-723.

(23) Harada, N.; Koumura, N.; Feringa, B. L. *J. Am. Chem. Soc*. **1997**, *119*, 7256-7264

(24) Davis, F. A.; Towson, J. C.; Weismiller, M. C.; Lal, S.; Carroll, P. J. *J. Am. Chem. Soc.* **1988**, 110, 8477-8482.

(25) Tartaggia, S.; Padovan, P.; Borsato, G.; De Lucchi, O.; Fabris, F. *Tetrahedron Lett*. **2011**, *52*, 4478-4480.

(26) Acerson, M. J.; Bingham, B. S.; Allred, C. A.; Andrus, M. B. *Tetrahedron Lett*. **2015**, *56*, 3277-3280

(27) Hassall, C. H. **2011**, The Baeyer-Villiger oxidation of aldehydes and ketones. *Organic Reactions*, *9*, 73-106.

(28) Grudzinski, A.; Roberts, S. M.; Howard, C.; Newton, R. F. *J. Chem. Soc., Perkin Trans. I* **1978**, 1182-1186.

(29) Krow, G. R. **2004**. The Baeyer–Villiger Oxidation of Ketones and Aldehydes. Organic Reactions. *43*, 251–798.

(30) Suri, S. C. *Tetrahedron Lett.* **1996**, *37*, 2335-2336.

(31) Paquette, L. A.; Vanucci, C.; Rogers, R. D. *J. Am. Chem. Soc.* **1989**, *111*, 5792-5800.

(32) Wagner, G. J. *Russ. Phys. Chem. Soc.* **1899**, *31*, 690.

(33) Meerwein, H. *Justus Liebigs Ann. Chem.* **1914**, *405*, 129-175.

(34) Davis, C. E.; Duffy, B. C.; Coates, R. M. *J. Org. Chem.* **2003**, *68*, 6935-6943.

(35) Srikrishna, A.; Viswajanani, R.; Sattigeri, J. A.; Yelamaggad, C. V. *Tetrahedron Lett.* **1995**, *36*, 2347-2350.

(36) Kim, H. J.; Su, L.; Jung, H.; Koo, S. *Org. Lett.*, **2011**, *13*, 2682-2685.

(37) Green, J. C.; Pettus, T. R. R. *J. Am. Chem. Soc*. **2011**, *133*, 1603–1608.

(38) Wustrow, D. J.; Smith III, W. J.; Wise, L. D. *Tetrahedron Lett.* **1994**, *35*, 61-64.

(39) Nicolaou, K. C.; Koftis, T. V.; Vyskocil, S.; Petrovic, G.; Tang, W.; Frederick, M. O.; Chen, D. Y. –K, Li, Y.; Ling, T.; Yamada, Y. M. A. *J. Am. Chem. Soc*. **2006**, *128*, 2859–2872.

(40)   Jackson, C. L.; Menke, A. E. *Proc. Am. Acad. Arts Sci.* **1882**, *18*, 93-95.
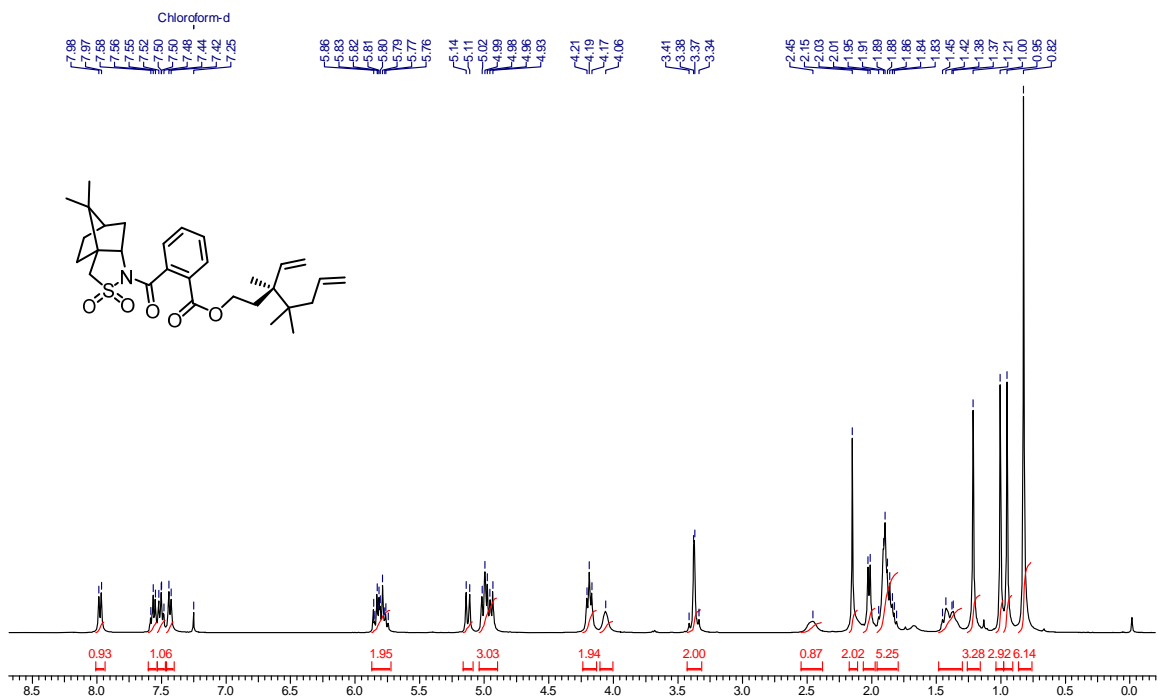
Figure 2.14. ^{1}H NMR spectra of **36a**
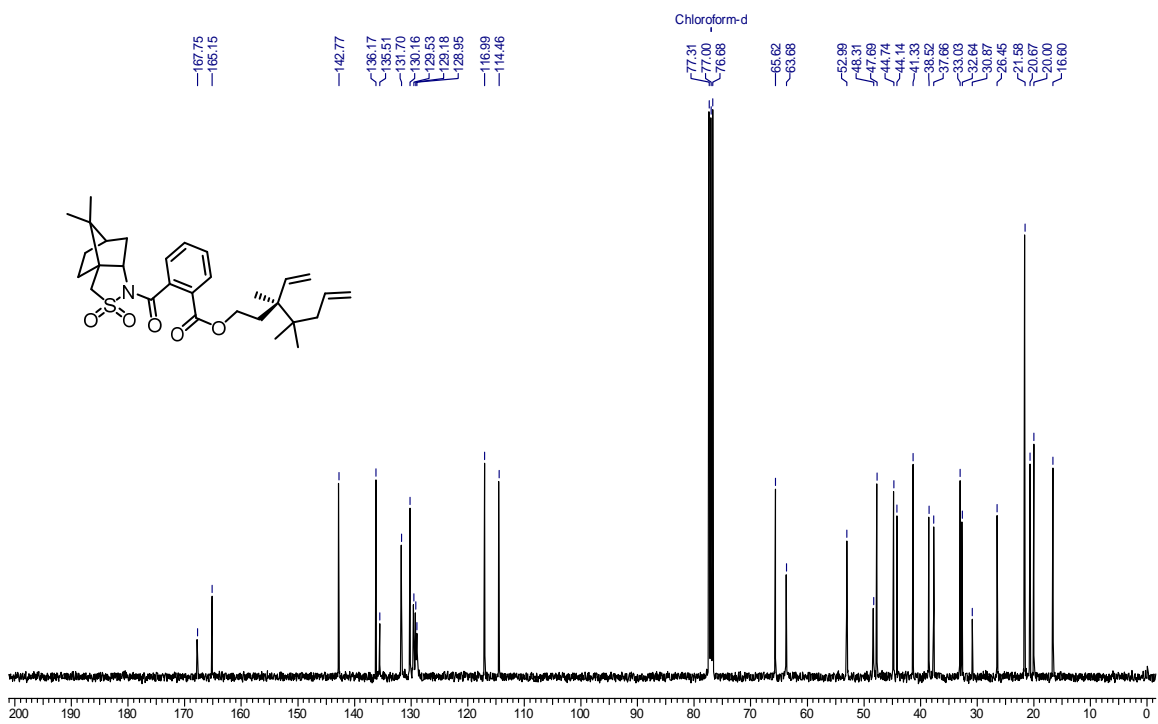
Figure 2.15. ^{13}C NMR spectra of **36a**
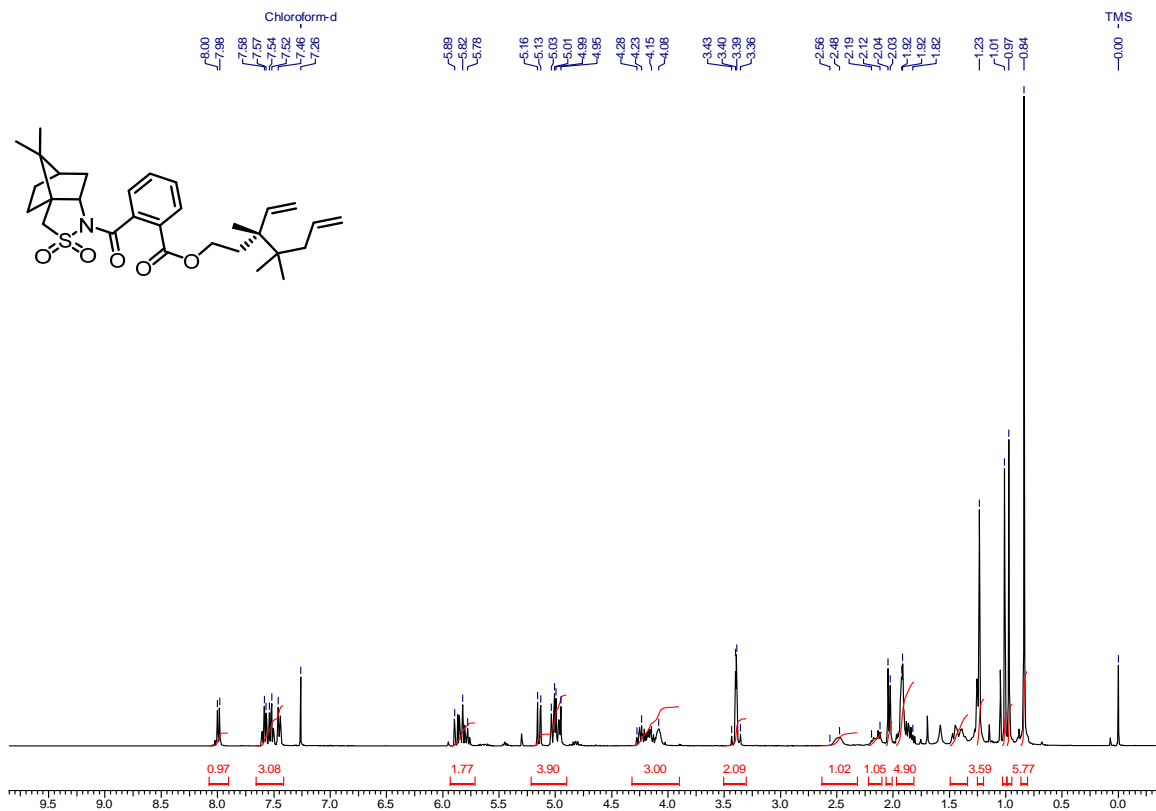
Figure 2.16. ^{1}H NMR spectra of **36b**
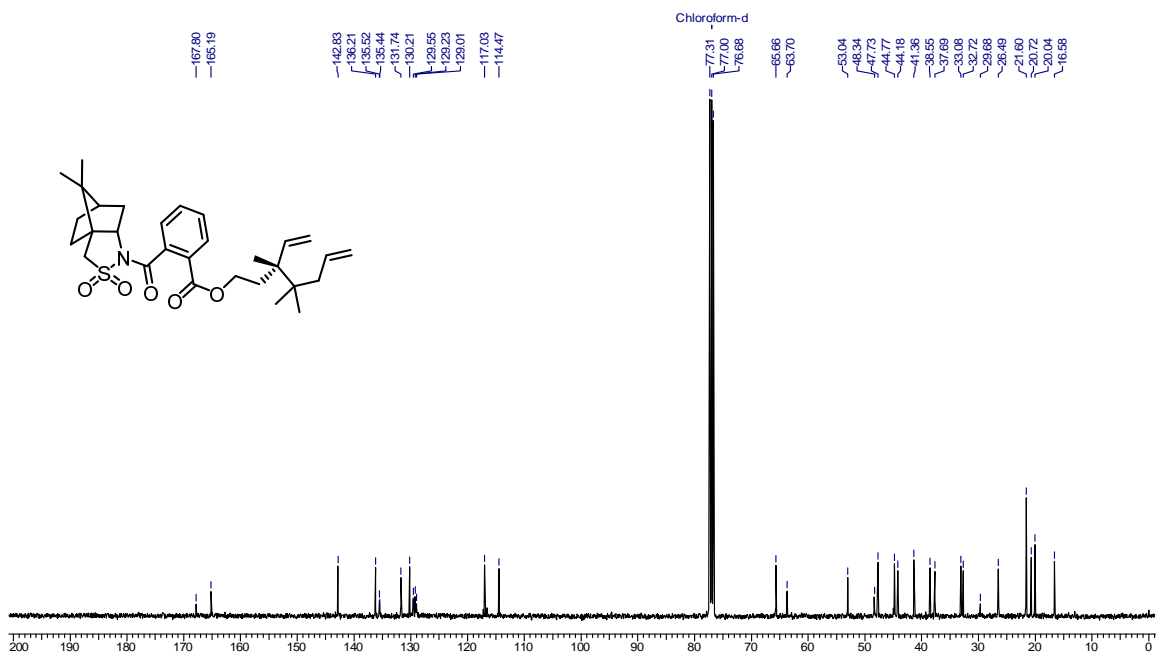
Figure 2.17. ^{13}C NMR spectra of **36b**
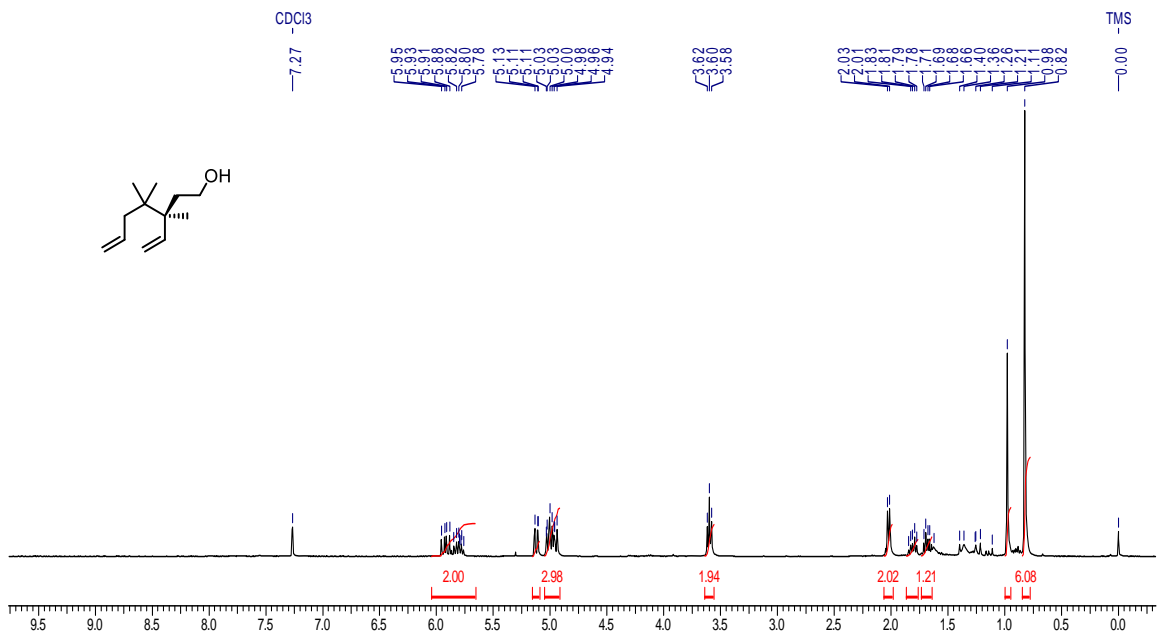
Figure 2.18. ^{1}H NMR spectra of **(S)-30**
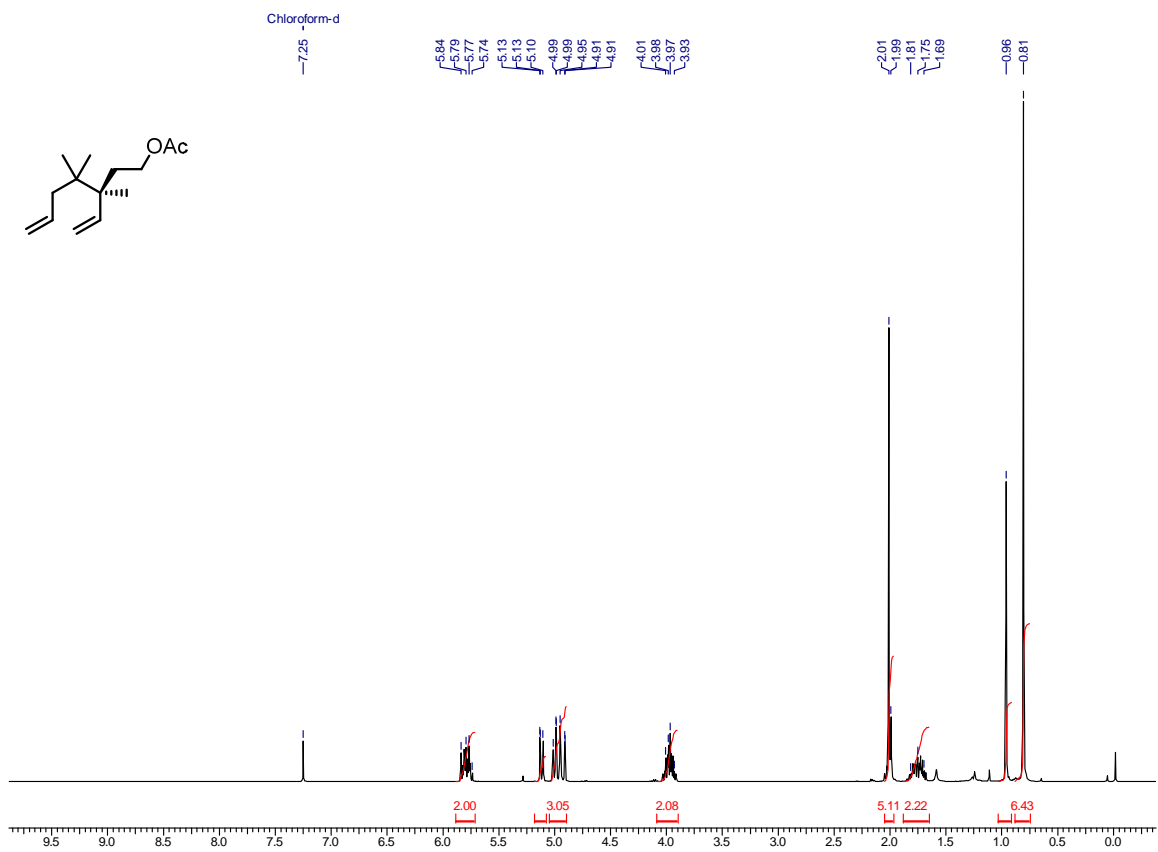
Figure 2.19. ^{1}H NMR spectra of **(S)-30a**
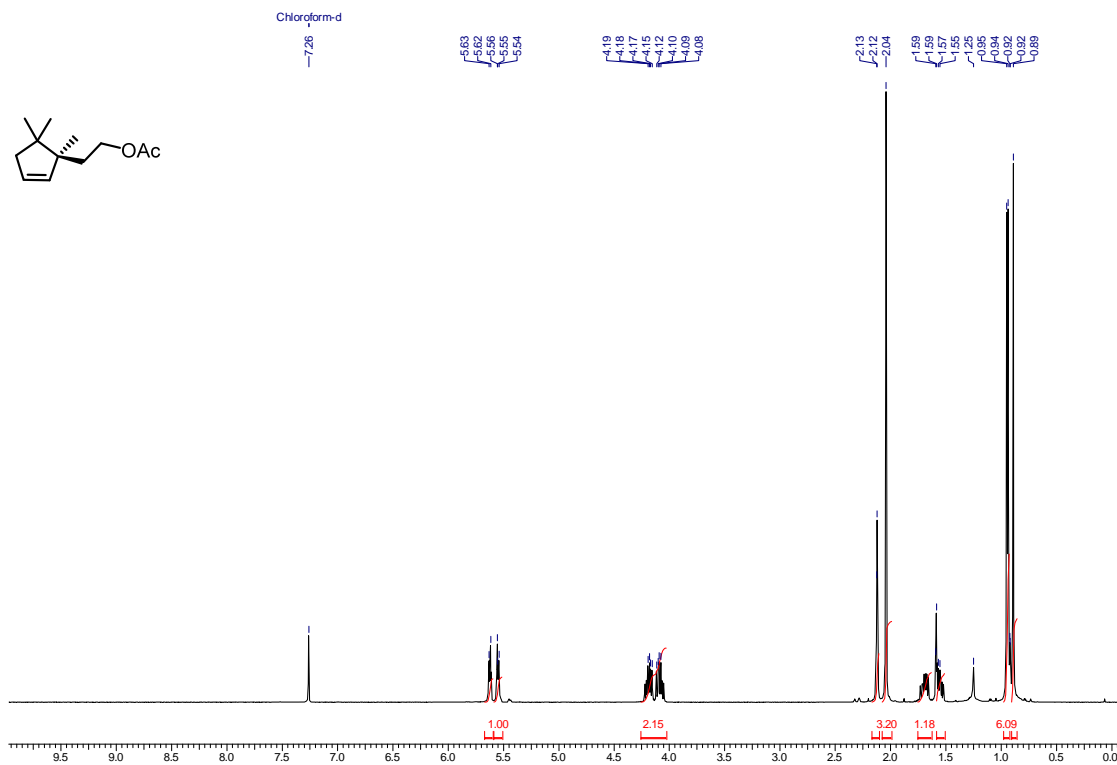
Figure 2.20. ^{1}H NMR spectra of **(S)-2** (400 MHz, CDCl$_3$)
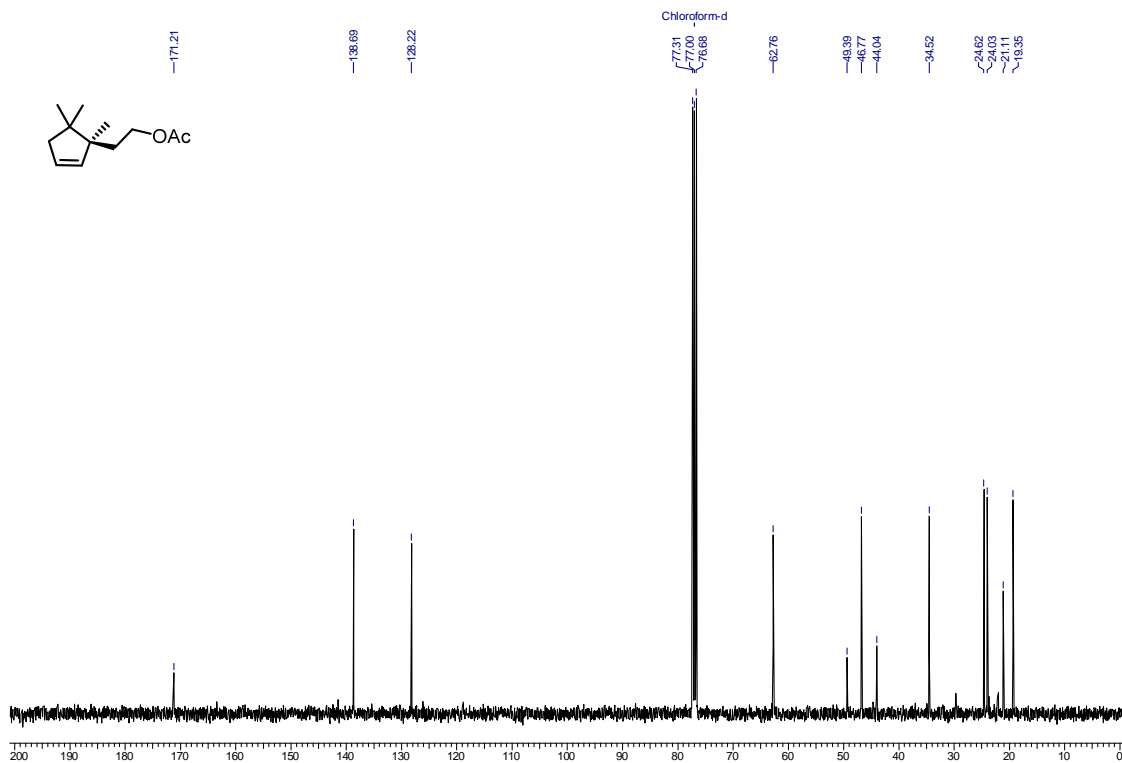
Figure 2.21. ^{13}C NMR spectra of **(S)-2** (100 MHz, CDCl$_3$)
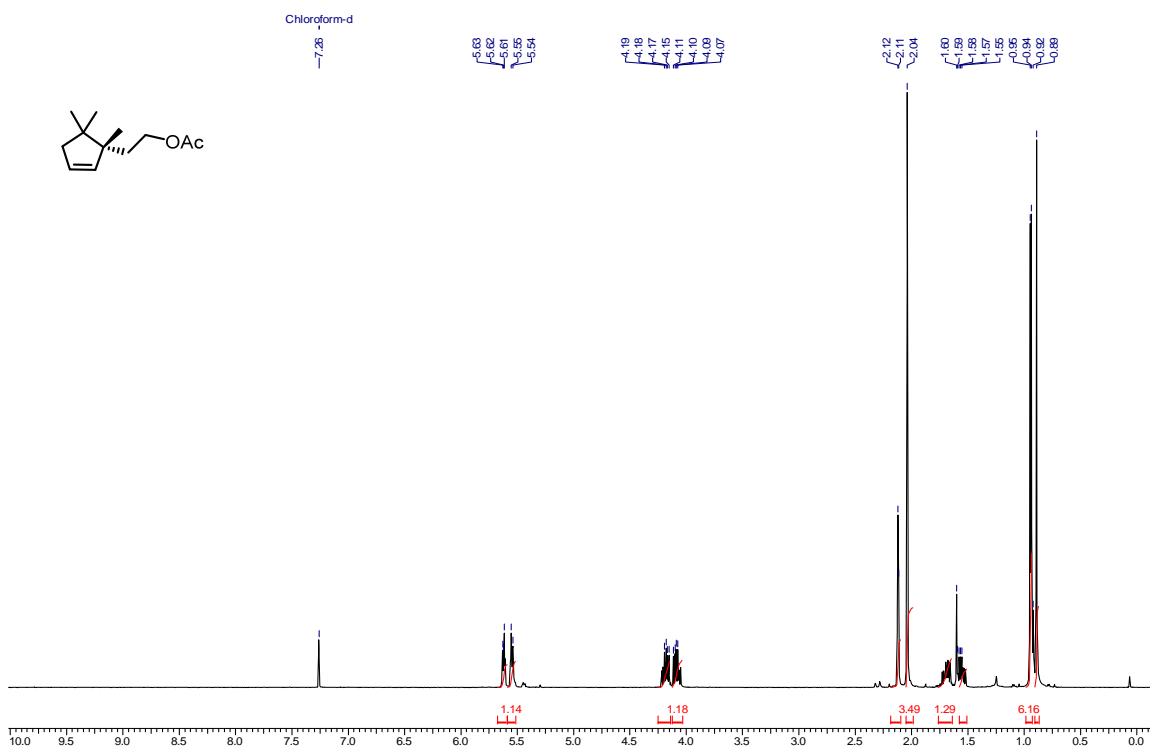
Figure 2.22. ^{1}H NMR spectra of **(R)-2** (CDCl$_3$, 400 MHz)
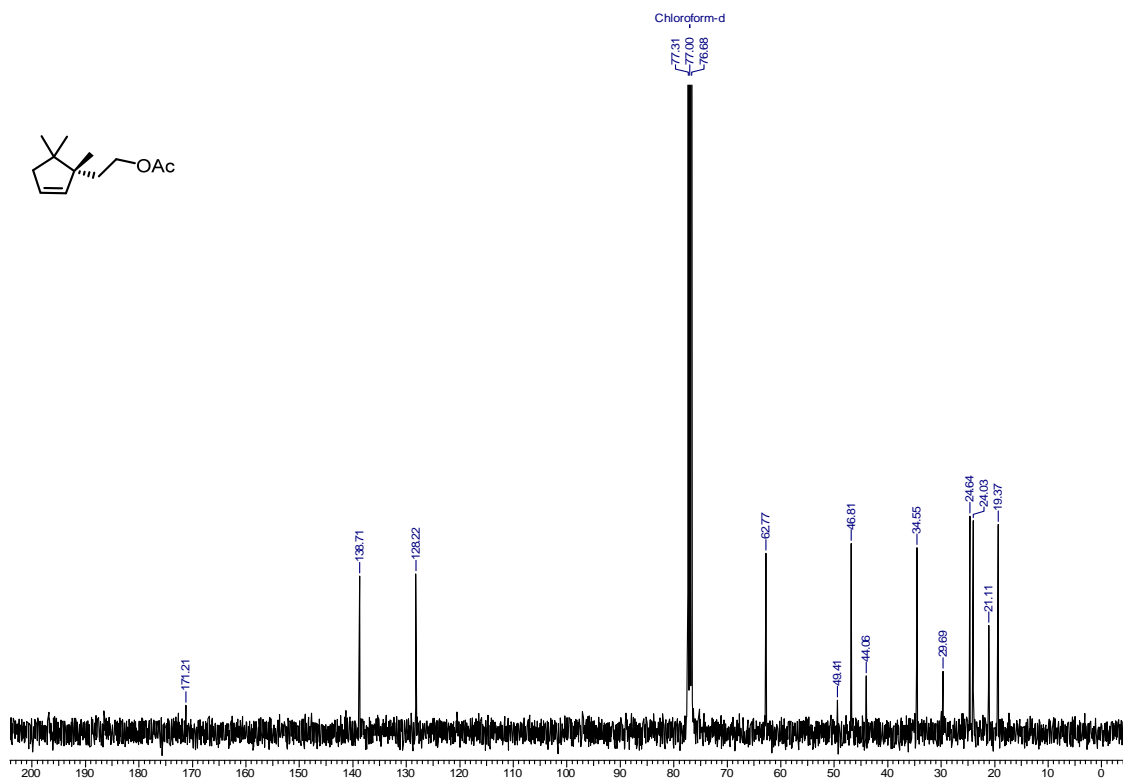
Figure 2.23. ^{13}C NMR spectra of **(R)-2** (CDCl$_3$, 100 MHz)
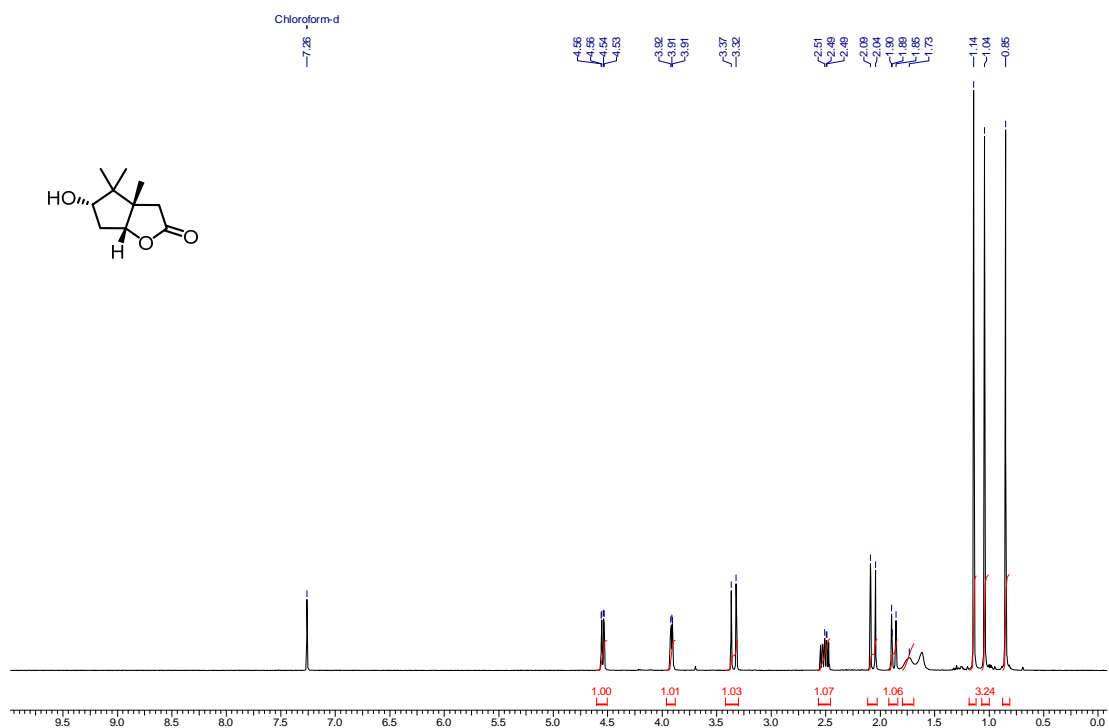
Figure 2.24. ^{1}H NMR spectra of **(-)-48** (CDCl$_3$, 400 MHz)
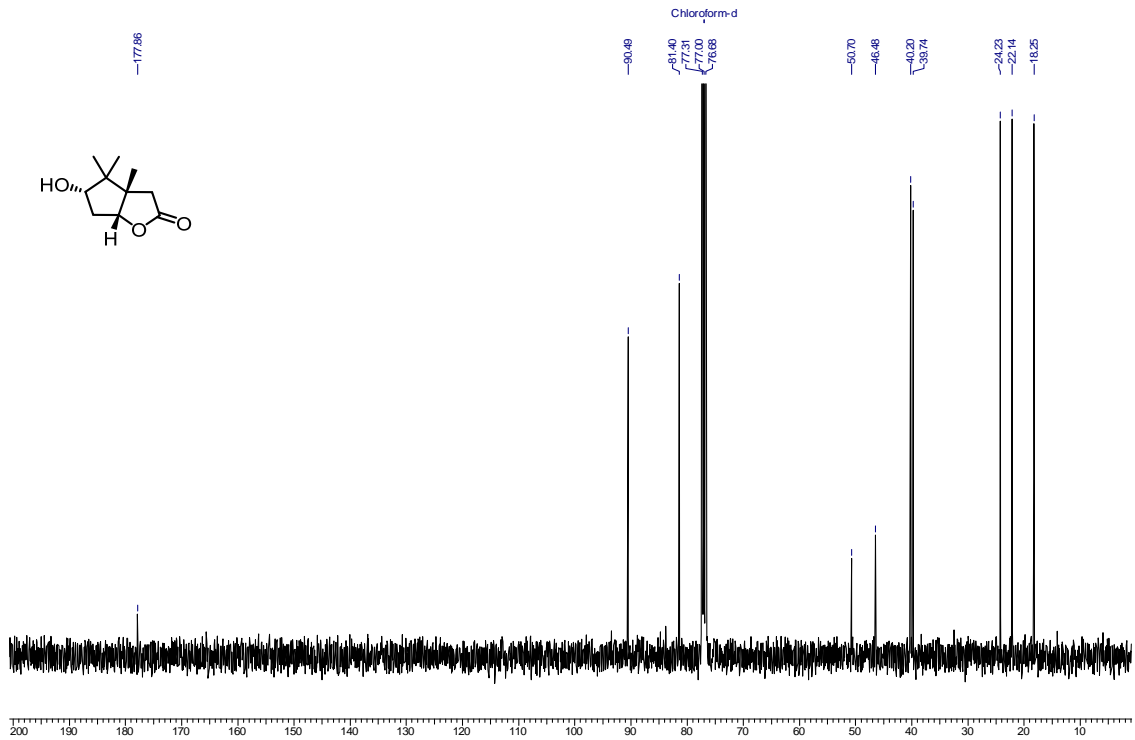
Figure 2.25. ^{13}C NMR spectra of **(-)-48** (CDCl$_3$, 100 MHz)
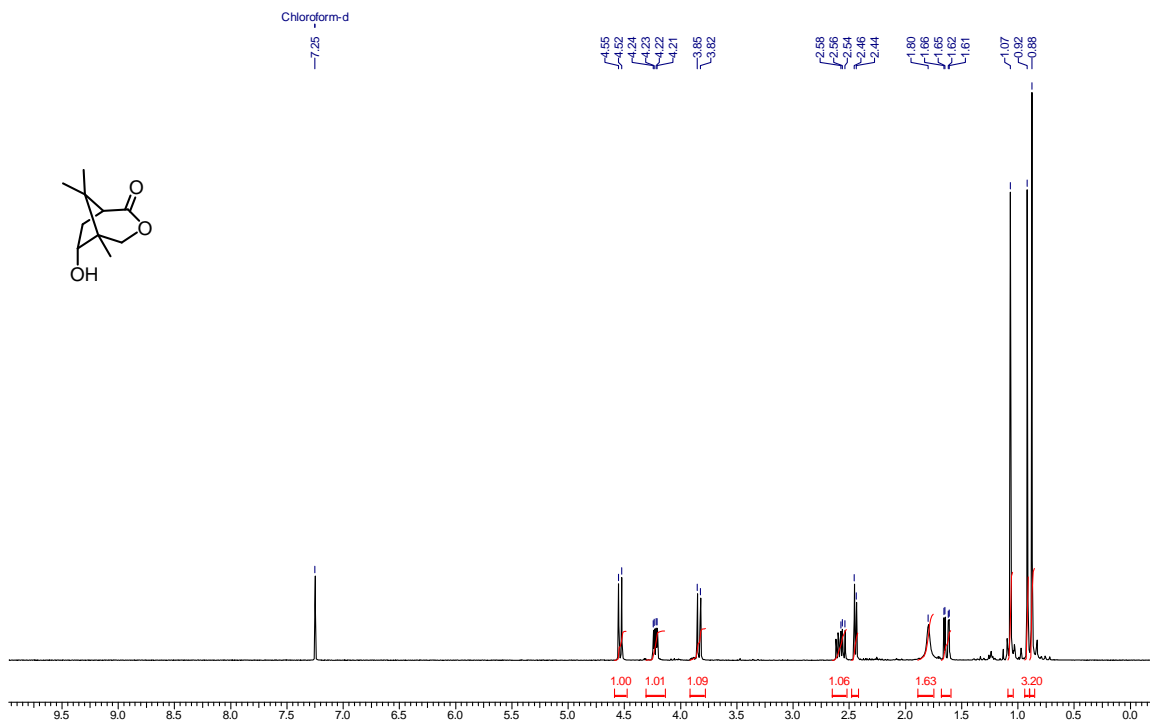
Figure 2.26. ^{1}H NMR spectra of **38'** (CDCl$_3$, 400 MHz)
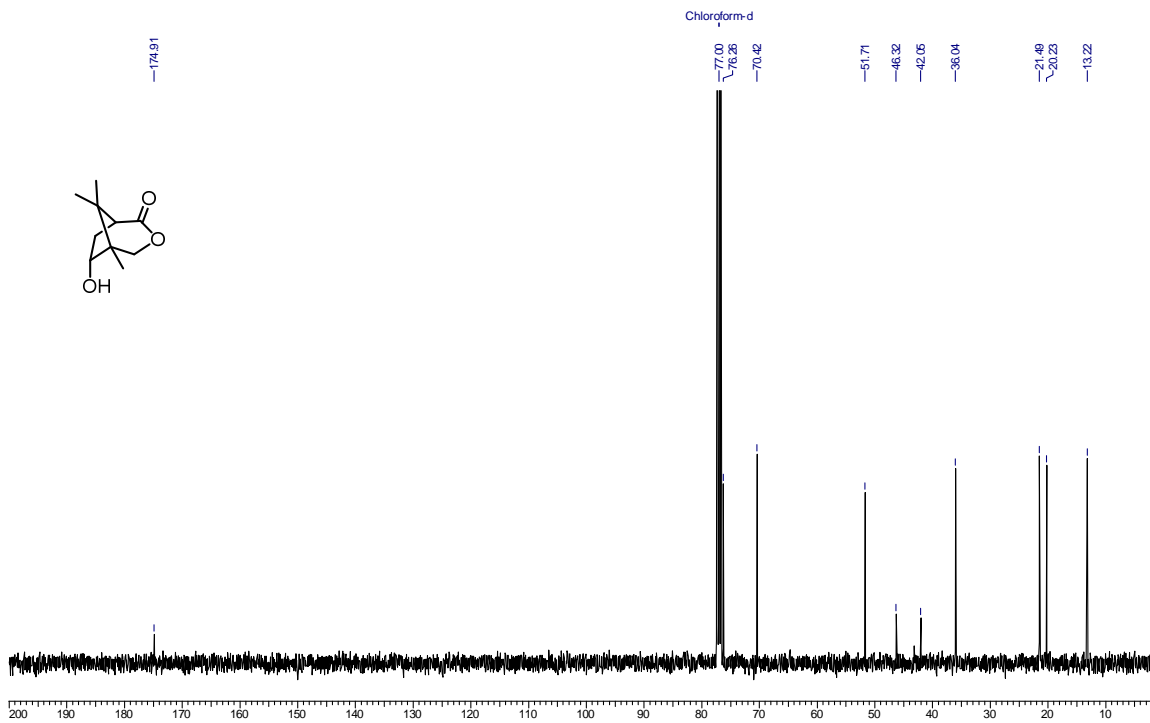
Figure 2.27. ^{13}C NMR spectra of **38'** (CDCl$_3$, 100 MHz)
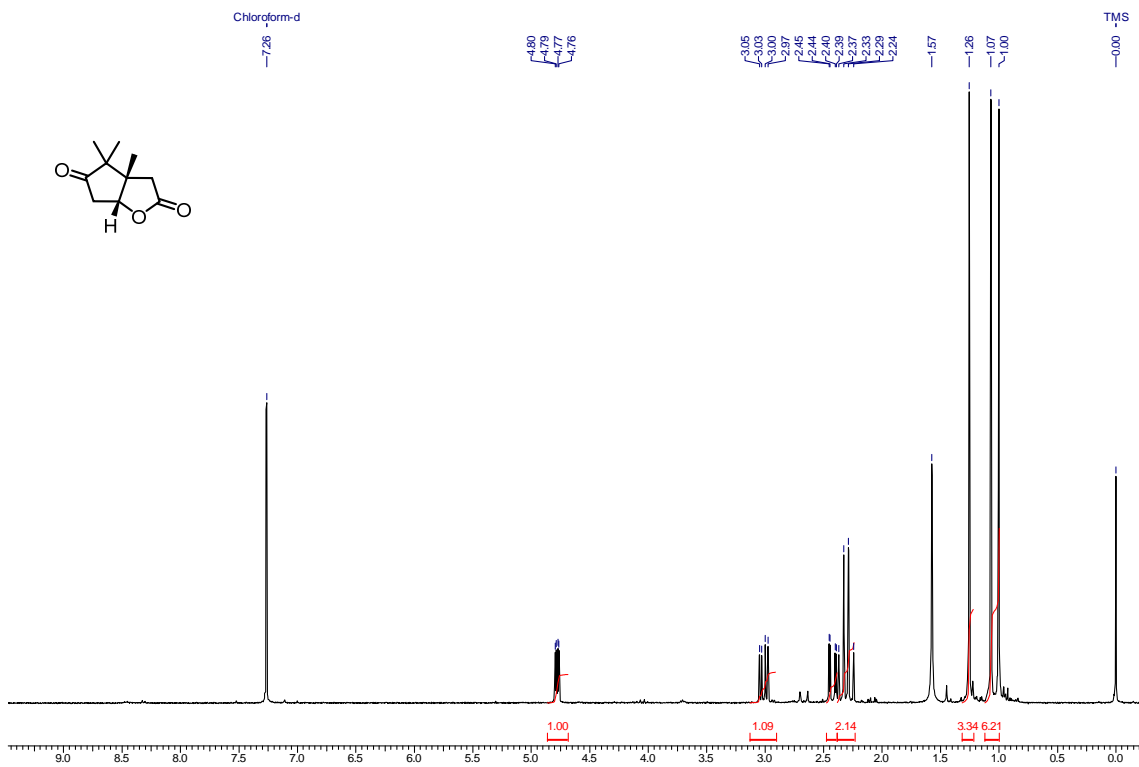
Figure 2.28. ^{1}H NMR spectra of **(-)-49** (CDCl$_3$, 400 MHz)
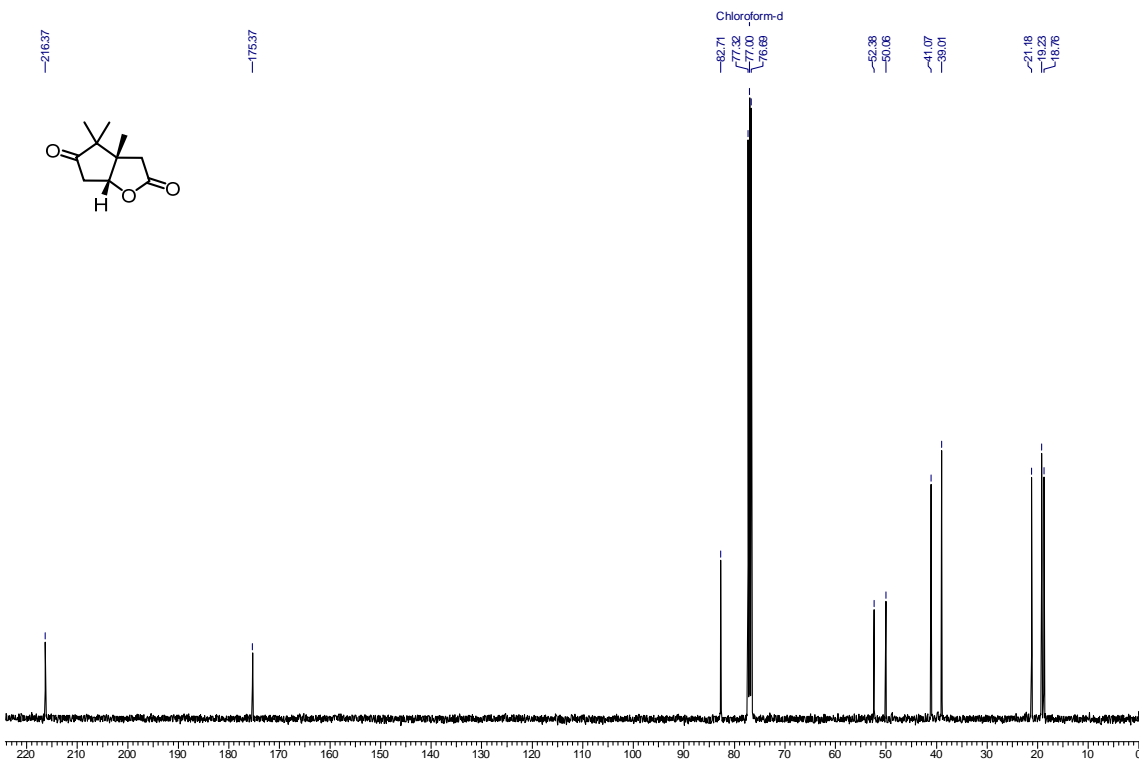
Figure 2.29. ^{13}C NMR spectra of **(-)-49** (CDCl$_3$, 100 MHz)

Figure 2.30. ^{1}H NMR spectra of **(-)-50** (CDCl$_3$, 500 MHz)

Figure 2.31. ^{13}C NMR spectra of **(-)-50** (CDCl$_3$, 125 MHz)

234

Figure 2.32. ^{1}H NMR spectra of revised **41** (CDCl$_3$, 400 MHz)

Figure 2.33. ^{13}C NMR spectra of revised **41** (CDCl$_3$, 100 MHz)
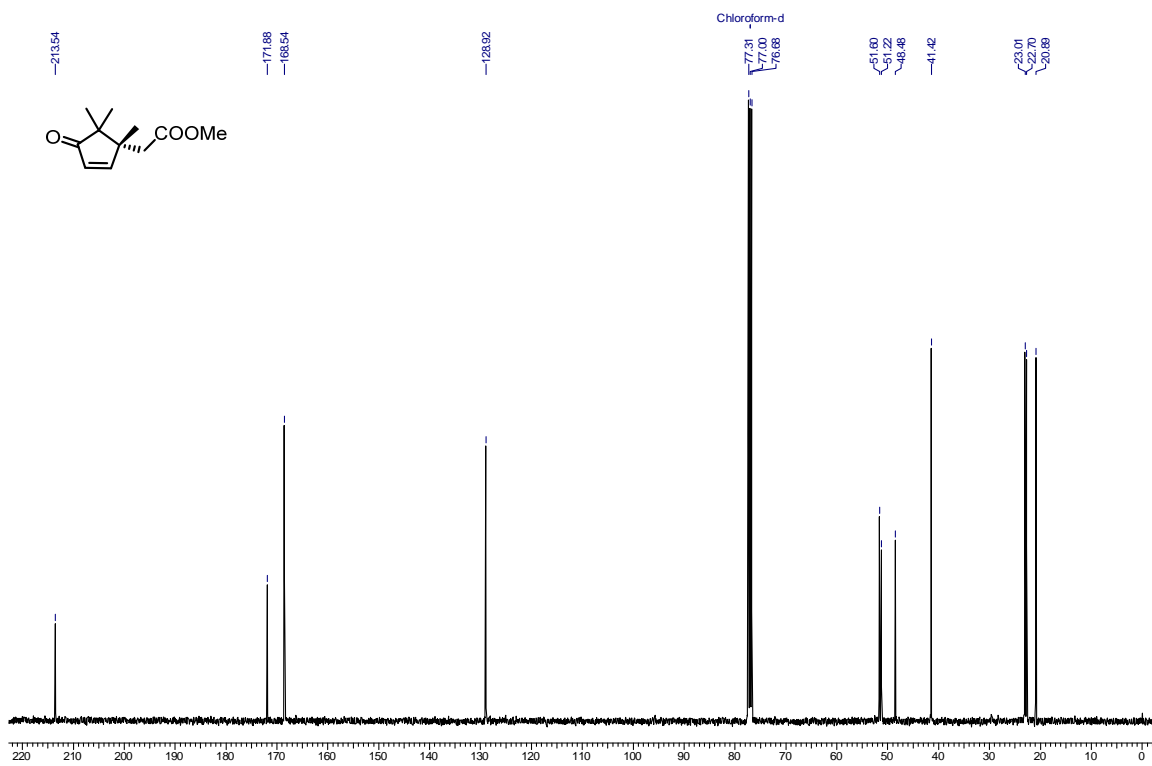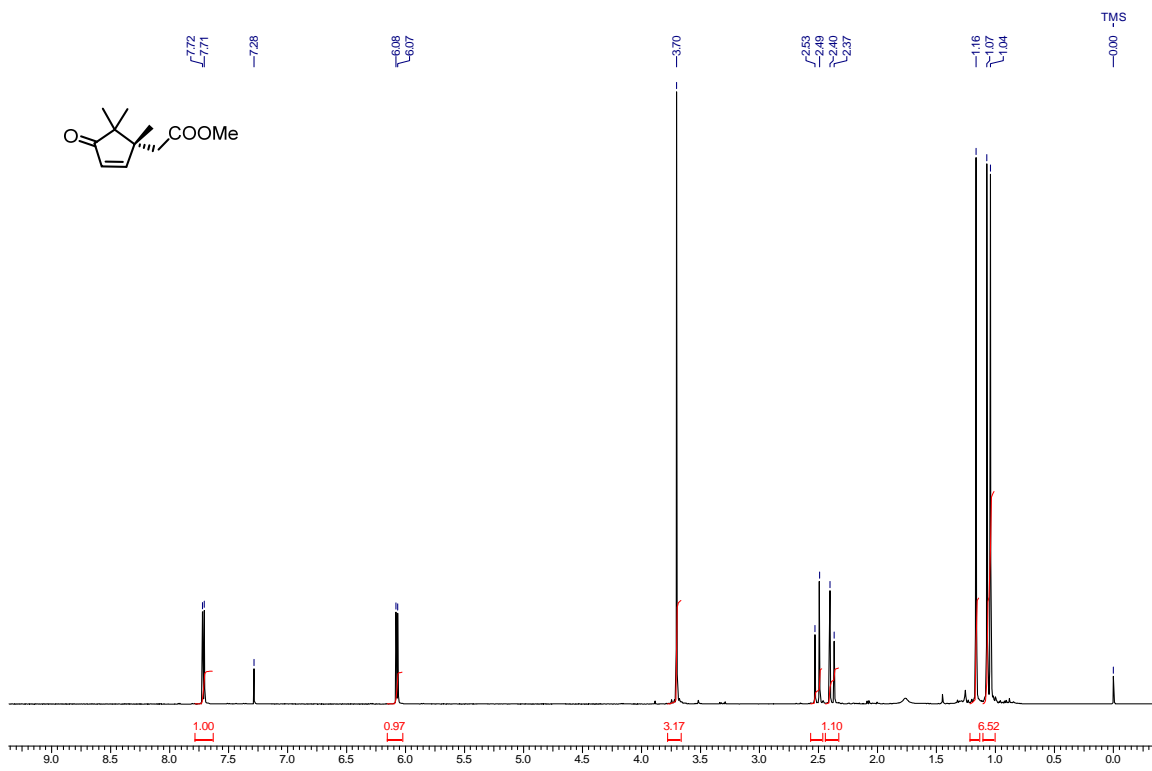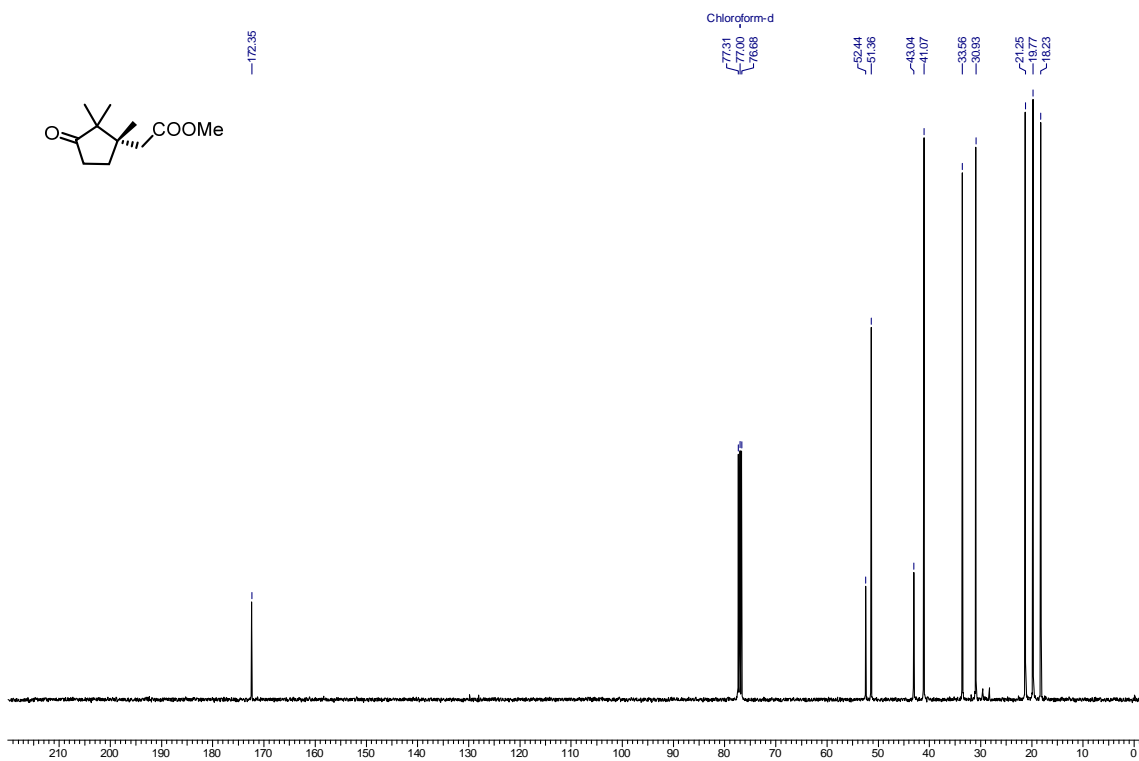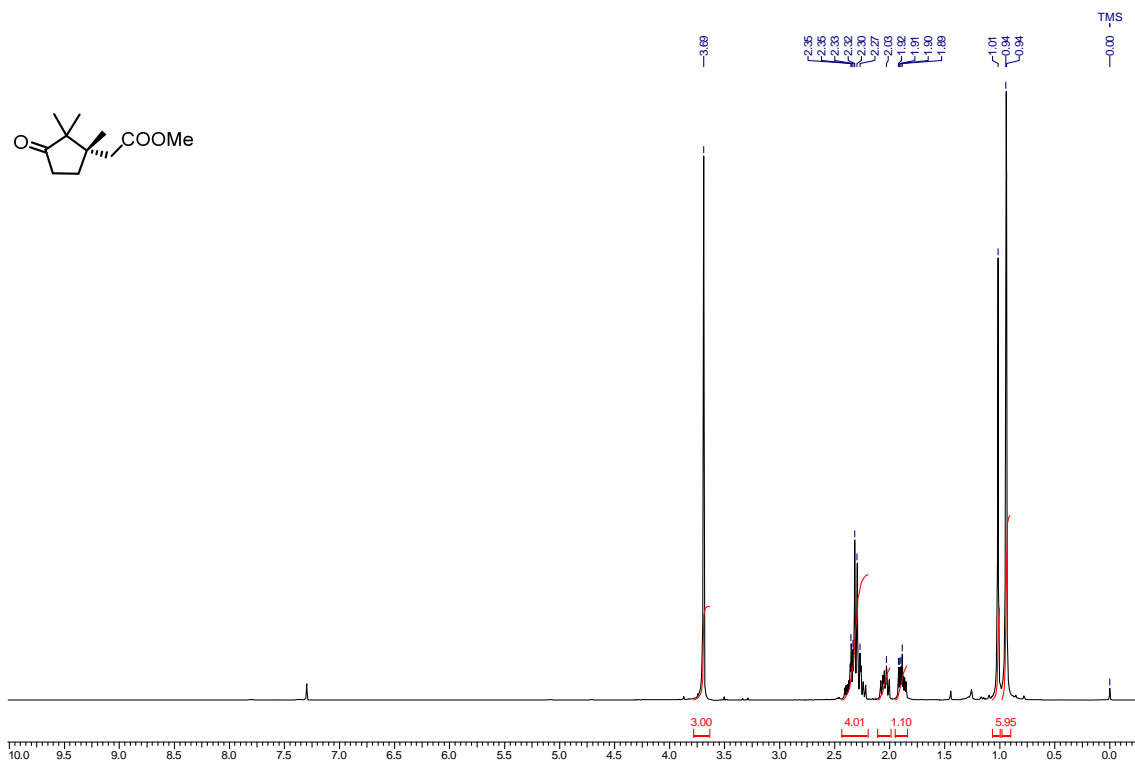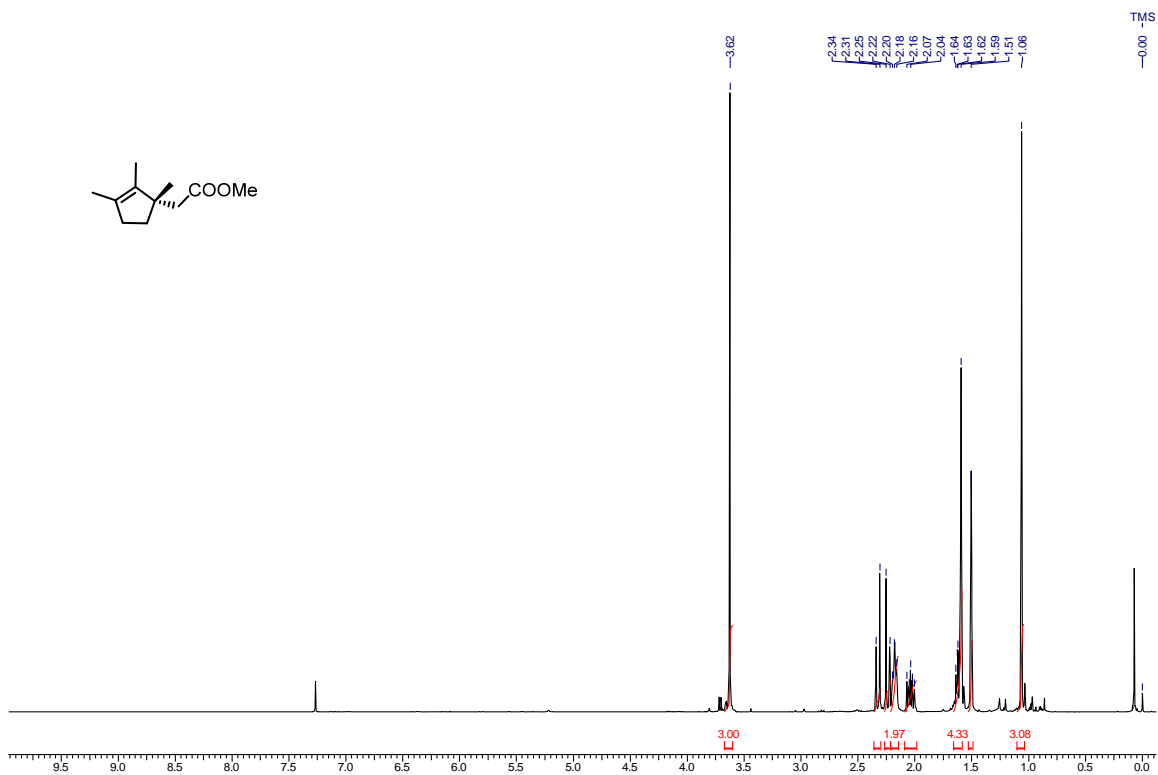
Figure 2.34. ^{1}H NMR spectra of **46** (CDCl$_3$, 400 MHz)
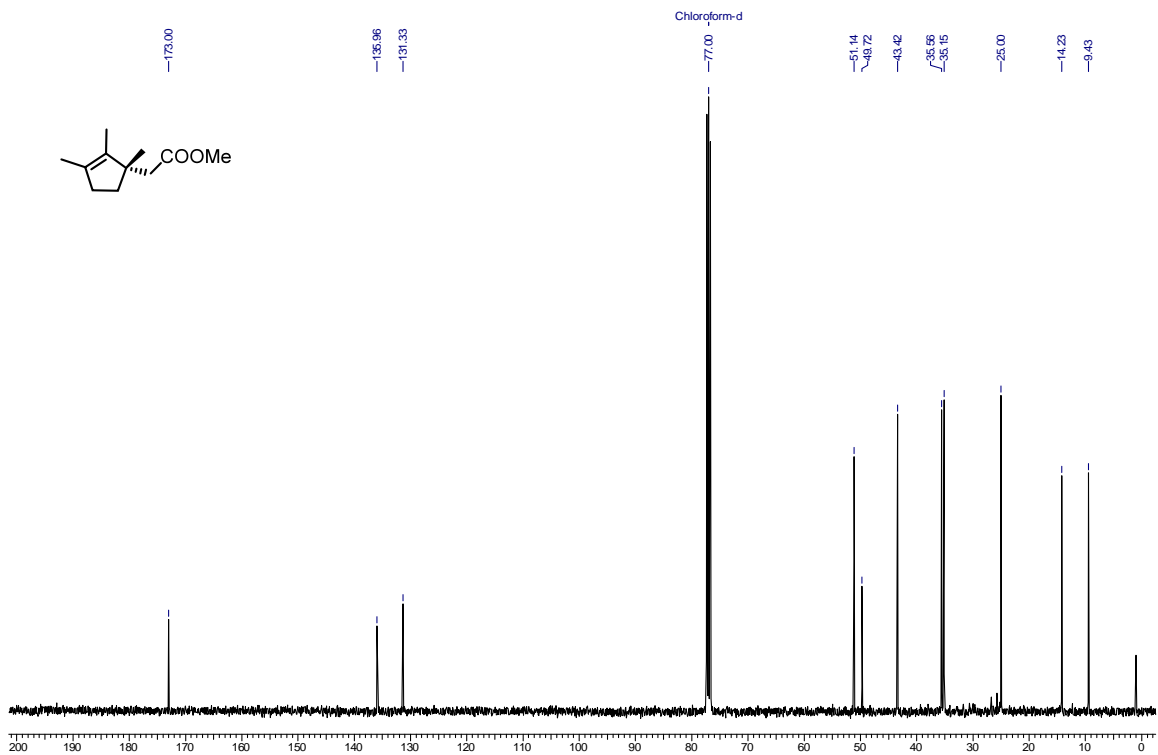
Figure 2.35. ^{13}C NMR spectra of **46** (CDCl$_3$, 100 MHz)
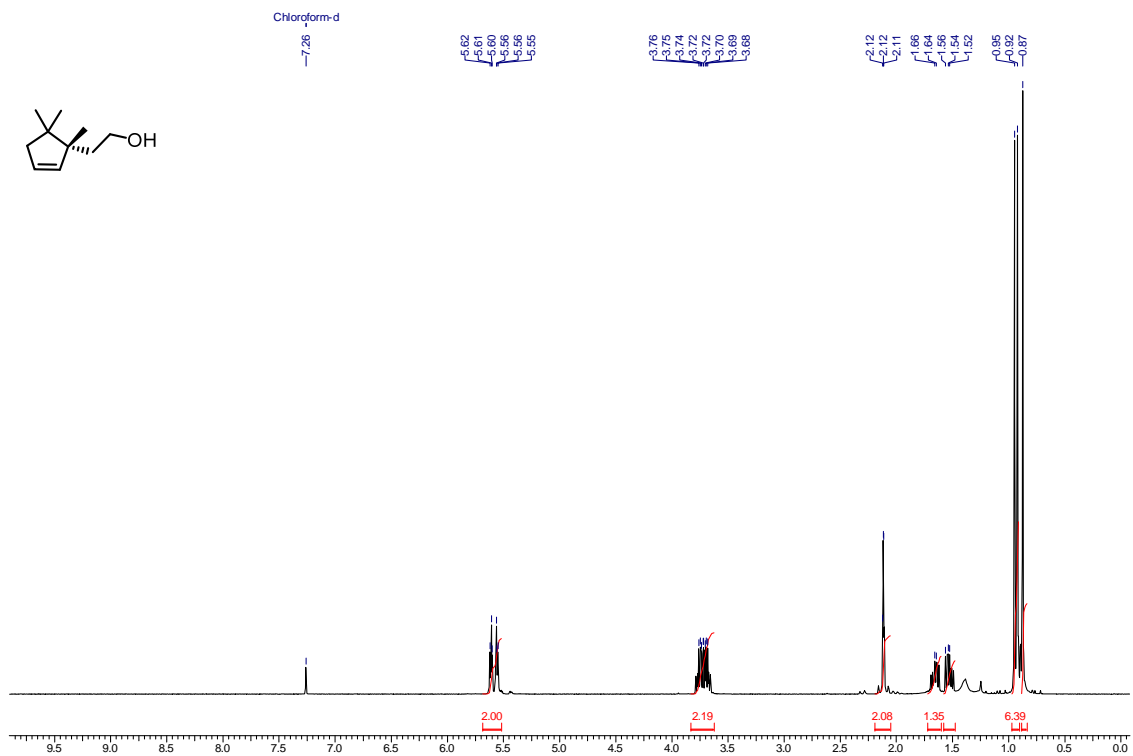
Figure 2.36. ^{1}H NMR spectra of **(-)-12** (CDCl$_3$, 400 MHz)
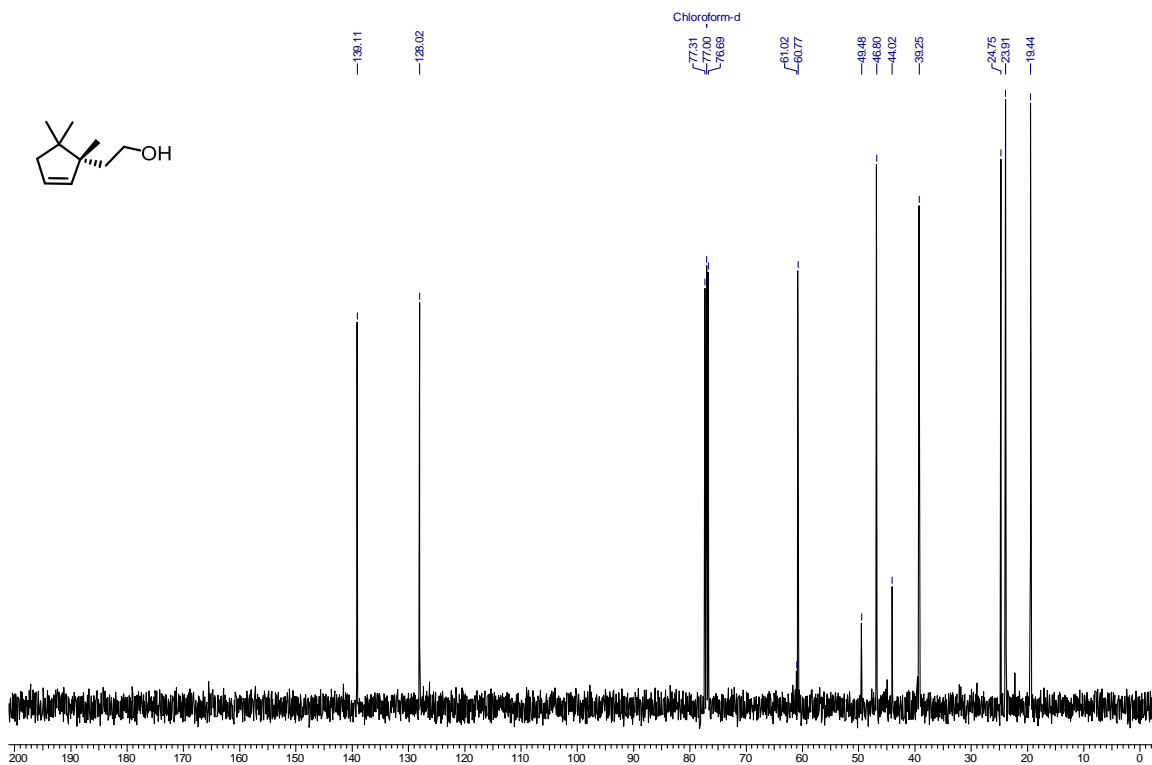
Figure 2.37. ^{13}C NMR spectra of **(-)-12** (CDCl$_3$, 100 MHz)
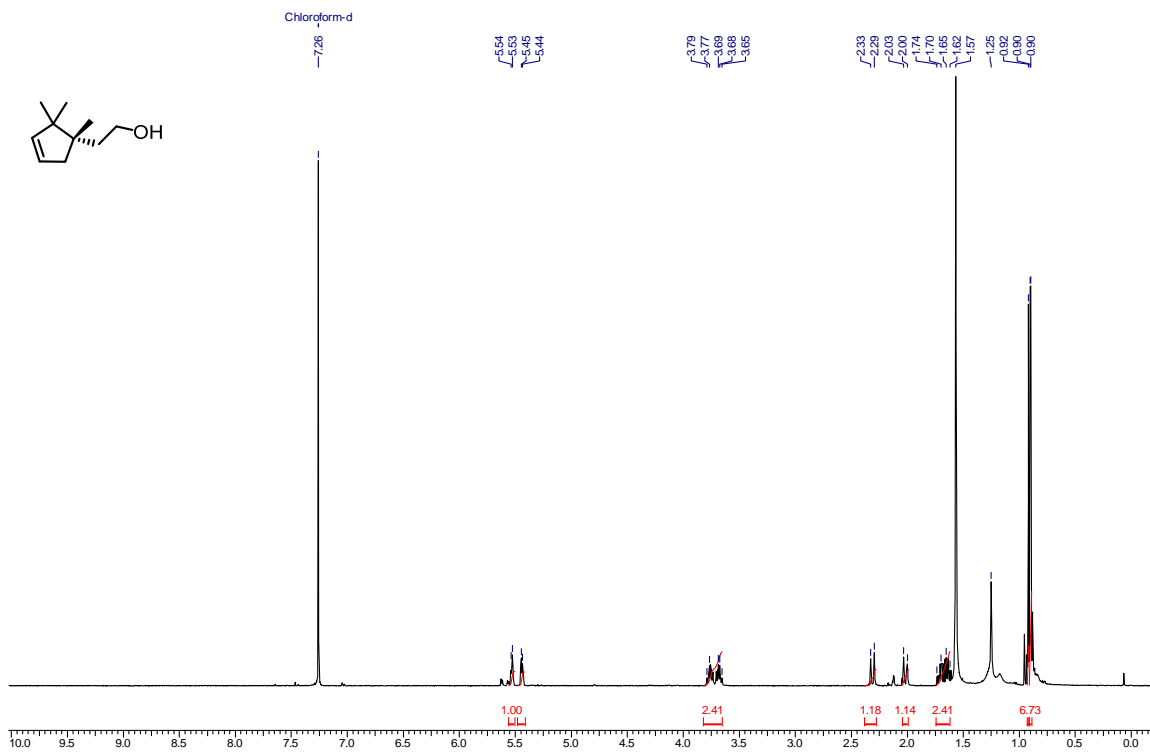
Figure 2.38. ^{1}H NMR spectra of **(+)-12a** (CDCl$_3$, 400 MHz)
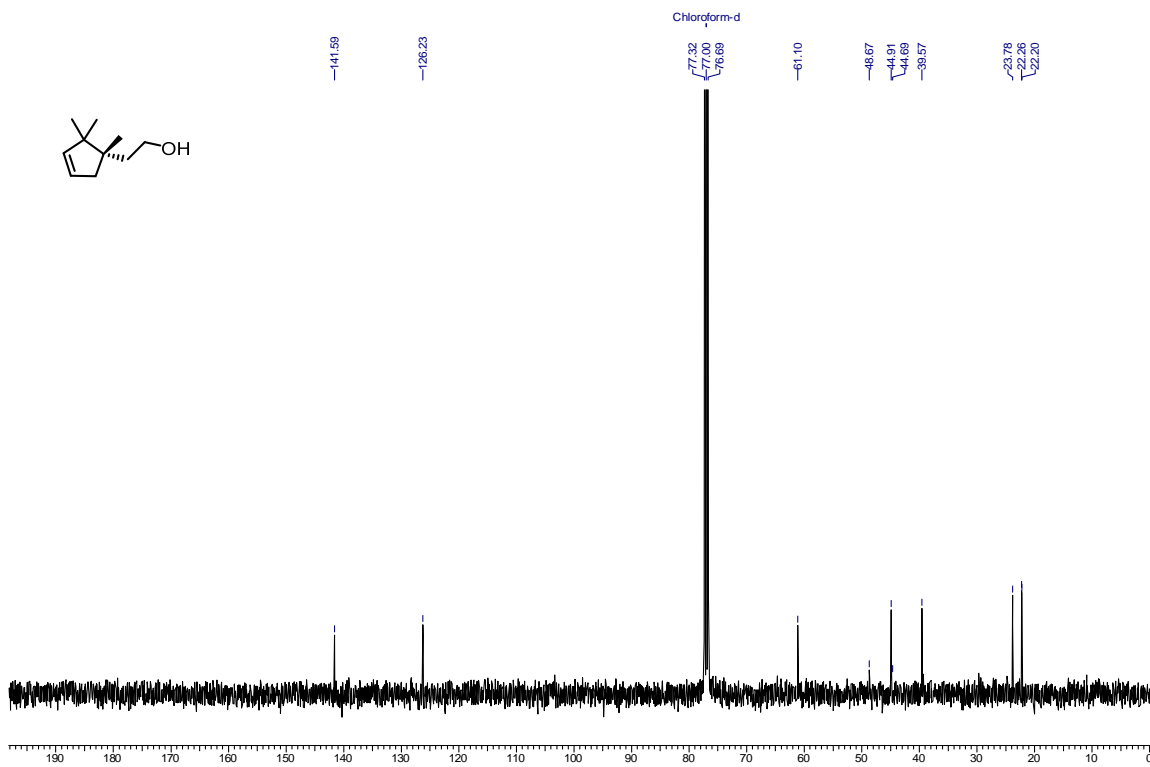
Figure 2.39. ^{13}C NMR spectra of **(+)-12a** (CDCl$_3$, 100 MHz)
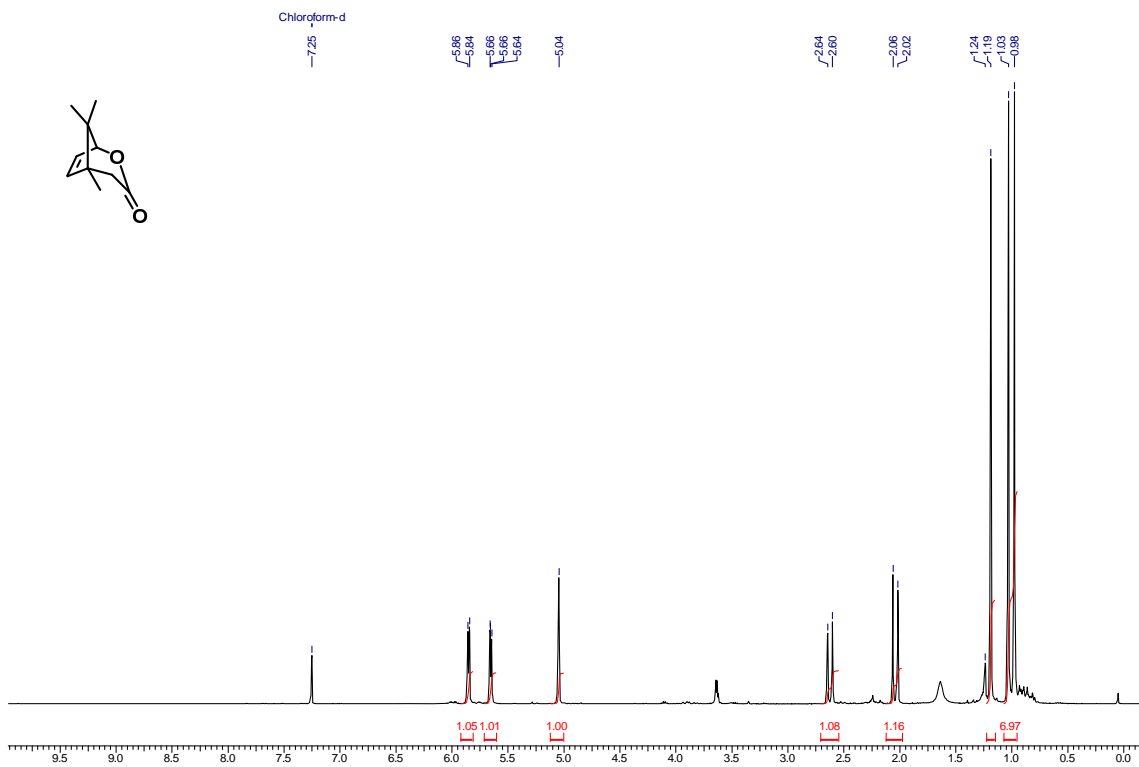
Figure 2.40. ^{1}H NMR spectra of **52** (CDCl$_3$, 400 MHz)
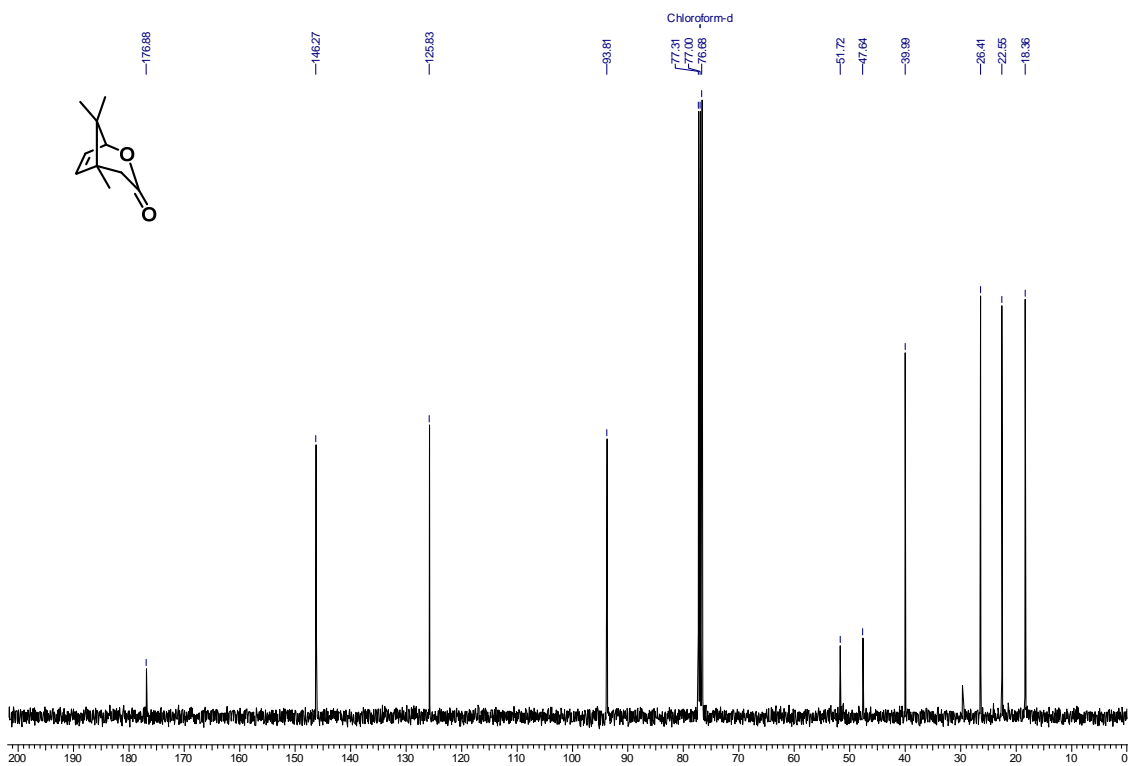
Figure 2.41. ^{13}C NMR spectra of **52** (CDCl$_3$, 100 MHz)

239
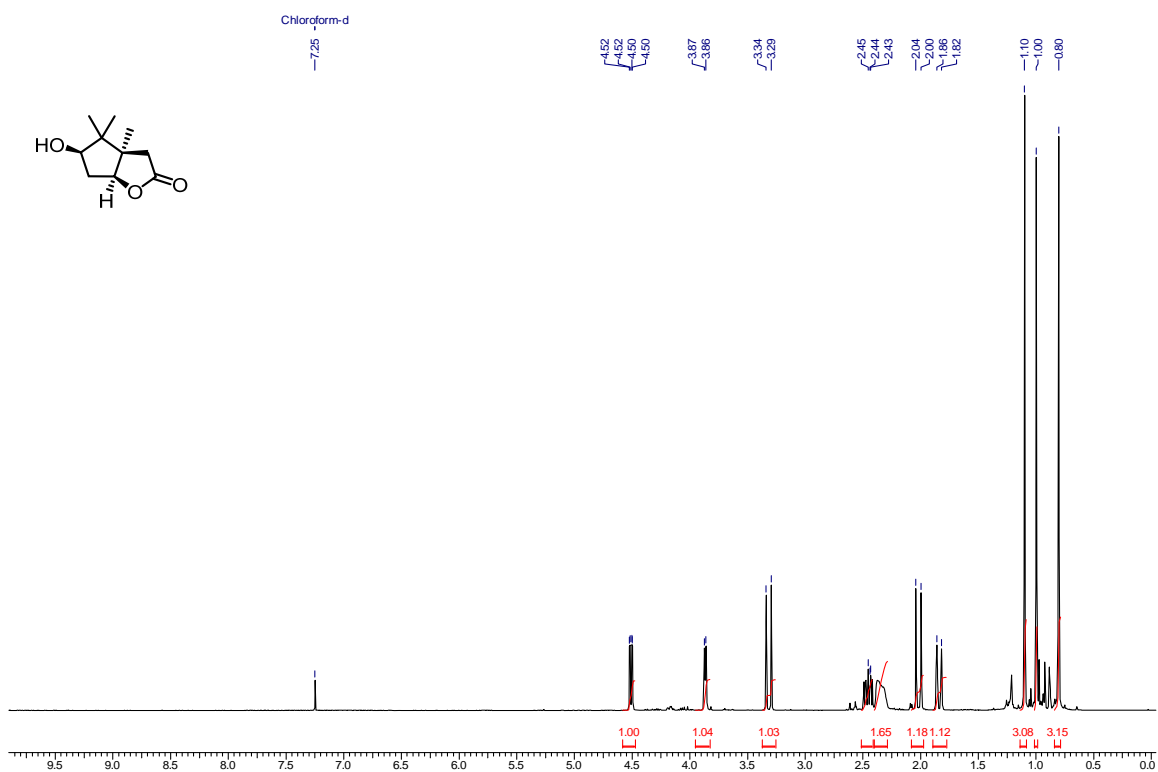
Figure 2.42. ^{1}H NMR spectra of **(+)-48** (CDCl$_3$, 400 MHz)
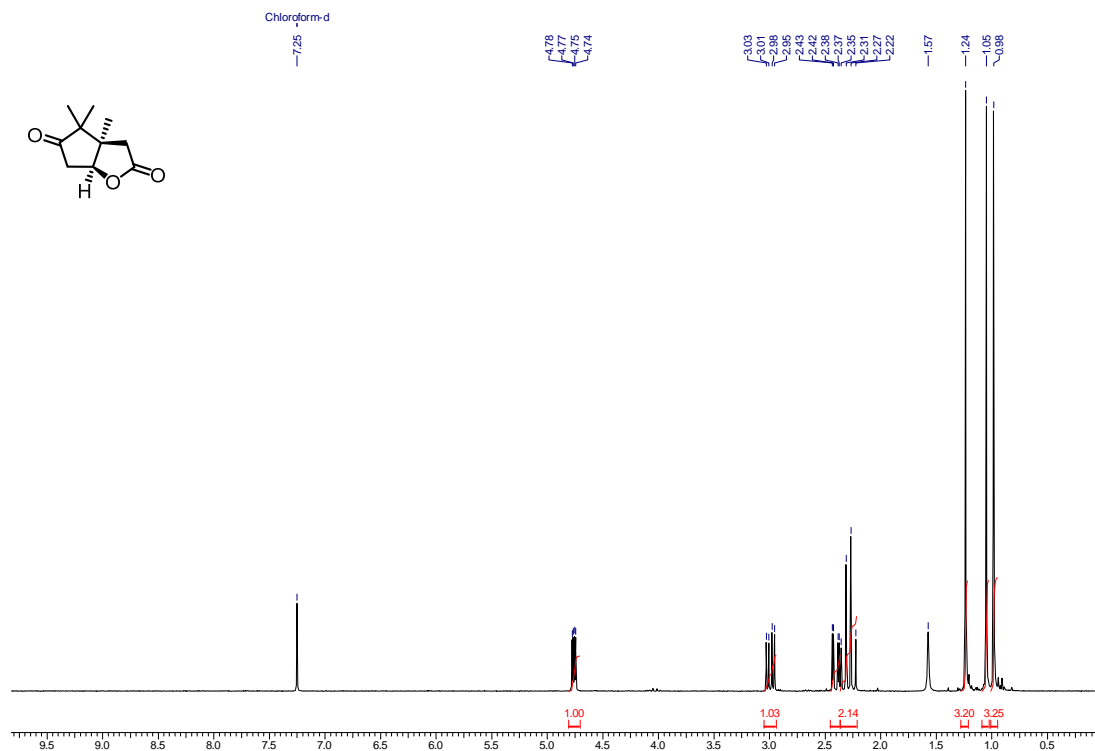
Figure 2.43. ^{1}H NMR spectra of **(+)-49** (CDCl$_3$, 400 MHz)
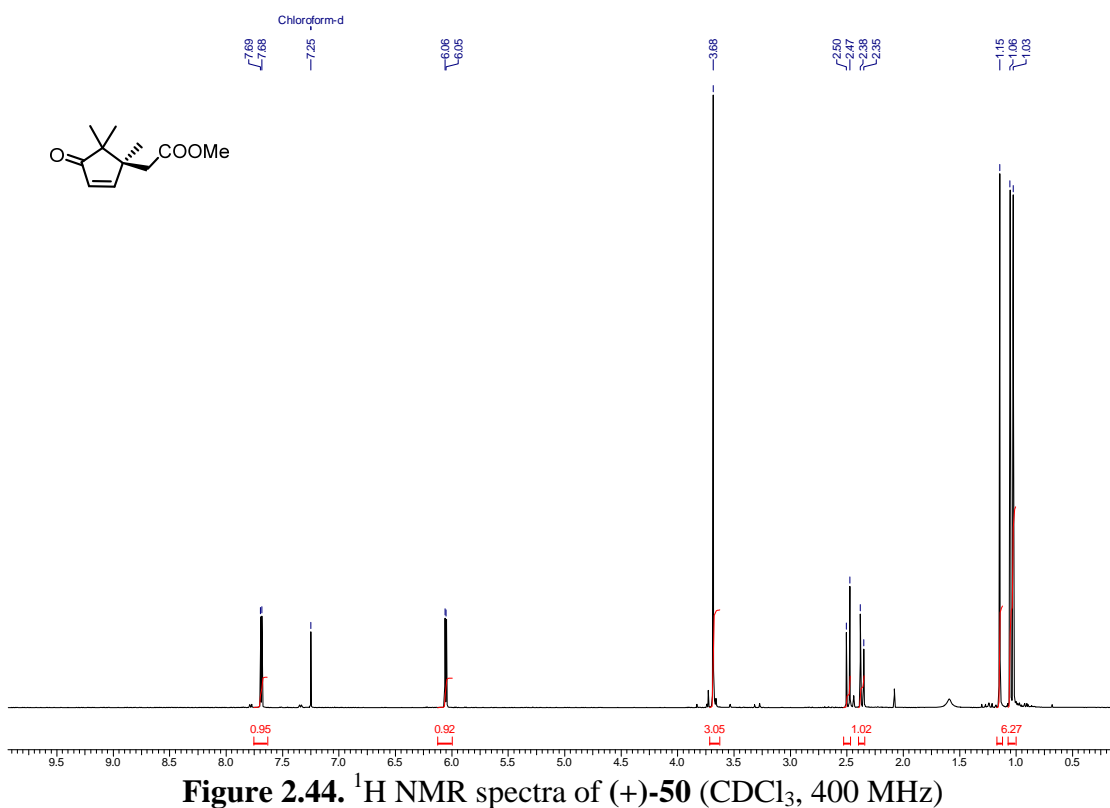
Figure 2.44. ^{1}H NMR spectra of **(+)-50** (CDCl$_3$, 400 MHz)
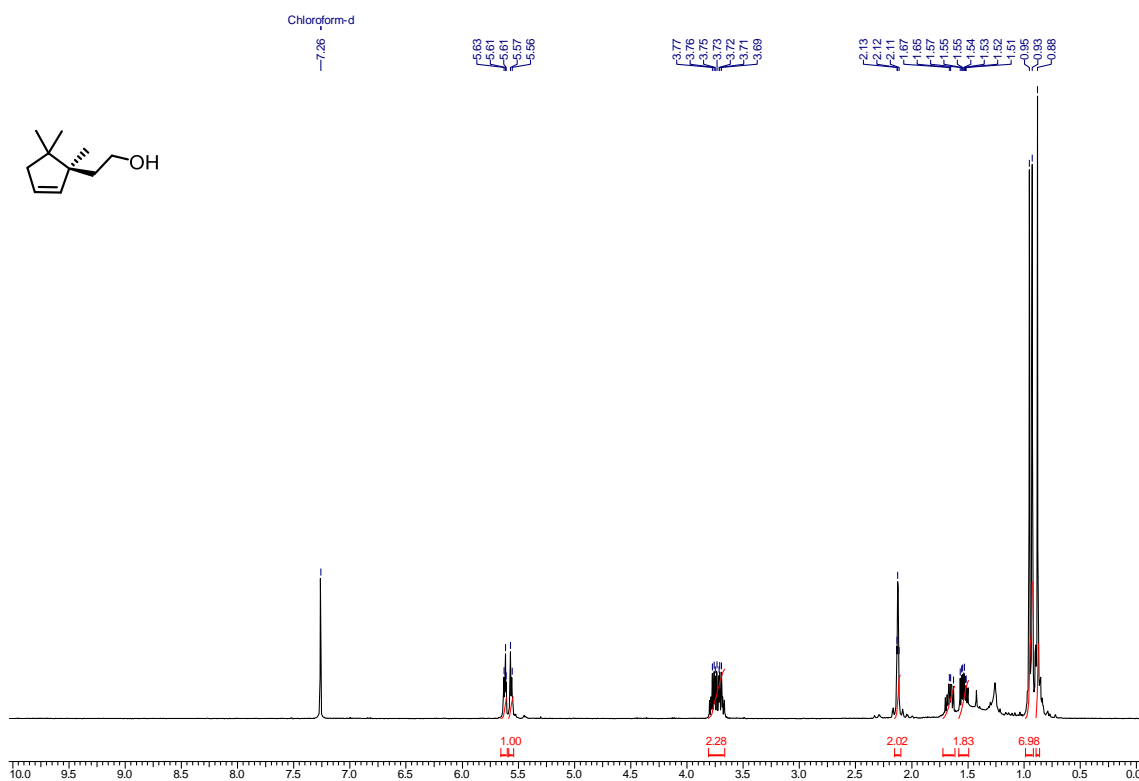
Figure 2.45. ^{1}H NMR spectra of **(+)-12** (CDCl$_3$, 400 MHz)
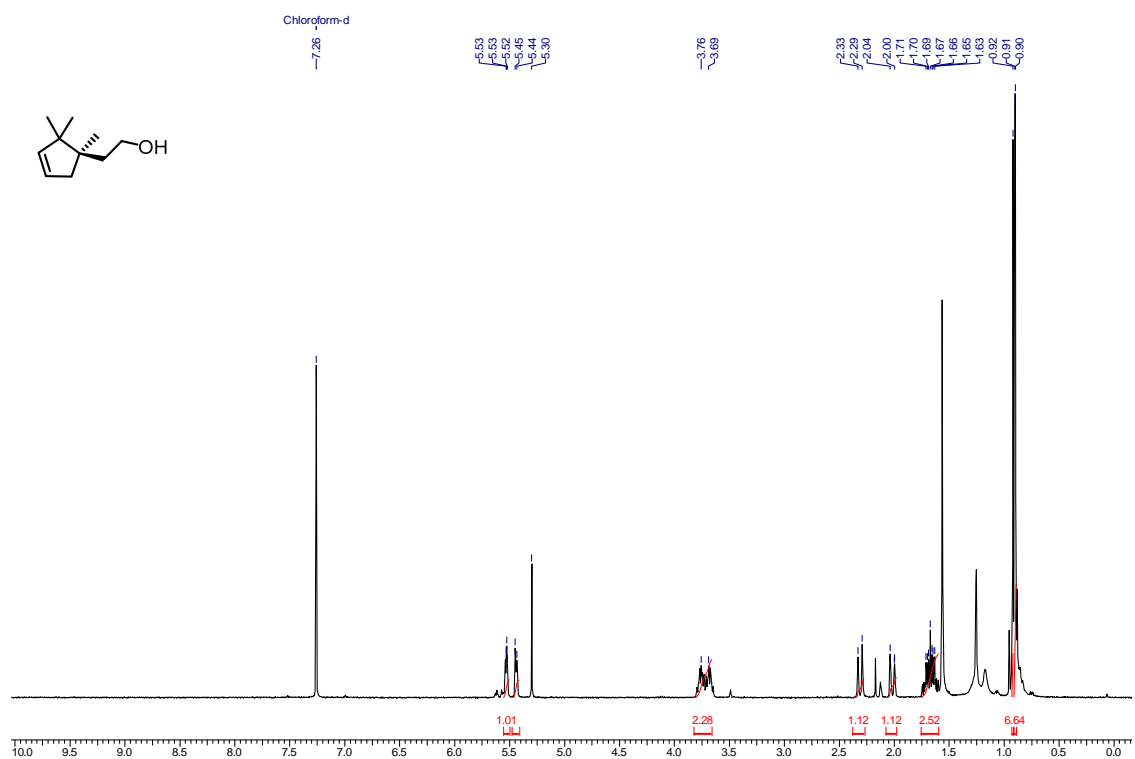
Figure 2.46. ^{1}H NMR spectra of **(-)-12a** (CDCl$_3$, 400 MHz)

List of publications

1. Syntheses and determination of absolute configurations and biological activities of the enantiomers of the longtailed mealybug pheromone. **Remya Ramesh**, Pandrangi Siva Swaroop, Rajesh G. Gonnade, Choppari Thirupathi, Rebeccah A. Waterworth, Jocelyn G. Millar, and D. Srinivasa Reddy*, *J. Org. Chem.* **2013**, *78*, 6281-6284.

2. Zinc mediated allylations of chlorosilanes promoted by ultrasound: Synthesis of novel constrained sila amino acids. **Remya Ramesh**, and D. Srinivasa Reddy*, *Org. Biomol. Chem.* **2014**, *12*, 4093-4097.

3. Enantiospecific synthesis of both enantiomers of the longtailed mealybug pheromone and their evaluation in a New Zealand vineyard. **Remya Ramesh**, Vaughn Bell, Andrew M. Twidle, Rajesh Gonnade, and D. Srinivasa Reddy*, *J. Org. Chem.* **2015**, *80*, 7785-7789.

4. Design, synthesis, and identification of silicon incorporated oxazolidinone antibiotics with improved brain exposure. B. Seetharamsingh, **Remya Ramesh**, Santoshkumar S. Dange, Pankaj V. Khairnar, Smita Singhal, Dilip Upadhyay, Sridhar Veeraraghavan, Srikant Viswanadha, Swaroop Vakkalanka, and D. Srinivasa Reddy*, *ACS Med. Chem. Lett.* **2015**, *6*, 1105-1110.

5. Silicon incorporated morpholine antifungals: Design, synthesis, and biological evaluation. Gorakhnath R. Jachak, **Remya Ramesh**, Duhita G. Sant, Shweta U. Jorwekar, Manjusha R. Jadhav, Santosh G. Tupe, Mukund V. Deshpande, and D. Srinivasa Reddy*, *ACS Med. Chem. Lett.* **2015**, *6*, 1111-1116.

6. Repurposing of a known drug scaffold: Identification of novel sila analogues of rimonabant as potent antitubercular agents. **Remya Ramesh**, Rahul Shingare, Vinod Kumar, Amitesh Anand, Swetha B, Sridhar Veeraraghavan, Srikant Viswanadha, Ramesh Ummanni, Rajesh Gokhale, and D. Srinivasa Reddy*, *Eur. J. Med. Chem.* **2016**, *122*, 723-730.

List of published patents

1. Sila analogs of oxazolidinone derivatives and synthesis thereof. Dumbala Srinivasa Reddy, B. Seetharamsingh, **Remya Ramesh**, *WO 2013/054275*; *US 2014/0296133 A1*; *EP2766373A1*

2. Cyclic aza-sila compounds as insect repellents. Dumbala Srinivasa Reddy, **Remya Ramesh**, B. Seetharamsingh, *WO 2014/097322 A1*; *US20150342191*

3. Antitubercular compounds and process for the preparation thereof. Dumbala Srinivasa Reddy, **Remya Ramesh**, *WO 2014/128724 A1*

4. Novel pyrazole derivatives with silicon incorporation. Dumbala Srinivasa Reddy, **Remya Ramesh**, Rahul Dilip Shingare, *WO 2014/181357 A1*

5. Novel pyrrole derivatives with silicon incorporation. Dumbala Srinivasa Reddy, Vasudevan Natarajan, Sachin Bhausaheb Wagh, **Remya Ramesh**, *WO 2014/195970 A1*

6. Silicon based fungicides and process for producing the same. Dumbala Srinivasa Reddy, Gorakhnath Rajaram Jachak, **Remya Ramesh**, Santosh Genba Tupe, Mukund Vinayak Deshpande, *WO 2015/102025 A1*

Publications

Syntheses and Determination of Absolute Configurations and Biological Activities of the Enantiomers of the Longtailed Mealybug Pheromone

Remya Ramesh,[†] Pandrangi Siva Swaroop,[†] Rajesh G. Gonnade,[†] Choppari Thirupathi,[‡] Rebeccah A. Waterworth,[§] Jocelyn G. Millar,[§] and D. Srinivasa Reddy*,[†]

[†]CSIR-National Chemical Laboratory, Dr. Homi Bhabha Road, Pune, 411008, India
[‡]Daicel Chiral Technologies (India) Pvt. Ltd., Hyderabad 500078, India
[§]Department of Entomology, University of California, Riverside California 92521, United States

Ⓢ *Supporting Information*

ABSTRACT: Preparation and assignment of absolute configurations to both enantiomers of the sex pheromone of the longtailed mealybug, an irregular monoterpenoid with extraordinary biological activity, has been completed. Comparison of the biological activities of both enantiomers and the

(S)-pheromone   *(R)*-pheromone

Highlights:
- Access to both enantiomers for the first time
- Harada's CSP-based enantioresolution
- Determination of absolute configurations
- Biological activities of both enantiomers

racemate in field trials showed that the (S)-(+)-enantiomer was highly attractive to male mealybugs, strongly suggesting that female longtailed mealybugs produce this enantiomer. The (R)-(−)-enantiomer was benign, being neither attractive nor inhibitory.
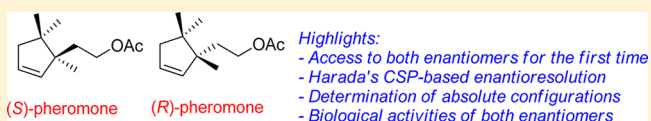
The longtailed mealybug *Pseudococcus longispinus* (Order Hemiptera: Family Pseudococcidae), is one of a group of small sucking insects that are widely distributed pests of agricultural crops and ornamental plants. Damage is caused by direct feeding, by the growth of sooty mold and other fungi on the honeydew excreted by the insects, and increasingly, through the transmission of plant pathogens.[1] Females of sexually reproducing mealybug species have been shown to produce powerful sex pheromones to attract males for mating, and some of these pheromones have been identified and commercialized for use in pest management.[2] In addition to their practical value, the structures of mealybug pheromones are intrinsically interesting because of their irregular terpenoid skeletons (Figure 1).[3]
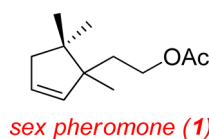
sex pheromone (1)

Figure 1. Gross structure of the sex pheromone of the longtailed mealybug.

The pheromone of the longtailed mealybug was identified after collection of headspace odors produced by thousands of live unmated females over many weeks. Isolation by liquid and preparative gas chromatography produced a few micrograms of the pure material, sufficient for identification of the basic structure as 2-(1,5,5-trimethyl-2-cyclopent-2-en-yl)ethyl acetate 1.[4] Several syntheses of the racemate have been developed, using different strategies.[4,5] The synthetic pheromone proved to be extremely biologically active; lures loaded with 25 μg of

the racemate remained active for several months under field conditions.[6]

However, to date it has not been possible to determine the absolute configuration of the insect-produced compound because the pheromone, its corresponding alcohol, and several analogues were not resolved by GC on chiral stationary phases.[4] We report here the syntheses of both enantiomers of the pheromone, the determination of their absolute configurations, and the results of field trials testing their biological activity.

The most recently developed synthesis of the racemic pheromone progressed through the key intermediate **2**, in which the adjacent quaternary carbons were generated by a Claisen rearrangement of a readily accessible allylic alcohol precursor, followed by ring-closing metathesis of **2** to close the cyclopentene ring with the endo double bond in the correct position.[5c] Although the alcohol function in **2** was separated from the stereogenic center by two carbon atoms, we reasoned that the enantiomers still might be separable as diastereomeric derivatives of the alcohol. Furthermore, at least one of the two resulting diastereomers must be crystalline so that the relative and absolute configurations could be unambiguously determined from an X-ray crystal structure determination. After careful examination of the literature, Harada's camphorsultam phthalic (CSP) acid appeared to be a suitable candidate for the optically active auxiliary.[7] Thus, alcohol **2**, available in gram quantities from the synthesis of the racemate,[5c] was readily esterified (DMAP, DCC) with CSP acid to produce the mixture of diastereomers **3a** and **3b**. Although the diaster-

eomers were not separable on achiral stationary phases, they were resolved to baseline on an enantioselective column, eluting with *n*-hexane:EtOH:MeOH (90:10:2). NMR data of compounds **3a** and **3b** were very similar (See Table S1 in the Supporting Information).

After recrystallization from petroleum ether, the relative and absolute configurations of **3b** were determined through X-ray crystal structure analysis, revealing that the chiral center in the synthetic intermediate had the (*R*)-configuration (Scheme 1).

Scheme 1
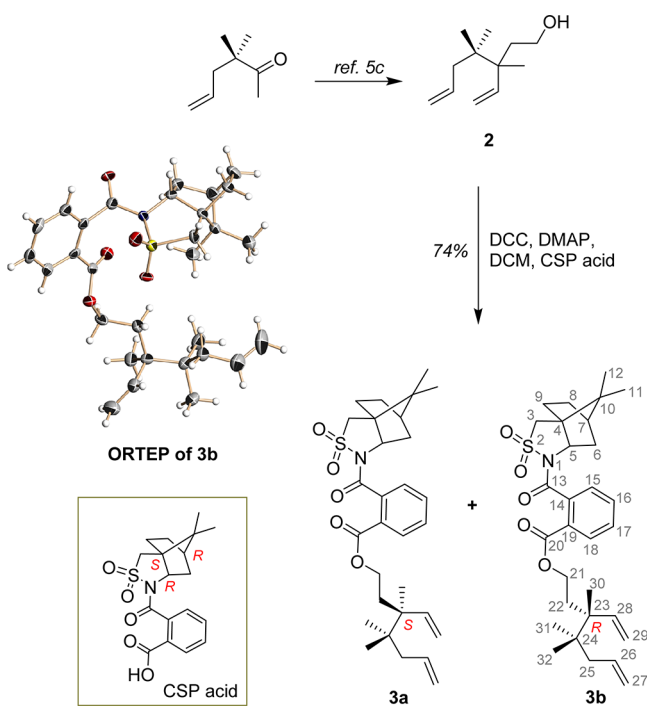
Diastereomer **3a** was hydrolyzed with K_2CO_3 in MeOH to obtain alcohol (*S*)-**2**, which was subsequently transformed to the target pheromone (*S*)-(+)-**1** by acetylation followed by ring-closing metathesis as previously described (Scheme 2).[5c] As expected, the spectral data of (*S*)-(+)-**1** were in agreement with those of the racemate. The other diastereomer **3b** was converted to (*R*)-(−)-**1** in similar fashion.

With both enantiomers of the pheromone in hand, the biological activities of each enantiomer and the racemate were tested in field trials. The results showed that the (*S*)-(+)-enantiomer was highly attractive to male mealybugs (Figure 2), strongly suggesting that female longtailed mealybugs produce this enantiomer. The (*R*)-(−)-enantiomer was

Scheme 2
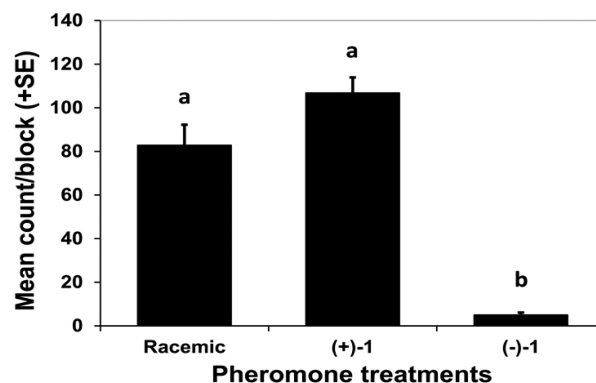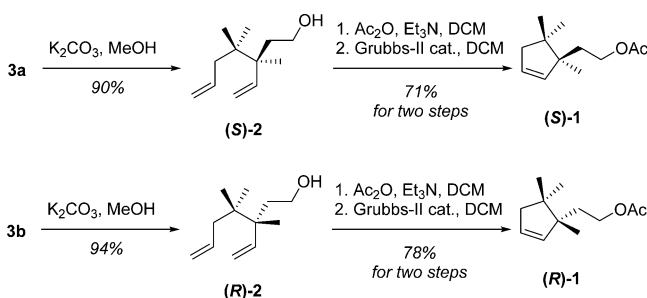
Figure 2. Male longtailed mealybugs caught in traps baited with each of the enantiomers of the pheromone, and the racemate. No mealybugs were caught in solvent treated controls.

only slightly more attractive than solvent-treated controls. This very slight attraction may have been due to the contamination of this enantiomer with 1.7% of the bioactive (*S*)-enantiomer. Furthermore, as seen with many other mealybug species,[2] the racemate was as attractive as the pure enantiomer, indicating that the (*R*)-(−)-enantiomer is not inhibitory. Thus, the cheaper and more readily synthesized racemic pheromone should be entirely adequate for practical applications in pest management.

■ EXPERIMENTAL SECTION

General Methods. All reactions were carried out in oven-dried glassware under argon or nitrogen unless otherwise specified, with magnetic stirring. Air sensitive reagents and solutions were transferred via syringe or cannula and were introduced to the apparatus via rubber septa. All reagents, starting materials, and solvents were obtained from commercial suppliers and used without further purification. Reactions were monitored by thin layer chromatography (TLC) with 0.25 mm precoated silica gel plates (60 F254). Visualization was accomplished with either UV light, iodine vapors, or by immersion in ethanolic solutions of phosphomolybdic acid, *para*-anisaldehyde, or $KMnO_4$ followed by heating with a heat gun for ~15 s. Flash column chromatography was performed on silica gel (100−200 or 230−400 mesh size). High resolution mass spectra (HRMS, ESI) were recorded with an ORBITRAP mass analyzer (Q Exactive). Mass spectra were measured with electrospray ionization with an MSQ LCMS mass spectrometer. Infrared (IR) spectra were recorded on a FT-IR spectrometer as thin films. Optical rotations were recorded on a polarimeter at 589 nm.

CSP Esters (3a and 3b). A solution of 3,4,4-trimethyl-3-vinyl-hept-6-en-1-ol **2** (50 mg, 0.27 mmol) and *N*-(2-carboxybenzoyl)-(−)-10,2-camphorsultam (131 mg, 0.36 mmol, prepared according to literature procedures[7a,b,8]) in CH_2Cl_2 (5 mL) was treated with dimethylaminopyridine (DMAP, 44 mg, 0.36 mmol) followed by dicyclohexylcarbodiimide (DCC, 61 mg, 0.30 mmol) at 0 °C. After stirring at rt for 24 h, the reaction mixture was filtered, and the filtrate was concentrated under reduced pressure. The residue was purified by flash chromatography yielding the mixture of diastereomers (105 mg, 74%). R_f = 0.2 (20% EtOAc:hexanes). The mixture was resolved by chiral preparative HPLC on a Daicel CHIRALPAK AD-H column (amylose tris(3,5-dimethylphenyl carbamate) coated on 5 μm silica gel; 30 mm id × 250 mm length), eluting with *n*-hexane/ethanol/methanol (90/10/2, v/v/v) at 40 mL/min and monitoring with a UV detector at 225 nm. The diastereomeric mixture was dissolved in the mobile phase (10 mg/mL), and 3 mL aliquots were injected. Diastereomers **3a** and **3b** eluted at 9 and 12 min, respectively. The purity of the collected fractions was checked on a 4.6 × 250 mm Chiralpak IA-3 column (3 μm particle size) eluted with *n*-hexane: EtOH (95/5), flow 1.0 mL/min, 25 °C, monitoring by UV at 224 nm.

Diastereomer-I (3a): $[\alpha]^{26}_{D}$ −106.6° (*c* 0.2, CHCl$_3$); IR γ_{max} (thin film applied as CHCl$_3$ solution) 2963, 1721, 1686, 1635, 1336, 1300, 1168, 1112, 1083, 912, 776 cm^{-1}; HRMS (ESI) *m/z* calculated for C$_{30}$H$_{42}$NO$_5$S [M + H]$^+$ 528.2778, found 528.2787; Chiral HPLC purity = 98.3% (96.6% ee); t_R:10.57 min. ^{1}H and ^{13}C NMR data are provided in Supporting Information.

Diastereomer-II (3b): $[\alpha]^{24}_{D}$ −71.0° (*c* 0.2, CHCl$_3$); IR γ_{max} (thin film applied as CHCl$_3$ solution) 2963, 1720, 1685, 1635, 1333, 1299, 1168, 1137, 1082 cm^{-1}; HRMS (ESI) *m/z* calculated for C$_{30}$H$_{42}$NO$_5$S [M + H]$^+$ 528.2778, found 528.2787; Chiral HPLC purity = 99.3% (98.6% ee); t_R:13.63 min. ^{1}H and ^{13}C NMR data are provided in Supporting Information.

X-ray Crystal Structure Details. Single crystals of compound **3b** were obtained from petroleum ether. X-ray intensity data were collected on a Bruker SMART APEX II CCD diffractometer with graphite-monochromatized (Mo Kα = 0.71073 Å) radiation at low temperature, 150(2) K. The X-ray generator was operated at 50 kV and 30 mA. Diffraction data were collected with a ω scan width of 0.5° and at different settings of φ and 2θ. The sample-to-detector distance was fixed at 5.00 cm. The X-ray data acquisition was monitored by the APEX2 program suite.[9] All the data were corrected for Lorentz-polarization and absorption effects using SAINT and SADABS programs integrated in the APEX2 program package.[9] The structures were solved by the direct method and refined by full matrix least-squares, on the basis of F^2, using SHELX-97.[10] Molecular diagrams were generated using XSHELL program integrated in SHELXTL package.[11] All the H-atoms were placed in geometrically idealized position (C−H = 0.95 Å for phenyl H-atoms, C−H = 0.99 Å for methylene H-atoms, C−H = 1.00 Å for methine H-atoms, and C−H = 0.98 Å for methyl H-atoms) and constrained to ride on their parent atoms [U_{iso}(H) = 1.2U_{eq}(C) for the phenyl, methylene, and methine group, and U_{iso}(H) = 1.5U_{eq}(C) for the methyl group]. Crystallographic data for **3b** (C$_{30}$H$_{41}$NO$_5$S): M = 527.70, Crystal dimensions 0.40 × 0.22 × 0.02 mm^3, monoclinic, space group P2$_1$, a = 9.8209(13), b = 11.2394(16), c = 13.1369(18) Å, β = 107.284(10)°, V = 1384.6(3) Å^3, Z = 2, ρ_{calcd} = 1.266 gcm^{-3}, μ(Mo Kα) = 0.157 mm^{-1}, $F(000)$ = 568, $2\theta_{max}$ = 50.00°, T = 150(2) K, 8872 reflections collected, 4482 unique, 3055 observed ($I > 2\sigma(I)$) reflections, 340 refined parameters, R value 0.0524, wR2 = 0.0902, (all data R = 0.0954, wR2 = 0.1053), S = 0.996, minimum and maximum transmission 0.940 and 0.997; maximum and minimum residual electron densities +0.26 and −0.23 e Å^{-3}. The absolute configuration was established by anomalous dispersion effect (Flack parameter of 0.07(11)) in X-ray diffraction measurements, caused by the presence of the sulfur atom in the molecule.

(+)-3,4,4-Trimethyl-3-vinyl-hept-6-en-1-ol (S)-2. K$_2$CO$_3$ (282 mg, 2.04 mmol) was added to a solution of **3a** (90 mg, 0.170 mmol) in methanol at rt. After stirring for 2 h, the reaction mixture was concentrated under reduced pressure and purified by column chromatography to give (+)-3,4,4-trimethyl-3-vinyl-hept-6-en-1-ol (S)-**2** (28 mg, 90%): R_f = 0.4 (20% EtOAc:hexanes); $[\alpha]^{25}_{D}$ +1.7° (*c* 0.38, CHCl$_3$). The ^{1}H NMR spectrum was identical to that of the racemate. ^{1}H NMR: (400 MHz, CDCl$_3$) δ 0.82 (s, 6H) (gem-dimethyl), 0.98 (s, 3H) (quaternary methyl), 1.64−1.71 (m, 1H) (-CH$_2$-CH$_2$−OH), 1.78−1.85 (m, 1H) (-CH$_2$-CH$_2$−OH), 2.02 (d, J = 7.3 Hz, 2H) (allylic CH$_2$), 3.60 (t, J = 7.3 Hz, 2H) (CH$_2$-CH$_2$−OH), 4.93−5.03 (m, 3H) (terminal olefin), 5.12 (dd, J = 10.8, 1.5 Hz, 1H) (terminal olefin), 5.76−5.95 (m, 2H) (internal olefin).

(+)-2-(1,5,5-Trimethylcyclopent-2-en-1-yl)ethyl acetate (S)-1. A solution of (+)-(S)-3,4,4-trimethyl-3-vinyl-hept-6-en-1-ol (S)-**2** (24 mg, 0.13 mmol) and Et$_3$N (73 μL, 0.52 mmol) in dry CH$_2$Cl$_2$ (3 mL) was treated with acetic anhydride (26 μL, 0.26 mmol) and a catalytic amount of DMAP (2.5 mg) at rt. After stirring for 2 h, the reaction mixture was concentrated under reduced pressure and directly purified by column chromatography to give (−)-(3,4,4-trimethyl-3-vinyl-hept-6-enyl) acetate (28 mg, 95%): R_f = 0.75 (20% EtOAc:hexanes); $[\alpha]^{23}_{D}$ −4.6° (*c* 0.1, CHCl$_3$). The ^{1}H NMR was identical to that of the racemate. ^{1}H NMR: (500 MHz, CDCl$_3$) δ 0.82 (s, 6H), 0.97 (s, 3H), 1.70−1.83 (m, 2H), 2.01−2.04 (m, 5H), 3.95−4.02 (m, 2H), 4.93−5.02 (m, 3H), 5.13 (dd, J = 11.0, 1.5 Hz, 1H), 5.77−5.84 (m, 2H).

A solution of (−)-(3,4,4-trimethyl-3-vinyl-hept-6-enyl) acetate (22 mg, 0.10 mmol) in dry CH$_2$Cl$_2$ (5 mL) was degassed for 10 min with a stream of argon and then treated with Grubbs' second generation catalyst (9 mg, 10 mol %; Aldrich, cat# 569747) in one portion. After stirring at 40 °C for 16 h, the mixture was treated with a drop of DMSO, and stirring was continued for 1 h. Evaporation of the solvent and purification by column chromatography furnished the (S)-(+)-2-(1,5,5-trimethylcyclopent-2-en-1-yl)ethyl acetate (S)-**1** (14.2 mg, 75%): R_f = 0.7 (20% EtOAc: hexanes); $[\alpha]^{25}_{D}$ +27.8° (*c* 0.16, CH$_2$Cl$_2$). The ^{1}H NMR matched that of the racemate. ^{1}H NMR: (400 MHz, CDCl$_3$) δ 0.89 (s, 3H), 0.94 (s, 3H), 0.95 (s, 3H), 1.52−1.58 (m, merged with CDCl$_3$ moisture, 1H), 1.66−1.74 (m, 1H), 2.04 (s, 3H), 2.13 (t, J = 1.6 Hz, 2H), 4.05−4.23 (m, 2H), 5.55−5.64 (m, 2H).

Diastereomer **3b** was converted to (R)-**1** in analogous fashion. Spectral data matched those of the corresponding enantiomers described above. Yields and optical rotations were as follows. Alcohol **2b**: Yield 94%; $[\alpha]^{25}_{D}$ −2.0° (*c* 0.15, CHCl$_3$). Acetate (R)-**2**: yield 94%; $[\alpha]^{25}_{D}$ +3.3° (*c* 0.15, CHCl$_3$). Pheromone (R)-**1**: yield 83%; $[\alpha]^{25}_{D}$ −24.0° (*c* 0.13, CH$_2$Cl$_2$).

Field Trial of the Pheromone Enantiomers and the Racemate. A field bioassay of the pheromone was conducted at a nursery in Bonsall, California, USA, in a 0.49 ha plot of *Ruscus hypoglossum* L. (plot coordinates: 33°17′18.36′′ N, 117°16′55.61′′ W elev 113 m) that was known to be infested with *P. longispinus*. The plot was divided into seven hoop houses (63 m long × 7 m wide), six of which were used in this study. Each house (block) was covered in plastic with open ends. Airflow between houses was not restricted because the plastic cover began 1 m above the plant canopy. Four delta sticky traps were spaced every 12.5 m along a transect within each house, suspended directly above the ruscus canopy. Each trap contained an 11 mm gray rubber septum impregnated with a hexane solution of one of four treatments: solvent control, 5 μg of (S)-(+)-enantiomer, 5 μg of (R)-(−)-enantiomer, 10 μg of the racemate. Treatments were assigned randomly along each transect. Traps were replaced, and treatments were repositioned once after 6 d. Traps remained in place for another 11 d. Trap count data were analyzed by analysis of variance after $\sqrt{(x + 0.5)}$ transformation of the data to meet the assumptions of normality and equal variances. Differences among means were tested using Tukey's honestly significant differences (HSD) test. There was no significant interaction between the two sampling periods (date) and the treatments (F = 3.23, df = 2, 30, and P = 0.054). Thus, data for each date were combined for the final analysis. There was both a significant effect of date (F = 10.19, df = 2, 32, P = 0.0032) and treatment (F = 130.04, df = 2, 32, P < 0.0001). Controls were not included in the analysis because their zero values and lack of variance violate the assumptions of ANOVA. Instead, confidence intervals were constructed, showing that the low trap counts for the (R)-(−)-enantiomer were significantly different than zero, i.e., that the (−)-enantiomer was slightly more attractive than controls.[12]

■ ASSOCIATED CONTENT

Ⓢ Supporting Information

Copies of chiral HPLC traces demonstrating enantiomeric purities of chiral intermediates; NMR data comparison of **3a** and **3b**; copies of NMR spectra and CIF file for the X-ray crystal structure of compound **3b**. This material is available free of charge via the Internet at http://pubs.acs.org.

■ AUTHOR INFORMATION

Corresponding Author

*E-mail: ds.reddy@ncl.res.in.

Notes

The authors declare no competing financial interest.

■ REFERENCES

(1) (a) Golino, D. A.; Sim, S. T.; Gill, R.; Rowhani, A. *Calif. Agric.* **2002**, 196−201. (b) Tsai, C.; Rowhani, A.; Golino, D. A.; Daane, K. M.; Almeida, R. P. P. *Phytopathology* **2010**, *100*, 830−834.

(2) (a) Millar, J. G.; Daane, K. M.; McElfresh, J. S; Moreira, J. A.; Bentley, W. J. Chemistry and applications of mealybug sex pheromones. In *ACS Symposium Series # 906, Semiochemicals in Pest Management and Alternative Agriculture*; Petroski, R., Ed.; American Chemical Society: Washington, D.C., 2005; pp 11−27. (b) Zou, Y.; Chinta, S. P.; Millar, J. G. Irregular terpenoids as mealybug and scale pheromones: Chemistry and applications. In *ACS Symposium Series, Natural Products for Pest Management*; Beck, J., Coats, J., Duke, S., Koivunen, M., Eds.; American Chemical Society: Washington D.C., in press.

(3) (a) Millar, J. G.; Midland, S. L.; McElfresh, J. S.; Daane, K. M. *J. Chem. Ecol.* **2005**, *31*, 2999−3005. (b) Millar, J. G.; Midland, S. L. *Tetrahedron Lett.* **2007**, *48*, 6377−6379. (c) Figadère, B.; Devlin, F. J.; Millar, J. G.; Stephens, P. J. *Chem. Commun.* **2008**, 1106−1108.

(4) Millar, J. G.; Moreira, J. A.; McElfresh, J. S.; Daane, K. M.; Freund, A. S. *Org. Lett.* **2009**, *11*, 2683−2685.

(5) (a) Zou, Y.; Millar, J. G. *J. Org. Chem.* **2009**, *74*, 7207−7209. (b) Zou, Y.; Millar, J. G. *Synlett* **2010**, 2319−2321. (c) Kurhade, S. E.; Siddaiah, V.; Bhuniya, D.; Reddy, D. S. *Synthesis* **2013**, DOI: 10.1055/s-0033-1338450. Another synthesis appeared during the review process of this manuscript. Bailey, W. F.; Bakonyi, J. M. *J. Org. Chem.* **2013**, *78*, 3493−3495.

(6) Waterworth, R. A.; Redak, R. A.; Millar, J. G. *J. Econ. Entomol.* **2011**, *104*, 555−565.

(7) (a) Harada, N.; Nehira, T.; Soutome, T.; Hiyoshi, N.; Kido, F. *Enantiomer* **1996**, *1*, 35−39. (b) Harada, N.; Koumura, N.; Robillard, M. *Enantiomer* **1997**, *2*, 303−309. (c) Kosaka, M.; Sugito, T.; Kasai, Y.; Kuwahara, S.; Watanabe, M.; Harada, N.; Job, G. E.; Shvet, A.; Pirkle, W. H. *Chirality* **2003**, *15*, 324−328. (d) Harada, N. *Chirality* **2008**, *20*, 691−723.

(8) Davis, F. A.; Towson, J. C.; Weismiller, M. C.; Lal, S.; Carroll, P. J. *J. Am. Chem. Soc.* **1988**, *110*, 8477−8482.

(9) *APEX2, SAINT and SADABS*; Bruker AXS, Inc.: Madison, WI, 2006.

(10) Sheldrick, G. M. *Acta Crystallogr.* **2008**, *A64*, 112−122.

(11) *SHELXTL*, Version 6.14; Bruker AXS, Inc.: Madison, WI, 2003.

(12) Zar, J. H. *Biostatistical Analysis*, 3rd ed.; Prentice Hall: Upper Saddle River, NJ, 1996; http://support.sas.com/documentation/cdl/en/proc/65145/HTML/default/viewer.htm#p0klmrp4k89pz0n1p72t0clpavyx.htm.

COMMUNICATION

Zinc mediated allylations of chlorosilanes promoted by ultrasound: Synthesis of novel constrained sila amino acids†

Remya Ramesh and D. Srinivasa Reddy*

A simple, fast and efficient method for allylation and propargylation of chlorosilanes through zinc mediation and ultrasound promotion is reported. As a direct application of the resulting bis-allylsilanes, three novel, constrained sila amino acids are prepared for the first time. The design and synthesis of the constrained sila analogue of GABA (γ-amino butyric acid) is a highlight of this work.

Organosilanes have wide applications in organic chemistry, from commonly used protecting groups to synthetic intermediates.[1] Compared to other organometallic reagents, they are stable in air and hence are easy to handle and store. Apart from their conventional use in organic synthesis and polymer chemistry,[2] organosilanes have uses in medicinal chemistry[3] as well. Since both carbon and silicon belong to the same group in the periodic table, medicinal chemists have used silicon as a bioisostere of carbon to improve the drug-like properties of molecules, hence the use of organosilanes is becoming popular in recent times.[4] As part of an ongoing program (silicon switch approach) in this group, we are interested in making novel silicon analogues of selected drug molecules to improve their desired properties. Some of the silicon analogues synthesized in this group have shown promising results (Fig. 1).[5] Biological profiling and lead optimization is currently in progress with respect to Silinezolid. Along these lines, there is a need to explore simple and practical methods to access organosilicon building blocks which will be useful for the drug discovery programs based on the silicon switch approach.[3]

Allylsilanes are versatile reagents with very rich chemistry,[6] with a variety of methods known in the literature for their preparation. The reaction of Grignard reagents, prepared from allylhalides with chlorosilanes or alkoxysilanes, is the most

Silinezolid
(WO2013/054275 A1)

GABA analogue
(present work)
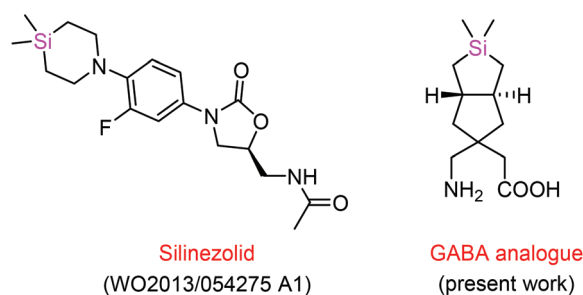
Fig. 1 Silicon analogues of known drugs from the present group.

widely used method for their preparation.[7] Reactions mediated by other organometallic reagents using indium,[8] samarium[9] and zinc[10] are also known. However, there was no report in the literature for using sonication in preparing allylsilanes. The ultrasound waves disperse the metal and clean its surface, which makes it more reactive.[11] The experimental safety, simplicity, low-cost and the rapid reaction rate are the added advantages of this technique. Herein, organozinc mediated allylations and propargylations on a variety of chlorosilanes promoted by ultrasound waves are reported.

The initial attempts started with diphenyldichlorosilane and allyl bromide using THF as the solvent. The chlorosilane, allyl bromide and zinc dust in THF solvent were sonicated by placing them in an ultrasound cleaning bath (37 kHz, 320 W). The reaction was complete within 10 minutes and the desired product diallyldiphenylsilane **1** was isolated in 88% yield. For the comparison purpose, the reaction was conducted without using ultrasonication and it was found that the present method is superior. After having this result in hand, the same conditions (2 eq. of allylbromide and 2 eq. of Zn per chloro) were applied to a variety of chlorosilanes, which include mono-chloro, dichloro as well as trichlorosilanes (Scheme 1). All the results are compiled in Chart 1. In most cases the product was obtained in good to excellent yields.

In the case of monochlorosilanes, the products **2**, **3**, **4**, **5** and **6** were obtained in the range of 71–98% yield. However in

Division of Organic Chemistry, CSIR-National Chemical Laboratory, Dr HomiBhabha Road, Pune, 411008, India. E-mail: ds.reddy@ncl.res.in; Fax: +91 20 25902629; Tel: +91 20 25902445

†Electronic supplementary information (ESI) available: Characterization data, NMR spectra and detailed experimental procedures. See DOI: 10.1039/c4ob00294f

This journal is © The Royal Society of Chemistry 2014

Org. Biomol. Chem., 2014, **12**, 4093–4097 | **4093**
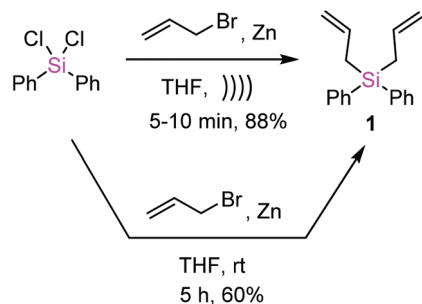
Scheme 1 Allylation of chlorosilane using Zn mediation.
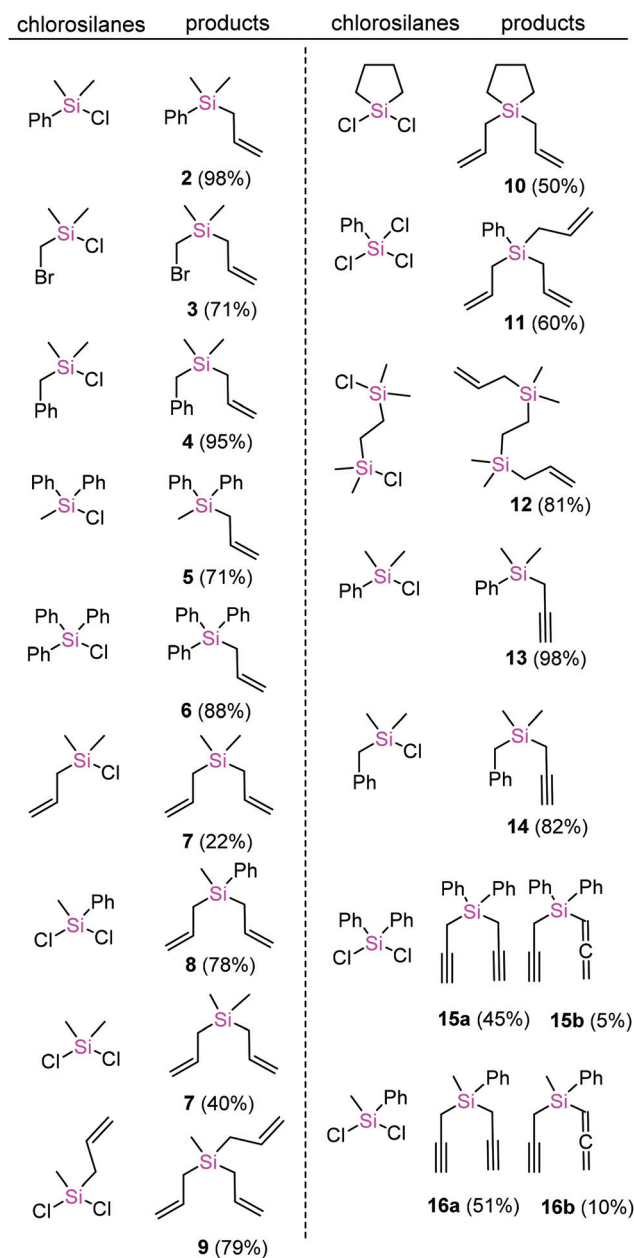
Chart 1 Scope of the method.

the case of dimethylallylchlorosilane, the product **7** was isolated in poor yield due to its volatile nature. Addition of two and three allyl groups was demonstrated using the same protocol to obtain products **7**, **8**, **9**, **10**, **11** and **12**. It is worth mentioning here that products like **9**, **11** and **12** are important building blocks in dendrimers and polymers. To expand the scope of the present method, the reaction of chlorosilanes with propargylbromide was also explored and the results are interesting. Propargylbromide reacted with dimethylphenylchlorosilane and dimethylbenzylchlorosilane under the same conditions to give exclusively the desired propargyl compounds **13** and **14**, respectively. In the case of dichlorosilanes, the propargylallenyl compounds (**15b** and **16b**) were obtained as minor compounds in addition to the desired dipropargyl compounds (**15a** and **16a**). It is interesting to note that a similar reaction mediated by indium metal as reported by Lai *et al*[8] gives the allene derivative exclusively. The ^{1}H NMR data of all the known compounds were compared with the literature values and were found to be exactly matching.

As a direct application of the resulting allylsilanes, we envisaged the preparation of novel constrained unnatural silicon-containing amino acids which are interesting candidates in drug discovery or as part of the drug candidates. In addition, the synthetic unnatural amino acids[12] can also be used for probing bioactive conformations in peptides of interest.[13] Synthesis and biological studies of silicon-containing amino acids, as well as the peptides incorporating them, have been documented in literature.[14,3d] However, they are still few in number with limited structural variation despite their attractive features. There is a need to find new routes to access novel and diverse silicon-containing amino acids. Along these lines, the crucial intermediate diiodo compound **17** was prepared from diallyldimethylsilane (**7**), by zirconacyclization followed by addition of iodine according to the literature protocol.[15] This intermediate **17** was used as a starting point to access various planned unnatural amino acids, particularly α-, β- and γ-amino acids with unusual 5,5-*trans* fusion.[16] Accordingly, compound **17**, on treatment with ethylisocyanoacetate in the presence of K_2CO_3 as base and a phase-transfer catalyst (18-crown-6), produced compound **18** as a sole product.[17] The ease of formation of such a strained system can be attributed to the larger Si–C bond length (189 pm as compared to 154 pm for an sp^3–sp^3 C–C bond),[18] which makes the reaction feasible under milder conditions. The isocyano group on hydrolysis (aq. HCl) gave the desired amino ester **19**, an unnatural α-amino acid in 91% yield. The free amine group was protected as the *t*-butyl carbamate to give orthogonally protected α-amino acid **20**. For the synthesis of the β-amino acid, compound **17** was treated with ethylcyanoacetate under the same conditions adopted for the synthesis of α-amino acid, to give α-cyanoester **21** in 86% isolated yield. The cyano group present in **21** was hydrogenated in the presence of RANEY® nickel under 60 psi pressure, to furnish β-amino ester **22**. When the hydrogenation reaction was carried out in the presence of Boc anhydride, the Boc protected amino acid **23** was obtained with improved yield (Scheme 2). Both the α-, and β-amino acid
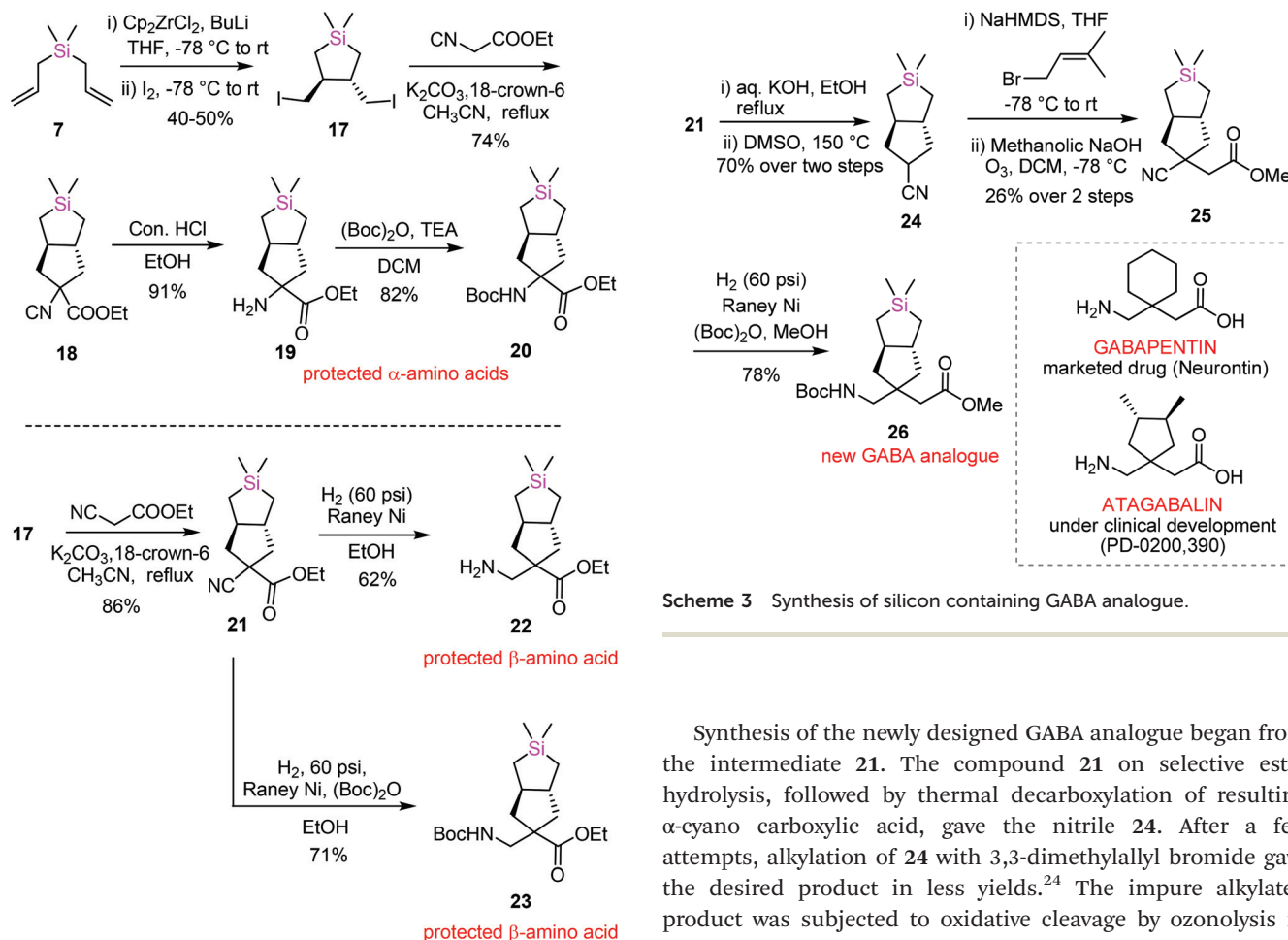
4094 | *Org. Biomol. Chem.*, 2014, **12**, 4093–4097

This journal is © The Royal Society of Chemistry 2014

Scheme 2 Synthesis of constrained sila α-, β-amino acids.

Scheme 3 Synthesis of silicon containing GABA analogue.

derivatives **20** and **23** were well characterized using spectral data.[19]

After succeeding in the preparation of both α- and β-amino acids with an unprecedented core, the next task was to synthesize a GABA analogue with the same skeleton. GABA (γ-amino butyric acid) is the chief inhibitory neurotransmitter present in the mammalian central nervous system.[20] The deficiency of GABA is associated with several neurological disorders. For disease states associated with the deficiency of GABA, lipophilic GABA analogues have been synthesized.[20] The polar and flexible structure of GABA prevents it from crossing the blood brain barrier (BBB). Atagabalin[21] and Gabapentin[22] are pharmaceutically important, conformationally rigid GABA analogues. The incorporation of silicon is believed to increase the lipophilicity of a molecule which can be an attractive feature in the development of CNS drugs as it is expected to increase brain exposures. To our knowledge, Tacke's group, the pioneer of silicon switch approach, has claimed the sila-cyclohexyl and sila-cyclopentyl analogues of Gabapentin in a patent publication.[23] Therefore, we became interested in accessing novel, constrained sila analogues of GABA, which can be good starting points for the medicinal chemistry programs.

Synthesis of the newly designed GABA analogue began from the intermediate **21**. The compound **21** on selective ester hydrolysis, followed by thermal decarboxylation of resulting α-cyano carboxylic acid, gave the nitrile **24**. After a few attempts, alkylation of **24** with 3,3-dimethylallyl bromide gave the desired product in less yields.[24] The impure alkylated product was subjected to oxidative cleavage by ozonolysis in methanolic NaOH to furnish the desired compound **25**.[25] Although the ozonolysis reaction was clean, the alkylation needs further optimization. The compound **25** on reduction (RANEY® Ni, 60 psi) in the presence of Boc anhydride furnished the novel GABA analogue **26** in 78% yield (Scheme 3).[19] The new GABA analogue is structurally close to that of the marketed drug Gabapentin and a developmental candidate Atagabalin. Hence, compound **26** can serve as a starting point which needs more attention to profile in biological assays.

In summary, a simple and rapid method for the preparation of allyl- and propargyl-silanes has been developed, which can be an addition to the existing toolbox to access these compounds. The unsaturated organosilanes are very good starting materials in the polymer industry, since they can undergo addition polymerization. Using allyl-silanes as starting material, silicon incorporated unnatural α-, β- and γ-amino acids with unusual 5,5-*trans* fusion have been prepared for the first time. The more lipophilic and conformationally rigid GABA analogue is expected to be an important compound, which may be useful for the modulation of various CNS disorders. Biological profiling, conformational studies and structure activity relationships (SARs) are the subject of future publications from this group.

This journal is © The Royal Society of Chemistry 2014

Org. Biomol. Chem., 2014, **12**, 4093–4097 | **4095**

thank B. Seetharamsingh (CSIR-NCL, Pune) for his help in some of the initial experiments. RR thanks CSIR, New Delhi, for the award of a research fellowship.

Notes and references

1 Selected reviews and publications: (*a*) R. West and T. J. Barton, *J. Chem. Educ.*, 1980, **57**, 165–169; (*b*) I. Fleming, *Chem. Soc. Rev.*, 1981, **10**, 83–111; (*c*) G. L. Larson, *Recent Synthetic Applications of Organosilanes, in Organic Silicon Compounds*, 2004, vol. 1 and 2; (*d*) S. E. Denmark and R. F. Sweis, *Chem. Pharm. Bull.*, 2002, **50**, 1531–1541; (*e*) S. E. Denmark and C. S. Regens, *Acc. Chem. Res.*, 2008, **41**, 1486–1499; (*f*) M. A. Brook, *Silicon in Organic, Organometallic and Polymer Chemistry*, Wiley Interscience, New York, 2000; (*g*) I. Fleming, in *Comprehensive Organic Synthesis*, ed. B. M. Trost and I. Fleming, Pergamon Press, Oxford, 1991, vol. 2, pp. 563–593; (*h*) H.-J. Zhang, D. L. Priebbenow and C. Bolm, *Chem. Soc. Rev.*, 2013, **42**, 8540–8571.

2 Selected references related to silicon based polymers: (*a*) D. Y. Son, *Chem. Commun.*, 2013, **49**, 10209–10210; (*b*) S. Thames and K. Panjnani, *J. Inorg. Organomet. Polym.*, 1996, **6**, 59–94; (*c*) R. Richter, G. Roewer, U. Böhme, K. Busch, F. Babonneau, H. P. Martin and E. Müller, *Appl. Organomet. Chem.*, 1997, **11**, 71–106 and references cited therein.

3 See selected recent reviews and publications for the use of silicon in medicinal chemistry: (*a*) J. S. Mills and G. A. Showell, *Drug Discovery Today*, 2003, **8**, 551–556; (*b*) J. S. Mills and G. A. Showell, *Expert Opin. Invest. Drugs*, 2004, **13**, 1149–1157; (*c*) S. Gately and R. West, *Drug Dev. Res.*, 2007, **68**, 156–163; (*d*) A. K. Franz and S. O. Wilson, *J. Med. Chem.*, 2013, **56**, 388–405; (*e*) R. Tacke, *Angew. Chem.*, 1999, **111**, 3197–3200, (*Angew. Chem., Int. Ed.*, 1999, **38**, 3015–3018).

4 Selected recent reports on silicon switch approach: (*a*) M. Chang, S.-R. Park, J. Kim, M. Jang, J. H. Park, J. E. Park, H.-G. Park, Y.-G. Suh, Y. S. Jeong, Y.-H. Park and H.-D. Kim, *Bioorg. Med. Chem.*, 2010, **18**, 111–116; (*b*) K. Maruyama, M. Nakamura, S. Tomoshige, K. Sugita, M. Makishima, Y. Hashimoto and M. Ishikawa, *Bioorg. Med. Chem. Lett.*, 2013, **23**, 4031–4036; (*c*) M. Nakamura, M. Makishima and Y. Hashimoto, *Bioorg. Med. Chem. Lett.*, 2013, **21**, 1643–1651; (*d*) M. Nakamura, D. Kajita, Y. Matsumoto and Y. Hashimoto, *Bioorg. Med. Chem. Lett.*, 2013, **21**, 7381–7391; (*e*) M. Fischer and R. Tacke, *Organometallics*, 2013, **32**, 7181–7185; (*f*) J. Wang, C. Ma, Y. Wu, R. A. Lamb, L. H. Pinto and W. F. DeGrado, *J. Am. Chem. Soc.*, 2011, **133**, 13844–13847; (*g*) P. Luger, M. Weber, C. Hübschle and R. Tacke, *Org. Biomol. Chem.*, 2013, **11**, 2348–2354; (*h*) A. P. Ayscough, G. A. Showell, M. R. Teall, H. E. Temple and S. Ahmed, *WO*, 092342, A1, 2010; (*i*) D. Troegel, F. Möller and R. Tacke, *J. Organomet. Chem.*,

2010, **695**, 310–313; (*j*) U. Olszewski, R. Zeillinger, M. D. Kars, A. Zalatnai, J. Molnar and G. Hamilton, *Anti-Cancer Agents Med. Chem.*, 2012, **12**, 663–671.

5 Unpublished results. However, a PCT document covering Silinezolid and related compounds is available in public domain. D. S. Reddy, B. Seetharamsingh and R. Ramesh, *WO*, 054275, A1, 2013.

6 Selected reviews and publications on allylsilanes: (*a*) H. Sakurai, *Pure Appl. Chem.*, 1982, **54**, 1–22; (*b*) A. Hosomi, *Acc. Chem. Res.*, 1988, **21**, 200–206; (*c*) J. R. Hwu, B.-L. Chen and S.-S. Shiao, *J. Org. Chem.*, 1995, **60**, 2448–2455; (*d*) S. BouzBouz, L. Boulard and J. Cossy, *Org. Lett.*, 2007, **9**, 3765–3768; (*e*) T. H. Chan and D. Wang, *Chem. Rev.*, 1995, **95**, 1279–1292; (*f*) C. E. Masse and J. S. Panek, *Chem. Rev.*, 1995, **95**, 1293–1316; (*g*) J. Wu, Y. Chen and J. S. Panek, *Org. Lett.*, 2010, **12**, 2112–2115; (*h*) R. E. Grote and E. R. Jarvo, *Org. Lett.*, 2009, **11**, 485–488; (*i*) J. W. A. Kinnaird, P. Y. Ng, K. Kubota, X. Wang and J. L. Leighton, *J. Am. Chem. Soc.*, 2002, **124**, 7920–7921; (*j*) J. S. Panek and M. Yang, *J. Am. Chem. Soc.*, 1991, **113**, 9868–9870.

7 (*a*) S. D. Rosenberg, J. J. Walburn and H. E. Ramsden, *J. Org. Chem.*, 1957, **22**, 1606–1607; (*b*) R. E. Scott and K. C. Frisch, *J. Am. Chem. Soc.*, 1951, **73**, 2599–2600.

8 Z. Li, C. Yang, H. Zheng, H. Qiu and G. Lai, *J. Organomet. Chem.*, 2008, **693**, 3771–3779.

9 Z. Li, X. Cao, G. Lai, J. Liu, Y. Ni, J. Wu and H. Qiu, *J. Organomet. Chem.*, 2006, **691**, 4740–4746.

10 Only once Zn was utilized in the literature for the allylation of chlorosilanes, but it was not generalized. See: T. Sanji, M. Iwata, M. Watanabe, T. Hoshi and H. Sakurai, *Organometallics*, 1998, **17**, 5068–5071.

11 (*a*) G. Cravotto, E. C. Gaudino and P. Cintas, *Chem. Soc. Rev.*, 2013, **42**, 7521–7534; (*b*) C. Einhorn, J. Einhorn and J.-L. Luche, *Synthesis*, 1989, 787–813.

12 N. Voloshchuk and J. K. Montclare, *Mol. BioSyst.*, 2010, **6**, 65.

13 (*a*) D. A. Dougherty, *Curr. Opin. Chem. Biol.*, 2000, **4**, 645–652; (*b*) M. Tanaka, K. Anan, Y. Demizu, M. Kurihara, M. Doi and H. Suemune, *J. Am. Chem. Soc.*, 2005, **127**, 11570–11571.

14 (*a*) M. Mortensen, R. Husmann, E. Veri and C. Bolm, *Chem. Soc. Rev.*, 2009, **38**, 1002–1010; (*b*) R. J. Smith and S. Bienz, *Helv. Chim. Acta*, 2004, **87**, 1681–1696; (*c*) R. Tacke, M. Merget, R. Bertermann, M. Bernd, T. Beckers and T. Reissmann, *Organometallics*, 2000, **19**, 3486–3497; (*d*) B. Vivet, F. Cavelier and J. Martinez, *Eur. J. Org. Chem.*, 2000, 807–811; (*e*) R. D. Walkup, D. C. Cole and B. R. Whittlesey, *J. Org. Chem.*, 1995, **60**, 2630–2634; (*f*) S. Falgner, G. Buchner and R. Tacke, *J. Organomet. Chem.*, 2010, **695**, 2614–2617; (*g*) S. Dörrich, S. Falgner, S. Schweeberg, C. Burschka, P. Brodin, B. M. Wissing, B. Basta, P. Schell, U. Bauer and R. Tacke, *Organometallics*, 2012, **31**, 5903–5917; (*h*) S. Falgner, C. Burschka, S. Wagner, A. Böhm, J. O. Daiss and R. Tacke, *Organo-*

4096 | *Org. Biomol. Chem.*, 2014, **12**, 4093–4097

This journal is © The Royal Society of Chemistry 2014

metallics, 2009, **28**, 6059–6066; (*i*) S. Falgner, D. Schmidt, R. Bertermann, C. Burschka and R. Tacke, *Organometallics*, 2009, **28**, 2927–2930.

15 (*a*) M. Mirza-Aghayan, R. Boukherroub, G. Etemad-Mogha-dam, G. Manuel and M. Koenig, *Tetrahedron Lett.*, 1996, **37**, 3109–3112; (*b*) A. G. Nair, K. M. Keertikar, S. H. Kim, J. A. Kozlowski, S. Rosenblum, O. B. Selyutin, M. Wong, W. Yu and Q. Zeng, *WO*, 112429, 2011.

16 5,5-*cis*-Fusion of all carbon scaffold is commonly encountered in the literature.

17 (*a*) S. Kotha and E. Brahmachary, *J. Org. Chem.*, 2000, **65**, 1359–1365; (*b*) S. Kotha, D. Goyal and A. S. Chavan, *J. Org. Chem.*, 2013, **78**, 12288–12313 and refs cited therein.

18 *Handbook of Chemistry and Physics*, CRC Press, 81st edn, 2000.

19 All the spectral data (IR, ^{1}H NMR, ^{13}C NMR, HRMS) are provided in ESI.†

20 (*a*) K. Gajcy, S. Lochynski and T. Librowski, *Curr. Med. Chem.*, 2010, **17**, 2338–2347; (*b*) J. S. Bryans and D. J. Wustrow, *Med. Res. Rev.*, 1999, **19**, 149–177.

21 D. C. Blakemore, J. S. Bryans, P. Carnell, C. L. Carr, N. E. A. Chessum, M. J. Field, N. Kinsella, S. A. Osborne, A. N. Warren and S. C. Williams, *Bioorg. Med. Chem. Lett.*, 2010, **20**, 461–464.

22 (*a*) G. J. Sills, *Curr. Opin. Pharmacol.*, 2006, **6**, 108–113; (*b*) N. S. Gee, J. P. Brown, U. K. Dissanayake, J. Offord, R. Thurlow and G. N. Woodruff, *J. Biol. Chem.*, 1996, **271**, 5768–5776.

23 R. Tacke, J. Daiss, G. A. Showell and A. Richards, *UK Patent*, 2397576-A, 2004.

24 The alkylated product could not be purified despite a few attempts. The reaction and purification need further optimization.

25 J. A. Marshall and A. W. Garofalo, *J. Org. Chem.*, 1993, **58**, 3675–3678.

This journal is © The Royal Society of Chemistry 2014

Org. Biomol. Chem., 2014, **12**, 4093–4097 | **4097**

Enantiospecific Synthesis of Both Enantiomers of the Longtailed Mealybug Pheromone and Their Evaluation in a New Zealand Vineyard

Remya Ramesh,[†] Vaughn Bell,[§] Andrew M. Twidle,[§] Rajesh Gonnade,[‡] and D. Srinivasa Reddy*,[†]

[†]Division of Organic Chemistry, and [‡]Center for Material Characterization, CSIR-National Chemical Laboratory, Dr. Homi Bhabha Road, Pune 411008, India

[§]The New Zealand Institute for Plant & Food Research Ltd., Gerald Street, Lincoln 7608, New Zealand

Ⓢ *Supporting Information*

(−)-5-oxobornyl acetate · (−)-pheromone · (+)-pheromone · (+)-5-oxobornyl acetate
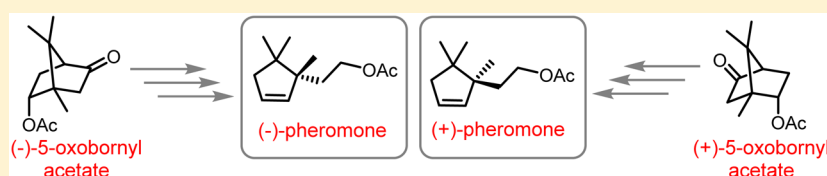
ABSTRACT: The irregular monoterpenoid sex pheromone of *Pseudococcus longispinus* and its enantiomer were prepared from the corresponding bornyl acetates. The use of readily accessible chiral starting materials and lactone−lactone rearrangement are the highlights of the present synthesis. The biological activities of the two enantiomers and racemic mixture were tested in a New Zealand vineyard. The (*S*)-(+)-enantiomer was significantly more attractive to *P. longispinus* males than the racemic mixture or the (*R*)-(−)-enantiomer.

Pheromones are chemicals released by organisms and serve as a means of communication between individuals of the same species. Among these, sex pheromones are of particular interest and find application in insect pest management. These pheromones are secreted by an individual so as to attract a potential mate. They can be very powerful, attracting conspecifics of the opposite sex from long distances.[1] The female-produced sex pheromone of *Pseudococcus longispinus*, the longtailed mealybug, a widely distributed pest of agricultural crops and ornamental plants, was identified by Millar et al.[2] In field trials, the racemic pheromone was very attractive to male longtailed mealybugs at low doses (25 μg) for more than three months. Because of this interesting biological activity and its utility in pest management strategies, to date five syntheses have been reported for the racemic compound.[2,3] Recently, in collaboration with the Millar group, we showed that the (*S*)-(+)-enantiomer was highly attractive and that the (*R*)-(−)-enantiomer was inactive, suggesting that female longtailed mealybugs produce the (*S*)-enantiomer.[4]

In our previous synthesis, racemic 3,4,4-trimethyl-3-vinyl-hept-6-en-1-ol was converted to its diastereomeric derivatives using Harada's camphorsultam phthalic acid (CSP acid), then both the diastereomers were separated by chiral HPLC (Scheme 1). Although we were able to synthesize both the enantiomers and determine the likely absolute configuration of the natural pheromone, this method was not suitable for making large quantities of the pure enantiomers. Here, we report enantiospecific routes to both the enantiomers of the pheromone starting from readily accessible chiral synthons and the results of field trials in New Zealand.

Choosing the appropriate starting material and reagents was crucial, as we were looking for a scalable and cheap synthesis. We reasoned that bicyclic terpenes, such as camphor, would be suitable starting materials. Initially, the commercially available (−)-bornyl acetate was chosen as starting material for optimization toward (−)-pheromone. The keto acetate (−)-2, prepared from (−)-bornyl acetate following literature procedures,[5] was subjected to Baeyer−Villiger oxidation using H_2O_2−H_2SO_4 conditions in acetic acid (Scheme 2).[6] We settled on these conditions after a few initial optimizations (*m*-CPBA along with additives such as $NaHCO_3$, PTSA, $BF_3 \cdot Et_2O$, $Sc(OTf)_3$). The reaction with *m*-CPBA was very sluggish and gave a mixture of products, and we could not isolate the desired compound in pure form. The present condition using H_2O_2/H_2SO_4 in acetic acid followed by acetate hydrolysis gave the trans-lactonized product (−)-3 along with a minor amount of the bicyclic lactone (−)-3a. The structure of (−)-3 was unambiguously confirmed by X-ray crystal structure analysis. This translactonization (lactone to lactone rearrangement) might have occurred under the reaction conditions to relieve the extra ring strain of the [3.2.1] bicyclic lactone.[7] The lactone (−)-3 was subjected to PDC oxidation to provide (−)-4 in 89% yield. Compound (−)-4 was refluxed in methanol in the presence of PTSA to obtain cyclopentenone derivative (−)-5, whose transesterification followed by dehydration took place in a single-pot operation.[8] The allylic alcohol 6 prepared by Luche reduction of (−)-5 was then subjected to deoxygenation using $BF_3 \cdot Et_2O$ and sodium cyanoborohydride.[9]

Scheme 1. Access to Enantipure Pheromones

Scheme 2. Synthesis of (−)-(R)-Pheromone

ORTEP of (-)-3[12]
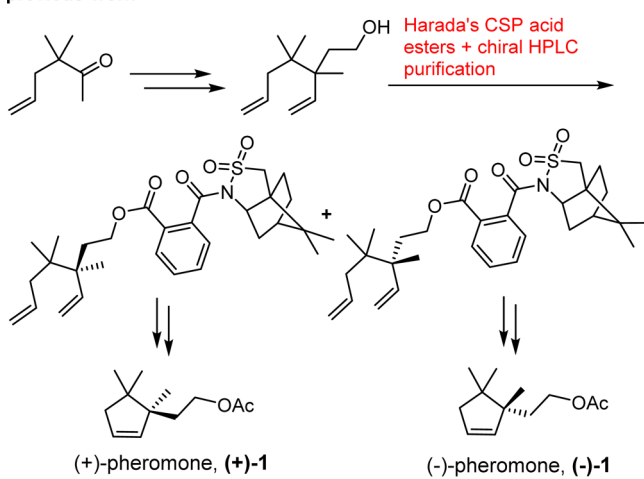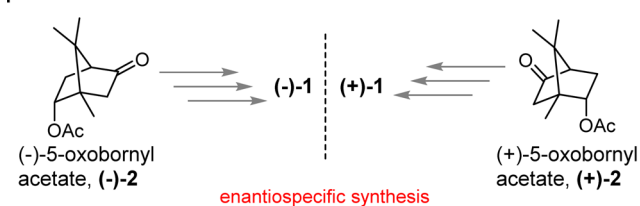
This reaction gave a mixture of both the olefin regioisomers **7** and **7a** in a 10:3 ratio, which on reduction with LiAlH$_4$ resulted in (−)-**8** and (+)-**8a**, with a combined yield of 82%.[10] Although alcohols were inseparable by TLC, we were able to separate them by careful column chromatography. The pure alcohol (−)-**8** was acylated to give the unnatural enantiomer of the pheromone (−)-**1**. The NMR data and optical rotation were in good agreement with the previously reported data.[4,11]

In analogous fashion, the synthesis of the natural enantiomer, (+)-**1** was accomplished from (+)-5-oxo-bornylacetate, (+)-**2**, which in turn was prepared from (+)-camphor using a published procedure (Scheme 3).[5,11,13]

Previously, both the enantiomers and the racemate had been tested in California (USA) vineyards, demonstrating that both the (+)-enantiomer and the racemate were active. We wanted to test all three forms in a completely different geographical location (a New Zealand vineyard infested with the longtailed mealybug) because during initial testing of the racemate in New Zealand, results did not appear as promising as they did in California. Accordingly, a field trial was established in a Hawke's Bay vineyard (39°33′0.93″ S, 176°53′34.13″ E) containing sauvignon blanc vines known to be infested with *Pseudococcus longispinus*. Thus, in March 2014, we tested delta sticky traps baited with red rubber septa dosed with one of the following: 10 μg of (+)-**1**, 10 μg of (−)-**1**, 20 μg of racemic pheromone, or a solvent blank.

The results from the New Zealand trials show that the (+)-enantiomer (+)-**1** was significantly more attractive than the racemate, or the (−)-enantiomer (−)-**1** (Figure 1). Previous work[4] also had shown the highest catches in trap baited with (+)-**1** but not significantly different from the racemate. Here, we report the highest catches again with (+)-**1**, but this time, statistical analysis does show a significant difference from the racemate. The minimal catch of the (−)-**1** treatment is likely a result of contamination with trace amounts of (+)-**1**.[14]
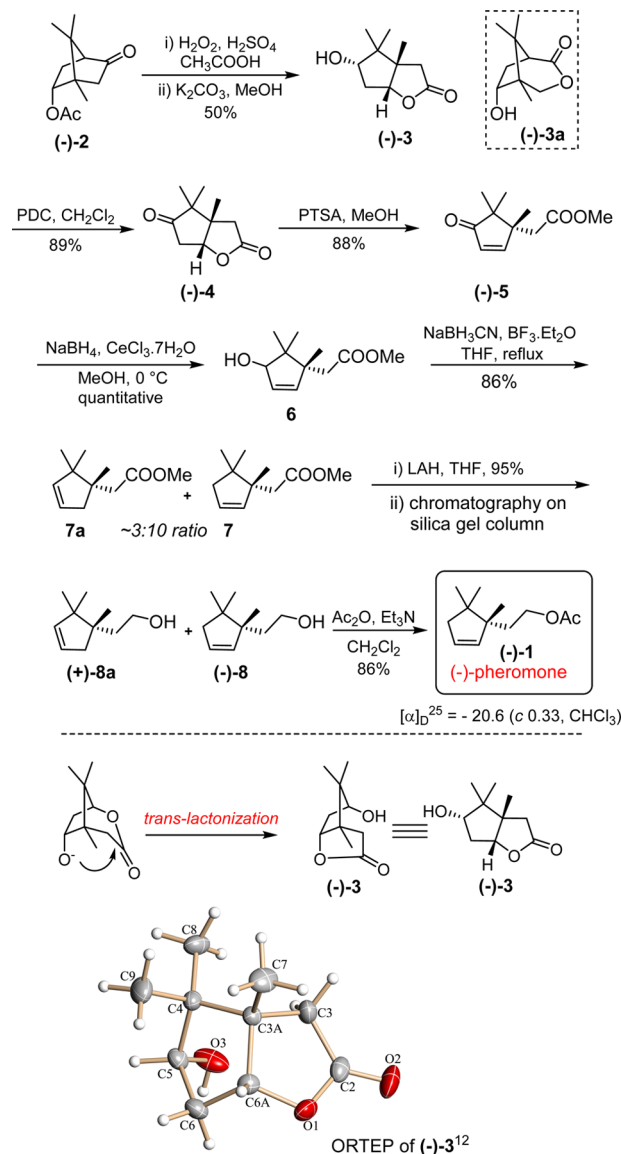
In summary, we have developed a new route for the enantiospecific synthesis of both the natural and unnatural enantiomers of the sex pheromone of the longtailed mealybug. Significantly, the route does not rely on the difficult separation of diasteromeric derivatives but on use of readily available enantipure starting materials from the chiral pool. Trapping trials with the enantiomers in New Zealand further confirmed that the (+)-enantiomer is highly attractive to male longtailed mealybugs.

■ EXPERIMENTAL SECTION

General. All reagents, starting materials, and solvents (including dry solvents) were obtained from commercial suppliers and used as such without further purification. Reactions were carried out in oven-dried glassware under a positive pressure of argon unless otherwise mentioned. Air sensitive reagents and solutions were transferred via syringe or cannula and were introduced to the apparatus via rubber septa. Reactions were monitored by thin layer chromatography (TLC) with 0.25 mm precoated silica gel plates (60 F254). Visualization was accomplished with either UV light, iodine adsorbed on silica gel, or by immersion in ethanolic solution of phosphomolybdic acid (PMA), *p*-anisaldehyde, or KMnO$_4$ followed by heating with a heat gun for ~15 s. Column

Scheme 3. Synthesis of (+)-(S)-Pheromone
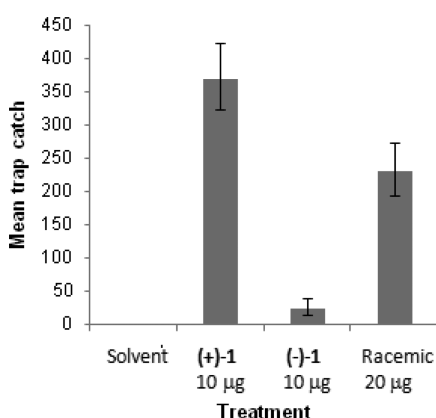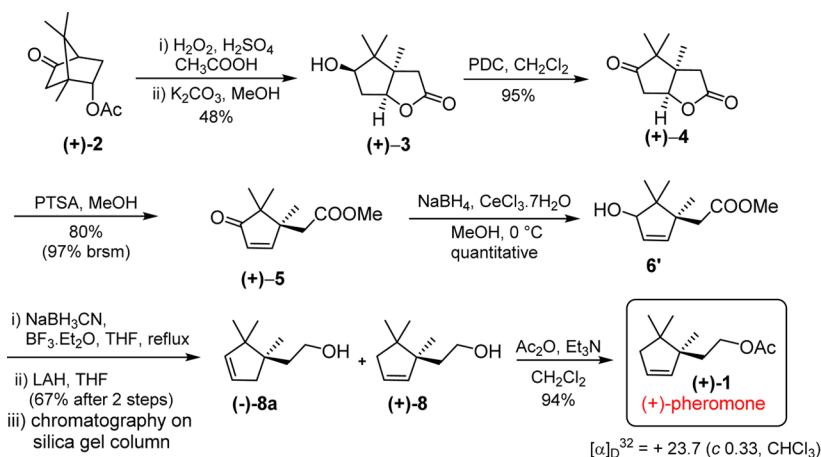
Figure 1. Mean numbers of male *Pseudococcus longispinus* caught per trap in a New Zealand vineyard using pheromone enantiomers, racemate, or solvent controls (*n* = 5 for each treatment). Error bars are 95% confidence limits for the means. Trap catches varied significantly between all treatments (*P* < 0.001).

chromatography was performed on silica gel (100−200 or 230−400 mesh size). Deuterated solvents for NMR spectroscopic analyses were used as received. All ^{1}H NMR and ^{13}C NMR spectra were obtained using a 200, 400, or 500 MHz spectrometer. Coupling constants were measured in Hertz. All chemical shifts were quoted in ppm, relative to TMS, using the residual solvent peak as a reference standard. The following abbreviations were used to explain the multiplicities: s = singlet, d = doublet, t = triplet, q = quartet, m = multiplet, and br = broad. HRMS (ESI) were recorded on an ORBITRAP mass analyzer. Infrared (IR) spectra were recorded on a FT-IR spectrometer as thin films using NaCl plates. Optical rotations were recorded on a polarimeter at 589 nm. Chemical nomenclature was generated using Chem Bio Draw Ultra 14.0.

Synthesis of (R)-(−)-Pheromone. *(3aS,5S,6aR)-5-Hydroxy-3a,4,4-trimethylhexahydro-2H-cyclopenta[b]furan-2-one ((−)-3).* Acetic acid (6 mL) and H_2O_2 (35 wt % in water, 5 mL) were taken in a single neck round-bottomed flask and cooled to 0 °C, and H_2SO_4 (1 mL) was added. Then a solution of (−)-2^5 (1.9 g, 9.03 mmol) in acetic acid (3 mL) was added and stirred at RT for 24 h. Ethyl acetate was added, and the aqueous layer was extracted thrice (30 mL × 3). The combined organic layer was dried over Na_2SO_4, and the solvent was evaporated under reduced pressure. The crude thus obtained was dissolved in methanol (20 mL), K_2CO_3 (3.74 g, 27.09 mmol) was added, and stirred at RT for 3 h. The reaction mixture was passed through Celite, and the filtrate was concentrated and purified by column chromatography (230−400 silica gel) using 25−30% ethyl acetate/pet ether to afford the product (−)-3 as a colorless crystalline solid (832 mg, 50%) along with minor amount of (−)-3a (5:2 ratio in this experiment). Mp = 224−226 °C; $[\alpha]_D^{29}$ −9.2 (c 0.33, CHCl$_3$); ^{1}H NMR (400 MHz,

CDCl$_3$) δ ppm 4.55 (dd, J = 8.6, 2.0 Hz, 1H), 3.92 (dd, J = 5.6, 1.7 Hz, 1H), 3.35 (d, J = 18.1 Hz, 1H), 2.51 (ddd, J = 15.9, 8.6, 5.9 Hz, 1H), 2.07 (d, J = 18.1 Hz, 1H), 1.88 (dt, J = 16.1, 2.0 Hz, 1H), 1.73 (brs, 1H), 1.14 (s, 3H), 1.04 (s, 3H), 0.85 (s, 3H); ^{13}C NMR (100 MHz, CDCl$_3$) δ ppm 177.9, 90.5, 81.4, 50.7, 46.5, 40.2, 39.8, 24.2, 22.1, 18.2; IR ν_{max} (thin film applied as CHCl$_3$ solution) 3470 (broad peak), 2969, 1764, 1069 cm^{-1}. HRMS (ESI): m/z calculated for C$_{10}$H$_{16}$O$_3$Na [M + Na]$^+$ 207.0992; found, 207.0985.

X-ray Crystal Structure Details of (−)-3. Single crystals of compound (−)-3 was obtained from chloroform. X-ray intensity data were collected on a APEX II CCD diffractometer with graphite-monochromatized (Mo Kα = 0.71073 Å) radiation at room temperature 296(2) K. The X-ray generator was operated at 50 kV and 30 mA. Diffraction data were collected with a ω scan width of 0.5° and at different settings of φ and 2θ. The sample-to-detector distance was fixed at 5.00 cm. The X-ray data acquisition was monitored by an APEX II program suite.[15] All the data were corrected for Lorentz-polarization and absorption effects using SAINT and SADABS programs integrated in the APEX II program package.[15] The structures were solved by a direct method and refined by full matrix least-squares, based on F^2, using SHELX-97.[16] ORTEP diagrams were generated using the XSHELL program integrated in the SHELXTL package[16] with 30% probability displacement ellipsoids, and H atoms are shown as small spheres of arbitrary radii. All of the H atoms were placed in geometrically idealized position (C−H = 0.97 Å for the methylene H atom, C−H = 0.96 Å for the methyl H atom, C−H = 0.98 Å for the methine H atom, and O−H = 0.82 Å for the hydroxyl H atom) and constrained to ride on their parent atoms [U_{iso}(H) = 1.2U_{eq}(C) for the methylene and methine group, U_{iso}(H) = 1.5 U_{eq}(C) for the methyl group and U_{iso}(H) = 1.5U_{eq}(O) for the hydroxyl group].

Crystallographic Data for (−)-3. (C$_{10}$H$_{16}$O$_3$): M = 184.23. Crystal dimensions 0.64 × 0.60 × 0.20 mm^3, orthorhombic, space group $P2_12_12_1$, a = 6.9872(7), b = 11.6575(12), c = 11.8586(12) Å, V = 965.92(17) Å^3, Z = 4, ρ_{calcd} = 1.267 gcm^{-3}, μ (Mo−K$_\alpha$) = 0.092 mm^{-1}, $F(000)$ = 400, 2θ_{max} = 50.00°, T = 296(2) K, 5178 reflections collected, 1648 unique, 1532 observed ($I > 2\sigma$ (I)) reflections, 122 refined parameters, R value 0.0329, wR2 = 0.0806, (all data R = 0.0356, wR2 = 0.0824), S = 1.091, minimum and maximum transmission 0.943 and 0.982; maximum and minimum residual electron densities +0.09 and −0.11 e Å^{-3}.

(1S,5R,6R)-6-Hydroxy-5,8,8-trimethyl-3-oxabicyclo[3.2.1]octan-2-one ((−)-3a). In the above experiment, compound (−)-3a was also isolated as a colorless solid (330 mg, 20%). Mp = 264−267 °C; $[\alpha]_D^{28}$ −10.8 (c 0.28, CHCl$_3$); ^{1}H NMR (400 MHz, CDCl$_3$) δ ppm 4.54 (d, J = 12.7 Hz, 1H), 4.23 (dd, J = 9.6, 2.9 Hz, 1H), 3.84 (d, J = 12.5 Hz, 1H), 2.63−2.55 (m, 1H), 2.46 (d, J = 7.6 Hz, 1H), 1.81 (brs, 1H), 1.64 (dd, J = 14.9, 3.9 Hz, 1H), 1.08 (s, 3H), 0.93 (s, 3H), 0.89 (s, 3H); ^{13}C NMR (100 MHz, CDCl$_3$) δ ppm 174.9, 76.3, 70.4, 51.7, 46.3, 42.0, 36.0, 21.5, 20.2, 13.2; IR ν_{max} (thin film applied as CHCl$_3$ solution) 3480 (broad peak), 2965, 1716, 1461, 1246, 1057 cm^{-1}. HRMS (ESI): m/z calculated for C$_{10}$H$_{16}$O$_3$Na [M + Na]$^+$ 207.0992; found, 207.0992.

(3aS,6aR)-3a,4,4-Trimethyltetrahydro-2H-cyclopenta[b]furan-2,5(3H)-dione ((−)-4). To a solution of (−)-3 (1.2 g, 6.5 mmol) in dry DCM (20 mL), 4 Å molecular sieves was added followed by PDC (3.7 g, 9.8 mmol) and stirred at RT overnight. The reaction mass was filtered through Celite. The filtrate was washed with 1 N HCl, dried over Na_2SO_4, and concentrated. The crude mass was purified by column chromatography (100−200 silica gel) using 15% ethyl acetate/pet ether to give the compound as a white crystalline solid (1.05 g, 89% yield). Mp = 169−171 °C; $[\alpha]_D^{29}$ −98.3 (c 0.32, CHCl$_3$); ^{1}H NMR (400 MHz, CDCl$_3$) δ ppm 4.79 (dd, J = 9.0, 4.2 Hz, 1H), 3.02 (dd, J = 20.3, 8.8 Hz, 1H), 2.44 (dd, J = 20.3, 4.2 Hz, 1H), 2.32 (AB quartet, 2H), 1.27 (s, 3H), 1.08 (s, 3H), 1.02 (s, 3H); ^{13}C NMR (100 MHz, CDCl$_3$) δ ppm 216.3, 175.3, 82.7, 52.4, 50.1, 41.1, 39.0, 21.2, 19.3, 18.8; IR ν_{max} (thin film applied as CHCl$_3$ solution) 2973, 2884, 1783, 1747, 1460, 1288, 1177, 1050 cm^{-1}. HRMS (ESI): m/z calculated for $C_{10}H_{15}O_3$ [M + H]$^+$ 183.1016; found, 183.1011.

Methyl (R)-2-(1,5,5-Trimethyl-4-oxocyclopent-2-en-1-yl)acetate ((−)-5). The compound (−)-4 (900 mg, 4.95 mmol) was dissolved in dry methanol (20 mL), and PTSA monohydrate (3.8 g, 19.8 mmol) was added and refluxed for 24 h. The reaction mass was cooled to RT, and solvent was removed under reduced pressure. Water (10 mL) and DCM (25 mL) were added, and the organic layer was separated, the aqueous layer was extracted with DCM (20 mL × 2), and the combined organics were dried over Na_2SO_4 and concentrated under reduced pressure. The pure product was obtained by column chromatography (silica gel 100−200) using 10% ethyl acetate/pet ether to afford the product as a colorless liquid (850 mg, 88% yield) along with the recovery of starting material (60 mg, 94% brsm). $[\alpha]_D^{29}$ −4.4 (c 0.34, CHCl$_3$); ^{1}H NMR (500 MHz, CDCl$_3$) δ ppm 7.71 (d, J = 5.8 Hz, 1H), 6.08 (d, J = 5.8 Hz, 1H), 3.71 (s, 3H), 2.51 (d, J = 14.9 Hz, 1H), 2.39 (d, J = 14.9 Hz, 1H), 1.18 (s, 3H), 1.09 (s, 3H), 1.06 (s, 3H); ^{13}C NMR (125 MHz, CDCl$_3$) δ ppm 213.5, 171.9, 168.5, 129.0, 51.6, 51.3, 48.5, 41.5, 23.0, 22.7, 20.9; IR ν_{max} (thin film applied as CHCl$_3$ solution) 2969, 2883, 1715, 1594, 1203 cm^{-1}. HRMS (ESI): m/z calculated for $C_{11}H_{17}O_3$ [M + H]$^+$ 197.1172; found, 197.1173.

Methyl (R)-2-(1,5,5-trimethylcyclopent-2-en-1-yl)acetate (7). A solution of (−)-5 (70 mg, 0.356 mmol) in dry methanol (3 mL) was cooled to 0 °C, added CeCl$_3$·7H$_2$O (146 mg, 0.392 mmol), followed by sodium borohydride (27 mg, 0.712 mmol) and stirred at RT for 1 h. The reaction mass was cooled to 0 °C and quenched with sat. NH$_4$Cl, and methanol was removed in a rotary evaporator. Ethyl acetate (10 mL) was added, and the aqueous layer was extracted (10 mL × 3), dried over Na_2SO_4, and concentrated to give the allyl alcohol **6** as a colorless liquid (70 mg, quantitative).

A solution of **6** (70 mg, 0.353 mmol) in dry THF (3 mL) was cooled to 0 °C, BF$_3$·Et$_2$O (0.13 mL, 1.059 mmol) was added, followed by sodium cyanoborohydride (66 mg, 1.059 mmol) and refluxed overnight. The reaction was quenched with 2 N NaOH, DCM (10 mL) was added, and the organic layer was separated. It was then dried over Na_2SO_4, concentrated, and purified by column chromatography (silica gel 230−400 gel) using 2% ethyl acetate/pet ether to give product **7** as a mixture with its regioisomer **7a** (55 mg, 86% combined yield, 10:3 ratio by NMR). Data for the major isomer **7**: ^{1}H NMR (400 MHz, CDCl$_3$) δ ppm 5.80−5.76 (m, 1H), 5.68−5.65 (m, 1H), 3.68 (s, 3H), 2.44−2.07 (m, 4H), 0.99 (s, 6H), 0.96 (s, 3H); ^{13}C NMR (100 MHz, CDCl$_3$) δ ppm 173.6, 138.7, 127.9, 51.2, 49.8, 46.7, 44.1, 40.6, 24.4, 24.0, 19.8.

(R)-2-(1,5,5-Trimethylcyclopent-2-en-1-yl)ethan-1-ol ((−)-8). The regioisomeric mixture (**7** and **7a**) obtained in the above step was used to prepare the title compound. This mixture (50 mg, 0.275 mmol) was dissolved in dry THF (3 mL), cooled to 0 °C, added to LAH (31 mg, 0.824 mmol), and stirred at RT for 2 h. The reaction mixture was quenched with saturated Na$_2$SO$_4$ solution, ethyl acetate (10 mL) was added, and the organic layer was separated, the aqueous layer was again extracted (10 mL X 2), dried over Na_2SO_4, concentrated in a rotary evaporator, and purified by column chromatography (silica gel 230−400 mesh) using 5% ethyl acetate/pet ether to give the product as a colorless liquid (40 mg, 95% yield along with its regioisomer (+)-**8a**). Both the regioisomers could be separated by flash column chromatography, although they were inseparable in TLC. $[\alpha]_D^{26}$ −10.4 (c 1.14, CHCl$_3$); ^{1}H NMR (400 MHz, CDCl$_3$) δ ppm 5.65−5.63 (m, 1H), 5.59−5.57 (m,

1H), 3.81−3.68 (m, 2H), 2.15−2.13 (m, 2H), 1.73−1.65 (m, 1H), 1.59−1.52 (m, 1H), 0.97 (s, 3H), 0.95 (s, 3H), 0.90 (s, 3H). HRMS (ESI): m/z calculated for $C_{10}H_{19}O$ [M + H]$^+$ 155.1435; found, 155.1430.

(S)-2-(1,2,2-Trimethylcyclopent-3-en-1-yl)ethan-1-ol ((+)-8a). $[\alpha]_D^{25}$ +14.5 (c 0.17, CHCl$_3$); ^{1}H NMR (500 MHz, CDCl$_3$) δ ppm 5.54−5.51 (m, 1H), 5.44−5.43 (m, 1H), 3.79−3.64 (m, 2H), 2.32−2.28 (m, 1H), 2.03−2.00 (m, 1H), 1.73−1.60 (m, 2H), 0.92 (s, 3H), 0.90 (s, 3H), 0.90 (s, 3H).

(R)-2-(1,5,5-Trimethylcyclopent-2-en-1-yl)ethyl acetate ((−)-1). To a solution of (−)-8 (10 mg, 0.065 mmol) in dry DCM (2 mL), triethylamine (36 µL, 0.26 mmol) and acetic anhydride (12 µL, 0.13 mmol) were added, followed by a pinch of DMAP, and stirred at RT for 3 h. The reaction mixture was diluted with DCM, water was added, the organic layer was separated, dried over Na_2SO_4, concentrated, and purified by column chromatography (100−200 silica gel) using 20% DCM/pentane to afford the product as a colorless liquid (11 mg, 86%). $[\alpha]_D^{25}$ −20.6 (c 0.33, CHCl$_3$); ^{1}H NMR (400 MHz, CDCl$_3$) δ ppm 5.66−5.63 (m, 1H), 5.58−5.56 (m, 1H), 4.24−4.07 (m, 2H), 2.14 (t, J = 2.2 Hz, 2H), 2.06 (s, 3H), 1.75−1.68 (m, 1H), 1.63−1.54 (m, 1H, merged with moisture peak), 0.97 (s, 3H), 0.96 (s, 3H), 0.91 (s, 3H). HRMS (ESI): m/z calculated for $C_{12}H_{20}O_2Na$ [M + Na]$^+$ 219.1356; found, 219.1355.

Synthesis of (S)-(+)-Pheromone. The same route was followed for the synthesis of the other antipode (S)-(+)-pheromone starting from (+)-**2**.[5,13] The NMR data of all the compounds in this series were found to be exactly matching with the other enantiomeric series. The optical rotations also showed the same magnitude but with an inverse sign.

(3aR,5R,6aS)-5-Hydroxy-3a,4,4-trimethylhexahydro-2H-cyclopenta[b]furan-2-one (+)-3. Yield: 48%; $[\alpha]_D^{28}$ +6.8 (c 0.34, CHCl$_3$).

(3aR,6aS)-3a,4,4-Trimethyltetrahydro-2H-cyclopenta[b]furan-2,5(3H)-dione (+)-4. Yield: 95%; $[\alpha]_D^{28}$ +98.3 (c 0.27, CHCl$_3$).

Methyl (S)-2-(1,5,5-trimethyl-4-oxocyclopent-2-en-1-yl)acetate (+)-5. Yield: 80%, 97% brsm; $[\alpha]_D^{25}$ +4.5 (c 0.50, CHCl$_3$).

(S)-2-(1,5,5-Trimethylcyclopent-2-en-1-yl)ethan-1-ol ((+)-8). $[\alpha]_D^{26}$ +11.3 (c 0.30, CHCl$_3$)

(R)-2-(1,2,2-Trimethylcyclopent-3-en-1-yl)ethan-1-ol ((−)-8a). $[\alpha]_D^{24}$ −13.8 (c 0.17, CHCl$_3$); ^{1}H NMR (400 MHz, CDCl$_3$) δ ppm 5.54−5.51 (m, 1H), 5.44−5.43 (m, 1H), 3.79−3.64 (m, 2H), 2.32−2.28 (m, 1H), 2.03−1.98 (m, 1H), 1.73−1.60 (m, 2H), 0.91 (s, 3H), 0.90 (s, 3H), 0.89 (s, 3H); ^{13}C NMR (100 MHz, CDCl$_3$) δ ppm 141.6, 126.2, 61.1, 48.7, 44.9, 44.7, 39.6, 23.8, 22.3, 22.2.

(S)-2-(1,5,5-Trimethylcyclopent-2-en-1-yl)ethyl acetate ((+)-1). Yield: 94%; $[\alpha]_D^{32}$ +23.7 (c 0.33, CHCl$_3$).

Methyl (S)-2-(1,2,2-Trimethyl-3-oxocyclopentyl)acetate. The compound (−)-5 (350 mg, 1.79 mmol) was dissolved in methanol (5 mL), and palladium on carbon (35 mg, 10 wt %) was added and was stirred under an atmosphere of hydrogen for 1 h. The reaction mass was then filtered through Celite and washed with DCM and dried over Na_2SO_4, and the solvent was removed under reduced pressure to give the product as a colorless liquid (330 mg, 93%). $[\alpha]_D^{27}$ −74.5 (c 1.33, CHCl$_3$); ^{1}H NMR (400 MHz, CDCl$_3$) δ ppm 3.64 (s, 3H), 2.36−2.17 (m, 4H), 2.04−1.96 (m, 1H), 1.87−1.80 (m, 1H), 0.97 (s, 3H), 0.90 (s, 3H), 0.89 (s, 3H); ^{13}C NMR (100 MHz, CDCl$_3$) δ ppm 222.3, 172.4, 52.5, 51.4, 43.1, 41.1, 33.6, 30.9, 21.3, 19.8, 18.2; IR ν_{max} (thin film applied as CHCl$_3$ solution) 2968, 1737, 1450, 1206, 1105 cm^{-1}; HRMS $C_{11}H_{18}O_3Na$ [M + Na]$^+$ 221.1148; found, 221.1147.

Methyl (S)-2-(1,2,3-Trimethylcyclopent-2-en-1-yl)acetate (S6). The saturated ketone (50 mg, 0.25 mmol) obtained in the above reaction was dissolved in dry methanol (3 mL) and cooled to 0 °C, and NaBH$_4$ (10 mg, 0.25 mmol) was added cautiously and stirred at RT for 1 h. The reaction mass was cooled to 0 °C and quenched with sat. NH$_4$Cl, and methanol was removed in a rotary evaporator. Ethyl acetate (10 mL) was added, the organic layer was separated, the aqueous layer was again extracted (20 mL × 3), and the combined extracts were dried over Na_2SO_4 and concentrated under reduced pressure to give S5 (40 mg). The crude mass was used for the next step without further purification.

The compound S5 (40 mg, 0.20 mmol) was dissolved in dry benzene (3 mL), and P$_2$O$_5$ (170 mg, 0.599 mmol) was added and refluxed

overnight.[17] The reaction mixture was cooled to RT, diluted with DCM (10 mL), and 2 N NaOH was added. The organic layer was separated, washed with brine, and dried over Na_2SO_4, and the solvent was removed in a rotary evaporator. The reaction mixture was purified by column chromatography (silica gel 100−200) using 2−3% ethyl acetate/pet ether to afford the product as a colorless liquid (28 mg, 78% yield). $[\alpha]_D^{30}$ −6.4 (c 0.19, $CHCl_3$); ^1H NMR (400 MHz, $CDCl_3$) δ ppm 3.61 (s, 3H), 2.26 (AB quartet, 2H), 2.16 (m, 2H), 2.05−1.98 (m, 1H), 1.64−1.55 (m, 1H, merged with methyl singlet), 1.58 (s, 3H), 1.49 (s, 3H), 1.05 (s, 3H); ^{13}C NMR (100 MHz, $CDCl_3$) δ ppm 173.0, 136.0, 131.3, 51.1, 49.7, 43.4, 35.6, 35.2, 25.0, 14.2, 9.4; IR ν_{max} (thin film applied as $CHCl_3$ solution) 3022, 2926, 2856, 1729, 1446, 1322, 1214, 1017 cm^{-1}; HRMS $C_{11}H_{19}O_2$ $[M + H]^+$ 183.1380; found, 183.1379.

(1S,5R)-5,8,8-Trimethyl-2-oxabicyclo[3.2.1]oct-6-en-3-one (S7). $[\alpha]_D^{27}$ −207.3 (c 1.1, $CHCl_3$); ^1H NMR (400 MHz, $CDCl_3$) δ ppm 5.85 (d, J = 5.9 Hz, 1H), 5.65 (dd, J = 5.8, 1.3 Hz, 1H), 5.05 (m, 1H), 2.62 (d, J = 17.1 Hz, 1H), 2.04 (d, J = 17.1 Hz, 1H), 1.19 (s, 3H), 1.03 (s, 3H), 0.98 (s, 3H); ^{13}C NMR (100 MHz, $CDCl_3$) δ ppm 176.9, 146.3, 125.8, 93.8, 51.7, 47.6, 40.0, 26.4, 22.6, 18.4; IR ν_{max} (thin film applied as $CHCl_3$ solution) 3023, 2967, 2876, 1774, 1611, 1457, 1346, 1215, 1178 cm^{-1}; HRMS $C_{10}H_{15}O_2$ $[M + H]^+$ 167.1067; found, 167.1066.

Field Trial of the Pheromone Enantiomers. A field trial of the pheromone was established in a Hawke's Bay vineyard (39°33′0.93″ S, 176°53′34.13″ E) containing sauvignon blanc vines known to be infested with *Pseudococcus longispinus*. Thus, in March 2014, we tested red delta traps with white sticky base baited with red rubber septa dosed with one of the following: 10 μg of (+)-**1**, 10 μg of (−)-**1**, 20 μg of racemic pheromone, or a solvent blank. Using a complete randomized block design, each of the four treatments was replicated five times. The four treatments per trapping row were separated by 25 m; replicate rows were separated by 40 m. The traps were periodically visited during the study. At each visit, traps were allocated a new position within the replicate row using a random number table, with a new sticky base replacing the old one in each trap. Back in the laboratory, male mealybugs were counted. The trapping trial concluded on May 23, 2014. Pheromone lures were not replaced during the trial. The trap counts from March 28 to May 23, 2014 (the first week of data was omitted due to low catch) were analyzed with a Poisson generalized linear model.[18] The model used a logarithmic link function, with dispersion estimated ("Quasi-Poisson").The analysis of deviance assessed various contrasts between the treatments using F-tests. All analyses were carried out with GenStat (version 14). Trap catches of the four treatments were compared examining the effect of the presence of (+)-**1** and the presence/absence of (−)-**1**. Overall, trap catches varied significantly among all of the treatments ($P < 0.001$).

ASSOCIATED CONTENT

Ⓢ Supporting Information

Initial synthetic plan toward pheromones, optimization conditions for deoxygenation, CIF file (CCDC 1058183), and NMR spectra. The Supporting Information is available free of charge on the ACS Publications website at DOI: 10.1021/acs.joc.5b01131.

AUTHOR INFORMATION

Corresponding Author

*E-mail: ds.reddy@ncl.res.in.

Notes

The authors declare no competing financial interest.

ACKNOWLEDGMENTS

DEDICATION

This work is dedicated to Professor D. Basavaiah, University of Hyderabad, on the occasion of his 65th birthday.

REFERENCES

(1) (a) Shorey, H. H. *Annu. Rev. Entomol.* **1973**, *18*, 349−380. (b) Mori, K. *Acc. Chem. Res.* **2000**, *33*, 102−110. (c) Zou, Y.; Millar, J. G. *Nat. Prod. Rep.* **2015**, *32*, 1067−1113. (d) Mori, K. *Proc. Jpn. Acad., Ser. B* **2014**, *90*, 373−388. (e) Mori, K. *Tetrahedron* **1989**, *45*, 3233−3298 and refs cited therein .

(2) (a) Millar, J. G.; Moreira, J. A.; McElfresh, J. S.; Daane, K. M.; Freund, A. S. *Org. Lett.* **2009**, *11*, 2683−2685. (b) Zou, Y.; Chinta, S. P.; Millar, J. G. Irregular Terpenoids as Mealybug and Scale Pheromones: Chemistry and Applications. In *Pest Management with Natural Products*; Beck, J., Coats, J., Duke, S., Koivunen, M., Eds.; ACS Symposium Series; American Chemical Society: Washington, DC, 2013; Vol. *1141*, Chapter 9, pp 125−143.

(3) (a) Zou, Y.; Millar, J. G. *J. Org. Chem.* **2009**, *74*, 7207−7209. (b) Zou, Y.; Millar, J. G. *Synlett* **2010**, *2010*, 2319−2321. (c) Bailey, W. F.; Bakonyi, J. M. *J. Org. Chem.* **2013**, *78*, 3493−3495. (d) Kurhade, S. E.; Siddaiah, V.; Bhuniya, D.; Reddy, D. S. *Synthesis* **2013**, *45*, 1689−1692.

(4) Ramesh, R.; Swaroop, P. S.; Gonnade, R. G.; Thirupathi, C.; Waterworth, R. A.; Millar, J. G.; Reddy, D. S. *J. Org. Chem.* **2013**, *78*, 6281−6284.

(5) (a) Tartaggia, S.; Padovan, P.; Borsato, G.; De Lucchi, O.; Fabris, F. *Tetrahedron Lett.* **2011**, *52*, 4478−4480. (b) Acerson, M. J.; Bingham, B. S.; Allred, C. A.; Andrus, M. B. *Tetrahedron Lett.* **2015**, *56*, 3277−3280.

(6) (a) Hassall, C. H. The Baeyer-Villiger oxidation of aldehydes and ketones. *Org. React.* **2011**, *9* (3), 73−106. (b) Grudzinski, A.; Roberts, S. M.; Howard, C.; Newton, R. F. *J. Chem. Soc., Perkin Trans. 1* **1978**, 1182−1186 and refs cited therein. .

(7) Although it was not planned in our initial approach, the unexpected observation (trans-lactonization) led to the present route. See more details in the Supporting Information.

(8) Suri, S. C. *Tetrahedron Lett.* **1996**, *37*, 2335−2336.

(9) Srikrishna, A.; Viswajanani, R.; Sattigeri, J. A.; Yelamaggad, C. V. *Tetrahedron Lett.* **1995**, *36*, 2347−2350.

(10) We have tried several conditions for optimizing the deoxygenation step. All of the details are given in the Supporting Information.

(11) In an attempt to determine enantiopurity, we have tried a few methods to resolve the racemic pheromone and alcohol using chiral GC. It was not satisfactory for us to determine the % ee as the baseline separation was not seen. Professor Millar also mentioned in his original paper (see ref 2a of this paper) that it was difficult to resolve the compounds under various methods. As we are starting from chiral pool material and also at no place during the sequence can it (possibly) racemize, we are confident that they are pure enantiomers.

(12) The displacement ellipsoids are drawn at the 50% probability level, and H atoms are shown as small spheres with arbitrary radii.

(13) Jackson, C. L.; Menke, A. E. *Proc. Am. Acad. Arts Sci.* **1882**, *18*, 93−95.

(14) The material used in the present study was from a previous batch (it was from the same batch of California trials; see ref 4).

(15) Bruker *APEX2, SAINT and SADABS*; Bruker AXS Inc.: Madison, WI, 2006.

(16) Sheldrick, G. M. *Acta Crystallogr., Sect. A: Found. Crystallogr.* **2008**, *64*, 112−122.

(17) Paquette, L. A.; Vanucci, C.; Rogers, R. D. *J. Am. Chem. Soc.* **1989**, *111*, 5792−5800.

(18) McCullagh, P.; Nelder, J. A. Generalized Linear Models. In *Monographs on Statistics and Applied Probability*, 2nd ed.; Chapman & Hall: London, 1989; Vol. 37, p 511.

Design, Synthesis, and Identification of Silicon Incorporated Oxazolidinone Antibiotics with Improved Brain Exposure

B. Seetharamsingh,[†] Remya Ramesh,[†] Santoshkumar S. Dange,[†] Pankaj V. Khairnar,[†] Smita Singhal,[‡] Dilip Upadhyay,[‡] Sridhar Veeraraghavan,[§] Srikant Viswanadha,[§] Swaroop Vakkalanka,[§] and D. Srinivasa Reddy*,[†]

[†]CSIR-National Chemical Laboratory, Dr. Homi Bhabha Road, Pune 411008, India
[‡]Daiichi Sankyo India Pharma Pvt. Ltd., Gurgaon, Haryana 122015, India
[§]Incozen Therapeutics Pvt. Ltd., Alexandria Knowledge Park, Turkapally, Rangareddy 500078, India

S *Supporting Information*

ABSTRACT: Therapeutic options for brain infections caused by pathogens with a reduced sensitivity to drugs are limited. Recent reports on the potential use of linezolid in treating brain infections prompted us to design novel compounds around this scaffold. Herein, we describe the design and synthesis of various oxazolidinone antibiotics with the incorporation of silicon. Our findings in preclinical species suggest that silicon incorporation is highly useful in improving brain exposures. Interestingly, three compounds from this series demonstrated up to a 30-fold higher brain/plasma ratio when compared to linezolid thereby indicating their therapeutic potential in brain associated disorders.

KEYWORDS: *Antibacterial, linezolid, oxazolidinone, brain exposure, sila analogue*
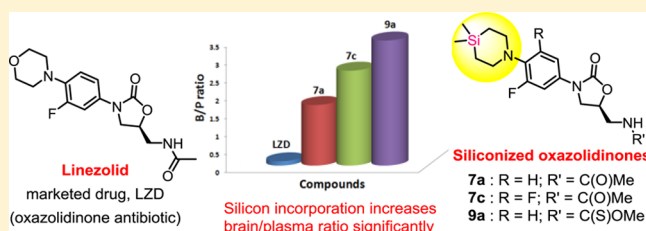
Bacterial meningitis is a very severe condition with sudden onset of symptoms and death within hours. According to WHO statistics, bacterial meningitis affects more than 400 million people per year in the "African meningitis belt". Of the 22 831 cases diagnosed in 2010 across 14 African countries, 2415 deaths were reported with a case-fatality ratio of 10.6%.[1] The diagnosis is done by investigating the cerebrospinal fluid of patients obtained by a lumbar puncture. Since meningitis is fatal, wide spectrum antibiotics are given even before the disease is actually confirmed. The choice of antibiotics depends on the pathogen that causes meningitis, the most common ones being *Streptococcus pneumoniae* and *Neisseria meningitidis*. Cephalosporin, ampicillin, vancomycin, and rifampin are some of the commonly used antibiotics for treating bacterial meningitis.[2] The central nervous system (CNS) is protected by the highly selective blood–brain barrier (BBB) that controls the entry of compounds into the brain. In a normal individual, the BBB efficiently protects the brain from pathogens that can easily cause infections in other parts of the body. While brain infections are not common, they can be difficult to treat in affected individuals due to the inability of drugs to cross the BBB. The BBB, therefore, makes drug delivery to the CNS a challenging task for medicinal chemists.[3,4] In addition to permeability, development of resistance to existing antibiotics is yet another problem encountered in treatment of brain infections. Hence, a global demand and medical need exists to develop novel lipophilic antibiotics with better BBB penetration for treating brain infections.

Linezolid[5,6] is the first oxazolidinone antibiotic to be marketed for clinical use that suppresses bacterial growth via inhibition of ribosomal protein synthesis. Linezolid binds to a site on the 50S ribosomal subunit near its interface with the 30S unit and thus prevents the formation of a 70S initiation complex.[7] Linezolid's broad spectrum of activity against virtually all Gram-positive bacteria, including methicillin resistant and vancomycin resistant bacteria, led to an increased usage of the drug and resulted in significant worldwide sales ever since its approval in 2000. However, only limited information has been established with respect to linezolid's efficacy in treating infections of the central nervous system (CNS). The cerebrospinal fluid (CSF) penetration of linezolid, a limitation observed with other frontline antibiotics in the treatment of CNS infections, is relatively better. Although, it was not evaluated in a large number of patients suffering from CNS infections, positive clinical experience with linezolid was documented in the literature by a few groups.[8,9] To increase the utility of linezolid in CNS infections, synthesis of novel compounds is necessary; in particular, by improving B/P ratios of drug concentrations. Sutezolid (PNU-100480)[10] is another closely related molecule that falls in the oxazolidinone category and is currently in phase II clinical trials for the treatment of both drug resistant and sensitive tuberculosis. While

oxazolidinone antibiotics are typically bacteriostatic, their clinical activity is governed by the clinical dose as well as the pharmacokinetics. Other bacteriostatic agents such as tetracycline and chloramphenicol also possess good CSF penetration and are used in the treatment of bacterial meningitis.[11]

Bioisosterism is one of the widely used methods for the efficient optimization of pharmacokinetic (PK) properties of a lead molecule.[12−14] The incorporation of silicon into known drug scaffolds called the "silicon switch approach" has gained momentum in recent times.[15−22] It is worth highlighting the efforts of Tacke's group for their work on this interesting approach. In general, silicon analogues are more lipophilic than their carbon counterparts. Hence this strategy would be beneficial in CNS drug discovery wherein siliconized compounds could potentially display better blood−brain barrier (BBB) penetration. In our group, we are interested in synthesizing novel bioactive molecules with the incorporation of silicon.[23] Along these lines, we have designed and synthesized silicon analogues of the oxazolidinone antibiotics linezolid/sutezolid. We reasoned that the incorporation of silicon instead of an oxygen atom or sulfur atom in the morpholine/thiomorpholine ring can lead to a more lipophilic molecule, which was further supported by simple clogP calculations (Figure 1).[24,25] Since the morpholine/thiomorpho-

silapiperidines 3a and 3b. These important intermediates were synthesized on multigram scale, which helped us to generate a library of silicon analogues of linezolid without much difficulty. The silapiperidines 3a and 3b on treatment with 3,4-difluoronitrobenzene and 3,4,5-trifluoronitrobenzene, resulted in compounds 4a−4c by a simple nucleophilic aromatic substitution. The nitro group was reduced with H_2−Pd/C in THF followed by Cbz protection of the resulting amine in one pot to give the intermediates 5a−5c. Compounds 5a−5c were treated with chiral building block A[29] in the presence of LiO^{t}Bu in dimethylformamide (DMF) to furnish the oxazolidinone core. Boc deprotection was achieved with trifluoroacetic acid (TFA) in CH_2Cl_2, and the salts were neutralized to afford the free amines 6a−6c (Scheme 1).

Scheme 1. Synthesis of Oxazolidinone Amines with Silicon Incorporation

Figure 1. Design of silicon incorporated oxazolidinones.

line ring is not essential for activity and is amenable to different sterics around this moiety while retaining potency, we anticipated that the newly designed compounds would show similar activity to that of the parent. The details of experimental results are disclosed herein.[26]

The chemical synthesis commenced with the preparation of 1,4-azasilinanes 3a[27] and 3b[28] from commercially available divinylsilanes 1a and 1b. The treatment of HBr gas to vinylsilanes in heptane in the presence of a catalytic amount of dibenzoyl peroxide (DBP) gave bis(bromoethyl)silanes, which on reaction with benzylamine in CHCl₃ resulted in silapiperidines with benzyl protection 2a and 2b, respectively. The compounds 2a and 2b were debenzylated to give the key

These oxazolidinone amines 6a−6c were treated with acetyl chloride and propionyl chloride to give the corresponding amides 7a−7f. Treatment of amines 6a and 6b with carbonyldiimidazole (CDI) followed by addition of methanol produced two methylcarbamate derivatives 8a and 8b.[29] The reaction of amines 6a and 6b with thiophosgene followed by methanol yielded the thiocarbamates 9a and 9b. Similarly, quenching with aqueous ammonia resulted in the thiourea derivatives 9c and 9d (Scheme 2).

For the generation of compounds with varying structural features, compounds 5a−5c were treated with n-BuLi and (R)-glycidyl butyrate to furnish the hydroxyl derivatives 10a−10c. The alcohols 10a and 10b were converted to the corresponding

Scheme 2. Synthesis of Target Oxazolidinones with Silicon Incorporation

R^2COCl, DIPEA
CH_2Cl_2, 0 °C to RT

7a, R = Me, R^1 = H, R^2 = Me (72%)
7b, R = Me, R^1 = H, R^2 = Et (69%)
7c, R = Me, R^1 = F, R^2 = Me (62%)
7d, R = Me, R^1 = F, R^2 = Et (63%)
7e, R = Ph, R^1 = F, R^2 = Me (72%)
7f, R = Ph, R^1 = F, R^2 = Et (76%)

a) CDI, Et_3N
0 °C to RT

b) MeOH
0 °C to RT

8a, R = Me, R^1 = H, R^2 = OMe (37%)
8b, R = Me, R^1 = F, R^2 = OMe (55%)

a) $CSCl_2$, Et_3N
0 °C to RT

b) MeOH/ aq.NH_3
0 °C to RT

9a, R = Me, R^1 = H, R^2 = OMe (40%)
9b, R = Me, R^1 = F, R^2 = OMe (33%)
9c, R = Me, R^1 = H, R^2 = NH_2 (78%)
9d, R = Me, R^1 = F, R^2 = NH_2 (74%)
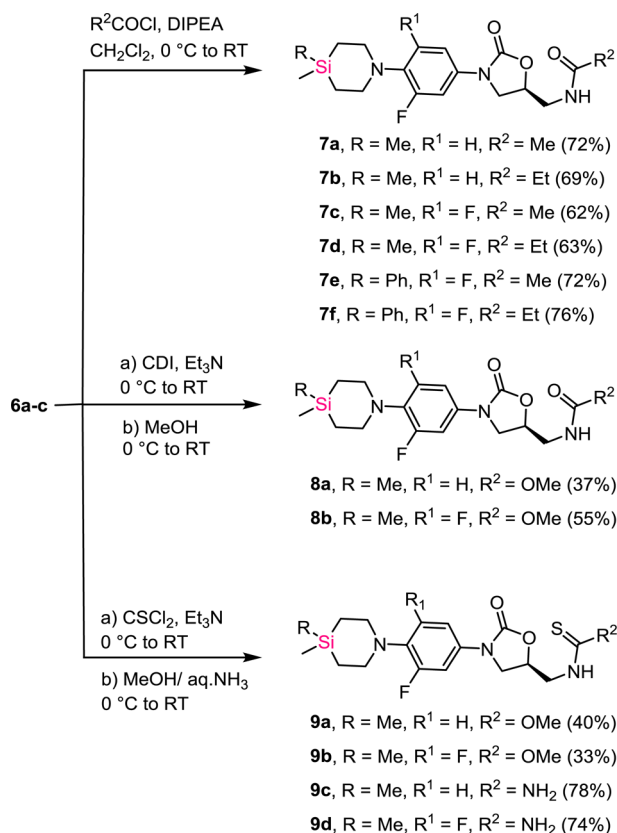
mesylates and the mesylate group was displaced with azide. The azide on heating with norbornadiene underwent a 1,3-dipolar cycloaddition followed by retro Diels−Alder reaction to furnish the triazoles **11a** and **11b**, respectively (Scheme 3).

Scheme 3. Synthesis of Triazole-Based Oxazolidinones

(R)-glycidyl butyrate
n-BuLi, THF, -78 °C to RT

5a, R = Me, R^1 = H
5b, R = Me, R^1 = F
5c, R = Ph, R^1 = F

a) MsCl, Et_3N, CH_2Cl_2
0 °C - RT

b) NaN_3, DMF, 60 °C
c) **B**, 1,4-dioxane, reflux

10a, R = Me, R^1 = H (58%)
10b, R = Me, R^1 = F (62% brsm)
10c, R = Ph, R^1 = F (53% brsm)

B

11a, R = Me, R^1 = H (26% over 3 steps)
11b, R = Me, R^1 = F (40% over 3 steps)
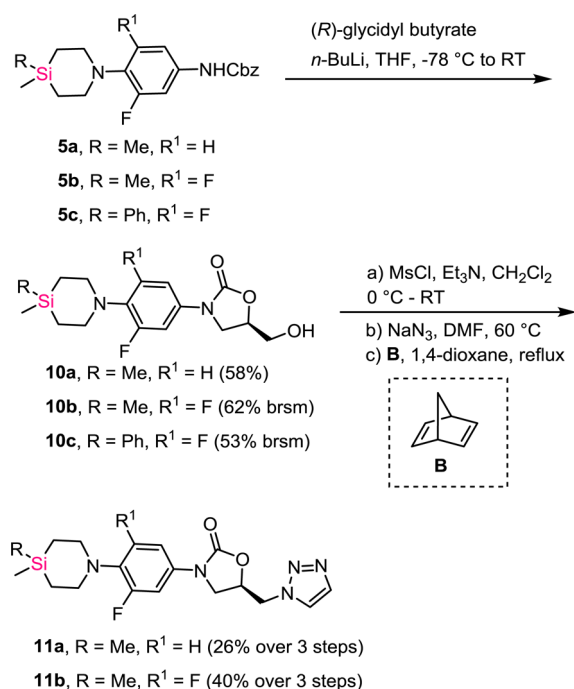
After synthesizing several silicon analogues, the antibacterial activity was assessed against various strains. MIC (minimum inhibitory concentration) of NCEs were determined by microbroth dilution method against facultative bacteria. The screening results of all compounds are provided in the Supporting Information. Among the screened oxazolidinones, the compounds **7a**, **7c**, **7d**, **9a**, and **9d** were more active against a majority of the bacterial strains tested. Compound **7a**, which is the closest linezolid analogue of all the compounds synthesized, showed good potency, but 4−8-fold less potent compared to linezolid across the strains. Introduction of additional fluorine atom on to aromatic ring (**7c**) resulted in a modest improvement in the potency. The compound with thiocarbamate functionality **9a** was the most potent compound in the series with activity comparable to that of linezolid. The presence of phenyl group on silicon resulted in a loss of potency (see Supporting Information). The alcohols **10a**−**10c** were found to be less potent. In general the addition of fluorine atom in the aromatic ring enhanced the antibacterial activity. However, addition of a fluorine atom onto the aromatic ring resulted in a marked decrease in potency (**9a** vs **9b**, see Supporting Information) in compounds belonging to the thiocarbamate series. After analysis of the structural features present in some of the potent oxazolidinones reported in literature, compounds **11a** and **11b** were prepared with triazole moieties in place of N-acyl group.[30] However, we did not observe significant activity with these compounds.

Upon completion of in vitro testing of antibacterial activities, three out of the five best compounds (**7a**, **7c**, and **9a**) from this series were selected for ADME and physicochemical property studies. Specifically, solubility across the pH range, stability in plasma, stability in microsomes, and plasma protein binding were evaluated (results compiled in Table 1). Compound **7a** was soluble across the pH range tested with values being similar to that of linezolid. The solubility of compounds **7c** and **9a** was also comparable to linezolid at acidic pH; however, it was decreased at higher pH conditions. All silicon compounds demonstrated very good plasma stability profile similar to that of linezolid. All three compounds (**7a**, **7c**, and **9a**), along with linezolid, were screened for their microsomal metabolic stability in three different species (mouse, rat, and human). Compounds **7a** and **7c** were moderately stable in both mouse and human liver microsomes with **7c** being superior among the two. Compound **9a** showed poor stability in rodent liver microsomes, but it showed better stability in human microsomes. In the case of plasma protein binding studies, we found striking difference between linezolid and sila compounds. All three compounds, **7a**, **7c**, and **9a**, were strongly bound to the plasma proteins. Hence, this can be an advantage for the improvement in BBB penetration. Although free drug concentrations are generally associated with greater antimicrobial activity, the success of telavancin and daptomycin reflect the benefit associated with high protein binding (lower clearance, longer half-life, and longer duration of action). The discrepancy in findings can be attributed to the difference in the static in vitro test systems vis-à-vis the dynamic nature in an in vivo setting wherein several factors such as binding affinity of the drug to the proteins, transport across barriers, physiological conditions, and metabolism play a major role.[31] Based on the overall in vitro profile, compound **7a** was selected for detailed in vivo pharmacokinetic studies in mice (results are compiled in the table provided in the Supporting Information). Although compound **7a** demonstrated 100% bioavailability and similar

Table 1. *In Vitro* PhysChem and ADME Data

| compd | solubility (μM) at pH | | | | | % plasma stability | | % metabolic stability in liver microsomes (after 30 min) | | | % human PPB |
	1.2	2.2	4.5	7.4	10.2	rat	human	mouse	rat	human	
LZD	50	50	50	49	50	100.0	100.0	100.0	88.3	100.0	26.04
7a	50	50	41	40	41	97.3	100.0	40.8	10.8	48.9	94.33
7c	48	43	20	17	20	94.7	100.0	68.4	9.6	69.8	99.60
9a	48	47	9	2	2	100.0	100.0	15.2	5.7	43.0	100.00

Table 2. Brain PK Comparison of 7a, 7c, 9a, and LZD[a]

| route | 7a | | | 7c | | | 9a | | | LZD | | |
	brain	plasma	B/P ratio	brain	plasma	B/P ratio	brain	plasma	B/P ratio	brain	plasma	B/P ratio
dose	10	10		10	10		10	10		10	10	
N	2	2		2	2		2	2		2	2	
C_{max}	1.33	1.05	**1.27**	5.58	2.02	**2.76**	1.47	0.37	**3.96**	0.45	3.65	**0.12**
AUC$_{0-t}$	3.01	1.78	**1.69**	14.74	5.80	**2.54**	3.11	0.87	**3.57**	0.83	7.58	**0.11**
AUC$_{0-inf}$	3.05	1.80	**1.69**	16.44	6.21	**2.65**	3.24	0.93	**3.49**	0.90	7.70	**0.12**

[a]Units for brain: C_{max} = μg/g, AUC$_{0-t}$ = μg·h/g, AUC$_{0-inf}$ = μg·h/g. Units for plasma: C_{max} = μg/mL, AUC$_{0-t}$ = μg·h/mL, AUC$_{0-inf}$ = μg·h/mL.

Table 3. Antibacterial Activity of Selected Compounds against *S. pneumoniae* and *N. meningitidis*

strain	7a[b]	7c[b]	9a[b]	LZD[b]
S.pneumoniae ATCC 49619	8	16	4	0.5
S.pneumoniae ATCC 6303	4	8	4	0.5
S.pneumoniae 6303 **LZD**^R	>32	>32	32	32
S.pneumoniae ATCC 700904 Pen^R, erm+ve	4	16	4	1
N.meningitidis[a] E-63	32	>32	32	8
N.meningitidis[a] M-1	>32	>32	32	8
N.meningitidis[a] 306	>32	>32	32	8
N.meningitidis[a] E-95	>32	>32	32	8
N.meningitidis[a] 184	>32	>32	32	8

[a]Clinical isolates. [b]MIC values are measured in μg/mL.

half-life as compared to linezolid, it was inferior in terms of C_{max}, AUC, and clearance. However, the volume of distribution (Vz) of **7a** was twice that of linezolid, which can be attributed to its high plasma protein binding. Next, we decided to understand BBB penetrating potential of the silicon compounds, which was the main objective of this project. Toward this goal, all three selected compounds, i.e., **7a**, **7c**, and **9a** were administered through oral route and various parameters were measured. The details of experimental protocol and all the measurements are placed in the Supporting Information. Interestingly, all the three compounds displayed significant brain penetration. Compounds **7a**, **7c**, and **9a** had a 14-, 22-, and 29-fold higher B/P ratios compared to linezolid (see Table 2). These ratios were calculated using AUC measurements. Calculations using C_{max} also gave similar ratios. It is worth highlighting that actual brain concentrations of the sila compounds **7a**, **7c**, and **9a** are much superior with respect to linezolid. Out of the three compounds, **7c** was the best in terms of actual drug concentration (C_{max} = 5.58 μg/g and AUC = 16.44 μg·h/g). As the siliconized linezolid analogues displayed impressive B/P ratio, we became interested in testing these compounds against selected bacterial strains (*S. pneumoniae* and *N. meningitidis*) that cause brain infections.[2] The MIC values generated using various strains suggest that all three compounds possess comparable activity with respect to *S. pneumoniae* (Table 3).[32] However, in the case of *N. meningitidis* strains, only compound **9a** showed significant activity and other two compounds **7a** and **7c** did not show the activity up to 32

μg/mL. Although the antibacterial potencies are less when compared to the marketed drug linezolid, the higher B/P ratio of silicon compounds suggest that incorporation of silicon is beneficial in terms of BBB penetration.

In conclusion, we have designed and synthesized various oxazolidinones with the incorporation of silicon. Three compounds **7a**, **7c**, and **9a** were identified as potential lead molecules from the present series, demonstrating up to 30-fold higher B/P ratio as compared to the marketed antibiotic drug, linezolid. These results can be considered as an initial step toward the development of brain penetrant oxazolidinone antibiotics. The demonstrated concept with the incorporation of silicon into known drug scaffold to improve CNS exposures can also be applied to other classes of compounds. Profiling of selected compounds in brain infected preclinical models is the future course of action and the goal is to further optimize the identified compounds toward the development of an antibiotic that can be useful in treating CNS infections.

■ ASSOCIATED CONTENT

Ⓢ Supporting Information

The Supporting Information is available free of charge on the ACS Publications website at DOI: 10.1021/acsmedchemlett.5b00213.

Experimental details; compound characterization details; screening details; antibacterial data for all the compounds; protocols for pharmacokinetic studies including brain PK; data from mice PK experiments (PDF)

AUTHOR INFORMATION

Corresponding Author
*E-mail: ds.reddy@ncl.res.in.

Author Contributions
The manuscript was written through contributions of all authors. All authors have given approval to the final version of the manuscript.

Funding

Notes
The authors declare no competing financial interest.

DEDICATION

This work is dedicated to Professor Sourav Pal, Indian Institute of Technology, Bombay and former Director, CSIR-NCL, Pune on the occasion of his 60th birthday.

ABBREVIATIONS

NCE, new chemical entity; brsm, based on recovered starting material; LZD, linezolid; ADME, absorption, distribution, metabolism, excretion; N, number of subjects; AUC, area under the curve; $t_{1/2}$, half-life; K_{el}, elimination rate constant; Clz, clearance; BA, bioavailability; B/P ratio, brain to plasma ratio; PPB, plasma protein binding

REFERENCES

(1) Data taken from WHO factsheet on meningitis. http://www.who.int/gho/epidemic_diseases/meningitis/en/ (accessed on May 2015).

(2) Hoffman, O.; Weber, J. R. Pathophysiology and treatment of bacterial meningitis. *Ther. Adv. Neurol. Disord.* **2009**, *2*, 401−412.

(3) Gabathuler, R. Approaches to transport therapeutic drugs across the blood-brain barrier to treat brain diseases. *Neurobiol. Dis.* **2010**, *47*, 48−57.

(4) Hawkins, B. T.; Davis, T. P. The blood-brain barrier/neurovascular unit in health and disease. *Pharmacol. Rev.* **2005**, *57*, 173−185.

(5) Gregory, W. A.; Brittelli, D. R.; Wang, C. L. J.; Wuonola, M. A.; McRipley, R. J.; Eustice, D. C.; Eberly, V. S.; Bartholomew, P. T.; Slee, A. M.; Forbes, M. Antibacterials. Synthesis and structure-activity studies of 3-aryl-2-oxooxazolidines. 1. The "B" group. *J. Med. Chem.* **1989**, *32*, 1673−1681.

(6) Barbachyn, M. R.; Ford, C. W. Oxazolidinone structure−activity relationships leading to linezolid. *Angew. Chem., Int. Ed.* **2003**, *42*, 2010−2023.

(7) Stevens, D. L.; Dotter, B.; Madaras-Kelly, K. A review of linezolid: the first oxazolidinone antibiotic. *Expert Rev. Anti-Infect. Ther.* **2004**, *2*, 51−59.

(8) Rupprecht, T. A.; Pfister, H.-W. Clinical experience with linezolid for the treatment of central nervous system infections. *Eur. J. Neuro.* **2005**, *12*, 536−542.

(9) Nau, R.; Sörgel, F.; Eiffert, H. Penetration of drugs through the blood-cerebrospinal fluid/blood-brain barrier for treatment of central nervous system infections. *Clin. Microbiol. Rev.* **2010**, *23*, 858−883.

(10) Barbachyn, M. R.; Hutchinson, D. K.; Brickner, S. J.; Cynamon, M. H.; Klemens, S. P.; Glickman, S. E.; Grega, K. C.; Hendges, S. K.; Toops, D. S.; Ford, C. W.; Zurenko, G. E. Identification of a novel oxazolidinone (U-100480) with potent antimycobacterial activity. *J. Med. Chem.* **1996**, *39*, 680−685.

(11) Pankey, G. A.; Sabath, L. D. Clinical relevance of bacteriostatic versus bactericidal mechanisms of action in the treatment of gram-positive bacterial infections. *Clin. Infect. Dis.* **2004**, *38*, 864−870.

(12) Patani, G. A.; LaVoie, E. J. Bioisosterism: A rational approach in drug design. *Chem. Rev.* **1996**, *96*, 3147−3176.

(13) Lima, L. M.; Barreiro, E. J. Bioisosterism: A useful strategy for molecular modification and drug design. *Curr. Med. Chem.* **2005**, *12*, 23−49.

(14) Meanwell, N. A. Synopsis of some recent tactical application of bioisosteres in drug design. *J. Med. Chem.* **2011**, *54*, 2529−2591.

(15) Franz, A. K.; Wilson, S. O. Organosilicon molecules with medicinal applications. *J. Med. Chem.* **2013**, *56*, 388−405.

(16) Ortega, R.; Sanchez-Quesada, J.; Lorenz, C.; Dolega, G.; Karawajczyk, A.; Sanz, M.; Showell, G.; Giordanetto, F. Design and synthesis of 1,1-disubstituted-1-silacycloalkane-based compound libraries. *Bioorg. Med. Chem.* **2015**, *23*, 2716−2720.

(17) Geyer, M.; Wellner, E.; Jurva, U.; Saloman, S.; Armstrong, D.; Tacke, R. Can silicon make an excellent drug even better? An in vitro and in vivo head-to-head comparison between loperamide and its silicon analogue sila-loperamide. *ChemMedChem* **2015**, *10*, 911−924.

(18) Tacke, R.; Heinrich, T.; Bertermann, R.; Burschka, C.; Hamacher, A.; Kassack, M. U. Sila-haloperidol: A silicon analogue of the dopamine (D_2) receptor antagonist haloperidol. *Organometallics* **2004**, *23*, 4468−4477.

(19) Mills, J. S.; Showell, G. A. Chemistry challenges in lead optimization: silicon isosteres in drug discovery. *Drug Discovery Today* **2003**, *8*, 551−556.

(20) Mills, J. S.; Showell, G. A. Exploitation of silicon medicinal chemistry in drug discovery. *Expert Opin. Invest. Drugs* **2004**, *13*, 1149−1157.

(21) Gately, S.; West, R. Novel therapeutics with enhanced biological activity generated by the strategic introduction of silicon isosteres into known drug scaffolds. *Drug Dev. Res.* **2007**, *68*, 156−163.

(22) Geyer, M.; Karlsson, O.; Baus, J. A.; Wellner, E.; Tacke, R. Si- and C- Functional organosilicon building blocks for synthesis based on 4-Silacyclohexan-1-ones containing the silicon protecting groups MOP (4-Methoxyphenyl), DMOP (2,6-Dimethoxyphenyl), or TMOP (2,4,6-Trimethoxyphenyl). *J. Org. Chem.* **2015**, *80*, 5804−5811.

(23) Ramesh, R.; Reddy, D. S. Zinc mediated allylations of chlorosilanes promoted by ultrasound: Synthesis of novel constrained sila amino acids. *Org. Biomol. Chem.* **2014**, *12*, 4093−4097.

(24) Vivet, B.; Cavelier, F.; Martinez, J. Synthesis of silaproline, a new proline surrogate. *Eur. J. Org. Chem.* **2000**, *2000*, 807−811.

(25) Calculated logP (ClogP) values were computed by using the ChemBioDraw Ultra14.0 by Perkin-Elmer.

(26) The initial results from this series are patented and available in public domain. Reddy, D. S.; Balamkundu, S.; Ramesh, R. Sila analogs of oxazolidinone derivatives and synthesis thereof. Patent WO 2013054275, 2013.

(27) Wendeborn, S. V.; Lamberth, C.; Nebel, K.; Crowley, P. J.; Nussbaumer, H. Novel triazolepyrimidine derivatives. Patent WO 2006066872, 2006.

(28) Namane, C.; Nicolai, E.; Pacquet, F.; Pascal, C.; Venier, O. Tetrahydroquinoxaline urea derivatives, preparation thereof and therapeutic use thereof. Patent US 20120135958, 2012.

(29) Perrault, W. R.; Pearlman, B. A.; Godrej, D. B.; Jeganathan, A.; Yamagata, K.; Chen, J. J.; Lu, C. V.; Herrinton, P. M.; Gadwood, R. C.; Chan, L.; Lyster, M. A.; Maloney, M. T.; Moeslein, J. A.; Greene, M. L.; Barbachyn, M. R. The synthesis of N-aryl-5(S)-aminomethyl-2-oxazolidinone antibacterials and derivatives in one step from aryl carbamates. *Org. Process Res. Dev.* **2003**, *7*, 533−546.

(30) Cho, Y. L.; Chae, S. E.; Baek, S. Y.; Kim, Y. O.; Kim, S. J.; Lee, H. S.; Park, J. H.; Park, T. K.; Woo, S. H.; Kim, Y. Z. Novel oxazolidinone derivatives with cyclic amidoxime or cyclic amidrazone and pharmaceutical composition thereof. Patent US 20110178293, 2011.

(31) Zeitlinger, M. A.; Derendorf, H.; Mouton, J. W.; Cars, O.; Craig, W. A.; Andes, D.; Theuretzbacher, U. Protein binding: do we ever learn? *Antimicrob. Agents Chemother.* **2011**, *55*, 3067−3074.

(32) We have also determined the cytotoxicity of compounds **7a**, **7c**, and **9a** following 24 h incubation with human hepatoma (HepG2) and tracheal epithelial cells (HTEpiC). Compounds **7c** and **9a** were nontoxic at >10 μM concentration in both HepG2 and HTEpiC cells. However, the IC$_{50}$ of compound **7a** incubation was 9 μM in HepG2 cells and 5 μM in HTEpiC cells. Details are provided in the Supporting Information.

Silicon Incorporated Morpholine Antifungals: Design, Synthesis, and Biological Evaluation

Gorakhnath R. Jachak,[†] Remya Ramesh,[†] Duhita G. Sant,[‡] Shweta U. Jorwekar,[‡] Manjusha R. Jadhav,[§] Santosh G. Tupe,*,[‡] Mukund V. Deshpande,*,[‡] and D. Srinivasa Reddy*,[†]

[†]Division of Organic Chemistry and [‡]Biochemical Sciences Division, CSIR-National Chemical Laboratory, Dr. Homi Bhabha Road, Pune-411008, India

[§]National Research Centre for Grapes, Manjri, Solapur Road, Pune-412307, India

S Supporting Information

ABSTRACT: Known morpholine class antifungals (fenpropimorph, fenpropidin, and amorolfine) were synthetically modified through silicon incorporation to have 15 sila-analogues. Twelve sila-analogues exhibited potent antifungal activity against different human fungal pathogens such as *Candida albicans*, *Candida glabrata*, *Candida tropicalis*, *Cryptococcus neoformans*, and *Aspergillus niger*. Sila-analogue **24** (fenpropimorph analogue) was the best in our hands, which showed superior fungicidal potential than fenpropidin, fenpropimorph, and amorolfine. The mode of action of sila-analogues was similar to morpholines, i.e., inhibition of sterol reductase and sterol isomerase enzymes of ergosterol synthesis pathway.
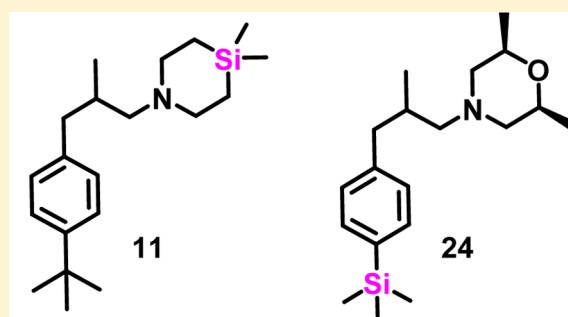
Sila-analogues of morpholine antifungals

KEYWORDS: *Antifungal drugs, Candida albicans, ergosterol biosynthesis, morpholines, sila-analogues*

Steep rise in invasive fungal infections (IFI) mainly in immunocompromised patients, change in epidemiology of IFI, emergence of fungal pathogens, which were previously insignificant, development of resistance against currently used antifungal drugs, and certain drawbacks (like less clinical efficacy, acute and chronic side effects) associated with them necessitate the development of new antifungal drugs.[1,2] Similarly, in agriculture, fungal infections is a major cause for crop loss with consequential heavy economic burden worldwide. Though several groups of fungicides are available, development of resistance against most of them stresses on the need to explore new antifungal agents.[3]

An ideal antifungal agent is one that selectively interacts with a fungal target not found in other eukaryotic cells. The fungal cell wall and cell membrane are attractive therapeutic targets as cell wall constituents such as chitin and major membrane lipid ergosterol are not present in mammalian cells. For instance, from currently used antifungals, three classes of compounds inhibit ergosterol synthesis through selective inhibition of different enzymes involved in the biosynthesis pathway. Allylamines such as terbinafine and naftifine act on squalene epoxidase, and azoles inhibit cytochrome P450 enzyme lanosterol 14-α-demethylase, whereas morpholines act on two different enzymes of this pathway, viz., sterol Δ^{14} reductase and sterol Δ^7-Δ^8 isomerase (Figure 1).[4] Thus, morpholines seem to be ideal antifungals, as acquiring resistance against them will be difficult for a pathogen because of the requirement to mutate two genes of these enzymes. However, only one drug, amorolfine, from this class is used clinically, and its use is restricted to topical application for nail infections, the reason is that though quite effective *in vitro* against different human pathogens, it is ineffective against IFI due to rapid metabolism inside the host.[5] Nevertheless, in agriculture, aldimorph, fenpropimorph, fenpropidin, tridemorph, and dodemorph from this class are in use as fungicides (Figure 1). With this background, we synthesized modified morpholines by incorporating silicon to increase their efficacy and stability.

The introduction of bioisostere is a key strategy used by medicinal chemists during lead optimization process in order to improve the desired biological and physical properties of a potential compound without altering its structure significantly,[6,7] which may lead to improvement in bioactivity and stability or reduction in toxicity of the compound. Chemists have used silicon as a classical bioisostere for carbon as it has similar steric and electronic features and has the same valency as carbon.[8–12] The change in biological activities due to sila-substitution may be attributed to larger bond length, altered bond angles, and different ring conformations due to larger covalent radius of silicon over carbon and increased lipophilicity, which in turn will increase its tissue distribution, particularly uptake through membranes.[13–15] In our group, we are interested in making silicon analogues of biologically active compounds so as to improve their drug-like properties.[16–18] Acker et al. have
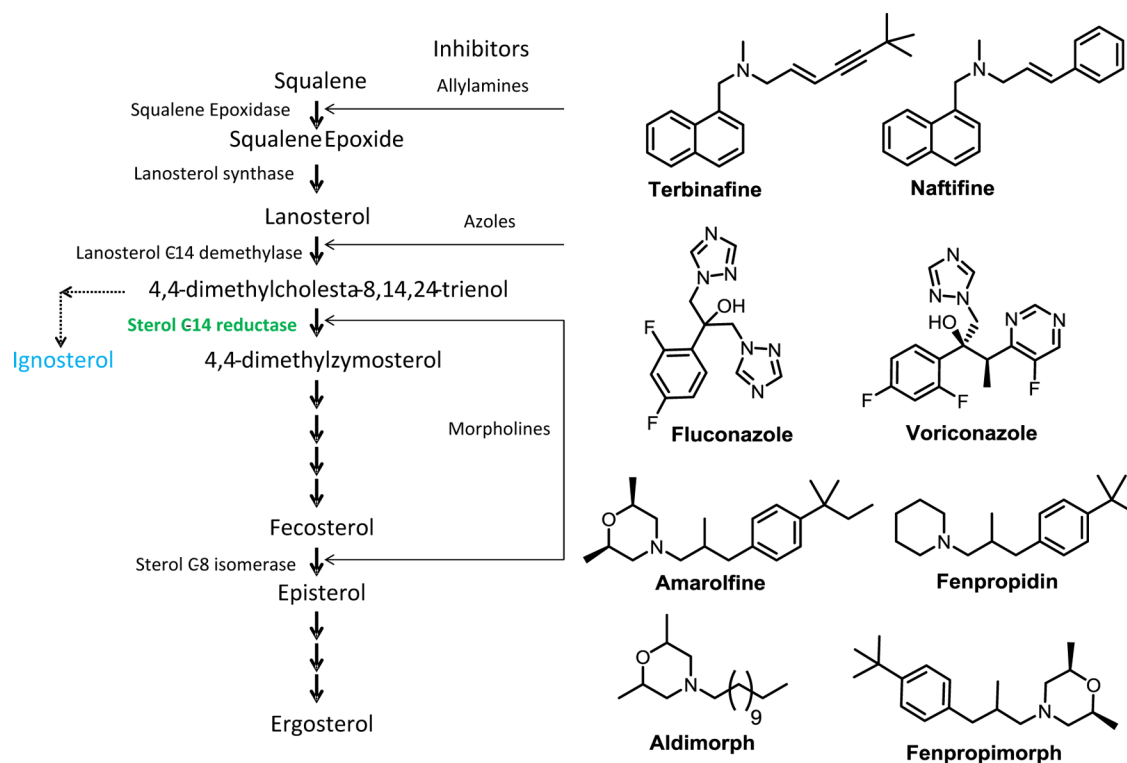
Figure 1. Ergosterol synthesis pathway and known inhibitors of the pathway enzymes.

previously reported the synthesis of siliconized antifungals in the patent literature, but their use was restricted to fungal plant pathogens.[19] Specifically, we have reasoned our design around fenpropimorph and amorolfine, which are closely related antifungals. Generally metabolism of fenpropidin takes place through hydroxylation of the piperidine ring or hydroxylation and oxidation of the methyls of aromatic *t*-butyl group (Figure 2).[20] Closely related amorolfine also undergoes oxidation at isopentyl group present at the *p*-position of the aromatic ring.[21]

We hypothesized that incorporation of silicon at these metabolic soft spots in morpholine antifungals will help to overcome their drawbacks and give more potent and stable

Figure 2. Metabolism of fenpropidin and rationale for our design.

compounds (Figure 2). In general, all the silicon analogues are expected to be more lipophilic compared with fenpropidin, fenpropimorph, and amorolfine. Based on calculated cLogP values, incorporation of one silicon atom showed only slight increase in lipophilicity, but two silicon atoms incorporation resulted in large increase in lipophilicity with respect to fenpropidin (see Table S2 in the Supporting Information). Incorporation of silicon in to heterocycle (piperidine ring) has more effect when compared to silicon incorporation in the aromatic ring. Sometimes, high lipophilicity can be detrimental to the druggable properties such as solubility. This undesired increase in lipohilicity can be counterbalanced by the addition of polar groups to the molecule, for example, morpholine containing silicon analogue showed lower cLogP values with respect to all three fungicides fenpropidin, amorolfine, and fenpropimorph.

To begin with, 4-(trimethylsilyl) benzaldehyde **1** was first prepared from 1,4-dibromobenzene as reported earlier.[22] Treatment of **1** with ylide ethyl-2-(triphenyl phosphanylidene) propanoate in anhydrous toluene at 110 °C, afforded ethyl 2-methyl-3-(4-(trimethylsilyl)phenyl) acrylate, **2**. Hydrogenation of **2** in the presence of 10% Pd/C in EtOH followed by ester hydrolysis using LiOH in THF-MeOH-H$_2$O led to formation of carboxylic acid **3**. Carboxylic acid **3** was then coupled with piperidine under standard conditions using EDC·HCl and HOBt in CH$_2$Cl$_2$ to give the amide **4**. Reduction of amide **4** using LAH in THF afforded the sila-amine **5** (Scheme 1). The furnished carboxylic acid **3** was further exploited to synthesize a library of sila-amines **15−24** (Scheme 1, see details in the Supporting Information). The sulfone derivative **17** was prepared from **16** by *m*-CPBA oxidation. In a similar way, carboxylic acid **6**[23,24] and **7**[23,24] on coupling with 4,4-dimethyl-4-silapiperidine **8**[17,18] using standard protocol followed by reduction of the resulting amide gave amines **11** and **12**, respectively. Carboxylic acid **6** was
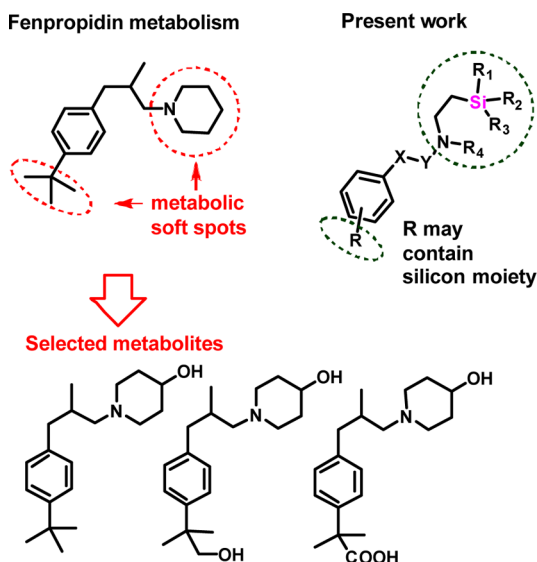
Scheme 1. Synthesis of Silicon Incorporated Morpholines
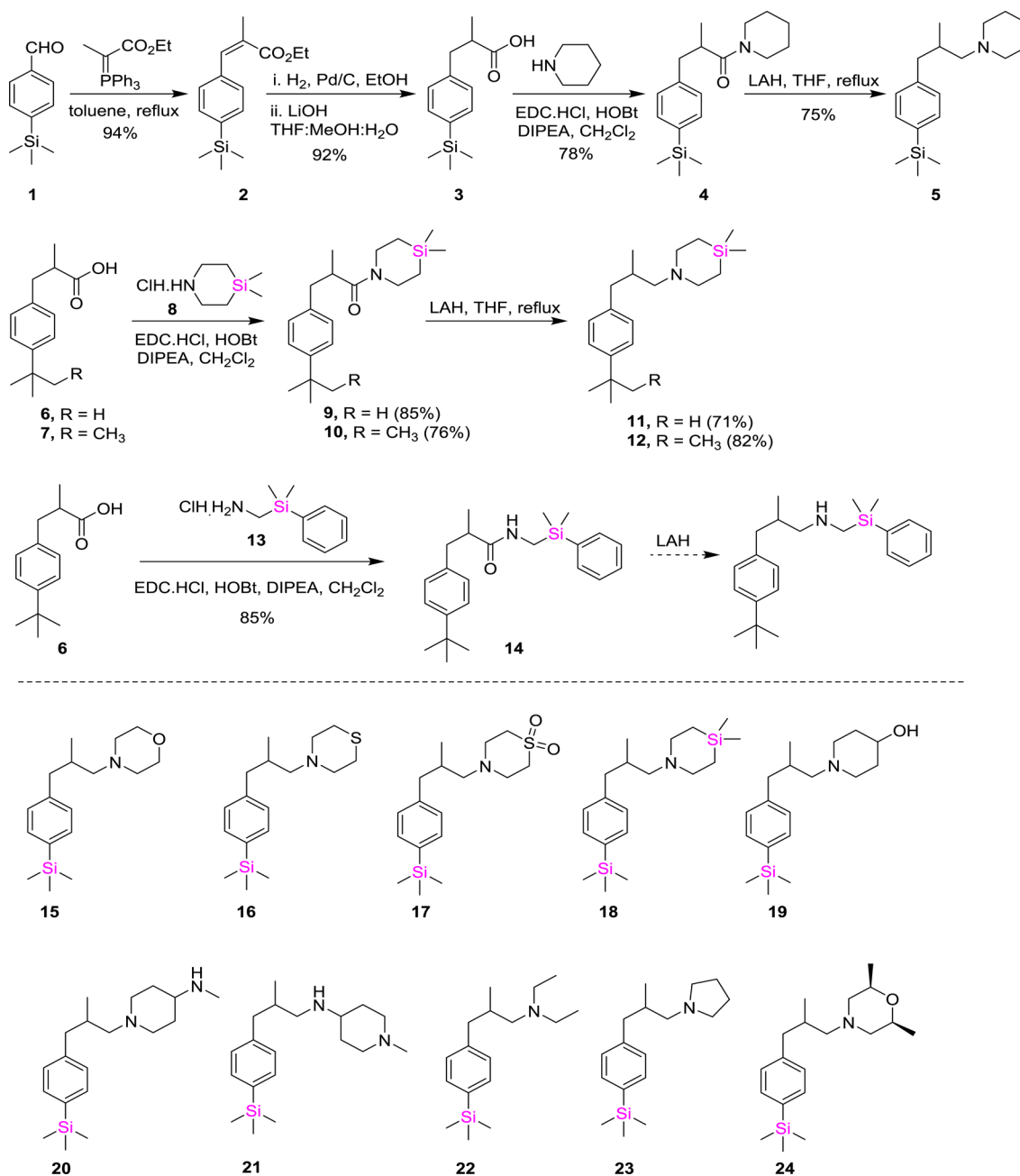
coupled to (dimethyl(phenyl)silyl)methanamine **13** to give the amide **14**. However, reduction of amide carbonyl of **14** to give corresponding amine was not successful. The structures of the compounds were confirmed by ^{1}H NMR, ^{13}C NMR, and HR-MS spectra.

All the synthesized sila-analogues were tested for antifungal activity against different human pathogenic yeasts and filamentous fungi by Clinical Laboratory Standards Institute's (CLSI) broth microdilution assay (CLSI document M27-A3 and CLSI M38-A2).[25,26] The results in terms of IC$_{50}$, i.e., concentration causing 50% growth inhibition, minimum inhibitory concentration (MIC), and minimum fungicidal concentration (MFC) are given in Table 1. From the 15 sila-compounds synthesized, 12 compounds, namely, **5**, **11**, **12**, **15**, **16**, and **18−24**, exhibited potent antifungal activity against *Candida albicans* ATCC 24433, *C. albicans* ATCC 10231,

Candida glabrata NCYC 388, *Candida tropicalis* ATCC 750, *Cryptococcus neoformans* ATCC 34664, and *Aspergillus niger* ATCC 10578 (Table 1). No antifungal effect was observed (MIC $\geq$ 256 μg/mL) for three compounds, viz., **9**, **14**, and **17** against all the pathogens tested. Compounds **9** and **14** are amides suggesting that the basic tertiary nitrogen is essential for the activity. In the case of compound **17**, presence of polar sulfone moiety on heterocycle was found to be detrimental for the activity. The sila fenpropimorph analogue **24** was most effective followed by sila fenpropidin analogues **5** and **15**. It is worth highlighting that silicon incorporation on aromatic ring seems to be more effective compared to silicon incorporation in heterocycle. Compound **24** exhibited better antifungal activity than fluconazole and morpholine fungicides fenpropimorph and fenpropidin against all the pathogens. Further, the MIC values of

Table 1. Antifungal Activity of the Sila-Morpholine Analogues against Different Human Pathogenic Fungi

compd	Candida albicans ATCC 24433			Candia albicans ATCC 10231			Cryptococcus neoformans ATCC 34664			Candida glabrata NCYC 388			Candida tropicalis ATCC 750			Aspergillus niger ATCC 10578		
	IC_{50}[a]	MIC[b]	MFC[c]	IC_{50}	MIC	MFC	IC_{50}	MIC	MFC	IC_{50}	MIC	MFC	IC_{50}	MIC	MFC	IC_{50}	MIC	MFC
5	0.12	0.25	2	0.11	0.25	32	0.0625	0.125	8	0.035	0.125	8	1	4	64	41.24	64	128
11	1.85	4	8	0.31	0.5	0.5	0.875	2	4	1.52	4	8	16	64	64	13.82	32	64
12	1.68	4	16	0.28	0.5	64	1.4	2	4	1.47	4	4	13.8	64	256	0.16	0.5	64
15	0.74	1	8	0.26	0.5	8	0.125	0.5	2	0.144	0.5	16	0.5	8	16	105.93	128	>256
16	0.245	1	8	0.5	1	2	0.80	2	64	0.25	0.5	8	0.25	2	>256	1	2	>256
18	1.25	4	8	0.45	1	4	1.98	8	64	1.75	8	16	44.8	64	>256	0.5	2	>256
19	0.396	1	2	0.19	0.25	4	0.93	2	16	0.196	0.5	8	0.198	4	256	0.25	0.5	256
20	1.55	4	8	1	2	2	3.77	8	8	1.63	2	4	5.87	16	16	1.25	2	64
21	5.13	8	8	1.59	2	2	6.9	16	16	5.92	8	16	1.50	64	256	4.5	8	>256
22	3.75	8	32	0.57	2	4	1.5	4	32	1.85	4	>256	4.85	16	256	64	256	>256
23	0.97	2	8	0.31	0.5	2	0.25	1	4	0.319	1	32	2.76	16	128	50.08	64	256
24	0.043	0.125	0.5	0.25	0.5	1	0.079	0.125	2	0.017	0.125	2	0.164	0.5	64	0.5	2	256
9, 14, 17	≥256	≥256	≥256	≥256	≥256	≥256	≥256	≥256	≥256	≥256	≥256	≥256	≥256	≥256	≥256		≥256	≥256
fenpropidin	0.19	0.25	0.5	0.27	1	2	0.22	1	32	0.1	0.5	16	0.125	4	256	16	32	128
fenpropimorph	0.21	0.5	4	0.833	2	2	0.25	1	64	0.25	1	128	0.125	2	>256	1	4	>256
amorolfine	0.028	1	8	0.1	0.25	32	0.031	0.125	64	0.038	0.125	32	0.173	0.5	>256	0.125	0.5	>256
fluconazole	0.73	2	4	4.21	8	16	4.6	32	>256	16	128	>256	64	>256	>256	>256	>256	>256

[a]IC_{50}, concentration causing 50% growth inhibition. All the values are in $\mu g/mL$. The assay was done twice in triplicate. [b]MIC, minimum inhibitory concentration. All the values are in $\mu g/mL$. The assay was done twice in triplicate. [c]MFC, minimum fungicidal concentration. All the values are in $\mu g/mL$. The assay was done twice in triplicate.

Table 2. Effect of 24 and Amorolfine Treatment on the Sterol Profile of *Candida albicans* ATCC 24433[a]

	control	compound 24 0.125 µg/mL	compound 24 0.25 µg/mL	amorolfine 0.125 µg/mL	amorolfine 0.25 µg/mL
squalene	07.17 ± 0.35	21.52 ± 1.37	13.82 ± 0.81	22.04 ± 1.07	17.08 ± 1.31
ergosterol	73.34 ± 2.53	15.52 ± 0.8	11.12 ± 0.54	30.16 ± 1.48	06.13 ± 0.29
cholesta-8,24-dien-3-ol, 4-methyl-(3a′,4a′)-,	07.19 ± 0.65	05.36 ± 0.61	27.78 ± 1.2	12.26 ± 0.73	12.03 ± 0.67
ergosta-5,8-dien-3-ol, (3a′)	05.15 ± 0.44	ND[b]	ND	ND	ND
cholesta-5,24-dien-3-ol	03.58 ± 0.52	15.34 ± 0.86	0.87 ± 0.18	0.44 ± 0.1	ND
ergosta-8,14-dien-3-ol (ignosterol)	ND	07.23 ± 0.68	42.29 ± 2.35	ND	11.11 ± 0.78
ergosta-5,8,22-trien-3-ol,(3a′,22E)- (Lichesterol)	ND	29.84 ± 1.33	ND	08.26 ± 0.33	32.13 ± 1.95
ergostenol	ND	05.19 ± 0.33	04.12 ± 0.38	11.56 ± 0.41	05.71 ± 0.42
ergosta-7,22-dien-3-ol,(3a′,22E)-	ND	ND	ND	15.28 ± 0.3	15.81 ± 1.1
unidentified/other sterols	03.57 ± 0.57	ND	ND	ND	ND

[a]All the values mentioned here are average % determined from two experiments with standard error of the mean. [b]ND, Not detected.

24 were comparable or better than amorolfine with more potent fungicidal effect (MFC) against all the tested strains.

Morpholine class of antifungals act on two enzymes of ergosterol biosynthesis pathway, viz., sterol Δ^{14} reductase and sterol Δ^7-Δ^8 isomerase, leading to ergosterol depletion and accumulation of intermediates ignosterol (Figure 1) and lichesterol.[27,28] To check whether the present sila-analogues act in a similar way, *C. albicans* ATCC 24433 cells were grown in the presence of different subinhibitory (<MIC) concentrations of **5**, **19**, **24**, and amorolfine and the cellular sterols were extracted and measured spectrophotometrically.[29] Ergosterol and the late sterol intermediate 24(28) dehydroergosterol (24(28)DHE) in a sample shows characteristic four-peaked curve in a spectrometric scan between wavelengths 230−300 nm.[29] In the presence of compounds **5**, **19**, and **24**, a dose-dependent decrease in the height of the absorbance peaks was observed indicating decrease in the ergosterol content in *Candida* cells (Figure S1 in Supporting Information). Accumulation of specific intermediates was checked by GC−MS quantification of cellular sterols in samples of **24** and amorolfine treatment. Results confirmed decrease in ergosterol content and also showed concomitant increase in the concentration of ignosterol and/or lichesterol (Table 2). The accumulation of these intermediates was like amorolfine treated cells implying the same mode of action, i.e., inhibition of sterol reductase and sterol isomerase. More accumulation of lichesterol (32.13%) than ignosterol (11.11%) for amorolfine indicated stronger action on isomerase enzyme than reductase (Table 2), whereas, in the case of **24**, accumulation of ignosterol (42.29%) can be attributed to the major effect on sterol reductase at higher concentration. Depletion of ergosterol compromises membrane integrity, affects membrane proteins functions due to membrane instability, and leads to cessation of growth.

The % microsomal stability of selected compounds was evaluated after 30 min incubation with mouse as well as human liver microsomes. All the tested compounds did not show good stability in mouse liver microsomes. However, three compounds with silicon incorporation (**15**, **18**, and **24**) showed relatively better stability than fenpropidin (Table 3). In case of human liver microsomes, metabolic stability was improved including for fenpropidin. Compound **18** showed better stability in human liver microsomes than fenpropidin, whereas compound **24** was found to be slightly inferior to fenpropidin. Thus, incorporation of silicon in the piperidine ring seems to be beneficial toward improving the metabolic stability.

Table 3. % Metabolic Stability of the Compounds in Liver Microsomes (after 30 min)

compds	metabolic stability	
	mouse	human
15	5.1	26.0
18	17.3	44.5
24	6.2	27.3
fenpropidin	1.1	34.4

To determine that the compounds are selectively toxic to the fungal cells and not to mammalian cells, hemolysis assay[30] using RBCs and MTT assay[30] using HEK293 cells were carried out. RBC hemolysis was not observed for any of the tested compounds up to 128 µg/mL, whereas partial hemolysis was observed for **19**, **20**, and **21** at 256 µg/mL (Supporting Information Table S1). As this concentration was many folds higher than the MICs of the compounds against different pathogens, they may be considered safe. In the case of lead compound **24**, only negligible hemolysis (∼7%) was observed at 512 µg/mL. The concentrations of the compounds required for 50% reduction in growth of HEK293 cells were also far higher than the MICs against fungi. Among the tested compounds, only compound **20** was found to be toxic to some extent against HEK293 cells with IC$_{50}$ of 9.81 µg/mL (Supporting Information Table S1).

In conclusion, total 15 silicon analogues of morpholine antifungals were designed and synthesized. Twelve compounds, viz., **5**, **11**, **12**, **15**, **16**, and **18−24**, exhibited potent antifungal activity against different fungal pathogens. The compounds act similar to morpholines by targeting sterol reductase and sterol isomerase of ergosterol synthesis pathway and cause depletion of ergosterol. Compound **24** showed better antifungal activity than fenpropidin, fenpropimorph, and amorolfine against different yeast and filamentous human pathogens and was identified as the lead. Further optimization of this series is in progress.

■ ASSOCIATED CONTENT

Ⓢ Supporting Information

The Supporting Information is available free of charge on the ACS Publications website at DOI: 10.1021/acsmedchemlett.5b00245.

Spectrophotometric sterol analysis, details of biological assays including cytotoxicity and metabolic stability, and experimental procedures and characterization data for all the new compounds (PDF)

AUTHOR INFORMATION

Corresponding Authors
*E-mail: sgtupe@yahoo.co.in.
*E-mail: mv.deshpande@ncl.res.in.
*E-mail: ds.reddy@ncl.res.in.

Notes
The authors declare no competing financial interest.

ACKNOWLEDGMENTS

ABBREVIATIONS

RBCs, red blood cells; HEK293, Human Embryonic Kidney 293 cells

REFERENCES

(1) Chaudhary, P. M.; Tupe, S. G.; Deshpande, M. V. Chitin synthase inhibitors as antifungal agents. *Mini-Rev. Med. Chem.* **2013**, *13*, 222–236.

(2) Tupe, S. G.; Deshpande, M. V. Current Status and New Directions in Antifungal Drug Development. In *Biotechnology: Beyond Borders*; Deshpande, M. V., Ruiz-Herrera, J., Eds.; National Chemical Laboratory: Pune, India, 2014; pp 241–252.

(3) Fungicide Resistance Action Committee. FRAC Code List: Fungicides sorted by mode of action (including FRAC Code numbering), 2011; pp 1–10.

(4) Gauwerky, K.; Borelli, C.; Korting, H. C. Targeting virulence: a new paradigm for antifungals. *Drug Discovery Today* **2009**, *14*, 214–222.

(5) Hartman, P. G.; Sanglard, D. Inhibitors of ergosterol biosynthesis as antifungal agents. *Curr. Pharm. Design* **1997**, *3*, 177–208.

(6) Lima, L. M.; Barreiro, E. J. Bioisosterism: A useful strategy for molecular modification and drug design. *Curr. Med. Chem.* **2005**, *12*, 23–49.

(7) Meanwell, N. A. Synopsis of some recent tactical application of bioisosteres in drug design. *J. Med. Chem.* **2011**, *54*, 2529–2591.

(8) Geyer, M.; Wellner, E.; Jurva, U.; Saloman, S.; Armstrong, D.; Tacke, R. Can silicon make an excellent drug even better? An *in vitro* and *in vivo* head-to-head comparison between loperamide and its silicon analogue sila-loperamide. *ChemMedChem* **2015**, *10*, 911–924.

(9) Tacke, R.; Popp, F.; Müller, B.; Theis, B.; Burschka, C.; Hamacher, A.; Kassack, M. U.; Schepmann, D.; Wünsch, B.; Jurva, U.; Wellner, E. Sila-haloperidol, a silicon analogue of the dopamine (D2) receptor antagonist haloperidol: synthesis, pharmacological properties, and metabolic fate. *ChemMedChem* **2008**, *3*, 152–64.

(10) Johansson, T.; Weidolf, L.; Popp, F.; Tacke, R.; Jurva, U. In vitro metabolism of haloperidol and sila-haloperidol: new metabolic pathways resulting from carbon/silicon exchange. *Drug Metab. Dispos.* **2010**, *38*, 73–83.

(11) Geyer, M.; Karlsson, O.; Baus, J. A.; Wellner, E.; Tacke, R. Si- and C- Functional organosilicon building blocks for synthesis based on 4-silacyclohexan-1-ones containing the silicon protecting groups MOP (4-methoxyphenyl), DMOP (2,6-dimethoxyphenyl), or TMOP (2,4,6-trimethoxyphenyl). *J. Org. Chem.* **2015**, *80*, 5804–5811.

(12) Nakamura, M.; Kajita, D.; Matsumoto, Y.; Hashimoto, Y. Design and synthesis of silicon-containing tubulin polymerization inhibitors: replacement of the ethylene moiety of combretastatin A-4 with a silicon linker. *Bioorg. Med. Chem.* **2013**, *21*, 7381–7391.

(13) Franz, A. K.; Wilson, S. O. Organosilicon molecules with medicinal applications. *J. Med. Chem.* **2013**, *56*, 388–405.

(14) Mills, J. S.; Showell, G. A. Exploitation of silicon medicinal chemistry in drug discovery. *Expert Opin. Invest. Drugs* **2004**, *13*, 1149–1157.

(15) Gately, S.; West, R. Novel therapeutics with enhanced biological activity generated by the strategic introduction of silicon isosteres into known drug scaffolds. *Drug Dev. Res.* **2007**, *68*, 156–163.

(16) Ramesh, R.; Reddy, D. S. Zinc mediated allylations of chlorosilanes promoted by ultrasound: Synthesis of novel constrained sila amino acids. *Org. Biomol. Chem.* **2014**, *12*, 4093–4097.

(17) Balamkundu, S. S.; Ramesh, R.; Dange, S. S.; Khairnar, P. V.; Singhal, S.; Upadhyay, D.; Veeraraghavan, S.; Viswanadha, S.; Vakkalanka, S.; Reddy, D. S. Design, Synthesis and Identification of Silicon Incorporated Oxazolidinone Antibiotics with Improved Brain Exposure. Unpublished results; communicated.

(18) Reddy, D. S.; Balamkundu, S.; Ramesh, R. Sila analogs of oxazolidinone derivatives and synthesis thereof. Patent WO2013054275, 2013.

(19) Acker, R.-D.; Buschmann, E.; Pommer, E. H.; Ammermann, E. Organosilyl compounds and their use as fungicides. Patent US4579842A.

(20) Roberts, T. R.; Hutson, D. H. Morpholines. In *Metabolic Pathways of Agrochemicals: Insecticides and Fungicides*; Roberts, T. R., Hutson, D. H., Eds.; Royal Society of Chemistry: London, UK, 1998; pp 1225–1238.

(21) Polak, A. Mode of action of morpholine derivatives. *Ann. N. Y. Acad. Sci.* **1988**, *544*, 221–228.

(22) Brenzovich, W. E.; Brazeau, J.-F., Jr.; Toste, F. D. Gold-catalyzed oxidative coupling reactions with aryltrimethylsilane. *Org. Lett.* **2010**, *12*, 4728–4731.

(23) Doherty, E. M.; Fotsch, C.; Bo, Y.; Chakrabarti, P. P.; Chen, N.; Gavva, N.; Han, N.; Kelly, M. G.; Kincaid, J.; Klionsky, L.; Liu, Q.; Ognyanov, V. I.; Tamir, R.; Wang, X.; Zhu, J.; Norman, M. H.; Treanor, J. J. S. Discovery of potent, orally available vanilloid receptor-1 antagonists. Structure-activity relationship of N-aryl cinnamides. *J. Med. Chem.* **2005**, *48*, 71–90.

(24) Kim, H. D.; Suh, Y. G.; Park, H. G.; Oh, U. T.; Park, S. R.; Kim, J. H.; Jang, M. J.; Park, Y. H.; Shin, S. S.; Kim, S. Y. Novel compounds, isomer thereof, or pharmaceutically acceptable salts thereof as vanilloid receptor antagonist; and pharmaceutical compositions containing the same. Patent WO 2006101318A1, 2006.

(25) Clinical and Laboratory Standards Institute. CLSI document M27-A3, Reference method for broth dilution antifungal susceptibility testing of yeasts: approved standard, 3rd ed., Wayne, PA, 2008.

(26) Clinical and Laboratory Standards Institute. CLSI document M38-A2, Reference method for broth dilution antifungal susceptibility testing of filamentous fungi. Approved Standard, 2nd ed., Wayne, PA, 2008.

(27) Liang, R.-M.; Cao, Y.-B.; Fan, K.-H.; Xu, Y.; Gao, P.-H.; Zhou, Y.-J.; Dai, B.-D.; Tan, Y.-H.; Wang, S.-H.; Tang, H.; Liu, H.-T.; Jiang, Y.-Y. 2-Amino-nonyl-6-methoxyl-tetralin muriate inhibits sterol C-14 reductase in the ergosterol biosynthetic pathway. *Acta Pharmacol. Sin.* **2009**, *30*, 1709–1716.

(28) Müller, C.; Staudacher, V.; Krauss, J.; Giera, M.; Bracher, F. A convenient cellular assay for the identification of the molecular target of ergosterol biosynthesis inhibitors and quantification of their effects on total ergosterol biosynthesis. *Steroids* **2013**, *78*, 483–493.

(29) Arthington-Skaggs, B. A.; Jradi, H.; Desai, T.; Morrison, C. J. Quantitation of ergosterol content: Novel method for determination of fluconazole susceptibility of *Candida albicans*. *J. Clin. Microbiol.* **1999**, *37*, 3332–3337.

(30) Maurya, I. K.; Thota, C. K.; Sharma, J.; Tupe, S. G.; Chaudhary, P.; Deshpande, M. V.; Prasad, R.; Chauhan, V. S. Mechanism of action of novel synthetic dodecapeptides against *Candida albicans*. *Biochim. Biophys. Acta, Gen. Subj.* **2013**, *1830*, 5193–5203.

Short communication

Repurposing of a drug scaffold: Identification of novel sila analogues of rimonabant as potent antitubercular agents

Remya Ramesh [a, d], Rahul D. Shingare [a, d], Vinod Kumar [a], Amitesh Anand [b, d], Swetha B [c], Sridhar Veeraraghavan [e], Srikant Viswanadha [e], Ramesh Ummanni [c, d], Rajesh Gokhale [b, d], D. Srinivasa Reddy [a, d, *]

[a] CSIR-National Chemical Laboratory, Dr. Homi Bhabha Road, Pune, 411008, India
[b] CSIR-Institute of Genomics and Integrative Biology, Mathura Road, New Delhi, 110025, India
[c] CSIR-Indian Institute of Chemical Technology, Tarnaka, Hyderabad, 500007, India
[d] Academy of Scientific and Innovative Research (AcSIR), New Delhi, 110 025, India
[e] Incozen Therapeutics Pvt. Ltd., Alexandria Knowledge Park, Turkapally, Rangareddy, 500078, India

ARTICLE INFO

ABSTRACT

The structural similarity between an MmpL3 inhibitor BM212, and a cannabinoid receptor modulator rimonabant, prompted us to investigate the anti-tubercular activity of rimonabant and its analogues. Further optimization, particularly through incorporation of silicon into the scaffold, resulted in new compounds with significant improvement in anti-tubercular activity against *Mycobacterium tuberculosis* (H37Rv). The sila analogue **18a** was found to be the most potent antimycobacterial compound (MIC, 31 ng/mL) from this series with an excellent selectivity index.

© 2016 Elsevier Masson SAS. All rights reserved.

1. Introduction

Drug discovery has become an increasingly tough endeavor. The average cost of bringing a drug into market is estimated to be about US$ 2600 million with a timeline of up to 15 years [1]. Identification of entirely novel compounds with unknown pharmacokinetic and safety profile poses more risk apart from being expensive and time consuming. The discovery of new indications for an existing drug termed "drug repurposing or drug reprofiling" is a lower risk strategy with increased probability of success within a short span of time. According to a recent report, 24 drugs had been remarketed for new uses and more than 15 are currently in the various developmental stages [2–4]. Also, molecules that failed in the clinic for a particular indication can be successfully repurposed for treatment of other conditions. Thalidomide, the most controversial drug of all time, is now used for pain relief in certain cancers and leprosy [5]. Pfizer's blockbuster drug sildenafil citrate (Viagra®), which was originally intended for hypertension was serendipitously repurposed after the Phase I clinical trials for erectile dysfunction [6].

Tuberculosis (TB) is an infectious disease caused by various strains of mycobacteria; the most common one being *Mycobacterium tuberculosis* (Mtb). Almost one-third of the total world population is asymptomatically infected by Mtb and it is the second leading cause of death due to an infectious agent [7]. Medications are known to treat TB; however, the response rate is slow with development of antibiotic resistance posing a serious threat. In view of these challenges, there is a need to develop new drug candidates with novel mechanisms for treating tuberculosis. The pre-clinical candidate BM212, a 1,5-aryl substituted pyrrole was

---

BM212 (**1**)
MmpL3 inhibitor

Rimonabant (**2**)
CB1 receptor modulator

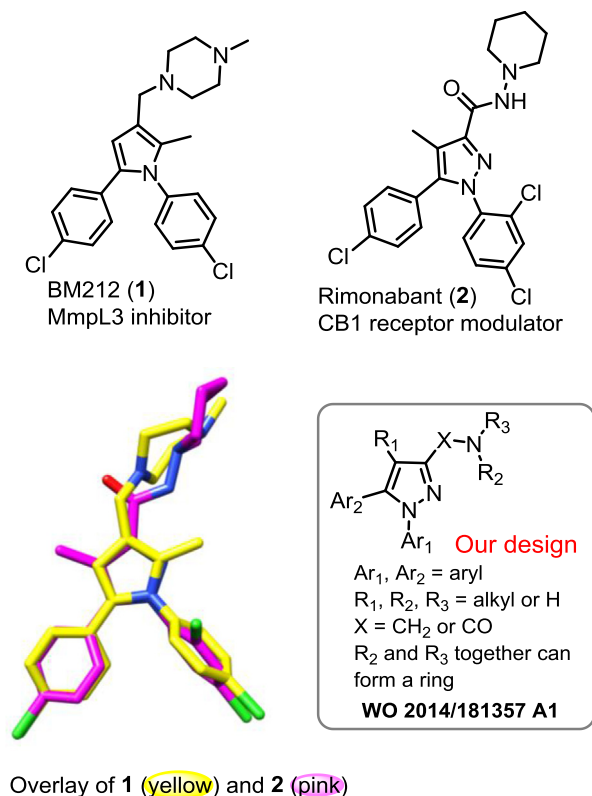Overlay of **1** (yellow) and **2** (pink)

Fig. 1. Design of diarylpyrazoles (rimonabant analogues) towards antitubercular agents.

reported to be active against Mtb with a minimum inhibitory concentration (MIC) of 0.7–1.5 μg/mL [8]. BM212 belongs to the MmpL3 class of inhibitors and blocks the transport of mycolic acids that are essential for the development of cell wall of mycobacteria thereby inhibiting their growth [9]. MmpL3 is a relatively new therapeutic target and other lead compounds such as SQ109, AU-1235, NITD-304 are also known to act on this transporter protein [10–14]. To identify new antitubercular agents with novel scaffolds that have already been tested in humans, a scaffold hopping technique was adopted using BM212. Towards this direction, an anti-obesity drug rimonabant (**2**) [15] attracted our attention. An overlay of BM212 (**1**) and rimonabant (**2**) suggested close structural similarities between the two (see Fig. 1). Rimonabant acts by blocking the cannabinoid receptor-1 (CB1). This receptor is expressed mainly in the central and peripheral nervous system and is involved in controlling food consumption, mood, and anxiety related disorders [16,17]. An advantage with the rimonabant scaffold is that it can penetrate blood-brain-barrier (BBB) and may be useful in developing agents for the treatment of brain tuberculosis. The objective of the current study was to repurpose the rimonabant scaffold towards the development of agents active against Mtb [18].

2. Results and discussion

2.1. Synthesis

Initial screening of rimonabant demonstrated moderate potency (MIC = 25 μg/mL, Mtb) and gave us encouragement to synthesize more analogues. Analogues of rimonabant with varying structural features were synthesized and evaluated for their activity against Mtb. All the synthetic details are outlined in Schemes 1–5. Compound **3** was synthesized according to the literature protocol and

was coupled with several amines to give a series of amides (**4a**–**4k**) [19]. Amide **4l** was prepared from the corresponding acid chloride employing procedures known in the literature [20]. The ester group in **4k** was hydrolyzed to obtain the acid **4m**. The hydrazide **4n** was obtained from the corresponding ester **6** and hydrazine hydrate [21]. Because of our group's continued interest in organosilicon molecules [22,23], we synthesized a few silicon analogues (**4c** and **4d**) as well. The bioisosteric replacement of carbon with silicon has gained attention in recent times [24–29]. The silaamide **4c** was converted to thioamide **5** by treating with Lawesson's reagent in THF (Scheme 1). Towards slightly more polar analogues, the known ester **6** was subjected to benzylic bromination using *N*-bromo-succinimide (NBS) and the bromo derivative was converted to alcohol in the presence of AgNO$_3$ and water. Hydroxylester **7** was hydrolyzed to obtain the acid **8** [30]. Carboxylic acid **8** was then coupled to the silicon amines **A** and **B** using EDC. HCl and HOBt to obtain amides **9a** and **9b**, respectively (Scheme 2). Alcohol **10** was prepared from ester **6** by following the literature procedures and was subjected to alkylation using benzyl bromide and NaH as base to obtain the ether **11** (Scheme 3) [31]. Alcohol was converted into its mesylate and displaced with various amines to generate a library of rimonabant amine analogues **12a**–**12g** (Scheme 3).

For the preparation of hydroxymethyl amine, the alcohol **7** was

4a: R =   **4b**: R =   **4c**: R =

4d: R =   **4e**: R =   **4f**: R =

4g: R =   **4h**: R =   **4i**: R =

4j: R =   **4k**: R =   **4l**: R =

4m: R =   **4n**: R =
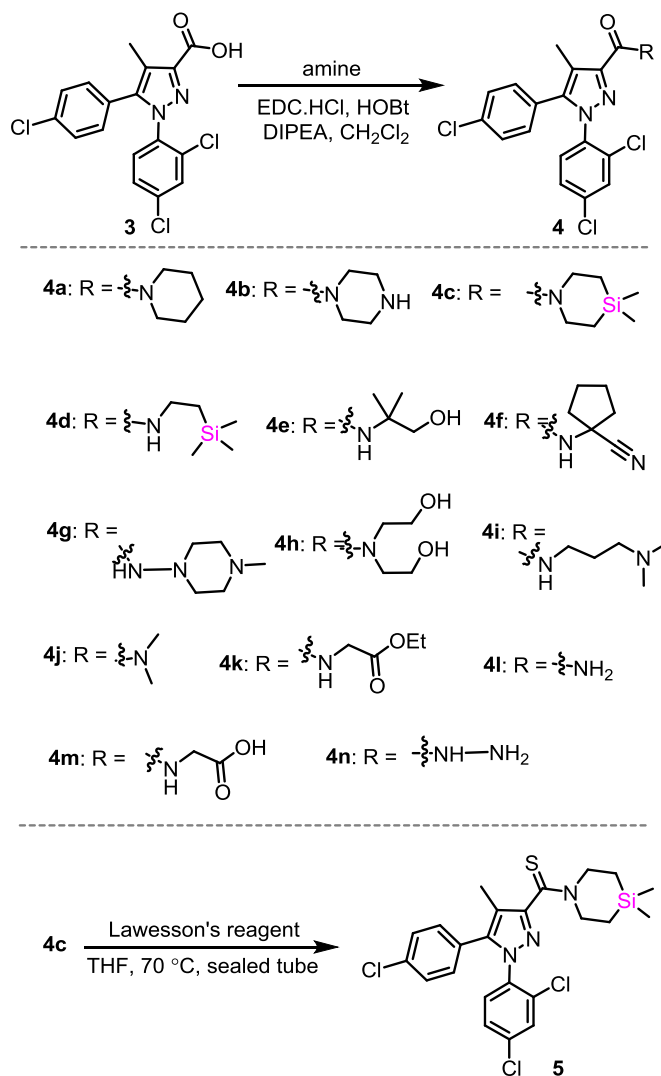
Scheme 1. Syntheses of amides and thioamide.

Scheme 2. Synthesis of hydroxymethyl amides.
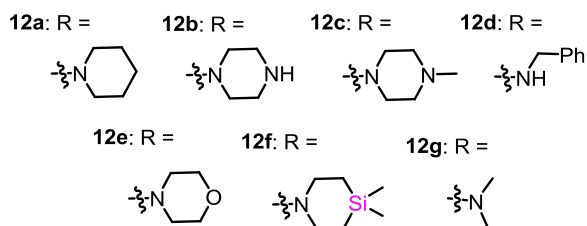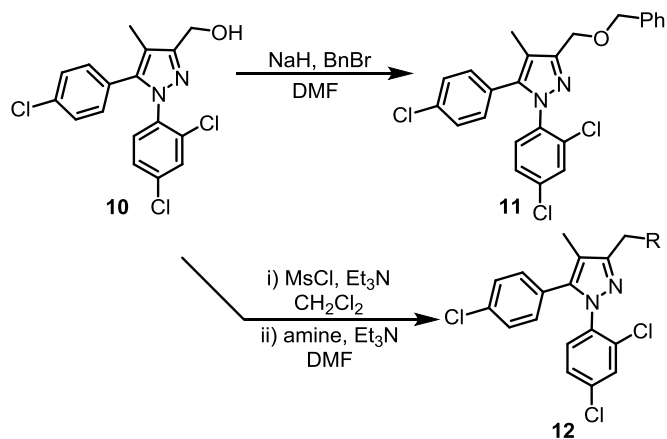
Scheme 3. Syntheses of ether **11** and amines **12**.

Scheme 4. Synthesis of compounds **14** and **16**.
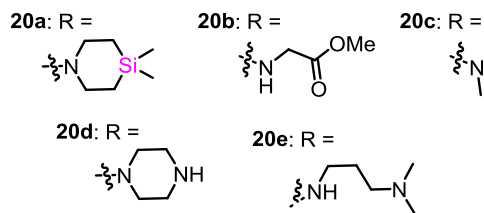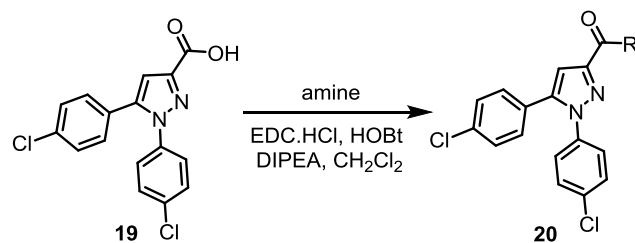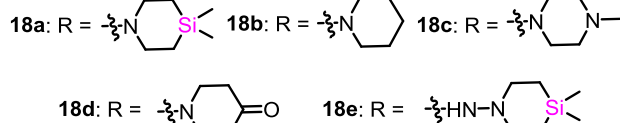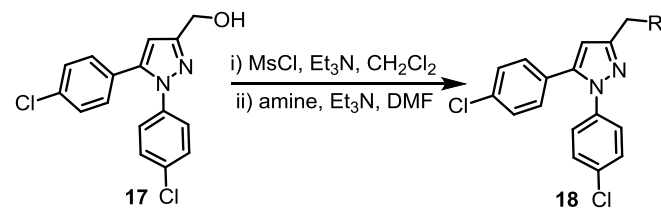
Scheme 5. Synthesis of des-methyl pyrazole derivatives.

Table 1
Antitubercular activity of selected compounds.
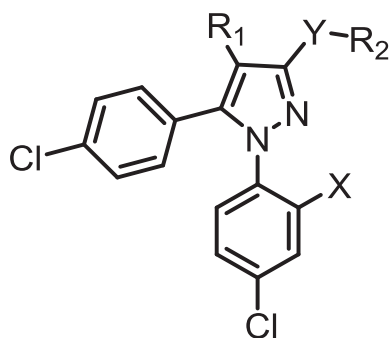
Compd	X	R_1	Y	R_2	MIC[a]	Compd	X	R_1	Y	R_2	MIC[a]
2	Cl	Me	CO	HN–N(piperidine)	25	**18a**	H	H	CH_2	N(sila-piperidine, Si)	0.031
4b	Cl	Me	CO	N(piperazine)–NH	25	**18b**	H	H	CH_2	N(piperidine)	1.56
4g	Cl	Me	CO	HN–N(piperazine)–N–CH₃	25	**18c**	H	H	CH_2	N(piperazine)–N–CH₃	25
4i	Cl	Me	CO	NH–CH₂CH₂CH₂–N(CH₃)₂	25	**18d**	H	H	CH_2	N(piperidinone, =O)	25
12a	Cl	Me	CH_2	N(piperidine)	12.5	**18e**	H	H	CH_2	HN–N(sila-piperidine, Si)	0.39
12b	Cl	Me	CH_2	N(piperazine)–NH	25	**20a**	H	H	CO	N(sila-piperidine, Si)	6.25
12c	Cl	Me	CH_2	N(piperazine)–N–CH₃	12.5	**20c**	H	H	CO	N(CH₃)₂	25
12d	Cl	Me	CH_2	NH–CH₂–phenyl	6.25	**20d**	H	H	CO	N(piperazine)–NH	25
12f	Cl	Me	CH_2	N(sila-piperidine, Si)	1.17	**20e**	H	H	CO	NH–CH₂CH₂CH₂–N(CH₃)CH₃	25
12g	Cl	Me	CH_2	N(CH₃)₂	6.25	**1**	–	–	–	–	0.70
14	Cl	CH₂OH	CH_2	N(sila-piperidine, Si)	6.25	**INH**	–	–	–	–	0.3

[a] MIC values are measured in μg/mL.

protected as its silyl ether **13** and the ester was reduced using Lithium aluminium hydride (LAH) in THF. The resulting alcohol was mesylated and displaced with the silicon amine **A** and finally the protecting group was removed using TBAF to obtain the hydroxymethyl sila analogue **14**. In order to make compounds with more structural variations, alcohol **10** was converted to its corresponding azide **15**. This azide on CuI catalyzed azide-alkyne cycloaddition with ethyl propiolate gave the 1,4 –substituted triazole ester **16** (Scheme 4). We also wanted to determine the influence of methyl group of pyrazole moiety on the activity of the compound because the C-4 methyl group is absent in BM212. Accordingly the alcohol

**17** and acid **19** were synthesized [32]. By utilizing the same strategy adopted for the previous compounds, amines **18a**–**18e** and amides **20a**–**20e** were prepared (Scheme 5).

2.2. Antitubercular activity of compounds

After generating a library of rimonabant analogues with various structural features, our next task was to check the anti-tubercular activity of the compounds. The MIC of the compounds against H37Rv was determined in an Alamar- Blue assay (see supplementary data). The MIC values of selected compounds are given in

Fig. 2. SAR conclusions (using anti-TB potential) of the current series.

Table 2
Cytotoxicity effects of the selected compounds.

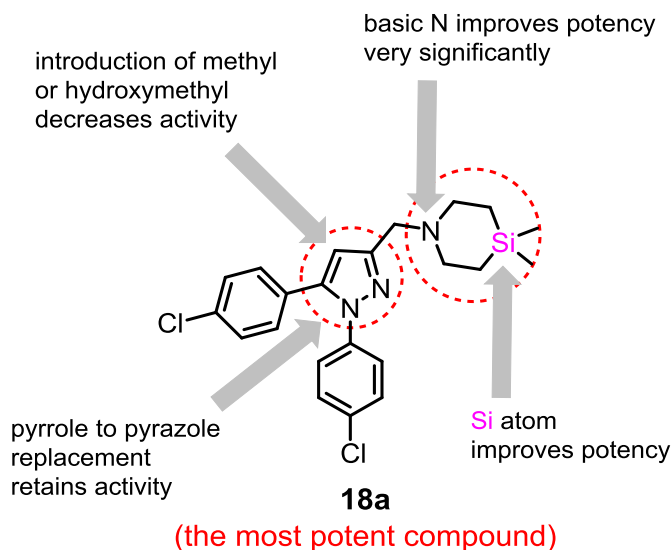| Compd	IC$_{50}$ (µM)		Selectivity index	
	A549 IC$_{50}$ ± Std dev	HEP G2 IC$_{50}$ ± Std dev	A549	HEP G2
BM212	91.55 ± 5.16	71.00 ± 5.26	57.22	44.38
12a	88.83 ± 6.37	>100	3.1	>3.5
12c	80.29 ± 3.12	85.05 ± 4.35	2.9	3.1
12d	55.82 ± 1.12	57.41 ± 3.39	4.1	4.2
12f	54.16 ± 9.64	51.87 ± 3.26	31.86	30.51
12g	57.18 ± 5.37	36.32 ± 2.37	3.62	2.30
14	61.94 ± 3.62	30.42 ± 1.21	4.92	2.41
18a	58.89 ± 0.52	21.44 ± 2.62	841.30	306.32
18e	73.22 ± 3.42	86.83 ± 3.69	84.16	99.80
20a	68.33 ± 2.07	58.97 ± 0.53	4.85	4.18
Doxorubicin	5.32 ± 3.2	5.34 ± 1.82	–	–

(Table 2). Cytotoxicity of the most active compounds **12f**, **18a**, **18e** and the standard compound BM212 (**1**) were also evaluated in RAW macrophages and THP-1 monocytes (see supplementary data). Cytotoxicity was apparent at ≥ 3 µM for all the compounds tested and varied in the range of 40–60% across both cell lines. After this exercise, five best compounds were selected for further profiling. Solubility across different pH, plasma stability, metabolic stability and plasma protein binding were evaluated (Table 3). The amide **20a** showed poor solubility at all the pH tested. The compound **18e** showed very good solubility at varying pH. The other compounds showed good solubility at lower pH, but solubility decreased at higher pH. Since these compounds are basic in nature, they are expected to show good solubility at acidic pH. All the compounds showed good plasma stability similar to that of BM212. The most potent compound **18a**, showed 100% stability in human plasma. Some compounds are degraded by plasma enzymes; therefore, stability in plasma is vital for determining efficacy of the parent compound. Metabolic stability of selected compounds was evaluated using mouse and human liver microsomes after 60 min incubation at 1 µM concentration. Most of the compounds including **18a** showed poor metabolic stability in both mouse and human liver microsomes with respect to BM212. Compound **18b** showed moderate stability in human liver microsomes. However, compound **18e** showed very good metabolic stability in liver microsomes. The compound **18e** was the best compound in terms of PK profile and the overall profile was better than BM212. Compounds demonstrating higher metabolic stability tend to have an increased half-life translating into superior efficacy *in vivo*. All the compounds including BM212 were strongly bound to the plasma proteins. High plasma protein binding is associated with a lower clearance rate resulting in a greater half-life *in vivo* compared to low protein bound compounds. It is generally believed that drugs with low plasma protein binding are more available and efficacious because of higher free drug concentration. But in an *in vivo* setting, several other factors such as metabolism and transport come into play [34,35].

3. Conclusion

In summary, we have successfully repurposed the rimonabant scaffold towards the development of potent antitubercular agents. After the synthesis and screening of several analogues around the rimonabant scaffold, we have identified the silicon analogue **18a** as the most potent compound against Mtb with an MIC value 31 ng/mL. It was observed that an increase in lipophilicity improves the potency of the compounds in this series. Based on present study, we have made a few SAR conclusions with respect to anti-TB potential, en route to the best compound **18a**. An *in vitro* analysis using ADME assays suggests that it needs further improvement in PK

Table 1. Rimonabant demonstrated moderate activity with an MIC of 25 µg/mL. Some of the compounds from the amide series (**4b**, **4i**, **4g** and **20a**, **20c**–**20e**) also showed moderate activity with high MIC values. The thioamide **5**, the ether analogue **11**, as well as the triazole **16** were not active. Many of the amines demonstrated good activity indicating that the basic nitrogen is essential for the desired antitubercular activity. The silicon amine **12f** (MIC 1.17 µg/mL) showed an activity similar to that of BM212. To our delight, compound **18a** showed excellent anti-tubercular activity with an MIC of 0.031 µg/mL, more than 22-fold increase in activity compared to the parent compound BM212. Interestingly this compound lacks the methyl group on pyrazole ring and is structurally more close to BM212. The compound **18e** (MIC 0.39 µg/mL) also showed good activity, but was 12 times less potent than **18a**. We have tested the compounds **18b** and **18c** in which silapiperidine ring was replaced with piperidine and piperazine rings, respectively. As expected, both the compounds **18b** (MIC 1.56 µg/mL) and **18c** (MIC 25 µg/mL) showed inferior activity with respect to corresponding silicon analogues **18a** and **18e**. The activity of **18b** is similar to that of BM212 which shows that the replacement of pyrrole to pyrazole in BM212 retains the anti-TB activity and can be modulated by changing the C3 substituents. The improved activity of silicon analogues may be explained by the improved cell wall permeability of lipophilic sila compounds. However, we do not have any experimental evidence with the present set of compounds. The introduction of a more polar hydroxyl group decreased the activity as seen in compound **14** (MIC 6.25 µg/mL), a 5-fold loss in potency when compared to **12f**. The amide **20a** showed moderate (MIC 6.25 µg/mL) activity and was the best from the amide series, whereas a similar compound **4c** did not show any activity. The introduction of methyl group on the pyrazole ring seems to be detrimental for the activity in most of the compounds (**20a** vs **4c** and **18a** vs **12f**). Based on this current exercise, we have made a few structure-activity relationship conclusions and they are compiled in Fig. 2.

2.3. Cytotoxicity and ADME data

We have also carried out cytotoxicity studies on selected compounds against lung epithelial cells (A549) and human hepatoma cells (HepG2) to determine their selectivity index [33]. The potent compounds **12f**, **18a** and **18e** showed excellent selectivity for Mtb over the cytotoxic effect against A549 and Hep G2 cell lines tested

Table 3
In-vitro physchem and ADME data.

Compd	Solubility (μM) at pH					% Plasma stability in human	% Metabolic stability in liver microsomes (after 30 min)		% Human PPB
	1.2	2.2	4.5	7.4	10.2		Mouse	Human	
BM212	45.19	42.21	36.73	26.68	5.38	100	62.4	79.8	99.23
12f	40.98	40.58	34.24	1.05	10.94	99.18	9.2	18.5	99.95
14	44.02	42.47	41.62	5.31	2.39	88.12	3.7	2.1	99.96
18a	43.04	42.28	41.87	3.72	1.99	100.0	6.3	20.3	99.93
18b	44.96	44.65	43.56	11.40	1.49	91.7	26	60.1	99.89
18e	43.14	43.20	44.28	39.76	38.00	100.0	100.0	93.1	99.31
20a	0.16	0.18	0.13	0.05	1.28	89.72	3.9	2.1	99.99

parameters, in particular, improvement in metabolic stability. However, compound **18e** (MIC 0.39 μg/mL) showed very good ADME profile. Optimization of the lead to improve the PK parameters and further biological profiling in *in vivo* models are in progress.

4. Experimental section

4.1. General

All reagents, starting materials, and solvents (including dry solvents) were obtained from commercial suppliers and used as such without further purification. Reactions were carried out in oven-dried glassware under a positive pressure of argon unless otherwise mentioned. Air sensitive reagents and solutions were transferred via syringe or cannula and were introduced to the apparatus via rubber septa. Reactions were monitored by thin layer chromatography (TLC) with 0.25 mm pre-coated silica gel plates (60 F254). Visualization was accomplished with either UV light, Iodine adsorbed on silica gel or by immersion in ethanolic solution of phosphomolybdic acid (PMA), *p*-anisaldehyde or $KMnO_4$ followed by heating with a heat gun for ~15 s. Column chromatography was performed on silica gel (100–200 or 230–400 mesh size). Deuterated solvents for NMR spectroscopic analyses were used as received. All ^1H NMR and ^{13}C NMR spectra were obtained using a 200 MHz, 400 MHz or 500 MHz spectrometer. Coupling constants were measured in Hertz. All chemical shifts were quoted in ppm, relative to TMS, using the residual solvent peak as a reference standard. The following abbreviations were used to explain the multiplicities: s = singlet, d = doublet, t = triplet, q = quartet, m = multiplet, br = broad. HRMS (ESI) were recorded on ORBITRAP mass analyser. Chemical nomenclature was generated using Chem Bio Draw Ultra 14.0. The purity of products was determined by reverse phase HPLC analysis using Agilent technologies 1200 series; column: ZORBAX Eclipse XBD-C-18 (4.6 × 250 mm, 5 μ). Flow rate 1.00 mL/min, UV 254 nm; using mobile phases, Method A: 95/5 CH_3OH/H_2O for 20 min; Method B: 90/10 CH_3CN/H_2O for 20 min.

4.2. General procedure for amide coupling

To a solution of the carboxylic acid (1 eq) in dry dichloromethane, was added *N*-(3-Dimethylaminopropyl)-*N'*-ethylcarbodiimide hydrochloride (EDC.HCl, 1.2 eq), Hydroxybenzotriazole (1.2 eq) and diisopropylethyl amine (3 eq) at 0 °C. Then the amine (1.1 eq) was added and stirred at RT for 6 h. To the reaction mixture, water was added and the organic layer was separated, washed with saturated $NaHCO_3$, 1 N HCl, dried over Na_2SO_4 and concentrated under reduced pressure. This crude mixture was purified by column chromatography to give the pure compound.

4.3. General procedure for preparation of amines

To a solution of the alcohol (1 eq) in dry dichloromethane (DCM), was added triethylamine (2.5 eq) followed by Mesyl chloride (1.1 eq) at 0 °C and stirred at the same temperature for 30 min. To the reaction mixture water was added and the organic layer was separated, dried over Na_2SO_4 and concentrated under reduced pressure. This crude product was immediately taken for the next step. The mesylate was dissolved in dry dimethyl formamide (DMF), triethylamine (4 eq) and corresponding amine partner (1.2 eq) was added at 0 °C and left to stir at RT for 4 h. To the reaction mixture water was added and the organic layer was separated, the aqueous layer was extracted using dichloromethane, dried over Na_2SO_4 and concentrated under reduced pressure. The crude was then purified by column chromatography to give the required compound.

4.4. Protocol for determination of MICs against H37Rv

The compounds were tested for antitubercular activity through inhibition of growth of the virulent strain of *Mycobacterium tuberculosis* H37Rv using Alamar-Blue assay method. MIC values of the compounds against H37Rv were determined in 7H9-OADC media supplemented with 0.5% glycerol and 1 mgml^{-1} tryptone at 37 °C in 96-well microtiter plates using the colorimetric resazurin microtiter assay, and growth was measured by visual readout. Isoniazid was used as a positive drug control. Statistically significant differences of individual drugs were not observed between the triplicates for any of the antimicrobial agents tested.

4.5. Protocol for determination of % inhibition against *Mycobacterium smegmatis* (mc^{2}155)

Anti-mycobacterial activity of series of compounds synthesized was performed with *Mycobacterium smegmatis* strain using turbidimetry for growth inhibition. Isolated single colonies of *M. smegmatis* mc^{2}155 (ATCC 14,468) from 7H10 agar plate were grown overnight in Middlebrook 7H9 medium (0.47% Middlebrook 7H9 broth base, 10% ADS, 0.2% glycerol, and 0.1% Tween-80) to mid exponential phase at 370 °C. Subsequently, 5 mL of Middlebrook 7H9 broth were inoculated with the overnight grown culture and allowed to grow at 37 °C to early log phase (OD600 ≈ 0.3). For antimicrobial assay, 98 μL of 1:1000-folds dilution of secondary culture was dispensed into 96-well microtiter plate. To each well 2 μL of test compound was added to attain a final concentration of 6.25, 12.5, 25, 50 and 100 μM, and allowed to grow at 37 °C for 32 h 240 μL of sterile water were added to each well of the peripheral rows of 96-well plate to minimize media evaporation during assay incubation. Bacterial growth was assessed after 32 h of incubation by measuring turbidity at 600 nm OD600 values using TECAN

Infinite 200 PRO™ (Tecan Instruments, Switzerland). Positive controls (Rifampicin and INH) were included in every assay plates using stock solutions. The results were analyzed as the percentage of growth inhibition. All experiments were carried out in triplicates and results were reported as ± SD.

4.6. In vitro metabolic stability [36,37]

10 mM of standard solution was prepared in DMSO. 1 mM of working solution-1 was prepared in acetonitrile from the standard solution, 50 μM of working solution-2 was prepared in acetonitrile, water mixture (1:1) from the working solution-1. 98 μL of cocktail mixture (buffer, microsomes and cofactor) was transferred in a pre labelled micro centrifuge tube, 2 μL of working solution (50 μM in ACN: Water) was added into the cocktail mixture. Samples were incubated at 37 °C for 15, 30, 45 and 60 min time intervals. After incubation, samples were terminated with 200 μL of methanol containing internal standard. Then the samples were Vortexed in a table top vortexer for 5 min and centrifuged at 14,000 RPM for 5 min. Supernatant samples were subjected to LC-MS/MS analysis.

4.7. In vitro plasma stability [38]

10 mM of standard solution was prepared in DMSO. 1 mM of working solution-1 was prepared in Acetonitrile from the standard solution, 50 μM of working solution-2 was prepared in Acetonitrile, water mixture (1:1) from the working solution-1. 98 μL of test system was transferred in a pre labelled micro centrifuge tube, 2 μL of working solution (50 μM in ACN: Water) was added in to the cocktail mixture. Samples were incubated at 37 °C for 60 min time intervals. After incubation samples were terminated with 200 μL of methanol containing internal standard. Samples were Vortexed in a table top vortexer for 5 min and centrifuged at 14,000 RPM for 5 min, supernatant samples were subjected to LCMS/MS analysis.

4.8. Plasma protein binding (equilibrium dialysis method) [38]

745 μL of plasma was transferred into 2 mL micro centrifuge tube. To that 5 μL of test compound (150 μM) was added, samples were mixed in the table top vortexer for 2 min 50 μL plasma (n = 2) was transferred in a pre labelled 1.5 mL micro centrifuge tube treated as 0 h sample. Remaining 650 μL plasma sample were incubated for 30 min at 37 °C in a water bath, after 30 min incubation 50 μL plasma (n = 2) was removed in a pre labelled 1.5 mL micro centrifuge tube treated as 0.5 h sample. 200 μL of plasma sample (n = 2) was transferred into the sample chamber which is indicated by the red ring, RED insert was placed into the base plate and 350 μL of buffer was transferred into the buffer chamber. Plates were incubated at 37 °C at approximately 100 RPM on an orbital shaker or 20 RPM on an up-and-down shaker for 4 h 50 μL of post dialysis sample from the buffer and the plasma chambers were transferred into pre labelled micro centrifuged tube. 50 μL of plasma to the buffer samples and an equal volume of buffer (KH_2PO_4 Buffer pH 7.4) were added to the collected plasma samples. 150 μL of methanol containing internal standard (Tolbutamide 250 ng/mL) was added to precipitate the protein and release compound. Samples were vortexed for 3 min in a table top vortexer and centrifuged for 5 min at 14,000 RPM. The supernatant was subjected to LC-MS/MS analysis.

4.9. In vitro solubility

10 mM of standard solution was prepared in DMSO, 5 mM of working solution-1 was prepared in DMSO from the standard

solution. 495 μL of Buffer (1.2, 2.2, 4.5, 7.4 and 10.2 pH) was transferred in a pre labelled micro centrifuge tube. 5 μL of working solution (5 mM) was added in to the test system. Samples were vortexed in a table top vortexer for 5 min and centrifuged at 14,000 RPM for 5 min; supernatant samples were subjected to HPLC analysis.

4.10. Cytotoxicity assays

Selected compounds were evaluated for their in vitro cytotoxicity against A549 human lung carcinoma epithelial cells and HepG2 human hepatoma cells. A549 and HepG2 cells used in this study were purchased from the American Type Culture Collection (ATCC, USA). Cells were grown in standard Dulbecco's modified Eagles medium containing 10% FBS in a humidified atmosphere of 5% CO_2 at 37 °C. When cells were sub-confluent in 90 mm dishes, cells were harvested by trypsinization and seeded in 96 well plates at a density of 7500 cells. They were further allowed to grow in complete medium under standard conditions. After 18 h to treat cells with test molecules, aliquots of 2 μL of the compound dilutions were added to the appropriate microtiter wells containing 198 μL of fresh medium with cells, resulting in the required final drug concentrations (0.1, 1, 10 and 100 μM as per NCI screening protocol) in triplicates. As a standard reference drug, Doxorubicin was used in all assay plates and served as internal control. Plates were incubated further for 48 h and assay was terminated by the addition of 10 μL of 3-(4, 5-Dimethylthiazol-2-yl)-2, 5-diphenyltetrazolium bromide (MTT, 5 mg/ml) and incubated for 60 min at 37 °C. The plates were air-dried and the dye bound to the cells was subsequently solubilized in 100 μL of DMSO, and the absorbance was red on a multimode reader (Tecan) at a wavelength of 560 nm, which is directly proportional to cell growth. Percentage growth was calculated for test wells relative to control wells. The above determinations were repeated three times and mean values ± SD are reported. The growth inhibitory effects of the compounds were analyzed by generating dose response curves as a plot of the percentage surviving cells versus drug concentration. Further selectivity index was calculated by ratio between cytotoxicity (IC_{50} in μM)/MIC in μM.

Conflict of interest

No conflict of interest.

Appendix A. Supplementary data

Supplementary data related to this article can be found at http://dx.doi.org/10.1016/j.ejmech.2016.07.009.

References

[1] Statistics taken from internet via http://csdd.tufts.edu/news/complete_story/pr_tufts_csdd_2014_cost_study.

[2] C.R. Chong, D.J. Sullivan, New uses for old drugs, Nature 448 (2007) 645–646.

[3] L.A. Tartaglia, Complementary new approaches enable repositioning of failed drug candidates, Expert Opin. Investig. Drugs 15 (2006) 1295–1298.

[4] A useful site on drug repurposing: www.drugrepurposingportal.com.

[5] C. Therapontos, L. Erskine, E.R. Gardner, W.D. Figg, N. Vargesson, Thalidomide induces limb defects by preventing angiogenic outgrowth during early limb formation, Proc. Natl. Acad. Sci. U. S. A. 106 (2009) 8573–8578.

[6] N.K. Terrett, A.S. Bell, D. Brown, P. Ellis, Sildenafil (viagra™), a potent and selective inhibitor of type 5 CGMP phosphodiesterase with utility for the treatment of male erectile dysfunction, Bioorg. Med. Chem. Lett. 6 (1996) 1819–1824.

[7] Information taken from WHO site http://www.who.int/mediacentre/factsheets/fs104/en/accessed on August 2015.

[8] D. Deidda, G. Lampis, R. Fioravanti, M. Biava, G.C. Porretta, S. Zanetti, R. Pompei, Bactericidal activities of the pyrrole derivative BM212 against multidrug-resistant and intramacrophagic Mycobacterium tuberculosis strains, Antimicrob. Agents Chemother. 42 (1998) 3035–3037.

[9] V. La Rosa, G. Poce, J.O. Canseco, S. Buroni, M.R. Pasca, M. Biava, R.M. Raju, G.C. Porretta, S. Alfonso, C. Battilocchio, B. Javid, F. Sorrentino, T.R. Loerger, J.C. Sacchettini, F. Manetti, M. Botta, A. De Logu, E.J. Rubin, E. De Rossi, MmpL3 is the cellular target of the antitubercular pyrrole derivative BM212, Antimicrob. Agents Chemother. 56 (2012) 324–331.

[10] S.T. Cole, Transporter targeted in tuberculosis, Nat. Chem. Biol. 8 (2012) 326–327.

[11] G.V. Rayasam, MmpL3 a potential new target for development of novel anti-tuberculosis drugs, Expert Opin. Ther. Targets 18 (2013) 1–10.

[12] K. Tahlan, R. Wilson, D.B. Kastrinsky, K. Arora, V. Nair, E. Fischer, S.W. Barnes, J.R. Walker, D. Alland, C.E. Barry III, H.I. Boshoff, SQ109 targets MmpL3, a membrane transporter of trehalosemonomycolate involved in mycolic acid donation to the cell wall core of Mycobacterium tuberculosis, Antimicrob. Agents Chemother. 56 (2012) 1797–1809.

[13] A.E. Grzegorzewicz, H. Pham, V.A.K.B. Gundi, M.S. Scherman, E.J. North, T. Hess, V. Jones, V. Gruppo, S.E.M. Born, J. Korduláková, S.S. Chavadi, C. Morisseau, A.J. Lenaerts, R.E. Lee, M.R. McNeil, M. Jackson, Inhibition of mycolic acid transport across the Mycobacterium tuberculosis plasma membrane, Nat. Chem. Biol. 8 (2012) 334–341.

[14] S. Lun, H. Guo, O.K. Onajole, M. Pieroni, H. Gunosewoyo, G. Chen, S.K. Tipparaju, N.C. Ammerman, A.P. Kozikowski, W.R. Bishai, Indoleamides are active against drug-resistant Mycobacterium tuberculosis, Nat. Commun. 4 (2013) 1–8.

[15] M. Bifulco, C. Grimaldi, P. Gazzerro, S. Pisanti, A. Santoro, Rimonabant: just an antiobesity drug? current evidence on its pleiotropic effects, Mol. Pharmacol. 71 (2007) 1445–1456.

[16] R.I. Wilson, R.A. Nicoll, Endocannabinoid signaling in the brain, Science 296 (2002) 678–682.

[17] R.G. Pertwee, The pharmacology of cannabinoid receptors and their ligands: an overview, Int. J. Obes. 30 (2006) S13–S18.

[18] While we were working on this project, an article on the activity of rimonabant analogues against TB appeared in the literature J.M. Gajbhiye, N.A. More, M.D. Patil, R. Ummanni, S.S. Kotapalli, P. Yogeeswari, D. Sriram, V.H. Masand, Discovery of rimonabant and its potential analogues as anti-TB drug candidates, Med. Chem. Res. 24 (2015) 2960–2971. We have filed a patent before this publication which is now published, WO 2014/181357A1.

[19] P.K. Sasmal, D.S. Reddy, R. Talwar, B. Venkatesham, D. Balasubrahmanyam, M. Kannan, P. Srinivas, K. Shiva Kumar, B. Neelima Devi, V.P. Jadhav, S.K. Khan, P. Mohan, H. Chaudhury, D. Bhuniya, J. Iqbal, R. Chakrabarti, Novel pyrazole-3-carboxamide derivatives as cannabinoid-1 (CB1) antagonists: journey from non-polar to polar amides, Bioorg. Med. Chem. Lett. 21 (2011) 562–568.

[20] S.Y. Kang, S.–H. Lee, H.J. Seo, M.E. Jung, K. Ahn, J. Kim, J. Lee, Tetrazole-biaryl pyrazole derivatives as cannabinoid CB1 receptor antagonists, Bioorg. Med. Chem. Lett. 18 (2008) 2385–2389.

[21] P.K. Sasmal, R. Talwar, J. Swetha, D. Balasubrahmanyam, B. Venkatesham, K.A. Rawoof, B. Neelima Devi, V.P. Jadhav, S.K. Khan, P. Mohan, D.S. Reddy, V. Nyavanandi, S. Nanduri, K. Shiva Kumar, M. Kannan, P. Srinivas, P. Nadipalli, H. Chaudhury, V.J. Sebastian, Structure–activity relationship studies of novel pyrazole and imidazole carboxamides as cannabinoid-1 (CB1) antagonists, Bioorg. Med. Chem. Lett. 21 (2011) 4913–4918.

[22] B. Seetharamsingh, R. Ramesh, S.S. Dange, P.V. Khairnar, S. Singhal, D. Upadhyay, S. Veeraraghavan, S. Viswanadha, S. Vakkalanka, D.S. Reddy, Design, synthesis and identification of silicon incorporated oxazolidinone antibiotics with improved brain exposure, ACS Med. Chem. Lett. 6 (2015) 1105–1110.

[23] G.R. Jachak, R. Ramesh, D.G. Sant, S.U. Jorwekar, M.R. Jadhav, S.G. Tupe, M.V. Deshpande, D.S. Reddy, Silicon incorporated morpholine antifungals: design, synthesis and biological evaluation, ACS Med. Chem. Lett. 6 (2015) 1111–1116.

[24] A.K. Franz, S.O. Wilson, Organosilicon molecules with medicinal applications, J. Med. Chem. 56 (2013) 388–405.

[25] S. Gately, R. West, Novel therapeutics with enhanced biological activity generated by the strategic introduction of silicon isosteres into known drug scaffolds, Drug Dev. Res. 68 (2007) 156–163.

[26] R. Tacke, T. Heinrich, R. Bertermann, C. Burschka, A. Hamacher, M.U. Kassack, Sila-haloperidol: a silicon analogue of the dopamine (D_2) receptor antagonist haloperidol, Organometallics 23 (2004) 4468–4477.

[27] C.M. Reid, K.N. Fanning, L.S. Fowler, A. Sutherland, Synthesis and reactivity of 4-oxo- 5-trimethylsilanyl derived α-amino acids, Tetrahedron 71 (2015) 245–251.

[28] M. Geyer, E. Wellner, U. Jurva, S. Saloman, D. Armstrong, R. Tacke, Can silicon make an excellent drug even better? an in vitro and in vivo head-to-head comparison between loperamide and its silicon analogue sila-loperamide, ChemMedChem 10 (2015) 911–924.

[29] J. Wang, C. Ma, Y. Wu, R.A. Lamb, L.H. Pinto, W.F. DeGrado, Exploring organosilane amines as potent inhibitors and structural probes of influenza A virus M2 proton channel, J. Am. Chem. Soc. 133 (2011) 13844–13847.

[30] F. Barth, C. Congy, S. Martinez, P. Pointeau, M. Rinaldi-Carmona. Derivatives of N-[(1,5-diphenyl-1H-pyrazol-3-yl)methyl]sulfonamide, Their Preparation and Their Application in Therapeutics. US 7297710 B1.

[31] K. Kobayashi, M. Uchiyama, H. Ito, H. Takahashi, T. Yoshizumi, H. Sakoh, Y. Nagatomi, M. Asai, H. Miyazoe, T. Tsujita, H. Hirayama, S. Ozaki, T. Tani, Y. Ishii, H. Ohta, O. Okamoto, Discovery of novel arylpyrazole series as potent and selective opioid receptor-like 1 (ORL1) antagonists, Bioorg. Med. Chem. Lett. 19 (2009) 3627–3631.

[32] M. Alvarado, P. Goya, M. Macías-González, F.J. Pavón, A. Serrano, N. Jagerovic, J. Elguero, A. Gutiérrez-Rodríguez, S. García-Granda, M. Suardíaz, F.R. de Fonseca, Antiobesity designed multiple ligands: synthesis of pyrazole fatty acid amides and evaluation as hypophagic agents, Bioorg. Med. Chem. 16 (2008) 10098–10105.

[33] A. Singh, B. Mahipal, S. Chandrasekhar, R. Ummanni, 5-epi-Torrubiellutin C shows antiproliferative activity on DU145 prostate cancer cells through inactivation of the AKT/mTOR pathway, Anticancer Drugs 25 (2014) 385–392.

[34] D.A. Smith, L. Di, E.H. Kerns, The effect of plasma protein binding on in vivo efficacy: misconceptions in drug discovery, Nat. Rev. Drug Discov. 9 (2010) 929–939.

[35] X. Liu, M. Wright, C.E. Hop, Rational use of plasma protein and tissue binding data in drug design, J. Med. Chem. 57 (2014) 8238–8248.

[36] R.P. Remmel, B.C. Crews, K.R. Kozak, A.S. Kalgutkar, L.J. Marnett, Studies on the metabolism of the novel, selective cyclooxygenase-2 inhibitor indomethacin phenethylamide in rat, mouse, and human liver microsomes: identification of active metabolites, Drug Metob. Despos. 32 (2004) 113–122.

[37] A.P. Li, In vitro approaches to evaluate ADMET drug properties, Curr. Top. Med. Chem. 4 (2004) 701–706.

[38] W.J. Jusko, M. Gretch, Plasma and tissue protein binding of drugs in pharmacokinetics, Drug. Metab. Rev. 5 (1976) 43–140.

The following are added based on suggestions of reviewers.

Section 1.2.3.3

Page no: 55 *correction of structure*

The representation of compound **42** in table 1.2.1 is wrong. The structure of **42** is as shown in scheme 1.2.9.

Page no: 56 *explanation of activity in correlation with lipophilicity*

It is known that silicon incorporation increases the lipophilicity of compounds which is also evident from the clogP values. The silicon analog **52** has a clogP 9.4 whereas the corresponding carbon analog **53** has a value of 6.8 (calculated by chemdraw). This increase in clogP value is clearly reflected in the MIC values of both the compounds (MIC of **52** = 0.031 µg/mL; MIC of **53** = 1.56 µg/mL). Similar trend was observed in other compounds as well (**31** and corresponding silicon analog **35**). Compound **35** (clogP = 10.1; MIC = 0.78 µg/mL) and compound **31** (clogP = 7.5; MIC = 12.5 µg/mL).

Section 1.3.2.1

Page no: 130 *explanation for observed selectivity*

Propargyl and allenyl organometallics often exist as an equilibrium mixture and reactions involving these organometallic reagents can result in the formation of both products. Li *et. al.* observed that organoindium was a useful reagent for the regioselective allenylation of chlorosilanes.[34] Although the explanation for this observation was not provided, this is probably due to the increased stability of allenylindium compared to propargylindium species. According to our observation, zinc reaction highly favours the formation of propargyl products than the rearranged allenes. Under our reaction conditions we did not observe the formation of allenes in case of monochlorosilanes (scheme 1.3.5). In the case of dichlorosilanes, we could isolate small amounts of allenylpropargyl compounds (compounds **35** and **37**, scheme 1.3.6). In case of monochlorosilanes the rearranged product might have been formed only in very minor amounts that we could not isolate it.